

3.4.3

**Full Length Research Papers
Published in the Journals
Notified on UGC Care List**

2022 – 23



JMJ COLLEGE FOR WOMEN (AUTONOMOUS)
TENALI-522202, GUNTUR DT.A.P.
PRIVATE AIDED – MINORITY INSTITUTION
Re-Accredited by NAAC with B++ Grade (IV Cycle)
Recognized by UGC New Delhi under Section 2(f) & 12 (b)
(An Autonomous College in the Jurisdiction of Acharya Nagarjuna University)
Ph: 08644 225994

3.4.3 Number of research papers published per teacher in the Journals as notified on UGC CARE list during the last five years (2018 – 23)

S.No	Title of paper	Name of the author/s	Department of the teacher	Name of journal	Year of publication	ISSN number
2022 -23						
1.	Economical Bioprocess development to enhance the alkaline protease enzyme production by using <i>Penciliumoxalicum</i> KRSS-S-FP10 with statistical tools''	Dr.Ch.Sarojini	Zoology	International Education and Research Journal	June.2022	ISSN: 24549916
2.	Women's Quest for Self Esteem from Restrictions	Dr.G.Jyothi Olivia	English	Journal of English Language and Literature	June. 2022	ISSN:2349-9753
3.	English Language: An Icon for Advertisements and Cinema	Dr.N.Vimala Devi	English	Journal of English Language and Literature	June. 2022	ISSN:2349-9753



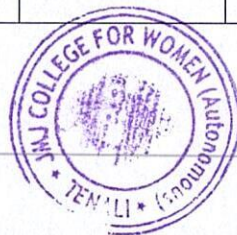
4.	“Survey of Helminth Parasites in Freshwater Fishes collected from Regions of Tenali Town, Guntur District, Andhra Pradesh”	Ms. M. Aruna	Zoology	International Journal of Creative Research Thoughts (IJCRT)	July.2022	ISSN: 2320-2882
5.	Cobalt (II) complexes with N-methyl thiosemicarbazide Schiff bases: Synthesis, spectroscopic investigation, cytotoxicity, DNA binding and incision, anti-bacterial and anti-fungal studies	Dr.V. Sumalatha	Chemistry	Inorganic Chemistry Communications	Sept.2022	Print ISSN: 1387-7003 Online ISSN: 1879-0259
6.	‘An Exploratory Study On Free And Paid Senior Citizen Homes in AP	Mrs. P. Hemalatha	Home Science	International Journal of Advanced Academic Studies	Sept.2022	P-ISSN:2706-8919, E-ISSN: 2706-8927,
7.	An Empirical Study On Elderly Abuse & Neglect: Issues and coping strategies	Mrs. P. Hemalatha	Home Science	International Journal of Applied Research	Oct.2022	ISSN Print:2394-7500, ISSN Online: 2394-5869
8.	Facile synthesis of hexagonal-shaped CuO NPs from Cu(II)-Schiff base complex for enhanced visible-light-driven degradation of dyes and antimicrobial studies	Dr.V. Sumalatha	Chemistry	Inorganica Chimica Acta	Dec.2022	Print ISSN: 1387-7003 Online ISSN: 1879-0259
9.	Kalipatnam Rama Rao Kathalalo Samakaalinatha	Dr.B.Mary Kumari	Telugu	International Journal of Multidisciplinary Educational Research	Dec.2022	ISSN No.2277-7881
10.	Kalipatnam Rama Rao Kathalalo Saamaajika Nepadhyam	Dr.B.Mary Kumari	Telugu	International Journal of Multidisciplinary Educational Research	Dec.2022	ISSN No.2277-7881



11.	Artificial Intelligence Technologies on Human Resource Management: A Study with Reference to Indian IT Sector at Hyderabad, Telegana.	P.Ch. Praveen Kumar PV. Vara Prabhakar	Commerce	IJRTI - International Journal for Research Trends and Innovation	Jan.2023	2456-3315
12.	A Study on Urban Health Management System in East Godavari District-AP-INDIA	P.Ch. Praveen Kumar PV. Vara Prabhakar	Commerce	The Seabold Report	Jan.2023	1533-9211
13.	Fabrication and characterization of CuO nano-needles from thermal decomposition of Cu(II) metal complex: Fluorometric detection of antibiotics, antioxidant, and antimicrobial activities	Dr.V. Sumalatha	Chemistry	Results in Chemistry	Jan. 2023	Online ISSN: 1873-3255, Print ISSN: 0020-1693
14.	Catalytic degradation of HIV drugs in water and antimicrobial activity of Chrysin-conjugated Ag-Au, Ag-Cu, and Au-Cu bimetallic nanoparticles	Dr.V. Sumalatha	Chemistry	Results in Chemistry	Jan. 2023	Online ISSN: 2211-7156
15.	Back Propagation Neural Network PO-based Grid Connected Dual PV Management and reliability Improvement	G.S.Rao	Computer Science	International Journal of Scientific Methods in Intelligence Engineering Networks (IJSMIEN)	May, 2023	2583-8113
16.	Synthesis of Schiff base stabilized AuNPs for enhanced catalytic degradation of pesticides, Cr(VI) detection, antioxidant, and antimicrobial activities	Dr.V. Sumalatha	Chemistry	Materials Today: Proceedings	May.2023	Online ISSN: 2214-7853



17.	Synthesis of Schiff base stabilized AgNPs for enhanced catalytic degradation of antibiotics, Hg(II) detection, antioxidant, and antimicrobial activities	Dr.V. Sumalatha	Chemistry	Materials Today: Proceedings	May .2023	Online ISSN: 2214-7853
18.	Hydrothermal fabrication of n-CeO ₂ /p-CuS heterojunction nanocomposite for enhanced photodegradation of pharmaceutical drugs in wastewater under visible-light and fluorometric sensor for detection of uric acid	Dr.V. Sumalatha	Chemistry	Inorganic Chemistry Communications	June, 2023	Online ISSN: 2214-7853
19.	Combining lightweight Encryption Methods to secure IOT Networks	G.S.Rao	Computer Science	International Journal of Scientific Methods in Engineering and Management (IJSMEM)	July,2023	2583-8083
20.	Fabrication of dual-functional heterostructured pCuO/n-ZnS nanocomposite for enhanced visiblelight active photocatalytic response and fluorometric sensor for selective sensing of thiolcontaining amino acids	Dr.V. Sumalatha	Chemistry	Chemical Engineering Research and Design	August,2023	https://doi.org/10.1016/j.cherd.2023.08.034 0263-8762/© 2023
21.	Financial Distress Analysis using the Altman Z Score Model, the Springat Model, and the Grainger Model in the Indian Cement Industry	Dr.M.Sambasivudu	Commerce	Journal of Namibian Studies	Sept.2023	ISSN: 2197-5523



22.	Class consciousness in the Novel The Space Between Us by Thirty Umrigar	S. Mary Sophia Rani	English	TIJER - INTERNATIONAL RESEARCH JOURNAL	Nov. 2023	2349-9249	
-----	---	---------------------	---------	---	-----------	-----------	--



S. S. Rani
Principal
JMJ COLLEGE FOR WOMEN (Autonomous)
TENALI



ECONOMICAL BIOPROCESS DEVELOPMENT TO ENHANCE THE ALKALINE PROTEASE ENZYME PRODUCTION BY USING *PENCILIUM OXALICUM* KRSS-S-FP10 WITH STATISTICAL TOOLS

Sarojini Chiluvuri

Department of Zoology, J.M.J. College for Women (A), Tenali, Guntur, A.P, India.

ABSTRACT

Alkaline protease producing microorganism's isolated total of 74 and 69 fungi from beach soils and black soils respectively were 10 from Kakinada beach soil and 9 from Vishakhapatnam beach soil and 40 isolates from Tenali black soil. The best producing organism identified and characterized as *Pencilium oxalicum* KRSS-S-FP10. Taguchi RSM was used to know active and independent variables screened by using PDA media variables was employed to derive statistical model (Response surface methodology: RSM) for optimizing the medium composition. The alkaline protease activity was in between 2.0U/mL to 10.76U/mL and The Delta value indicates the effect of component in the form of ranking has given to the variables. To confirm these results, experiments were carried out using RSM these nutrients with same concentrations and it was observed that the mean value of alkaline protease was 10.13U/mL as compared to the predicted value of 10.76U/mL using MINITAB. The final optimized medium has given approximately three-fold increase in alkaline protease production in comparison with one-factor-at-a-time (5.12U/mL) method.

KEY WORDS: MINITAB, Taguchi, *Pencilium oxalicum* KRSS-S-FP10, PDA media, optimization.

INTRODUCTION:

Currently enzymes can be used in basic and applied arenas of research as well as in a wide range of product design and manufacturing processes, such as food, beverage, pharmaceutical, detergent, leather processing and peptide synthesis industries with the estimated value of the global sales over 3 billion USD (Jordan Chapman *et al.*, 2018). Of the whole industrial enzymes, 75% are hydrolytic.

Three soil samples were collected in depth of 5-6 cm from soil. Alkaline pH was observed across the sampling sites and a total of 3 samples were found with plenty of micro flora occurrence (Ashok Pandey *et al.*, (2013)). The total micro-organism counts of the soils were estimated by standard dilution plate technique. The isolated microbes were identified by their cultural and fungi and actenomyces were obtained from the positive three soil samples (Dilution Worksheet and Problems (2021)). These are 10 fungal forms from Kakinada, 9 from Vishakhapatnam and 40 from Tenali black field morphological characteristics. Total 74 microorganism forms (includes bacteria soils. Alkaline proteases fungi were isolated using milk agar plate assay consists of 0.5% casein from different soils collected from Kakinada, Vishakhapatnam beach soil and Tenali black soil fields of Andhra Pradesh. Three soil fungal isolates were examined for protease producing microorganism. Isolation and RAPD-identification of the highest alkaline protease producer under submerged fermentation, using PDA media.

MATERIALS AND METHODS:

Reagents: Unless otherwise stated, the chemicals and medium ingredient used in this study were purchased from Sigma Chemical Co. (St. Louis, Mo, USA) and BD Bioscience (Le Pont de Claix, France). All other chemicals were also of analytical grade.

Optimization of enzyme production: Characterization of the different factors for alkaline protease production was optimized by applying RSM. Then statistical model was obtained using Central composite design (CCD) with three independent variables alkaline protease (X_1), (X_2) and $MnSO_4$ concentration (X_3). CCD maximizes the amount of information that can be obtained while limiting the number of individual experiments (Kunamneni and Singh, 2005). Each factor in the design was studied at five different levels (Table-1). A set of 20 experiments were performed. All variables taken at a central coded values were listed in Table-2. Upon completion of experiments, the average of alkaline protease production was taken as the dependent variable or response.

Statistical analysis: One factor ANOVA in Taguchi and MINITAB software was used to analyse the experimental results. Statistical analysis is considered as an important tool to interpret and summarise the experimental data. All the experiments results were carried out in duplicate and data obtained is represented as mean \pm SD in this paper. P-values of the experimental data are reported respective figures. The P-value less than 0.05 is considered to be statistically significant.

RESULTS AND DISCUSSION:

4.5.1 Optimization of the factors of Taguchi L_{12} :

Using L_{12} orthogonal array design approach, the relationships between medium component variables and their concentrations could be worked out. The optimal combinations and the concentration of the factors required to achieve the highest alkaline protease activity was represented in Table 4.5.1.1. The alkaline protease activity was in between 2.0 U/mL to 10.76 U/mL at different levels of various independent factors. The Taguchi approach suggests to analyze variation by using an appropriately chosen signal-to-noise (S=N) ratio and also serve to analyze the average response for each run in the inner array. The Table-4.5.1.2 and 4.5.1.3 represent the response table for mean and S/N ratio to understand the delta and the rank value of the system. The Delta value indicates the effect of that component whereas rank (Table-4.5.1.4) based on the delta values serialized the factors from the greatest effect to the least effect on the response.

In the present study, it can be seen that for each of the seven variables at three levels, one level increases the mean compared to the other level (Table-4.5.1.5). Thus the factors $NaNO_3$ at level-1, $MgSO_4$ at level-1, $ZnSO_4$ at level-1, TA at level-1, KH_2PO_4 at level-2, $FeSO_4$ at level-1, KCl at level-1 shows a main effect. These levels also represent the optimal concentrations of the individual components in the medium. The Fig.10 and Fig.11 represent the main effect plot of means and S/N ratio in the system. Final optimized levels of each factor in the medium for alkaline protease production had shown in Table-4.5.1.1. To confirm these results, experiments were carried out using these nutrients with same concentrations and it was observed that the mean value of alkaline protease was 10.13 U/mL as compared to the predicted value of 10.76 U/mL using MINITAB. The final optimized medium (Table-4.5.1.6) has given approximately three-fold increase in alkaline protease production in comparison with one-factor-at-a-time (5.12U/mL) method. Therefore, it should be considered that the selected conditions were the most suitable in practice and $NaNO_3$, casein and KCl were identified as the major influencing factors in the enzyme production.

Table 4.5.1.1. Optimization of the factors of Taguchi L_{12}

Run	pH	Casein	Glucose	$FeSO_4$	$NaMoO_4$	$MnCl_2$	$CaCl_2$	$MgSO_4$	NH_4NO_3	KH_2PO_4	Mean	R1
1	9	1	1	0.005	0.005	1	1	2	5	2	6.880	6.010
2	9	1	4	0.050	0.005	4	4	2	5	2	9.117	10.000
3	9	10	1	0.005	0.050	1	1	2	5	6	9.910	10.620
4	9	10	4	0.005	0.005	4	4	6	5	6	3.540	3.220
5	9	1	1	0.050	0.050	1	1	6	5	6	8.520	8.490
6	9	10	4	0.050	0.050	4	4	6	5	2	2.000	2.114
7	10	10	4	0.005	0.050	4	4	2	10	2	8.800	9.210
8	10	1	4	0.050	0.050	4	4	2	10	6	10.880	9.160
9	10	10	1	0.050	0.005	1	1	2	10	6	6.760	7.120

10	10	1	1	0.005	0.050	1	1	6	10	2	8.240	8.520
11	10	10	1	0.050	0.005	1	1	6	10	2	10.630	10.270
12	10	1	4	0.005	0.005	4	4	6	10	6	10.760	10.130

Table 4.5.1.2. Response Table for Signal to Noise Ratios

Level	pH	Casein	Glucose	FeSO ₄	NaMoO ₄	MnCl ₂	CaCl ₂	MgSO ₄	NH ₄ NO ₃	KH ₂ PO ₄
1	40.4238	43.5218	40.6685	25.1055	28.9432	22.9226	18.0618	39.9127	37.3846	41.8684
2	36.6501	36.4160	36.0426	36.9830	37.0424	34.8195	35.8304	35.4223	36.5373	35.5176
3	31.9141	30.1763	30.6532	31.2489	33.0206	31.4222	31.6511	30.6031	30.9134	30.1116
4	35.9046	36.1387	36.5120	35.5717	35.5123	37.7351	36.7242	37.1324	36.0173	37.0370
5	9.5424	39.4626	33.2552	37.5012	0.0000	36.3909	36.9020	34.9638	31.5957	42.3454
Delta	30.8814	13.3455	10.0152	12.3958	37.0424	14.8126	18.8402	9.3096	6.4712	12.2338
Rank	2	5	8	6	1	4	3	9	10	7

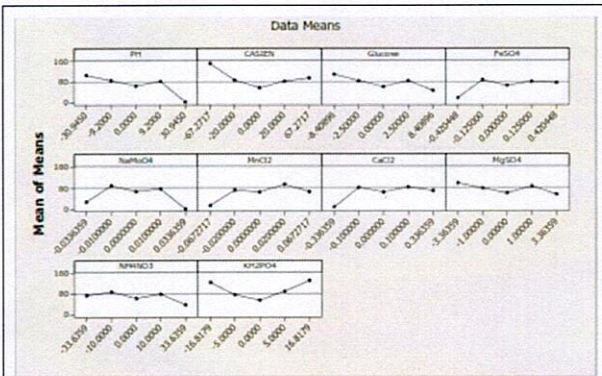


Fig. 11: Main Effects Plot for Means

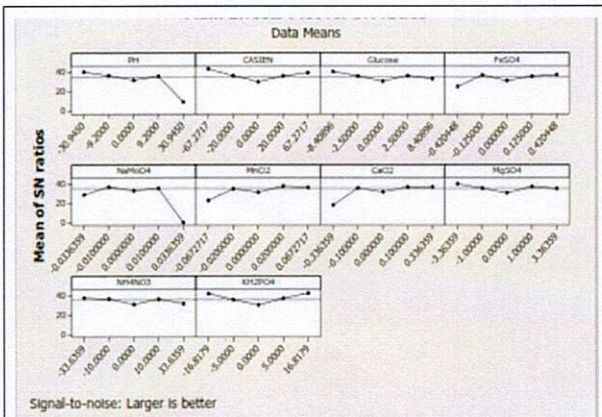


Fig. 12: Main Effects Plot for SN ratios

4.5.2. Optimization of the selected medium components by RSM:

The Taguchi results showed that among seven different culture components, four have significant impact on enzyme production (Mishra, Rashmi, (2020)). Response surface methodology was used to investigate the effects of four components viz. MnCl₂, Casein, NaMoO₄, and pH by taking as independent variables on alkaline protease enzyme production (Malhotra and Chapadgaonkar, 2020). It was found that alkaline protease production was enhanced up to 10.76 U/mL in the medium optimized by RSM.

The CCD matrix in terms of code and actual values of independent variables is given in Table-4.5.2.1. The second order model equation was quantified by using Analysis of variance (ANOVA). ANOVA of the quadratic model indicated that the model is significant. In this study it was found that A, C, D, A², H², AB, AC, AH, BH and CH (A=MnCl₂, 0.005 g/L, B=casein 13.1521g/L, C= NaMoO₄, 0.0205 g/L, and D=pH 9.0/10.0) are the model terms. The second order response model was made after analysis of regression. The model can be illustrated as follows.

Final Equation in Terms of Coded Factors:

$$R1 = +523.9752.65 * A^3 + 3642.48 * B^4 + 5.32 * C^1 + 73.27 * D + 79.31 * AB + 183.06 * AC + 118.23 * AD + 77.81 * BC + 842.31 * BD + 101.88 * CD + 123.35 * A^2 + 2398.65 * B^2 + 17.$$

$$52 * C^2 + 200.31 * ABD + 158.81 * ACD + 181.31 * BCD + 130.35 * A^2 + 2D + 396.40 * B^2 + 138.66 * C^2 + 2D.$$

Final Equation in Terms of Actual Factors (pH 9.0):

$$R1 = +1.221666E+0051.83737E+006 * MnCl_2 + 1884.72947 * Casein + 14828.82972 * NaMoO_4 + 2420.00000 * MnCl_2 * Casein + 2.48718E+005 * MnCl_2 * NaMoO_4 + 530.76923 * Casein * NaMoO_4 + 1.01484E+007 * MnCl_2^2 + 27.95051 * Casein^2 + 6.73725E+005 * NaMoO_4^2 \text{ and}$$

Final Equation in Terms of Actual Factors: pH10.0:

$$R1 = +37550.07733 - 76878.05410 * MnCl_2 - 2039.89282 * Casein + 2.87974E+005 * NaMoO_4 + 5592.50000 * MnCl_2 * Casein + 3.50641E+006 * MnCl_2 * NaMoO_4 + 1328.84615 * Casein * NaMoO_4 + 2.79959E+005 * MnCl_2^2 + 20.02245 * Casein^2 + 25597.90761 * NaMoO_4^2$$

Table 4.5.2.1: Actual and predicted values

Run Order	Actual Value	Predicted Value	Residual	Leverage	Internally Studentized Residual	Externally Studentized Residual	Cook's Distance	Influence on Fitted Value	Standard Order
1	8808.00	8484.71	323.29	0.670	0.723	0.714	0.053	1.018	5
2	702.00	697.24	4.76	0.166	0.007	0.007	0.000	0.003	15
3	709.00	1525.14	-816.14	0.607	-1.675	-1.760	0.217	-2.189	10
4	350.00	350.70	-0.70	0.166	-0.001	-0.001	0.000	-0.000	39
5	386.00	350.70	35.30	0.166	0.050	0.048	0.000	0.022	37
6	370.00	618.29	-248.29	0.607	-0.509	-0.500	0.020	-0.622	29
7	15850.00	16145.34	-295.34	0.607	-0.606	-0.596	0.028	-0.741	11
8	55.00	-598.38	653.38	0.670	1.458	1.503	0.216	2.141	28
9	356.00	350.70	5.30	0.166	0.007	0.007	0.000	0.003	36
10	759.00	697.24	61.76	0.166	0.087	0.085	0.000	0.038	19
11	12018.00	10725.21	1294.79	0.607	2.657	3.219	0.546	4.003	31
12	12.00	1060.34	-1048.34	0.607	-2.151	-2.391	0.358	-2.974	12
13	45.00	-136.68	181.68	0.670	0.407	0.398	0.017	0.567	24
14	2822.00	3926.26	-1104.26	0.670	-2.471	-2.889	0.919	-4.115	26
15	5508.00	5511.03	-293.03	0.670	-0.454	-0.445	0.021	-0.634	25
16	152.00	-609.22	761.22	0.670	1.703	1.795	0.294	2.557	8
17	304.00	538.46	-234.46	0.607	-0.481	-0.472	0.018	-0.587	33
18	5208.00	5422.66	-214.66	0.670	-0.480	-0.471	0.023	-0.671	22
19	312.00	350.70	-38.70	0.166	-0.054	-0.053	0.000	-0.024	40
20	8305.00	8116.10	188.90	0.670	0.423	0.414	0.018	0.589	1
21	308.00	43.34	264.66	0.607	0.543	0.533	0.023	0.663	34
22	45.00	-1037.91	1082.91	0.670	2.423	2.810	0.595	4.002	23
23	701.00	697.24	3.76	0.166	0.005	0.005	0.000	0.002	17
24	9208.00	8809.17	398.83	0.670	0.892	0.887	0.081	1.263	6
25	740.00	1516.95	-776.95	0.607	-1.594	-1.663	0.197	-2.068	14
26	332.00	350.70	-18.70	0.166	-0.026	-0.026	0.000	-0.011	38
27	160.00	-466.83	626.83	0.670	1.403	1.440	0.199	2.050	4
28	63.00	-130.31	193.31	0.670	0.433	0.424	0.019	0.603	27
29	363.00	350.70	12.30	0.166	0.017	0.017	0.000	0.008	35
30	708.00	697.24	10.76	0.166	0.015	0.015	0.000	0.007	18
31	4067.00	5639.93	-672.93	0.670	-1.306	-1.559	0.230	-2.220	21
32	8894.00	8537.76	356.24	0.670	0.797	0.790	0.064	1.124	2
33	40.00	1504.59	-1264.59	0.607	-2.595	-3.105	0.521	-3.862	32
34	789.00	697.24	91.76	0.166	0.129	0.126	0.000	0.056	20
35	144.00	-449.89	593.89	0.670	1.329	1.356	0.179	1.932	7
36	760.00	1326.73	-566.73	0.607	-1.163	-1.174	0.105	-1.460	13
37	147.00	-404.50	551.50	0.670	1.234	1.251	0.151	1.782	3
38	755.00	697.24	57.76	0.166	0.081	0.079	0.000	0.035	16
39	322.00	43.51	278.49	0.607	0.571	0.562	0.020	0.608	30
40	777.00	1304.55	-527.55	0.607	-1.082	-1.082	0.045	-1.082	9

The significance of second order model equation was verified by F (ANOVA) test (Table-4.5.2.3.). For this model, if the F test is significant at 5% level i.e. P<0.0001, then the model 5 is considered as fit ANOVA analysis can explain whether the more complex model is required for a better fit and it gives the values of the model (Rouaa Daou et al., 2021). According to the ANOVA of the quadratic regression model, it was identified that the present model is highly significant and it is justified by the F test value of 49.79 (with 0.0001 probability value (Pmodel> F is 0.0001) (Table-4.5.2.3). The "Pred R-Squared" of 0.9793 is not as close to the "Adj R-Squared" of 0.9596 as one might normally expect (Abiola Ezekiel Taiwo et al., 2020). This may indicate a large block effect or a possible problem with the model and/or data. Things to consider are model reduction, response transformation, outliers, etc "Adeq Precision" measures the signal to noise ratio. A ratio greater than 4 is desirable (Sunil Chamoli, 2015). A ratio of 31.246 indicates an adequate signal (Table-4.5.2.4.). The three dimensional plots of the responses were drawn to predict the alkaline protease for different test variable values to understand the interaction among the independent factors (Ram Kumar et al., 2018). The plots of A², B², C², AC, BC, BD were constructed by taking response (alkaline protease production) at z-axis against two variables (Fig.

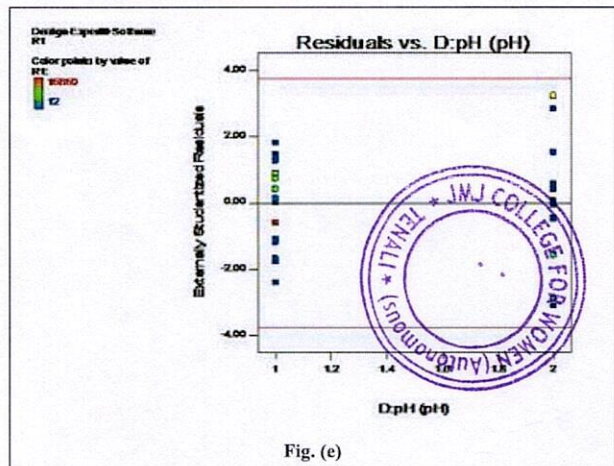
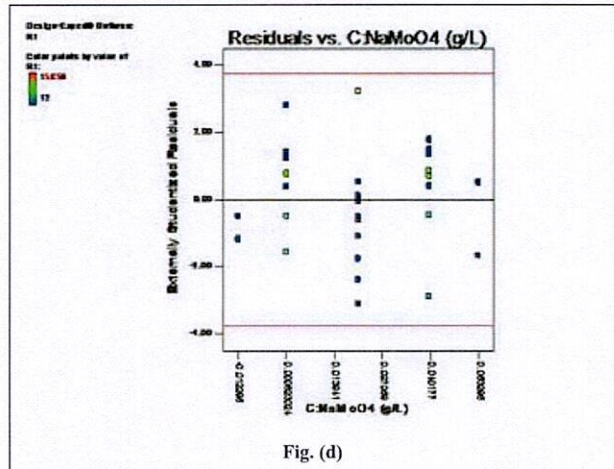
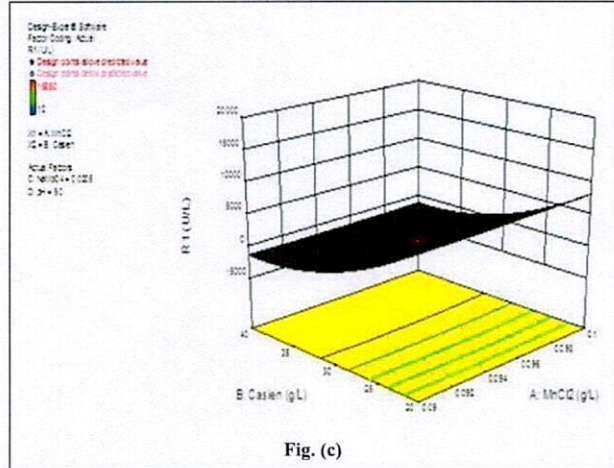
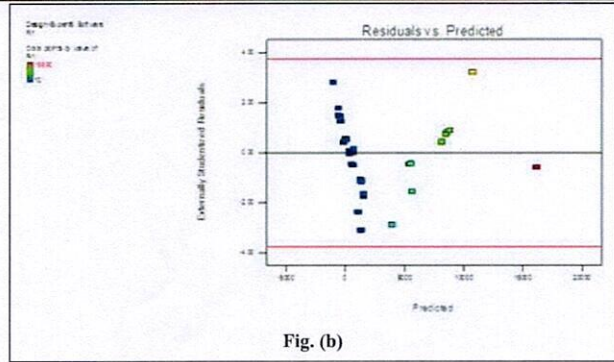
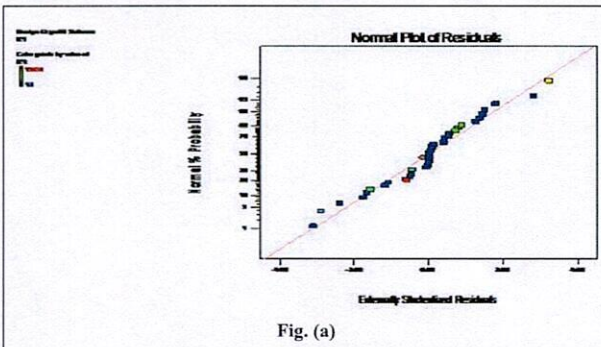
12). It was observed that medium containing MnCl₂ 0.005 g/L, casein 13.1521 g/L, NaMoO₄ 0.0205 g/L, and pH 9.0/10.0. The predicted results comparatively show 0.5-fold increase with Taguchi (10.76 to 15.82 U/mL) alkaline protease activity (Hammami, Bayouhd, and Abdelhedi, 2018). Similarly, the effects of parameters such as, relative humidity, pH of the liquid medium, and volume of inoculums were positive and smaller than the error limits and the change in mean effect was also small, in which case according to the decision-making procedure of the evolutionary operation technique it was advisable to select a new search region and start a new phase of experiments reported (Dhayalan, Velramar, Govindasamy, 2022). RSM has been applied for designing of experiments to evaluate the interactive effects through a full 31 factorial design and reported the similar results by Gilmour, Steven, in the year (2006). The optimum conditions were casein concentration, 3.22%; fermentation period, 96h; temperature, 30°C; and pH 9.0. The high value of the regression coefficient (R²=0.9793) indicate excellent evaluation of experimental data by second-order polynomial regression model. The RSM revealed that a maximum alkaline protease production of 15.82 U/mL was obtained at the optimum conditions and found the similar results with Gomaa, (2013).

Table 4.5.2.2: ANOVA for Response Surface Reduced cubic model
Analysis of variance table.

ANOVA for Response Surface Reduced Cubic model						
Analysis of variance table [Partial sum of squares - Type III]						
Source	Sum of Squares	df	Mean Square	F Value	p-value Prob > F	
Model	5.722E+008	19	3.012E+007	49.79	< 0.0001	significant
A-MnCl2	75716.45	1	75716.45	0.13	0.7272	
B-Casien	3.624E+008	1	3.624E+008	599.15	< 0.0001	
C-NaMoO4	56104.35	1	56104.35	0.093	0.7638	
D-pH	3.610E+005	1	3.610E+005	0.60	0.4488	
AB	1.006E+005	1	1.006E+005	0.17	0.6877	
AC	5.362E+005	1	5.362E+005	0.89	0.3577	
AD	3.818E+005	1	3.818E+005	0.63	0.4362	
BC	96876.56	1	96876.56	0.16	0.6932	
BD	1.938E+007	1	1.938E+007	32.04	< 0.0001	
CD	2.835E+005	1	2.835E+005	0.47	0.5014	
A^2	4.386E+005	1	4.386E+005	0.73	0.4046	
B^2	1.658E+008	1	1.658E+008	274.17	< 0.0001	
C^2	3.981E+005	1	3.981E+005	0.66	0.4268	
ABD	6.420E+005	1	6.420E+005	1.06	0.3152	
ACD	4.035E+005	1	4.035E+005	0.67	0.4237	
BCD	5.260E+005	1	5.260E+005	0.87	0.3622	
A^2D	4.898E+005	1	4.898E+005	0.81	0.3789	
B^2D	4.529E+006	1	4.529E+006	7.49	0.0127	
C^2D	5.542E+005	1	5.542E+005	0.92	0.3499	
Residual	1.210E+007	20	6.048E+005			
Lack of Fit	1.209E+007	10	1.209E+006	1192.90	< 0.0001	significant
Pure Error	10132.17	10	1013.22			
Cor Total	5.843E+008	39				

Table 4.5.2.3. Response curve standards with factor 1 and R1

Factor	Coefficient Estimate	df	Standard Error	95% CI Low	95% CI High	VIF
Intercept	523.97	1	224.29	56.12	991.82	
A-MnCl2	-52.65	1	148.81	-363.06	257.76	1.00
B-Casien	-3642.48	1	148.81	-3952.89	-3332.07	1.00
C-NaMoO4	-45.32	1	148.81	-355.73	265.09	1.00
D-pH	-173.27	1	224.29	-641.13	294.58	3.33
AB	79.31	1	194.43	-326.26	484.88	1.00
AC	-183.06	1	194.43	-588.63	222.51	1.00
AD	-118.23	1	148.81	-428.64	192.18	1.00
BC	77.81	1	194.43	-327.76	483.38	1.00
BD	842.31	1	148.81	531.90	1152.72	1.00
CD	-101.88	1	148.81	-412.29	208.53	1.00
A^2	123.35	1	144.86	-178.82	425.53	1.02
B^2	2398.65	1	144.86	2096.47	2700.82	1.02
C^2	117.52	1	144.86	-184.65	419.70	1.02
ABD	200.31	1	194.43	-205.26	605.88	1.00
ACD	-158.81	1	194.43	-564.38	246.76	1.00
BCD	181.31	1	194.43	-224.26	586.88	1.00
A^2D	-130.35	1	144.86	-432.53	171.82	1.67
B^2D	-396.40	1	144.86	-698.58	-94.23	1.67
C^2D	-138.66	1	144.86	-440.84	163.51	1.67



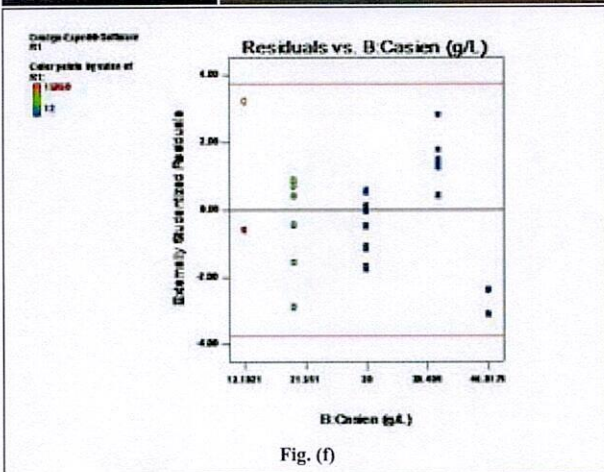


Fig. (f)

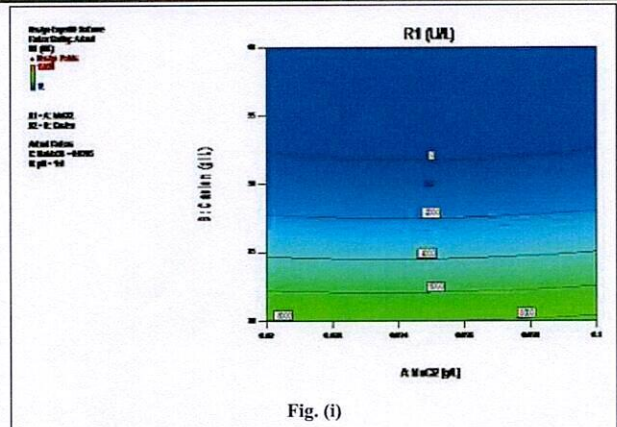


Fig. (i)

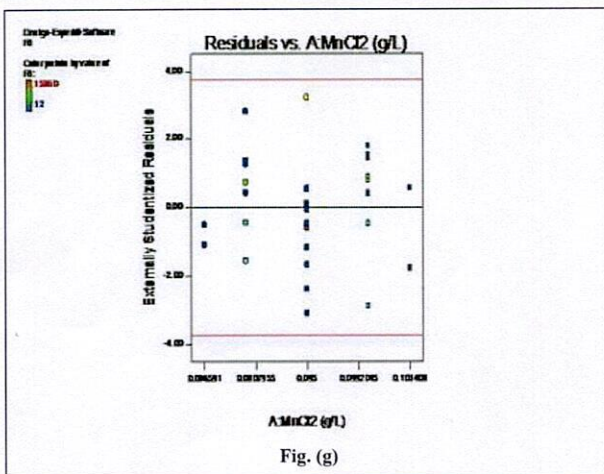


Fig. (g)

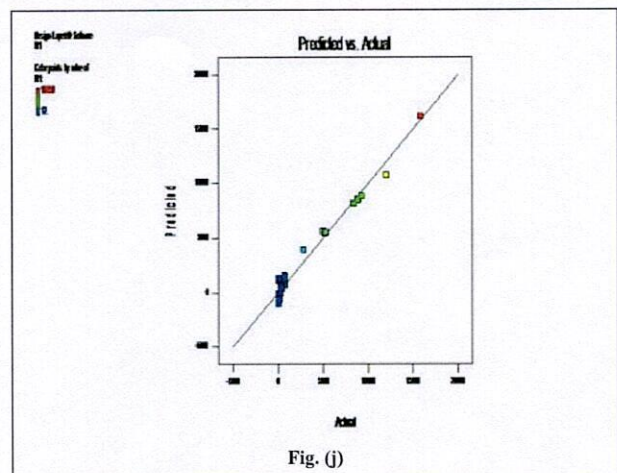


Fig. (j)

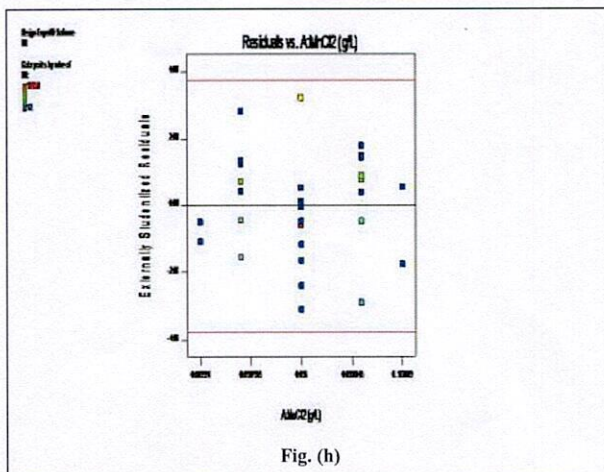


Fig. (h)

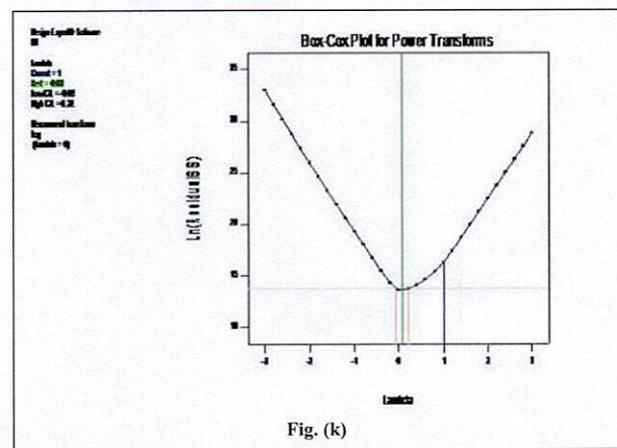


Fig. (k)

Table 4.5.2.4: Standard Deviation, Mean

Std. Dev.	777.71	R-Squared	0.9793
Mean	2326.35	Adj R-Squared	0.9596
C.V. %	33.43	Pred R-Squared	0.8407
PRESS	9.307E+007	Adeq Precision	31.246

CONCLUSION:

Present investigation aims to develop new bioprocess and economically feasible media by using optimization of production medium composition. It effects the cost of production medium and found effective production of enzyme. By taking PDA media and serially optimized the media by using some statistical tools are Taguchi, RSM and Minitab reduces the unwanted variables in the media for good fermentation, this step reduces the cost of production. As a result, use of dependent and independent variables enhance the production of alkaline protease shake flask fermentation. The bioprocess optimization predicted results comparatively show 0.5-fold increase with Taguchi to RSM (10.76 to 15.82 U/mL) alkaline protease activity and also have prepared different production media for enzyme fer-

mentation.

REFERENCES:

- I. Dhayalan, A., Velramar, B., Govindasamy, B. (2022). Isolation of a bacterial strain from the gut of the fish, *Systemus sarana*, identification of the isolated strain, optimized production of its protease, the enzyme purification, and partial structural characterization. *J Genet Eng Biotechnol* 20, 24.
- II. Gilmour, Steven. (2006). Response Surface Designs for Experiments in Bioprocessing. *Biometrics*. 62. 323-31.
- III. Gomaa E Z. (2013). Optimization and characterization of alkaline protease and carboxymethyl-cellulase produced by *Bacillus pumillus* grown on *Ficus nitida* wastes. *Braz J Microbiol*. 2013;44(2):529-537.
- IV. Ram Kumar A, Siva Kumar N, Gujarathi AM, Victor R. (2018). Production of thermotolerant, detergent stable alkaline protease using the gut waste of *Sardinella longiceps* as a substrate: Optimization and characterization. *Sci Rep*. 2018;8(1):12442.
- V. Parameswaran Binod, Piyush Palkhiwala, Raghavendra Gaikawai, K Madhavan Nampoothiri, Arvind Duggal, Kakali Dey and Ashok Pandey (2013). Industrial Enzymes - Present status and future perspectives for India; *Journal of Scientific & Industrial Research*; Vol. 72: 271-286.
- VI. Dilution Worksheet and Problems (2021). *Biology*.
- VII. Jordan Chapman, Ahmed E. Ismail and Cerasela Zoica Dinu (2018). *Industrial Applications of Enzymes: Recent Advances, Techniques, and Outlooks; catalysts*.
- VIII. Mishra, Rashmi. (2020). Optimization of culture parameters for α -glucosidase production from suspension culture of moss *Hyophilla nymaniana* (Fleish.) Menzel. *Journal of Genetic Engineering and Biotechnology*. 18.
- IX. Malhotra, G., Chapadgaonkar, S.S. (2020). Taguchi optimization and scale up of xylanase from *Bacillus licheniformis* isolated from hot water geyser. *J Genet Eng Biotechnol* 18, 65.
- X. Mishra, R., Chandra, R. (2020) Optimization of culture parameters for α -glucosidase production from suspension culture of moss *Hyophilla nymaniana* (Fleish.) Menzel. *J Genet Eng Biotechnol* 18, 82.
- XI. Hammami, A., Bayouh, A., Abdelhedi, O. (2018). Low-cost culture medium for the production of proteases by *Bacillus mojavensis* SA and their potential use for the preparation of antioxidant protein hydrolysate from meat sausage by-products. *Ann Microbiol* 68, 473-484.
- XII. Rouaa Daou, Karine Joubrane, Richard G. Maroun, Lydia Rabbaa Khabbaz, Ali Ismail, André El Khoury (2021). Mycotoxins: Factors influencing production and control strategies, *AIMS Agriculture and Food*; Volume 6, Issue 1: 416-447
- XIII. Abiola Ezekiel Taiwo, Tafirenyika Nyamayaro Madzimbamuto, Tunde Victor Ojumu, (2020). Optimization of process variables for acetoin production in a bioreactor using Taguchi orthogonal array design, *Heliyon*, Volume 6, Issue 10.
- XIV. Sunil Chamoli, (2015). ANN and RSM approach for modeling and optimization of designing parameters for a V down perforated baffle roughened rectangular channel, *Alexandria Engineering Journal*, Volume 54, Issue 3, Pages 429-446.

Principal
 JMJC COLLEGE FOR WOMEN (Autonomous)
 TENALI



Vol.9 Spl.Issue 1 2022

ISSN : 2349-9753

Veda's Journal of English Language and Literature (JOELL)

A Peer Reviewed International Research Journal

Impact Factor
(SJIF)
6.12

Proceedings of a

TWO-DAY National Seminar

on

Issues, Challenges & Remedial Approaches in Contemporary Literatures

On 24th & 25th June, 2022



Organised by :

Department of English

Andhra Christian College

Guntur

www.joell.in



Veda Publications

In Collaboration with
Acharya Nagarjuna University
Nagarjuna Nagar, Guntur

Table of Contents

S.No.	Title	Pg.No.
1	The Role of Race And Ethnicity in Aboriginal Society Structure Dr. Raju Bollavarapu & Mr D P Praveen	1-4
2	Reflection of Contemporary Issues in Kiran Desai's Novel "The Inheritance of Loss" Dr. Y. Sumithra	5-8
3	Syntactic Characteristics of English and Telugu Smt. K.Madhavi, Prof. K. Ratna Shiela Mani	9-18
4	English Language : An Icon for Advertisements and Cinema Dr. N. Vimala Devi	19-24
5	Cross-Cultural Implications in The Scarlet Song By Mariama Ba Dr. M. Sandra Carmel Sophia	25-28
6	Women's Quest for Self-Esteem from Restrictions - Dr.G.Jyothi Olivia	29-33
7	The Portrayal of Women in The Novels of Amulya Malladi B. Subhashini & Dr.Ande Bala Sowri	34-39
8	Diaspora in English Literature - Dr. M. Maheswaran,	40-42
9	Feminism Dr. A.V. Rajyalakshmi	43-47
10	From the Shackles of Bondage to Defining Womanhood Dr.P.Prasanna Kumari	48-56
11	Socio-Domestic Struggle of Women as an Outcast in Indian English Fiction:A Feministic Appraoch to Anita Desai, Shashi Deshpande and Girish Karnad's Select Works - Dr. S. Farhad	57-66
12	Trauma of Women During Partition - Rangumudri Ganapathi Rao	67-69
13	Ecofeminism and Deconstruction – A Melded Study of Schism Mrs. N. Vasanthi, Mr.S. Srinivasa Rao	70-78
14	Female Characters Representation in Indian Literature - Epuri Sunitha	79-84
15	Importance of Motivation as a Contributing Factor in Second Language Acquisition in the ESL Classroom Mr Saloman Raju Yarlagadda	85-91
16	Women in Literature - M.Sudharani	92-95
17	Amitav Ghosh's The Hungry Tide as a Historical Narrative - P Pradeep	96-106
18	Use of Language in Artemis Fowl by Eoin Colfer - Jangam Judah	107-114



WOMEN'S QUEST FOR SELF ESTEEM FROM RESTRICTIONS

Dr.G.Jyothi Olivia

(Lecturer in English, JMJ College For Women(A) Tenali.)

oliviajyothi@gmail.com

DOI: <https://doi.org/10.54513/JOELL.2022.v9spli1.06>

ABSTRACT

The Present paper deals with the Self-Esteem from Restrictions, the maximum prominent elements related to each Indian Woman inside the cutting-edge state of affairs according to many contemporary fiction writers in India. The internal adventure of the 'self' in literature reaches the final destination referred to as self-realization'. It deals with the inner exploration of the Characters in Indian novels and the following adjustments that manifest of their life. Self-esteem is essential at each factor in an individual's life. Its presence varies once in a while; at a young age for a few individuals, all through the center a long time for some others and at old age for others. The evaluation of self enables a person to discover the potentiality of his/her self to achieve any intention in existence. Esteem further motivates the 'self' to yearn for the reason in existence. Whereas motive pushes the person in addition to the reality that is an unavoidable truth that the self has to agree upon absolutely the makeover. The main objective of the movement is to focus on the rights and protection of woman rights and identification of their share in the life of man and also to make everyone realize their responsibility in the protection of woman rights. It gives a full stop to the silent suffering and helplessness. Simone De Beauvoir rightly pointed in her magnum opus "The Second Sex"; "Of course, the miserable condition of woman all over the world inspired the women of talent like Virginia Woolf to do something in this field and the result was the emergence of Feminism, a great movement in the western world in 1960's. It is a movement for the emancipation of women and their fight for equal rights." (1955: 80)

Keywords: *Subjugation, Exploitation, Suppression, Emancipation, rights etc.*

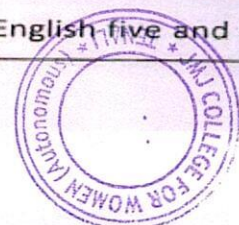


This whole alternate of one's self leads an individual to benefit greater information, dedication and judgment. Literature is the consultant artwork of existence and humanity. The comprehension of life is perceived by the mind and emotions of the characters. The principle of existence concentrates extra at the self and the identity of the self. Also, the opinion of a character to begin with receives approval from the society which in flip reaches all the humans round the arena. According to modernists' notion, humans are independent, rational individuals or 'selves' who suppose and act as unaccompanied of all different people. While a number of us are at ease in spotting this concept as obvious and natural, yet for the acculturated and educated within the Western continent, it's miles an insignificant assemble. In the postmodern period, this notion or this assemble is named as subjective. In the recent instances, the concept of individuality has turn out to be identifiable as compared to the sooner many years. People have aware of a couple of methods of being, and they may be at ease in relationships and connections with one another. They are also mixture of many, often conflicting elements. As they often confront the specific contexts, cultures, and sets of thoughts (and/or between the special parts of themselves), they behave otherwise, and suppose differently with regards to others.

THE PROGRESS OF NOVEL AND INDIAN WOMEN W

The Novel as a literary genre is popular in modern-day India. The count greater variety of epics, lyrics, dramas, stories and fables that have their respective ancestries, for closing several centuries. It for the duration of the contemporary period a touch more than a century that the radi extended 4 enduring piece of prose fiction started out to strengthen its roots in India won't agree if he or she is pupil of literature to mention that Sanskrit work Bana's Kadambari and Subandhu's Vasuv are also novels. But this description might longer absolutely gain in analyzing and re the existing fiction writing. The fact is the ones mentioned above are remoted ma For the unconventional, and its amazing into the arena, one needed to wait until latter and half of the nineteenth century the Western influence commenced running precise or horrific on India's cultural front additionally resulted in lots of other inside the development of formal written in the regional languages. The number cognizance to begin with is on purpose factors and presently as an inventive means for its recognition and progress.

Novels had been posted in more than languages and also in English because of reciprocal have an effect on between the nations that came in English five and the novels the





published in the regional languages. The dating among those two is extra intimate and purposive than this sort of within the manufacturing of the works in the related fields, such as poetry or drama. And this has elevated the opportunities to facilitate writing with greater comparative ease with which a unique (as distinctive paintings of artwork) can be translated into one or more Indian languages within the United States at present. As there may be a few attempt to explore a simply exhaustive and definitive literary records of modern-day India which is yet to be approached, the principle signpost appears to be comprehensible sufficient for the scholars. Bengal is the location diagnosed with for greater productivity works as part of 'Literary Renaissance' but the signs of in reality at once afterwards, the signs and signs and symptoms of 'new existence' were to be visible in Madras, Bombay and other additives of India as well. The Indian women novelists had been portraying women in numerous manifestations. The latest change that can be traced inside the submit - colonial duration is that the wonderful and first-rate dispositions of female characters especially women writers are humdingers to study.

The great Indian girls novelists like Kamala Ambedkara, Nayantara Sahagal, Anita Desai, Bhabha Deshpande, Bharati Mukharjee, Manju Manjunath, Sita Hariharan and others are vociferous about their girls characters, demonstrating the

standards of 'self-Esteem' and 'liberation'. Their demonstration of these two characteristics in the modern-day day girls signify their combat against suppression and oppression of by the patriarchal society. It is commonplace to observe that biological variations between males and females are natural. But those biological dissimilarities which might be made out of gender distinction reasons them to treat one another otherwise due to their inherent contrastive nature. It is the idea for structural inequality which differentiates males and females. Subsequently, women undergo hardships due to systematic social despotism. Inequality between the sexes is not the outcome of organic prerequisite however it's miles the result of cultural manipulation of gender variations. Simon de Beauvoir rightly says, in *The Second Sex*, of girls with reference to the remedy that they get from men at home or in society. This makes the existence of ladies more sympathetic and insightful in their method. She further states that, "One isn't born a lady; instead one will become, a female, it is Civilization as an entire that produces this creature most effective the intervention of a person else can set up an person as some other." (Beauvoir: 295)

The social and cultural system in India is inspired and controlled by means of a patriarchal society wherein the dominance of male is unsure in the socio - financial situations

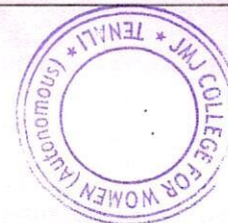


(elements), denying girls in their self-esteem and liberation humiliating them to the placement of 2d class residents. In such male ruled society, liberation, quest for self-identification, protests and concepts referring to resistance are beyond the manipulate of women. Surprisingly, the girls of the sooner instances were now not even aware about such phrases, since ladies are obviously very 'touchy, sacrificing and home makers'. They are always taken into consideration as obedient, quiet, submissive and passive humans. Their self-Esteem and liberation are usually subjected to the male dominance. Such is their humiliation that has conditioned them down simplest to accord a few benefit over their male opposite numbers.

The women in their works is a being with no area for herself, without any self-identification, reverence for his or her obligations as human beings and so forth. These women novelists have targeted a good deal upon the afflictions and the maladies of the ladies of that day and at the identical time they by no means attempted to disappointed or deviate from the traditional and cultural ethics in their period. This illustrates why a primary recognition in recent Indian girls writing is shifted to peep into the inner self this is lively enough in its look for identity and emancipation whilst being steady in interpersonal dating. The cutting-edge ladies writers try to disclose the secrets and enclose the conscious negation that

is not having plenty help in these days's co
Certain characteristics of girls are no
projected as beings who surrender, public
suffer themselves to martyrdom.
emphasize the significance of portrayal of
because the characters revolting toward
conventional rule, disintegrating the man
exploitation and oppression, kindling with
identity, to assert their individuality.
novels noticeably gift the resentment, r
retaliations and their infringement
conventional projections of the Indian Wor

The Concepts of Self-esteem
Restrictions of Women in Indian Writing
for Self-esteem and Female-liberatio
Contemporary Indian Fiction in English ar
special subjects denoting the conditions o
The cause is to direct its gaze closer t
sociological factors of ladies which include
non-stop conflict to pick out their own fu
inside the social system that is long
negated due to inner and external conflict
expressions 'Self-esteem' and 'liberation'
come to be high-toned and elegant terms
the contemporary literary research. Of pa
even the media is vociferous on s
problems of women inside the society ar
way, pointing to the need for 'self-id
Smitha. G denotes that there are v
expressions gaining momentum in the pur
identification. Their stories inform
approximately 'countrywide identity', 're



ification', 'tribal identification', 'cultural identity', 'man's identity', 'women's identification', 'Indian identity', 'European identity', 'organization identification' and hoards other identities. One has no idea how many identities are at gift floating in the air. It may be hard to have a depend of them, to seize and to recognize them. (Smitha: 321)

of the novelists who belong to the older generation are worried in discussing the troubles of identity and emancipation however their subject is more physical than mental. Not endorsed by those, the novelists of the modern era, like Chaman Lal, Nayantara Sehgal, Anita Desai, Ruth Praver Jhabwala, Salman Rushdie, are deeply concerned with the 'self-identity'. Any try to undergo their terrific works help us discover how their characters move across the subject matter of identity. Balachandra Rajan has explored the hard affairs of alienating one's personal 'self' in novels.

"Self-Esteem and liberation" illustrates how a female as an embodied object makes use of her body as a weapon or a car of resistance to move in opposition to violence in any form inflicted inside the patriarchal strengths and emerge as visible subjects. Even when a girl's body is invaded and destabilized by patriarchal pressures and interventions, the text authentically illustrates how girls fight and their declare over their bodies and

assert their rights to empower their self and establish their identity as self reliant beings. The conquest (control) ladies has on her frame is the most important victory they can flavor breaking themselves from the orthodox ideology of being physically weak makes them vulnerable in decision making strength additionally.

REFERENCES

- Abraham, E. John. "Sexual Abuse in South Asian Immigrant Marriages". *Violence Against Women*. vol.5.Issue.6.Boston.Massachusetts:Sage Journals 1999. pp.591-618.
- Ashcroft, et.al. "Key Concepts in Post Colonial Studies". London: Routledge. 2004, p.69.
- Beauvoir, de Simone. *The Second Sex*.UK: Vintage Classics, Random House, 1949, p.167.
- Bhagabat, Nayak. "Love and Longing in Manju Kapur's *Difficult Daughters*", *Indian English Literature*. vol, 3. ed. Basavaraj Naikar. Atlantic Publishers & Distributors: New Delhi, 2002, pp. 156-165.
- . "Feminine assertion in Manju Kapur's *A Married Woman*", *The Indian Journal of English Studies*, R.K. Dhawan. ed. New Delhi: IAES,vol.41. 2003, p.137



PRINCIPAL
JMJC COLLEGE FOR WOMEN (Autonomous)
TENALI

Veda's Journal of English Language And Literature (Joell)

About Andhra Christian College:

Andhra Christian College was established in the year 1885, under the aegis of Andhra Evangelical Lutheran Church, to cater to the educational and spiritual needs of young men and women of India, particularly of Andhra Pradesh. It is affiliated to Acharya Nagarjuna University. It has produced several International and National Leaders, Academicians, Sports Persons, Scientists, Ambassadors, World Food Laureate awardee of repute and others. Chief ministers and central ministers like Sri Kasu Brahmananda Reddy, Sri Bhavanam Venkata Rami Reddy, Sri N.T. Rama Rao and Sri Kotha Raghu Ramaiah are products of this college to mention. Also, it has produced many IAS and IPS officers.

Known for its sprawling campus with four hostels, large playgrounds, well-equipped laboratories and State-of-the-art facilities, the college ensures holistic development of its students. The college offers five Intermediate courses, nine UG courses and eight post-graduate courses in History, English, Zoology, Chemistry, Mathematics, Botany, Telugu and Commerce. Along with these, there are University career-oriented programmes in Taxation and Tally and Water Quality Analysis funded by UGC. This is the only college with the largest intake of students from Scheduled Caste, Scheduled Tribe and Backward Classes. At present there are 2000 students, 100 teaching staff and 60 office staff working in the college. The college is Accredited with 'A' Grade by NAAC.

The first Prime Minister of India Sri. Jawaharlal Nehru, Consecutive Prime Ministers Sri. Lal Bahadur Sastry, Mrs. Indira Gandhi, President of India Sri. Giani Zail Singh, UGC Chairman Sri. Arun Nigavekar and Mr. James Irwin, the first man who landed on the Moon visited our college.

Published by:
VEDA PUBLICATIONS
Ph : +91 9948850996 : 9985200048.
www.vedapublications.com



S. S. S.
PRINCIPAL
JMJC COLLEGE FOR WOMEN (Autonomous)
TENALI



ENGLISH LANGUAGE: AN ICON FOR ADVERTISEMENTS AND CINEMA

Dr. N. Vimala Devi

(HOD of English, JMJ College For Women , Tenali.)

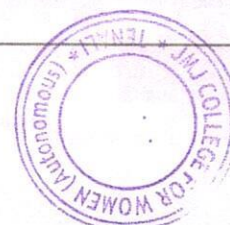
Email: vimal.chowdary@gmail.com

DOI: <https://doi.org/10.54513/JOELL.2022.v9spli1.04>

ABSTRACT

In the present modern society advertising is with us everywhere, which is fast gaining significance and helping to establish a new global culture that spreads across national boundaries. Advertising is rampant now a days. It's a known fact that the purpose and importance of advertising is felt around the globe. It has spread even to the remote areas. The coin of advertising is both positive and negative. Advertising is the sales and promotion of goods, ideas and images through impersonal media. The language used in advertisements is not for the uneducated as it is full of Rhetorical figures and Incongruity. The language used in advertisements make linguistics to frown seriously as it is highly persuasive, full of deviations, ambiguities, euphemisms and with ungrammatical structures. Though it violating the rules of language, one of the best ways is the language used in advertisements can be eye-catching, memorable and expresses new ideas, new creations in new ways. It has spread even to the remote areas. Awe inspiring advertisement is witnessed by the world. The positive aspects give immense delight to us and negative features make us think and critique. Sometimes the impact of the advertising on the people is beyond expectations.

Keywords: *Advertising, English, Language, Globalization.*



Advertising is a prevalent phenomenon nowadays that has gained the attention and interest of a large number of individuals in different societies around the globe. Critics and writers have usually treated the idea of cinema and literature from one point of view, considering the influence of literature on cinema. Critics usually compare cinematographic work to literature, assessing the degree to which a movie is faithful to a text or novel. The paper attempts to shed light on the dynamic and mutual relation that ties language to advertisements and cinema.

In the present modern society advertising is with us everywhere, which is fast gaining significance and helping to establish a new global culture that spreads across national boundaries. Advertising is rampant nowadays. It's a known fact that the purpose and importance of advertising is felt around the globe. It has spread even to the remote areas. The coin of advertising is both positive and negative. Advertising is the sales and promotion of goods, ideas and images through impersonal media. The language used in advertisements is not for the uneducated as it is full of Rhetorical figures and Incongruity. The language used in advertisements make linguistics to frown seriously as it is highly persuasive, full of deviations, ambiguities, euphemisms and with ungrammatical structures. Though it violating the rules of language, one of the best ways is

the language used in advertisements can be eye-catching, memorable and expresses new ideas, new creations in new ways. It has spread even to the remote areas. Awe inspiring advertisement is witnessed by the world. The positive aspects give immense delight to us and negative features make us think and critique. Sometimes the impact of the advertising on the people is beyond expectations.

The question of the relationship between language and film remains an open and active one. We can never fully understand or explain the impact of the new medium of film on its early viewers and commentators: We look back from the perspectives of those who have grown up in a film age and, most recently, in a digital age. Cinema and language are connected to each other but still they are different in their own ways. It has always been one of the most fascinating forms of knowledge which has made great impact on human psyche.

Cinema is the art of showing life of humans and the respective happenings in life and it reflects the actual happenings in an idealized form, the standards of social thought and morality. Cinema or movie is the most remarkable, illuminating and fascinating discovery of science and technology. The tone of language changes with the stages of society. Life style and incidents are portrayed and given a clear view by means of perfect moulding in the mode of films. All the credit goes to the



American scientist Thomas Alva Edison. Language and Cinema seems like the two sides of a coin. Cinema is also used in response to poetry.. Poetry as the art of utterance and cinema the art of showing, both whole on their own, don't easily make a good couple. Cinema and language meet head on, not unified as in conventional film, but remaining distinct and dancing, stepping on toes, wooing each other with a charms of mouth, eye and mind. There are some best adaptations of literary works that have ever happened in the Indian film industry. For example, Hindi language film industry, Bolly wood which routinely picks up movies and novels from around the world and copies them and sometimes doing adaptations that are better than the originals they are based on.

Advertisements are not only an ' ideal tool ' for reaching people but also a device of attaining and maintaining contacts with persons. The cultural content of advertising, its language and its connection with gender issues are deeply rooted in our society and in the present day, the universal presence of advertising is increasingly influencing the daily life of people. According to Nicosla, advertisers should not only inform their audiences about the product, but also stimulate ideas among them as well as develop their curiosity and interests through creating new meanings from the advertised commodity. Surveys state that consumers come to identify themselves with the merits and significance of

the advertised product in their everyday life through images, verbal language or symbols. Due to the force of globalization and consequent media revolution, the meta-theoretical lens through which patriarchal Indian society traditionally viewed its social world seems to be transforming. Advertisements too create an environment in India. Just as it is difficult to be healthy in a toxic physical environment, if we are breathing poisoned air or drinking polluted water, it is difficult to be healthy in a "toxic cultural environment" that surrounds us with unhealthy images and constantly sacrifices our health and well being for the sake of profit. They sell more than products because they sell values, images, and concepts of love, sexuality, success, besides telling us who we are and who we should be. In all kinds of advertising , women's bodies refer to "things" and "objects".

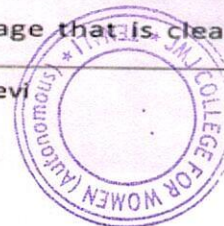
Advertisizing has become a part of present day life. From everywhere around us, advertisements of diverse type attack our privacy. Inspite of it, there is an attractive power, which is able to manipulate the consumer, an invisible voice of advertisement advocates, encourages, asks, announces, and deeply embeds into people's minds. "Advertising is telling and selling". It comes from the Latin word "Adverto", which means to turn round. An advertiser intends to spread his ideas about his products and hence designs it to influence the purchasing power and thought



patterns of the audience. For an advertiser, the human minds are his work fields, his ideas, styles are his tools, and he operates from a remote distance. It is nearly impossible to go through a day without being bombarded with advertisements unless we live in the deepest and remotest part of the world! In last decades the market glut of advertising caused the increased intention and interest in linguistic aspect of advertising. Advertising has become a science. People have begun to describe, analyze the linguistic means and evaluate the language to find out the principles so as to create new kinds of relationship between elements of language and improve the techniques, with the aim to be unique and maximize the effect at full blast. Therefore, media largely reflects the lifestyles, socialization patterns, participation levels, cultural boundaries, political manoeuvrings, religious manifestations, educational standards, social hierarchy, and of course society images of any given society. During the phases of economic liberalization, the overall scenario of media in India has changed tremendously. The images of the various sections of society, which are constantly beamed on television through advertisements, tend to have a deep influence upon the perception of society towards the role and identity of women. Ultimately, products are related to people's personal happiness, and social success, consequently, commodities are

not only satisfiers of needs but communicators of meaning.

In this age of opening up economy to global market forces which on the logic of what sells best and quickest, it is no wonder that women and girls have become the most important media and for the advertisement in particular. As Sheelan says "advertisements have effects on consumers, but only if consumers choose to be affected by advertisements" The function of language in advertising is to express feelings, offer information and persuade, describe or inform. Advertising language can either follow the prescribed path of advertising clichés or it can have the freedom to "deviate from it and create its own rules of the language itself". Language in advertising with socio cultural senses and interpretations is far from having a passive function in society such as just reflecting the social life. Language is not "a transparent carrier of meanings", rather it is "a medium which imposes its own constraints on the user and the user which is constructed". Generally, advertising language tends to be more formal than spoken language. This brings me to another point about print advertising language where the language used in the advertisements is a mixture of spoken and written patterns of language. Within advertisements, we find a language that is clearly written to be



spoken, like logos. At the same time, we also
 ns that are typical of spoken language and
 e intended to represent spoken language.
 er language reflects or shapes ideas and
 ts in society is a complex issue to explore.
 e importance of language is clearly not
 a mirror that reflects reality. Rather it
 ns to impose structure on our
 tions of the world.

Language seems to play both roles in
 . It holds the key to challenging and
 ng male hegemony. The role of images in
 ising is to display a human context which
 s meanings from the product, and it is for
 e reason that the majority, if not all
 sements, contain images of persons,
 ally young people. Language, gender and
 are closely interwoven terms. Instead of
 being viewed as an essential
 eristic of an individual's psyche, it is
 ood as a thoroughly social construct, one
 produced by language and discourse.
 ge, a product of society, is considered to
 significant role in human interaction, the
 being, language and society are an
 oven texture. Language has an impact on
 e view the world, it therefore "affects the
 al conditions of women's lives.
 quently, language "rather than simply
 ng society, actually brings about and
 changes in the way we see and think, it is
 on knowledge that language in general

reflects and reinforces men's power and
 authority, and at the same time maintains
 negative images about women. Concerning
 language, women and men may adopt different
 characteristics when speaking to each other, and
 many factors such as power and social status
 play a significant role in defining the choice of
 language as well as intensifying these
 differences. These differences at the level of the
 linguistic form take place in the speech system
 of almost all societies, in developing and under
 developed countries, alike both in tradition and
 modern societies.

Finally the language and discourse of
 advertising remain crucial to understanding the
 objective of advertising as well as the social and
 cultural dimensions used to achieve and
 influence audiences. However, the role of the
 language of gender is very important to clarify
 the language used in advertising and the impact
 it has on women and men.

Advertising texts are of great value for
 the analysis from linguistic, sociological,
 sociolinguistic, psychological, ethnologic and last
 but not least marketing point of view. Linguists
 are interested in language used in the
 advertisement, and marketing experts are
 interested in finding the tricks on how to make
 advertising more effective. English enables the
 creators of advertisements to use word puns,
 figurative language and to mix individual styles
 and types of texts. Advertising unifies language,



pictures, music: it contains information, invokes emotions and imaginations. Above all, it has a social and practical aim. As a genre, it seems much diversified. Various aspects and forms of advertising discourse can be seen as a part of the study. There are many forms such as television, billboards, radio, mobile phones, etc., These are traditional forms of advertising. The latest trend is internet advertising, various sponsored links, paid advertising on specific websites and social networking advertising are a few to mention. Advertising can sometimes give a negative impact and may turn dangerous.

Today every Indian youth is straddling tradition and modernity all the time. While it is fairly western in its outlook towards life, it is firmly rooted in Indianness in the heart. Also, Indians have a way of "indianizing" all things western. The strategic thought behind the concept is that when Indians see anything international, they give it a 'desi' twist. The same is true of Indian ads also., which is in for some exciting and creative times as a wave of new thinking is blowing over the industry. Indian brands are now on a global playing field. India's economic growth is having a positive impact on world economy and the advertising business. The major as well as preferred language used previously in advertising was English, the importance of which has still not diminished: rather, the advent of the internet and globalization has only strengthened it. However,

very slowly but steadily, Hindi has become a new power language. It no longer considers English as its archrival. Globalization has changed the equation and chemistry between the two languages. It is perhaps the "Buy One Get One Free" syndrome that the two languages enjoy in India. In fact, English and Hindi come closer and they deliver 'just perfect' when they work in tandem. Right from Da Aisi', it is this 'winning blend' which has become a new mantra in social acceptance, prestige and success.

REFERENCES

Bhatia, Tej.1987. English in advertising: Mixing and media. *World Englishes* 6, 48

Bhatia, Tej.2001. *Language mixing in advertising. The Three Circles of English* By Edwin Thumboo: 195-215. Singapore: UniPress

Geis, Michael. 1982. *The Language of Television Advertising*. London: Academic Press

Leech, Geoffrey N. (1972), *English in Advertising: A Linguistic Study of Advertising in Britain*. London: Longman.

Leiss, W. (1997), *Social Communication in Advertising*. London and New York: Routledge.

S. S. S.
 PRINCIPAL
 JMJ COLLEGE FOR WOMEN (Autonomous)
 TENALI





INTERNATIONAL JOURNAL OF CREATIVE RESEARCH THOUGHTS (IJCRT)

An International Open Access, Peer-reviewed, Refereed Journal

SURVEY OF HELMINTH PARASITES IN FRESHWATER FISHES COLLECTED FROM REGIONS OF TENALI TOWN, GUNTUR DISTRICT, ANDHRA PRADESH, INDIA

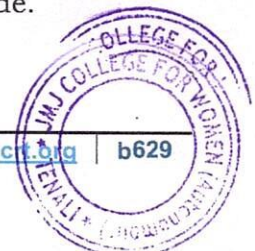
Mallavalli Aruna*

Department of Zoology, J.M.J. College for Women (A), Marris pet, Tenali, Guntur, Andhra Pradesh, India.

ABSTRACT

The occurrence of zoonotic parasites in edible fish are been used to consume daily by the local fisher man families and rural area people collected from the different fresh waters resources like lakes and ponds etc. The presenting results from a survey of helminth parasites of fishes in present investigation was undertaken between July 2009 and April 2011 with an aim to study the helminth parasites associated with different freshwater fishes collected from various places of Tenali Town, Guntur District and Andhra Pradesh. Infection of helminth parasites in freshwater fishes in relation to environmental factors. Fish samples were collected from in and around the Tenali town examined for helminth parasites included three classes i.e. Cestode, Trematode and Nematode. During the present study 343 fishes were examined, in which 11 fishes were infected with six helminth parasites (trematodes), two nematodes and two acanthocephalones. Present studies are helpful for the status of diversity of helminth parasites.

Key words: zoonotic parasites, helminth parasites, trematodes, nematode.

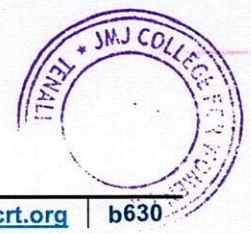


INTRODUCTION

Human activities and natural disasters like earthquakes, floods etc... increased day by day which alarmed the environmental destruction (Knap and Rusyn (2016)). Ecological conditions are being continuously changed results of novel species appearance and ancient might be disappear due to this reason systematic study would be complex to identify the newly formed species characteristics led foundation for the biodiversity studies to initiate significance research findings (Chu and Karr (2017)). Studies and research progress to conduct fauna distribution of species worldwide. As parasites lifestyle has been incredibly successful in the history of life on earth, the efforts and inquisitive talents of parasitologists can make the biodiversity research quite fascinating and appealing (Khurshid Ahmad Tariq (2020)).

In the present study a total of six varieties of fishes were examined for the various metazoan parasites of which total of ten species have been collected and have been concisely listed and described, of these parasites, a digenean, *Clinostomum gideoni* from *Anabas*, *Euclinostomum* from *Channa punctatus*, *Genarchopsis goppo* from *Channa punctatus*, *Genarchopsis faruquis* from *Mastacembelus armatus*, *Allocreadium handiai* from *Channa punctatus*, *Haplorchoides macrones* from *Labeo rohita*, *Camallanus unispiculus* from *Channa punctatus*, *Paracamallanus* from *Channa punctatus*, *Pallisentis ophiocephali* from *Channa punctatus*, *Pallisentis colisai* from *Mastacembelus armatus* have been described as parasitic species.

Parasites infection and incidence of fresh water fishes has been contributed by a number of scientists from all over the world. Parasitology of fresh water fishes in India has a long history of almost a century. Since the first report of *Isoparorchis hypselobagri* dates. It is not much difficult to give the information about the digenetic trematodes of fresh water fishes (Sohn and Na (2018)). Taxonomic work on these digenetic trematodes has flourished throughout the world.



Fairly extensive amount of literature is available on the Nematodes of the Camallanidae from the fishes only to varieties of Nematodes are collected from *Channa punctatus* belongs to the genus *Camallanus* and *Paracamallanus*. However, the vast amount of literature available from various parts of the world cannot be quoted here (Shah; Qayoom; Balkhi and Kumar. (2015)).

The spiny headed worms Acanthocephalans are one of the important parasites of fishes causing serious damage to the hosts. The spiny proboscis of the parasite attaches to the intestinal villi causing severe pathological changes in the fish. Enormous work has been reported from the various parts of the world including India. Only one genera *Pallisentis* and two species have been collected as adults in fishes (Gautam et al., 2020). Extensive work has done on Acanthocephalans is available till now.

The present study on the taxonomy of metazoan parasites of the fresh water fishes of canals of Krishna River and culture ponds has unveiled the biodiversity of various parasites from the fishes of this dynamic macro habitat and thus also enabled to compile a post parasite list. Such type of studies will fill the lacunae in the field of taxonomy by adding and updating the already existing knowledge with the additional information gathered and enables to prepare data base of parasites in the hosts.

MATERIALS AND METHODS

Parasite collection: Two hundred parasites in total from two species of edible imported Channidae (Sp. A) (n = 103) and Bagridae fish (Sp. B) (n = 18) were collected in McClelland, Michael and Sass, Greg. (2012). for identification in the present study. Table No-1 provides fish details. Collected parasites were stored in 1.5 mL sterile Eppendorf® tubes containing 70% ethanol pending morphological/and or molecular identification in the present study. “Any information which may lead to the identification of an included country has been omitted from the manuscript, auxiliary tables and figures. This information includes country descriptions, fish species names, or citations.”



Parasite preparation: Preparation of parasites for morphological examination were according to each morphotype and followed methods described in **Table No-1**. For molecular study of nematodes, a small piece was excised from the mid-body of a representative specimen of each larval nematode as described in Shamsi *et al.*, (2008). The anterior and posterior portion of nematode specimens were slide mounted and cleared with lactophenol. Digenean specimens were removed from 70% ethanol and rehydrated with a 50% ethanol and distilled water series before staining with Semichon's acetocarmine. Specimens were then dehydrated with a graded ethanol series (50%, 70%, 80%, 90%, 95% (twice), absolute (twice)), and cleared with xylene based on the method in Sohn and Na (2018). Cycling time for re/and dehydration was adjusted according to specimen size. Specimens were slide mounted with Canada Balsam.

Morphological identification: Selected specimens were studied morphologically and characteristics of importance, following publications in **Table No-2, were Table No-1** Details of fish in the present study measured using an eyepiece micrometre (BX-43 Olympus Microscope, Olympus Corporation, Japan). All measurements are given in millimetres, unless stated otherwise. The range of measurements are given in the format of length x width mm or specified as length or width only. Drawings were made using BX-43 Olympus Microscope, Olympus Corporation, Japan fitted with a drawing tube. Image capture of specimens was conducted using an Upright Motorized Microscope ECLIPSE Ni-E, Nikon, Japan. Morphological description is provided for *Isoparorchis* sp. and *Euclinostomum* sp. Due to the poor quality of larval *Eustrongylides* specimens, molecular method only was used for identification.



Table No:1- Information of Collected Fish

Sl.No	Fish ID	Number of fish	Country of origin	Packaging and fish ~length	Fish details
1	Mastacembelus	3	India	Consumer ready but a wide variation of processing standards. Many partially eviscerated and with gills still remaining. Fish frozen in single layer and surrounded with ice. Fish ranged between 9 and 12 cm in length	Primarily freshwater aquaculture or polyculture. Considered voracious, predatory carnivore of small fish and also feeds on worms and insects. Habitat includes stagnant or muddy aquatic environments
	Chana punctatus	3	India		
2				Non-consumer ready. Fish uneviscerated with head and gills present. Fish frozen in single layer and surrounded with ice. Fish were generally uniform in size (~6 cm in length).	Freshwater commercial species which feeds on crustacea, insects, or plant matter. Habitat includes freshwater lowland basins/rivers.

Parasite examination and calculations

The prevalence (P), mean intensity (MI), and mean abundance (MA) of the parasites described in this paper were calculated

following Bush *et al.*, (1997)



$P = (\text{Number of infected fish} / \text{Total number of examined fish}) \times 100;$

$MI = (\text{Number of parasites} / \text{Number of infected hosts});$

List and number of zoonotic parasites identified from imported fish Species A & B.

RESULT AND DISCUSSION

A total of 10 parasites species were found in 6 fish species namely Channa punctatus, Catla catla, Labeo rohita, Cirrhina, mrigala, Anabas, Mastacembelus armatus. A total of 343 fish samples were examined for parasites. A total of 10 were observed parasites.

Table No: 2 Name of the Fish and Number of Fish with parasite

S.N O	Date	Name of the Fish and Number of Fish	Name of the Parasite	Number of Parasite s Collecte d
26	19.7.2010	Catla catla---4 Anabas---4	Nil	Nil
27	3.8.2010	Labeo rohita---4 Channa	Nil	Nil
28	23.8.2010	punctatus---4 Mastacembelus	Nil	Nil
29	0	armatus---5 Channa	Nil	Nil
30	20.9.2010	punctatus---4 Catla catla---4	Nil	Nil
31	19.10.2010	Labeo rohita---4 Mastacembelus	Nil	Nil
32	10	armatus---3 Labeo rohita---5	Unidentifie d	
33	4.11.2010	Cirrhina mrigala- --5 Channa	Nematode cyst- Larval	1
	12.11.2010	punctatus---5 Mastacembelus---	stage. Trematode	3
34	11.12.2010	3 Chana	s Haplorchoi	1
35	10	punctatus---3 Cirrhina mrigala-	des Unidentifie	2
36		--3 Labeo rohita---5 Channa	d Nematode	
	20.12.2010	punctatus---11 Anabas---3	cyst-larval stage. Tramatode	2
37	22.1.2011	Channa punctatus---10	Allocreadi um	3
38	1	Mastacembelus	handiai	



39		armatus---4	Trematode	1
	29.1.201	Channa	Euclinostomum	
38	1	punctatus---5		1
		Channa	Trematode	
		punctatus---10	Genarchop	Nil
39		Mastacembelus	sis	
		armatus---4	faruquis	1
40	14.2.201	Labeo rohita---2	Nematode	
41	1	Catla catla---4	Paracamall	Nil
42		Labeo rohita---4	anus	Nil
43	23.2.201	Mastacembelus	Acanthocephalan	Nil
44	1	armatus---4		Nil
45		Labeo rohita---2	Pallisentis	Nil
46	7.3.2011	Catla catla ---4	ophioceph	Nil
47		Labeo rohita---4	ali	Nil
	23.2.201	Cirrhina mrigala -	Pallisentis	Nil
	1	--4	colisai	Nil
		Labeo rohita---2	Nil	
	7.3.2011	Cirrhina mrigala-	Pallisentis	
		--3	colisai	
	15.3.201	Catla catla---3	Nil	
	1	Catla catla ---4	Nil	
	22.3.201	Labeo rohita---4	Nil	
	1	Cirrhina mrigala-	Nil	
	28.3.201	--3	Nil	
	1	Catla catla---2	Nil	
	29.3.201	Labeo rohita---4	Nil	
	1	Cirrhina mrigala-	Nil	
	4.4.2011	--3	Nil	
	7.4.2011	Labeo rohita---4		
	8.4.2011	Catla catla---5		
	9.4.2011	Cirrhina mrigala-		
		--6		

Table No:3 NAME AND NUMBER OF FISH HOSTS EXAMINED

S.NO	Name of the host	No. of fishes examined	No. of fishes infected
1	Channa	51 + 52	2+4 =6
2	punctatus	=103	Nil
3	Catla catla	26 +26 =52	1
4	Labeo rohita	34 + 38 =72	Nil
5	Cirrhina	46 + 27 =73	1
6	mrigala	11 + 7 =18	3
	Anabas	6 + 19 =25	
	Mastacembelus armatus		
		343	11



Table No: 4. LIST OF PARASITS COLLECTED

S. No	Name of the Fish	Name of the Parasite	No. of Parasites Collected
1	Anabas	Clinostomum	3
2	Channa punctatus	gideoni	
3	Channa punctatus	Genarchopsis goppo	2
4	Channa punctatus	Camallanus unispiculus	3
5	Channa punctatus	Allocreadium handiai	2
6	Channa punctatus	Euclinostomum Para	2
7	Labeo rohita	camallanus	1
8	Mastacembelus armatus	Haplorchoides macrons	3
9	Channa punctatus	Genarchopsis faruquis	3
10	Mastacembelus armatus	Pallisentis ophiocephali	1
		Pallisentis colisai	1

In the course of routine examination 343 fish species belonging to 22 genera, 5 orders, 7 families found in different localities of around Tenali, Guntur District Andhra Pradesh, were studied for helminth parasites. Out of which only 10 species of fish were found to infect with list of parasites information given in the **Table No: 4.**

1. Metacercaria Clinostomum Gideoni Bhalerao'1942: **(Fig: 1).**
2. Metacercaria Euclinostomum (Rud, 1809) **(Fig: 2).**
3. Genarchopsis goppo (Ozaki, 1925): **(Fig: 3).**
4. Genarchopsis faruquis Gupta, 1951: **(Fig: 4).**
5. Allocreadium handiai pande, 1937: **(Fig:5).**
6. Haplorchoides macrones (Dayal, 1949) Yamaguti, 1958: **(Fig:6).**
7. Nematoda Camallanus unispiculus khera, 1956: **(Fig: 7).**
8. Paracamallanus: **(Fig: 8).**
9. Acanthocephala: Pallisentis ophiocephali (Thapar, 1930) Bayliss, 1933: **(Fig:-9)**
10. Paracamallanus **(Fig: 10)**



METACERCARIA CLINOSTOMUM GIDEONI BHALERAO'1942

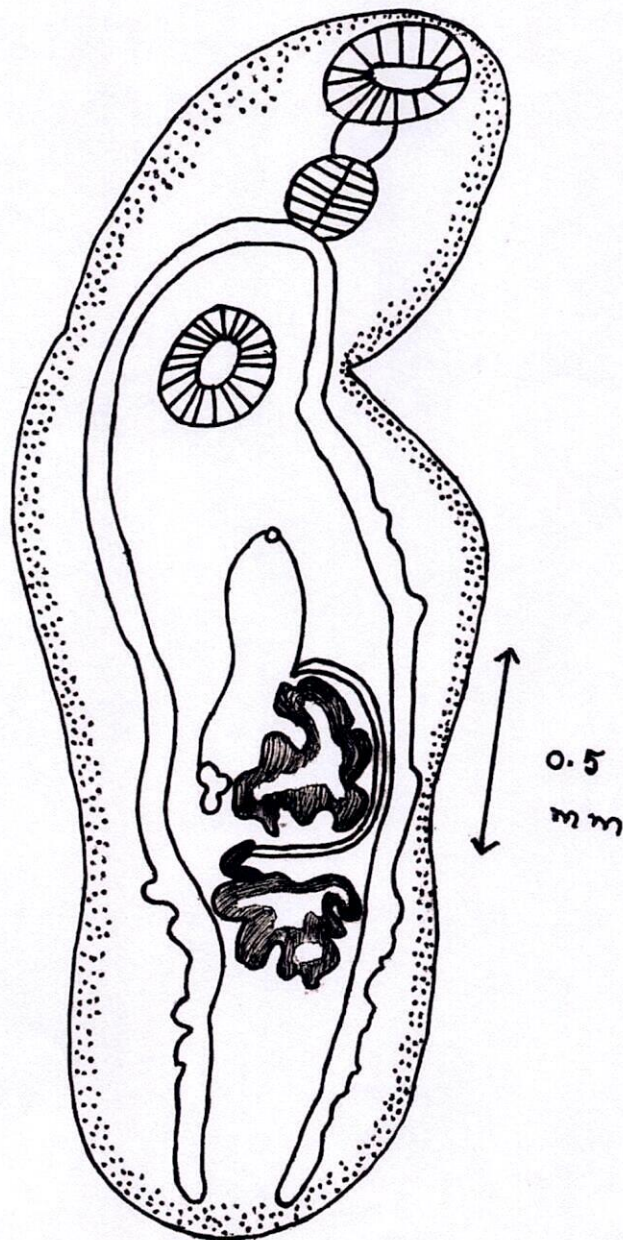


Fig-9



ALLOCREADIUM HANDIAI PANDE, 1937

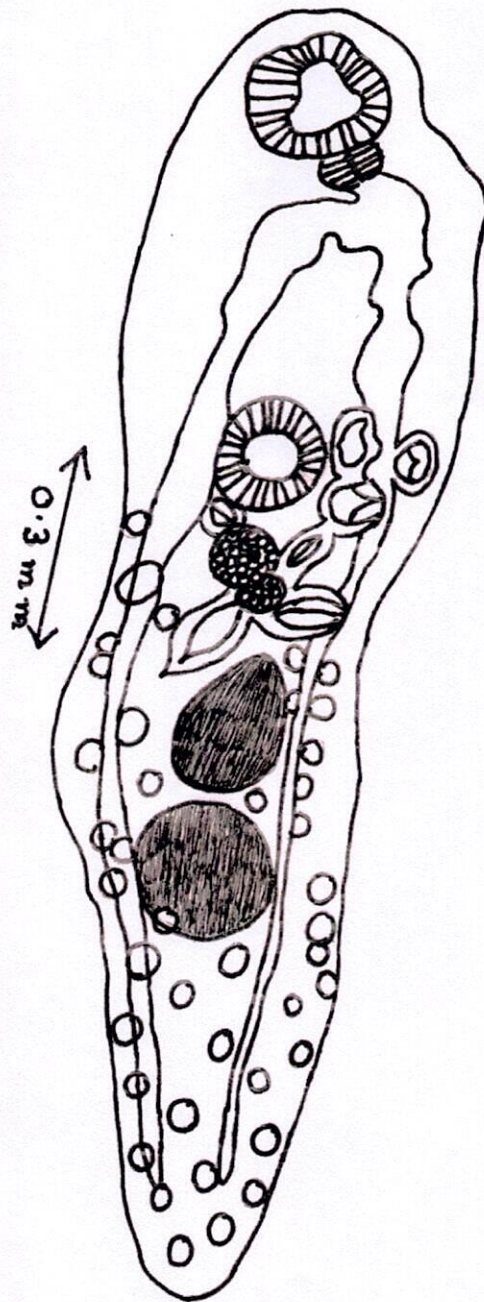


Fig-2



METACERCARIA EUCLINOSTOMUM (Rud,1809)

Travossos, 1928

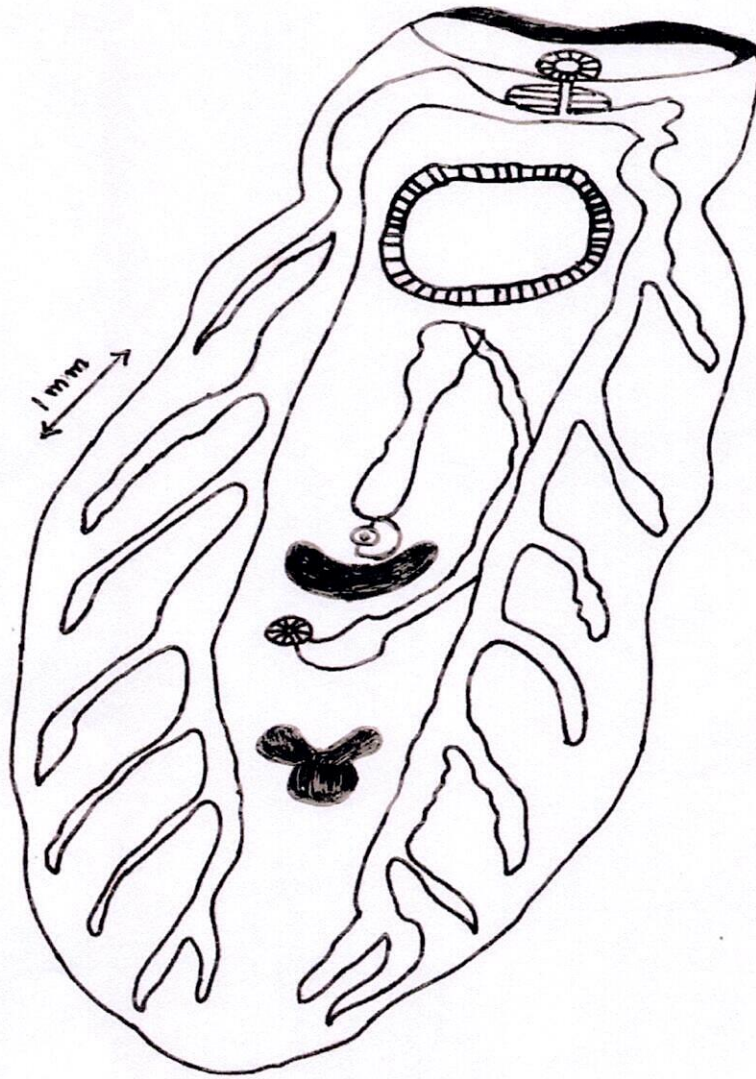


Fig-3



GENARCHOPSIS GOPPO (OZAKI,1925)

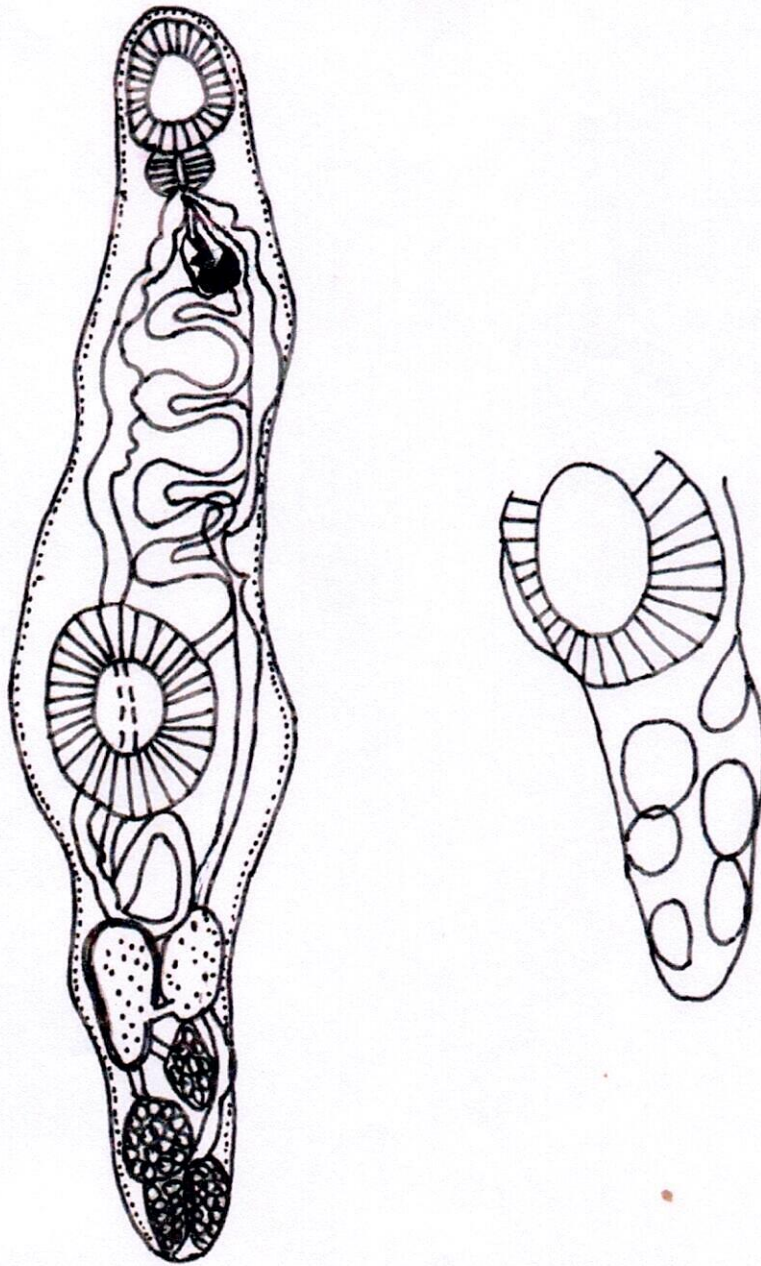


Fig-4



GENARCHOPSIS FARUQUIS GUPTA, 1951

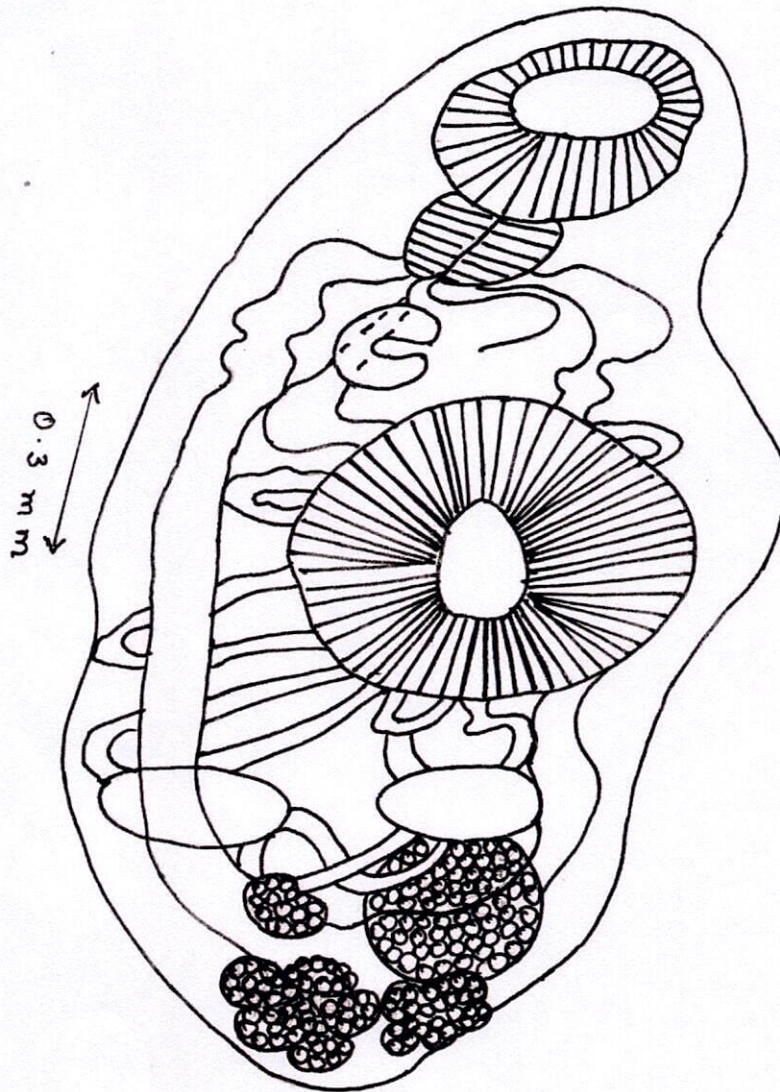


Fig-5



HAPLORCHOIDES MACRONES (DAYAL, 1949) YAMAGUTI, 1958

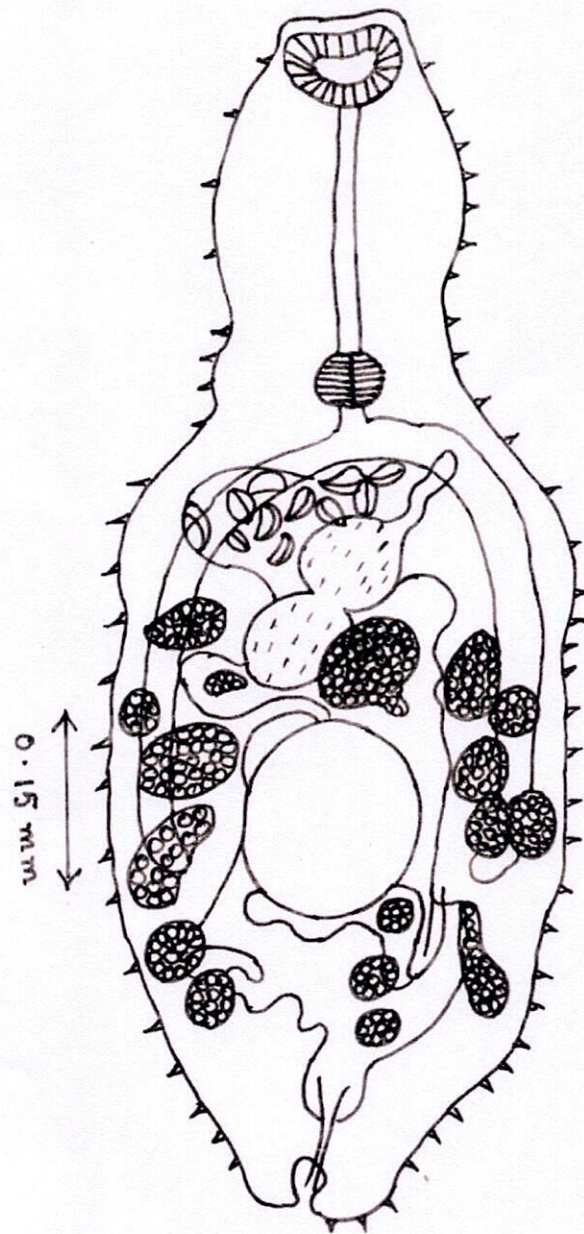
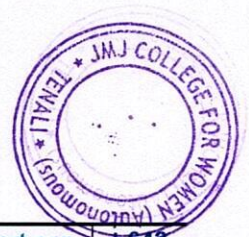


Fig-6



ACANTHOCEPHALA

PALLISENTIS OPHIOCEPHALI (THAPAR, 1930)

BAYLISS, 1933

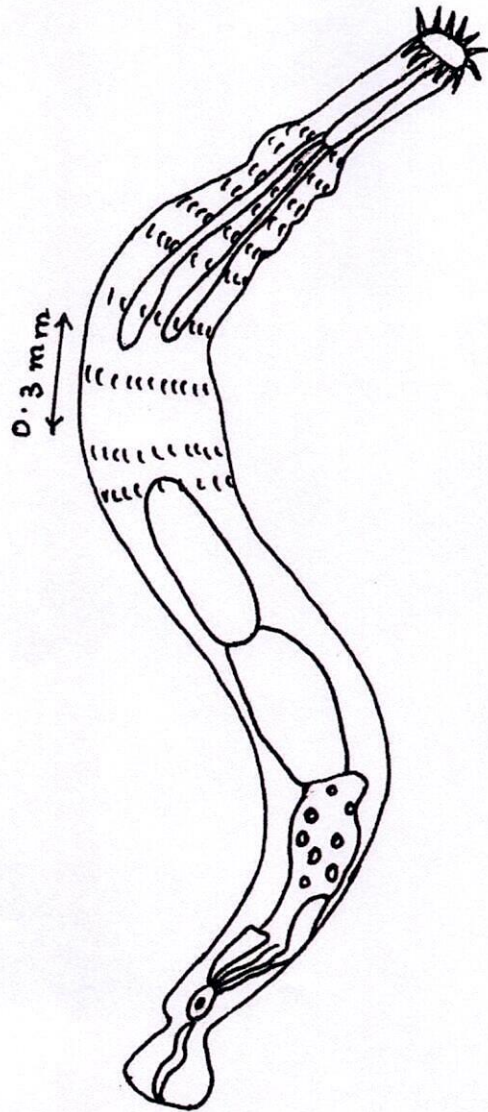


Fig-7

RT



PALLISENTIS COLISAI - SARKAR, 1954

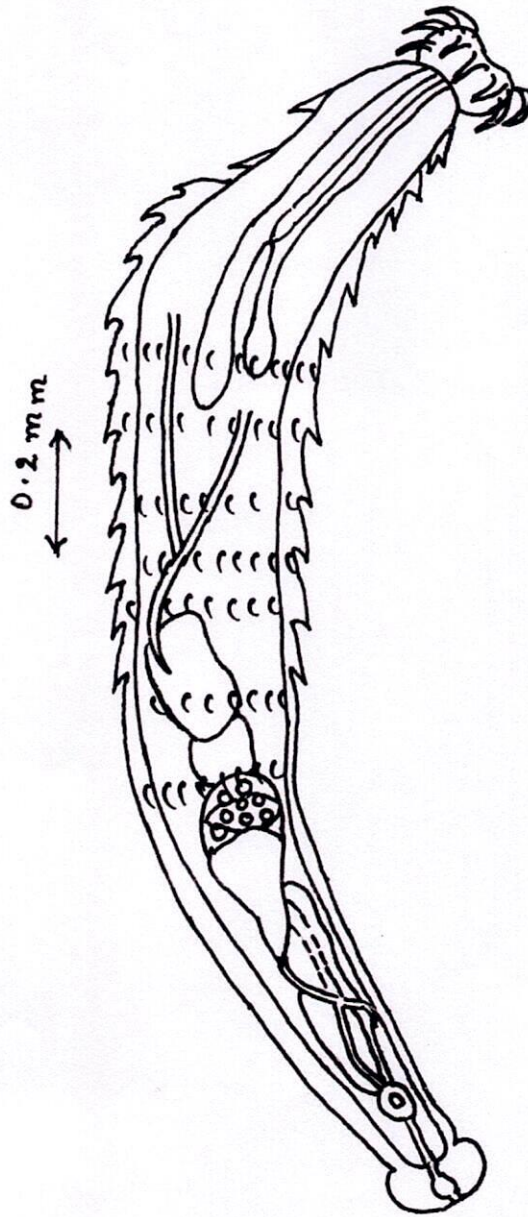


Fig-8



NEMATODA

CAMALLANUS UNISPICULUS KHERA, 1956

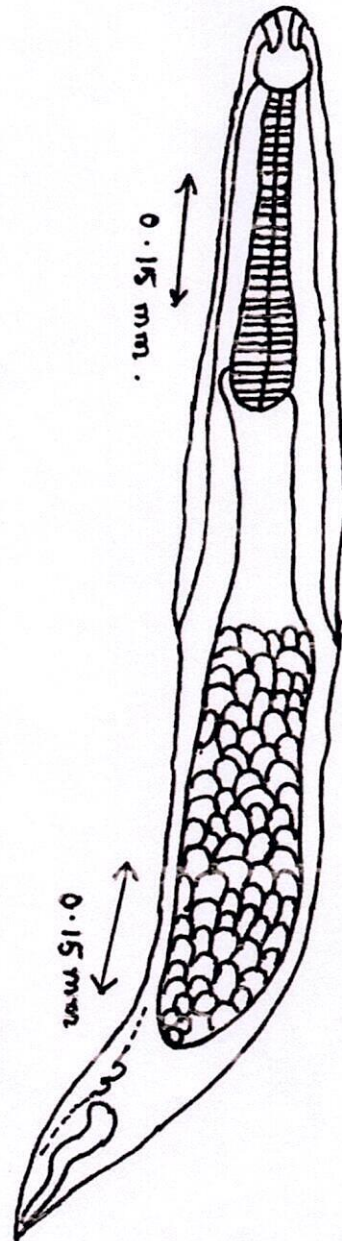


Fig-9



PARACAMALLANUS

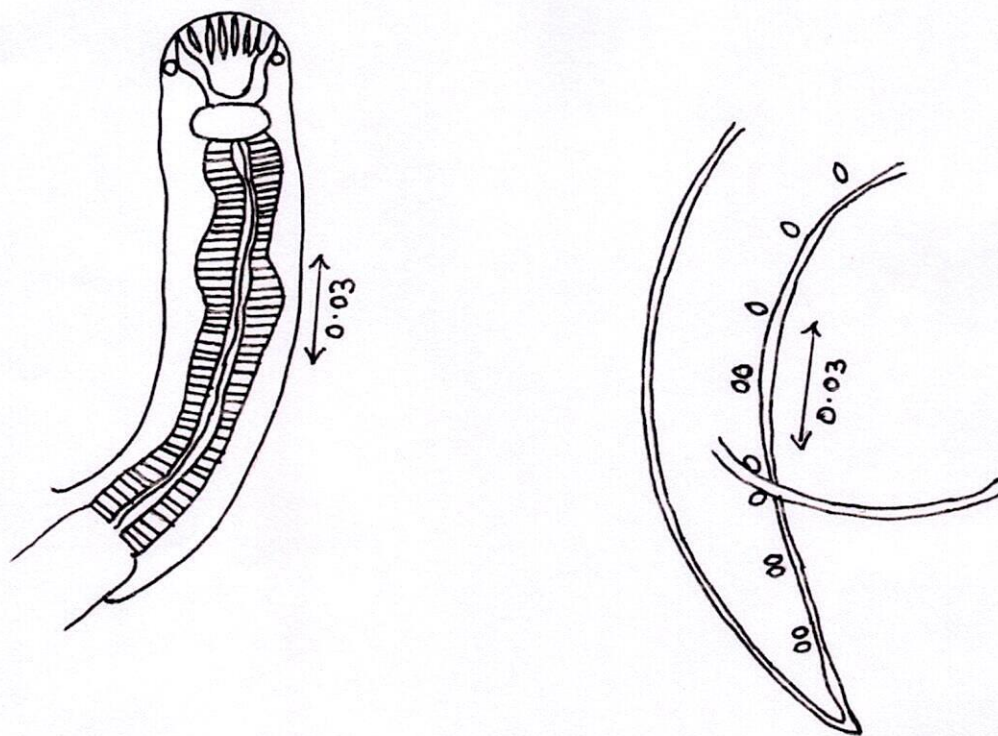


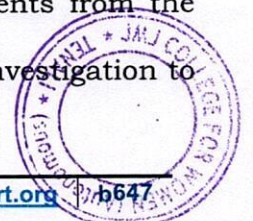
Fig-10

The survey was carried out with 343 freshwater fishes in which *Channa punctatus*, *Catla catla*, *Labeo rohita*, *Cirrhina mrigala*, and *Anabas* and *Mastacembelus armatus* from various places of Tenali town in and around (Jyrwa, Donald (2016)). Out of 343 fresh water fishes 11 were infected with helminth parasites in which cestode, trematode and nematode were found in one annual cycle. A total 21 helminth parasites were found during the present investigation. They were belonging with three classes in

which total seven genera are found, out of them four from cestode (Balai et al., 2017). During the present investigation the high rate of infection of trematode found as compare to nematode parasites. The values for the incidence, intensity, density of infection in **Table No-1** whereas the **Table No-2** shows influence of season on parasitic infection of helminth parasites from freshwater fishes. In the summer and autumn season high rate of infection takes place and also the diversity of parasites and increased trematode population can be seen when compared to nematode (CDC (2019)). The infective stages would attack in the summer and the growth and maturation takes place in during autumn and winter seasons (Burrell et al., 2017). The factors which affect the distribution and environment of the host diet and mode of feeding, often play important role to limit the parasite (Kołodziej-Sobocińska, M. (2019)). Eggs hatching is favorable in the summer season because the temperature and enhances the rate of parasites production but in the case of rainy season found low infection rate (Short et al., 2017).

According to the environmental conditions parasites are get diversified and differentiated or specific differentiation and phylogenetic development as free living animals. The wide external environment surrounding causes the differences but host also acting as the environment (Chang et al., (2019)). The latter produces stimuli which promote further development. Parasites differentiation depends on their host surrounding environment (Muche, et al., 2022). Parasites inhabiting the host organism, in which they form a certain aggregation, the parasitofauna (Tad et al., 2019). Parasitofauna depend upon Ecological parasitology to study the whole changes in the external conditions surrounding the host and on changes in the physiological state of the host (Carlos Rauquea et al., 2018).

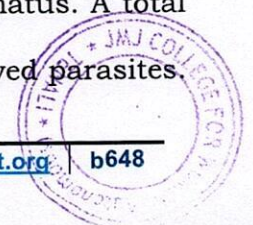
Morphological, physiological and ecological factors play important role in the host specificity and parasites are site specific probably derive certain nutrients from the organs (Vanessa Zuzarte-Luís, Maria Mota, (2018)). This needs further investigation to



establish the reasons for organ specificity. Host and parasite organ specificity depends on ecological surroundings of host (Muhammad Moosa Abro *et al.*, 2019).

During this study different variations observed in parasitic infection at different sampling stations. Fish was heavily infected with the cestode and nematode while the other parasites occurred in low numbers or absent (Larry I Lutwick (2019)). Similar results found with fish collected in Aurangabad heavily infected by the cestode parasites (Deshmukh, Shaziya and Gaikwad, (2019)). The variations can be attributed to changes in physico-chemical parameters or variation in food habits of the host (Di Renzo *et al.*, 2020). Fish from more polluted water tend to harbour more helminth parasites than those from less polluted waters (Jasrotia, *et al.*, 2017). Factors determining the variety of parasite fauna the diet of the host, lifespan of the host, the mobility of the host throughout its life including the variety of habitats it encounters, its population density and the size attained, large hosts provide more habitats suitable for parasites (Scholz *et al.*, 2018). Parasites cause diseases and affect the health and reproduction, leads to observable symptoms are fall easy prey to predators and some infect man (Rashid *et al.*, 2019). Economic losses occur due to parasites epidemics and mortalities (Narladkar, B.W. (2018)). The purpose of this survey was to estimate the present status of parasite incidence in this region and to provide parasitologic and epidemiologic information (Jaywant Shivajirao Dhole *et al.*, 2020).

CONCLUSION: The Two-year duration the survey had been conducted in the Tenali in and around area fresh water resources. Where that fresh water fishes collected from various ponds, lakes and canals Krishna canals were taken as a source of wide range of parasites especially the helminth parasites. The study was established A total of seven 10 parasites species were found in 6 fish species namely *Channa punctatus*, *Catla catla*, *Labeo rohita*, *Cirrhina*, *mrigala*, *Anabas*, *Mastacembelus armatus*. A total of 343 fish samples were examined for parasites. A total of 10 were observed parasites.



This study thus highlights on the details of therefore is, the only one that has given some details on the endoparasitic organisms infecting freshwater fish species. Due to seasonal variation generally parasite infection, variation in intensity of infection, variation in parasite fauna with the diet of the host, variation in infection with the habitat type.

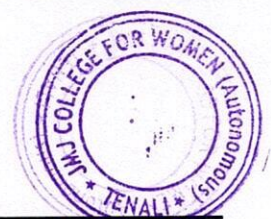
ACKNOWLEDGEMENT: I am very much grateful to the U.G.C. for financial support to complete this minor research project. The author is very much thankful to the management of J.M.J. College for women (A) Tenali, Guntur, and Andhra Pradesh, India for providing the laboratory facilities during this work.

REFERENCES:

1. Jyrwa, Donald B (2016). "Helminth parasite spectrum of fishes in Meghalaya, Northeast India: a checklist." *Journal of parasitic diseases: official organ of the Indian Society for Parasitology* vol. 40,2 (2016): 312-29.
2. Balai, V.K., Sharma L.L., and Ujjania N.C. (2017). Morphometric relationship of Indian major carps (Catla catla, Labeo rohita and Cirrhinus mrigala) from Jaisamand Lake, Udaipur (India), *Journal of Entomology and Zoology Studies*; 5(3): 547-550.
3. CDC (2019). Parasites-Diphyllobothrium Infection, Biology, Causal Agents: Global Health, Division of Parasitic Diseases and Malaria.
4. Jaywant Shivajirao Dhole, Sushil Jawale, Somnath Balbhim Waghmare and Ramrao Chavan (2020). Survey of helminth parasites in freshwater fishes from Marathwada region, MS, <https://www.researchgate.net/publication/272158741>.
5. Carlos Rauquea, Gustavo Viozzia, Verónica Floresa, Rocío Vegaa, Agustina Waicheima, Guillermo Salgado-Maldonadob (2018). Helminth parasites of alien freshwater fishes in Patagonia (Argentina) *IJP: Parasites and Wildlife* 7 (2018) 369-379.




6. Vanessa Zuzarte-Luís, Maria M. Mota, (2018). Parasite Sensing of Host Nutrients and Environmental Cues, *Cell Host & Microbe*, Vol (23) 6: 749-758,
7. Scholz, T. Vanhove, M.P.M. Smit, N. Jayasundera Z. and Gelnar M. (2018). A Guide to the Parasites of African Freshwater Fishes,
8. Larry I Lutwick (2019). Moderator, Program for Monitoring Emerging Diseases; Medscape.
9. Deshmukh, Shaziya & Gaikwad, J. (2019). studies on prevalence of cestode parasites in freshwater fishes from parbhani district (M.S) India.
10. Rashid, M., Rashid, M., Akbar, H., Ahmad, L., Hassan, M., Ashraf, K., . . . Gharbi, M. (2019). A systematic review on modelling approaches for economic losses studies caused by parasites and their associated diseases in cattle. *Parasitology*, 146(2), 129-141.
11. Narladkar, B.W. (2018). Projected economic losses due to vector and vector-borne parasitic diseases in livestock of India and its significance in implementing the concept of integrated practices for vector management. *Vet World*. 2018;11(2):151-160.
12. Muhammad Moosa Abro, Nadir Ali Birmani and Muhammad Bachal Bhutto (2019). Incidence of Helminth Parasites in freshwater Fishes of the River Indus at Jamshoro, Sindh, Pakistan, *Biological Forum – An International Journal* 11(2): 113-116.
13. Jasrotia, D., & Kaur, H. (2017). Molecular analysis of a novel species, *Gangesia punjabensis* (Family: Proteocephalidae, Subfamily: Gangesiinae) infecting an Indian freshwater cat fish, *Wallago attu* evidencing species complex. *Journal of parasitic diseases: official organ of the Indian Society for Parasitology*, 41(3), 888–898.



14. Tad A. Dallas, Anna-Liisa Laine and Otso Ovaskainen (2019). Detecting parasite associations within multi-species host and parasite communities, proceeding of the royal society B, Biological sciences.
15. Burrell CJ, Howard CR, Murphy FA. (2017). Epidemiology of Viral Infections. *Fenner and White's Medical Virology*. 2017;185-203.
16. Kołodziej-Sobocińska, M. (2019). Factors affecting the spread of parasites in populations of wild European terrestrial mammals. *Mamm Res* **64**, 301–318.
17. Short EE, Caminade C, Thomas BN.(2017). Climate Change Contribution to the Emergence or Re-Emergence of Parasitic Diseases. *Infect Dis (Auckl)*. 2017; 10.
18. Di Renzo, L., Gualtieri, P., Pivari, F. et al. (2020). Eating habits and lifestyle changes during COVID-19 lockdown: an Italian survey. *J Transl Med* 18, 229 (2020). <https://doi.org/10.1186/s12967-020-02399-5>
19. Lei Chang, Hui Jing Lu, Jennifer E. Lansford, Marc H. Bornstein, Laurence Steinberg, Bin-Bin Chen, Ann T. Skinner, Kenneth A. Dodge, Kirby Deater-Deckard, Dario Bacchini, Concetta Pastorelli, Liane Peña Alampay, Sombat Tapanya, Emma Sorbring, Paul Oburu, Suha M. Al-Hassan, Laura Di Giunta, Patrick S. Malone, Liliana Maria Uribe Tirado and Saengduean Yotanyamaneewong (2019). External environment and internal state in relation to life-history behavioural profiles of adolescents in nine countries. *Proc. R. Soc. B* 286: 20192097.
20. Muche, M., Muasya, A.M. & Tsegay, B.A. (2022). Biology and resource acquisition of mistletoes, and the defense responses of host plants. *Ecol Process* **11**, 24.
21. Ahn S, Kim YJ, Sohn CH, Seo DW, Lim KS, Donnino MW, Kim WY.(2018). Sodium bicarbonate on severe metabolic acidosis during prolonged



- cardiopulmonary resuscitation: a double-blind, randomized, placebo-controlled pilot study. *J Thorac Dis.* 2018 Apr;10(4):2295-2302.
22. Na W, Kim M, Sohn C.(2018). Dietary inflammatory index and its relationship with high-sensitivity C-reactive protein in Korean: data from the health examinee cohort. *J Clin Biochem Nutr.* 2018 Jan;62(1):83-88.
23. McClelland, Michael & Sass, Greg. (2012). Assessing fish collections from random and fixed site sampling methods on the Illinois River. *Journal of Freshwater Ecology - J FRESHWATER ECOL.* 27. 1-9.
24. Chu E.W., and Karr J.R. (2017). Environmental Impact: Concept, Consequences, Measurement. Reference Module in Life Sciences. 2017; B978-0-12-809633-8.02380-3.
25. Knap A.H. and Rusyn I. (2016). Environmental exposures due to natural disasters. *Rev Environ Health.* 2016;31(1):89-92
26. Shah F. A, Qayoom I, Balkhi M. H, Kumar A. (2015). Impact of Parasitic Diseases on Fishes of North West Himalayan Streams. *Curr World Environ* 2015;10(3).
27. Gautam, Neelam & Misra, Pawan & Saxena, Anand & Monks, Scott. (2020). Description of *Pallisentis thapari* n. sp. and a re-description of *Acanthosentis seenghalae* (Acanthocephala, Quadrigyridae, Pallisentinae) using morphological and molecular data, with analysis on the validity of the subgenera of *Pallisentis*. *Zootaxa.* 4766. 139-156.
28. Khurshid Ahmad Tariq (2020). Parasite biodiversity: A parasitologists perspective; We know that around 50% of life on this earth is parasitic.
29. Sohn W.M., and Na B.K. (2018). Morphological Characteristics and Fish Hosts of *Isoparorchis* sp. (Digenea: Isoparorchidae) in Korea. *Korean J Parasitol.* 2018;56(5):501-507.


PRINCIPAL
J.M.J. COLLEGE FOR WOMEN (Autonomous)

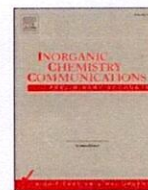


2022



Contents lists available at ScienceDirect

Inorganic Chemistry Communications

journal homepage: www.elsevier.com/locate/inoche

Short communication

Cobalt (II) complexes with N-methyl thio semicarbazide Schiff bases: Synthesis, spectroscopic investigation, cytotoxicity, DNA binding and incision, anti-bacterial and anti-fungal studies

P. Jyothi^{a,b,*}, V. Sumalatha^a, D. Rajitha^a^a Department of Chemistry, Osmania University, Telangana 500007, India^b Government Polytechnic, Nalgonda, Telangana 508001, India

ARTICLE INFO

Keywords:

Schiff bases
Metal complexes
DNA binding
DNA cleavage
Cytotoxicity, antimicrobial

ABSTRACT

Three Co(II) complexes [Co(L₁) (I), [Co(L₂) H₂O] (II), and [Co(L₃) H₂O] (III)], where L₁H is 2-(2-Hydroxy-5-Bromo Benzylidene) Hydrazine N-Methyl Carbo-Thioamide, L₂H is 2-(2-Hydroxy-5-Chloro Benzylidene) Hydrazine N-Methyl Carbo-Thioamide and L₃H is 2-(2-Hydroxy-Phenylethylidene) Hydrazine N-Methyl Carbo-Thioamide were synthesized and spectroscopically characterized using FT-IR, UV-Dr, ¹H NMR, ¹³C NMR, ESI Mass, TGA, Magnetic susceptibility values. Based on these values a tetrahedral geometry is proposed for all the complexes. The DNA binding studies against calf thymus DNA (CT DNA) revealed an intercalative mode of binding has existed between DNA and metal complex and also metal complexes can cleave the supercoiled pBR 322 DNA effectively. The Schiff bases and metal complexes were also examined for antimicrobial studies against bacterial species of two gram-positive and two gram-negative strains and also two fungal strains and observed that complexes showed better activity than a free ligand. Further, the cytotoxic activity of synthesized compounds has been done using MTT assay and found that complexes acted as good anticancer agents against both MCF7 and HeLa cell lines.

1. Introduction

In the investigation of anticancer drugs, DNA plays a vital role as it is the genetic material [1]. The drugs effects the cell growth, replication and transcription process and so that it can interfere with protein synthesis. Generally, Platinum-based drugs are the most commonly used anticancer drugs and are widely studied. Since they possess severe side effects, there is an extreme need for the invention of the most effective alternate metal-based DNA binding agents that possess low side effects [2]. There are several examples that metal complexes can act as good DNA cleavage agents [3]. Usage of Cobalt metal complexes as antitumor drugs leads to lower side toxicity and is more vital compared to other analogous compounds [4], further studies on Co metal revealed that they are having variety of applications and easy formation procedures [5–7].

“Metal complexes with Schiff base ligands have a wide range of biological applications in different fields as it contains azomethine linkage which provides an opportunity for biological activities” [8–10]. Thiosemicarbazone derivatives proved to be more potent in various applications [11,12]. “Thiosemicarbazone derivatives with

salicylaldehyde possess excellent pharmacological activities like anti-inflammatory, anti-cancer, anti-microbial, anti-HIV and also pesticides and insecticidal activities” [13,14]. Recently we have communicated synthesis, characterization, cytotoxicity, DNA binding, incision and anti-microbial activities of N-Methyl thio semi carbazide schiff base metal complexes [15,16]. Given above, we are focussing on a simple drugs which binds DNA effectively with more curative power and minimum side effects. The present research discusses on synthesis, characterization, DNA binding and cleavage, cytotoxicity, antibacterial and antifungal activities of Co (II) metal complexes of Schiff bases of N-Methyl thiosemicarbazide.

2. Procedure

2.1. Synthesis

2.1.1. Synthesis of Schiff base ligands

The Schiff's base ligands have been synthesized by adding methanolic solution of (40 ml) N-Methyl Thiosemicarbazide (2.10 g, 0.02 mol) and a few drops of sulphuric acid was to a Methanolic solution of 5-

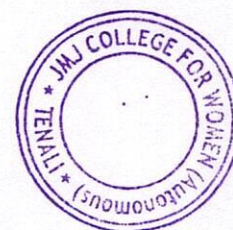
* Corresponding author.

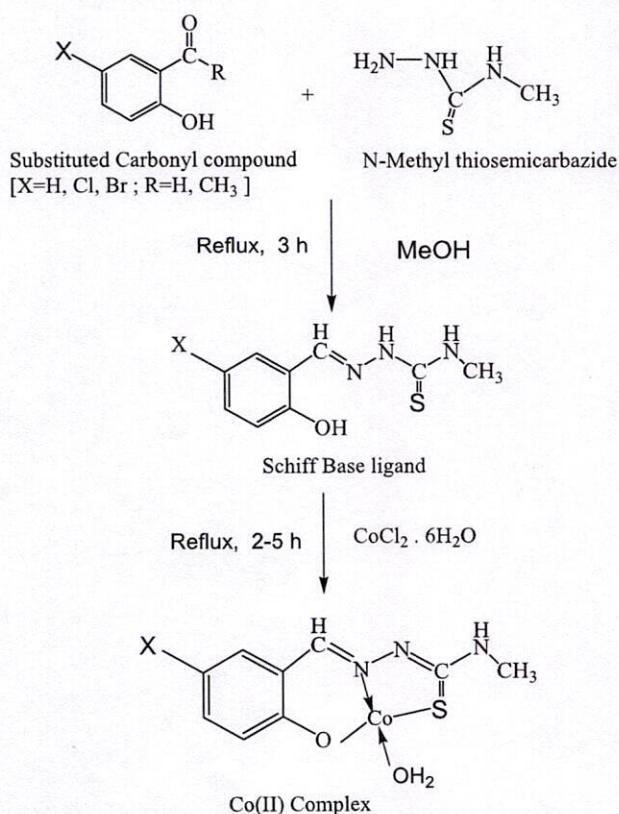
E-mail address: jyothi.p59@gmail.com (P. Jyothi).<https://doi.org/10.1016/j.inoche.2022.110029>

Received 27 June 2022; Received in revised form 13 September 2022; Accepted 25 September 2022

Available online 29 September 2022

1387-7003/© 2022 Elsevier B.V. All rights reserved.





Scheme 1. Schematic route for the preparation of Schiff bases and their Co(II) metal complexes.

Bromo Salicylaldehyde (4.02 g, 0.02 mol), 5-Chloro Salicylaldehyde (3.13 g, 0.02 mol), o-hydroxy acetophenone to get L₁, L₂, L₃ respectively. The resultant mixture was refluxed for 3 h; the resulting solid product was isolated by filtration and recrystallized from methanol.

2.1.1.1. (2Z)-2-(2-Hydroxy-5-Bromo Benzylidene) Hydrazine N-Methyl Carbo-Thioamide (L₁). Yield 84 %; ESI-MS (DMSO): $m/z = 286$ (calcd.286) [M]⁺; IR (KBr, cm⁻¹): 1627(C=N), 1475(C=C), 1654(-CH=N), 3275(-NH), 3390(-OH);

Anal. Calc. (C₉H₁₁N₃O₂Br): C, 37.6; H, 3.80; N, 14.51. Found: C, 37.3; H, 3.72; N, 14.4.

¹H NMR (400 MHz, CDCl₃, ppm): 8.3 (d, H_c; 1H), 8.0 (d, H_d; 1H), 8.6 (s, H_f; 1H), 11.5 (s, -OH; 1H), 7.2 (s, -NH_a; 1H), 6.8 (s, -NH_b; 1H), 10.2 (s, CH=N; 1H), 3.0 (s, -CH₃; 3H).

2.1.1.2. (2Z)-2-(2-Hydroxy-5-Chloro Benzylidene) Hydrazine N-Methyl Carbo-Thioamide (L₂). Yield 80 %; ESI-MS (DMSO): $m/z = 245$ (calcd.244) [M + 1].

Anal. Calc. (C₉H₁₁N₃O₂Cl): C, 44.2; H, 4.50; N, 17.2. Found: C, 44.3; H, 4.41; N, 17.5.

¹H NMR (400 MHz, CDCl₃, ppm): 8.3 (d, H_c; 1H), 8.0 (d, H_d; 1H), 8.6 (s, H_f; 1H), 11.5 (s, -OH; 1H), 7.3 (s, -NH_a; 1H), 6.9 (s, -NH_b; 1H), 10.3 (s, CH=N; 1H), 3.0 (s, -CH₃; 3H).

2.1.1.3. (2Z)-2-(2-Hydroxy-Phenylethylidene) Hydrazine N-Methyl Carbo-Thioamide (L₃). Yield 82 %; ESI-MS (DMSO): $m/z = 224$ (calcd.223) [M + 1].

Anal. Calc. (C₁₀H₁₃N₃O₂): C, 54.05; H, 5.85; N, 18.91. Found: C, 53.89; H, 5.97; N, 19.01.

¹H NMR (400 MHz, CDCl₃, ppm): 7.2–7.3 (d, H_c; 1H), 7.0–7.1 (d, H_d; 1H), 7.1–7.2 (d, H_e; 1H), 7.4–7.5 (d, H_f; 1H), 10.8 (s, -OH; 1H), 6.9–7.0 (s, -NH_a; 1H), 6.8–6.9 (s, -NH_b; 1H), 9.0 (s, CH=N; 1H), 3.0–3.5 (s,

-CH₃-N; 3H) 2.2–2.5 (s, -CH₃-C; 3H).

2.1.2. Synthesis of Co(II) metal complexes

These complexes were prepared by mixing CoCl₂·6H₂O (1 mM) in MeOH (50 ml) and Schiff bases L₁, L₂, and L₃ (1 mM) in 15 ml methanol in 1:1 ratio to get complex-I, complex-II and complex-III respectively. The resultant mixed solutions were refluxed for 2–5 h at 70–80 °C. The products were separated and washed with ethanol and dried in a vacuum. (Scheme.1).

Yield 82 %; ESI-MS (DMSO): $m/z = 400$ (calcd.361) [M + K]⁺ [Co(L₁)H₂O].

Anal. Calc. (C₉H₁₂N₃O₂SBrCo): C, 29.90; H, 3.32; N, 11.63; Co, 16.31. Found: C, 29.70; H, 3.20; N, 11.8; Co, 16.5.

Yield 80 %; ESI-MS (DMSO): $m/z = 341$ (calcd.318) [M + Na]⁺ [Co(L₂)H₂O].

Anal. Calc. (C₉H₁₂N₃O₂S Cl Co): C, 33.90; H, 3.72; N, 13.23; Co, 18.51. Found: C, 33.80; H, 3.80; N, 13.31; Co, 18.40.

Yield 75 %; ESI-MS (DMSO): $m/z = 337$ (calcd.298) [M + K]⁺ [Co(L₃)H₂O].

Anal. Calc. (C₁₀H₁₄N₃O₂S Co): C, 40.26; H, 4.69; N, 14.09; Co, 19.46. Found: C, 40.54; H, 4.99; N, 14.56; Co, 19.32.

Materials and instrumentation are listed in supplementary material.

2.2. DNA binding studies

2.2.1. Electron absorption studies

"Electron Absorption spectroscopy is one efficient technique for evaluating the DNA binding nature of synthesized metal complexes" [17]. Test compounds were dissolved in DMSO and make up the solution with TAE buffer (40 mM tris base, 20 mM acetic acid and 1 mM EDTA). "UV absorbance DNA in buffer solution gave a ratio of 1.8–1.9 / 1 at 260 and 280 nm indicating DNA was free from the protein and also concentration of DNA was evaluated by its known molar extinction coefficient of 6600 M⁻¹ cm⁻¹ at 260 nm" [18].

The intrinsic binding constant (K_b) of complexes with DNA were obtained by controlling the changes in absorbance at their respective MLCT band. Complex concentration is fixed at 10 μM while nucleotide is varied from 0 to 10 μM. The absorbance of CT-DNA was deleted by giving equal amounts of DNA solution to the complex and reference solution. "The binding strength can be known quantitatively by using the following equation.

$$[\text{DNA}] / (\epsilon_a - \epsilon_f) = [\text{DNA}] / (\epsilon_b - \epsilon_f) + 1 / K_b (\epsilon_b - \epsilon_f)$$

where ϵ_a , ϵ_f , ϵ_b are the compound with DNA, alone compound and fully bound DNA with compound respectively" [19].

K_b is given by the ratio of the slope to the intercept.

2.2.2. Fluorescence quenching studies

The EtBr displacement method was carried out in a TAE buffer to determine the binding affinity between DNA and complex on fluorescence spectrometry by changing the concentration of the metal complexes from 0 to 60 μM and maintaining the concentration of EB-bound DNA as constant (1: 10 ratio of EtBr and CT-DNA). "The effect of the metal complex on the emission intensity of the EB bound CT-DNA was recorded in the range of 520–700 nm where excitation wavelength was set at 510 nm" [20]. The quenching efficiency can be determined by using the Stern-Volmer equation [21].

[Q].

I₀ and I are emission intensity in the absence and the presence of compound respectively.

[Q] is the concentration of the compound.

2.2.3. Viscosity studies

Viscosity experiments were performed by maintaining the

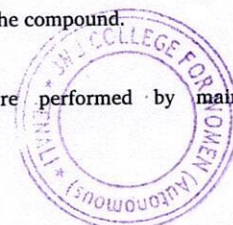


Table 1
IR spectra data of the Schiff bases and their complexes.

compound	OH/H ₂ O	C=N	C=S	CH = N	-NH	M-O	M-N	M-S
L ₁	3390	1552	1267	1606	3275	-	-	-
Complex-I	3383	1548	-	1608	-	576	472	374
L ₂	3394	1554	1267	1600	3259	-	-	-
Complex-II	3552	1548	-	1608	-	576	472	364
L ₃	3307	1566	1267	1598	3091	-	-	-
Complex-III	3215	1525	-	1604	-	561	478	341

Table 2
Mass spectra data of the Schiff bases their complexes.

complex	Obtained mass	Calcd. Mass	Peak assigned
L ₁	286	286	[M] ⁺
Complex-I	400	361	[M + K] ⁺
L ₂	245	244	[M + 1]
Complex-II	341	318	[M + Na] ⁺
L ₃	224	223	[M + 1]
Complex-III	337	298	[M + K] ⁺

Table 3
IC₅₀ values of the Schiff bases their complexes.

compound	IC ₅₀ values (μM)	
	MCF7	HeLa
L ₁	54.8	62.98
Complex-I	47.73	53.33
L ₂	50.56	55.80
Complex-II	42.78	44.81
L ₃	52.48	53.6
Complex-III	44.77	46.81
Cisplatin	41.36	29.34

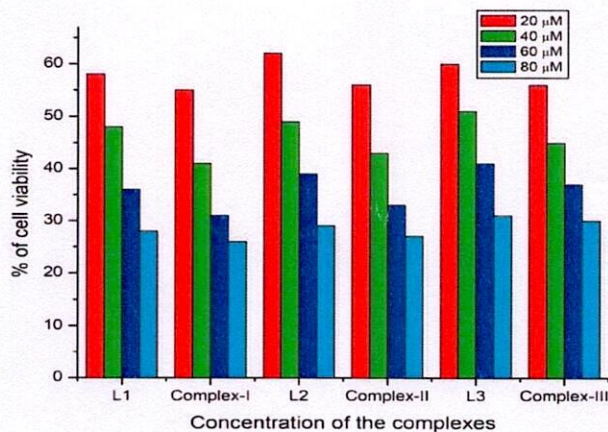


Fig. 1. Effect on the cell viability of HeLa cell lines on increasing the concentration of the Schiff base and their complexes.

concentration of the CT-DNA constant at 200 μM and varying the complex concentrations from 0 to 200 μM. In these experiments, Ostwald capillary Viscometer immersed in a thermostatic water bath maintained at 30.0 ± 0.1 °C using the TAE buffer (40 mM Tris-acetate, 1 mM EDTA) solution of pH 7.2 [22].

The flow time of test samples in TAE buffer was measured with a digital timer, and each experiment was carried out at least three times to get accuracy, and an average flow time was calculated. Data obtained is plotted between $(\eta/\eta_0)^{1/3}$ vs $[Co(L)H_2O]/[DNA]$, where η and η_0 are the viscosity of CT-DNA in the presence of complex solution and alone in TAE buffer respectively. ' η ' and ' η_0 ' were calculated by using the

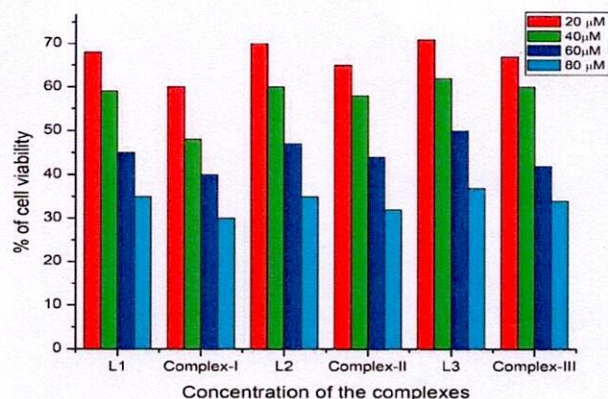


Fig. 2. Effect on the cell viability of MCF7 cell lines on increasing the concentration of the Schiff base and their complexes.

following equations,

$$\eta = (t_1 - t_0)/t_0$$

$$\eta^0 = (t - t_0)/t_0$$

t_0 = Flow time of the buffer solution alone,

t = Flow time of DNA solution in the absence of complex,

t_1 = Flow time of DNA solution in the presence of the complex.

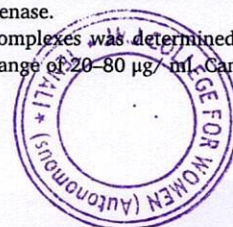
2.3. DNA cleavage

Gel electrophoresis technique was used to know the DNA cleavage efficiency of all the complexes which was performed by treating the supercoiled pBR322 DNA with variable concentrations of metal (II) complexes in the presence of H₂O₂ (Oxidative cleavage) and UV light (Photolytic cleavage) and followed by dilution with Tris-HCl / NaCl buffer (5: 50 mM, pH 7.2). Then mixed samples were incubated for 2 h at 37 °C and followed by mixing with bromophenol blue (2 μL). Later, loaded the mixed samples (10 μL out of 16 μL) in the wells of 1 % agarose gel which was placed in TAE buffer (pH 8.0) containing tray, then subjected to electrophoresis for 45 min at 70 V. Once an electric field is applied across the gel, the DNA which is negatively charged at neutral pH slowly migrates towards the anode. The resulting gel was stained with Ethidium bromide before the images were taken under UV light using a Bio-Rad Gel documentation system [23].

2.4. In vitro cytotoxicity

The cytotoxic activity of Schiff bases and metal complexes were examined on HeLa & MCF7 cells using colorimetric 3-(4, 5-dimethylthiazole-2-yl)-2, 5-biphenyl tetrazolium bromide (MTT) assay. MTT technique based on colorimetry, that measures the reduction of yellow 3-(4, 5-dimethylthiazol-2-yl)-2, 5-diphenyl tetrazolium bromide (MTT) by mitochondrial succinate dehydrogenase.

The cytotoxic activity of metal complexes was determined by the complex in the concentration in the range of 20–80 μg/mL. Cancer cell



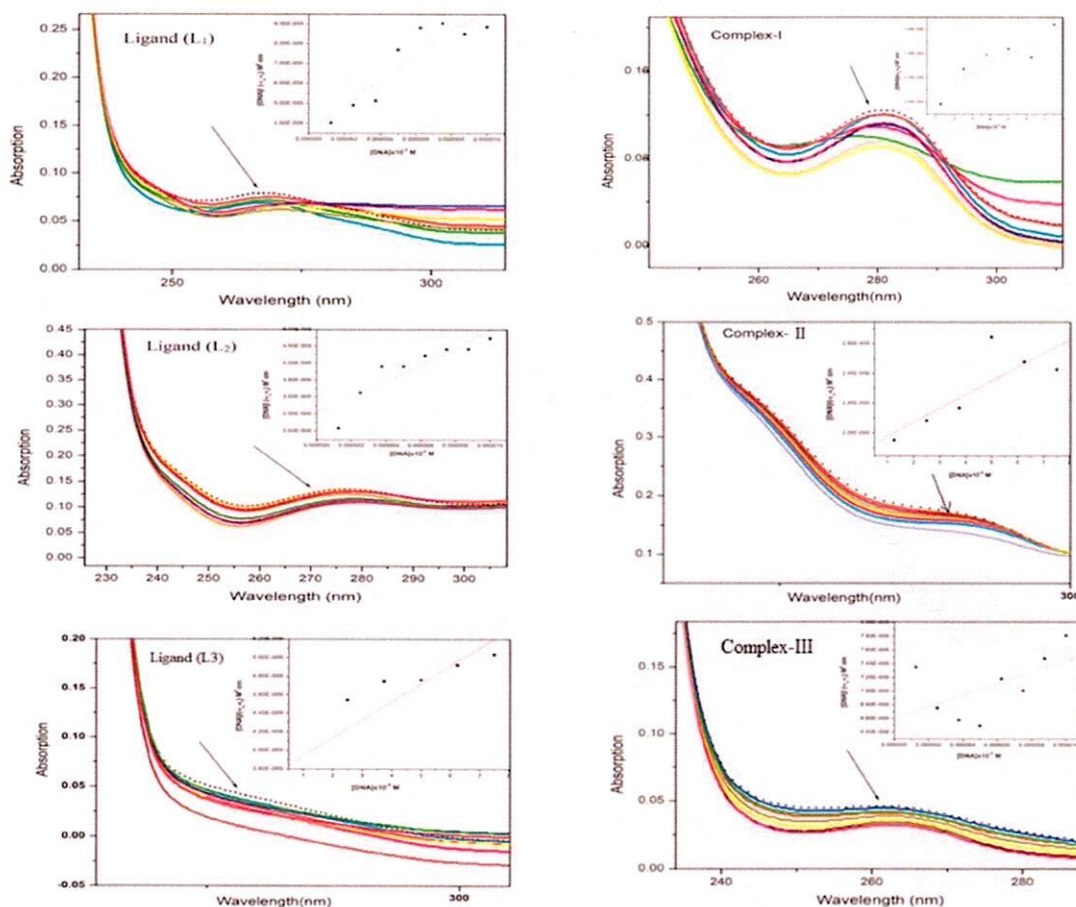


Fig. 3. UV-absorption spectra of Ligands and their complexes in the absence (dashed line) and presence of CT-DNA in Tris-HCl buffer. [Complex] = 10 μ M, [DNA] = 0–10 μ M. Arrow mark shows the change in absorbance upon increasing the concentration of DNA. Inset: linear plots of $[DNA] / (\epsilon_a - \epsilon_f)$ vs $[DNA]$.

lines were cultivated in DMEM with 10 % fetal bovine serum in 96 well plates for 24 h followed by treating with different concentrations of test compounds in represented wells in 96 plates. After 48 h of incubation, the cells were washed twice with buffer solution and exposed to freshly prepared MTT solution (0.5 mg/ml in phosphate buffer solution) allowed to incubate at 37 $^{\circ}$ C for 4 h. The formazan crystals obtained by MTT incubation were dissolved in DMSO and measured for optical density at 570 nm on a microplate reader [24]. The percentage of growth inhibition was calculated using the following formula.

$$\% \text{ of Inhibition} = 100(\text{Control-Treatment}) / \text{Control}.$$

2.5. Anti-microbial activity

In-vitro antimicrobial activity of both Schiff bases and Co (II) complexes were evaluated by paper disc method against bacteria *Bacillus Subtilis*, *Streptococcus Aureus* (gram-positive bacteria) and *Escherichia Coli*, *Pseudomonas Aeruginosa* (gram-negative bacteria) and fungi *Fusarium Oxysporium Lycopersicum* and *Fusarium recini* using penicillin and ketoconazole as standard drugs for antibacterial and antifungal respectively. 5 mg of each sample was dissolved in DMSO to get a stock solution of 500 μ g / ml. Cultures of tested microbes were maintained in nutrient agar media and then transferred to Petri dishes before testing [25,26]. All the test compounds were impregnated on the paper discs and incubated at 37 $^{\circ}$ C for 48 h. The zone of inhibition was measured in mm [27].

3. Result and discussion

3.1. Characterisation of ligands and its metal complexes

3.1.1. NMR spectra

The result of the ^1H NMR Spectra of Schiff base ligands confirms their formation which exhibits a signal at δ 10.8–11.5 corresponding to the phenolic OH group. The signal at δ 9.0–10.3 attributes to azomethine proton. The multiplets of strong bands in the zone of δ 8.0–8.6 correspond to the protons of the benzene ring. And also the peaks of protons for –NH group were observed at δ 6.8– δ 7.2.

The ^{13}C NMR Spectra also revealed the expected number of peaks which corresponds to the presence of various kinds of carbon atoms present in the ligands. The spectrum consists of a strong band at δ 178–179 ppm which is assigned to the C=S group. The signal for azomethine carbon was obtained at δ 155–158 ppm. The carbons of the aromatic ring showed signals in the region of δ 110–140 ppm and the intense peak of methyl carbon showed at δ 40 ppm. (Fig. s1 - Fig. s6).

3.1.2. FTIR spectra

On comparison of FTIR spectra of ligands and complexes, free ligands exhibited bands at 3307–3394 cm^{-1} , due to phenolic OH found to be absent confirms co-ordination of this group to metal centre. And also the bands at 1552–1566 cm^{-1} , and 1267 cm^{-1} by azomethine nitrogen and thioketo sulfur were found to be altered in the spectra of metal compounds, implying their coordination in the complex formation. Moreover, the appearance of moderate potent ν (Co-O), ν (Co-N), and ν (Co-S) bands in the zone of 561–576 cm^{-1} , 472–478 cm^{-1} and 341–374



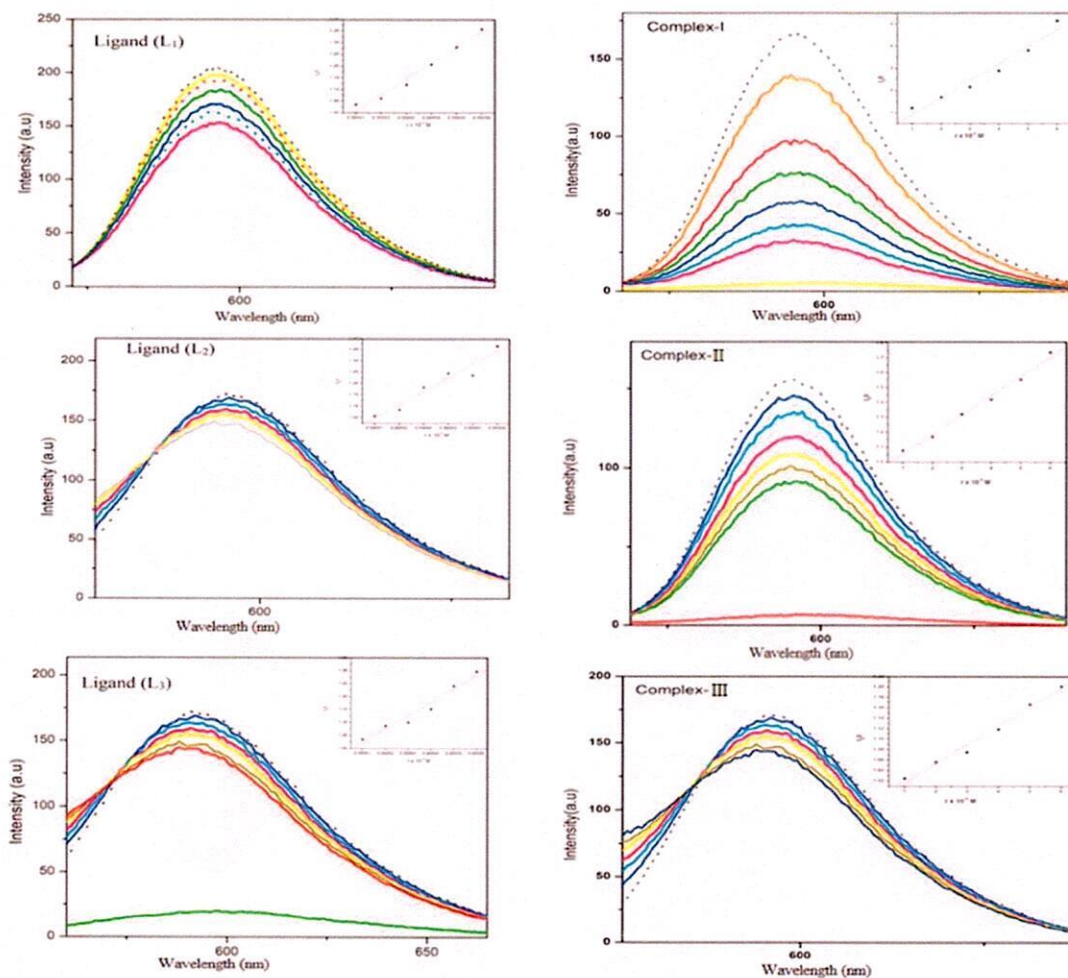


Fig. 4. Fluorescence emission spectra of EB bound DNA in the absence (dashed line) and presence of Schiff bases and their complexes. [EB] = 12.5 μ M, [DNA] = 125 μ M, [compound] = 0–60 μ M. The arrow mark shows the change in intensity upon increasing the concentration. Inset: (I_0 / I) vs r .

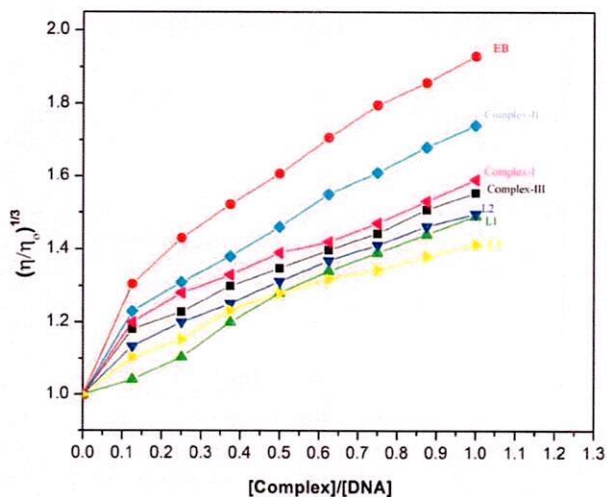
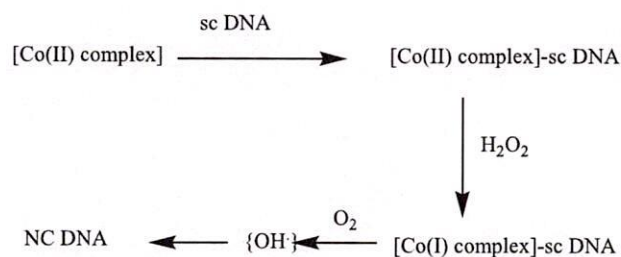


Fig. 5. Effect of enhancing amounts of EB, Complexes I, II, III and Schiff bases L_1 , L_2 , L_3 , on the relative viscosity of CT-DNA at 30 ± 0.1 °C.

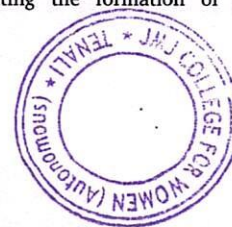


Scheme 2. Schematic route for the Mechanism of DNA cleavage in presence of H_2O_2 .

cm^{-1} respectively indicated the complex existence [28]. In the spectra of all the complexes the band corresponding to ν (NH) was found to be absent and also new band observed for ν (C-S) at $727\text{--}767$ cm^{-1} revealing that the co-ordination occurs through thiolate sulphur after enolization and deprotonation. The FTIR spectral results of prepared compounds are listed in Table.1 (Fig. s7 - Fig. s12).

3.1.3. Mass spectra

Mass spectral results for prepared compounds were given in Table.2. Calculated mass values for the compounds were in good agreement with the obtained mass values indicating the formation of prepared



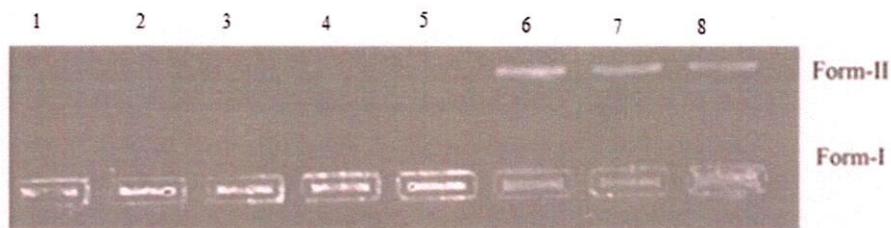


Fig. 6. Oxidative cleavage of supercoiled pBR 322 DNA at 37 °C in 5 mm Tris HCl / NaCl buffer by the Schiff bases and Complexes. Lane 1: DNA control; Lane 2: DNA + H₂O₂ (1 mM); Lane 3: DNA + H₂O₂ (1 mM) + L₁ (60 μM); Lane 4: DNA + H₂O₂ (1 mM) + L₂ (60 μM); Lane 5: DNA + H₂O₂ (1 mM) + L₃ (60 μM); Lane 6: DNA + H₂O₂ (1 mM) + Complex -I (60 μM); Lane 7: DNA + H₂O₂ (1 mM) + Complex -II (60 μM); Lane 8: DNA + H₂O₂ (1 mM) + Complex -III (60 μM).

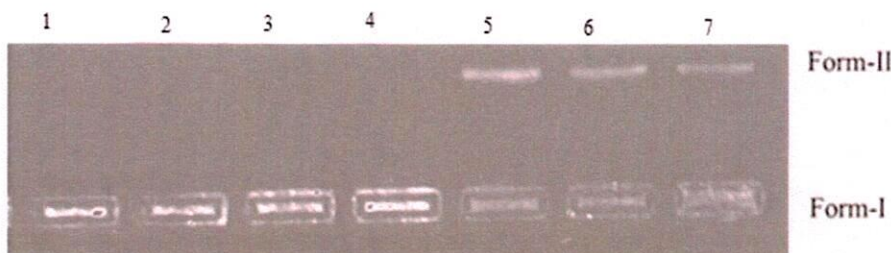


Fig. 7. Photolytic cleavage of supercoiled pBR 322 DNA at 37 °C in 5 mm Tris HCl / NaCl buffer by the Schiff bases and Complexes using UV irradiation of 365 nm. Lane 1: DNA control; Lane 2: DNA + L₁ (60 μM); Lane 3: DNA + L₂ (60 μM); Lane 4: DNA + L₃ (60 μM); Lane 5: DNA + Complex -I (60 μM); Lane 6: DNA + Complex -II (60 μM); Lane 7: DNA + Complex -III (60 μM).

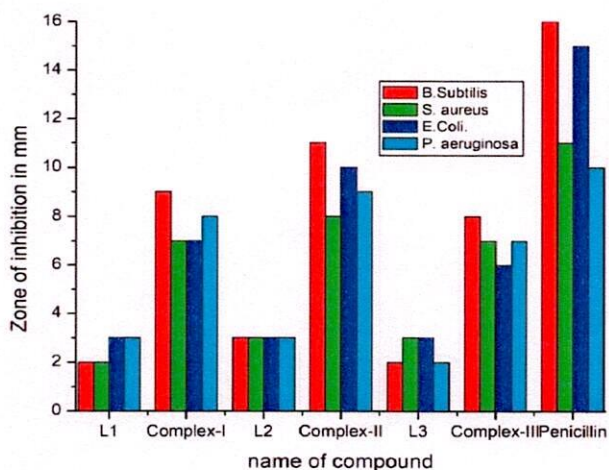


Fig. 8. Zone of inhibition values of Schiff bases and their complexes against bacterial strains.

compounds (Fig. s13 to Fig. s18).

3.1.4. UV-Dr's spectra

The electronic spectral data gives information regarding the shape of metal complexes. The diffuse reflectance spectrum of metal compounds showed bands in the region of 200 to 400 nm, indicating the charge transfer transitions and also Complexes showed bands assigned to ν_1 [$^4A_{2g}(F) \rightarrow ^4T_{1g}(F)$] in the region of 500–700 nm indicating its tetrahedral geometry [29]. On the other hand, ligand shows peaks in the region of 200–400 nm which are assigned to INCT transitions (Fig.s19-Fig. s24).

TGA analysis is given in supplementary material.

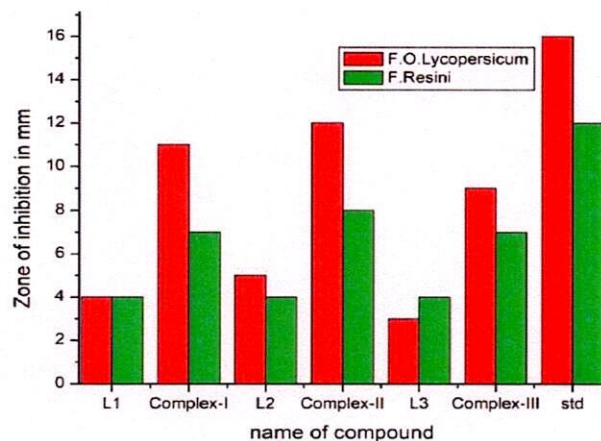


Fig. 9. Zone of inhibition values of Schiff bases and their complexes against fungal strains.

3.2. Biological activity of Schiff bases and their Co (II) metal complex

3.2.1. Solubility

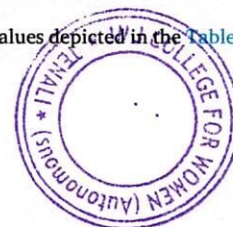
Ligands are soluble in methanol whereas complexes are soluble in DMSO but both are insoluble in water. All the compounds are stable at room temperature.

3.2.2. Cytotoxicity

Cancer is the most widespread disease in the world. So the research for the novel compounds that kills cancer cells selectively is still needed due to the side effects of current chemotherapeutics.

Because of the above, the study of the cytotoxic activity of all synthesized metal complexes was examined on HeLa & MCF7 cell lines adopting MTT assay [30], using Cisplatin as a standard. Cytotoxic activity of metal complexes depends on capability to intercalate with DNA leads to its failure of its function [31].

The results were analyzed by IC₅₀ values depicted in the Table 3. The



% of inhibition on the tested cell lines in the compound concentration range of 20–80 μM of the Schiff bases and complexes are given in Fig. 1 & Fig. 2. According to the result as the compound concentration increases, the inhibition of that cell will increase.

From this study, it is to be observed that II is found to be more capable than other complexes against MCF7 & HeLa cell lines that related to its binding capability with DNA and results are almost resembles with the earlier reported drugs but remarkable by their simple synthetic procedures as they are binary metal complexes [15].

3.2.3. DNA binding studies

3.2.3.1. Electron absorption studies. Electron absorption spectra is widely accepted technique to know the strength and mode of binding of complexes with DNA which involves the observing of $\pi\text{-}\pi^*$ transition absorption band of the complex in the absence and presence of DNA. In general hypochromism with red shift is due the presence of strong stacking force between the aromatic chromophore of the complex molecule and DNA base pairs through non-covalent $\pi\text{-}\pi^*$ interactions which leads to intercalative mode of binding. To know the binding strength of the compounds intrinsic binding constant (K_b) values were calculated [32].

The k_b values for synthesized complexes are determined as 0.9×10^4 , 1.2×10^4 , 1.1×10^4 , 4.9×10^4 , 0.8×10^4 , 1.7×10^4 , for L₁, I, L₂, II, L₃, III respectively which are slightly lower than that of potent intercalators like ethidium bromide. The intercalation of metal complexes with DNA was resulting in hypochromic in intensity (6–50 %) and red shift in wavelength (2–12 nm) indicating the intercalative mode of binding was existed between the metal complexes and DNA. (Fig. 3).

3.2.3.2. Fluorescence study. Fluorescence experiments were performed to get proof for an interacting mode of compounds with DNA [10]. Ethidium Bromide is one of the potent fluorescent probes that intercalate with DNA resulting in the enhancement of the intensity of fluorescent spectra due to its strong intercalating ability with DNA base pairs [11]. By adding metal compounds to EB-DNA, the intensity of fluorescent spectra of EB-DNA will reduce owing to the compound aggressive binding by replacing the bound EB from DNA [33].

The Stern Volmer quenching constant (K_{sv}) values of all the compounds are found to be in between 0.7 and $3.1 \times 10^4 \text{ M}^{-1}$. The result of this study is consistent with Electron absorption studies i.e. intercalative mode of binding has existed (Fig. 4).

3.2.3.3. Viscosity. Viscometric experiments have been done to confirm the mode of binding of metal compounds with CT-DNA and the most crucial tests of the binding mode of solution in the unavailability of crystallographic structural data.

The binding of metal complexes with DNA is sensitive to the viscosity of DNA in which there is an increase in Viscosity of DNA due to the separation of base pairs of DNA and extension in the double helix length. Viscosity measurements of prepared complexes are represented in Fig. 5.

On analyzing the results, it is to be declared that by enhancing the concentration of complexes the relative viscosity of DNA solution was increased, further suggesting that, an intercalative mode of binding has existed between DNA and metal compounds [34].

3.2.4. DNA cleavage activity

The nucleotide incision activity of synthesized complexes with supercoiled pBR322 has been investigated using oxidative and photolytic cleavage methods by implying the Agarose gel electrophoresis technique.

Binding of the drug compound to ds circular DNA resulting in the conversion of the sc form (Form-I) of DNA into nicked circular form (Form-II) and linear form (Form-III). If incision takes place on the single strand of the ds circular DNA (SC), it relaxes to form-II (NC), while if

incision takes on both the strands, it relaxes to Form-III (LC). Generally form-I migrate faster than form-II, which migrates slowly and form-III migrates in between the SC form and nicked form. Hence, the DNA incision ability of metal compounds was monitored by studying the alteration of the SC form into NC form and linear form. Mechanism of oxidative cleavage is representing in Scheme.2.

The complexes almost showed similar cleavage efficiency except for the slight variation attributed to the diverse DNA intercalating ability of the compounds by oxidative and photolytic cleavage methods. In Oxidative cleavage Lane 1 and Lane 2 have not shown any incision since they consist only of DNA and DNA + H₂O₂ (without complexes) respectively was indicating the catalytic role of metal compounds in the DNA incision [35].

From the study, it is to be noticed that metal compounds converted DNA Form-I to Form-II while the ligands did not show such activity (Figs. 6 & 7).

3.2.5. Antimicrobial studies

The prepared compounds are tested for their Antimicrobial activity towards two gram-positive and two gram-negative strains and also two antifungal strains and depicted in Figs. 8 and 9. The results stated that the compounds are more active towards the selected strains that are compatible to standard drug consistent with the cause might be likely Lipophilicity property [36]. Metal ion improves the lipophilic nature of ligands by involving them in chelation and by increasing delocalization of p- electrons.

4. Conclusions

Three Schiff bases and their Co (II) complexes have been synthesized and characterized spectroscopically. DNA intercalation study of the prepared compounds with DNA revealed that intercalation mode of binding existed between DNA and complex. Metal complexes also acted as good cell inhibitors and also complexes can cleave the PBR 322 DNA efficiently. In addition, metal complexes were act as excellent antimicrobial agents. Further, it is to be stated that Metal complexes were more potent than their respective Schiff bases.

Declaration of Competing Interest

The authors declare that they have no known competing financial interests or personal relationships that could have appeared to influence the work reported in this paper.

Data availability

Data will be made available on request.

Acknowledgements

We express our sincere thanks to the Head, Department of chemistry and the Director, CFRD, Osmania University for the providing required facilities and also the Director, IICT, Hyderabad, India.

Funding

This research did not receive any specific grants from public or commercial sectors.

Appendix A. Supplementary data

Supplementary data to this article can be found online at <https://doi.org/10.1016/j.inoche.2022.110029>.



References:

- [1] I. Ali, L.M.A. Mahamood, Y.T.H. Mehdar, H.Y. Aboul-Enein, M.A. Said, Synthesis, characterization, simulation, DNA binding and anticancer activities of Co(II), Cu(II), Ni(II) and Zn(II) complexes of a Schiff base containing *o*-hydroxyl group nitrogen ligand, *Inorg. Chem. Commun.* 118 (2020), 108004.
- [2] Z.H. Siddik, Cisplatin: Mode of cytotoxic action and molecular basis of resistance, *Oncogene*, 22 (2003) 7265-7279.
- [3] M.R. Rodriguez, M.J. Vavecchia, B.S.P. Costa, A.C. Gonzalez, M.R. Gonzalez-Baro, E.R. Cattaneo, DNA Cleavage mechanism by metal complexes of Cu(II), Zn(II) and Vo(IV) with a Schiff base ligand, *Biochimie*, 186 (2021) 43-50.
- [4] A. Hussain, M.F.A. Ajmi, Md.T. Rahman, A.A. Khan, P.A. Shaikh, R.A. Khan, Evaluation of Transition Metal Complexes of Benzimidazole-derived Scaffold as Promising Anticancer Chemotherapeutics, *Molecules*, 23(5) (2018) 1232.
- [5] T.A. Yousef, O.A. El-Gammal, S.F. Ahmed, G.m., Abu El-Reash, Structural, DFT and biological studies on Co (II) complexes of semi and thiosemicarbazide ligands derived from diketone hydrazide, *J. Mol. Struct.* 1076 (2014) 227-237.
- [6] K. Chithra, D. Sathesh, K. Jayanthi, S.V. Kumar, V. Muthulakshmi, K. Kalavani, R. Saravanan, P. Sellam, Cobalt(II) Complexes of (E)-2-(2-Hydroxy-3-methoxybenzaldehyde)hydrazinecarbo(thio)amides: Synthesis, FT-IR studies and their antimicrobial activity, *Chem. Data Collect.* 32 (2021), 100652.
- [7] M. Jarestan, K. Khalatbari, A. pouraei, et al., Preparation, characterization, and anticancer efficacy of novel cobalt oxide nanoparticles conjugated with thiosemicarbazide, *Biotech* 10 (2020) 230.
- [8] H. Kargar, M.F. Mehrjardi, et al., Synthesis, spectral characterization, crystal structures, biological activities, theoretical calculations and substitution effect of salicylidine ligand on the nature of mono and dinuclear Zn (II) Schiff base complexes, *Polyhedron* 213 (2022), 115636.
- [9] H. Kargar, M.F. Mehrjardi, et al., Binuclear Zn(II) Schiff base complexes: Synthesis, spectral characterization, theoretical studies and antimicrobial investigations, *Inorg. Chim. Acta* 530 (2022), 120677.
- [10] H. Kargar, M.F. Mehrjardi, et al., Zn(II) complexes containing O, N, N,O-donor Schiff base ligands: synthesis, crystal structures, spectral investigations, biological activities, theoretical calculations and substitution effect on structures, *J. Coord. Chem.* 74 (2021) 2720-2740.
- [11] H. Kargar, R.B. Ardakani, V. Torabi, M. Kashani, Z.C. Natanzi, Z. Kazemi, V. Mirkkhani, A. Sahraei, M.N. Tahir, M. Ashfaq, K.S. Munawar, Synthesis, characterization, crystal structures, DFT, TD-DFT, molecular docking and DNA binding studies of novel Copper(II) and Zinc(II) complexes bearing halogenated bidentate N, O-donor Schiff base ligands, *Polyhedron* 195 (2021), 114988.
- [12] S.S. Saleem, M. Sankarganesh, P.A. Jose, J.D. Raja, Design, synthesis, antioxidant, antimicrobial, DNA binding and molecular docking studies of Morpholine based Schiff base ligand and its metal(II) complexes, *Inorg. Chem. Comm.*, 124 (2021) 108306.
- [13] L.V. Kumar, S. Sunitha, G. Rathikanath, Antioxidant, antidiabetic and anticancer studies of nickel complex of Vanillin-4-Methyl-4-Phenyl-3-Thiosemicarbazone, *Mat. Today: Proc.* 41 (2021) 669-675.
- [14] S. Savir, J.W. Kent liew, I. Vythilingam, Y.A.L. Lim, C.H. Tan, K.S. Sim, V.S. Lee, M. J. Maah, K.W. Tan, Nickel(II) Complexes with Polyhydroxybenzaldehyde and O,N, S tridentate Thiosemicarbazone Ligands: Synthesis, Cytotoxicity, Antimalarial activity, and Molecular Docking Studies, *J. Mol. Struct.*, 1242 (2021) 130815.
- [15] P. Jyothi, K. Suneetha, V. Sumalatha, B. Ushaiah, C. GyanaKumari, Synthesis, characterization, cytotoxicity, DNA binding and antimicrobial studies of binary and ternary metal complexes of Co (II), *Inorg. Chem. Comm.* 110 (2019), 107590.
- [16] P. Jyothi, C. Gyana Kumari, Synthesis, Characterization And Biological Evaluation Of Schiff Base Of 5-Chloro Salicylaldehyde Hydrazine N-Methyl CarboThioamide And Its Metal Complexes: Cytotoxicity, DNA Interaction & Incision, Antifungal And Antifungal Studies, *Euro. J. Mo.r & Clin. Medicine*, 7(2020) 4339-4355.
- [17] H. Kargar, R.B. Ardakani, et al., Synthesis, characterization, crystal structures, DFT, TD-DFT, molecular docking and DNA binding studies of novel copper(II) and zinc (II) complexes bearing halogenated bidentate N, O-donor Schiff base ligands, *Polyhedron* 195 (2021), 114988.
- [18] H. Kargar, R.B. Ardakani, et al., Novel copper(II) and zinc(II) complexes of halogenated bidentate N, O-donor Schiff base ligands: Synthesis, characterization, crystal structures, DNA binding, molecular docking, DFT and TD-DFT computational studies, *Inorg. Chim. Acta* 514 (2021), 120004.
- [19] A. Jamshid, M. Sahihi, et al., Studies on DNA binding properties of new Schiff base ligands using spectroscopic, electrochemical and computational methods: Influence of substitutions on DNA-binding, *J. Mol. Liq.* 253 (2018) 61-71.
- [20] K. Venkateshwarlu, D. Sreenu, G. Ramesh, P.V.A. Lakshmi, Shivraj, Investigation of DNA binding, and Bio activities of Furan cored Schiff base Cu(II), Ni(II), Co(III) complexes: Synthesis, Characterization and spectroscopic properties, *Appl. Org. Met. Chem.* 35 (2021) e6326.
- [21] A. Rambabu, D. Sreenu, D. Shivashanker, Shivraj, DNA Binding, -Cleavage, and Antimicrobial investigation on mononuclear Cu (II) Schiff base complexes originated from Riluzole, *J. Mol. Struct.* 1244 (2021), 131002.
- [22] G. Ramesh, S. Daravath, N. Ganji, A. Rambabu, Venkateshwarlu, Shivraj, Facile synthesis, structural characterization, DNA Binding, Incision evaluation, antioxidant and antimicrobial activity studies of Co(II), Ni(II), Cu(II) complexes of 3-amino-5-(4- fluorophenyl) isoxazole derivatives, *J. Mol. Struct.* 1202 (2020), 127338.
- [23] A. Rambabu, M.P. Kumar, N. Ganji, S. Daravath, Shivraj, DNA binding and cleavage, cytotoxicity and antimicrobial studies of Co(II), Ni(II), Cu(II) and Zn(II) complexes of 1-((E)-4-(trifluoromethoxy) phenyl imino) methyl) naphthalene 2-ol Schiff base, *J. Bimol. Struct. and Dyn.* 38 (2020) 307-316.
- [24] Q.T. Nguyen, P.N. Pham Thi, V.T. Nguyen, P. Bednarski, Synthesis, Characterization, and Invitro-Cytotoxicity of unsymmetrical tetra dentate Schiff base Cu(II) and Fe(III) complexes, *Bio inorg. Chem. and appli.* 2021 (2021) 1-10.
- [25] A.A. Ardakani, H. Kargar, N. Feizi, M.N. Tahir, Synthesis, characterization, crystal structures and antibacterial activities of some Schiff bases with N₂O₂ donor sets, *J. Iran. Chem. Soci.*, 15 (2018)1495-1504.
- [26] H. Kargar, F. Aghaei-Meybodi, R. Behjatmanesh-Ardakani, M.R. Elahifard, V. Torabi, M. Fallah-Mehrjardi, M.N. Tahir, M. Ashfaq, K.S. Munawar, Synthesis, crystal structure, theoretical calculation, spectroscopic and antibacterial activity studies of copper(II) complexes bearing bidentate schiff base ligands derived from 4-aminoantipyrine: Influence of substitutions on antibacterial activity, *J. Mol. Struct.* 1230 (2021) 129908.
- [27] H. Kargar, F.A. Meybodi, M.R. Elahifard, M.N. Tahir, M. Ashfaq, K.S. Munawar, Some new Cu(II) complexes containing O, N-donor Schiff base ligands derived from 4-aminoantipyrine: synthesis, characterization, crystal structure and substitution effect on antimicrobial activity, *J. Coord. Chem.* 74 (9-10) (2021) 1534-1549.
- [28] V. Sumalatha, S. Daravath, A. Rambabau, G. Ramesh, Shivraj, Antioxidant, antimicrobial, DNA binding, and cleavage studies of novel Co(II), Ni(II), and Cu(II) complexes of N, O donor Schiff bases: Synthesis, and spectral characterization, *J. Mol. Struct.* 1229 (2021), 129606.
- [29] E. Yousef, A. Majeed, K.A. Sammarae, N. Salih, J. Salimon, B. Abdullah, Metal complexes of Schiff bases: Preparation characterization and antibacterial activity, *Arab. J. Chem.*, 10 (2017) S1639-S1644.
- [30] J. Devi, J. Yadav, K. Lal, N. Kumar, A.K. Paul, D. Kumar, P.P. Dutta, D.K. Jindal, Design, synthesis, crystal structure, molecular docking studies of some diorganotin (IV) complexes derived from the pyperonylic hydrazide Schiff base ligands as cytotoxic agents, *J. Mol. Struct.*, 1232 (2021) 129992.
- [31] N. Vamsikrishna, S. Daravath, N. Ganji, N. Pasha, Shivraj, Synthesis, structural characterization, DNA interaction, and antibacterial and cytotoxicity studies of bivalent transition metal complexes of 6-amino benzothiazole Schiff base, *Inorg. Chem. Commun.* 113 (2020), 107767.
- [32] S. Gurusamy, K. Krishnaveni, M. Sankarganesh, R.N. Asha, A. Mathavan, Synthesis, characterization, DNA interaction, BSA/HSA binding activities of VO(IV), Cu (II) and Zn (II) Schiff base complexes and its molecular docking with biomolecules, *J. Mol. liq* 345 (2021), 117045.
- [33] G. Ramesh, S. Daravath, M. Swathi, V. Sumalatha, D.S. Sankar, Shivraj, Investigation on Co (II), Ni (II), Cu (II) and Zn(II) complexes of derived from quadridentate salen type Schiff base: structural characterization, DNA interactions, antioxidant proficiency, and biological evaluation, *Chem. Data Collec.* 28 (2020), 100434.
- [34] A. Das, D.K. Mishra, P. Gurung, V.K. Dakua, B. Sinha, DNA binding and DNA cleavage activities of newly synthesized Co(II), Cu (II) complexes of a β -Cyclodextrin based azo functionalized Schiff base, *Aust. J. Chem.* 74 (5) (2021) 341-350.
- [35] T. Chadrasekar, A. Aruna devi, N. Raman, Synthesis, spectral characterization, DNA binding and antimicrobial profile of biological active mixed ligand Schiff base metal (II) complexes incorporating 1,8- diamionaphthalene, *J. Coord. Chem.* 74 (2021) 804-822.
- [36] V. Sumalatha, A. Rambabu, N. Vamsikrishna, N. Ganji, S. Daravath, Shivraj, Synthesis, characterization, DNA binding propensity, nuclease efficacy, antioxidant and antimicrobial activities of Cu (II), Co (II) and Ni(II) complexes derived from 4-(trifluoro methoxy) aniline Schiff base, *Chem. Data Collec.* 20 (2019), 100213.

PRINCIPAL
JMJC COLLEGE FOR WOMEN (Autonomous)
TENALI





International Journal of Advanced Academic Studies

E-ISSN: 2706-8927
P-ISSN: 2706-8919
www.allstudyjournal.com
IJAAS 2022; 4(4): 80-84
Received: 11-08-2022
Accepted: 16-09-2022

P Hema Latha
Research Scholar, Department
of Sociology and Social Work,
Acharya Nagarjuna,
University, Guntur, Andhra
Pradesh, India

Dr. V Venkateswarlu
Professor, Department of
Sociology and Social Work,
Acharya Nagarjuna
University, Guntur, Andhra
Pradesh, India

An exploratory study on free and paid senior citizen homes in Andhra Pradesh

P Hema Latha and Dr. V Venkateswarlu

Abstract

The major objective of this paper was to know the reasons of elderly to stay in senior citizen homes both paid and free homes. And to identify their preference stay and aspirations etc. The study was conducted in six senior citizen homes which were located in different areas of Guntur District. In these six, three were paid homes and another three were free homes. The data was collected through case study and interview methods. The findings reveal that differences and adjustment problem with Daughter-in-law/son, Negligence of family members and poverty, insufficient housing and economic hardships were some of the reasons for joining in the homes as expressed by the elderly. Financial autonomy and living with children were the major aspiration of elderly living in paid homes and free homes along with other aspirations.

Keywords: Elderly, living arrangement, free homes, paid homes

Introductions

Ageing is one of the emerging problems of the world and it is applicable to India also. In the present era, rapid change is observed everywhere. The biggest challenge of any nation is to provide essential support services for the growing graying population. With the advancement in medical technology and improved standard of living automatically the lifespan of individuals is increased. The trend is bound to increase further in the future years. As per World Population Prospects: the 2019 Revision report the number of persons aged 80 years or above is projected three times, from 143 million in 2019 to 426 million in 2050. According to United Nations projections, by the year 2020, the number of older persons is expected to increase more than threefold, from 600 million to almost 2 billion.

During the last two decades both the developed and developing countries are facing the challenges in preparing policies due to the phenomena of population ageing. Even though the challenge is same, its implications vary in developed, developing and under developed countries. In the traditional Indian society the old age was not at all a problem. Younger ones used to give more respect to the elderly. Elderly were the chief patrons of the family. The stable joint family system provides security and care and use to protect the elderly from all angles. This family structure has been the socioeconomic backbone of the average Indian (Shah, 1998) [14]. In India a large percentage of the aged are poor and destitute and bereft of even the basic necessities of life, namely food, shelter, clothing. Due to limited resources, the government is also unable to fulfill the basic needs of the aged population. How the social systems respond to the consequences of ageing and face the challenges is crucial for any nation in creating ageing friendly society. It is very important to understand how these changes happen and how they mix up with traditional and cultural issues to face the challenges of elderly.

Living arrangements is one of the component which influences overall wellbeing of the elderly. When there is no well-developed system in the country to provide needy social services to the elderly they must opt whatever is available for them in their close proximity, for social, Physical and psychological support including economic (Domingo and Caster line, 1992) [2]. Policy makers and government officials along with NGOs should take initiative to support and care of elderly. The government should give financial security to the vulnerable sections of elderly population in possible ways like health care, transport, recreation, etc.

Ageing is a serious reality and last step of life cycle which cannot be avoided by none. Most of the elderly prefer to live with their children. Usually elderly men who have their wives

Corresponding Author:
Dr. V Venkateswarlu
Professor, Department of
Sociology and Social Work,
Acharya Nagarjuna
University, Guntur, Andhra
Pradesh, India



will depend on them but older women likely to rely on children and others. Many elderly suffer due to inadequate income to meet their basic needs. Nowadays, Nuclear families are seen more in urban areas than in rural areas thereby affecting the care of elderly. Dual career of women, increased self-centeredness, contemporary changes in the family system are forcing elderly to live alone or to join in old age homes. The long term caring of the aged in terms of community based services is a matter of great concern. Health and wellbeing of elderly are affected by many inter woven aspects like physical, emotional and social environment.

Review of Literature

Previous research results of studies conducted with institutionalized elderly are presented in brief. Minal P and Kamala R (1995) [9] conducted a study and found that the institutionalized elderly are having poor adjustments than the elderly living in the families. Kanwar P and Chadha N.K (1998) [6] assessed the psycho-social determinants of 60 institutionalized and 60 non institutionalized elderly. The results revealed that institutionalized elderly are more depressed and lonely. More or less same results were observed in Agarwal S and Srivastava S. K (2002) [5] where they found that elderly living in institutions are more depressed and suffer due to anxiety: Naik A (2007) [10] study also supports this. Mathew M A. *et al.*, (2009) [7] did a comparative study on stress, coping strategies and quality of life of institutionalized and non-institutionalized elderly in Kottayam district, Kerala, India with a sample of 150 (75+75) and found that there is significant difference between these two groups which was consistent with the previous studies stating that institutionalized are more depressed. Kavitha A. K. (2007) [15]’s results also reports that elderly living in senior citizen homes showed less mean scores regarding quality of life. Neelam, wason and Karuna Jain (2011) [13] studied Nutritional Status, dietary adequacy and health problems of 56 institutionalized elderly in Jodhpur (31 males and 25 females). Questionnaire, interview, anthropometry, dietary surveys were used to collect the data. Results revealed that elderly living in care homes had better nutritional status and care. All the personal needs and health care are being met by the homes and the nutritional condition of the elderly seems to be satisfactory. Mehta (1999) [8] found low protein,

low calories, and low nutrient intake in institutionalized elderly as compared to elderly living in families. Saletti *et al.*, (2000) [12], Hewitt *et al.*, (2006) [5] reported that nearly one fourth of the elderly are either malnourished or overweight in free old age homes.

Objectives of the Study

- The main objectives of the present study are:
- To know the socio-demographic profile of the elderly living in senior citizen homes.
 - To find out the reasons of elderly for staying in free and paid senior citizen homes.
 - To explore the aspirations of elderly living in free and paid senior citizen homes

Methodology

For the present study, Six senior citizen homes were selected which were located in different areas of Guntur District. In these six, three were paid homes and another three were free homes. Convenience sampling method was adopted and the data was collected by making use of both qualitative and quantitative techniques i.e., case study method and interviews.

Results and Discussion

Socio- Demographic profiles of the elderly

Table 1: Distribution of the sample respondents by Age

Age	Paid Homes		Free Homes		Total	
	N	%	N	%	N	%
60-69	19	48.72	21	67.74	40	57.14
70-79	15	38.46	07	22.58	22	31.42
80+	05	12.82	03	09.68	08	11.42
Total	39	100.00	31	100.00	70	100.00

The above table shows that majority (57.14%) of the respondents are in 60-69 age group, followed by 31.42% in 70-79 age group and very few were (11.42%) in 80+ age group. In the paid homes and free homes also the same trend was noticed where in paid homes 48.72% belongs to 60-69 age group, 38.46% in 70-79 age group followed by 12.82% in 80+ group. In free homes majority (67.74%) were in 60-69 age group, 22.58% in 70-79 age group followed by 9.68% in 80+ group.

Table 2: Distribution of the sample respondents by Sex

Sex	Paid Homes		Free Homes		Total	
	N	%	N	%	N	%
Male	18	46.15	12	38.71	30	42.86
Female	21	53.85	19	61.29	40	57.14
Total	39	100.00	31	100.00	70	100.00

The above table shows that majority (57.14%) of the respondents were females and males were only 42.86%. In both the categories of elderly living in paid homes and free homes, female crossed the number of males such as 53.85%

and 61.29% respectively and the correspondent males were 46.15% and 38.71% in paid and free home category respectively.

Table 3: Distribution of the sample respondents by religion

Religion	Paid Homes		Free Homes		Total	
	N	%	N	%	N	%
Hindu	23	58.98	12	38.70	35	50.00
Christian	11	28.20	13	41.94	24	34.28
Muslim	05	12.82	06	19.36	11	15.72
Total	39	100.00	31	100.00	70	100.00



From the above table it was observed that majority (50.00%) of the respondents were Hindus followed by Christians 34.28% and Muslim 15.72%. Same trend was seen in the Elderly living in Paid homes where 58.98%

belong to Hindu Religion followed by 28.20% in Christian Religion and 12.82% in Muslim Religion. But in the Free Homes category Christians were higher (41.94%) followed by Hindus 38.70% and Muslims 12.82%.

Table 4: Distribution of the sample respondents by caste

Caste	Paid Homes		Free Homes		Total	
	N	%	N	%	N	%
Non Schedule Caste	30	76.92	20	64.52	50	71.43
Schedule Caste	09	23.08	11	35.48	20	28.57
Total	39	100.00	31	100.00	70	100.00

The above table determines that majority (71.43%) of the respondents belong to Non Schedule Caste and 28.57% of the respondents belong to Schedule caste category. In paid homes 76.92% of the respondents belong to non-schedule caste and 23.08% belong to schedule caste. In free home

category 64.52% belong to Non schedule caste community and 35.48% belong to schedule caste category. On the whole nonscheduled caste elderly were more than schedule caste elderly.

Table 5: Distribution of the sample respondents by background area of living

Background Area of Living	Paid Homes		Free Homes		Total	
	N	%	N	%	N	%
Rural	16	41.02	18	58.06	34	48.57
Urban	23	58.97	13	41.94	36	51.43
Total	39	100.00	31	100.00	70	100.00

From the above table it was observed that majority (51.43%) of the respondents belong to urban area and (48.57%) belong to rural area. In paid home category urban background elderly were more (58.97%) than rural

background (41.02%). In free homes this is in reverse where rural background elderly (58.06%) were more than urban background elderly (41.94%).

Table 6: Distribution of the sample respondents by educational qualification

Educational Qualification	Paid Homes		Free Homes		Total	
	N	%	N	%	N	%
Illiterate	09	23.07	22	70.96	31	44.28
Primary	17	43.60	09	29.03	26	37.14
High School	05	12.82	00	0.00	05	7.14
Intermediate	08	20.51	00	0.00	08	11.42
Graduate & above	00	0.00	00	0.00	00	0.00
Total	39	100.00	31	100.00	70	100.00

The above table depicts the educational qualification of the respondents. 44.28% were illiterates, 37.14% of elderly completed their Primary school 11.42% intermediate

followed by 7.14% high school. None of the respondents have educational qualification of graduation and above.

Table 7: Distribution of the sample respondents by marital status

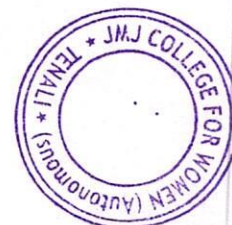
Marital Status	Paid Homes		Free Homes		Total	
	N	%	N	%	N	%
Unmarried	02	05.13	04	12.90	06	8.57
Married & living with spouse	19	48.72	12	38.71	31	44.29
Widow/Widower	18	46.15	15	48.39	33	47.14
Total	39	100.00	31	100.00	70	100.00

The above table depicts that majority (47.14%) of the respondents were widow/widowers. 44.29% of the respondents were married and living with spouse. Only 8.57% of the respondents were unmarried. In paid home category 48.72% of the respondents were married and living

with spouse, 46.15% of the respondents were widow/widower and only 5.13% were unmarried. In free home category majority (48.39%) of the respondents were widow/widowers. 38.71% of the respondents were married and living with spouse and 12.90% were unmarried.

Table 8: Distribution of the sample respondents by No. of married children

No. of married children	Paid Homes		Free Homes		Total	
	N	%	N	%	N	%
None	2	5.12	4	12.90	6	8.57
One	6	15.38	2	6.45	8	11.42
Two	16	41.02	6	19.35	22	31.42



Three	11	28.20	8	25.80	19	27.14
More than Three	4	10.25	11	35.48	15	21.42
Total	39	100.00	31	100.00	70	100.00

The above table clearly indicates that majority (31.42%) of the respondents have two married children, 27.14% of the respondents have three married children, 21.42% of the respondents have more than three married children, 11.42% of the respondents have one married child and only 8.57% of the respondents have no married children. In the paid home category, 41.02% of the respondents have two married children and in free homes 19.35% of the respondents have two married children, 28.20% of the respondents have three married children and in free homes

35.48% of the respondents have more than three married children, 15.38% of the respondents have one married child and in free homes only 6.45% of the respondents have one married child, 10.25% of the respondents have more than three married children and in free homes 35.48% of the respondents have more than three married children, and in paid category only 5.12% of the respondents have no married children, in free homes 12.90% of the respondents do not have married children.

Table 9: Distribution of the elderly by reasons for joining in paid homes

S. No	Reason (Paid Homes)	No.	%
1.	Daughter-in-law problem	18	46.15
2.	Misbehavior of son	07	17.94
3.	Adjustment problem	02	5.12
4.	Disrespect and neglect by the family members	04	10.25
5.	Unwillingness expressed to take care	03	7.69
6.	Free and independent life	01	2.56
7.	Settlement of children at abroad	04	10.25

The above table reveals that the majority (46.15%) of the elderly respondents stated that Daughter-in-law problem was the reason for joining in paid homes and 17.94% of the elderly respondents stated that misbehavior of son was the reason for joining in paid home. 10.25% of the respondents stated that disrespect and neglect by the family members was the reason for joining in paid home and 7.69% of the respondents stated that unwillingness expressed to take care

was the reason for joining in paid home. 10.25% of the respondents stated that settlement of children at abroad was the reason for joining in paid home and 5.12% of the respondents stated that adjustment problem was the reason for joining in paid home only 2.56% of the respondents stated that free and independent life was the reason for joining in paid home.

Table 10: Distribution of the elderly by reasons for joining in free homes

S. No	Reason (Free homes)	No.	%
1.	Shortage of accommodation	02	6.45
2.	In-law problems	03	9.67
3.	Negligence of son/daughter-in-law	17	54.83
4.	Unwillingness expressed to take care	03	7.69
5.	Afraid of children	01	3.22
6.	Abuse by care givers	01	3.22
7.	Poverty	04	12.90

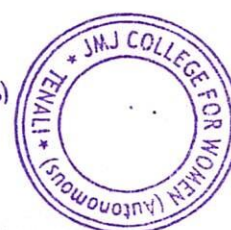
The above table determines that majority (54.83%) of the respondents stated that negligence of son/daughter-in-law was the reason for joining in free home, 12.90% of the respondents stated that poverty was the reason for joining in free homes, 9.67% of the respondents stated that in-law problems was the reason for joining in free homes and 7.69% of the respondents stated that unwillingness


expressed to take care was the reason for joining in free homes. 3.22% of the respondents stated that afraid of children was the reason for joining in free homes, 6.45% of the respondents stated that shortage of accommodation was the reason for joining in free homes and only 3.22% of the respondents stated that abuse by care givers was the reason for joining in free homes.

Table 11: Distribution of the sample respondents by aspirations

Aspirations	Paid Homes (39)				Free Homes (31)				Total (70)			
	Yes	%	No	%	Yes	%	No	%	Yes	%	No	%
Want to be with children	31	79.48	8	20.51	29	93.54	2	6.45	60	85.71	10	14.71
Attending gatherings	20	51.28	19	48.71	16	51.61	15	48.38	36	51.42	34	48.57
To spend time with relatives	25	64.10	14	35.89	18	58.06	13	41.93	43	61.42	27	38.57
Spend time with grand children	30	76.92	9	23.07	25	80.64	6	19.35	55	78.57	15	21.42
Financial Autonomy	32	82.05	7	17.94	26	83.87	5	16.12	58	82.85	12	17.14
Free transport	20	51.28	19	48.71	31	100	0	00	51	72.85	19	27.14
Free Medical Aid	39	100	0	00	31	100	0	00	70	100	00	00
Enough food	35	89.74	4	10.25	26	83.87	5	16.12	61	87.14	09	12.85
Soft corner from the staff	30	76.92	9	23.07	27	87.09	4	12.90	57	81.42	13	17.57

Principal
JMJC COLLEGE FOR WOMEN (Autonomous)
TENALI



 You are accessing a free view of the Web of Science [Learn More](#)

Results for The element of ... > THE ELEMENT OF EMOTIONAL INTELLIGENCE AND THEIR IMPACT ON SOCIA...

THE ELEMENT OF EMOTIONAL INTELLIGENCE AND THEIR IMPACT ON SOCIAL RELATION

By: Hemalatha, P. (Hemalatha, P.) ; Chandra, K. Ram (Chandra, K. Ram) ; Azim, Shakila (Azim, Shakila) ; Annapurna, B. (Annapurna, B.) ; Nagalakshmi, V. (Nagalakshmi, V.) ; Kalyani, M. Esther (Kalyani, M. Esther)
INTERNATIONAL JOURNAL OF EARLY CHILDHOOD SPECIAL EDUCATION

Volume: 14 Issue: 3 Page: 4303-4309

DOI: 10.9756/INT-JECSE/V14I3.555

Published: 2022

Indexed: 2022-06-05

Document Type: Article

Abstract

Particularly the most basic and significant aspect of human experience is our capacity to experience emotions. Humans can feel a myriad of emotions can be joy, pleasure anger, stress. Defining emotion is a complicating task but the concept somewhere lies between the field of psychology, philosophy, and neuroscience. In this paper, we are discussing emotions from the perspective of psychology. Emotions and intelligence have different meanings and roles from the viewpoint of psychology but after combining both words, EI can be referred to as an ability that provides an advantage in the world to deal with many negative emotions and in spread harmony. Emotional intelligence has drawn the attention of many researchers in every field. The Emotional intelligence first article was published by Salovey& Mayer in 1990 after that so much work has been done in the academic area of professional relations, instruments, or Scales for EI. So, the researcher decided to study factors of emotional intelligence and its role in social relationships. [1] [2]

Keywords

Author Keywords: Social relation; Emotional intelligence

Addresses:

- 1 JMJ Coll Women, Dept Home Sci, Tenali, Andhra Pradesh, India
- 2 VR Siddhartha Engrn Coll, Dept English, Vijayawada, Andhra Pradesh, India
- 3 MDDM Coll, Dept Psychol, Muzaffarpur, Bihar, India
- 4 Aditya Coll Engrn Surampalem, Dept CSE, Surampalem, Andhra Pradesh, India
- 5 Ch SD St Therasas Coll Women, Dept Chem, Eluru, Andhra Pradesh, India

...more addresses

Categories/Classification

Research Areas: Education & Educational Research

[+ See more data fields](#)

Citation Network

In Web of Science Core Collection

0 Citations

15 Cited References

Use in Web of Science

Web of Science Usage Count

0 Last 180 Days

0 Since 2013

This record is from:

Web of Science Core Collection

- o Emerging Sources Citation Index (ESCI)

Suggest a correction

If you would like to improve the quality of the data in this record, please Suggest a correction



© 2022
Clarivate
Training
Portal
Product
Support

Data
Correction
Privacy
Statement
Newsletter

Copyright
Notice
Cookie
Policy
Terms of
Use

Manage
cookie
preferences

Follow
Us



[Handwritten Signature]
PRINCIPAL
JMJC COLLEGE FOR WOMEN (Autonomous)
TENALI





ISSN Print: 2394-7500
ISSN Online: 2394-5869
Impact Factor: 8.4
IJAR 2022; 8(11): 13-15
www.allresearchjournal.com
Received: 09-09-2022
Accepted: 15-10-2022

P Hema Latha
Research Scholar, Department
of Sociology and Social Work,
Acharya Nagarjuna
University, Guntur,
Andhra Pradesh, India

V Venkateswarlu
Professor, Department of
Sociology and Social Work,
Acharya Nagarjuna
University, Guntur,
Andhra Pradesh, India

An empirical study on elderly abuse & neglect: Issues and coping strategies

P Hema Latha and V Venkateswarlu

Abstract

World elderly population is growing both in developing and developed countries. India is also facing the same situation. Changing family structures from joint to nuclear, urbanization, women employment and various other factors are making the lives of elderly more measurable. In the present scenario there is no guarantee that children will definitely take care of their parents. The longevity increases dependency. Hence this is an attempt to identify the prevalence, types of abuse and coping strategies in an urban area of Guntur. Self structured questionnaire was administered to 35 male and 45 female elderly. The results revealed that emotional abuse is more prevalent than other forms of abuse and majority of elderly were using tolerance as a coping strategy.

Keywords: Elder abuse, coping strategies, ageing, prevention

Introduction

Aging is a complex, natural, inevitable, multi factorial phenomena which occurs in biological species. The concept of ageing is multi-disciplinary and multi-faceted. It can be viewed from biological, physiological, sociological, demographic and psychological point. Biological research focuses on the reduction of capacities, psychological concentrates on emotional, attitudinal and behavioural characteristics. Sociologists study the gradual unfolding of socialization with regard to change in position, status and role. Over a period of hundred years the annual growth rates of the elderly are alarming, including gender imbalance. Over the decades significant gain in longevity by the elderly is noted (Malaker and Guharoy, 1990) [6]. This is true for both males and females but with a difference.

India is a country where the people of diversifying cultures live together. Being a developing country, it suffers from many financial constraints. The review of Indian researchers focused largely on few areas and moderately on some areas. The areas where the work is to be accentuated are conflict resolutions, frustrations, service needs of disabled, elderly friendly environments, elder abuse and its prevention etc. The present paper focuses on prevalence of elder abuse, various forms of it, how to prevent abuse and create a safe, healthy atmosphere for the elderly.

In the traditional society elderly were treated as repositories of wisdom and experience. They played active role in family decision making and participated in economic and political activities with legitimate authority. When the traditional society is adopting modernism several changes are seen in almost all spheres of society. The changes in social roles of elderly automatically leading to change in the self-image of elderly. The elderly who were treated reverentially in traditional societies and enjoyed a golden era are now much worse off in present society. They are being neglected by their family members, kin and kith and derogated by grandchildren.

Elderly were accorded prestige through four components advisory, contributory, control and residual. They use to give advises with their vast experience of the life. They used to participate actively in familial, economic and cultural activities. They have the sole control of authority over the members, possessed property in their name; distribute it as per their will and wish. The residual component depends on their previous position in the community. Elder abuse is now understood globally as a social and public health problem threatening Elderly (Lachs & Pillemer, 2004) [8]. It is very serious challenge and concern to the younger sections on those elderly depends for support and sustenance.

Corresponding Author:
V Venkateswarlu
Professor, Department of
Sociology and Social Work,
Acharya Nagarjuna
University, Guntur,
Andhra Pradesh, India



It is true in case of institutional setting along with the domestic scenario. Abuse means the wilful infliction of injury, negligent, unreasonable confinement or cruel punishment resulting in physical or emotional pain to the individual mostly by the care givers. The problem of elder abuse is more pervasive than recognised. Many older adults experience their pathetic situation as a way of life. Rise of dual-career families, more empty-nest years due to increased life expectancy, dependency are making the elderly more susceptible to abusive treatment than before (Jamuna, 2003) [5]. In India aged are accepted happily only in the politics

where a positive state of self-acceptance can result in happiness and life satisfaction. Rise of dual-career.

Types of Abuse

1. **Covert Abuse:** Which are hidden and not direct, mostly they may be non-verbal also.
2. **Overt Abuse:** Are obvious and direct. They may be physical, non-cooperation deprivation of needs.

These can be otherwise classified as:

Table 1: Types of Abuse

S. No	Type of Abuse	Examples	Signs and Symptoms
1.	Physical	Pushing, Hitting, punching, slapping, burning, restraining or giving over medication or wrong medication.	Injuries on two sides of the body, sprains or dislocations unexplained bruises, bone fractures, bite marks, broken eyeglasses, signs of restrained like rope marks.
2.	Emotional	Ignoring or humiliation a person, shouting, swearing, blaming, frightening, threatening and isolation	Agitated, being upset, apathy, withdrawal, depression and non-communication.
3.	Financial	Deprivation of money Illegal or unauthorized use of a person's property, money, pension book or other valuables, changing the person's will, fraudulently obtaining power of attorney, or other property or by eviction from own home.	Large cash withdrawal from the elder's bank account, objects or other money missing from the senior's house hold, abrupt change in will, unpaid bills, forged signatures, elder's sudden reluctance to discuss financial matters, increasing tiredness or depression on the part of the elder.
4.	Elder neglect	Inadequate provision of food or water, inappropriate housing or shelter, clothing, dental of medical care, abandonment, physical restraint and inadequate help with hygiene or bathing	Unhygienic Conditions, unusual weight loss, malnutrition, not meeting minimum basic needs Starving, untreated illness, such as bedsores, unsanitary and unclean living conditions,

Methodology

80 elderly (35 Male & 45 Female) living in Guntur Urban area are selected as sample for the present study by purposive sampling method. The investigator prepared a self-structured questionnaire with Yes/No type questions along with general information to find out the prevalence and types of abuse and neglect in elderly. The results were discussed with percentages.

The above table reveals that 51.43% of males and 57.78% of females are experiencing abuse and neglect in one or the other way. 48.57% of Males and 42.22% of females expressed that they are not experiencing any abuse and neglect in the family.

Results and Discussion

Table 2: Sample particulars of elderly by Gender and Income level

Gender	Income Level							
	Low Income		Middle Income		High Income		Total	
	N	%	N	%	N	%	N	%
Male	14	43.75	10	43.47	11	44.00	35	43.75
Female	18	56.25	13	56.53	14	56.00	45	56.25
Total	32	100.00	23	100.00	25	100.00	80	100.00

Source: Primary Data

The above table shows that out of 80 elderly 43.75% were males and 56.25% were females. The income level of the elderly for categorized into low, middle- and high-income groups. It shows that 43.75% of males are in low income level, 43.47% belongs to middle income level and 44.00% high income levels. Among the females 56.25% are in low income level, 56.53% are in middle income and 56.00% are in high income levels.

Table 3: Prevalence of Abuse and Neglect

Gender	Abuse and Neglect				Total	
	YES		NO		N	%
	N	%	N	%		
Male	18	51.43	17	48.57	35	43.75
Female	26	57.78	19	42.22	45	56.25
Total	44	55.00	36	45.00	80	100.00

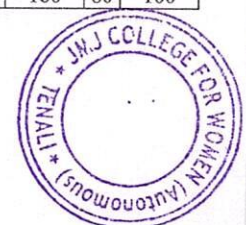
Table 4: Forms of Abuse/Neglect Experiencing by the Elderly

Forms of Abuse/Neglect	Forms of abuse					
	Male		Female		Total	
	N	%	N	%	N	%
Physical	5	41.67	7	58.33	12	15.00
Emotional	11	44.00	14	56.00	25	31.30
Verbal	5	35.72	9	64.28	14	17.5
Social	3	62.50	5	37.50	8	10.00
Financial	11	47.62	10	52.38	21	26.30
Total	35	43.75	45	56.25	80	100.00

The above table denotes that 41.67% of males and 58.33% of females were experiencing physical abuse, 44.00% males and 56.00% of females are undergoing emotional abuse, 35.72% of males and 64.28% of females are abused verbally, 62.50% of males and 37.50% of females are facing social avoidance followed by 47.62% of males and 50.38% of females are neglected by not meeting their financial needs.

Table 5: Perpetrators of Abuse and Neglect of elderly

Relationship of Perpetrator	Gender					
	Male		Female		Total	
	N	%	N	%	N	%
Spouse	06	17.14	03	6.70	09	11.25
Son	14	40.00	09	20.00	23	28.75
Daughter in Law	05	14.30	15	33.33	20	25.00
Daughter	02	5.71	06	13.33	08	10.00
Son in Law	01	2.85	02	4.44	03	3.75
Grand Children	05	14.30	07	15.55	12	15.00
Others	02	5.71	03	6.70	05	6.25
Total	35	100	45	100	80	100



The above table depicts that 87.14% of the elderly respondents felt that they need enough food to eat, 85.71% desired to live with their children, 82.85% are in need of financial autonomy to fulfil their needs without depending on others, 81.42% expressed that they feel happy if the staff who are working in the senior citizen homes behaves softly with them, 78.57% are fond of their grandchildren and want to spend some time with them, 72.85% expressed that government should give them free transport to go wherever they want to meet people, 61.42% desire to spend time with their relatives 51.42% like to attend gatherings like previous life but 100% of the elderly expressed that the government should provide free medical aid for all the elderly irrespective of age groups and living arrangement.

Irrespective of the type of home whether paid or free majority of the elderly expressed that they want to be with children (79.48% paid homes) (93.54% free homes). There is no much difference in paid and free homes regarding the desire to attend gatherings (51.28% and 51.61%), majority are in need of financial autonomy (82.05% paid homes and 83.87% free homes), regarding spending time with grandchildren (76.92% & 80.64%), enough food (89.74% & 83.87%) there is no much difference between categories of homes. 51.28% of elderly living in paid homes felt that it would be better if elderly are given free transport facility where as 100% of the elderly living in free homes desired the same. Unanimously all the elderly expressed that they need free medical aid irrespective of type of home. 76.92% of the elderly living in paid homes and 87.09% of the elderly living in free homes expressed that the behaviour of the staff should not be harsh towards them which is hurting them and causing panic towards their status.

Conclusion

The findings of the present study states that majority of the elderly living in senior citizen homes were from urban background. But in elderly living in free homes the situation is just opposite. Majority were from rural area. Gender wise females crossed the males on the whole as well as in paid homes and free homes. Differences and adjustment problem with Daughter-in-law/son, Negligence of family members and poverty, insufficient housing and economic hardships were some of the reasons for joining in the homes as expressed by the elderly. Loneliness is another reason of joining the homes and is supported by Dubey *et al.*, (2011)^[3] and Gupta *et al.*, (2014)^[4]. Adjustment problem with daughter-in-law/son was expressed by the elderly as the major reason to join in the homes. This is inconsistent with the results of Siddhu (2010)^[16]. The elderly who are residing in paid homes state that they joined in the home to lead a peaceful life with freedom and without interference of others. Panigrahi *et al.*, (2012)^[11] also revealed the same. 100% of the elderly expressed that the government should provide free medical aid for all the elderly irrespective of age groups and living arrangement. In spite of the differences and conflicts with children, majority of them want to live with their children and grandchildren.

References

1. Agarwal S, Srivastava SK. Effect of living arrangement and gender differences on emotional states and self-esteem of old aged persons, *Indian Journal of Gerontology*. 2002;16:312-320.
2. Domingo Lita J, John B. Casterline. Living Arrangements of the Filipino Elderly. *Elderly in Asia Report No. 92-16*. 4 1992
3. Dubey Aruna, Bhasin Seema, Gupta Neelima, Sharma, Neeraj. A Study of elderly living in old age home and within family set-up in Jammu. *Stud. Home Com. Sci.* 2011;5(2):93-98.
4. Gupta A, Mohan U, Tiwari SC, Singh SK, Singh VK. Quality of life of elderly people and assessment of facilities available in old age homes of Lucknow, India. *National Journal of Community Medicine*. 2014;5(1):21-24.
5. Hewitt G, Ismail S, Patterson S, Draper A. The Nutritional vulnerability guyaneses in residential homes. *West Indian Medical Journal*; c2006. p. 55 (5).
6. Kanwar P, Chadha NK. Psychosocial determinants of institutionalized elderly. An empirical study. *Indian Journal of Gerontology*. 1998;12:27-39.
7. Mathew AM, George SL, Paniyadi N. Comparative study on stress, coping strategies and quality of life of institutionalized and non-institutionalized elderly in Kottayam district, Kerala. *Indian Journal of Gerontology*. 2009;23(2009):79-8.
8. Mehta. Diet, Nutrition and Health profile of elderly population of urban Baroda. *Ageing, Nutrition and health*; c1999. p. 54-60.
9. Minal P, Kamala R. Situation of institutionalized and non-institutionalized ageing women. *Indian journal of Gerontology*. 1995;9:28-31.
10. Naik NA. Comparative study to assess emotional well-being of senior citizens staying in old age home versus senior citizens staying with family. *Nightingale's nursing Times*; c2007. p. 37-38.
11. Panigrahi AK, Syamala TS. Living Arrangement Preferences and Health of the Institutionalised Elderly in Odisha. *ISEC Working Paper Series*; c2012. p. 291.
12. Saletti A, Lindgren EY, Johanson L, Cederholm M. Nutritional status according to mini nutritional assessment in an institutionalized elderly population in Sweden, *Gerontology*. 2000;46:139-145.
13. Wason Neelam, Karuna Jain. Malnutrition and Risk of Malnutrition among Elderly, *Indian Journal of Gerontology*. 2011;25(2):208-17.
14. Shah J, Higgins T, Friedman RS. Performance incentives and means: how regulatory focus influences goal attainment. *Journal of personality and social psychology*. 1998 Feb;74(2):285.
15. Kavitha AK. Comparative study on quality of life among senior citizens living in home for the aged and family set up in Erode District. *Nightingale Nursing Times*. 2007;3(4):47.
16. Siddhu G. Can Families in Rural India Bear the Additional Burden of Secondary Education? Investigating the Determinants of Transition. *CREATE Pathways to Access. Research Monograph No. 50*. 2010 Nov.



The above table indicates that among the male elderly majority (40%) expressed that son is the abuser, 17.14% as spouse, 14.30% by daughter in law and Grandchildren. 5.71% by daughter and others. Only 2.85% felt that they are abused by their son in law. In female Elderly majority (33.33%) revealed that Daughter in law is the abuser, 20.00% are abused by Son, 15.55% by grandchildren. 13.33% by daughter and 6.70% by spouse and others. Son in law is the abuser only for (4.44%). However, son is the main abuser for males, and Daughter in law for the female elderly as per the results of the present study.

Table 6: Coping Strategies of abused elderly

Coping Strategy	Gender				Total	
	Male		Female		N	%
	N	%	N	%		
Tolerating	22	62.90	15	33.33	37	46.25
Sharing with others	06	17.14	12	26.70	18	22.5
Spirituality	05	14.28	08	17.77	13	16.25
Crying	00	00	06	13.33	06	7.5
Self-Blaming	02	5.71	04	8.88	06	7.5
Total	35	100	45	100	80	100

The above table analysed the coping strategies adopted by the abused elderly. It was observed that 62.90% of males and 33.33% females are tolerating the abusing the behaviour of Perpetrators in silence. This might be they had the opinion that nothing is possible even though they express it loudly. 17.14% of males 26.70% of females are getting console by sharing with others. 14.28% males and 17.77% of females opted spirituality as coping mechanism and getting relief by participating in religious activities, going to temples listening to the religious preachers etc. only 5.71% of males and 8.88% of females are blaming themselves for their present status. In females 13.33% are getting relief whenever they abused.

Causes for elder abuse

- Declining Human and spiritual values in the name of modernization is main factor for showing disrespect and dish honour towards elderly.
- Growing materialistic nature of the adults who are indirectly teaching self-centeredness, selfishness, individualism etc. through their interactive behaviours.
- Wrong role models in the immediate environment for the children
- Silent suffering of elderly due to too much affection of their children
- The irony of pretending and false prestige before others by not sharing about abusive behaviours.

Preventive measures

- Counselling the family members to develop empathetic attitude towards elderly
- Sharing the presser of the care giver by other family members
- Creating a stress-free environment in the home
- Setting up a comfortable living arrangement with in the available infrastructure
- Parents should be conscious in their child rearing practices to develop love, respect, kindness, humility, sympathy, compassion, non-violence, understanding etc.

- Younger generation must allot some times to listen to the elderly in the family
- Elderly should be encouraged to speak about their suffering instead of bearing their silence
- Educating the care givers health workers and other professionals and administrators who are involved in elderly care
- Prosecution and punishment to the abusers by the legal authorities when they find it
- Being socially active and avoiding social isolation which makes elderly more vulnerable to elder abuse
- Creating awareness to the elderly to protect their rights and about constitutional provisions

Conclusion

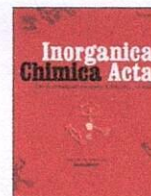
It is unfortunate to witness the abusive behaviour from the people we trust. It is really a problem, which is ignored or not recognized until it becomes serious. Always legal protection cannot save the elderly from abuse. The right way would be a judicious mixture of family and community involvement and interventions by the Government to protect and take care of the helpless.

References

1. Biggs S, Phillipson C, Kingston P. Elder abuse in perspective. Rethinking ageing series. Buckingham, Philadelphia: Open University Press, 1995.
2. Cohen M, Levin SH, Gagin R, Friedman G. Elder abuse: Disparities between older people's disclosure of abuse, evident abuse, and high risk of abuse. Journal of American Geriatrics Society. 2007;55:1224-1230.
3. Fernandez M. Cultural beliefs and domestic violence. Annals of New York Academy of Science. 2006;1087:250-260.
4. Inglehart R, Welzel C. Modernization, Cultural change and democracy. New York and Cambridge: Cambridge University Press, 2005.
5. Jamuna D. Issues of elder care and elder abuse in the Indian context. Journal of Ageing and Social Policy. 2003;15:125-140.
6. Malaker CR, Guha Roy S. Reconstruction of Indian life table for 1901-81 and projections for 1981-2001, Sankhya. 1990;52(B):3.
7. Kosberg JI, Garcia JL, eds. Elder abuse: International and cross-cultural perspectives. New York: The Haworth Press; c1995.
8. Lachs MS, Pillemer K. How would you like to be treated when you are 75? The Lancet. 2004;364:1263-1272. Retrieved September 22, 2006, from the PubMed database.
9. Reis M, Nahmiash D. When seniors are abused. Toronto: Captus Press; c1995.
10. WHO. World Report on Violence and Health (Definition developed by Action on Elder Abuse in the United Kingdom) World Health Organisation: Geneva, Switzerland; c2002.

PRINCIPAL
JMJC COLLEGE FOR WOMEN (Autonomous)
TENALI





Facile synthesis of hexagonal-shaped CuO NPs from Cu(II)-Schiff base complex for enhanced visible-light-driven degradation of dyes and antimicrobial studies

V. Sumalatha^{a,*}, Dasari Ayodhya^b, V. Balchander^c

^a Department of Chemistry, JMJ College for Women, Tenali, Guntur-522201, Andhra Pradesh, India

^b Department of Chemistry, University College of Science, Osmania University, Hyderabad-500007, Telangana State, India

^c Department of Pharmaceutical Engineering, BV Raju Institute of Technology, Narsapur, Medak-502313, Telangana State, India

ARTICLE INFO

Keywords:

Monoclinic CuO NPs
Cu(II)-Schiff base complex
Hexagonal structure
Thermal decomposition
Photodegradation
Antimicrobial activity

ABSTRACT

The current research work reports a simple and facile synthesis of hexagonal shaped monoclinic bare CuO NPs and Cu(II)-CuO NPs (CuO NPs from binuclear copper complex derived from Schiffbase,2-(4-(trifluoromethoxy) phenylimino)methyl)-4-methylphenol, TMPM4MP). It is found that the geometrical structure of [Cu (TMPM4MP)₂] is square planar around the copper atoms using the results of ¹H NMR, ES-Mass, UV-vis, and FTIR studies. In addition, hexagonal shaped CuO NPs were produced in the nano range (10–15 nm) by the thermal decomposition of the Cu(II) complex. The synthesized Schiff base, Cu(II) complex and CuO NPs were characterized using the physicochemical methods, including ¹H NMR, ¹³C NMR, ES-Mass, FT-IR, UV-vis, PL, powder XRD, BET, elemental analysis, SEM, and TEM measurements. The photocatalytic activity of CuO NPs was assessed toward degradation of CV and FL dyes and the results exhibited 90.8 % and 94.2 % efficiencies with degradation rate of 0.1241 and 0.1354 min⁻¹ with in 60 min of reaction time under visible light, which is higher than the bare CuO NPs. In addition, the synthesized Schiff base, Cu(II) complex, and CuO NPs show more antibacterial activity against gram positive and gram negative bacteria, as well as fungi using disc diffusion method. Moreover, the synthesized CuO NPs and Cu(II) complex show more antibacterial activity against gram positive and gram negative bacteria in comparison to their Schiff base and precursor; and comparable to standard drugs.

1. Introduction

Recently, nanotechnology has emerged as a tool for the development in the biological synthesis of metal-based nanoparticles [1,2]. Nanoparticles have attracted great interest in recent years because of their unique chemical and physical properties, which are different from those of either bulk materials or single atoms and have potential applications in optoelectronics, catalysis, ceramics and so on [1,2]. The synthesis of metal oxide nanoparticles from the Schiff base transition metal complexes was one of the most suitable methods, because the products obtained were of good purity and with perfect structure [3]. Apart from it, the synthesis of various metal complexes including Cu(II), Ni(II), Co(II), Fe(II), Zn(II), U(VI), VO(IV), Ce(III), and Th(IV) derived from Schiff bases exhibited tremendous biological activities such as antimicrobial, antioxidant, and antitumor studies [4–6]. This technique offers several

unique advantages over other methods including easy work-up, low temperature processing, short reaction time, and production of inorganic nanomaterials with narrow size distribution. There are some examples reported in the literature on the direct calcination of metal complexes as precursors for the preparation of metal oxide nanoparticles [7–9]. For that reason, thermal decomposition of metal complexes precursors offers a good alternative to control size and uniformity in shape. Therefore, we have studied herein the synthesis of metal oxide nanoparticles via a simple, economical, one-step method which includes the thermal decomposition of metal complexes precursors.

Recently, the preparation of transition metal oxide nanoparticles including ZnO, CuO, NiO, and other oxides with controlled size and morphology have attracted much interest because of their outstanding unique characteristics and numerous applications [7–10]. CuO is a narrow p-type semiconductor with a band gap value of 1.2 eV [7]. CuO

* Corresponding author.

E-mail address: sumalathav99@gmail.com (V. Sumalatha).

<https://doi.org/10.1016/j.ica.2022.121358>

Received 6 July 2022; Received in revised form 8 December 2022; Accepted 19 December 2022

Available online 22 December 2022

0020-1693/© 2022 Elsevier B.V. All rights reserved.



has been reported in numerous applications such as catalysis, gas sensors, batteries, and transistors [11–14]. Till now, different synthetic methods have been reported for the preparation of CuO NPs including hydrothermal, electrochemical, thermal evaporation, and decomposition [15–18]. Currently, the solid-state thermal decomposition of coordinated complexes as new precursors is being investigated [19–21], and as compared to conventional methods, it is much more rapid, cost-effective, and controllable. Different shapes of CuO nanosized such as nanorods, nanospheres, and nanowires also have been synthesized by various coordinated precursor structures [15–18].

Among nano-sized metal oxides, the synthesized CuO NPs from Cu(II) complexes were still play an important role because of their vast applications in waste water remediation and sensor applications [11], enhanced energy storage, lithium-ion batteries [12], and photocatalytic degradation of dyes from aqueous solutions [13,14]. Although there are numerous valid methods for synthesis of copper oxide nanostructures such as microwave-assisted template-free, hydrothermal, and others, these methods are require long time and/or complicated [15–18]. Using coordination of Cu(II) complexes as precursors for the synthesis of CuO NPs has been considered as one of the greatest convenient and excellent practical approaches [7]. Furthermore, it has been widely investigated for many optoelectronic devices such as optical switch, energy storage, field emission devices and solar cells, gas sensors, lithium-ion electrode materials, magnetic storage media, rectifiers, heterogeneous catalysts, etc. [11–14]. CuO NPs are the most widely used metal oxide nanoparticles for wastewater treatment because of their superior catalytic properties [22–24]. According to previous reports, CuO NPs were synthesized from Cu(II) complexes coated materials and without selective morphology and size of the particles [7,9,23,24]. Hence, we have synthesized particular hexagonal shaped and better photocatalytic and antimicrobial activities CuO NPs.

In this study, we report to used facile and reproducible synthetic procedure for the preparation of hexagonal shaped monoclinic CuO NPs from [Cu(TMPM4MP)₂] complex derived from 2-(4-(trifluoromethoxy)phenylimino)methyl-4-methylphenol (TMPM4MP) and copper acetate precursors. The synthesized CuO NPs were fully characterized using UV-vis DRS, PL, FTIR, powder XRD, and TEM. The shape and size of the particles were characterized using XRD and TEM techniques. The photocatalytic activity of the synthesized CuO NPs was assessed toward the photocatalytic degradation of CV and FL dyes in an aqueous medium as model pollutants. Furthermore, antibacterial and antifungal activities with effect of concentration variation of the synthesized CuO NPs are also performed and the obtained results were prominent and comparable to standard drugs.

2. Experimental

2.1. Materials and methods

Copper acetate (Cu(CH₃COO)₂·H₂O), methanol, ethanol, ether, acetone, crystal violet, fluorescein, hexamethylenetetramine, NaOH, 4-(trifluoromethoxy)benzenamine, and 2-hydroxy-5-methylbenzaldehyde were obtained from Sigma-Aldrich Chemicals Pvt. Ltd (India). Double distilled water was used as a solvent for all experiments. All reagents were of analytical grade and they were purchased and used as received without further purification.

2.2. Synthesis of Schiff base, 2-(4-(trifluoromethoxy)phenylimino)methyl-4-methylphenol (TMPM4MP)

The Schiff base (TMPM4MP) was synthesized by mixing the hot methanolic solution of 4-(trifluoromethoxy)benzenamine (10 mM, 25 mL) and 2-hydroxy-5-methylbenzaldehyde (10 mM, 25 mL) in 1:1 ratio with stirring and refluxing at 60–70 °C temperature on hot oil bath for 2–4 h. After that, the reaction mixture was left for some time to attain room temperature. The colored precipitates resulted were isolated by

filtration and recrystallized from methanol and the entire procedure was summarized in Scheme 1.

2.2.1. Analytical data of Schiff base (TMPM4MP)

Elemental analysis (%): Molecular formula C₁₅H₁₂F₃N₂O₂; Found: C, 60.82; H, 4.03; N, 4.68. Calculated: C, 61.02; H, 4.10; N, 4.74.

¹H NMR (400 MHz, CDCl₃): δ = 12.73 (s, 1H); 8.52 (s, 1H); 7.24 (m, 4H); 7.19 (dd, 1H, J = 8.533 Hz); 7.16 (s, 1H); 6.92 (d, 1H, J = 8.282 Hz); 2.30 (s, 3H), Fig. S1.

¹³C NMR (100 MHz, CDCl₃): δ = 163.46, 158.93, 147.73, 147.35, 134.49, 132.42, 128.35, 124.33, 122.37, 122.03, 121.78, 119.22, 118.64, 117.1, 20.31, Fig. S2.

IR (KBr)(cm⁻¹): ν(O–H) 3451, ν(CH=N) 1622, ν(C–O) 1174, Fig. S3.

UV (DMSO) λ_{max}(nm)(cm⁻¹): 260 (38461), 347 (35714), Fig. S4.

MS (ESI): m/z = 296 [M + H]⁺, Fig. S5.

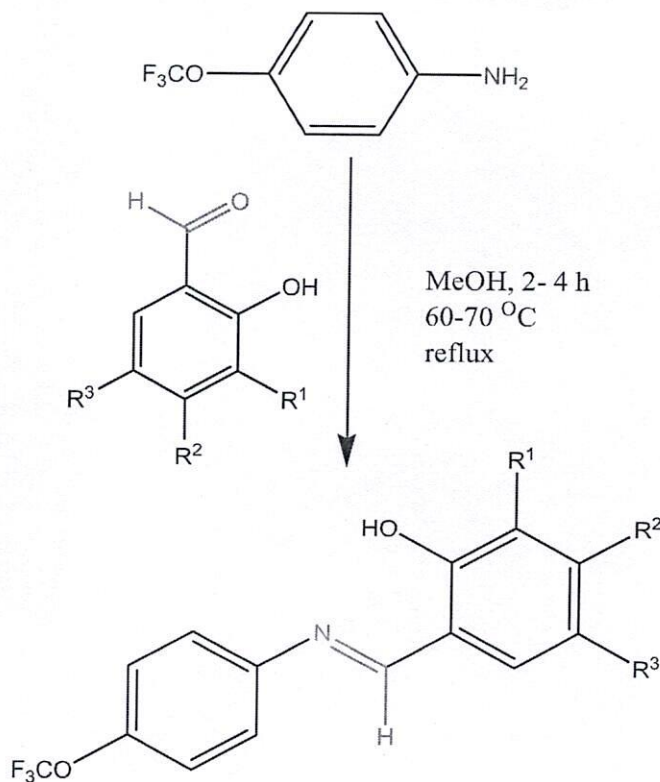
2.3. Synthesis of [Cu(TMPM4MP)₂] complex

The synthetic route for the Cu(II) complex such as [Cu(TMPM4MP)₂] as shown in Scheme 2. The Cu(II) complex was synthesized by using metal salt (copper acetate) and Schiff base (TMPM4MP) in 1:2 M ratio. The hot methanolic solution of metal acetate such as [Cu(CH₃COO)₂·H₂O, 10 mM] and Schiff base ligand (TMPM4MP, 20 mM) were mixed and refluxed for 2–4 h at 70–80 °C. This solution was kept aside at RT for slow evaporation. The separated red colored Cu(II) complex as precipitate was filtered off, washed thoroughly with water, ethanol and ether; and finally dried in vacuum over desiccators.

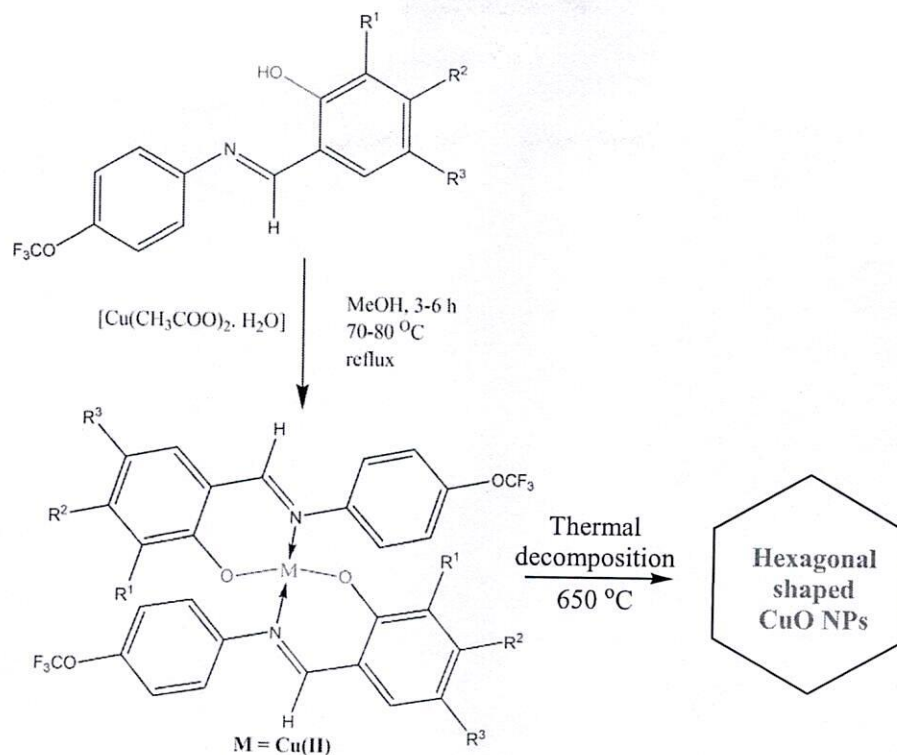
2.3.1. Analytical data of [Cu(TMPM4MP)₂] complex

Elemental analysis (%): Molecular formula [C₃₀H₂₂F₆N₂O₄Cu], Found: C, 55.07; H, 3.35; N, 4.24, Cu, 9.66. Calculated: C, 55.26; H, 3.40; N, 4.30; Cu, 9.75.

IR (KBr)(cm⁻¹): ν(CH=N) 1612, ν(C–O) 1175, ν(M–O) 520, ν(M–N) 509, Fig. S6.



Scheme 1. Schematic route for the synthesis of Schiff base ligand (TMPM4MP), wherein R¹ = H, R² = H, R³ = CH₃.



Scheme 2. Synthetic route for the hexagonal-shaped CuO NPs from Cu(II) complex $[\text{Cu}(\text{TMPM4MP})_2]$ complex, wherein $\text{R}^1 = \text{H}$, $\text{R}^2 = \text{H}$, $\text{R}^3 = \text{CH}_3$.

UV (DMSO) $\lambda_{\text{max}}/\text{nm}(\text{cm}^{-1})$: 268 (37313), 310 (32258), 406 (24630), 590 (16949) Fig. S7.

2.3.2. Magnetic moment (μ_{eff}): 1.72 BM

MS (ESI): $m/z = 653 [\text{M} + \text{H}]^+$, Fig. S8.

ESR: g_{\parallel} (2.148), g_{\perp} (2.065), G (2.20), A [$\text{Gauss}(\text{cm}^{-1})$] 180 (0.0168), g_{\parallel}/A (cm) (127) Fig. S9.

SEM: Spherical shape, average diameter 85 nm, Fig. S10.

2.4. Synthesis of CuO NPs

In a typical synthesis of CuO NPs, the stoichiometric ratio of copper acetate (0.1 M) and hexamethylenetetramine $[\text{C}_6\text{H}_{12}\text{N}_4]$ (0.05 M) were dissolved in 100 mL deionized water and allowed to stir for the complete dissolution of the compound, followed by the drop-wise addition of NaOH aqueous solution into the reaction mixture until the \sim pH 9. The reaction was allowed to proceed for 5 h in a hot air oven at 110 °C and then the resulting precipitate was washed several times with ethanol and dried at room temperature.

2.5. Synthesis of CuO NPs from $[\text{Cu}(\text{TMPM4MP})_2]$ complex

The as-prepared $[\text{Cu}(\text{TMPM4MP})_2]$ complex was thermally decomposed at 650 °C for 2 h in an electrical muffle to give the corresponding CuONPs (Cu(II)-CuO NPs) as shown in Scheme 2. In this method, the dried precursor was transferred to a silica crucible and heated to red hot condition at 650 °C for about 65 min with a heating rate 10 °C/min according to the thermal behavior of the precursors. The precursor started decomposing violently. The preliminary step is the characterizing of nanoparticles is the color transformation of solution indicating the reduction of copper ions into CuO NPs using $[\text{Cu}(\text{TMPM4MP})_2]$ complex. The total decomposition of the precursor complex led to the formation of the corresponding oxide nanoparticles, which are quenched to room temperature, ground well, and stored.

2.6. Characterization

UV-vis diffuse reflectance spectra (DRS) of the synthesized samples are obtained from Shimadzu UV-3600 UV-vis near-infra-red (NIR) spectrophotometer. Photoluminescence (PL) spectra were measured on a Shimadzu RF-5301 PC spectrometer with an excitation wavelength of 310 nm. X-ray diffraction (XRD) patterns of the as-synthesized samples were obtained with a X'pert Philips diffractometer using Cu-K α radiation. The HR-TEM images were taken on a transmission electron microscope (JEOL; model 1200 EX) at an accelerator voltage of 220 kV. FT-IR spectra of Schiff base, their Cu (II) complex and CuO NP were recorded on a Shimadzu spectrophotometer in the range of wavenumber is 4000–400 cm^{-1} with KBr disks. The ^1H NMR spectra of Schiff base and Cu(II) complex were recorded in DMSO on a Bruker 300 MHz spectrometer at room temperature using TMS as an internal reference. Elemental analyses for C, H, N, and S were done using ElementerVario EL III Carlo Erba 1108 instrument. ESR of Cu(II) complex was recorded on Varian E-9 spectrophotometer.

2.7. Photocatalytic activity experiment

In a typical experiment of photocatalytic degradation of CV (crystal violet) and FL (fluorescein) dye solutions is performed using the synthesized CuO NPs as a catalyst prepared from $[\text{Cu}(\text{TMPM4MP})_2]$ complex and bare CuO NPs. In a photocatalytic reaction, 15 mg of the prepared catalyst was added to 50 mL of 10 mg/L aqueous dye solutions (CV and FL) separately. The solution in which the prepared photocatalysts are dispersed is first kept in the dark for 60 min to allow the system to reach an adsorption-desorption equilibrium. Afterward, the reaction mixture was under visible light (at 440 nm) irradiation of the solution is started. The degradation was investigated in a Pyrex beaker under UV-vis illumination using a 250 W Hg-vapour lamp (Thoshiba, SHLS-002) ($\lambda = 440$ nm). After exposure to visible radiation for a desired time interval, samples were withdrawn from the reaction mixture and CuO NPs were separated from the suspension by centrifugation. After



recovering the catalyst by centrifugation, the light absorption of a clear solution is measured at 590 nm (λ^{\max} for CV) and 492 nm (λ^{\max} for FL) at a set time using a UV-vis spectrophotometer. The degradation rates of the dyes at given time intervals were calculated by measuring the changes in the absorption profile at their maximum absorbance wavelengths and concentration variance of the CV and FL solutions from UV-vis spectra, and the dye degradation efficiency (D) was calculated from the following equation:

$$D(\%) = C_0 - C_t / C_0 \times 100$$

where C_0 and C_t were initial and final concentrations after a certain reaction time, respectively.

2.8. Antimicrobial activity experiment

Antimicrobial activities of the synthesized Schiff base, precursor, their Cu(II) complex, and as-prepared CuO NPs were determined using a modified Bauer-Kirby method [25]. Briefly, 100 μ L of the pathogenic bacteria/fungi were grown in 10 mL of fresh media until they reached a count of 10^8 cells/mL for bacteria or 10^5 cells/mL for fungi [25]. 100 μ L microbial suspensions were spread onto agar plates corresponding to both pathogens in which they were maintained. Isolated colonies of each organism were selected and tested for susceptibility by the disc diffusion method. A filter paper disc impregnated with the tested chemical was placed on agar. The prepared agar plates were filled with gram positive and gram negative bacteria such as *Escherichia coli* (ATCC 27853), *Pseudomonas aeruginosa* (ATCC 25922), *Staphylococcus aureus* (ATCC 25923), and *Bacillus subtilis* (ATCC 19659); and fungi such as *Aspergillus niger* and *Candida albicans* were incubated at 25–27 °C for 24–48 h. The prepared Schiff base, Cu(II) complex, and CuO NPs suspension (10 μ L) was added to the discs. The samples were initially incubated for 15 min at 4 °C (to allow diffusion) and later on at 37 °C for 24 h. Positive test results were scored when a zone of inhibition was observed around the discs.

3. Results and discussion

The synthesized Schiff base ligand and its Cu(II) complex were completely characterized, confirmed, and represented in the supplementary information. The prepared bare CuO NPs and CuO NPs from [Cu(TMPM4MP)₂] complex were characterized by using XRD, FTIR, UV-vis DRS, PL, and HR-TEM and discussed. With this fast and simple method, CuO NPs can be produced without expensive and toxic solvents or complicated equipment.

3.1. Powder XRD analysis

The crystalline structure and phase of the synthesized CuO NPs were characterized using powder XRD as shown in Fig. 1. The diffraction peaks for CuO exist at 32.8°, 35.9°, 39.1°, 46.3°, 52.9°, 58.7°, 62.74°, 66.6°, 68.3°, 72.6°, and 75.2° which are indexed at (-111), (002), (111), (-202), (020), (202), (-113), (-311), (113), (311), and (220) respectively. All these diffraction peaks, including not only the peak positions but also their relative intensities, can be perfectly indexed into the monoclinic phase of CuO with cell constants: $a = 4.678 \text{ \AA}$, $b = 3.431 \text{ \AA}$, and $c = 5.136 \text{ \AA}$ (JCPDS card No. 80-0076); these data are in agreement with previously [26]. No characteristic peaks of other impurity phases have been detected, indicating that the final product is of high purity. The average crystal size was estimated using the Debye-Scherrer formula [27]:

$$D = 0.96\lambda / \beta \cos\theta$$

where λ , β , θ are the X-ray wavelength, the full width at half maximum (FWHM) of the diffraction peak, and the Bragg diffraction angle, respectively. The estimated average crystal size of CuO NPs prepared

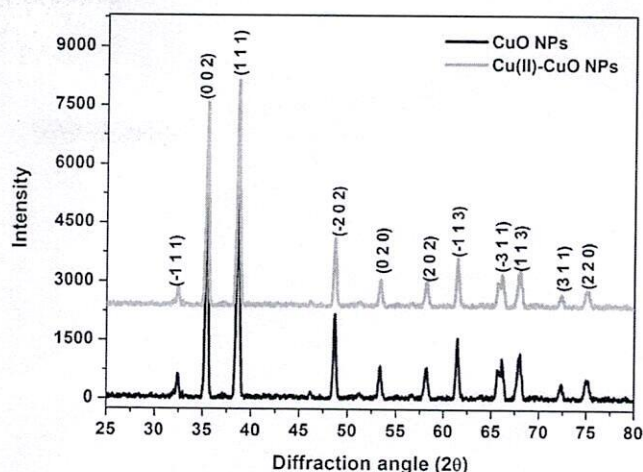


Fig. 1. The powder XRD pattern of the synthesized bare CuO NPs and CuO NPs from [Cu(TMPM4MP)₂] complex.

from [Cu(TMPM4MP)₂] complex using the XRD technique was found around 18 ± 3 nm, further compared with the TEM analysis.

3.2. FTIR

The FT-IR spectral measurements of dried CuO-NPs from Cu(II) complex were carried out to find out the related functional groups mainly responsible for the reduction, capping, and stabilization of the CuO-NPs as shown in Fig. 2. It revealed the presence of several significant absorption peaks mainly at 3440 cm^{-1} , 2922 cm^{-1} , 1628 cm^{-1} , 1262 cm^{-1} , 1158 cm^{-1} , and the broad absorption bands in the range of 518–590 cm^{-1} . These absorption peaks are attributed to the band O–H stretching vibrations (3440 cm^{-1}) and the weak band of H–O–H bending vibrations mode (1628 cm^{-1}), C–O stretching vibration band (1158 cm^{-1}), and the range of 518–590 cm^{-1} due to $\nu(\text{Cu} - \text{O})$ stretching vibration mode [23]. In view of the reducing and capping properties of Cu(II) complex, it can be articulated that the oxygenated functional groups of an energy-efficient reduction and nucleation of Cu^{2+} into CuO NPs.

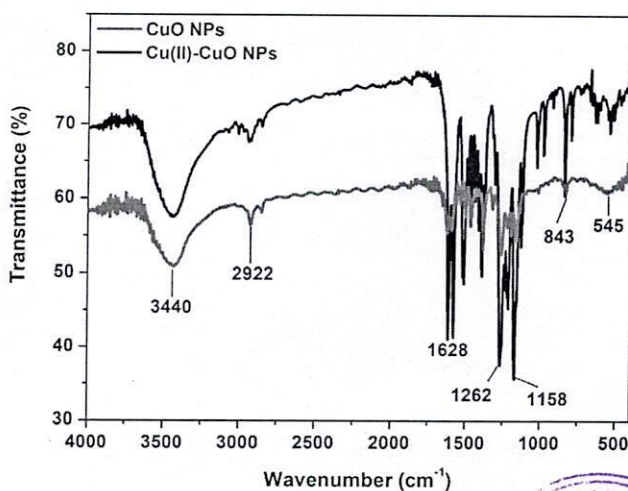


Fig. 2. FTIR spectra of the synthesized bare CuO NPs and CuO NPs from [Cu(TMPM4MP)₂] complex.

3.3. UV-vis DRS

The optical properties of the synthesized CuO NPs were studied by recording the UV-vis diffuse reflectance spectrum of the formed powder in the wavelength range 200–800 nm using UV-vis absorption spectrophotometer and the obtained results are presented in Fig. 3. From Fig. 3, It can be seen that the CuO NPs has good absorption capacity in the visible region [28]. Thereafter, the band gap energy is important for the photocatalytic activity because the energy of incident light must be greater than or equal to the band gap energy is the criteria of material selectivity for the photocatalyst. It clearly shows the optical reflectance of the CuONPs was found to exhibit optical absorption was the strong absorption band around 0.5–1 a.u., and the lowest optical reflectivity of around 10–35 % was in the visible region, which was the characteristic peak of Cu^{2+} ions. The sharp rise in the absorption curve below 382 nm was confirmed the highly crystalline and monoclinic phase of both CuONPs. The band gap (E_g) can be estimated as 3.52 eV [26,29] and it suggests to superior photocatalytic properties. These values reveal that the as-prepared CuO NPs products are semiconductors and are in good agreement with the reported data [29].

3.4. Photoluminescence

The photoluminescence (PL) emission spectra of the synthesized both CuO NPs at room temperature with an excitation wavelength of 310 nm was displayed in Fig. 4. The PL spectra show the maximum intensity with a broad band peak of emission at 496 nm and 502 nm (2.51 eV and 2.47 eV) in the green spectral region for bare CuO NPs and CuO NPs from $[\text{Cu}(\text{TMPM4MP})_2]$ complex, respectively. In addition, the PL intensity of $[\text{Cu}(\text{TMPM4MP})_2]$ complex derived CuO NPs is very less when compared to bare CuO NPs, which is suggesting to the strong recombination of photogenerated electron-hole pairs. In general, CuO NPs were showed the similarly broad luminescence band with a broad pronounced shoulder peak in the blue-green spectral region of semiconductors [30]. The absorbance, emission, and excitation spectrums of CuO NPs were indicated that the optical band gap value can be used for optoelectronic devices such as optical switches, energy storage, field emission devices, and solar cells and photocatalysts.

3.5. Tem

The morphology and shape of the synthesized CuO NPs from $[\text{Cu}(\text{TMPM4MP})_2]$ complex was evaluated using high-resolution TEM images. According to this HR-TEM analysis, the formed nanoparticles

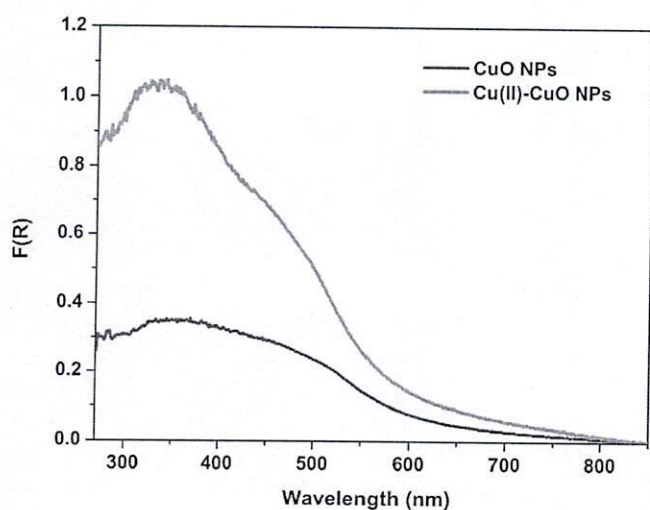


Fig. 3. The UV-vis DRS of the synthesized bare CuO NPs and CuO NPs from $[\text{Cu}(\text{TMPM4MP})_2]$ complex.

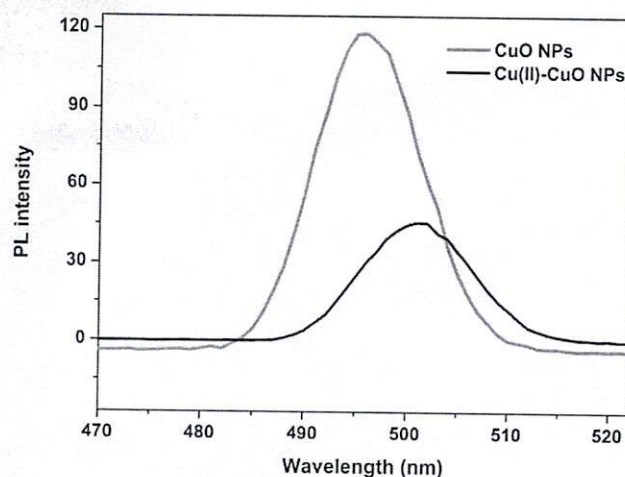


Fig. 4. The PL spectra of the synthesized bare CuO NPs and CuO NPs from $[\text{Cu}(\text{TMPM4MP})_2]$ complex.

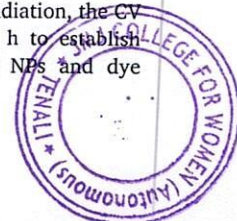
appear as spherical and hexagonal, but there are also large particles formed by the combination of small particles. It is also apparent that, with our optimal synthesis conditions, nanoparticles into noticeable different morphologies as spherical, hexagonal and oval shapes (Fig. 5). In detail, the particle size was supported using HR-TEM such as cubic, sphere and irregular shaped aggregates with average particle size of 16 ± 2 nm as shown in Fig. 5(a-d). The diffraction patterns obtained from the XRD, HR-TEM showed exactly the same d-spacing values such as 1.26 to 2.54 Å, which is suggesting to the prepared CuO NPs from $[\text{Cu}(\text{TMPM4MP})_2]$ complex is the crystalline nature [31].

3.6. BET

The BET isotherms were employed to characterize the detailed surface parameters including surface area, porosity, and distribution of the particles of the synthesized bare CuO NPs and CuO NPs derived from $[\text{Cu}(\text{TMPM4MP})_2]$ complex was shown in Fig. 6. According to the obtained BET isotherms of the CuO NPs is exhibited as a type of IV with a hysteresis loop and presence of mesopores with the pore size distribution is in the range of 5–20 nm [32]. The specific surface area of the synthesized CuO NPs and CuO NPs from Cu(II) complex were found to be $36.48 \text{ m}^2 \text{ g}^{-1}$ and $45.21 \text{ m}^2 \text{ g}^{-1}$, respectively. It suggests that the obtained specific area of the CuO NPs from Cu(II) complex is awfully greater than that of the bare CuO NPs. In general, the extent surface area and porous structure of the composites can meritoriously encourage the rate of catalytic reaction and it will simplifying charge transfer and suppression the charge carriers by increasing the number of active sites. Therefore, based on the obtained surface area results, the CuO NPs from Cu(II) complex could give more prominent catalytic performance.

3.7. Photocatalytic activity

The heterogeneous photocatalytic treatment of dyes (CV and FL) was carried out utilizing the synthesized bare CuO NPs and Cu(II)-CuO NPs as photocatalysts. A blank analysis was also run by exposing the dye sample under direct visible light without adding the photocatalyst. In this study, the blank was used as a control and to prove the potentiality of CuO NPs as a photocatalyst for the degradation of CV and FL dyes. In fact, dark adsorption is an initial step and one of the most critical aspects of the photocatalysis mechanism [33]. Further, the synthesized both CuO NPs were used to study the photodegradation of CV and FL dyes when exposed to visible light. In the presence of light radiation, the CV and FL dye solutions were stirred in the dark for 1 h to establish adsorption-desorption equilibrium between the CuO NPs and dye



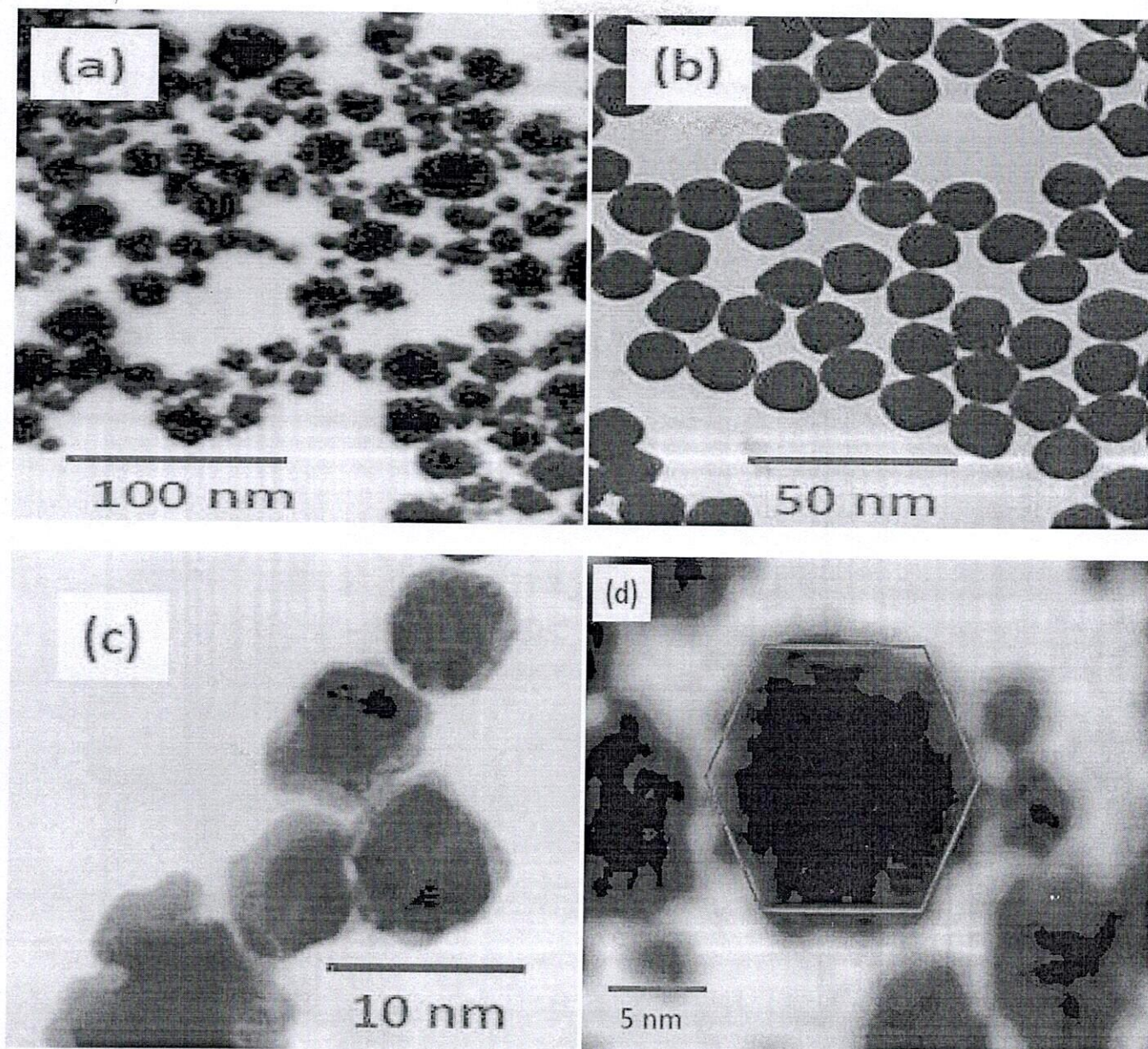


Fig. 5. The HR-TEM images of the synthesized CuO NPs from $[\text{Cu}(\text{TMPM4MP})_2]$ complex.

molecules. A UV-visible absorption spectrum was recorded to estimate the CV and FL dye concentrations during the 60 min of photocatalytic reaction. Control experiments were carried out in the dark (both with and without CuO NPs) to rule out any possibility of dye self-degradation, dye adsorption, or NP catalytic activity in the dark. In the absence of CuO NPs, we observed negligible CV and FL dye degradation after the experiment was completed as shown in Fig. 7(a) and Fig. 7(b), respectively. Furthermore, dye degradation experiments in the absence of a catalyst revealed negligible dye degradation. Therefore, CV and FL dyes were nearly complete to degradation, light and in the presence of catalyst are required. The photocatalytic activity of the synthesized Cu(II)-CuO NPs and the absorption peaks at 590 nm (λ^{max} for CV) and 492 nm (λ^{max} for FL) decreased as shown in Fig. 7(c) and Fig. 7(d). After completion of the photocatalytic reaction, the estimated degradation efficiency was 90.8 % and 94.2 % for CV and FL dyes in the presence of Cu(II)-CuO NPs, respectively within 60 min of light irradiation. In addition, the synthesized bare CuO NPs were also examined for the photocatalytic degradation of CV and FL dyes under similar reaction conditions (Fig. 8(a) and Fig. 8(b)). It was lesser active than the Cu(II)-

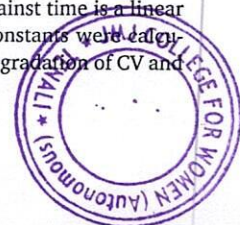
CuO NPs towards the degradation of CV and FL dyes due to less absorption capacity and size of the particles.

3.8. Photocatalytic kinetics

The photocatalytic rate of reaction was observed that the synthesized CuO NPs and Cu(II)-CuO NPs in the degradation processes of dyes follow pseudo-first-order kinetics. The Langmuir-Hinshelwood model was employed to clarify the photo-degradation kinetic of the catalyzed reactions (Fig. 9(a) and Fig. 9(b)). In a simple form, the model for the apparent pseudo-first-order is expressed as follows:

$$\ln(C_t/C_0) = -K_{\text{app}}t$$

where (K_{app}) is the apparent pseudo-first-order constant (min^{-1}), C_0 is the initial concentration (at time) of the dye, and C_t is the concentration of the dye at reaction time. The plot of $\ln(C_t/C_0)$ against time is a linear function with the slope equal to (K_{app}). The rate constants were calculated to be 0.1241 min^{-1} and 0.1354 min^{-1} for the degradation of CV and



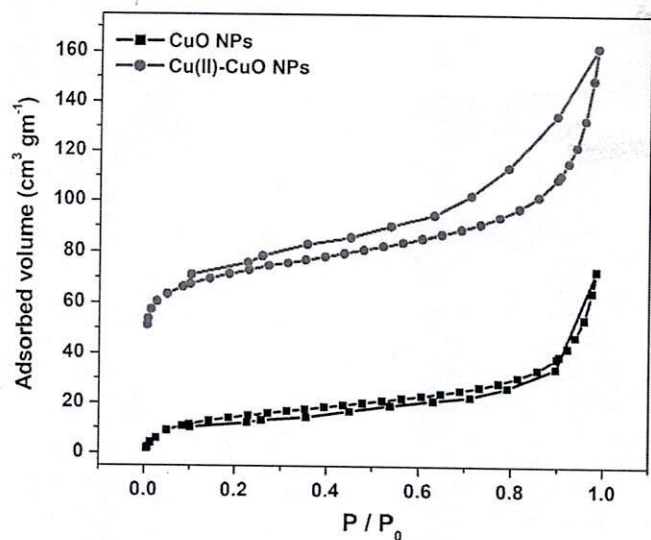


Fig. 6. BET isotherms of CuO NPs and CuO NPs from [Cu(TMPM4MP)₂] complex.

FL dyes using Cu(II)-CuO NPs under visible light irradiation.

3.9. Reusability of catalyst

An examination of the photocatalytic activities of the recycled Cu(II)-CuO NPs was investigated by collecting the catalyst from a sample solution after centrifugation up to 5 consecutive cycles. The separated catalyst was thoroughly washed with water and ethanol. The reusability test of CuO NPs under UV-visible irradiation on the CV and FL dyes shows the stability of the catalyst. As shown in Fig. 10, the reused catalyst showed very little change in the degradation efficiency in photocatalysis. This emphasizes the excellent chemical stability of the catalyst, making it beneficial for practical wastewater remediation applications. A slight decrease in the photocatalytic activity in each successive cycle can be attributed to several reasons like a degradation of the photocatalyst itself, unavoidable loss of photocatalyst during the recycling processes, and slight aggregation of NPs after the photocatalytic process. In addition, it shows the slight aggregation of Cu(II)-CuO NPs, possibly by the interactions between CuO NPs and intermediates formed during the degradation process, thus decreasing the electrostatic energy barrier between NPs and increasing the aggregation behavior [34]. As this recycled Cu(II)-CuO NPs form clusters, hence, the surface to volume ratio of NPs decreases, and their catalytic activity also

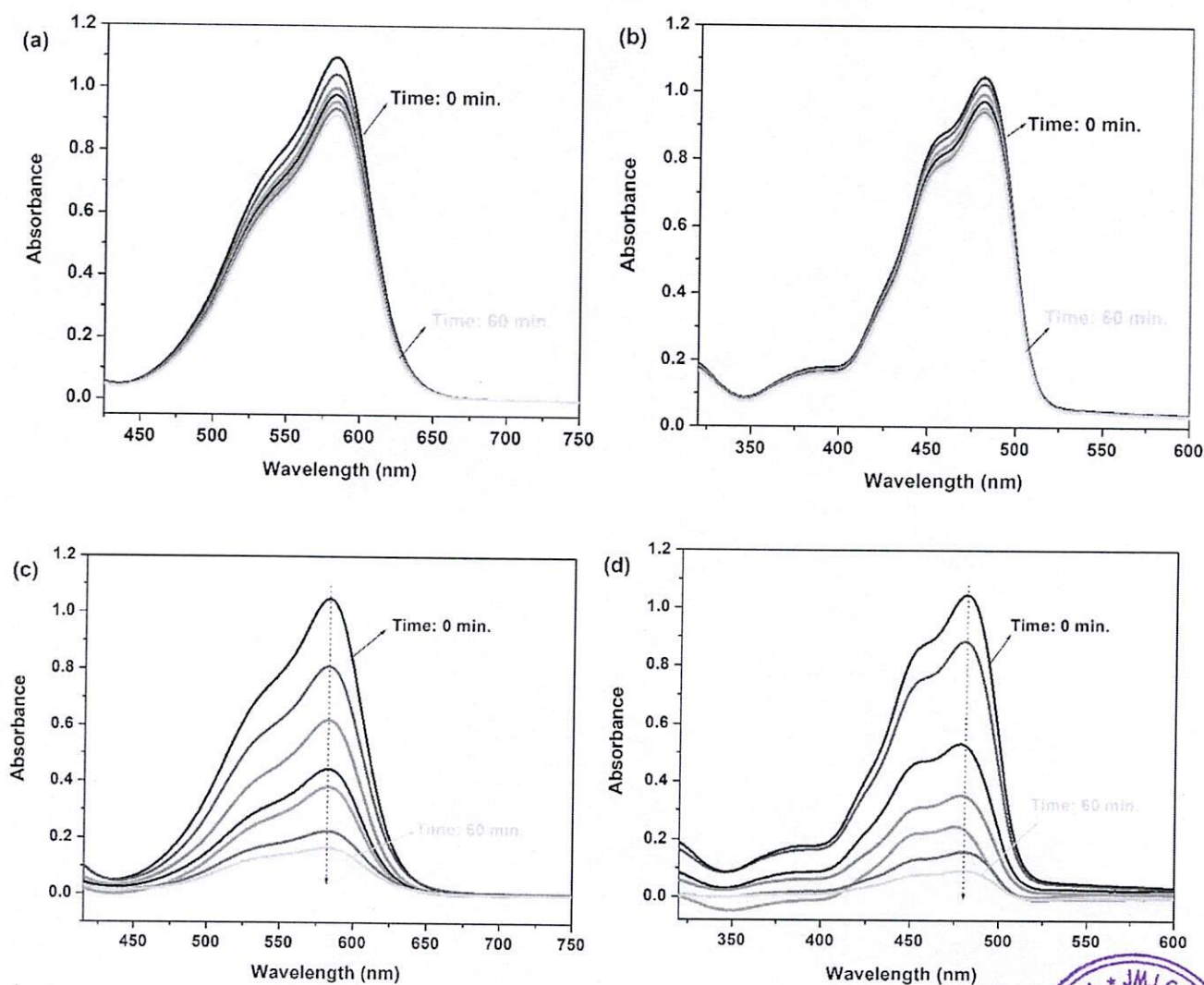
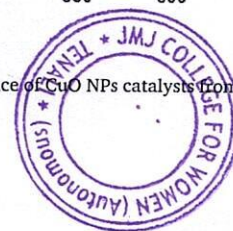


Fig. 7. The UV-vis absorption spectra of the photocatalytic degradation of CV (a and c) and FL (b and d) dyes in the absence and presence of CuO NPs catalysts from [Cu(TMPM4MP)₂] complex under visible light irradiation.



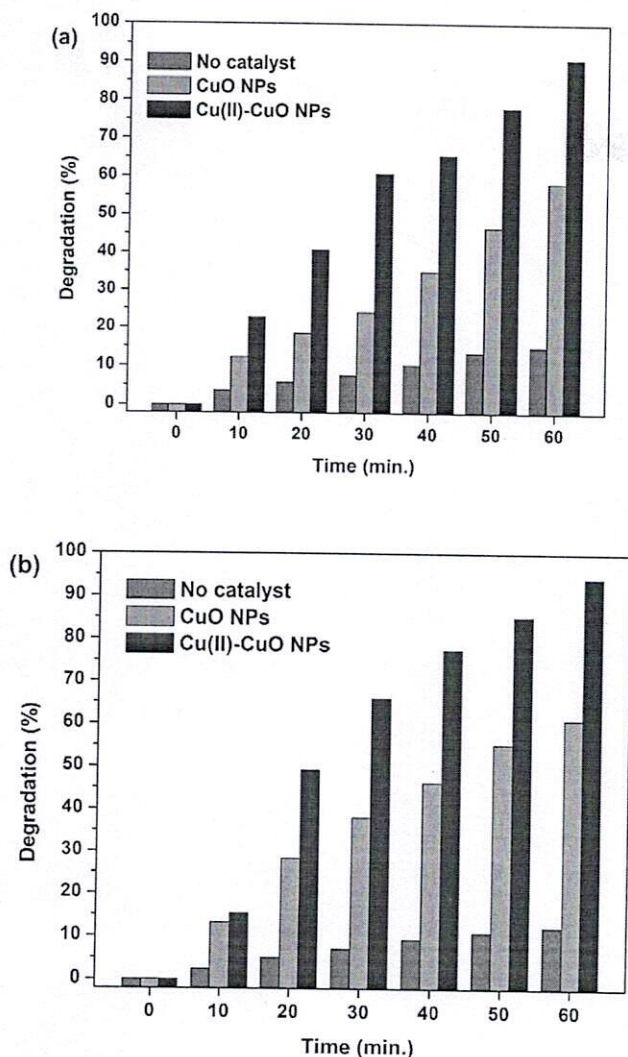


Fig. 8. The bar diagrams of the photocatalytic degradation of CV (a) and FL (b) dyes in the absence and presence of CuO NPs catalysts from $[\text{Cu}(\text{TMPM4MP})_2]$ complex under visible light irradiation.

decreases.

3.10. Photocatalytic reaction mechanism

In the photocatalytic reaction mechanism of dyes using the synthesized CuO NPs, the CuO NP is a semiconductor, which is able to generate electron-hole pairs (e^-/h^+) due to the transition of excited electrons from the valence band to the conduction band, creating holes in the valence band, after absorbing the photon energy ($h\nu$) upon the irradiation of light. The oxygen and water molecules in the dyes (CV and FL) reacted with the electron-hole pairs and subsequently formed hydroxyl radical ($\bullet\text{OH}$), which was responsible for breaking down the organic complex in dyes. The oxygen (O_2) reacted with the excited electrons (e^-) and dissociated hydrogen ions (H^+) from water molecules to form hydrogen peroxide (H_2O_2). Under the irradiation of light, hydrogen peroxide was generated, which was further reduced to hydroxyl radicals and hydroxide ions. The hydroxyl radicals were involved in degrading the organic materials in the dyes into simple harmless degradation products. In the end, the possible products of the photocatalytic degradation process could be water, carbon dioxide, methane gas, and other simple molecules [35] and it was similar to previous reports [35,36]. The schematic representation of the degradation of dyes by photocatalytic degradation mechanism over the synthesized CuO NPs is

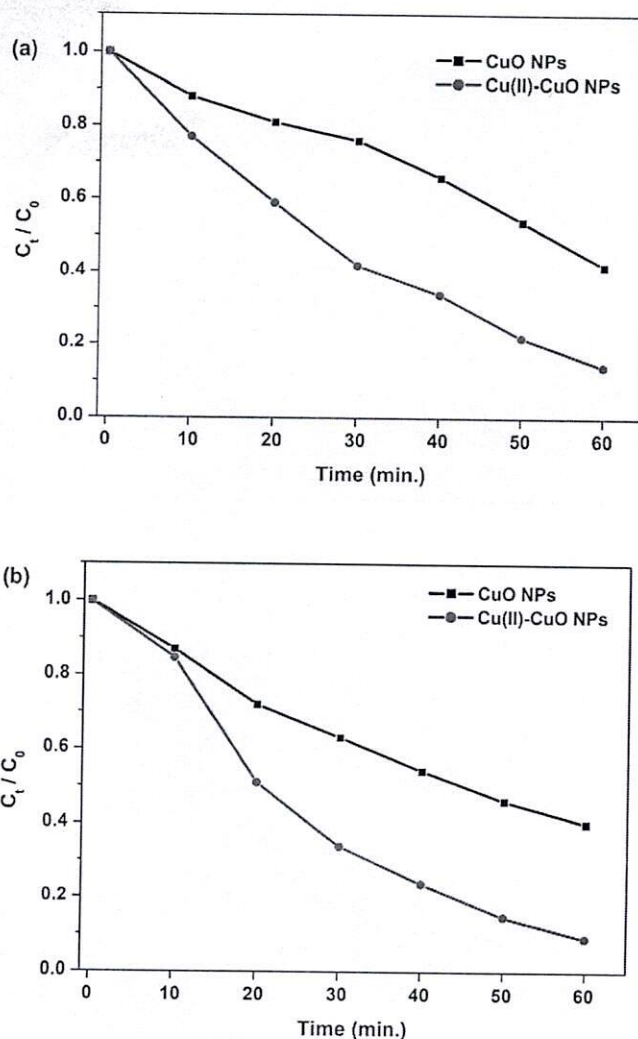


Fig. 9. The photocatalytic rate of reactions for the degradation of CV (a) and FL (b) dyes using CuO NPs from $[\text{Cu}(\text{TMPM4MP})_2]$ complex under visible light irradiation.

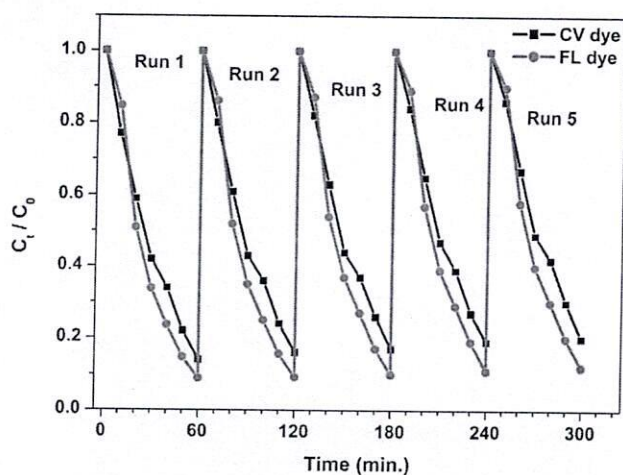
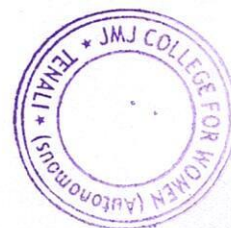
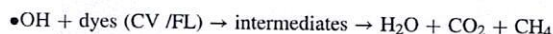
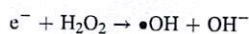
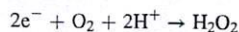
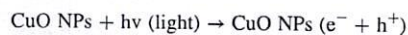


Fig. 10. The stability and recycling graphs for the degradation of CV (a) and FL (b) dyes using CuO NPs from $[\text{Cu}(\text{TMPM4MP})_2]$ complex under visible light irradiation.



illustrated as follows:



3.11. Antimicrobial activity

All the synthesized Schiff base, precursor, Cu(II) complex, and as-prepared CuO NPs were screened in-vitro for their biological activities such as antibacterial and antifungal activities using gram positive and gram negative bacteria such as *Escherichia coli* (ATCC 27853), *Pseudomonas aeruginosa* (ATCC 25922), *Staphylococcus aureus* (ATCC 25923),

and *Bacillus subtilis* (ATCC 19659); and fungi such as *Aspergillus niger* and *Candida albicans* by using disc diffusion method. Ampicillin (antibacterial agent) and Amphotericin B (antifungal agent) served as positive controls for antimicrobial activity and a filter disc impregnated with 10 μL of solvent (DMSO) was used as a negative control. During the incubation time, the tested samples (Schiff base, Cu(II) complex, and Cu(II)-CuO NPs) were exhibited prominent antimicrobial activity for the inhibition of bacteria and fungi growth and it was shown in Fig. 11(a). In addition, the effect of concentration variation of the synthesized Cu(II)-CuO NPs (10–50 μL) for the inhibition of bacteria and fungi growth was also examined under similar conditions (Fig. 11(b)) and it was shown as a concentration reliant effect. Among them, the synthesized CuO NPs were exhibited maximum activity than its Schiff base and Cu(II) complex against gram positive bacteria due to their small size and effectiveness, they show efficient inhibition mechanisms inside the cell of microorganisms [37].

In general, Schiff base compounds and their transition metal

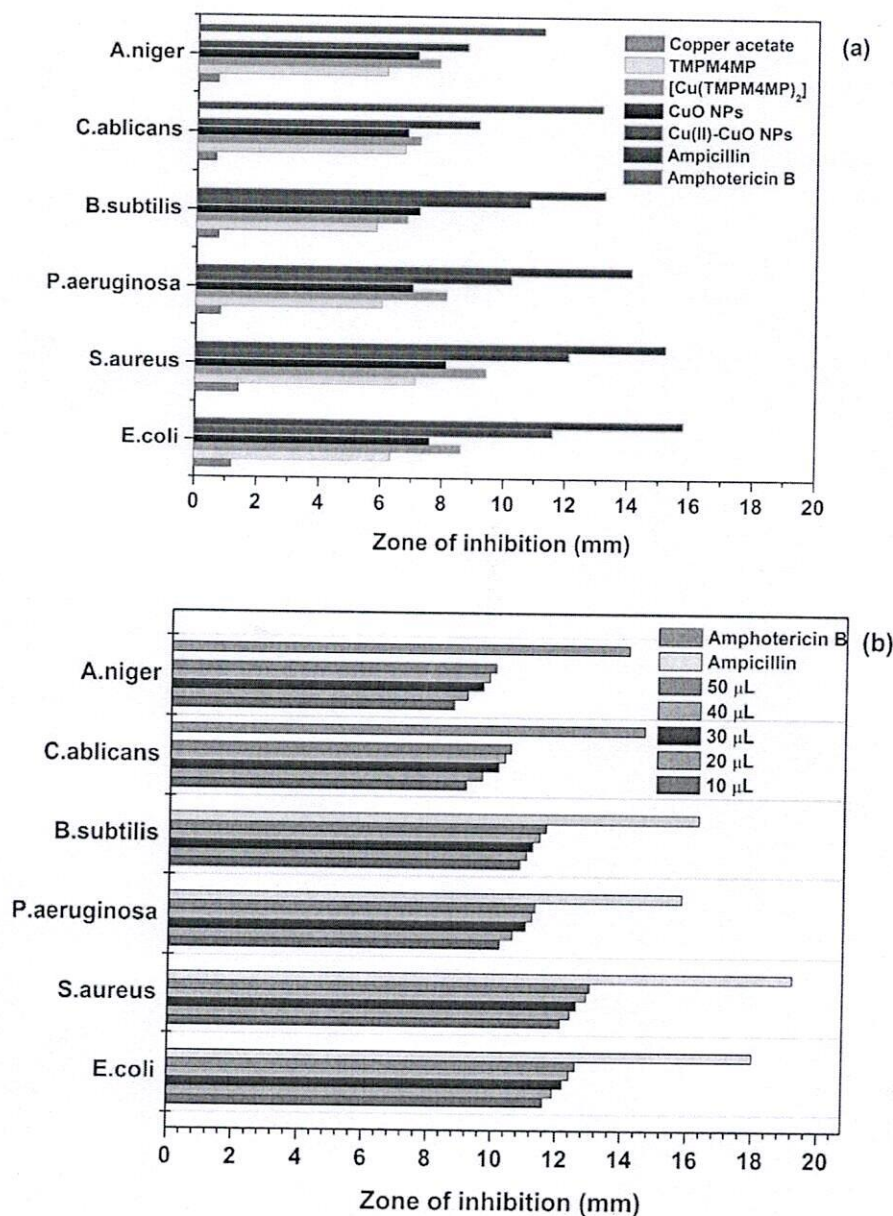


Fig. 11. (a) The antibacterial and antifungal activities, (b) effect of concentration variation of the synthesized CuO NPs (10–50 μL) from [Cu(TMPM4MP)₂] complex against various gram positive and gram negative bacteria as well as fungi by using disc diffusion method.



complexes exhibit major importance for their biological properties, encompass antibacterial, antifungal, and anticancer properties [38,39]. The different complexes based on similar or related ligands with Cu(II), Co(II), and Zn(II) ions showed better inhibition zone in microbial activities against various micro-organisms such as *C. albicans*, *S. aureus*, *P. aeruginosa*, and *E. coli* [40]. Also, they utilized the nanoparticles derived from complexes and Schiff bases as an antibacterial agent against various bacterial and fungal strains [41]. Thermal decomposition of complexes is considered one of the simplest methods for producing nanomaterials with small crystallite sizes and various morphologies. Asma et al synthesized Cu(II) and Zn(II) complexes exhibited enhanced activity against the tested bacterial (*S. aureus* and *E. Coli*) and fungal strains (*C. albicans* and *A. fumigatus*) as compared to free ligand [42]. It is noteworthy that biological activities of the majority of the Schiff bases increased upon coordination with different transition elements. In addition, it was revealed that such compounds, which were already active, became more active and those which were not biologically active became very active upon coordination. The improvement in biological activities upon coordination may be explained on the basis of Overton's concept and chelation theory [43]. Copper is considered as one of the most important transition metals, which possess the ability to form biologically active coordination compounds especially with Schiff bases [44]. Based on the previous reports, we have synthesized CuO NPs as well as Cu(II) complex from Schiff base (TMPM4MP) exhibited prominent antimicrobial activity both pathogenic bacterial and fungal strains.

On the basis of these observations, it can be concluded that synthesized CuO NPs had strong antibacterial activity against bacteria belonging to both gram positive and gram negative bacteria as well as fungi. CuO NPs have an important antibacterial property due to their large surface area, which helps them to make closer contact with microorganisms. Furthermore, the gram negative bacteria seemed to be more resistant to CuO NPs than gram positive bacteria [37]. It was earlier reported that the interaction between Gram positive bacteria and NPs was stronger than that of Gram negative bacteria because of the difference in cell walls between Gram positive and Gram negative bacteria [43]. These findings suggest the use of synthesized CuO NPs as a potential antimicrobial agent. The smaller size and homogeneous morphology of the nanoparticles are consistent with their excellent antimicrobial activity [37]. Although the structures of the bacterial cell walls are different and the biocidal effect could be dependent on the bacterial species, the CuO NPs have the potential to cause cell death as a consequence of electrostatic interactions between the liberated metal ions and the negatively charged bacterial cell wall, subsequent disruption of the cell membrane and protein denaturation [45]. In addition, the CuO NP solution reaches inhibition levels similar to those of a conventional antimicrobial drug.

4. Conclusions

In the present study reported a simple and low-cost approach for the synthesis of hexagonal shaped monoclinic bare CuO NPs and CuO NPs from Cu(II) complex derived from Schiff base, 2-(4-(trifluoromethoxy) phenylimino)methyl)-4-methylphenol (TMPM4MP) by the thermal decomposition method without expensive and toxic solvents or complicated equipment. The as-prepared both CuO NPs were characterized using XRD, FTIR, UV-vis DRS, PL, BET, and HR-TEM techniques to estimate the band gap energy, structure, phase, and shape of the CuO NPs. From XRD and TEM, the synthesized CuO NPs have monoclinic structure and hexagonal shaped with average diameter of the particles is 15 ± 2 nm. The photocatalytic degradation of CV and FL dyes under visible light irradiation over the synthesized bare CuO NPs and Cu(II)-CuO NPs was studied. The synthesized Cu(II)-CuO NPs were exhibited the maximum degradation of CV and FL dyes under 60 min of reaction time, which is 90.8% and 94.2%, respectively. In comparison, the bare CuO NPs as exhibited lesser photocatalytic activity than the Cu(II)-CuO

NPs due to low absorption capacity and large particle size. Moreover, the recycling experiments were carried out up to 5 consecutive cycles by using the synthesized Cu(II)-CuO NPs, there is no significant loss in the catalytic activity. Finally, using microbiological tests, it was determined that Cu(II)-CuO NPs have outstanding antibacterial and antifungal activity against several pathogen bacteria and fungi than Schiff base, Cu(II) complex, and bare CuO NPs by disc diffusion method and with a similar effect to that of a conventional drug, therefore potentially it may be used in bio-medicinal applications.

5. Authors' contributions

DA, VS, and VB conceptualized the study, designed the methods, conducted experiments, wrote the first and revised draft. DA and VS conducted experiments. DA and VS supervised the study and worked on the revised draft. VB assisted in data interpretation and worked on the revised draft. All authors read and approved the final manuscript.

Funding

This research did not receive any external funding.

Availability of data and materials

The raw data is available by contacting the authors.

Declarations Ethical approval

This article does not contain any studies with human participants or animals performed.

Declaration of Competing Interest

The authors declare that they have no known competing financial interests or personal relationships that could have appeared to influence the work reported in this paper.

Data availability

No data was used for the research described in the article.

Acknowledgments

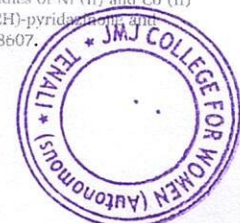
The authors acknowledge the Head, Department of Chemistry, Osmania University, Hyderabad and JMJ College for Women, Tenali, Andhra Pradesh, India for providing infrastructure support to conduct the research work.

Appendix A. Supplementary data

Supplementary data to this article can be found online at <https://doi.org/10.1016/j.ica.2022.121358>.

References

- [1] D. Ayodhya, G. Veerabhadram, A review on recent advances in photodegradation of dyes using doped and heterojunction based semiconductor metal sulfide nanostructures for environmental protection, *Mater. Today Energy* 9 (2018) 83–113.
- [2] M. Ijaz, M. Zafar, T. Iqbal, Green synthesis of silver nanoparticles by using various extracts: a review, *Inorg. Nano-Metal Chem.* 51 (5) (2021) 744–755.
- [3] M. Malathy, R. Jayasree, R. Rajavel, Facile synthesis of CuO nanoparticles from Cu(II) Schiff base complexes: Characterization, antibacterial and anticancer activity, *Smart Science* 5 (2017) 100–115.
- [4] M. Shebl, Mononuclear, homo- and hetero-binuclear complexes of 1-(5-(1-(2-amino phenylimino) ethyl)-2,4-dihydroxyphenyl) ethanone: synthesis, magnetic, spectral, antimicrobial, antioxidant, and antitumor studies, *J. Coord. Chem.* 69 (2016) 199–214.
- [5] O.M. Adly, M. Siebl, E.M. Abdelrhman, B.A. El-Shetary, Synthesis, spectroscopic, X-ray diffraction, antimicrobial and antitumor studies of Ni(II) and Co(II) complexes derived from 4-acetyl-5,6-diphenyl-3(2H)-pyridazinone and ethylenediamine, *J. Mol. Struct.* 1219 (2020), 128607.



- [6] S. Abdel Halim, M. Shebl, Synthesis, spectral, structural, DFT and NLO studies of cerium(III) and thorium(IV) complexes of 1-(5-(1-(2-aminophenylimino)ethyl)-2,4-dihydroxyphenyl)ethanone, *J. Coordinat. Chem.* 74 (17-20) (2021) 2984–3001.
- [7] M. Kiani, M. Bagherzadeh, S. Meghdadi, F. Fadaei-Tirani, M. Babaie, K. Schenk-Joss, Synthesis, characterisation and crystal structure of a new Cu(II)-carboxamide complex and CuO nanoparticles as new catalysts in the CuAAC reaction and investigation of their antibacterial activity, *Inorg. Chim. Acta* 506 (2020), 119514.
- [8] M. Salavati-Niasari, N. Mir, F. Davar, A novel precursor in preparation and characterization of nickel oxide nanoparticles via thermal decomposition approach, *J. Alloy. Compd.* 493 (1-2) (2010) 163–168.
- [9] S.Y. Ebrahimipour, I. Sheikhshoae, J. Castro, W. Haase, M. Mohamadi, S. Foro, M. Sheikhshoae, S. Esmaeili-Mahani, A novel cationic copper (II) Schiff base complex: Synthesis, characterization, crystal structure, electrochemical evaluation, anti-cancer activity, and preparation of its metal oxide nanoparticles, *Inorg. Chim. Acta* 430 (2015) 245–252.
- [10] T. Iqbal, S. Ghazal, S. Atiq, N.R. Khalid, A. Majid, S. Afsheen, N.A. Niaz, Influence of manganese on structural, dielectric and magnetic properties of ZnO nanoparticles, *Digest J. Nanomater. Biostruct.* 11 (2016) 899–908.
- [11] W. Jia, E. Reitz, P. Shimpi, E.C. Rodriguez, R.X. Gao, Y. Lei, Spherical CuO synthesized by a simple hydrothermal reaction: concentration-dependent size and its electrocatalytic application, *Mat. Res. Bull.* 44 (2009) 1681–1686.
- [12] W. Wang, O.K. Varghese, C. Ruan, M. Paulose, C.A. Grimes, Synthesis of CuO and Cu₂O crystalline nanowires using Cu(OH)₂ nanowire templates, *J. Mater. Res.* 18 (12) (2003) 2756–2759.
- [13] X. Jiang, T. Herricks, Y. Xia, CuO nanowires can be synthesized by heating copper substrates in air, *Nano Lett.* 2 (12) (2002) 1333–1338.
- [14] A. El-Trass, H. Elshamy, I. El-Mehasseb, M. ElKemary, CuO nanoparticles: synthesis, characterization, optical properties and interaction with amino acids, *Appl. Surf. Sci.* 258 (2012) 2997–3001.
- [15] S. Sathiyakumar, P. Selvam, J. Radhika, S. Anantharajan, F.L. Hakkim, K. Srinivasan, T. Premkumar, A first report on the synthesis of a complex of unsubstituted 1, 2, 3-triazolo [1, 5-a] pyridine formed in situ via oxidative N–N bond coupling: Structural, photoluminescent, and biological properties of a new Cu(II) complex and its use as a single-source precursor for Cu and CuO nanoparticles, *J. Phys. Chem. Solids* 148 (2021) 109730.
- [16] R. Shoja Razavi, M.R. Loghman-Estarki, Synthesis and characterizations of copper oxide nanoparticles within zeolite Y, *J. Clust. Sci.* 23 (4) (2012) 1097–1106.
- [17] H.-Q. Wu, X.-W. Wei, M.-W. Shao, J.-S. Gu, M.-Z. Qu, Synthesis of copper oxide nanoparticles using carbon nanotubes as templates, *Chem. Phys. Lett.* 364 (1-2) (2002) 152–156.
- [18] N.V. Suramwar, S.R. Thakare, N.T. Khaty, Synthesis and catalytic properties of nanoCuO prepared by soft chemical method, *Int. J. Nano Dimens.* 3 (2012) 75–80.
- [19] Z. Rezaeizadeh, F. Soleimani, B. Mahmoudi, M.A. Nasser, M. Kazemnejadi, Facile synthesis, characterization, and antibacterial activities of CuO, NiO, and Cu₂O metal oxide nanoparticles using polysalicylaldehyde-metal Schiff base complexes as a precursor, *Appl. Phys. A* 127 (2021) 1–13.
- [20] A. Dehno Khalaji, Preparation and characterization of NiO nanoparticles via solid-state thermal decomposition of Ni(II) complex, *J. Clust. Sci.* 24 (1) (2013) 189–195.
- [21] A. Khansari, M. Enhessari, M. Salavati-Niasari, Synthesis and characterization of nickel oxide nanoparticles from Ni(salen) as precursor, *J. Clust. Sci.* 24 (1) (2013) 289–297.
- [22] H. Veisi, B. Karmakar, T. Tamoradi, S. Hemmati, M. Hekmati, M. Hamelian, Biosynthesis of CuO nanoparticles using aqueous extract of herbal tea (*StachysLavandulifolia*) flowers and evaluation of its catalytic activity, *Sci. Rep.* 11 (2021) 1–13.
- [23] P. Selvam, S. Sathiyakumar, K. Srinivasan, T. Premkumar, Effect of alkyl substituent on molecular configuration in a Cu(II) complex: Synthesis of Cu and CuO nanoparticles using a single, solid-source precursor, *J. Mol. Struct.* 1224 (2021), 129011.
- [24] I.M. El-Nahhal, J. Salem, F.S. Kodeh, A. Elmanama, R. Anbar, CuO-NPs, CuO-Ag nanocomposite and Cu(II)-curcumin complex coated cotton/starched cotton antimicrobial materials, *Mater. Chem. Phys.* 285 (2022), 126099.
- [25] A.L. Barry, M.B. Coyle, C. Thomsberry, E.H. Gerlach, R.W. Hawkinson, Methods of measuring zones of inhibition with the Bauer-Kirby disk susceptibility test, *J. Clin. Microbiol.* 10 (6) (1979) 885–889.
- [26] H. Ahmad, K. Venugopal, A.H. Bhat, K. Kavitha, A. Ramanan, K. Rajagopal, R. Srinivasan, E. Manikandan, Enhanced biosynthesis synthesis of copper oxide nanoparticles (CuO-NPs) for their antifungal activity toxicity against major phytopathogens of apple orchards, *Pharma. Res.* 37 (2020) 1–12.
- [27] A.A. Mohamed, M. Abu-Elghait, N.E. Ahmed, S.S. Salem, Eco-friendly mycogenic synthesis of ZnO and CuO nanoparticles for in vitro antibacterial, antibiofilm, and antifungal applications, *Biolog. Trace Element Res.* 199 (7) (2021) 2788–2799.
- [28] I.M. El-Nahhal, J. Salem, F.S. Kodeh, A. Elmanama, R. Anbar, CuO-NPs, CuO-Ag nanocomposite and Cu(II)-curcumin complex coated cotton/starched cotton antimicrobial materials, *Mater. Chem. Phys.* 285 (2022), 126099.
- [29] K. Karthik, A.M. Qadir, Synthesis and crystal structure of a new binuclear copper (II) carboxylate complex as a precursor for copper (II) oxide nanoparticles, *J. Struct. Chem.* 60 (7) (2019) 1126–1132.
- [30] E.E. Elemike, D.C. Onwudiwe, M. Singh, Eco-friendly synthesis of copper oxide, zinc oxide and copper oxide-zinc oxide nanocomposites, and their anticancer applications, *J. Inorg. Organomet. Poly. Mater.* 30 (2) (2020) 400–409.
- [31] A.A. Badawy, N.A. Abdelfattah, S.S. Salem, M.F. Awad, A. Fouda, Efficacy assessment of biosynthesized copper oxide nanoparticles (CuO-NPs) on stored grain insects and their impacts on morphological and physiological traits of wheat (*Triticumaestivum* L.) plant, *Biology* 10 (2021) 233.
- [32] K.S.W.E. Sing, D.H. Haul, R.A.W. Moscou, L. Pierotti, R.A. Rouquerol, J. Siemieniowska, Reporting physisorption data for gas/solid systems with special reference to the determination of surface area and porosity, *Pure Appl. Chem.* 57 (1985) 603–619.
- [33] Y.K. Phang, M. Aminuzzaman, M. Akhtaruzzaman, G. Muhammad, S. Ogawa, A. Watanabe, L.H. Tey, Green synthesis and characterization of CuO nanoparticles derived from papaya peel extract for the photocatalytic degradation of palm oil mill effluent (POME), *Sustainability* 13 (2021) 796.
- [34] A. Chakraborty, D.A. Islam, H. Acharya, Facile synthesis of CuO nanoparticles deposited zeoliticimidazole frameworks (ZIF-8) for efficient photocatalytic dye degradation, *J. Solid State Chem.* 269 (2019) 566–574.
- [35] J. Zhang, S. Gao, G. Wang, X. Ma, S. Jiao, D. Sang, S. Liu, M. Mao, H. Fang, J. Wang, Tunable fabrication of CuO nanoparticles on ZnO nanorods: heterostructure formation by photodeposition for enhanced photocatalytic activity, *Eur. J. Inorg. Chem.* 2019 (2019) 2654–2660.
- [36] M. Alavi, M. Moradi, Different antibacterial and photocatalyst functions for herbal and bacterial synthesized silver and copper/copper oxide nanoparticles/nanocomposites: a review, *Inorg. Chem. Commun.* 142 (2022), 109590.
- [37] A. Venkatramanan, A. Ilangoan, P. Thangarajan, A. Saravanan, B. Mani, Green synthesis of copper oxide nanoparticles (CuO NPs) from aqueous extract of seeds of *Clutteriacardamomum* and its antimicrobial activity against pathogens, *Cur. Biotechnol.* 9 (4) (2021) 304–311.
- [38] S. Jiang, H. Ni, F. Liu, S. Gu, P. Yu, Y. Gou, Binuclear Schiff base copper(II) complexes: syntheses, crystal structures, HSA interaction and anti-cancer properties, *Inorg. Chim. Acta* 499 (2020), 119186.
- [39] D. Wu, L. Guo, S.J. Li, Synthesis, structural characterization and anti-breast cancer activity evaluation of three new Schiff base metal (II) complexes and their nanoparticles, *J. Mol. Struct.* 1199 (2020), 126938.
- [40] B.D. Sali, A.H. Dalaf, M.A. Alheety, W.M. Rashed, I.Q. Abdullah, Biological activity and laser efficacy of new Co(II), Ni(II), Cu(II), Mn(II) and Zn(II) complexes with phthalic anhydride, *Mater. Today: Proceed.* 43 (2021) 869–874.
- [41] A. Muthuvel, M. Jothibas, C. Manoharan, Synthesis of copper oxide nanoparticles by chemical and biogenic methods: photocatalytic degradation and in vitro antioxidant activity, *Nanotechnol. Environ. Eng.* 5 (2020) 1–19.
- [42] A.A. Allothman, M.D. Albaqami, Nano-sized Cu(II) and Zn(II) complexes and their use as a precursor for synthesis of CuO and ZnO nanoparticles: A study on their sonochemical synthesis, characterization, and DNA-binding/cleavage, anticancer, and antimicrobial activities, *Appl. Organomet. Chem.* 34 (2020) e5827.
- [43] H.M. Aly, M.E. Moustafa, M.Y. Nassar, E.A. Abdelrahman, Synthesis and characterization of novel Cu(II) complexes with 3-substituted-4-amino-5-mercapto-1, 2, 4-triazole Schiff bases: a new route to CuO nanoparticles, *J. Mol. Struct.* 1086 (2015) 223–231.
- [44] M.M. Abdelghany, I.S. Ahmed, H.A. Dessouki, E.A. Abdelrahman, Facile synthesis of CuO and Ag nanoparticles by thermal decomposition of novel Schiff base complexes, *J. Inorg. Organomet. Polymers Mater.* 31 (11) (2021) 4281–4299.
- [45] A.A. Oun, J.W. Rhim, Carrageenan-based hydrogels and films: Effect of ZnO and CuO nanoparticles on the physical, mechanical, and antimicrobial properties, *Food Hydrocol.* 67 (2017) 45–53.



PRINCIPAL
JMJ COLLEGE FOR WOMEN (Autonomous)
TENALI

ISSN : 2277 - 7881 : Peer Reviewed & Refereed International Journal
IJMER, Volume 11, Issue 12 (3), December - 2022
Impact Factor : 8.017, IC Value : 5.16, ISI Value : 2.286

**International Journal of
Multidisciplinary Educational Research**
(Social Sciences, Humanities, Commerce & Management, Engineering &
Technology, Medicine, Sciences, Art & Development Studies, Law)

జాతీయ సదస్సు

అంశం

**కాళీపట్నం రామారావు కథలు -
సామాజిక నేపథ్యం**

తేదీ : 6,7 డిసెంబర్ 2022

Editor-in-Chief

Prof. Dr. Victor Babu Koppula

M.A., M.A., M.Phil., P.D.F., D.Litt



Volume 11, Issue 12(3), December 2023
INTERNATIONAL JOURNAL OF MULTIDISCIPLINARY
EDUCATIONAL RESEARCH

జాతీయ సదస్సు

అంశం

కాళీపట్నం రామారావు కథలు -
సామాజిక నేపథ్యం

తేదీ : 6,7 డిసెంబర్ 2022

నిర్వహణ

తెలుగు శాఖ

బి.యం.జి. మహిళా కళాశాల (స్వయం ప్రతిపత్తి)
తెనాలి

Published by

Sucharitha Publications

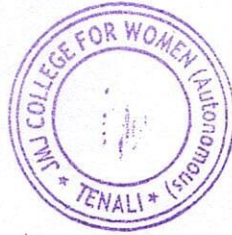
48-12-3/7, Flat No: 302, Alekya Residency

Srinagar, Visakhapatnam - 530 016

Andhra Pradesh - India

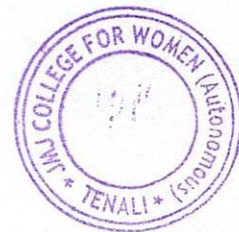
Email: victorphilosophy@gmail.com

Website: www.ijmer.in



విషయ సూచిక ...

Sl. No	Author and Article Name	Page No
1.	యజ్ఞం కథలో ఆర్థిక - సామాజిక అంశాలు విశ్లేషణ బి. భీమమ్మ	1
2.	వీరుడు - మహావీరుడు - కారా కనపాల జోసఫ్	5
3.	జ్ఞాననేత్రాన్ని తెరిపించే 'అప్రజ్ఞాతాం' నల్లపనేని విజయలక్ష్మి	8
4.	కాళీపట్నం రామారావు కథలు - చైతన్య దీపికలు పటం అన్నపూర్ణ	13
5.	కాళీపట్నం రామారావు గారి తీర్పు - సమాజ కుటుంబానికి నేర్పు రాళ్లపాటి లోకనాథం	18
6.	కాళీపట్నం రామారావు కథలు - సామాజిక చైతన్యం - పి.నాగ చందన	21
7.	కాళీపట్నం రామారావు - శ్రామిక వర్గ ప్రాధాన్య కథలు సూక్ష్మ పరిశీలన లెంక సత్యనారాయణ	23
8.	ఉత్తరాంధ్ర ప్రజాసాహిత్యపు ఋగత, కథోపనిషత్ కారా జాడ సీతాపతి రావు	31
9.	సంకల్పం కథ - సామాజిక విశ్లేషణ మన్నెమోని కృష్ణయ్య	34
10.	కాళీపట్నం రామారావు - జీవిత విశేషాలు పి. కేశవులు	40
11.	కారా - జీవధార ఎం.సి. సుధాకర్	43
12.	కాళీపట్నం రామారావు కథలు - విశ్లేషణ యస్. సరళాదేవి	48
13.	అన్నెమ్మనాయురాలు కథ - పరిశీలన సముద్రాల ప్రిసికెల్ల	54
14.	కథా దిక్కుచి - కా. రా ఎం. ప్రదీప్	58
✓15.	కాళీపట్నం రామారావు కథలలో సమకాలీనత బి.మేరికుమారి	62
16.	భయం కథలో సామాజిక స్పృహ బి. శ్రీ లవ పద్మశ్రీ	66





DOI: <http://ijmer.in.doi./2022/11.12.52>
www.ijmer.in

కాశీపట్నం రామారావు కథలు - విశ్లేషణ

డా॥ యస్. సరళాదేవి

తెలుగు అధ్యాపకురాలు

జె.యం. జె మహిళా కళాశాల, తెనాలి

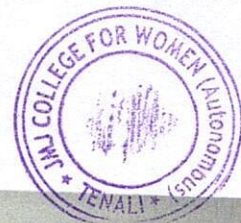
కథ ధాతువు నుంచి 'కథ' పుట్టింది. దీనికి సంభాషించు, చెప్పట అనే అర్థాలున్నాయి. అగ్నిపురాణంలో కథానిక ప్రస్తావన ఉందనీ, సంస్కృతంలో ఇతివృత్తి భేదాన్ని బట్టి "కథా, ఆభ్యాసితా, ఖండకథ, పరికథ" అనే భేదాలున్నాయని చెప్పారు. ప్రస్తుతం తెలుగులో కథ-కథానిక అనేవి సమానార్థకంగా వాడబడుతున్నాయి. ఏ భాషా వ్యవహారాలైనా కథ అంటే ఎక్కువ ఇష్టపడతారు. భారతదేశంలో అతి ప్రాచీన కాలం నుంచి కథా భేదాలున్నాయనీ, ప్రపంచానికి కథా సాహిత్యాన్ని అందించింది. భారతదేశమేనని అనుటలో సందేహంలేదు. వేదకాలం నుండి కథలుండటం, గుణాడ్కుడు 'బృహత్కథ' రాయటం, నన్నయ ప్రసన్న కథకి ప్రాముఖ్యం ఇవ్వడం, కొయ్యల్లోని కథలు, జానపద కథలు, తెనాలి రామలింగని కథలు, కాశీమజిలీ కథలు, పంచతంత్ర కథలు ఈ విధంగా మన దేశంలోనూ కథా మూలాలు ఉన్నాయి.

కథా సాహిత్యం ఎంత గొప్ప ప్రయోజనాన్ని కలిగిస్తుందో కారా గారి సాహిత్యం నిరూపించింది. ఇందులో ఆయన సమాజాన్ని నిశితంగా పరిశీలించిన తీరు తెన్నులు ఈ కథా సంపుటిలో స్పష్టంగా కనిపిస్తాయి. మానవ సామాజిక పరిస్థితులను క్షుణ్ణంగా చదివిన గొప్ప తాత్వికత కలిగిన కథకుడు అనుటలో సందేహం లేదు.

కథా రచనలో కారా మాఫారిది ప్రత్యేక మార్గం. మనుషుల జీవిత చిత్రణ అను, వారి మనస్తత్వ విశ్లేషణను కథాంతర్గతంగా చిత్రించగలిగిన నేర్వరి.

విభిన్న వర్గాలకు చెందిన మనుషులకు, విభిన్న సమస్యలు. ఇందులో మధ్యతరగతి వారి సమస్యలు విలక్షణమైనవి. కొన్ని కల్పించుకున్నవి, కొన్ని తెచ్చిపెట్టుకున్నవి. కొన్ని వ్యవస్థాగత భౌతిక వాస్తవాలూ, కష్టాలు, కన్నీళ్లు, ఆనంద విషాదాలు అతిశయం, ఆత్మన్యూనత, అణకువ, శత సహస్ర వైకల్యాలు, అల్ల సంతోషం ఇవన్నీ వారి కథలలో కనిపిస్తాయి.

వీటి అన్నిటినీ తీసుకొని కథాంశాలుగా మలచే నేర్వరితనం రచయితల్లో అందరికీ





ఉండదు. మరీ ముఖ్యంగా ఇటీవల మధ్యతరగతి గురించి కథ రాయాలంటే రచయితలకు ఒక పిరికితనం, విముఖత, బెరుకు, భయం, విరక్తి కలుగుతున్న దాఖలాలు కనిపిస్తున్నాయి.

మధ్యతరగతి మనుషుల గురించి, వారి అంతరంగ సంవేదనల్ని గురించి రాస్తు పాఠకుల్ని మెప్పిస్తున్నారు. ఈ సంపుటిలోని కథలలో మనకు తారసపడే వ్యక్తులంతా ఈ తరగతికి చెందినవారే వీరంతా కారా గారికి బాగా తెలిసిన వారినే కథా సంపుటాలను చేసి మన ముందుంచారు.

కాళీపట్నం రామారావు గారు వృత్తి లీత్యా ఉపాధ్యాయులు, ప్రవృత్తి కథాకర్షకుడు, కథల్ని కవనంలో కలిగించి కళ్ళకు కట్టించి ఆలోచించేలా చేసే కథా రచయిత కాళీపట్నం రామారావు గారు.

I. స్త్రీ వైతన్యం:

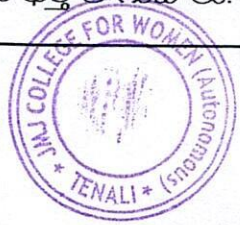
కారా కాలం సొమ్మంగా ఉన్నా, ఆగ్రహావేశాలకు కథనం పుట్టినిల్లు. సామాజిక సంఘర్షణల్లో దోపిడీనీ రూపుమాపాలనుకుని కంకణం కట్టుకున్న కథలు చావు, భయం.

పుట్టుట గిట్టుట కొరకే అన్నట్టు చావు కథలో మనిషి చనిపోవటం సహజం. చలీ, చీకటి ఎప్పడు పోతాయో, ఎర్రగా పొద్దెప్పుడు పొడుస్తోందీ, ఎప్పడు ఎండ వస్తుంది అనే ఆలోచనే ఉంటుంది. పూడల్ చలి నుంచి సమాజం బయటపడి, చైతన్యమై, జ్ఞాన మార్గంలో వెలుగుతూ నూతన సమాజ ఆహ్వానాన్ని దర్శింపచేసేలా చెప్పడం ఈ కథలో అంతరార్థం.

అట్టడుగు స్త్రీ పాత్రల్ని వారు ఎదుర్కొంటున్న సమస్యల్లో అణచివేత పీడన చుట్టూరా ఉన్నాయి. మాగాణి జీవితంలో భార్యగా వచ్చిన స్త్రీని ఒక వస్తువుగా చూసే స్థితిని ప్రత్యక్షంగా చూపారు. ఇందులో ముగ్గురు స్త్రీలు బలైన విధానాన్ని చూపారు. నారెమ్మ భర్త ప్రవర్తనకు అణిగి మణిగి ఓపికతో జీవించి మరణించింది.

రెండోది ముసలమ్మ పాత్ర. ఈ పాత్రలో ముసలమ్మ చలికి తట్టుకోలేక ఈ చలికే నేను చచ్చిపోతాను. శీతాకాలం, కర్ర లెక్కడా దొరకవు, కర్రలు దొరికితే నన్ను కర్రలలో కప్పిపెట్టండి. లేకపోతే ఎక్కడయినా కొనుక్కునో, లేదా అడుక్కునో, చివరికి దొంగతనం చేసినా సరే, కర్రలతో నన్ను కాలేయండి. ఇది చలి నుండి విముక్తి కోసం ముసలమ్మ కోరిక. ఈ విముక్తే స్త్రీల చైతన్య జనంలాగా సూచన. సహజత్వాన్ని కలిగించేలా వర్ణించాడు.

మూడో స్త్రీ ముసలమ్మ కూతుర్లలో చివరమ్మాయి. ఆమె భర్త తాగుబోతు. వాడి పెట్టే

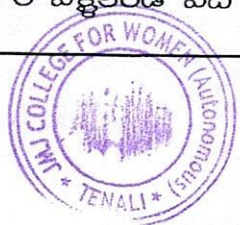




బాధల్ని తట్టుకోలేక వేరే వాడితో లేచిపోయి, ఆమె సహనంతో తన బతుకును పునఃనిర్మించుకుంది. ఈమె నిర్ణయం తల్లికి నచ్చకపోయినా జీవితాన్ని సుఖమయం చేసుకొడానికి అదో మార్గంగా చూపాడు. స్త్రీకి ఒక ఆలోచన ఉంటుందని, ఆమెకు ఒక మనస్సుంటున్నది అనే స్పృహను స్త్రీ కోణంలో నుంచి ఆలోచించాలనే తత్వాన్ని ఇక్కడ పాఠకులకు తెలిపినారు.

II. సామాజిక స్పృహ - కొంత పాలం వ్యవసాయం చేయాలనుకునే వెంకయ్య నాయుడు అనే రైతు ఎలా మానసికంగా కృంగిపోయాడో “కీర్తి కాముడు” అనే కథనం ద్వారా చూపించారు. దేశానికి వెన్నెముక రైతు. “బలహీనులు” కథలో కథానాయిక ఒక అందమైన నర్స్. నాకు దేవుడి మీద నమ్మకం ఉంది. అంటూ కథను మొదలు పెట్టి దేవుడు యిది నాకిచ్చిన శిక్షయేమోనని అనుమానం కలుగుతుంది అని ముగించాడు. ఇక్కడ ఏ పాత్రకూ పేరు లేదు. అందులో ఉన్న అమ్మాయిని వర్ణిస్తూ లోకంలోని సాందర్భ ధనులలో నేను ఒకర్లని. రంగు నల్లనైనా అందులో అందం ఉంది. తీర్చిదిద్దిన వంపులతో నా సుందరమైన నల్లని కాంతుల శరీరానికి తెల్లని చీర కడితే నా రూపం ఆరి తేరిన చిత్రకారుడితో చిత్రించిన బ్లాక్ అండ్ వైట్ షేడ్స్ చిత్రంలో ఆకర్షణగా ఉండేవి. ఎదురైన వ్యక్తులల్లా నా వైపు రెండవసారి చూడకుండా నడచిపోవడం ఆ నా పద్దెనిమిదేళ్లలో ఎప్పుడూ యెరగను. బలహీనులు అని ఆడవారి పట్ల మగవారు ఎలా ఉంటారో చెబుతూనే ఇందులో ఆ నర్స్ అతడి అభిప్రాయాన్ని తెలిసి కూడా పట్టించుకోక పోవటం ఆమె కన్నులో రంద్రం పడడంలో చూపిస్తాడు.

‘అల్లి’ కథలో పైగడయ్య గంగమ్మతో తనలోని మానసిక స్థితిని వ్యక్తంచేసే సంధర్భంలో నేను ఆరు నెలలు అయ్యి ఆడ మనిషి కోసం ఉపవాసం ఉన్నాను. ఇయ్యాల ఇంటికొస్తే మాయమ్మా, అత్తా కుమ్ములాడుకొని మమ్మల్ని విడదీసినారు. నిన్న రాత్రికి దానిని తవిటప్ప ఇంటికి రమ్మన్నాను. దానికీ నా బాధ అర్థమైనట్టు లేదు కావాలంటే, పట్టణంలో నా ఇష్టం వచ్చినట్టు ఉండగలను. నా తోటి వాళ్ళంతా యెలాగో తంటాలు పడుతున్నారో నేను చూస్తునే ఉన్నాను. అన్నిటో అలా గుండొచ్చుగాని, ఆడ దాని దగ్గర అలా, గుండాలంటే మనసు ఒప్పుకోవడంలేదు. ఇరుగమ్మతో పోరుగమ్మ పాటుపడితే ఇల్లిరగతీ మాలబీ కన్నె పిల్లని సెరిపితే, కలకాలం దాని ఉసురు కలకాలం దాని ఉసురు తగుల్తాది. మరింక రోడ్డోర మనసులుంటారు. ఆల ఊలికెల్లె ఆసుపత్రికి పోవడం సరేసరి - పనిలోకి వెళ్ళకండి పది రోజులుండే కూలి





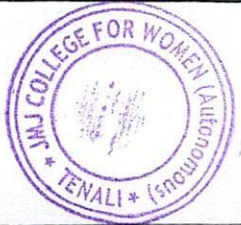
డబ్బులు మాట ఏమిటి ? అందుకే నా బాధ నాకు తెలియాలనీ ఆ దేవుడికి తెలియాలన్నారు. “ఇక్కడ శ్రమిక జీవన విధానం వారి ఆర్థిక స్థితిని ఒక ఆడ మనిషి కోసం ఉపవాసం ఉండటం ఇంట్లో తగాదాలు, పట్టణంలో నా వ్యక్తిగతమైన ఇష్టాలు ఉంటాయి. పల్లెలో అలా ఉండడానికి అవకాశంలేని పరిస్థితి వారి మానసిక స్థితి విలక్షణం. మాండలిక పదాలతో గ్రామీణ జీవితాన్ని చూపారు. ఇది బలహీనుల కథకు విభిన్నమైనతత్వం.

III. కుటుంబ పరిస్థితులు :-

“పలాయతాడు” కథలో సమస్యల నుంచి పారిపోయిన రాజశేఖరాన్ని చూపారు. డిగ్రీ చదువుకున్నా ఆ చదువుకు కారణమైన మేనమామ, ఇష్టంలేని అతడి తత్వానికి ఏ మాత్రం పొసగని మేనమామ కూతురుతో పెళ్ళి స్నేహితులు, చుట్టాలుకు పెట్టే ఖర్చులు, ఖర్చులకు చాలని జీతం... ఇలా ఎన్నో ఆర్థిక కష్టాలను ఆలంబనంగా సాగిన కథనమిది. పోట్లాడి స్నేహితులెలా కావచ్చో చూపిన పాత్ర రాజశేఖరం.

సినిమా హాల్లో సీటు మీద కర్చీఫ్ వేసి ఆపిన సీట్లో మరొకరు వచ్చి కూర్చోగా ఆరంభమైన చిన్న పాటి తగాదా నేపథ్యంలో కొంత వరకు సాగిన ప్రస్థానం రాజశేఖర్ గది వరకు వచ్చి, ఇబ్బంది పడిన క్షణం వరకు విచిత్రమైన మనిషి అనుకుంటూనే టూకీగా కథ సాగింది. పైగా మరింతా సినిమా హాలు సంఘటన మరచిపోతేలేదనుకుంటాను అనటం సాధారణమైన సంభాషణగానే సాగింది. ‘ఒక్క సారిగా మీకు స్వీట్లు, హాట్లు తాదు కదా బట్టి కాఫీ కూడా నేను పోయదలచుకోలేదు. నా జేబులో చాలా డబ్బులున్నాయి. కానీ మీకు దమ్మిడి అయినా ఇవ్వను. దమచేసి మీరు నన్ను వేదించకండి. ఇంతకు ముందు నిత్యం మిరిట్ల నా గదికి వచ్చి నాకిబ్బంది కలిగించడం నేను భరించను. మీరింక నా గదికి రాకండి’ అనడం కథకు మరో మలుపు.

‘మనిషి కృతజ్ఞత చూపించిన విధం చూస్తే జాలీ, అందులో వ్యక్తమైన నా తోడి ఆయన స్నేహం తలచుకుంటే మహాదానందం కలిగాయి’ అంటూ కథకుడి మానసిక స్థితిని చెప్పే ప్రయత్నం చేశాడు. విన్నవా బాబూ! పిల్లదాని వంటి మీద బంగారం అంతా అమ్మేశాడు. నాలుగు తులాల గొలుసు, రెండు తూలాల పుస్తెలను, తులంన్నర ఎత్తు గాజుల జత, సమస్తం అమ్మేశాడు, ముక్కువీ, చెవివే మాత్రం ఇంకా ముట్టుకోలేదు. మంగళ సూత్రం కోలికి వెళ్ళలేదు. సర్వగుటకాయ స్వాహా అంటూ రాజశేఖరం మేనమామ చెప్పడంతో





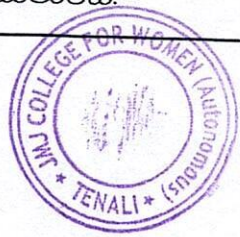
రాజశేఖర్ మిత్రులకు చుట్టూలకు ఎలా ఖర్చులకోసం డబ్బులు వాడుతున్నాడో తెలుస్తుంది. ఇద్దరు మిత్రులు ఒకరికొకరు ఉత్తరాలు రాయడం ఉండేది. కాకపోతే రాజశేఖర్ ఒకేసారి ఉత్తరం రాశాడు. మూడేళ్ల తర్వాత, మానవుడు సామాజిక జీవి అని, అతడి కష్ట సుఖాలు, ఆనంద విషాదాలు, లక్ష్యాల సాధించటం, సాధించకపోవడం, అతని ప్రయత్నం, ఒక్క దాని మీదే ఆధారపడి ఉండవనీ, ఎవడి జీవిత పగ్గాలు వాని చేతుల్లోనే ఉన్నట్లు కనిపించినా నిజానికి అవి అతడి చేతులలో లేవనీ, బహుశా మీరు గ్రహించగలిగి ఉండరు. అందుకు కారణం మీరెప్పుడు మళ్ళాపారబడుతున్నట్లు మీ ప్రయాణం లోపం ఒక్కటే కాదు. మీ పుట్టుక, మీ పుట్టుకకు ముందే మీకై పోర్టడిపోయిన జీవన పథ ప్రమేయం కూడా చాలా ఉంది. అంటూ సుదీర్ఘ జీవితాను భవగీతను బోధిస్తున్నట్లు ఒక వేగంతో కథనాన్ని నడిపించారు.

ఇంతా అనుభవంలో తను సంపాదించిన సత్యాలు, ఇలా చైతన్య స్రవంతి ధోరణిలో సాగుతుంది లేఖావ్యాసంగం, చివరికి ఈ ఇంద్ర జాలానికంతటికీ కారణం ఇప్పుడు మానవుడనుసరిస్తున్న ఆర్థిక విధానం అంటూ ఆర్థిక సంబంధాల స్థితిలోకి తీసుకువస్తాడు. తనదైన వ్యక్తిత్వాన్ని చంపుకుంటూనే ఎన్నో ఉద్యోగాలు చేసిన కచ్చితత్వాన్ని వదలని వాడు, చివరికి కుటుంబం నుంచి పలాయనం చిత్తగించడమే ఈ పలాయతుడు కుటుంబ అనుబంధాల ప్రధానంగా సాగే కథలులో మరొకొన్ని “అభిమానాలు” కథ సుదీర్ఘమైంది. 18 సంఘటనల సమాహారం చలపతి అనే చిన్న పిల్లాడి పట్ల భాస్కరం అనే చిన్నాన్న పాత్ర ఎలా ప్రవర్తించాడు, ఆలోచించాడు అనే విషయాలు ఉన్నాయి.

‘జీవధార’ ఈ కథలో మానవ విలువల చర్చి ఉంది. అందరూ సమ్మతిగా సంతోషంగా ఉండాలనే మానవ లక్ష్యాన్ని చూపారు నీళ్ల కోసం స్త్రీలు పడే బాధను బాగా వర్ణించారు. స్త్రీలను వ్యక్తిగా, శ్రమజీవిగా చూడడం ఈ కథలో ప్రత్యేకం.

IV. మానవతా విలువలు :-

మహదాశిర్వచనం అనే కథలో కుటుంబంలోని స్త్రీ, పురుషుల సంబంధాలతోపాటు దేశంలో ఆర్థిక పతనం, రూపాయి విలువ పడిపోవడం లాంటి విషయాలున్నై, ఆర్థిక మాంద్యంలో ఒక మధ్యతరగతి, స్త్రీలపై మాంద్యం ప్రభావం బాధ్యత వహించాల్సిన ప్రభుత్వం ఏమి చెబుతుంది. పార్లమెంటుల ప్రజాస్వామ్యం, కుటుంబ వ్యవస్థపై విమర్శలు, రక్షణలేని జీవితం అంశాలపై మహదాశిర్వచనం కథ చెబుతుంది.





“అభిశంఖులు” అనే కథలో అభిశాపమో ఊరక మోపిన నింద. బ్రహ్మాణితో లేచిపోయిన వచ్చిన రాఘవమ్మ అనే స్త్రీ జీవితం ఇందులో ప్రధానాంశం, ఆమె పడిన అగచాట్లు కూతుర్ల పెళ్ళి, ఇవన్నీ పంచాయితీలో తగవుకు వస్తాయి, ఇవే ఆమె ముసలితనంలో అభిశంఖుల, కులం, భర్తలేని స్త్రీ జీవితం సమాజంలో చిన్నచూపు, ‘నేనేం మణులు కోరలేదు, మాన్యాలు కోరలేదే, పట్టణాలు పాయసాలు కోరలేదే కట్టెందుకి చుట్టు చెంగాయి చీరలూ అలంకరించుకునేందుకి ఆభరణాలు కోరలేదే, ఏం కోరాను, పిడికెడు మెతుకులు, వాడి కంచం దగ్గర, వాడి పిల్లల కంచం దగ్గర, వాడి పెళ్ళం కంచం దగ్గర రాలేపాటి మెతుకులు కోరాను. వాడి పెళ్ళం కుడి చేత్తో వేసినా, ఎడంచేత్తో వేసినా, మలకలో పోసినా, మహాన విసిరేసినా మహాభాగ్యం అని అందుకుంటానన్నాను. ఆమె నన్ను ఎంత తిట్టినా పడతానన్నాను. తలంతా బొప్పిలు కట్టిట్టు మొట్టికాయలు మొట్టిన పెదవి కదపనన్నాను. ఇది రాఘవమ్మ జీవిత అంతిమ దశ, వృద్ధాప్యం, చిన్న చిన్న వాక్యాల్లో అంతులేని బాధను దైన్యాన్ని కళ్ళకు కట్టించి కంటతడిని పెట్టించాడు రచయిత,

తెలుగు సాహిత్యంలో ప్రచురించబడిన కథలను భావి తరాల వారికి పొందుపరచాలన్న బృహత్తర ఆశయంతో కాళీపట్నం రామారావు గారు కథానిలయన్ని స్థాపించాడు. తెలుగు కథకు అక్షుత్తమమైన ఘనత దక్కింది.

ఆధార గ్రంథాలు

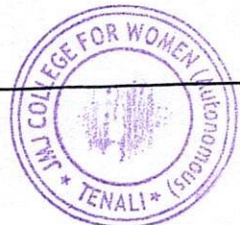
సాహిత్య ప్రస్థానం - జూన్ 2021 (సాహిత్య పత్రిక)

కీర్తికాముడు - ఆంధ్రపత్రిక 1949

అభిశంఖులు - ఆంధ్రపత్రిక ఉగాది

పొద్దు - అంతర్జాల తెలుగు పత్రిక

S. S. S.
PRINCIPAL
JMJ COLLEGE FOR WOMEN (Autonomous)
TENALI



ISSN : 2277 - 7881 : Peer Reviewed & Refereed International Journal
IJMER, Volume 11, Issue 12 (3), December - 2022
Impact Factor : 8.017, IC Value : 5.16, ISI Value : 2.286

**International Journal of
Multidisciplinary Educational Research**
(Social Sciences, Humanities, Commerce & Management, Engineering &
Technology, Medicine, Sciences, Art & Development Studies, Law)

జాతీయ సదస్సు

అంశం

**కాళీపట్నం రామారావు కథలు -
సామాజిక నేపథ్యం**

తేదీ : 6,7 డిసెంబర్ 2022

Editor-in-Chief

Prof. Dr. Victor Babu Koppula

M.A., M.A., M.Phil., PDF, D.Litt



Volume 11, Issue 12(3), December 2023
INTERNATIONAL JOURNAL OF MULTIDISCIPLINARY
EDUCATIONAL RESEARCH

జాతీయ సదస్సు

అంశం

కాళీపట్నం రామారావు కథలు -
సామాజిక నేపథ్యం

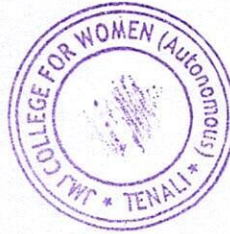
తేదీ : 6,7 డిసెంబర్ 2022

నిర్వహణ

తెలుగు శాఖ

బి.యం.బి. మహిళా కళాశాల (స్వయం ప్రతిపత్తి)
తెనాలి

Published by
Sucharitha Publications
48-12-3/7, Flat No: 302, Alekya Residency
Srinagar, Visakhapatnam - 530 016
Andhra Pradesh - India
Email: victorphilosophy@gmail.com
Website: www.ijmer.in



విషయ సూచిక ...

Sl. No	Author and Article Name	Page No
1.	యజ్ఞం కథలో ఆర్థిక - సామాజిక అంశాలు విశ్లేషణ బి. భీమమ్మ	1
2.	వీరుడు - మహావీరుడు - కారా కనపాల జోసఫ్	5
3.	జ్ఞాననేత్రాన్ని తెరిపించే 'అప్రజ్ఞాతాం' నల్లపనేని విజయలక్ష్మి	8
4.	కాళీపట్నం రామారావు కథలు - చైతన్య దీపికలు పటం అన్నపూర్ణ	13
5.	కాళీపట్నం రామారావు గారి తీర్పు - సమాజ కుటంబానికి నేర్పు రాళ్లపాటి లోకనాథం	18
6.	కాళీపట్నం రామారావు కథలు - సామాజిక చైతన్యం - పి.నాగ చందన	21
7.	కాళీపట్నం రామారావు - శ్రామిక వర్గ ప్రాధాన్య కథలు సూక్ష్మ పరిశీలన లెంక సత్యనారాయణ	23
8.	ఉత్తరాంధ్ర ప్రజాసాహిత్యపు ఋగత, కథోపనిషత్ కారా జాడ సీతాపతి రావు	31
9.	సంకల్పం కథ - సామాజిక విశ్లేషణ మన్నెమోని కృష్ణయ్య	34
10.	కాళీపట్నం రామారావు - జీవిత విశేషాలు పి. కేశవులు	40
11.	కారా - జీవధార ఎం.సి. సుధాకర్	43
12.	కాళీపట్నం రామారావు కథలు - విశ్లేషణ యస్. సరళాదేవి	48
13.	అన్నెమ్మనాయురాలు కథ - పరిశీలన సముద్రాల ప్రిసిక్విల్	54
14.	కథా దిక్కుచి - కా. రా ఎం. ప్రదీప్	58
15.	కాళీపట్నం రామారావు కథలలో సమకాలీనత బి.మేరికుమారి	62
16.	భయం కథలో సామాజిక స్పృహ బి. శ్రీ లవ పద్మశ్రీ	66





కాళీపట్నం రామారావు కథలలో సమకాలీనత

డా॥ బి. మేరికుమారి,

జె.యం.జె. మహిళా కళాశాల (స్వయంప్రతిపత్తి), తెనాలి.

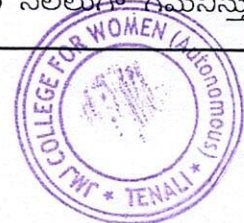
కథ ఉజ్వల భవిష్యత్తుకు శ్రీకారం చుట్టిన ఘనుడు కాళీపట్నం రామారావు. ఆడంబాలు లేని సాధారణ జీవితం ఆయన సొత్తు. కేంద్ర సాహిత్య అకాడమీ అవార్డు అందుకోవడం ఆయన మహత్తు. కాళీపట్నం రామారావు సమాజంలో దిగువ, మధ్యతరగతి వాళ్ళ శ్రమకు తగ్గ ఫలితం లేదని గుర్తించి, కథను ఒక ఆయుధంగా చేపట్టారు.

అధ్యశ్నము :

నేటి సమాజంలో వున్న మనుషుల మధ్య వున్న అంతరంతాలను ఈ కథలో చూపించారు.

లలిత అయిదవ తరగతి వరకు చదువుకున్న అమ్మాయి. గవర్నమెంటు ఆఫీసులో నెలకు యాభై రూపాయలు జీతం తీసుకుంటున్న అబ్బాయి నచ్చలేదు. ఇంతలో లలిత పెద్ద బావగారికి విశాఖపట్నానికి ఉద్యోగం ట్రాన్స్ఫరు అయ్యింది. విశాఖపట్నం చూడాలని అక్క బావలతో కలిసి విశాఖపట్నం వచ్చింది. విశాఖ వెళ్ళాక అక్కడి ప్రజల దుర్భరజీవితాన్ని కళ్ళార చూసింది. పెరుగుకు బదులు మజ్జిగ, నేతికి బదులు ఆముదం వాసన వేసే నేయి లలితకు ఇవి బాగుండలేదు అనిపించింది. వీటి అన్నింటితో ఆమెకు విశాఖలో ఉండబుద్ధి కాలేదు. వాళ్ళ అక్క ప్రక్క పోర్ట్ లో అనూరాధ అనే ఆమె ఉండేది. ఆమెతో చనువు ఏర్పడి, నువ్వు నువ్వు అనే స్థితికి వచ్చారు.

లలిత మధ్యాహ్నం ఒంటిగంటకు అనూరాధ ఇంటికి వెళ్ళింది. ఆమె అప్పుడు వీధి కిటికీ దగ్గర నిల్చుని నవ్వుముఖంతో బయటికి చూస్తుంది. మెల్లగా దగ్గరకు వెళ్ళి ఆమె వంక చూడగా ఎదురింటి గదిలో తనకన్నా రెండు సంవత్సరాల చిన్న అయిన యువకుడితో సంజ్ఞలు చేస్తుంది. లలితను గమనించిన యువకుడు వెళ్ళిపోయాడు. అనూరాధ తేలు కుట్టిన దొంగలా, తెల్లముఖం వేసుకుని బేబులు దగ్గరకు వచ్చి కూర్చుంది. నువ్వు చూశావా అని అడిగింది. లలిత లేదని అబద్ధం చెప్పింది మరల ఇంకొకసారి చూడటంతో అతనిని ప్రేమిస్తున్నావని ఆమెను అడిగింది. అందుకు అనూరాధ నేను అతనిని గత ఆరు నెలలుగా గమనిస్తున్నాను. అతడు





ఏనాడు శుభ్రంగా ఉండడు మాసిన గడ్డంతో ఉంటాడు. ఒకసారి అతని వంక పరిశీలనగా చూశాను అతనిలో మార్పు వచ్చి గాలి మేడలు కట్టుకున్నాడు అనుకొని నేను రెండు రోజులు కనపడకుండా ఉండేటప్పటికి అతడు పాత రూపం ఏర్పరుచుకున్నాడు. నా సముఖ్యంలో అతడు ఆనందంగా ఉంటాడు నాకు పోయేదేమిటి నాకు వచ్చేదేమిటని అతనివైపు చూస్తూ వుంటాను. ఉదయాన్నే మేలుకొలుపు పాట పాడతాడు. ఆరోగ్యానికి పాటించవలసిన విషయాలు వీలు కుదిరినప్పుడు చెప్తూ ఉంటాడు. రాత్రి వేళ నిద్రపోయేటప్పుడు నాకోసం జోలపాట పాడతాడు. ఈవిధంగా రోజులు మాకు కులాసాగ్గుగా సాగుతున్నాయి. దీనివల్ల నష్టం లేదు అని అంటుంది. తన మాటకారితనంతో లలితను యధాస్థితికి తీసుకొని రావాలని ప్రయత్నించింది. కాని చేయలేక పోయింది. శారీరకంగా కన్నా మానసికంగా చేసే వ్యభిచారమే ఎక్కువ నీది అని లలిత అంది. 'దానికి అనూరాధ నీవు చెయ్యటం లేదా వ్యభిచారం ? కథలు చదివేటప్పుడు అందమైన యువకులతో ఎన్నిసార్లు వ్యభిచారం చేశావో? ఎన్ని నిద్రలు లేని రాత్రులు గడిపారో. నూటికి లాంఛై తొమ్మిది మానసికంగా చలించిన వారే అని అన్నది. అనూరాధ సమర్థన బలంగా ఉందని వాళ్ళకి శారీరక సంబంధం కూడ ఉందని తన జాణ తనం ఎక్కువగా ఉపయోగించిందని అది బయట పడనీయలేదు అని తనలో తాను అనుకుంటుంది. అనూరాధ చదివిన బి.ఎ. అవినీతి సమర్థనకు ఉపయోగించి అవినీతి మార్గానపడి పతిత అయ్యిందని అనుకుంది. తర్వాత కొద్ది రోజులకు వాళ్ళ బావ సంబంధం ఎక్కడ దరకొనట్లు అతనినే ప్రతిపాదిస్తాడు. గుణశీలానికి ప్రాధాన్యత ఇచ్చే భారతనారి దుర్మార్గుడు, నీచుడు, రౌడీగా వున్న అతనిని ఎలా స్వీకరిస్తుంది అని? సమాజానికి వదిలివేయటం ఆయన కథ చివరిలో కనిపించే వ్యంగ్యం అని అనుకోవచ్చు.





Cover Page



DOI: <http://ijmer.in.doi./2022/11.12.55>
www.ijmer.in

బలానికి లక్ష్యం :

ఈ కథలో మనుష్యుల మధ్య వున్న తేడా, పట్టణము పల్లెటూరి వాళ్ళను, ధనవంతులు బీదవారిని, ఉద్యోగులు రైతు కూలీలను అగౌరవరచ దానికి వీలు లేదు అని తెలియజేసే కథ.

అయ్యారు హోటల్ నడుపుతుంటాడు. అతని యొక్క మనుష్యులు రైతును అతనిని తీసుకొని వచ్చి అయ్యారు ముందు నిలబెట్టారు. అందుకు ఆ హోటల్ కి వచ్చిన పెద్ద మనిషి అతనికి క్షమాపణ చెప్పండి అని అయ్యార్ కు చెప్పాడు. అక్కడ వున్న వారిలో వెనుక నుండి అసలు జరిగినదేమిటి, ఎందుకు క్షమాపణలు చెప్పాలి అని అడిగినప్పుడు పెద్ద మనిషి ఈ విధంగా చెప్పాడు. రైతు బిల్లు చూపిస్తూ బహుశ చదువు రాదేమో యెంత బాబూ అని అడిగాడు దానికి అయ్యగారి జవాబు అధికారం ఉట్టిఫడే స్వరంతో మూట విప్పురా! ఆ రూపాయి అక్కడ పెట్టరా! మిగతా చిల్లర పట్టుకు పోరా! ఇదివరస ఆ రైతు ఇచ్చిన గౌరవానికి యీయన ఇచ్చిన జవాబు చూడండి అని అయ్యారు వంక తిరిగి మేము నీ దగ్గర కొనుక్కాని నీకిచ్చే డబ్బులలో మిగుల్చుకున్న లాభం వల్లే బ్రతుకుతున్నావు. మేము నీవల్ల బ్రతకడం లేదు కాబట్టి నీ బ్రతుకుకకి ఆధారమైన మమ్ములను గౌరవించాలి. నాగరికత ఎందుకు గౌరవించి పలకరించిన వానికి జవాబుగౌరవ పూర్వకంగా ఇవ్వాలి. ఈరోజులలో ఒక మనిషిని మరొక మనిషి అగౌరవిస్తే సహించడం మరిచిపోతున్నాం. ఇతనికి క్షమాపణ చెప్పండి. ఇది తప్పని అయ్యారతో పెద్దది మనిషి మాట్లాడాడు. అందుకు అయ్యారు తన వెనుక బలం, బలగం ఉందని మిమ్మల్ని నేను ఏమైనా అన్నానా ఎవరినో ఏమో అంటే మీకెందుకూ మీ దారిని మీరు పొండి అని పెద్ద మనిషితో అన్నాడు. అందుకు పెద్ద మనిషి ఈరోజుల్లో వాడు నేను అనే చీలిక బుద్ధి సంకుచితత్వం కొద్దిరోజుల క్రిందటే పోయాయి. ఇప్పుడు మనము, మేము అనేవి మాత్రమే మిగిలాయి. అందుకు అతనికి క్షమాపణలు చెప్పండి అని మరల అడుగుతాడు. నిజాన్ని నిలబెట్టి అడిగితే దాని వెనుక అనేక మంది ఉంటారు అనేదానికి అక్కడ వున్న విద్యార్థి, అతనితోపాటు ఇంకా కొంతమంది అయ్యారును క్షమాపణ చెప్పమని ప్రశ్నించారు. అందుకు ముఖం ముడ్చుకుని నాటకంలో లాగ క్షమాపణ చెప్పేసాడు. బాబుకు ఎందుకు ఈ గొడవంతా అని అతనిని పోని అని రైతు పెద్ద





INTERNATIONAL JOURNAL OF MULTIDISCIPLINARY EDUCATIONAL RESEARCH
ISSN:2277-7881; IMPACT FACTOR:8.017(2022); IC VALUE:5.16; ISI VALUE:2.286

Peer Reviewed and Refereed Journal: VOLUME:11, ISSUE:12(3), December: 2022
Online Copy of Article Publication Available (2022 Issues)

Scopus Review ID: A2B96D3ACF3FEA2A

Article Received: 2nd December 2022

Publication Date: 10th January 2023

Publisher: Sucharitha Publication, India

Digital Certificate of Publication: www.ijmer.in/pdf/e-CertificateofPublication-IJMER.pdf

DOI: <http://ijmer.in.doi/2022/11.12.55>
www.ijmer.in

మనిషి అన్నప్పుడు ఈరకమైన అనాసక్తి వల్లే మీ గౌరవాన్ని మంటకలిపింది అని అంటాడు.

అప్పటి కాలం కన్నా ఇప్పుడు కాలంలో ప్రతి విద్యార్థిలో సహకారం, బిక్యత, ముందంజ నేడు ప్రత్యక్షంగా చూశాము అని పెద్ద మనిషి విద్యార్థులతో అంటూ ఇక ముందు కూడ కొనసాగించండి అంటాడు. ఎవ్వరిని తక్కువ చేయకూడదు అనే బలీయమైన వాంఛ అతనిని ఇంతవరకు నడిపించింది.

రచయిత చివరలో బలానికి లక్ష్యం ఇది అని కొనమెరుపు చూపిస్తాడు.

కాళిపట్నం రామారావు కథా ప్రియుడు. తను ఎన్నుకున్న తనకు నచ్చిన అంశాన్ని ఎన్ని కథలుగా మలిచాడు. ఈ కథలను పరిశీలిస్తే సమాజానికి ఉపయోగదేవి, సమాజాన్ని చైతన్యపరిచేవి ఉన్నాయి. మనిషి యొక్క నడవడికను, మనుషుల మధ్య సమానత్వాన్ని, తెలియచేసే కథలు ఎక్కువగా వున్నాయి. శ్రామికులు, కార్మికులు, రైతులు ఎక్కువగా కష్టపడుతున్నారని కష్టానికి ఫలితం దక్కటం లేదని వాటిని గురించి చూపించాడు.

ఉపయుక్త గ్రంథాలు :-

కాళిపట్నం రామారావు రచనలు.

కథానిక శిల్పం - వల్లంపాటి వెంకట సుబ్బయ్య

కథానికీ వాగ్మయం - పోరంకి దక్షిణామూర్తి



S. S. S. S.
PRINCIPAL
JMJ COLLEGE FOR WOMEN (Autonomous)
TENALI

Artificial Intelligence technologies on Human Resource Management: A study with Reference to Indian It Sector at Hyderabad, Telangana.

¹P. NARASIMHA BABU, ²DR.P.V. VARA PRABHAKAR, ³DR.PCH.PRAVEEN KUMAR

¹Research scholar in business management, ²Associate professor

^{1,2}Yogi Vemana University, Kadapa

^{2,3}Department of business management

Yogi Vemana University, Kadapa

³Sri Hari Degree College, Kadapa

ABSTRACT: Artificial Intelligence is fleetly revolutionizing so numerous diligences at such an intimidating rate that one similar advanced AI robot, Sophia, joined the panel and was pitched questions during the United Nations's convention on sustainable development. Artificial intelligence is producing multiple results for hiring directors including introductory recruiting tools, intermediate operations and advanced AI results. AI can cover workers' performance, and engagement, furnishing HR brigades with precious perceptivity. nearly all companies are using artificial intelligence to increase effectiveness of mortal coffers in IT Sector. The action begins with automated process in reclamation till performance appraisal of workers. Organizational leaders and mortal resource directors have faith that incorporating artificial intelligence (AI) into HR functions like on- boarding and administration of benefits can and will ameliorate the overall hand experience. Artificial intelligence is producing multiple results for hiring directors including introductory recruiting tools, intermediate operations and advanced AI results. Artificial intelligence (AI) is transubstantiating the mortal coffers field altogether. In this period of constant change and digital Dearth's, Chancing the right gift is more grueling than ever. By using AI and robotization, businesses can identify a different range of top campaigners snappily and fluently, and at a pace that keeps stride with the frenzied speed of ultramodern business.

Key words: Artificial intelligence, HR brigades, Robotization, Transubstantiating, Introductory recruiting tools , Performance appraisal of workers.

INTRODUCTION:

Artificial Intelligence is a system of making a computer, a computer- controlled robot, or a software suppose intelligently like the mortal mind. AI is fulfilled by studying the patterns of the mortal brain and by assaying the cognitive process. In computer system , artificial intelligence (AI), occasionally called machine intelligence, is intelligence demonstrated by machines, in discrepancy to the natural intelligence displayed by humans and other creatures. Computer wisdom defines AI exploration as the study of " intelligent agents " any device that perceives its terrain and takes conduct that maximizes its chance of successfully achieving its pretensions. Kaplan and Haenlein define AI as "a system's capability to rightly interpret external data, to learn from similar data, and to use those literacy to achieve specific pretensions and tasks through flexible adaption". Colloquially, the term " artificial intelligence " is applied when a machine mimics " cognitive " functions that humans associate with other mortal minds, similar as " literacy " and " problem working ". Artificial intelligence is a computer term which is used for software, machines and computers.

In the time 1920 during a wisdom fabrication play named Rossum Ovi UniversalLink Robotti which means- Rossum's Universal Robots, also more known as R.U.R. by Czech pen Karel Capek the term ROBOT was originally used. The term artificial intelligence was first introduced by John McCarthy in 1956 in his first academic conference on the subject. But this trip of knowing this area in further depth had started much before than that. How HR can include AI in their business strategy? By exploiting machine literacy, the company will see an acceleration in its processes. A long- term approach will involve regarding AI and mortal labor as a collaboration. By applying a factual approach, the first service to be affected by AI is IT. The compass of AI is disputed as machines come decreasingly able, tasks considered as taking " intelligence " are frequently removed from the description, a miracle known as the AI effect, leading to the idiosyncrasy in Tesler 's Theorem, " AI is whatever hasn't been done yet. " For case, optic character recognition is constantly barred from "artificial intelligence ", having come a routine technology. ultramodern machine capabilities generally classified as AI include successfully understanding mortal speech, contending at the loftiest position in strategic game systems (similar as chess and Go), autonomously operating buses, and intelligent routing in content delivery networks and military simulations. Kaplan and Haenlein classify artificial intelligence into three different types of AI systems logical, human inspired, and humanized artificial intelligence.

Analytical AI has only characteristics harmonious with cognitive intelligence generating cognitive representation of the world and using literacy grounded on once experience to inform unborn opinions. mortal- inspired AI has rudiments from cognitive as well as emotional intelligence, understanding, in addition to cognitive rudiments, also mortal feelings considering them in their decision timber. Humanized AI shows characteristics of all types of capabilities (i.e., cognitive, emotional, and social intelligence), suitable to be tone-conscious and tone- apprehensive in relations with others. Artificial intelligence is a computer term which is used for software, machines and computers.

Humanized AI shows characteristics of all types of capabilities (i.e., cognitive, emotional, and social intelligence), suitable to be tone-conscious and tone- apprehensive in relations with others introductory artificial intelligence programs that can help babe with the sourcing and Webbing processes include screening chatbots and automated social media scraping tools. These tools are designed to give weak or average pointers about an aspirant's liability of success with the company. Mya, an AI recruiting adjunct created by FirstJob, is one similar chatbot that interacts with aspirants to corroborate they meet job conditions, answer questions and keep them informed on their operation's status, according to the Society for Mortal Resource Management. This bot provides 24/7 support through converse, textbook communication, Skype or e-mail, and will communicate a mortal when it ca n't complete a task. Social media scraping tools are another type of artificial intelligence retaining tool. These bots can collect vast quantities of data through an aspirant's social media biographies and use this data to prognosticate certain actions like unborn engagement situations.

Artificial Intelligence in HRM

Using AI to ameliorate sourcing can greatly enhance an association's capability to find the right gift at just the right time. Artificial intelligence (AI) technology has remade the human's coffers (HR) department, enabling HR professionals to influence machine literacy and algorithms to streamline their work processes, reduce their impulses, and enhance their analysis and decision- timber. still, current limitations and vulnerabilities have given some associations break when it comes to espousing AI for fresh use cases. In this composition, we 'll bandy some of the ways AI is changing HR, considerations when espousing it and how far the trend may go.

SOURCING

The associations must continuously vend their open places due to one of the tightest labor requests in history. Using AI to ameliorate sourcing can greatly enhance an association's capability to find the right gift at just the right time. It can help to

- Find the stylish campaigners Uncover campaigners with the stylish match between job conditions and their chops and experience. Beyond a simple hunt for crucial terms, ML algorithms learn synonymous words that are generally used in resumes.
- Recommend jobs to campaigners' Prospective campaigners, set up either through organic hunt exertion or a targeted crusade, admit recommendations to apply for open positions. AI can warn the right people with the right skill sets to available jobs previous to them advertisement.
- prognosticate seeker performance AI- grounded seeker matching uses HR data to calculate a seeker's liability to accept a job offer, design performance issues, and estimate their anticipated term.

Webbing AND Canvassing

A major benefit of AI at the interview stage is the use of digital sidekicks for a further engaging seeker experience, which can

- Help campaigners come more tone- sufficient The entire canvassing process is in their control, from cataloging or canceling to transferring monuments, participating notes, and recommending coffers for review.
- help hiring directors AI reminds them of forthcoming interviews and provides details on campaigners.

AI can also help overcome subjectivity by gathering data from former workers in analogous places and preparing targeted questions for hiring directors. This provides lesser focus on the seeker's skill set, further environment on the nature of the job, and measures against analogous places in other associations. It allows them to

- Compare campaigners to being top players Use standard data and AI to compare job campaigners with others who have succeeded in analogous places in the association.
- produce personalized offers estimate the wealth of data points relative to the original request and listed hires by contender, furnishing a nuanced and strategic view into how places should be banded. Getting indeed more grainy, AI can also increase retaining efficacy by matching a specific offer with individual job and hand histories to calculate the odds of whether a seeker will accept.
- Anticipate seeker geste prognosticate a seeker's liability to accept, perform, and remain in the position being offered

ON BOARDING

Onboarding is critical because it sets the tone for the hand's term. According to exploration by Work Institute encompassing data from 34,000 exit interviews, roughly of new workers quit within the first time of being hired⁶. Work Institute estimates that three-diggings of that development was preventable if onboarding had been handled more effectively. AI helps to Ease the executive burden Automate delivery and damage of necessary paperwork, company programs, and login information. AI can track which documents were read, prisoner electronic autographs once way are completed, and remove the need for HR to follow up manually.

Cognitive- supporting decision- making IBM officers, who naturally are promoting their own AI capabilities through IBM Watson, also demonstrated ways cognitive machines could help workers arrive at crucial day- to- day opinions in the plant. generally, HR platoon members would have to handle these tasks holiday requests workers that want to put in for holiday days are informed that it is doubtful to be approved as numerous others have formerly reserved holiday in that time frame. Determining your

mood- An hand takes a customer call. After the call, the hand receives feedback that he seems anxious and should take a break before his meeting. Team training- When an association wants to take a more methodical approach to hand training, platoon directors are handed a list of training openings for platoon members. Hiring processes- A hiring director is presented with information that the company's reclamation approach falls short because it interviews too many campaigners. Cognitive results can help associations tap into multiple data sources and reveal new perceptivity to help companies develop seeker biographies, among other effects

AI TOOLS

AI tools automate down common HR tasks like benefits operation and triaging common questions and requests, HR brigades will be "free to do further of the creative and strategic work that has a bigger impact on the success of their companies." There are tools available that make it easy to make a stoner-friendly experience and to dissect, understand and communicate data, he added. " You no longer have to calculate on just an Excel spreadsheet full of calculation. " Getting a picture of what's actually passing in the association is important, Crews noted. " When advanced technology is paired with good liar and visualization, it empowers HR professionals to have the discussion with the compensation platoon, directors and other decision- makers. " Chatbots Certain technology, similar as chatbots, can help workers access important information about programs and procedures from anywhere and at any time. Chatbots communicate by textbook and can be useful for answering common hand questions.

Two- thirds of repliers said that they believe workers are more comfortable using chatbots than other forms of contact for transactional inquiries about paid- time- off programs, open registration and leaves of absence, according to a 2017 ServiceNow check of 350 HR leaders. Legal risks When using AI to drive mortal coffers strategy, HR professionals must cover systems for bias. They need to look out for distant impact which happens when a putatively fair or neutral standard is actually discriminative in illustration, a recruiting tool may weed out campaigners that are further than 10 long hauls down from the worksite. What if the neighborhoods girding the worksite are generally made up of rich white families? This hiring criterion could have a distant impact grounded on race and race (Nicastro, 2018). Recruiting We make numerous opinions on gut sense.

One study showed that utmost hiring directors decide on a seeker within the first 60 seconds of meeting a seeker, frequently grounded on look, handshake, vesture, or speech. Does we really know what characteristics, gests , education, and personality traits guarantee success in a given part? No, we do n't. directors and HR professionals use billions of bones of assessment, tests, simulations, and games to hire people – yet numerous tell me they still get 30- 40 of their campaigners wrong. Smarter people analytics For times, companies have been collecting data on their guests to gain perceptivity to prognosticate unborn geste . HR brigades have a lot of catching up to do in using these people analytics.

Review of Literature

Merlin & Jayam, " Artificial Intelligence in Human Resource operation " - International Journal of Pure and Applied Mathematics(2018) This paper tries to address the possibilities of how Artificial intelligence is transubstantiating and supporting the Human Resource functions like reclamation, training, gift operation & retention through real time exemplifications, gives perceptivity on crossroad of Artificial intelligence & Human resource operation cases and eventually it addresses the unborn impact on the HR pool. Geetha R & Bhanu Sree Reddy D, "Reclamation through artificial intelligence A abstract study "(2018) The major ideal of this paper is to study. how Artificial intelligence influences the recruitment strategy. The study also throws light on the techniques used by companies in AI while recruiting. This study is entirely done based upon secondary sources of information like conceptual papers, various peer reviewed journal articles, books and websites are used to further explore the concept. Secondary sources such as Websites, Journals, Reports, Publication of professionals and books are referred for drafting the entire paper.

□ Ian Bailie Head of HR - "An Examination of Artificial Intelligence and its Impact on Human Resources" (2018) This report tells about big firms that adopt AI and examine the basics of AI and explore how AI is being applied in HR. It has been developed for those that would like to learn more about the potential application of AI in HR. It examines both industry and academic sources to develop representation of AI and its application in business with a specific focus on HR.

□ Malathi Sriram and L. Gandhi, Shri Dharmasthala Manjunatheshwara "Exploring the dynamic Virtus of Machine Learning (ML) in Human Resource Management - A Critical Analysis of IT industry" (2017) This paper focuses on the use of machine learning that has replaced certain functions related to Human Resources Management, specifically in the IT industry. The objective is to understand the use of AI and ML in HR functions in the IT industry. - To attempt a model based on the findings. A few companies' cases have been selected in this paper to show howthey transformed their HR processes through the use of Machine Learning.

□ Shweta Jain-The Engine Driving the Next Wave of Transformation inBusiness (2017), in this paper author discuss about how artificial intelligence bring out total digital transformation when the organization well coordinate with the different units like HR, marketing, Finance, Manufacturing or process. In the report author concluded that HR professionals can make use of different AI technology and tools for all the functions of HR be it recruitment, selection, training, development, performance management, compensation and reward management

□ Robert Charlier and Sander Kloppenburg, PwC, Artificial Intelligence in HR: A Nobrainer (2017) - To find right talent against low costs and in less time, this is a huge argument in today's organisation. As per this paper which was based on research after the various aspects of artificial intelligence by the global network of PwC, the input of business partners, interviews with experts in the field, and the valuable remarks of the participants of our Round Table session in October 2017, and which was organised in cooperation with Seed link.

This study helps us to understand how do we embrace AI successfully with a case study on Loreal Business. Buzko et al. (2016) found that the main factor for influencing the amount of training in the company is the net income of the company for the previous year and the transition from discrete paradigm of information processing to continuous paradigm allow faster and more accurate

adapting to environment requirements. The authors have concluded that in the modern business conditions, it becomes more relevant to use artificial intelligence technologies for decision making Dianna L. et. al (2015) review the current effects of technology on HR processes and discuss the advantages and potential limitations of using information systems. The authors suggested that the movement towards her is expected to grow in the future but many of the traditional HR research findings also apply to HR

Objectives

- 1) To understand the role of AI in today's Human Resource Management.
- 2) To understand the reasons of adopting Artificial intelligence.
- 3) To identify the business outputs of Artificial intelligence.

Sampling Method

The proposed study consist sample from the Indian companies and multinational companies which are established in India. Convenient and judgement sampling technique has been used to collect the primary data. Sample selection of the companies in IT sector based on the turnover as well as employee strength of the company.

COMMON CHALLENGES:

1. Talent management: Still, many organizations have yet to fully embrace the opportunity of modern talent management and continue to experience high turnover due to:

- Passive career development: Organizations struggle to deliver on expectations for career growth across the workforce.
- Traditional succession planning: Many organizations continue to rely on reactive succession planning, leaving organizations unprepared when employees do leave
- Rigid, undifferentiated learning: Traditional learning offerings fail to meet evolving expectations for more differentiated learning styles and learning content anticipating future skills requirements.
- Compensation expectations: While employers leverage market data to determine compensation expectations, workers continue to search even after accepting an offer for better opportunities.

2. CAREER DEVELOPMENT:

One of the emerging nuances of work is the evolution of how job seekers and employees achieve career growth. In the distant past, workers often stayed with their employers for the entirety of their careers and grew from entry level roles into leadership. In order to retain employees, organizations must take a strategic approach to career development. Employees expect to be offered learning and career opportunities that help them grow their career and realize their goals. AI offers:

- Personalized recommendations: Employees can get curated career development recommendations that shift with the business and maximize career potential. Carefully tailored content not only acts as a supplement to manager guidance but will also show employees that their employers are invested in their career.
- Individualized career pathing: AI collects insights around each employee's career progression and deliver it in a personalized way. Each person can map their own career path, mapped to specific learning experiences required to bridge current and projected skills gaps. Providing employees with clarity and necessary tools to make career shifts is one of the best ways to encourage learning

3. SUCCESSION PLANNING:

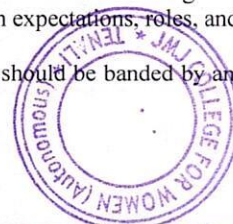
Even with the best retention strategies, an organization will experience some kind of turnover as employees decide to move on or retire. When employees with critical skills or domain expertise leave, it can often create huge gaps in the organization that impede company success and create a negative experience for the employees left in their wake. It is imperative that organizations have solid succession plans in place to ensure this transition is as smooth as possible. Yet, succession planning can be one of the trickiest parts of talent management. Leaders struggle to communicate succession plans to their teams and manage an effective process that can be fraught with bias. AI can help:

- Identify flight risk: Flight risk prediction draws on different attributes and behaviors in order to formulate its conclusions. The attributes include employee sentiment, an employee's mentors and influences, their number of years in a position, how long they've been reporting to their current manager, their potential career path, their salary history, and whether and when they last received a raise. These all factor into a predicted attrition rate and offer leaders a number of useful cues and clues on how to retain their most valuable people.
- Uncover most capable successors: Leveraging data models to analyze employee behavior and determine which employees are ready to step up based on cultural fit, leadership capability, and the accomplishments of past successors.

4. COMPENSATION:

A continuing concern of the labor market is compensation, as workers seek to be paid for their value. In this tight labor market, employees feel confident in seeking jobs elsewhere or asking for pay raises to improve their quality of life. In this environment, employers also face the challenge of ensuring the right compensation for the right positions to avoid paying too little or too much. Leaders must work strategically and seek to understand competitor trends so they can meet employee expectations and keep top talent. With HR continuing to evolve, it's important to also change how compensation is determined. Organizations need a wider range of data to create a strategy that works for their people and matches differences in expectations, roles, and skill sets. AI helps to:

- Provide market insights: AI provides a nuanced and strategic view into how roles should be banded by analyzing a wealth of salary data points relative to the local market and available competitor data.



□ Increase recruiting efficacy: By matching a specific offer with individual job and employee histories to calculate the odds of whether a candidate will accept.

Research Design

Research Method is quantitative for this study. Scale was designed as per the objective of our study and the data is secondary which is being analyzed by multiple researches done by many IT companies. Sources of Data Secondary data is collected through research papers, journals and articles published. We have also taken information from cross-sectional study from various peer reviewed survey questionnaire. As there were 50% eligible responses that we can use for the single t- test

RESULTS AND DISCUSSION:

TABLE-1

One-Sample Statistics				
	N	Mean	Std. Deviation	Std. Error Mean
SCORE	50	30.4980	26.84736	3.79679

Table 1 shows the one sample statistics where the mean , and std deviation ,and the error deviation is shown since the error mean is less than the actual mean this hypothesis is supported sop H1 is valid.

Table -2

One-Sample Test							
Test Value = 0							
	t	df	Significance		Mean Difference	95% Confidence Interval of the Difference	
			One-Sided p	Two-Sided p		Lower	Upper
SCORE	8.033	49	<.001	<.001	30.49800	22.8681	38.1279

Table 2 show the one sided and the two sided p value both are in equilibrium so the hypothesis 2 is valid so the H2 is supported

TABLE -3

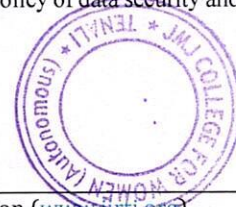
One-Sample Effect Sizes					
SCORE		Standardizer ^a	Point Estimate	95% Confidence Interval	
				Lower	Upper
	Cohen's d	26.84736	1.136	.776	1.489
	Hedges' correction	27.26721	1.118	.764	1.466

a. The denominator used in estimating the effect sizes. Cohen's d uses the sample standard deviation. Hedges' correction uses the sample standard deviation, plus a correction factor.

Table 3 shows the methods which are used in the one sample effects sizes by these correction methods as the point estimate value is accurate which resides with the standardizer value.

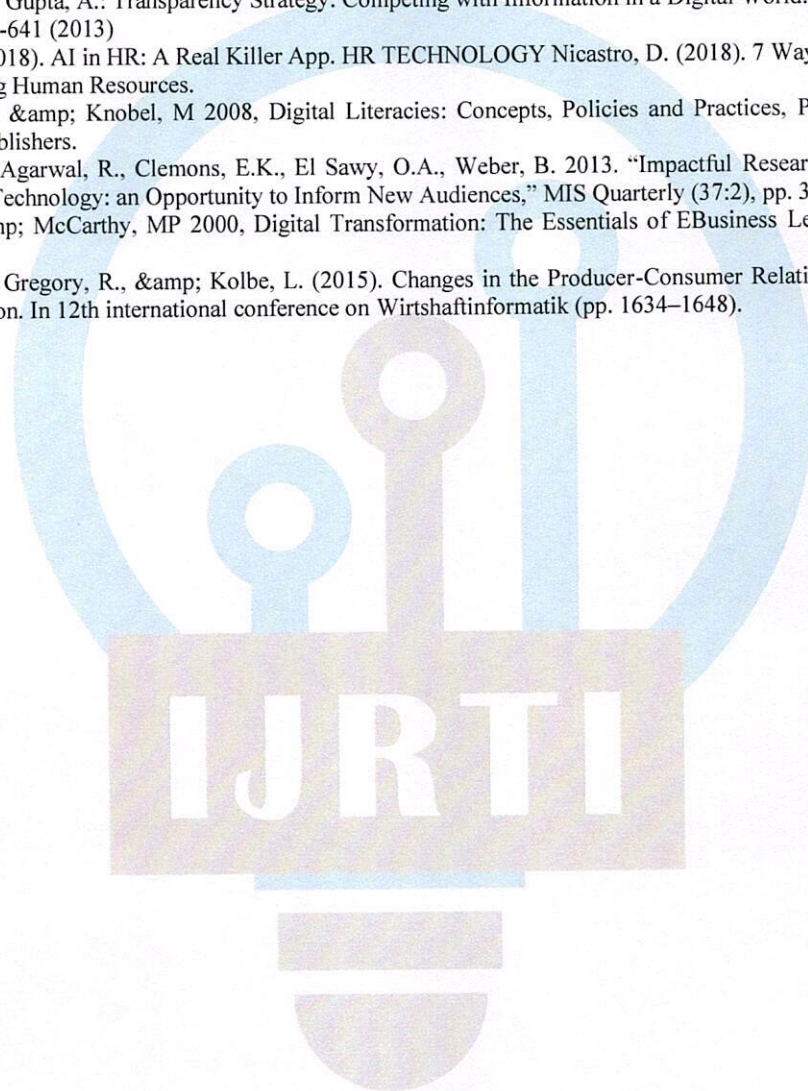
CONCLUSION:

Artificial Intelligence (AI) provides an impressive way of application in a wide range of area. The inclusion of Artificial Intelligence (AI) in business has opened doors to limitless opportunities. The future holds infinite possibilities for Artificial Intelligence (AI) especially when it comes to play in the field of Human Resource (HR). It cannot be denied that Artificial Intelligence (AI) aid and abet a Human Resource (HR) manager in carrying out different functions effectively and efficiently thus enabling them to focus on higher value task. But this not the stage where Artificial Intelligence (AI) can replace human beings. Right from recruitment to performance management there are administrative and repetitive in nature. The complexity of Human Resource (HR) and its multitude of variables add butter oil to burning flame. Digitalization and automation of work in Human Resource (HR) provides integrated orientation, experience and real time solution. The integration and adoption of Artificial Intelligence (AI) has transfigured the role of a Human Resource (HR) manager from manual administrative task to a more strategic approach. Although Artificial Intelligence (AI) is foreseen as an opportunity and is regarded as a game changer for business to gain competitive advantage, it also offers certain challenges (Bersin, 2017) which a company need to overcome to avail the full advantage of it. At the outset, the initial challenges to deal with the redundancy of the data. As the Human Resource data is stored at multiple locations which is required by different departments, any changes in one set of data may not be reflected in other set thus acknowledging the problem of data inconsistency. The second concern is to deal with the policy of data security and confidentiality.



References

1. Bharadwaj, A., El Sawy, O. A., Pavlou, P. A., and Venkatraman, N. 2013. "Digital Business Strategy: Toward a Next Generation of Insights," MIS Quarterly (37:2), pp. 471-482.
2. Clemons, E. K. (2008). How Information Changes Consumer Behavior and How Consumer Behavior Determines Corporate Strategy. Journal of Management Information Systems, 25(2), 13-40.
3. CMS Pay, V. B. (2018). How Artificial Intelligence Is Reinventing Human Resources.
4. Entrepreneur WirePiazza, L.N.(2018). How Can Artificial Intelligence Work for HR
5. Fichman, R. G., Dos Santos, B. L., and Zheng, Z. E. 2014. "Digital Innovation as a Fundamental and Powerful Concept in the Information Systems Curriculum," MIS Quarterly, pp. 329-353.
6. Fitzgerald, M., Kruschwitz, N., Bonnet, D., and Welch, M. 2013. "Embracing Digital Technology," MIT Sloan Management Review, 1-12.
7. Granados, N., Gupta, A.: Transparency Strategy: Competing with Information in a Digital World. MIS Quarterly, vol. 37, no. 2, pp. 637-641 (2013)
8. Joshbersin.(2018). AI in HR: A Real Killer App. HR TECHNOLOGY Nicasro, D. (2018). 7 Ways Artificial Intelligence is Reinventing Human Resources.
9. Lankshear, C & Knobel, M 2008, Digital Literacies: Concepts, Policies and Practices, Peter Lang International Academic Publishers.
10. Lucas, H.C., Agarwal, R., Clemons, E.K., El Sawy, O.A., Weber, B. 2013. "Impactful Research on Transformational Information Technology: an Opportunity to Inform New Audiences," MIS Quarterly (37:2), pp. 371-382.
11. Patel, K & McCarthy, MP 2000, Digital Transformation: The Essentials of EBusiness Leadership, McGraw-Hill Professional.
12. Piccinini, E., Gregory, R., & Kolbe, L. (2015). Changes in the Producer-Consumer Relationship-Towards Digital Transformation. In 12th international conference on Wirtschaftsinformatik (pp. 1634-1648).




PRINCIPAL
JMJ COLLEGE FOR WOMEN (Autonomous)
TENALI

A STUDY ON URBAN HEALTH MANAGEMENT SYSTEM IN EAST GODAVARI DISTRICT-AP-INDIA

Dr. K RAJESH KUMAR

Assistant Professor, Department of Arts KL (Deemed to be) University, KLEF Vaddeswaram Guntur.

Dr. K JHANSI RANI

Professor, Department of Public Administration, Arts and Science College for Women, Andhra Mahila Sabha, Hyderabad, Telangana, India.

Dr. K V V RAJU

Associate Professor, KL Business School, KL (Deemed to be) University, KLEF. Vaddeswaram Guntur.

Dr. P.V. VARAPRABHAKAR

Associate Professor, Department of Business Management, Yogi Vemana University, Kadapa.

Dr. P.CH. PRAVEEN KUMAR

Lecturer, Sri Hari Degree & PG College, Kadapa.

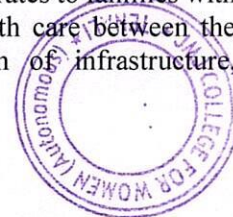
Abstract

Man's greatest asset is his health. It is the origin of man's joy. Nothing may be deemed to be of greater importance in terms of resources for socio economic growth than the general well-being of the populace. A financial investment in one's health is a growth of the nation's human resources is essential. Therefore, it is crucial to focus on improving one's health in order to increase one's quality of life. Article 25 of the Indian Constitution focuses on the right to health in particular. Everyone has the right to a standard of living adequate for his or her own and his or her family's health and well-being, including food, clothing, housing, medical care, and necessary services, as well as the right to security in the event of unemployment, sickness, disability, widowhood, old age, or other loss of livelihood due to circumstances beyond his or her control. Motherhood and childhood are entitled to special attention and care. According to various definitions, health can be defined as a state of well-being in which a man can enjoy the richness of his life. It includes living a longer life and being disease-free. Because health is influenced by a variety of factors such as adequate food, housing, basic sanitation, healthy lifestyles, protection from environmental hazards, and communicable diseases, the boundaries of health extend beyond the narrow confines of medical care. As a result, "health care" implies more than "medical care." It encompasses a wide range of "provided services." Health is multifaceted, with each aspect having a significant impact on the person both internally and outwardly in the society in which they live. It is said that the interaction of two sets of circumstances determines what a man is and the diseases to which he may be susceptible. These variables interact, and their effects on health can be either beneficial or detrimental.

Keywords: Healthcare, Service Delivery, Policies, Infrastructure, and Resources

INTRODUCTION

The federal and state governments run the facilities that make up the public healthcare system. In both urban and urban areas, these public facilities offer reduced or free rates to families with lower incomes. The Indian Constitution divides responsibility for health care between the central and state governments. State governments bear the burden of infrastructure,



employment, and service delivery, while the national government is still in charge of medical research and technical education. Issues that affect multiple states are included in the concurrent list, which is found in the ninth Schedule to the Indian Constitution. For instance, preventing the spread of infectious or contagious diseases between states is one example the national government has significant fiscal control over the health systems of the states, despite the states' considerable autonomy in their management. In the areas of health and family welfare, major communicable disease prevention and control, and the promotion of indigenous and traditional medical practices, the Ministry of Health & Family Welfare is instrumental in the implementation of numerous national programs. In addition, the Ministry provides technical assistance to states in order to prevent and control the spread of seasonal disease outbreaks and epidemics. Service of Well-being and Family Government assistance causes use either straightforwardly under Focal Schemes or via awards in-helps to the independent/legal bodies and so forth. NGOs and the Ministry is implementing several World Bank-supported programs for the control of AIDS, Malaria, Leprosy, and Tuberculosis in designated areas in addition to the 100% centrally sponsored family welfare program.

OBJECTIVES

- 1) To know the status of the urban health management system in the study area
- 2) To evaluate the policies implemented by the government of AP.
- 3) To identify the problems and suggestions for better health management.

Need for the study

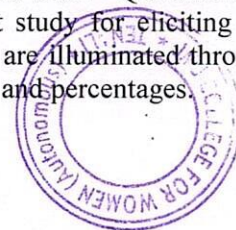
To analyse about the status and working of health care system in Andhra Pradesh, the investigator wants to study the implementation of health care policies conducted by the Government through aspects like Awareness, Knowledge, Quality and Satisfaction among the beneficiaries and attitude, supervision and coordination by the officials of healthcare officials in Andhra Pradesh.

Hypothesis of the study

- 1) It is perceived that majority of the respondents do not have awareness about the health policies and schemes
- 2) It is perceived that majority of the respondents have less satisfaction with the services of health centres.
- 3) It is perceived that majority of the respondents expressed negative opinion on the services available.

Tools and Techniques

Basing on the nature of work and objectives of the study, two popular tools –Questionnaire method and personal interview have been employed in the present study for eliciting the required information from the primary source. The facts and figures are illuminated through the bar charts for the purpose of analysing the data based on averages and percentages.



RESEARCH METHODOLOGY

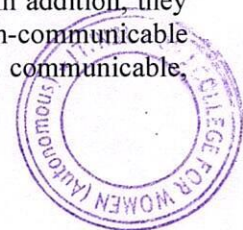
The data collected have been processed by using simple arithmetic techniques and by using computer. Averages and percentages are worked out to bring accuracy in understanding and presentation of the data. The collected data have been analyzed in the light of stated objectives using suitable classifications and tabulations.

REVIEW OF LITERATURE

In his 2009 paper, Duggal examined the National Urban Health Mission (NRHM)'s public health budgets. It stated that the NRHM flagship will continue to sink unless radical changes in budgetary and financing mechanisms are put in place by granting full autonomy to those who directly run the public health system. Among the many reasons for the failure of NRHM to increase funds in the public health sector are fungibility with the states, central control on health resources, and so on. Claeson and others, According to the Millennium Development Goals (MDGs) to be achieved by 2015, of which nearly half concern health, combating HIV/AIDS, malaria, and other diseases, reducing child mortality, and eradicating extreme poverty and hunger While some objectives have been accomplished, such as the nutrition objective, the lowest quintile of a nation's population is on track to achieve it; In most low-income nations, it is unlikely that the goal of reducing child mortality will be met. The capacity to scale up by 2015 will depend on a combination of sound policies and additional funding, but all nations can make progress.

Duggal (2006) examines the budget's health allocations in light of the National Common Minimum program's commitments and trend 54 in state government spending, with a focus on the National Urban Health Mission. Using data on public health expenditures at the state level, Bhat and Jain (2004) conducted an analysis of public health expenditures. According to the findings, state governments aim to allocate approximately 0.43 percent of State GDP (SGDP) to health and medical care, which does not include allocations received from centrally sponsored programs like family welfare. They believe that the goal of spending 2% to 3% of GDP on health seems like an extremely lofty goal given the current level of spending and state governments' financial situation. Additionally, the analysis suggests that when the SGDP changes, the elasticity of health expenditures is only 0.68, meaning that for every one percent increase in state per capita income, per capita public healthcare expenditures rise by approximately 0.68 percent.

According to Chauhan (2001), factors outside of the medical field, such as the environment, socioeconomic factors, information and communication, the availability of health services, utilisation of health services, age structure of the population, and so on, influence health. The public health approach addresses all of these health determinants, requiring inter-disciplinary coordination and collaboration across sectors. They said that an effective public health system is the only way to reduce India's high rate of disease, disability, and death. In addition, they stated that, while urban areas have a higher proportion of deaths from non-communicable diseases (56 percent), urban areas have a higher proportion of deaths from communicable, maternal, prenatal, and nutritional conditions (41 percent).



Rahman has examined the use of location-allocation models in health service development planning in developing nations and Smith (2000). Their review aims to determine whether these approaches are appropriate for designing health care systems and how they relate to issues of overall development in developing nations. Duggal and Jesani (1992) discuss the significance of morals in clinical practices. They emphasize that principles of non-maleficence, beneficence, autonomy, and justice must serve as the foundation for ethics enforcement. At the same time, it highlights serious issues like malpractice, organ trading, unethical practice, and the commercialization of health care, among others, and it calls for a powerful patient movement to uphold ethics and implement systemic reforms. There were only 28 colleges affiliated with the university when it first opened its doors. The number has now increased to 348! It is anticipated that it will continue to expand, expanding the university's boundaries. The number of affiliated colleges in each field can be found below.

S. No	Speciality	Number of affiliated colleges
1	Modern and advanced medicine	40
2	Department of Dentistry	21
3	Ayurveda department	7
4	Homeopathy department	6
5	Unani medicine	2
6	Department of Nursing	213
7	Naturopathy and Yoga	2
8	Department of Physiotherapy	38
9	Medical laboratory and technology	54

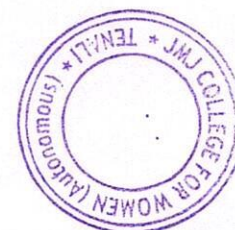
Super specialties in modern medicine and postgraduate courses in all other faculties are two examples of the university's rapid expansion of services. New certificate and fellowship programs in the fields that are in high demand and tailored to Andhra Pradesh's current disease profile are currently being actively considered. In addition to regular academic activities, the university organizes and funds CMEs, teacher training programs, speeches, guest lectures by well-known people, and other similar events.

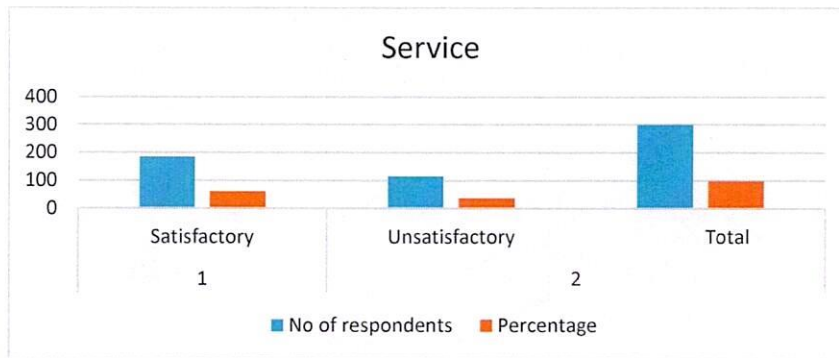
Analysis of Data Interpretation

Service management

S. no	Response	No of respondents	Percentage
1	Satisfactory	185	62.00
2	Unsatisfactory	115	38.00
	Total	300	100.00

Source: Primary Data



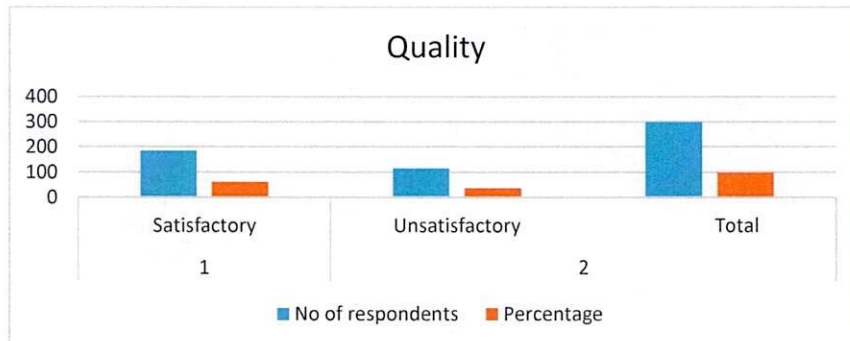


Above table shows that 62.00 percent of respondents expressed about the service delivery was more satisfactory and 38.00 percent of respondents stated that service delivery and treatment facilities are not upto the mark of satisfaction level.

Table 5.24: Quality service

S. no	Response	No of respondents	Percentage
1	Satisfactory	215	72.00
2	Unsatisfactory	85	28.00
	Total	300	100.00

Source: Primary Data

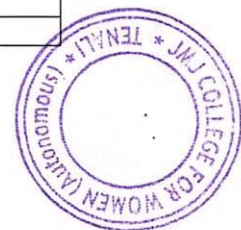


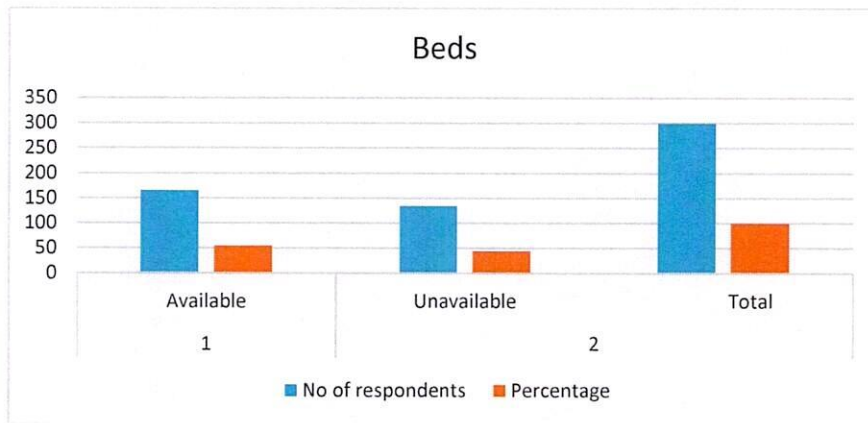
Above table shows that 72.00 percent of respondents expressed about the ambulance service was satisfactory and 28.00 percent of respondents stated that ambulance service facilities are not upto the mark of satisfaction level.

Table 5.25: Infrastructure facilities availability

S.no	Response	No of respondents	Percentage
1	Available	165	55.00
2	Unavailable	135	45.00
	Total	300	100.00

Source: Primary Data



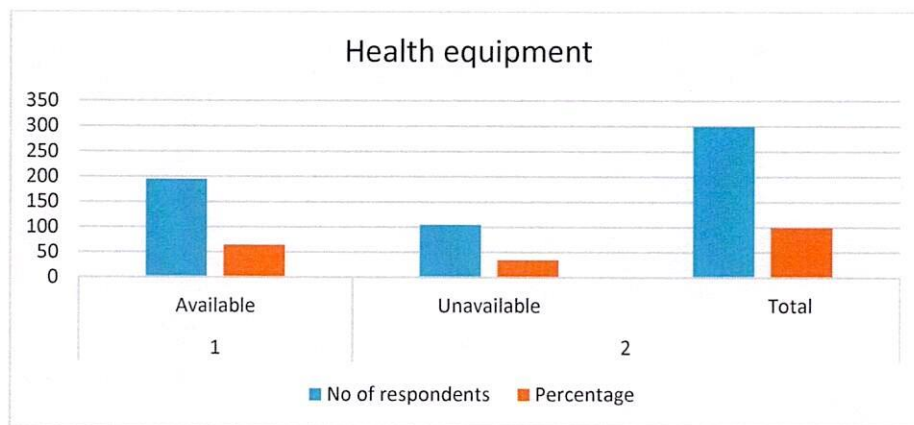


Above table shows that 55.00 percent of respondents expressed about the infrastructure facility available and 45.00 percent of respondents stated that the facilities was not sufficient as per the requirement of the health centers in the study area.

Table 5.26: Health Equipment's availability

S.no	Response	No of respondents	Percentage
1	Available	195	65.00
2	Unavailable	105	35.00
	Total	300	100.00

Source: Primary Data



Above table shows that 65.00 percent of respondents expressed about the equipments of healthcare management available and 35.00 percent of respondents stated that the health centers in the study area were not equipped the wards in the compound..

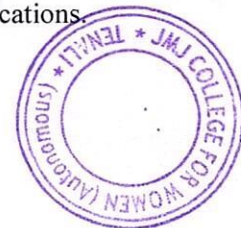


FINDINGS OF THE STUDY

- 1) More than half of those polled agreed that health centres have a sufficient number of medical testing labs, with 58,000 of those polled expressing concern about the lack of such facilities.
- 2) It was reported that more than half of respondents, or 58.00 percent, complained about longer registration times for Outpatients in the healthcare system. 33% of the patients who were surveyed expressed concern about the waste management process and stated that the district's PHCs did not properly manage waste.
- 3) Respondents agreed, with 79.00% saying that hospitals had adequate drinking water facilities and 21.00% saying that public health centres (PHCs) in the district did not have adequate drinking water facilities.
- 4) It was discovered that 38.00% of respondents stated that treatment facilities and service delivery do not meet satisfaction standards.
- 5) Quality service facilities were not up to the mark of satisfaction for 28.00 percent of respondents, according to their perception of satisfaction.
- 6) According to the findings, 45.00% of respondents said that the infrastructure facility did not meet the needs of the health centres' in the study area, and 55.00% of respondents said that the infrastructure facility was available.

SUGGESTIONS

- 1) In the study, the importance of ensuring a consistent supply of all essential medications and improving the quality of medicines should be emphasized.
- 2) The healthcare system's technical staff must regularly supervise and monitor clinical and laboratory facilities to improve them. In order to ensure that patients who are waiting for a consultation have access to sufficient furniture and clean drinking water, officials must keep an eye on the facilities.
- 3) The environment must be kept clean and hygienic on a regular basis. The toilets must be cleaned according to the schedule on a regular basis.
- 4) There was a need for health care workers, including doctors, to become motivated to help the underprivileged community and provide services with complete dedication to their responsibilities.
- 5) In order to better understand the beneficiaries, there is a need for increased promotion and awareness of the health plans in the study area.
- 6) In order to win the support of the populace, it is necessary to raise the quality of the medicines and guarantee a consistent supply of all necessary medications.



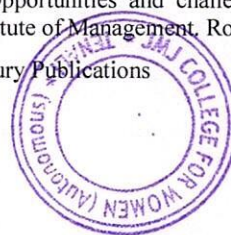
CONCLUSION

It is necessary to take action in the health sector: If the international community does not act quickly, "famine, malnutrition, and the resulting diseases will continue," "natural resources will continue to decline," and "conflicts over scarce resources like water will become even more common." The Organization calls for eradicating pockets of poverty within nations, including among refugees, and reducing poverty in the poorest nations. Legislation that promotes health and equity is the key to economic growth and the end of poverty.

References

1. Charnes, A., Cooper, W. W., Lewin, A. Y., & Seiford, L. M. (1995). Data envelopment analysis: Theory, methodology and applications.
2. Boston, MA: Kluwer. Chaudhuri, A and Gupta, R (2009). Motivation for care giving of the elderly in India. *Journal of Aging in Emerging Economies*
3. T., D. S. P., Rao, & Battese, G. (1998). An introduction to efficiency and productivity analysis. Boston, MA: Kluwer.
4. Dash, U., Vaishnavi, S. D., Muraleedharan, V. R., & Acharya, D. (2007). Benchmarking the performance of public hospitals in Tamil Nadu: an application of data envelopment analysis. *Journal of Health Management*, 9(1), 59–74.
5. Dash, U., Vaishnavi, S. D., & Muraleedharan, V. R. (2010). Technical efficiency and scale efficiency of district hospitals: A case study. *Journal of Health Management*, 12(3), 231–248.
6. Evans, D. B., Tandon, A., Murray, C. J. L., & Lauer, J. A. (2001). The comparative efficiency of national health systems in producing health: An analysis of 191 countries (GPE Discussion Paper Series No.29).
7. World Health Organization. Retrieved from <http://www.who.int/healthinfo/paper29.pdf> Farell, M. J. (1957). The measurement of productive efficiency. *Journal of the Royal Statistical Society Series A*, 120(3), 253–278.
8. Fried, H. O., Lovell, C. A. K., & Schmidt, S. S. (1993). The measurement of productive efficiency and productivity growth. New York: Oxford University Press.
9. Hollingsworth, B., & Wildman, J. (2003). The efficiency of health production: Re-estimating the WHO panel data using parametric and nonparametric approaches to provide additional information (Working Paper No. 131). Australia: Centre for Health Programme Evaluation, Monash University
10. Jamison, D. T., Sandbu, M., & Wang, J. (2001). Cross country variation in mortality decline, 1961–87: The role of country specific technical progress (CMH Working Paper Series Paper No WGI: 4).
11. Commission on Macroeconomics and Health, WHO. Retrieved from http://library.cphs.chula.ac.th/Ebooks/HealthCareFinancing/WorkingPaper_WG1/WG1_4.pdf
12. Murray, C. J. L., & Frenk, J. (1999). A WHO framework for health system performance assessment. Global Programme on Evidence and Information for Policy, the World Bank.
13. Prachitha, J., & Shanmugam, K. R. (2012). Efficiency of raising health outcomes in the Indian states (Working Paper 70/2012). Chennai: Madras School of Economics
14. Ramani, K. V., & Mavalankar, D. (2005). Health system in India: Opportunities and challenges for improvements (Working Paper No. 2005-07-03). Ahmadabad: Indian Institute of Management, Rout, H. S. (2011). Healthcare systems: A global survey. New Delhi: New Century Publications


PRINCIPAL
JMJ COLLEGE FOR WOMEN (Autonomous)
TENALI





Fabrication and characterization of CuO nano-needles from thermal decomposition of Cu(II) metal complex: Fluorometric detection of antibiotics, antioxidant, and antimicrobial activities

V. Sumalatha^a, Dasari Ayodhya^{b,*}

^a Department of Chemistry, JMJ College for Women, Tenali 522201, Andhra Pradesh, India

^b Department of Chemistry, University College of Science, Osmania University, Hyderabad 500007, Telangana State, India

ARTICLE INFO

Keywords:

CuO needles
[Cu(TMPM6MOP)₂] complex
Antibiotics detection
Fluorometric sensing
Antioxidant activity
Bacterial growth inhibition

ABSTRACT

In the present study, CuO NPs and CuO nano-needles were synthesized using thermal decomposition of Cu(II) complex derived from 2-(4-(trifluoromethoxy)phenylimino)methyl)-6-methoxyphenol (TMPM6MOP) and characterized by UV-vis DRS, PL, FTIR, XRD, and SEM. The monoclinic crystalline nature of the CuO NPs and CuO needles was illustrated by the XRD. The average size of the CuO NPs (30 nm) and CuO needles (diameter 10 nm, length 250 nm) were estimated from XRD and SEM. The prepared CuO needles were used as a fluorescent sensor for the selective and sensitive detection of ciprofloxacin (Cipro) among various antibiotics at diverse pH (4.0–9.0) conditions and the optimized pH = 5.0. The response of Cipro using the CuO needles was linear over the range from 10 to 100 $\mu\text{M L}^{-1}$. This sensor showed the lowest limit of detection of 0.21 nM and was much lower than the other antibiotic sensors. In addition, the sensor is highly sensitive, selective, and durable in the presence of a range of potentially interfering fluorometric active compounds due to the large surface area and positive surface charge of the CuO needles. Moreover, antimicrobial activities and antioxidant activities were investigated to evaluate the biological potential of the CuO NPs and CuO needles.

Introduction

A great deal of work has been carried out on the synthesis and characterization of transition metal complexes with Schiff base ligands and further development of nanomaterials from metal complexes, mainly due to their applications in fluorescence sensors, catalysts, and biologically active agents [1–2]. In recent years, Schiff base ligands containing imine moiety have attracted considerable attention because of their facile synthesis leading to various structures as well as their useful activities, especially biological ones. Furthermore, these Schiff base derivative compounds show remarkable biological activities which are greatly related to their metal complexation ability [3]. The complexes with transition metals (such as manganese, copper, and nickel) were found to have antibacterial, antifungal, and cytotoxicity activity [4]. Comparing to other metal complexes, Cu(II) complex have proved to be one of the best metallic species that have wide anticancer activity due to the selective permeability of cancer cell membranes to copper compounds [5]. In addition, copper can trigger the generation of ROS in human cells [6]. The several biological activities of Cu(II) complexes

including DNA binding [7], DNA cleavage [8] anti-cancer [9] and antimicrobial activities [10] have been documented extensively in the literature. The Cu(II) complexes are considered the best alternative to cis-platin complexes in the scope of anticancer activity mainly due to their biocompatibility and significant functions in biological systems [11]. For instance, they can accumulate in cancerous cells due to the selective permeability of their membranes to copper compounds [12]. Also, Cu(II) complexes have been widely utilized in metal-mediated DNA cleavage for generating activated oxygen species.

Recently, nanostructure-based metal oxides have been studied in the field of nanotechnology both from a fundamental and industrial point of view. The metal oxide nanoparticles (MONPs) prepared from earth-abundant and inexpensive metals have attracted considerable attention because of their prospect as viable alternatives to the expensive metal-based catalysts used in many conventional chemical processes. The great interest in catalysis using MONPs has prompted the synthesis and investigation of a diverse range of highly functionalized CuO nanostructures [13]. The copper-based materials which are cheap and environmentally friendly are especially attractive in this context due to

* Corresponding author.

E-mail address: ayodhyadasari@gmail.com (D. Ayodhya).

<https://doi.org/10.1016/j.rechem.2023.100821>

Received 12 January 2023; Accepted 31 January 2023

Available online 3 February 2023

2211-7156/© 2023 The Author(s). Published by Elsevier B.V. This is an open access article under the CC BY-NC-ND license (<http://creativecommons.org/licenses/by-nc-nd/4.0/>).



the high abundance of Cu in nature and the available simple and straightforward techniques to synthesize these materials. Also, Cu-based materials can promote and undergo a variety of reactions due to the wide range of accessible oxidation states of Cu such as Cu(0), Cu(I), Cu(II), and Cu(III) which enable reactivity via multiple pathways. Because of these distinctive properties, Cu-based metal oxide NPs are widely used as catalysts in various organic transformations, sensors in the detection of metal ions, antibiotics, and toxic pollutants; and biological agents [14]. However, it is challenging to develop a synthesis method for CuO NPs with a unique shape that is highly active, selective, stable, and robust for utilizing various applications [13–15].

Recently, nanoparticles synthesized from Schiff base derived transition metal complexes have been reported [13,16]. The synthesis of MONPs from the Schiff base transition metal complexes was one of the most suitable method, because the products obtained were of more purity and with perfect structure [16–18]. Among various MONPs, CuO NPs is one of the simplest and industrially important semiconductor materials belonging to the monoclinic structure system with a narrow bandgap energy of 1.2 eV with potential applications in various fields such as heterogeneous catalysis, field electron emitters, magnetic storage media, sensors, batteries, solar cells and supercapacitors [19–25]. CuO nanostructures with various sizes and morphologies have been prepared via several methods such as chemical precipitation [19], sonochemical [20], solvothermal [21], hydrothermal [22], thermal decompositions [23], electrochemical/biological [24], and exploding wire techniques [25]. The thermal decomposition of transition metal complexes is one of the simplest and least expensive techniques for preparing nano-sized transition-metal oxides, which is simple and no need for a template and costly apparatus [26]. However, the use of expensive and toxic chemicals as stabilizing or capping agent in most of these methods limits their use in wide range, so simple thermal decomposition method was used for the synthesis of CuO NPs for various applications such as sensors and biological fields.

Antibiotics, which possess the advantages of strong antibacterial activity and low cost, have been widely used for human medical treatment and veterinary. However, the abuse of antibiotics could result in their accumulation in human body or foods and thus lead to public health issues, for instance, causing cytotoxicity, nephrotoxicity, allergic reactions and bacterial resistance [27]. Therefore, it is crucial to develop sensitive, simple, facile, selective and rapid analytical methods for monitoring antibiotic level in foods and human body, which may further improve food safety and facilitate proper drug administration. Common analytical methods include high performance liquid chromatography (HPLC), liquid chromatography-mass spectrometry (LC/MS), capillary electrophoresis (CE), and gas chromatography (GC), etc., which are capable of simultaneous detection and quantification of antibiotics. However, these methods usually require expensive/large equipment, professional operators, time-consuming and laborious procedures, limiting their on-site detection and real-time monitoring potential. Apart from them, fluorescent sensors seem to be a good candidate meeting the requirements of antibiotic monitoring, which offer the benefits like high sensitivity, good selectivity for rapid analysis of wide variety of samples [28].

Based on the above facts, herein we have reported the synthesis of CuO NPs and CuO needles from the Schiff base derived Cu(II) complex by thermal decomposition via calcination method and characterized by various physicochemical methods such as UV–vis absorption, PL, FTIR, powder XRD, and SEM techniques. The fluorescence sensing performance of CuO needles was also evaluated against various antibiotics in an aqueous media. Further, the CuO NPs and CuO needles were analyzed for their antioxidant and antimicrobial activities.

Experimental

Materials and methods

All chemicals were of analytical reagent grade and were used as received. Copper acetate ($\text{Cu}(\text{CH}_3\text{COO})_2 \cdot \text{H}_2\text{O}$), methanol, ethanol, ether, acetone, hexamethylenetetramine, NaOH, 4-(trifluoromethoxy) benzenamine, and 2-hydroxy-3-methoxybenzaldehyde were obtained from Sigma-Aldrich Chemicals Pvt. Ltd. (India). Double distilled water was used as a solvent for all experiments. Antibiotics (levofloxacin, ciprofloxacin, norfloxacin, lomefloxacin, enrofloxacin, ofloxacin, moxifloxacin, and gatifloxacin) collected from Medchem Laboratory, Hyderabad.

Synthesis of Schiff base

The Schiff bases were synthesized by mixing the hot methanolic solutions of (25 mL) of 4-(trifluoromethoxy)benzenamine (10 mM) and (25 mL) of 2-hydroxy-3-methoxybenzaldehyde (10 mM) in 1:1 ratio with stirring and refluxing at 60–70 °C temperature on an oil bath for 2–4 h. The colored precipitates resulted were isolated by filtration and recrystallized from methanol. An outline of the synthetic procedure is presented in Scheme 1.

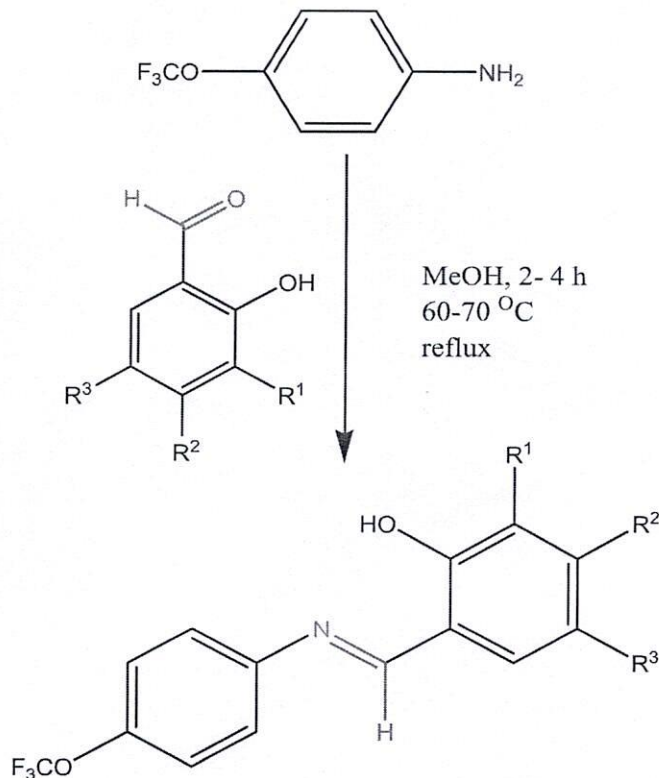
Analytical data of TMPM6MOP:

Elemental analysis (%): Molecular formula $\text{C}_{15}\text{H}_{12}\text{F}_3\text{NO}_3$; Found: C, 57.79; H, 3.80; N, 4.41. Calculated: C, 57.88; H, 3.89; N, 4.50.

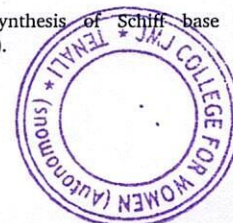
^1H NMR (400 MHz, CDCl_3): δ = 13.37 (s, 1H), 8.63 (s, 1H), 7.34–6.91 (m, 7H), 3.96 (s, 3H), Fig. S1

^{13}C NMR (100 MHz, CDCl_3): δ = 163.1, 161.5, 148.6, 146.2, 134.8, 131.8, 130.2, 121.4, 120.0, 119.7, 118.2, 117.9, 117.5, 33.9, 28.3, Fig. S2

IR (KBr)(cm^{-1}): $\nu(\text{OH})$ 3451, $\nu(\text{HC}=\text{N})$ 1623, $\nu(\text{C}=\text{O})$ 1160, Fig. S3



Scheme 1. Schematic route for the synthesis of Schiff base ligand (TMPM6MOP: $\text{R}^1 = \text{OCH}_3$, $\text{R}^2 = \text{H}$, $\text{R}^3 = \text{H}$).



UV (DMSO) $\lambda_{\max}/\text{nm}(\text{cm}^{-1})$: 244 (40983), 283 (35335), Fig. S4
 MS (ESI): $m/z = 312 [M + H]^+$, Fig. S5

Synthesis of CuO NPs

In a typical synthesis, copper(II) acetate solution (10 mL; 0.375 M) and appropriate volume of water were mixed together in a stopper glass vessel under continuous stirring at 65 °C. After 10 min of stirring, 13 mL of NaOH solution (1.125 M) was added dropwise to raise the pH of the reaction mixture to 12. The reaction mixture was further heated at the same temperature under constant stirring for 2 h. After that, the reaction mixture was allowed to cool down to room temperature naturally. The product was isolated by centrifugation at 10000 rpm for 10 min. The isolated product was purified by two cycles of washing with water and centrifugation. Finally, the solid mass was dried in a vacuum oven at 60 °C for overnight. The dried product was subjected to calcination in a muffle furnace at 400 °C for 2 h to remove the hydroxyl ions or water molecules if attached to the product.

Synthesis of [Cu(TMPM6MOP)₂] complex

The synthetic route for the preparation of [Cu(TMPM6MOP)₂] complex as shown in Scheme 2. The Cu(II) complex was synthesized by using metal salt (copper acetate) and Schiff base (TMPM6MOP) in 1:2 M ratio. The hot methanolic solutions of 10 mM of metal acetate such as [Cu(CH₃COO)₂·H₂O] and Schiff base (TMPM6MOP; 20 mM) were mixed and refluxed for 2–4 h at 70–80 °C. The reaction solution was kept aside at room temperature for slow evaporation. The red colored precipitate was filtered off, washed thoroughly with methanol and dried in desiccators.

Synthesis of CuO needles

The CuO needles were prepared from the precursor [Cu(TMPM6MOP)₂] complex by the simple thermal decomposition method via the calcination process. The prepared Cu(II) complex (50 mg) was taken in a porcelain crucible and heated to 580 °C in an electric furnace for 2 h. The decomposition product generated from the complexes was cooled to room temperature and kept in desiccators. The pure CuO needles were obtained and further characterized by various spectral studies.

Analytical data of [Cu(TMPM6MOP)₂] complex

Elemental analysis (%): Molecular formula [C₃₀H₂₂F₆N₂O₆Cu], Found: C, 52.55; H, 3.24; N, 4.02, Cu, 9.20. Calculated: C, 52.68; H, 3.24; N, 4.10; Cu, 9.29.

IR (KBr)(cm⁻¹): $\nu_{(\text{CH}=\text{N})}$ 1595, $\nu_{(\text{C}=\text{O})}$ 1172, $\nu_{(\text{M}-\text{O})}$ 552, $\nu_{(\text{M}-\text{N})}$ 466, Fig. S6

UV (DMSO) $\lambda_{\max}/\text{nm}(\text{cm}^{-1})$: 259 (38610), 305 (32786), 380 (26315), 580 (17241) Fig. S7

Magnetic moment (μ_{eff}): 1.76 BM

MS (ESI): $m/z = 685 [M + H]^+$, Fig. S8

ESR: g_{\parallel} (2.149), g_{\perp} (2.069), $G(2.10)$, $A[\text{Gauss}(\text{cm}^{-1})]$ 181(0.0168), $g_{\parallel}/A_{\parallel}$ (cm) (128) Fig. S9

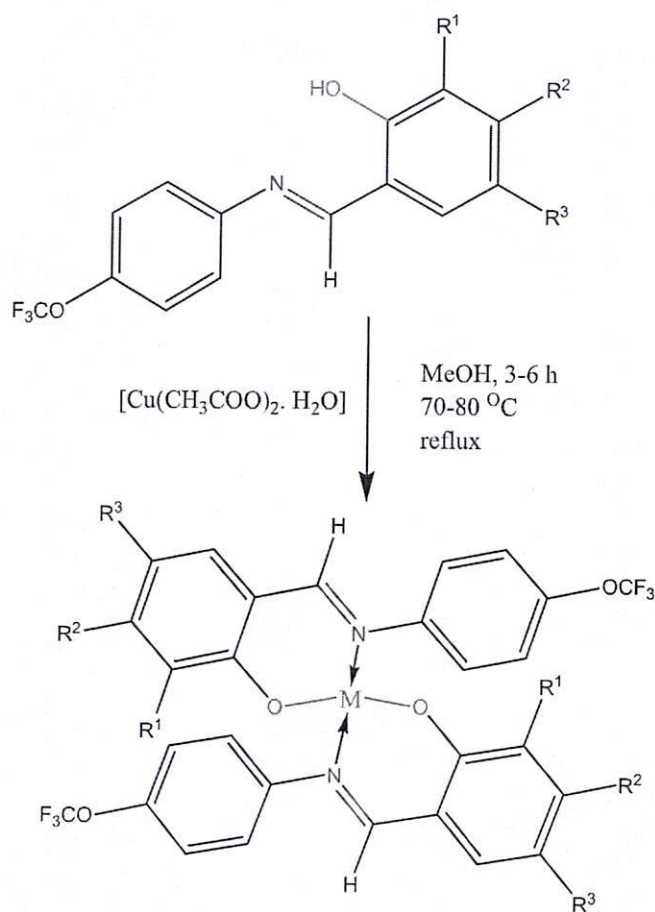
TGA: 70 % decomposition up to 800 °C Fig. S10

Characterizations

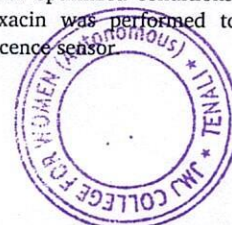
X-ray powder diffraction (XRD) pattern was obtained using a Philips/X'PertPro X-ray diffractometer (CuK α , $\lambda = 0.15406$ nm). FT-IR spectra were recorded at a Bruker-Tensor 27 by embedding the material in KBr discs in the range of 400–4000 cm⁻¹. Electronic spectra were recorded at 25 °C using a Cary 50 UV-Vis spectrophotometer. Micro analyses for C, H, and N were performed using a ThermoFinnigan Flash Elemental Analyzer 1112EA. Melting points were determined with the help of an Electrothermal Apparatus-9200. ¹H NMR spectra for the ligand were recorded on a Bruker Advance III, 400-MHz NMR spectrometer using DMSO-*d*₆ solvent and TMS as internal standard. The EPR spectrum was recorded on a Bruker spectrometer operating in the X-band and using 100-kHz magnetic field modulation. The thermogravimetric analysis of the complexes was recorded on a Perkin Elmer STA 6000 thermal analysis system within the temperature range 25–800 °C. The SEM micrographs were recorded on a ZEISS EVO scanning electron microscope at 200 kV acceleration.

Fluorometric detection of antibiotics

In a typical experiment of fluorometric detection of antibiotics, first, we add 10 μL various antibiotics including levofloxacin, ciprofloxacin, norfloxacin, lomefloxacin, enrofloxacin, ofloxacin, moxifloxacin, and gatifloxacin (5 μM), 50 μL of CuO NPs solution (3 nM), 10 μL of 0.1 M PBS buffer (pH 5.0), and 20 μL ultrapure water to a 100 μL centrifuge tube. The mixture was vortexed and then incubated for 5 min at room temperature. Next, the reaction mixture was incubated at 4 °C for 45 min. Use a pipette to move the mixed solution to a quartz cuvette to measure the fluorescence spectrum. The whole experiment process was carried out at 4 °C. The CuO NPs bound to the antibiotic solution were removed using ultracentrifuge and the supernatant then analyzed using fluorescence spectroscopy with excitation at 340 nm and an emission scan range of 200–800 nm. The results were compared with the calibration plot in order to evaluate the error within the assay. Further, to evaluate the detection range and sensitivity of the platform, we analyzed different concentrations of ciprofloxacin under optimized conditions. The fluorescence gradient test of ciprofloxacin was performed to investigate the detection range of this fluorescence sensor.



Scheme 2. Schematic route for the synthesis of Cu(II) complex from Schiff base ligand (TMPM6MOP: R¹ = OCH₃, R² = H, R³ = H; and M = Cu).



Antioxidant activity

The capacity of CuO NPs to scavenge the stable free radical DPPH was monitored using the different concentrations of the sample (4 mL) dissolved in 1 mL of methanol solution of DPPH radical (500 μM). After vortexing the mixture, it was left to stand at incubator at ambient temperature for 30 min. The λ^{max} of the resulting solution was read spectrophotometrically at 517 nm. Through the present study the ascorbic acid was applied as a control. The percentage of DPPH decolorization was calculated using the following equation, which represents the radical scavenging activity (RSA):

$$\text{RSA (\%)} = A_0 - A_s / A_0 \times 100$$

where A_0 is the absorbance of the control, and A_s is the absorbance of the sample. Furthermore, RSA% and RSA50% are percentage of the extract required to decay a special amount of DPPH free radicals and 50 % DPPH free radicals, respectively.

Antimicrobial activity

The antimicrobial activities of the synthesized Schiff base (TMPM6MOP), precursor (copper acetate), their $[\text{Cu}(\text{TMPM6MOP})_2]$ complex, and as-prepared CuO NPs were determined using a modified Bauer-Kirby method [25]. Briefly, 100 μL of the pathogenic bacteria/fungi were grown in 10 mL of fresh media until they reached a count of 10^8 cells/mL for bacteria or 10^5 cells/mL for fungi [29]. The 100 μL microbial suspensions were spread onto agar plates corresponding to both pathogens in which they were maintained. The isolated colonies of each organism were selected and tested for susceptibility by the disc diffusion method. A filter paper disc impregnated with the tested chemical was placed on agar. The prepared agar plates were filled with gram-positive and gram-negative bacteria such as *Escherichia coli* (ATCC 27853), *Pseudomonas aeruginosa* (ATCC 25922), *Staphylococcus aureus* (ATCC 25923), and *Bacillus subtilis* (ATCC 19659); and fungi such as *Aspergillus niger* and *Candida albicans* were incubated at 25–27 $^\circ\text{C}$ for 24–48 h. The prepared Schiff base, Cu(II) complex, CuO NPs, and CuO needles suspension (10 μL) was added to the discs. The samples were initially incubated for 15 min at 4 $^\circ\text{C}$ (to allow diffusion) and later on at 37 $^\circ\text{C}$ for 24 h. Positive test results were scored when a zone of inhibition

was observed around the discs.

Results and discussion

XRD study

The X-ray diffraction (XRD) study was undertaken to determine and to confirm the crystalline structure of synthesized CuO NPs and CuO needles; and displayed in Fig. 1. It shows the appearance of diffraction pattern at angle of $2\theta = 32.7, 35.8, 38.9, 49.0, 53.7, 58.5, 61.8, 66.3, 72.6$ and 75.4 which are assigned to the crystal planes of (110), (002), (111), (200), (020), (202), (311), (220), (311) and (004), respectively, which is correlated to monoclinic phase of CuO NPs (JCPDS file no.: 48–1548) [26]. No characteristic peak due to any impurity was observed in the XRD, it is suggesting the formation of pure crystalline CuO. The average size of the CuO NPs and CuO needles was calculated at the diffraction peak of $2\theta = 38.9^\circ$ by using the Debye–Scherrer equation. The average crystallite size in the synthesized CuO NPs and CuO needles is 10 ± 2 nm.

$$D = 0.9 \lambda / \beta \cos \theta$$

where λ is the wavelength of the X-ray radiation (0.154 nm), θ is the diffraction angle, and β is the full width at half maximum (FWHM).

SEM study

In order to confirm the surface topography and study the morphological evolution of the synthesized CuO NPs by using SEM analysis. The SEM image of the synthesized bare CuO NPs (Fig. 2a-b) shows the presence of smaller sized spherical CuO NPs which are assembled in a particular fashion to form some larger sized spheres of sizes about less than 100 nm. As it can be seen, there are voids within these spherical structures. The SEM images of the synthesized needles shaped CuO composite from Cu(II) complex was shown in Fig. 2(c-d). The length and diameter of the needles shaped CuO was measured in the ranges from less than 250 nm and 10–20 nm, respectively. This clearly indicated that the presence of Schiff base derived Cu(II) complex restricts the growth of the composite during needles formation and get less aggregation in a particular orientation to form needle-like structures. It may be

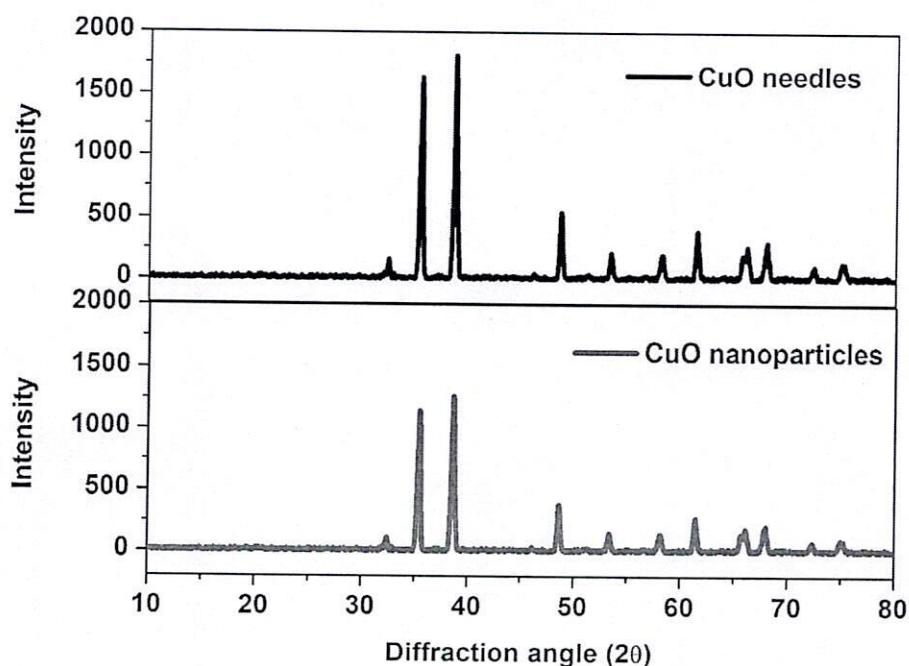
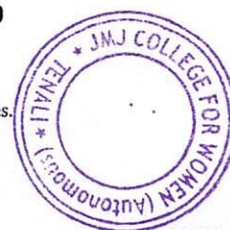


Fig. 1. The powder XRD pattern of the synthesized bare CuO NPs and Cu(II) complex derived CuO needles.



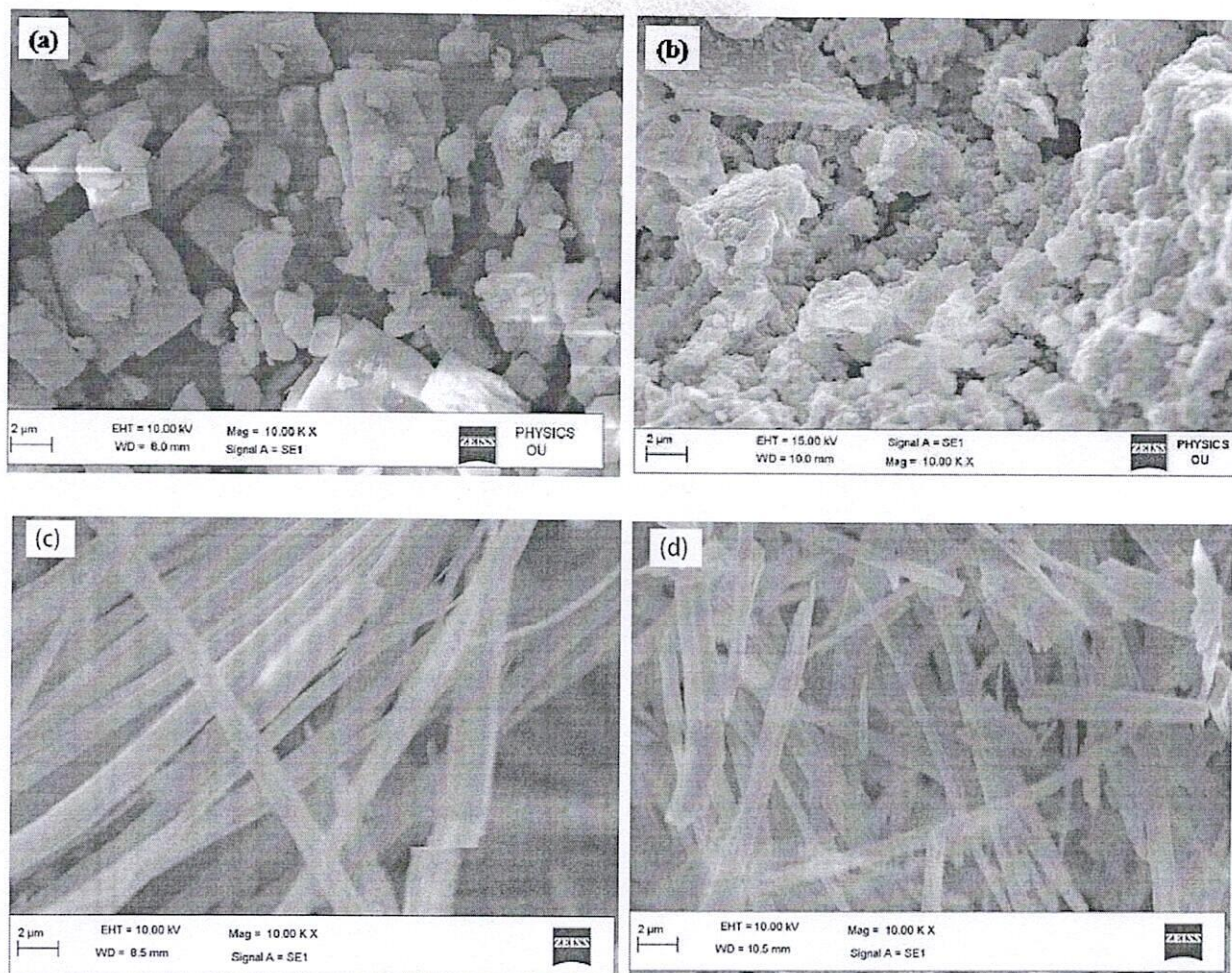


Fig. 2. SEM images of the synthesized (a-b) bare CuO NPs and (c-d) Cu(II) complex derived CuO needles.

mentioned that the size of CuO NPs calculated from the XRD study is different from those observed in SEM study. The possible reason is that, SEM measures the particle size, whereas XRD also can measure the crystallite size which is the coherent diffracting crystalline domains (crystallite) that is different from the particle size [30].

UV-vis DRS

The light-absorption characteristics were measured to identify the important features responsible for the various applications of CuO NPs and CuO needles were synthesized via the thermal decomposition method. The UV-vis absorption spectra is a potential measure for the identification of the synthesized CuO NPs and CuO needles and it was displayed in Fig. 3. It can be seen as, the formation of CuO NPs, which was confirmed by the characteristic surface plasmon absorbance at the wavelength of 374 nm with an absorption edge at 450 nm. The value of optical bandgap for CuO NPs and CuO needles, as obtained from the absorption onset is 3.21 eV and 3.32 eV, respectively, which is much larger than the bulk value (1.85 eV) [31]. It is observed that the UV-visible peak of CuO needles is shifted to a lower wavelength (blueshift) and higher intensity corresponding to an increase in bandgap value. It might be appealed that the blueshift is a result of less electron-phonon coupling, lattice distortions, and localization of charge carriers due to defect-interface interactions [32].

Photoluminescence

The photoluminescence (PL) emission spectra were widely carried

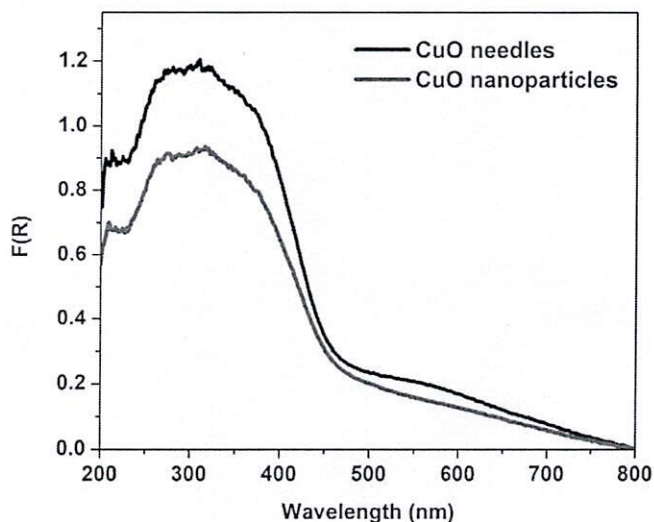


Fig. 3. UV-vis DRS of the synthesized bare CuO NPs and Cu(II) complex derived CuO needles.

out to examine the efficiency of charge carrier transfer and the lifetime of photoinduced electron-hole pairs in CuO systems. Fig. 4 displays the PL spectra of the synthesized CuO NPs and CuO needles at an excitation wavelength of 385 nm, and one distinct emission band at about 548 nm



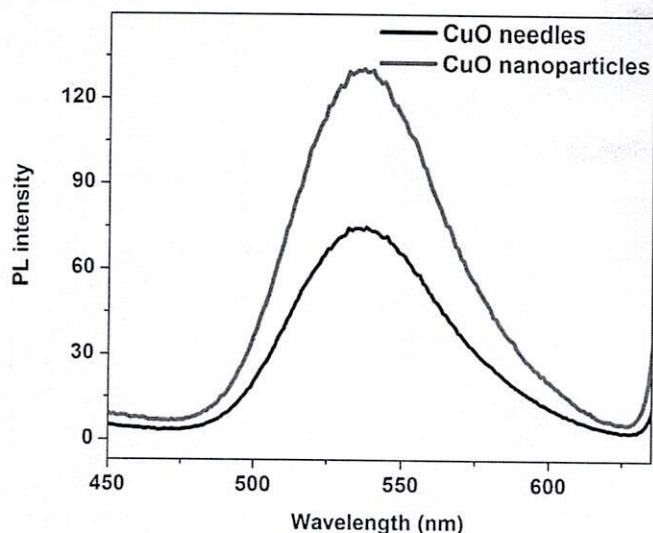


Fig. 4. PL spectra of the synthesized bare CuO NPs and Cu(II) complex derived CuO needles.

can be observed, which is in agreement with the literature [33]. The intense nature of the PL signal observed for the CuO NPs revealed that rapid photoinduced electron-hole pair recombination occurred following light irradiation [33]. The PL intensity of CuO needles is much lower than that of CuO NPs, indicating that efficient charge transfer takes place in the CuO needles. The PL results indicated that CuO needles uniformly arranged and effectively suppressed electron-hole pair recombination [34].

FTIR

FT-IR analysis was carried out to detect the probable functional groups present in the synthesis of CuO NPs and CuO needles. Fig. 5 shows the FT-IR spectra of the synthesized CuO NPs and CuO needles. In the FTIR spectra, the strong absorption bands range from 3200 to 3485 cm^{-1} , which are attributed to free hydroxyl groups and their intra/intermolecular H-bonds of phenolic compounds. The sharp peaks appeared at 2922, 1618, and 1398 cm^{-1} were related to saturated hydrocarbons (C-H), C=O, and C=C aromatic stretching frequencies respectively. The observed bands are due to lattice vibrational modes

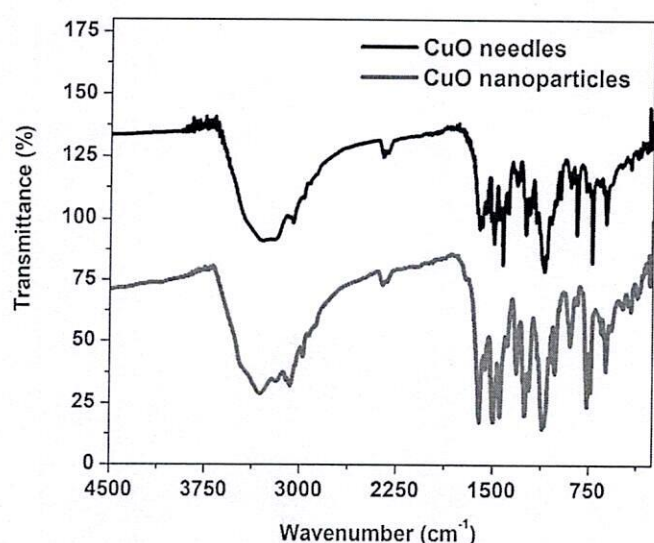


Fig. 5. FTIR spectra of the synthesized bare CuO NPs and Cu(II) complex derived CuO needles.

representing the functional groups of Cu(II) complex supported CuO needles. The peak at 1473 cm^{-1} and 1627 cm^{-1} was assigned to the bending vibrations of sp^2 -bonds of aromatic moieties and carbonyl stretching frequencies respectively. The different organic functional moieties surrounded over CuO NP are specified by the peaks observed at 1263, 1174 and 1051 cm^{-1} . The phonon bands were seen at 505 cm^{-1} and 585 cm^{-1} represent the stretching vibration of Cu-O bond in monoclinic CuO NPs and CuO needles [35].

Fluorescence detection of antibiotics by CuO needles

Before using the synthesized CuO needles to selective and sensitive detect Cipro, a single material CuO needles was used to perform the fluorescent selective detection on Cipro among various antibiotics including levofloxacin, ciprofloxacin, norfloxacin, lomefloxacin, enrofloxacin, ofloxacin, moxifloxacin, and gatifloxacin. In order to improve the accuracy of the detection results, the pH and response time during the experiment were optimized. The fluorescence intensity changed with the change of the pH value within the range of 4–9, and it has the most response when pH = 5 and it was displayed in Fig. 6. So, pH = 5 was selected as the optimal pH value for the whole fluorescence sensing activity. During the detection experiment, 20 μL antibiotics such as levofloxacin, ciprofloxacin, norfloxacin, lomefloxacin, enrofloxacin, ofloxacin, moxifloxacin, and gatifloxacin (10^{-3} M) were separately added dropwise to the synthesized CuO needles solution (Fig. 7(a)). Once Cipro was added, the fluorescence intensity of the nanosheets decreased rapidly, and did not change apparently with the increase of time other than antibiotics. It is obvious that the fluorescence intensity of CuO needles can be barely impacted by the response time.

The effect of some interferences like various antibiotics to the fluorescence intensity at 548 nm of CuO needles material was studied. The results show that the fluorescence intensity ratio is obviously changed by adding Cipro, while other interferences have little effect on the fluorescence intensity ratio, indicating that the CuO needles can achieve selective Cipro detection. Ciprofloxacin was selectively detected with the above-mentioned optimal conditions. With the Cipro concentration increase from 0 to 100 $\mu\text{M L}^{-1}$, the fluorescence intensity at 548 nm gradually decreases (Fig. 7(b)). Within the range of 15–70 $\mu\text{M L}^{-1}$ concentration of Cipro, the change in fluorescence intensity ($F_0 - F$) shows a good linear relationship with the Cipro concentration (Fig. 8). The linear regression equation is $(F_0 - F) = 0.341 [\text{TC}] + 1$, and the calculated minimum detection limit (LOD) is 0.21 nM, which is much lower than

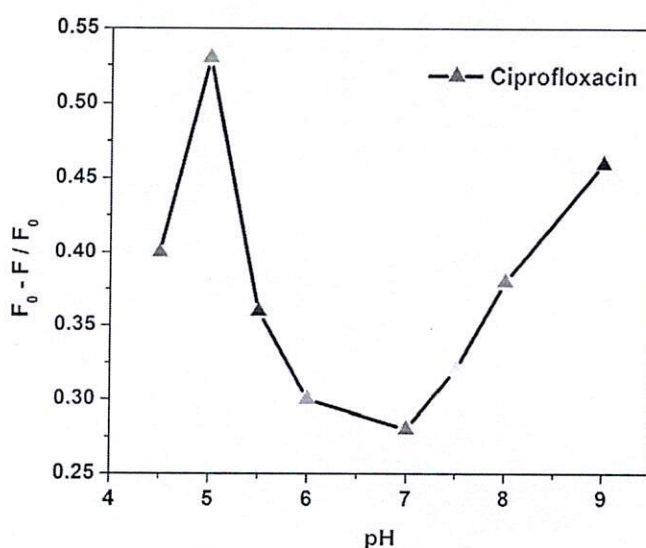


Fig. 6. The pH optimization of antibiotics (ciprofloxacin) for fluorometric detection using the synthesized Cu(II) complex derived CuO needles.

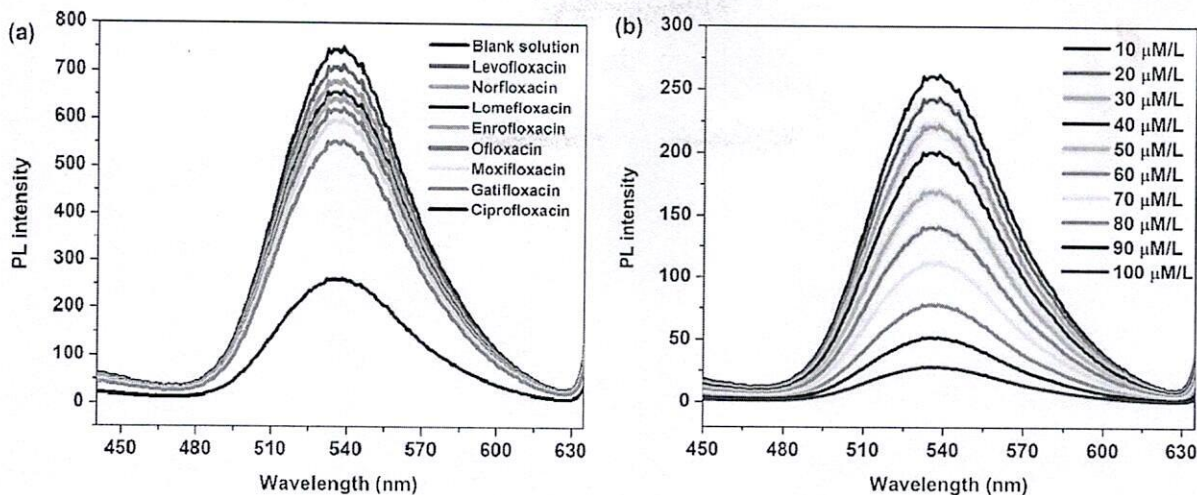


Fig. 7. The fluorescence emission spectra of the synthesized CuO needles with the effect of various antibiotics (a) and effect of increase the concentration of Cipro from 10 to 100 $\mu\text{M L}^{-1}$.

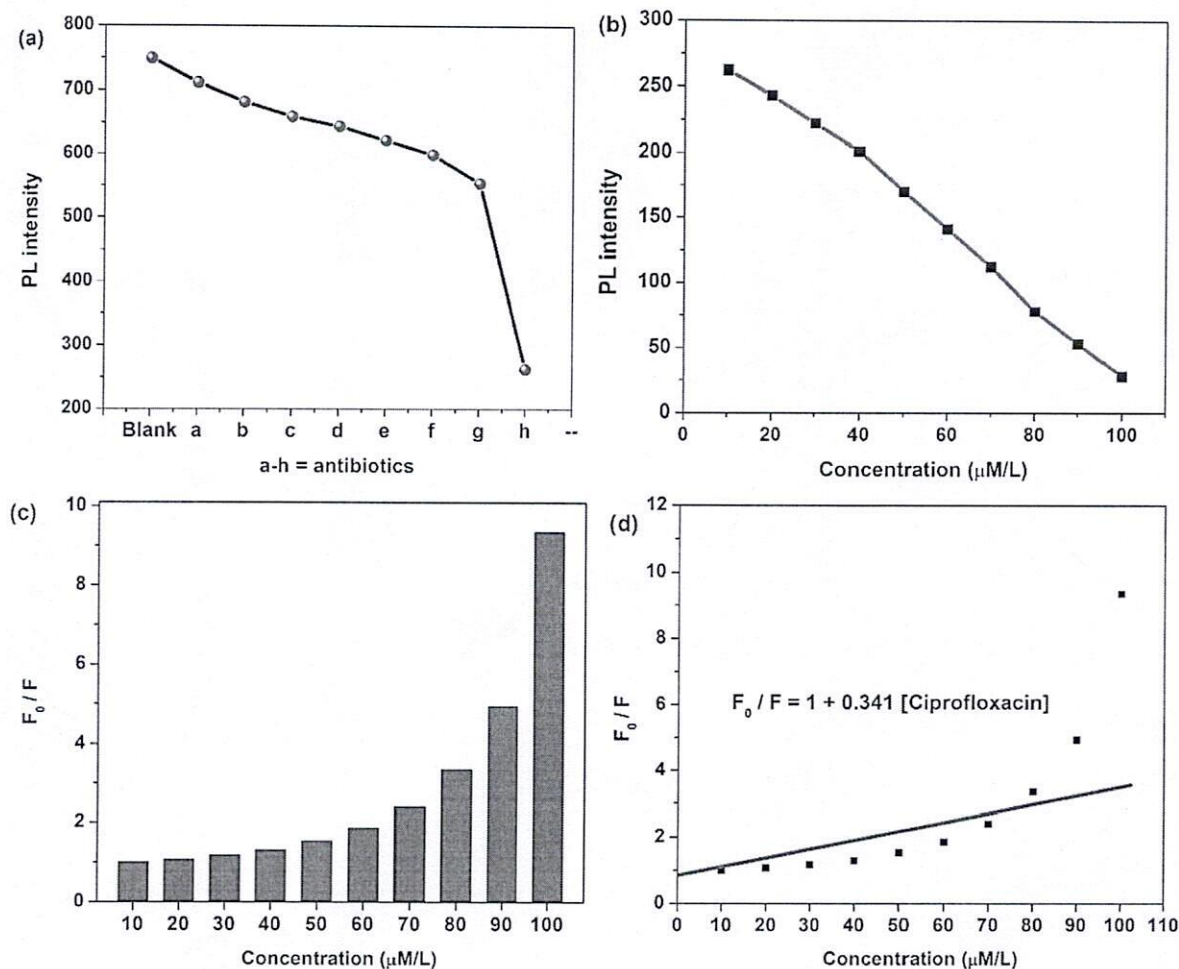


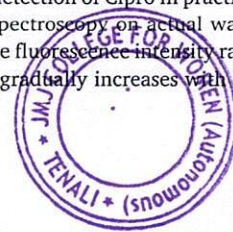
Fig. 8. (a) The change in PL intensity of CuO needles by using various antibiotics (a-h =), (b-c) the effect of Cipro concentration on PL intensity and relative fluorescence; (d) the linear relationship between changes in relative fluorescence intensity and Cipro concentrations (Stern-Volmer plot).

the other antibiotic sensors [36–37].

Detection of ciprofloxacin in water samples

In order to further evaluate the anti-interference ability of

fluorescent probes and the feasibility of this dual emission ratio fluorescent probe for rapid and ultra-sensitive detection of Cipro in practical applications, we performed fluorescence spectroscopy on actual water samples (tap water) test. It can be seen as the fluorescence intensity ratio of tap water and deionized water solution gradually increases with the



increase of Cipro concentration. In addition, the ratio of the fluorescence intensity of the probes in the two water samples was approximately the same, and no significant difference was observed (Table 1). The fluorescence intensity ratio has a linear relationship with the Cipro concentration and a good recovery rate of standard addition is obtained. The results show that the detection system has the same results as the laboratory conditions of deionized water, which can effectively eliminate the interference of coexisting substances, which proves that the probe has excellent selectivity. At the same time, it proved the accuracy and reliability of the probe in measuring Cipro in environmental samples.

Antioxidant activity

DPPH is a stable compound and accepts hydrogen or electrons from donor materials. In the present study, antioxidant activity of the CuO NPs was evaluated against DPPH with different concentrations (0–3 μM). The effective free radical inhibition was observed for both CuO NPs and CuO needles was shown in Fig. 9. The average percentage inhibition of CuO NPs and CuO needles was 58.82 % and 76.23 % and the activity was increased with increasing concentrations of CuO NPs and CuO needles (CuO NPs < CuO needles). The superoxide anions which are free radicals generated by transferring an electron play an important role in the formation of other reactive oxygen species such as hydrogen peroxide, hydroxyl radical, or singlet oxygen in living systems [38]. Due to their scavenging power, antioxidants are useful for the management of diseases, such as neurodegenerative, cancer and AIDS diseases. Antioxidants can also react with nitric oxide to form peroxynitrite, which can generate toxic radicals, such as hydroxyl radical [39]. Among these materials, the maximum DPPH radical scavenging activities were obtained from CuO NPs and CuO needles is 1.64 and 1.31 μM . The antioxidant activity of the CuO needles was prominent and comparable with that of the standard ascorbic acid; as well as the antioxidant activity of the CuO NPs was lower than that of the ascorbic acid in the DPPH free radical scavenging assay and CuO needles. However, CuO needles also showed higher antioxidant activity than the Schiff base and Cu(II) complex.

Antimicrobial activity

All the synthesized Schiff base, precursor, Cu(II) complex, as-prepared CuO NPs and CuO needles were screened in-vitro for their biological activities such as antibacterial and antifungal activities using gram positive and gram negative bacteria such as *Escherichia coli* (ATCC 27853), *Pseudomonas aeruginosa* (ATCC 25922), *Staphylococcus aureus* (ATCC 25923), and *Bacillus subtilis* (ATCC 19659); and fungi such as *Aspergillus niger* and *Candida albicans* by using disc diffusion method. Ampicillin (antibacterial agent) and ketocanazole (antifungal agent) served as positive controls for antimicrobial activity and a filter disc impregnated with 10 μL of solvent (DMSO) was used as a negative control. During the incubation time, the tested samples (Schiff base, Cu(II) complex, CuO NPs, and CuO needles) were exhibited prominent antimicrobial activity for the inhibition of bacteria and fungi growth and it was shown in Fig. 10(a-b). Among them, the synthesized CuO needles were exhibited maximum activity than its Schiff base, Cu(II) complex, and CuO NPs against gram positive bacteria due to their small size and effectiveness, they show efficient inhibition mechanisms inside the cell

Table 1
The Results for the determination of Cipro in real water sample.

Sample	Added (μM)	Founded (μM)	Recovery (n = 3, %)	RSD (n = 3, %)
Tap water	15	16.598	104.21	3.895
	25	26.158	102.32	2.157
	35	37.021	98.35	2.956

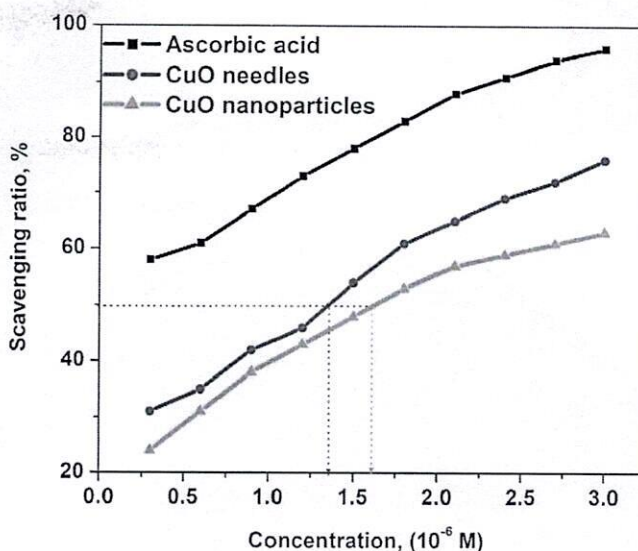


Fig. 9. The antioxidant activity of the synthesized bare CuO NPs and Cu(II) complex derived CuO needles.

of microorganisms [40].

Based on these observations, it can be concluded that synthesized CuO needles had strong antibacterial activity against bacteria belonging to both Gram-positive and Gram-negative bacteria as well as fungi. CuO needles have an important antibacterial property due to their large surface area, which helps them to make closer contact with microorganisms. Furthermore, the Gram-negative bacteria seemed to be more resistant to CuO needles than Gram-positive bacteria [41]. It was earlier reported that the interaction between Gram-positive bacteria and NPs was stronger than that of Gram-negative bacteria because of the difference in cell walls between Gram-positive and Gram-negative bacteria [41]. These findings suggest the use of synthesized CuO needles as a potential antimicrobial agent. The smaller size and homogeneous morphology of the nanoparticles are consistent with their excellent antimicrobial activity [39]. Although the structures of the bacterial cell walls are different and the biocidal effect could be dependent on the bacterial species, the CuO needles have the potential to cause cell death as a consequence of electrostatic interactions between the liberated metal ions and the negatively charged bacterial cell wall, subsequent disruption of the cell membrane and protein denaturation [42]. In addition, the CuO needles reach inhibition levels similar to those of a conventional antimicrobial drug.

Conclusions

The present study reported a simple and low-cost approach for the synthesis of monoclinic bare CuO NPs and CuO needles from Cu(II) complex derived from 2-(4-(trifluoromethoxy)phenylimino)methyl)-6-methoxyphenol (TMPM6MOP) by the thermal decomposition method without expensive and toxic solvents or complicated equipment. The prepared both CuO NPs and CuO needles were characterized using XRD, FTIR, UV-vis DRS, PL, and SEM techniques to estimate the band gap energy, structure, phase, and shape of the CuO NPs and CuO needles. From XRD and SEM, the synthesized CuO NPs and CuO needles have a monoclinic structure with an average diameter of the particles is 10 ± 2 nm and the length of the CuO needles is ≈ 250 nm. The fluorescence detection method is proposed for detecting Cipro among various antibiotics by the synthesized CuO needles. The selective detection of Cipro, when Cipro is added to CuO needles from Cu(II) complex acts as a response unit to coordinate with Cipro to form a complex, thereby sensitizing the characteristic emission peak at 548 nm. With the increase of Cipro concentration (0–100 μM), the fluorescence at 548 nm

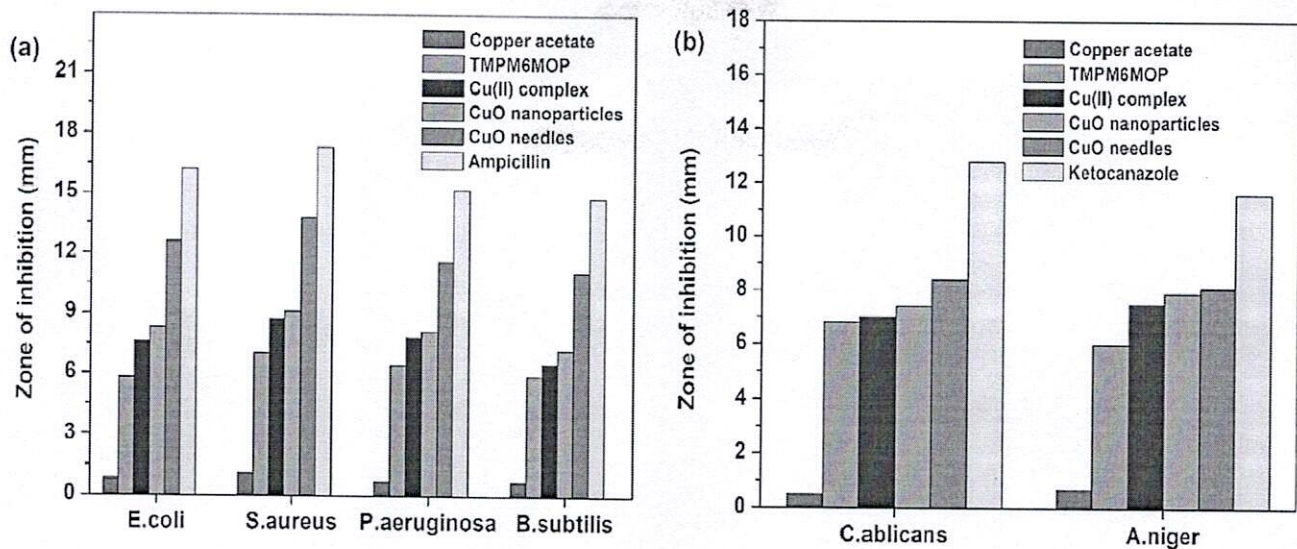


Fig. 10. (a) Antibacterial and (b) antifungal activities of the synthesized bare CuO NPs and Cu(II) complex derived CuO needles.

decreases continuously. So, the purpose of detecting Cipro can be achieved by changing the ratio of fluorescence signals. The linear range of this ratio fluorescent probe for detecting tetracycline is 15–70 μM , the minimum detection limit is 0.21 nM. The antibacterial activity of the synthesized CuO NPs and CuO needles was performed by disk diffusion method using Gram +ve and Gram -ve bacteria and the results are suggesting as CuO needles have prominent than other samples. The antioxidant activity results revealed that the CuO needles show a maximum than CuO NPs and are comparable to standard. Consequently, CuO needles have the potential for external uses as sensors and antibacterial agents in surface coatings on various substrates to prevent microorganisms from attaching, colonizing, spreading, and forming biofilms in indwelling medical devices.

Declaration of Competing Interest

The authors declare that they have no known competing financial interests or personal relationships that could have appeared to influence the work reported in this paper.

Data availability

No data was used for the research described in the article.

Acknowledgements

The authors acknowledge the Head, Department of Chemistry, Osmania University, Hyderabad and JMJ College for Women, Tenali, Andhra Pradesh, India for providing infrastructure support to conduct the research work.

Authors' contributions

DA is conceptualized the study, designed the methods, conducted experiments, wrote the first and revised draft. DA and VS conducted experiments. DA was supervised the study and worked on the revised draft. VS assisted in data interpretation and worked on the revised draft. All authors read and approved the final manuscript.

Ethics approval and consent to participate

This article does not contain any studies with human participants or animals performed.

Availability of data and material

The raw data is available by contacting the authors.

Funding

This research did not receive any external funding.

Appendix A. Supplementary data

Supplementary data to this article can be found online at <https://doi.org/10.1016/j.rechem.2023.100821>.

References

- [1] J. Rakhtshah, A comprehensive review on the synthesis, characterization, and catalytic application of transition-metal Schiff-base complexes immobilized on magnetic Fe_3O_4 nanoparticles, *Coord. Chem. Rev.* 467 (2022), 214614.
- [2] M.K. Patil, V.H. Masand, A.K. Malhure, Schiff base metal complexes precursor for metal oxide nanomaterials: a review, *Cur. Nanosci.* 17 (4) (2021) 634–645.
- [3] D. Ayodhya, G. Veerabhadram, Fabrication of Schiff base coordinated ZnS nanoparticles for enhanced photocatalytic degradation of chlorpyrifos pesticide and detection of heavy metal ions, *J. Materiomics* 5 (3) (2019) 446–454.
- [4] G. Bonaccorso, F. Marzò, D. La Mendola, Biological applications of thiocarbohydrazones and their metal complexes: a perspective review, *Pharmaceuticals* 13 (2019) 4.
- [5] S. Cao, X. Li, Y. Gao, F. Li, K. Li, X. Cao, Y. Dai, L. Mao, S. Wang, X. Tai, A simultaneously GSH-depleted bimetallic Cu(II) complex for enhanced chemodynamic cancer therapy, *Dalton Trans.* 49 (2020) 11851–11858.
- [6] M.K. Lesiów, A. Bieńko, K. Sobańska, T. Kowalik-Jankowska, K. Rolka, A. Legowska, N. Ptaszyńska, Cu(II) complexes with peptides from FomA protein containing -His-Xaa-Yaa-Zaa-IHis and -IHis-IHis-motifs. ROS generation and DNA degradation, *J. Inorg. Biochem.* 212 (2020), 111250.
- [7] C.-Y. Zhou, J. Zhao, Y.-B. Wu, C.-X. Yin, Y. Pin, Synthesis, characterization and studies on DNA-binding of a new Cu(II) complex with N1, N8-bis (1-methyl-4-nitropyrrrole-2-carbonyl) triethylenetetramine, *J. Inorg. Biochem.* 101 (1) (2007) 10–18.
- [8] M. Shakir, M. Azam, M.F. Ullah, S.M. Hadi, Synthesis, spectroscopic and electrochemical studies of N, N-bis [(E)-2-thienylmethylidene]-1,8-naphthalenedianiline and its Cu(II) complex: DNA cleavage and generation of superoxide anion, *J. Photochem. Photobiol. B* 104 (3) (2011) 449–456.
- [9] S. Abdelrahman, M. Alghrably, M. Campagna, G.A. Hauser, M. Jaremko, J. I. Lachowicz, Metal complex formation and anticancer activity of Cu(I) and Cu(II) complexes with metformin, *Molecules* 26 (2021) 4730.
- [10] H. Kargar, A.A. Ardakani, M.N. Tahir, M. Ashfaq, K.S. Munawar, Synthesis, spectral characterization, crystal structure determination and antimicrobial activity of Ni(II), Cu(II) and Zn(II) complexes with the Schiff base ligand derived from 3, 5-dibromosalicylaldehyde, *J. Mol. Struct.* 1229 (2021), 129842.
- [11] D.H. Cai, C.L. Zhang, Q.Y. Liu, L. He, Y.J. Liu, Y.H. Niong, X.Y. Le, Synthesis, DNA binding, antibacterial and anticancer properties of two novel Cu(II) complexes containing gluconate, *Eur. J. Med. Chem.* 270 (2021), 115195.

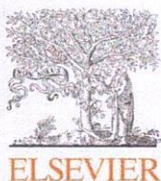


- [12] P.A. Ajibade, F.P. Andrew, A.A. Fatokun, A.E. Oluwalana, Synthesis, characterization and in vitro screening for anticancer potential of Mn (II), Co (II), Cu (II), Zn (II), and Pt (II) methoxy phenyl dithiocarbamate complexes, *J. Mol. Struct.* 1230 (2021), 129894.
- [13] D. Saravanakumar, H. Abou Oualid, Y. Brahmī, A. Ayeshamariam, M. Karunanaiithy, A.M. Saleem, K. Kaviyarasu, S. Sivaranjani, M. Jayachandran, Synthesis and characterization of CuO/ZnO/CNTs thin films on copper substrate and its photocatalytic applications, *OpenNano* 4 (2019), 100025.
- [14] L.i. Dong, H. Chu, Y. Li, S. Zhao, D. Li, Third-order nonlinear optical responses of CuO nanosheets for ultrafast pulse generation, *J. Materiomics* 8 (2) (2022) 511–517.
- [15] L.M. Dwivedi, N. Shukla, K. Baranwal, S. Gupta, S. Siddique, V. Singh, Gum acacia modified Ni-doped CuO nanoparticles: an excellent antibacterial material, *J. Clust. Sci.* 32 (2021) 209–219.
- [16] H. Heidari, F. Teimuri, A.R. Ahmadi, Nanocellulose-based aerogels decorated with Ag, CuO and ZnO nanoparticles: synthesis, characterization and the antibacterial activity, *Polyhedron* 213 (2022), 115629.
- [17] K. Karthik, A.M. Qadir, Synthesis and crystal structure of a new binuclear copper (II) carboxylate complex as a precursor for copper (II) oxide nanoparticles, *J. Struct. Chem.* 60 (7) (2019) 1126–1132.
- [18] Z. Rezaezadeh, F. Soleimani, B. Mahmoudi, M.A. Nasserī, M. Kazemnejadi, Facile synthesis, characterization, and antibacterial activities of CuO, NiO, and Co₂O₃ metal oxide nanoparticles using polysalicylaldehyde-metal Schiff base complexes as a precursor, *Appl. Phys. A* 127 (2021) 1–13.
- [19] M. Kundu, G. Karunakaran, E. Kolesnikov, M.V. Gorshenkov, D. Kuznetsov, Negative electrode comprised of nanostructured CuO for advanced lithium ion batteries, *J. Clust. Sci.* 28 (3) (2017) 1595–1604.
- [20] N. Silva, S. Ramirez, I. Diaz, A. Garcia, N. Hassan, Easy, quick, and reproducible sonochemical synthesis of CuO nanoparticles, *Materials* 12 (2019) 804.
- [21] E.H. Dias, G.T. Da Silva, J.C. Da Cruz, C. Ribeiro, One-pot solvothermal synthesis of carbon black-supported CuO for catalysis of CO₂ electroreduction, *Chem. Electrochem.* 9 (2022) e202200206.
- [22] M. Chandrasekar, M. Subash, S. Logambal, G. Udhayakumar, R. Uthrakumar, C. Immozhi, W.A. Al-Onazi, A.M. Al-Mohameed, T.W. Chen, K. Kanimozhi, Synthesis and characterization studies of pure and Ni doped CuO nanoparticles by hydrothermal method, *J. King Saud. Univ. Sci.* 34 (2022), 101831.
- [23] E.M. Ibrahim, L.H. Abdel-Rahman, A.M. Abu-Dief, A. Elshafaie, S.K. Hamdan, A. M. hmed, The synthesis of CuO and NiO nanoparticles by facile thermal decomposition of metal-Schiff base complexes and an examination of their electric, thermoelectric and magnetic properties, *Mater. Res. Bulletin* 107 (2018) 492–497.
- [24] S.H. Jaber, A.M. Rheima, D.H. Hussain, M.F. Al-Marjani, Comparing study of CuO synthesized by biological and electrochemical methods for biological activity, *Al-Mustansiriyah J. Sci.* 30 (1) (2019) 94–98.
- [25] M. Kasiri, M. Rahaie, A visible and colorimetric nanobiosensor based on DNA-CuO nanoparticle for detection of single nucleotide polymorphism involved in sickle cell anemia disease, *Mater. Today Commun.* 27 (2021), 102423.
- [26] D. Ayodhya, G. Veerabhadram, Facile thermal fabrication of CuO nanoparticles from Cu (II)-Schiff base complexes and its catalytic reduction of 4-nitrophenol, antioxidant, and antimicrobial studies, *Chem. Data Collections* 23 (2019), 100259.
- [27] F. Hernandez, N. Calisto-Ulloa, C. Gómez-Fuentes, M. Gómez, J. Ferrer, G. González-Rocha, H. Bello-Toledo, A.M. Botero-Coy, C. Boix, M. Ibáñez, M. Montory, Occurrence of antibiotics and bacterial resistance in wastewater and sea water from the Antarctic, *J. Hazard. Mater.* 363 (2019) 447–456.
- [28] D. Ayodhya, G. Veerabhadram, One-pot green synthesis, characterization, photocatalytic, sensing and antimicrobial studies of *Calotropis gigantea* leaf extract capped Cds NPs, *Mater. Sci. Eng. B* 225 (2017) 33–44.
- [29] A.L. Barry, M.B. Coyle, C. Thornsberry, E.H. Gerlach, R.W. Hawkinson, Methods of measuring zones of inhibition with the Bauer-Kirby disk susceptibility test, *J. Clin. Microbiol.* 10 (6) (1979) 885–889.
- [30] F. Bayansal, H.A. Çetinkara, S. Kahraman, H.M. Çakmak, H.S. Güder, Nano-structured CuO films prepared by simple solution methods: plate-like, needle-like and network-like architectures, *Ceram. Inter.* 38 (2012) 1859–1866.
- [31] H. Azadi, H.D. Aghdam, R. Malekfar, S.M. Bellah, Effects of energy and hydrogen peroxide concentration on structural and optical properties of CuO nanosheets prepared by pulsed laser ablation, *Results Phys.* 15 (2019), 102610.
- [32] S. Das, T.L. Alford, Structural and optical properties of Ag-doped copper oxide thin films on polyethylene naphthalate substrate prepared by low temperature microwave annealing, *J. Appl. Phys.* 113 (2013), 244905.
- [33] A.K. Bhunia, S. Saha, CuO nanoparticle-protein bioconjugate: characterization of CuO nanoparticles for the study of the interaction and dynamic of energy transfer with bovine serum albumin, *Bio. Nano Sci.* 10 (2020) 89–105.
- [34] J. Wu, C. Li, X. Zhao, Q. Wu, X. Qi, X. Chen, T. Hu, Y. Cao, Photocatalytic oxidation of gas-phase Hg⁰ by CuO/TiO₂, *Appl. Catal. B* 176–177 (2015) 559–569.
- [35] Y. Abboud, T. Saffaj, A. Chagraoui, A. El Bouari, K. Brouzi, O. Tanane, B. Ihsane, Biosynthesis, characterization and antimicrobial activity of copper oxide nanoparticles (CONPs) produced using brown alga extract (*Bifurcaria bifurcata*), *Appl. Nanosci.* 4 (5) (2014) 571–576.
- [36] J. Chen, Y. Xu, S. Li, F. Xu, Q. Zhang, Ratio fluorescence detection of tetracycline by a Eu³⁺/NH₂-MIL-53 (Al) composite, *RSC Adv.* 11 (4) (2021) 2397–2404.
- [37] W. Wang, Y. Xu, X. Liu, L. Peng, T. Huang, Y. Yan, C. Li, Efficient fabrication of ratiometric fluorescence imprinting sensors based on organic-inorganic composite materials and highly sensitive detection of oxytetracycline in milk, *Microchem. J.* 157 (2020), 105053.
- [38] M. Maruthapandi, A.P. Nagvenkar, I. Perelshtein, A. Gedanken, Carbon-dot initiated synthesis of polypyrrole and polypyrrole@ CuO micro/nanoparticles with enhanced antibacterial activity, *ACS Appl. Poly. Mater.* 1 (5) (2019) 1181–1186.
- [39] T. Revathi, S. Thambidurai, Cytotoxic, antioxidant and antibacterial activities of copper oxide incorporated chitosan- neem seed biocomposites, *Inter. J. Biolog. Macromol.* 139 (2019) 867–878.
- [40] G.S. Sree, S.M. Botsa, B.J.M. Reddy, K.V.B. Ranjitha, Enhanced UV-Visible triggered photocatalytic degradation of Brilliant green by reduced graphene oxide based NiO and CuO ternary nanocomposite and their antimicrobial activity, *Arab. J. Chem.* 13 (4) (2020) 5137–5150.
- [41] A. Bouafia, S.E. Laouini, M.R. Ouahrani, A review on green synthesis of CuO nanoparticles using plant extract and evaluation of antimicrobial activity, *Asian J. Res. Chem.* 13 (2020) 65–70.
- [42] M. Maruthapandi, A. Saravanan, P. Das, M. Natan, G. Jacobi, E. Banin, J.H. T. Luong, A. Gedanken, Antimicrobial activities of Zn-doped CuO microparticles decorated on polydopamine against sensitive and antibiotic-resistant bacteria, *ACS Appl. Poly. Mater.* 2 (12) (2020) 5878–5888.



Principal
JMJC COLLEGE FOR WOMEN (Autonomous)
TENALI

2023



Contents lists available at ScienceDirect

Results in Chemistry

journal homepage: www.sciencedirect.com/journal/results-in-chemistry

Catalytic degradation of HIV drugs in water and antimicrobial activity of Chrysin-conjugated Ag-Au, Ag-Cu, and Au-Cu bimetallic nanoparticles

Dasari Ayodhya^{a,*}, V. Sumalatha^b, Raju Gurrapu^c, M. Sharath Babu^d

^a Department of Chemistry, University College of Science, Osmania University, Hyderabad 500007, India

^b Department of Chemistry, JMJ College for Women, Tenali, Guntur, Andhra Pradesh 522201, India

^c Organic and Biomolecular Chemistry Division, CSIR-IICT, Hyderabad, Telangana 500007, India

^d Department of Chemistry, Sardar Patel College, Secunderbad, Telangana 500061, India

ARTICLE INFO

Keywords:

Bimetallic nanoparticles
Chrysin
SPR effect
HIV drugs degradation
Biological agents

ABSTRACT

Biogenic synthesis of bimetallic nanoparticles (BMNPs) have important applications in medicine and catalytic reactions due to their emerging properties. In this study, we report a new approach for the synthesis of bio-functionalized bimetallic silver, gold, and copper (Chry@Ag-Au, Chry@Ag-Cu, and Chry@Au-Cu) nanoparticles using Chry as bioreductant and capping agent, which is a natural anticancer bioflavonoid emerged as potential drug therapy for cancer treatment. The synthesized BMNPs were characterized by Fourier Transform Infrared Spectrophotometer (FTIR), Scanning Electron Microscopy (SEM), Transmission Electron Microscopy (TEM), X-ray diffraction (XRD), BET analysis, zeta potential, and UV-Vis spectrometer to know the shape, size, structure, surface area, and bandgap energy. BMNPs were tested for the catalytic degradation of HIV drugs (stavudine (STV) and zidovudine (ZDV)) in the presence of NaBH₄ as a reducing agent in an aqueous medium. The maximum degradation (≈ 96 %) of STV and ZDV was observed in 18 min of reaction time using Chry@Ag-Au BMNPs in the presence of NaBH₄ and reused up to 5 consecutive runs without significant loss of catalytic activity. The synthesized BMNPs (20 μg/mL) were determined to estimation of antimicrobial activity against *Escherichia coli*, *Staphylococcus aureus*, *Pseudomonas aeruginosa*, and *Bacillus subtilis* bacteria, as well as fungi such as *Aspergillus niger* and *Candida albicans* respectively by well diffusion method.

1. Introduction

Increasing the use of organic contaminants in industry and agriculture; environmental safety becomes one of the serious problems for the scientific community [1–2]. Among various organic contaminants, dyes as well as antibiotics are frequently used organic pollutants which are discharged into the environment [2]. Currently the removal of these contaminants becomes a key scientific interest and their removal from the wastewater is definitely related to the quality of life. For the last few decades, there has been increasing demand for the removal of toxins, carcinogenic and mutagenic molecules from waste effluents [1,3]. Thus, different biological, physical and chemical treatment methods have been employed for elimination of dye effluents from the aqueous environment, including adsorption, filtration, coagulation–flocculation, reverse osmosis, precipitation, chlorine or hydrogen peroxide treatment, ion-exchange adsorption, membrane systems and bacterial cells [1,3–5]. The aforementioned conventional methods available for wastewater

treatment are slow and non-destructive. Therefore, an efficient method is needed for the removal of these highly carcinogenic substances [6]. The catalytic degradation of organic pollutants using MNPs is an important way for elimination of pollutant molecules without production of secondary toxic substances [7]. Currently, large numbers of BMNPs have been effectively used for the degradation of organic molecules [8–11].

Recently, BMNPs in the development of nanobiotechnology is among the fastest-growing research fields that involve the development of tiny nanomaterials with medical and industrial applications via a green approach [11]. These BMNPs exhibit unique properties because of their higher surface area to volume ratio and ultra-small size. Thus, different biological assets, such as bacteria, fungi, algae, marine organisms, and plants, have been explored for their ability to generate these particles [12–14]. The advantage of green synthesis over conventional chemical synthesis is that it is eco-friendly and cost-effective [12]. These bioactive compounds could reduce metal ions as well as stabilize the structure and

* Corresponding author.

E-mail address: ayodhyadasari@gmail.com (D. Ayodhya).

<https://doi.org/10.1016/j.rechem.2023.100792>

Received 23 December 2022; Accepted 12 January 2023

Available online 16 January 2023

2211-7156/© 2023 The Author(s). Published by Elsevier B.V. This is an open access article under the CC BY-NC-ND license (<http://creativecommons.org/licenses/by-nc-nd/4.0/>).



stability of nanoparticles [13]. The interaction of biomolecules with metal ions results in the formation of conjugated nanoparticles, which exhibit higher efficiency than the free biomolecule. Among the biomolecules, Chrysin (CHY) (5, 7-dihydroxy flavone), a phenolic compound (flavone), is a natural part of dietary supplements. It is abundantly found in honey, passion flowers (*Passiflora incarnate* and *P. caerulea*), *Oroxylum indicum*, and propolis [15]. CHY possesses excellent medicinal properties, including anti-cancer, antioxidant, antibacterial, antifungal, anti-parasitic, and anti-diabetic activities [15].

BMNPs play an important role in many application areas such as catalytic, energy, sensor technology, electronics, biological, and optical devices [1,7,11–13,16]. BMNPs are technologically superior to monometallic nanoparticles thanks to their advanced optical, electronic, and catalytic properties [17–19]. Other than the usual morphological manipulations, the variations in the molar ratio of the individual components provide a diverse dimension in tailoring the properties of BMNPs. BMNPs possess enhanced catalytic activity and selectivity compared to their single metallic counterparts [10]. Recently, the catalytic activity of Au–Ag alloy compositions for aromatic amines prepared by the reduction of nitrocompounds has significant industrial importance as they are widely used as the intermediates for the synthesis of dyes, pharmaceuticals and agrochemicals was reported [20]. Also, the azo dyes characterized by the presence of (N=N) group used in dyeing, textile, paper, leather, cosmetics and food processing are found to be hazardous for human health and environment [21]. From our research group has been reported mono metallic NPs for various catalytic, sensing, and biological applications [7,13,22–24].

In the present study, we have synthesized and characterized Chry@Ag–Au, Chry@Ag–Cu, and Chry@Au–Cu BMNPs using Chry as a direct bioreductant and capping agent. BMNPs were used to investigate catalytic degradation of HIV drugs (STV and ZDV) in the presence of NaBH₄ as a reducing agent in an aqueous medium. BMNPs were determined to have prominent antimicrobial activity against *Escherichia coli*, *Staphylococcus aureus*, *Pseudomonas aeruginosa*, and *Bacillus subtilis* bacteria, as well as fungi such as *Aspergillus niger* and *Candida albicans*, respectively to know the efficiency in biomedical applications.

2. Experimental

2.1. Materials and methods

All chemicals were of analytical grade and used without further purification. Chloroauric acid (HAuCl₄, CAS number: 16903–35-8, 99 % purity), copper sulfate pentahydrate (CuSO₄·5H₂O, CAS number: 7758–99-8, 98 % purity), silver nitrate (AgNO₃), NaOH, Chrysin, and sodium borohydride (NaBH₄) are procured from Sigma Aldrich Chemicals Pvt. Ltd, India. Double distilled water was used as a solvent throughout experiments.

2.2. Synthesis of Ag–Au, Ag–Cu, and Au–Cu BMNPs

In a typical synthesis of Chry@Ag–Au BMNPs was performed by adding 12.5 mL of 0.02 M AgNO₃ and 12.5 mL of 0.01 M HAuCl₄ in a Falcon tube. Then, the tube was mixed and heated until reaching 60 °C. When the temperature was reached, 2.5 mL of the Chrysin was added to the mixture (2:1:1 proportion), kept at constant stirring, and heated at 80 °C for 1 h. The NPs formation was monitored and confirmed by a change of color from transparent to brown (for silver) or black (for gold). The reaction mixture was cool at room temperature, centrifuged at 15000 rpm for 10 min, and the supernatant was discharged. The obtained product was solidified and washed with 70 % ethanol, left to dry at room temperature for 24 h, and finally lyophilized (Free Zone 6, Lab-conco, Kansas City, MO, USA) for another 24 h. In a similar way, we have synthesized Chry@Ag–Cu and Chry@Au–Cu BMNPs with their corresponding precursors under identical reaction conditions as mentioned above.

2.3. Instrumentation

The synthesized BMNPs are optically analyzed using Perkin Elmer Lambda-35 UV–Visible spectrophotometer (L3R 3 V6, Canada) to estimate bandgap energy. The morphology of the synthesized particles was better determined from images recorded using Zeiss EVO18 and TecnaiG2 transmission electron microscope (TVIPS GmbH, Germany). FTIR spectra recorded using IR-Prestige-21 Shimadzu spectrometer (Tampa, Florida 33626) help to recognize the bioactive compounds in Chrysin that are associated with the reduction and stabilization of metal ions. The crystallographic structure of the prepared samples is probed using the XRD patterns obtained from XPERT-PRO diffractometer (United Kingdom). The catalytic potential of synthesized BMNPs in the chemical degradation of HIV drugs is investigated using PerkinElmer Lambda-35 UV–Visible spectrophotometer (L3R 3 V6, Canada). The specific surface area of the BMNPs were recorded by using N₂ adsorption–desorption isotherms with ASAP-2000 instrument (Malvern instrument ltd., Malvern, UK). The stability of BMNPs was determined using the zeta potential (DLS, Malvern instrument Ltd., Malvern, UK).

2.4. Catalytic activity

To investigate the catalytic activity of synthesized Chry@Ag–Au, Ag–Cu, and Au–Cu BMNPs for the degradation of HIV drugs including STV and ZDV. The samples were neutralized with acid/alkali and/or diluted two times with water. The catalytic degradation studies were conducted in acidic (0.1 M HCl for ZDV and 0.01 M HCl for STV), neutral (water) and alkaline (0.1 M NaOH) solutions by using the synthesized Chry@Ag–Au, Ag–Cu, and Au–Cu BMNPs. After completion of the study, in the catalytic reaction, the suspension was collected and monitored for chemical changes using a UV–vis spectrophotometer at approximately 254 nm for STV and 266 nm for ZDV, which are the characteristic absorption peaks of the drugs. The degradation of STV and ZDV from water was evaluated by using the change in color of the solution with the reaction proceeds. The entire reaction procedure is monitored by using UV–visible spectrophotometer. The catalysts could be readily recovered by simple filtration after completion of the reaction and reused for 5 consecutive cycles. The percentage of degradation (D%) in each reaction is calculated using the following equation.

$$D(\%) = \frac{A_0 - A_t}{A_0} \times 100$$

Wherein, A₀ is the absorbance at time is 0 min and A_t is the absorbance at different time intervals.

2.5. Antimicrobial studies

The antimicrobial potential of fabricated Chry@Ag–Au, Ag–Cu, and Au–Cu BMNPs were comparatively studied by using a well diffusion assay against various bacterial and fungal strains. All the bacterial pathogens (*Escherichia coli*, *Staphylococcus aureus*, *Pseudomonas aeruginosa*, and *Bacillus subtilis* bacteria, as well as fungi such as *Aspergillus niger* and *Candida albicans*) were cultured in the Mueller-Hinton (M–H) broth at 37 °C and then sub-cultured in M–H agar overnight. Then, the bacterial colonies were suspended in 2 mL of sterile saline, and the inoculum of test pathogens was prepared by adjusting the turbidity of bacterial suspensions to 0.5 McFarland (1.5 × 10⁶ colony forming units CFU/mL) by diluting the sterile saline. All the bacterial and fungal pathogens inoculum was uniformly swabbed onto Mueller-Hinton (MH) agar plates separately using sterilized cotton swabs. Meanwhile, the synthesized Chry@Ag–Au, Ag–Cu, and Au–Cu BMNPs (20 µg/mL) were loaded into each well, and ampicillin and ketoconazole were used as positive controls. After overnight incubation at 37 °C ± 0.2 °C, the formation of clear zones around the well was measured with a zone scale and compared.



3. Results and discussion

3.1. Optical absorption studies

The optical properties and LSPR (localized surface plasmon resonance) effect of Chry@Ag–Au, Ag–Cu, and Au–Cu BMNPs were investigated by using UV–vis absorption spectrometer. Fig. 1 shows the UV–vis absorption spectra of different Chry@Ag–Au, Ag–Cu, and Au–Cu BMNPs. It can be seen from Fig. 1, a physical mixture of the individual colloids have different surface plasmon peaks, those are corresponding to their combination of BMNPs [25]. In addition, a SPR band tuning from pure Ag to pure Au as a function of Ag–Au ratio can be obtained in an alloying process having an different electron density and it leads to the broadening and red shift of plasmon frequency [25]. It was found that Ag–Cu (584 nm) and Au–Cu BMNPs (456 nm) have high bandwidth as compared to Ag–Au BMNPs (426 nm) but the scattering efficiency of Ag–Au BMNPs is maximum as compare to the other BMNPs with the same size and surrounding medium. Therefore, from the comparison, it was found to be that Ag–Au BMNPs have high bandwidth and large tunability of LSPR, which are the most important factors while considering the efficiency of catalytic activity [25]. Thus, with consideration to low cost and high efficiency in catalysis, the Ag–Au BMNPs may be good candidate for catalytic applications as compared to Ag–Cu and Au–Cu BMNPs.

3.2. XRD analysis

The crystalline nature and structure of the prepared Chry@Ag–Au, Ag–Cu, and Au–Cu BMNPs are further confirmed by using XRD analysis. Fig. 2 shows the XRD spectra of the synthesized Chry@Ag–Au, Ag–Cu, and Au–Cu BMNPs. In all XRD patterns of BMNPs, the strongest peak was observed at 38.26° which corresponds to the predominant growth in the direction of (111) plane. The (200) plane can be attributed to the peak at 44.40° and other two reflections were observed at 64.56° and 77.66° are assigned to the (220) and (311) planes respectively [26]. All the four diffraction peaks for BMNPs reveal that they are crystallized in fcc structure. In addition, individual metals (Ag, Au and Cu) have very similar lattice constants and hence no lattice constants mismatch is observed for BMNPs and all reflections in the XRD pattern resemble to that of monometallic counterparts. The obtained XRD results were demonstrated that the Chry@Ag–Au, Au–Cu and Ag–Cu BMNPs are FCC structure and have good crystallinity with a strong (111) crystal plane orientation.

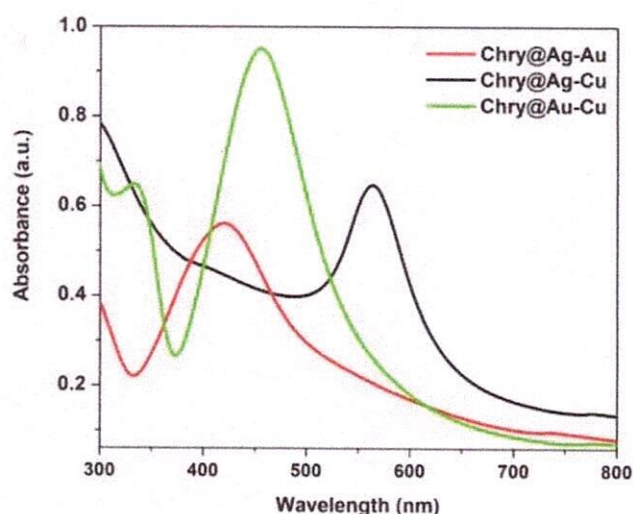


Fig. 1. UV–vis absorption spectra of the synthesized Chry@Ag–Au, Ag–Cu, and Au–Cu BMNPs.

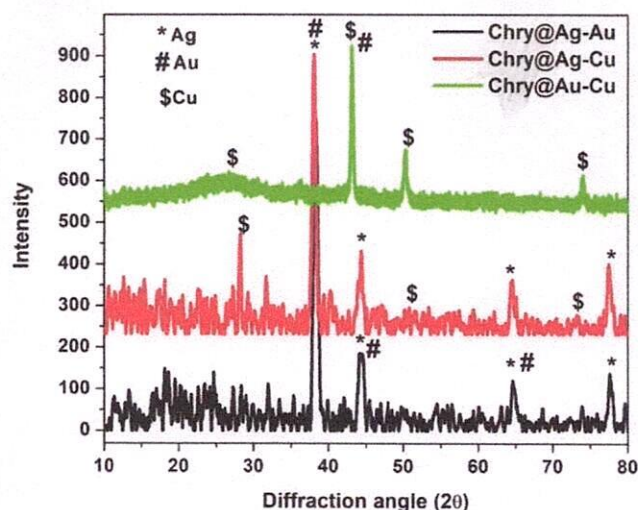


Fig. 2. Powder XRD patterns of the synthesized Chry@Ag–Au, Ag–Cu, and Au–Cu BMNPs.

3.3. FTIR spectrum

FTIR measurements are carried out to identify the possible functional groups in Chrysin, which is responsible for capping and efficient stabilization of the synthesized Ag–Au, Au–Cu, and Ag–Cu BMNPs as shown in Fig. 3. The FTIR absorption bands at 3405 cm^{-1} , 2358 cm^{-1} , 1626 cm^{-1} , and 1084 cm^{-1} in the spectrum corresponded to the O–H stretching vibration of the phenolic hydroxyls, stretching vibrations of C=C bonds, carbonyl stretching vibrations and C–OH vibrations, respectively, which are present in Chrysin [15]. The relative decrease in the intensity of phenolic hydroxyl stretching band in the spectrum of Chry@Ag–Au, Ag–Cu, and Au–Cu BMNPs indicate the partial role of phenolic hydroxyls in the reduction mechanism by donating electrons and forming quinones. The appearance of a band at 1378 cm^{-1} in the functionalized spectrum of BMNPs corresponds to the C–O stretching modes derived from the Chrysin. The complete disappearance of the C=C stretching vibrations in the FTIR spectrum of BMNPs can be attributed to the breaking of organic residues of Chrysin during the reaction [27]. The similar mechanism involves the role of phenolic hydroxyls and Chrysin in the reduction and stabilization of individual

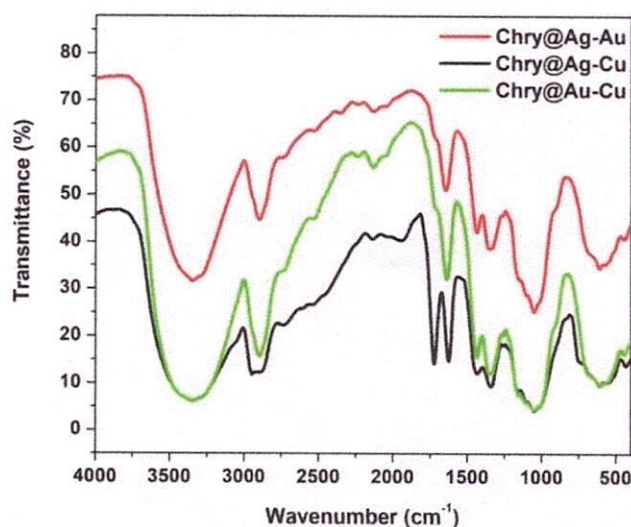


Fig. 3. FTIR spectra of the synthesized Chry@Ag–Au, Ag–Cu, and Au–Cu BMNPs.

BMNPs.

3.4. SEM analysis

In general, the structure of nanoparticles have much attention due to their interesting catalytic and biological properties, which are mostly dependent on their surface morphology and size. In order to evaluate the surface morphologies of Chry@Ag-Au, Ag-Cu, and Au-Cu BMNPs by using SEM analysis (Fig. 4a–c). The obtained SEM images of BMNPs have smooth surface, spherical morphology, and dispersed on the surface of Chry in BMNPs. The three kinds of BMNPs arrays exhibit hexagonal non-closed arrangement with the central distance between the two nearest-neighboring structural units of 500 nm. It indicates that each structural unit has near-spherical shape with uniform size, and the average diameter of Chry@Ag-Au, Ag-Cu and Au-Cu BMNPs was 196 ± 4 nm, 213 ± 5 nm, and 230 ± 8 nm, respectively.

3.5. TEM analysis

The UV–vis spectroscopic investigations on the formation and morphology of NPs can be more elaborately evidenced with the help of TEM analysis. Fig. 5(a–c) shows TEM images of Chry@Ag-Au, Ag-Cu, and Au-Cu BMNPs formed by the simultaneous reduction of Cu, Au, and Ag ions respectively in the molar ratio 1:1 by aqueous Chrysin solution. The morphology of BMNPs can be seen at higher magnifications. The particles are predominantly spherical and occasional aggregations lead to a very small percentage formation of pentagonal and spherical shape structures. The particles in Fig. 5 show a uniform contrast for each NP suggesting homogenous electron density within the volume of the particles with an average size <10 nm indicating the formation of tiny-sized BMNPs. The obtained results were commensurate well with the data obtained from UV–vis absorption and SEM studies from which we can reasonably estimate the interaction of Cu, Ag, and Au in the BMNPs.

3.6. BET analysis

In general, the catalytic reactions of the BMNPs as catalysts is related to the structure, size of the particles, as well as its specific surface area and porosity as pore size distribution of the catalyst. Therefore, the surface area and structure of the Chry@Ag-Au, Ag-Cu, and Au-Cu BMNPs were investigated by N_2 adsorption–desorption isotherms and specific surface area were estimated by the BET equation and the obtained results were shown in Fig. 6. From the obtained results, the isotherms of Chry@Ag-Au, Ag-Cu, and Au-Cu BMNP exhibits a type IV with a hysteresis loop, which indicates the presence of mesopores and the obtained results have pore diameter in the range of <15 nm [28]. The BET surface area (S_{BET}) of the Chry@Ag-Au, Ag-Cu, and Au-Cu BMNPs were estimated as $25.14 \text{ m}^2/\text{g}^{-1}$, $16.55 \text{ m}^2/\text{g}^{-1}$, and $12.53 \text{ m}^2/\text{g}^{-1}$, respectively. In this regard, the maximum surface area having BMNPs is assigned to the high surface roughness of the Chry@Ag-Au BMNPs, which may be beneficial for the prominent heterogeneous catalytic

response for the various degradation reactions.

3.7. Zetapotential analysis

The zeta potential was used to estimate the charge on synthesized Chry@Ag-Au, Ag-Cu, and Au-Cu BMNPs, and the findings are displayed in Fig. 7. It shows that repulsive forces exist and may be utilized to predict nanoparticle stability [29]. The synthesized Chry@Ag-Au, Ag-Cu, and Au-Cu BMNPs have a negative zeta potential of -11.21 mV, -20.84 mV, and -21.2 mV as a dispersant respectively. The produced Ag-Au, Ag-Cu, and Au-Cu BMNPs can be attributed to their enormous stability and lack of agglomeration for up to several months due to their negative potential.

3.8. Catalytic activity for the degradation of HIV drugs

In order to compare the catalytic activity of the synthesized Chry@Ag-Au, Ag-Cu, and Au-Cu BMNPs for the degradation of HIV drugs such as STV and ZDV in the presence of NaBH_4 as a reducing agent. The degradation capability of the synthesized samples (Chry@Ag-Au, Ag-Cu, and Au-Cu BMNPs) towards STV and ZDV was also studied under identical reaction conditions. The degradation of STV and ZDV drugs spiked wastewater effluents by UV–vis spectroscopy by using the synthesized Chry@Ag-Au, Ag-Cu, and Au-Cu BMNPs, and it was shown in Fig. 8(a and b), respectively. On the addition of an adequate aqueous suspension of Ag-Au BMNPs, the color of the reaction mixture gradually diminishes with time and becomes colorless. For STV and ZDV, the maximum degradation efficiency is approximately 95.76 % and 91.45 % in 18 min of reaction time by using Chry@Ag-Au BMNPs compared to the other Ag-Cu and Au-Cu BMNPs as shown in Table 1 and Fig. 9(a and b) due to the small particle size and large surface area [30]. In addition, the results showed that the degradation efficiency of the Chry@Ag-Au BMNPs was higher than that in both cases, which is mainly attributed to the relatively low molar absorption coefficients for the drugs and an efficient adsorbent for adsorption of drugs from aqueous medium [30].

The kinetics of the catalytic degradation of STV and ZDV using the synthesized Chry@Ag-Au, Ag-Cu, and Au-Cu BMNPs is periodically followed by UV–vis spectroscopy and shown in Fig. 10(a and b). The decrease in intensity of absorption around their corresponding wavelengths and gradually decreasing is monitored as a function of time. The BMNPs concentration is in excess during the reaction and hence considered constant compared to the concentration of HIV drugs. The reaction kinetics is hence assumed to follow pseudo-first order and can be described by the following equation:

$$kt = \ln \frac{C_t}{C_0}$$

where k is the pseudo-first order rate constant, t -reaction time, C_t and C_0 -concentration of the HIV drugs at time 't' and '0' respectively. The plot of $\ln(C_t/C_0)$ against time shows a linear relation as shown in Fig. 10(a and b) and the slope of the linear graph directly gives the rate constant



Fig. 4. (a–c) SEM images of the synthesized Chry@Ag-Au, Ag-Cu, and Au-Cu BMNPs, respectively.

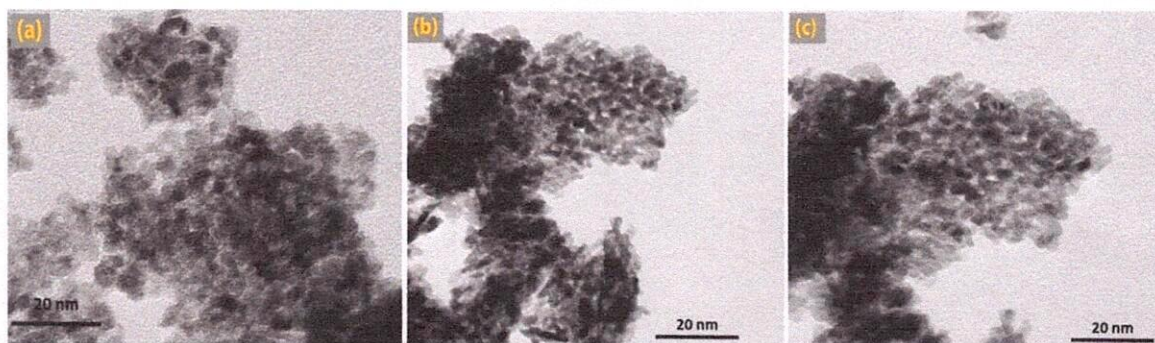


Fig. 5. (a-c) TEM images of the synthesized Chry@Ag-Au, Ag-Cu, and Au-Cu BMNPs, respectively.

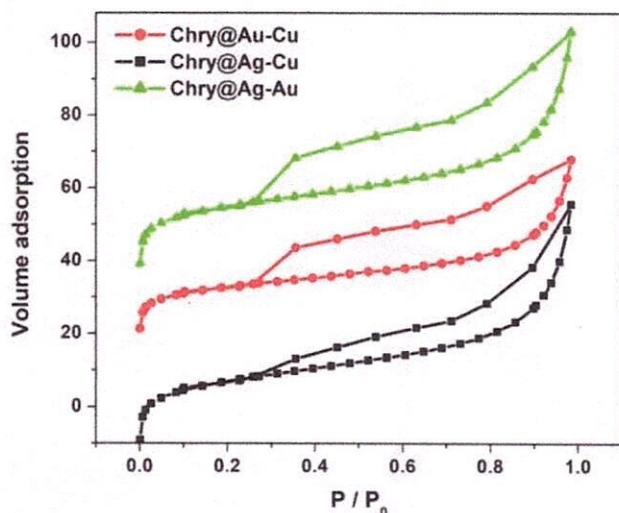


Fig. 6. N₂ adsorption-desorption isotherms of the synthesized Chry@Ag-Au, Ag-Cu, and Au-Cu BMNPs.

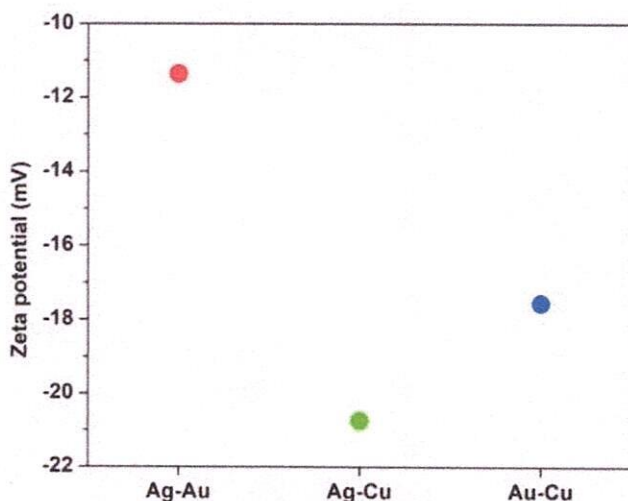


Fig. 7. Zetapotentials of the synthesized Chry@Ag-Au, Ag-Cu, and Au-Cu BMNPs.

for each reaction. The observed rate constants for the synthesized Chry@Ag-Au, Ag-Cu, and Au-Cu BMNPs were summarized in Table 1. The better catalytic efficiency can be attributed to the large surface-to-volume ratio of BMNPs and the improved activity of BMNPs relative to their particular counterparts [31]. The improved catalytic activity of

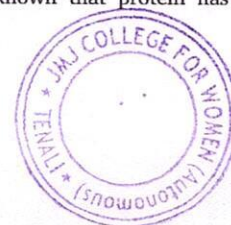
BMNPs than that of their mono-metallic counterparts can be accounted for by the electronic charge transfer between the nearby elements [32]. For Chry@Ag-Au BMNPs, the ionization potential of Au and Ag is 9.22 and 7.58 eV respectively. The electronic charges could transfer from Ag atoms to Au atoms in a particle, leading to an increase in electron density on the Au, thus acting as catalytically active sites for the redox reaction to proceed in a kinetically favorable manner [31].

3.9. Reusability of the BMNPs as catalyst

The reusability of a catalyst is a key aspect to evaluate its efficiency that is a crucial factor from eco-friendly and economical points of view. In this regard, we carry out the reusability of the synthesized Chry@Ag-Au, Ag-Cu, and Au-Cu BMNPs catalysts in the degradation reactions of HIV drugs (STV and ZDV) under the optimized conditions (Fig. 11). After completion of the reaction, the catalyst easily is separated by centrifugation from the reaction solution, washed with acetone, dried and reused in the next run (up to 5 consecutive cycles). It is found, that the present BMNPs system is one of the most effective catalysts for the degradation of HIV drugs and could be successfully recovered from the reaction mixture and reused for five consecutive catalytic cycles without significant loss and the slight decrease in the catalytic activity of the catalyst. The observed partial activity loss might be due to incomplete catalyst collection, surface deactivation, and decreased adsorption capacity [31].

3.10. Antimicrobial activity

The estimation of antimicrobial activities of the synthesized Chry@Ag-Au, Ag-Cu, and Au-Cu BMNPs by well diffusion method against various bacterial pathogens (*Escherichia coli*, *Staphylococcus aureus*, *Pseudomonas aeruginosa*, and *Bacillus subtilis*) as well as fungal strains (*Aspergillus niger* and *Candida albicans*). The antibacterial results showed that Chry@Ag-Au BMNPs inhibited the growth of all tested pathogens. A higher zone of inhibition was exhibited in Ag-Au BMNPs compared to Ag-Cu BMNPs and Au-Cu BMNPs. These Ag-Au BMNPs showed a higher zone of inhibition (ZOI) against *Pseudomonas aeruginosa* with the tested concentration (20 µg/mL) of all samples (Fig. 12). According to the obtained results of inhibition growth of fungi, it was observed that the synthesized Chry@Ag-Au BMNPs had a lethal effect against *Aspergillus niger* fungi among all tested fungal strains than Ag-Cu and Au-Cu BMNPs under identical experimental conditions. Hence, the results indicated that Chry@Ag-Au BMNPs possess a wide range of antimicrobial activity due to their synergistic properties. In addition, the observed inhibiting action of Ag-Au might be due to the electrostatic interaction (complex formation and/or attachment to cell membrane) between Ag-Au and various constituents of bacteria cell wall such as DNA, cellular protein and especially -SH groups of cysteine, S-containing amino acid, which imparts antibacterial efficacy in a concentration-dependent manner [33]. It is well known that protein has sulfur-



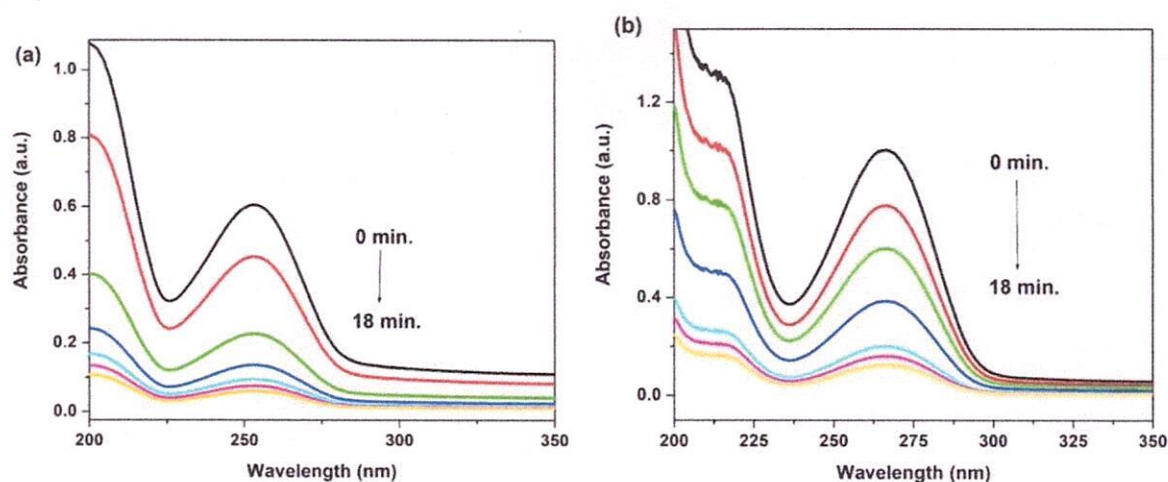


Fig. 8. Catalytic degradation performances of the HIV drugs such as (a) STV and (b) ZDV by using the synthesized Chry@Ag-Au, Ag-Cu, and Au-Cu BMNPs.

Table 1

The catalytic degradation parameters for the degradation of HIV drugs using the synthesized Chry@Ag-Au, Ag-Cu, and Au-Cu BMNPs.

HIV drugs	Degradation efficiency (%) / Rate constants (min ⁻¹)		
	Ag-Au	Ag-Cu	Au-Cu
STV	95.76/0.325	91.78/0.311	86.61/0.273
ZDV	91.45/0.304	87.98/0.281	85.41/0.266

containing amino acid cysteine, which contains three possible coordination sites at the -NH₂, -COOH, and -SH centers [33]. Out of these, sulfur has been established as the most susceptible to gaining electrons from the oxidizing species. As a result, the primary structure of the protein changes due to denaturation, inhibits the respiration processes, and finally causes cell death [33–34].

4. Conclusions

The present work deals with a facile synthesis of Ag-Au, Ag-Cu, and Au-Cu BMNPs using Chrysin as a capping and stabilizing agent. The synthesized BMNPs were characterized by UV-vis, FTIR, SEM, TEM, XRD, BET analysis, and zeta potential techniques. From these

techniques, the shape, size (<10 nm), surface area (25.14 m²/g⁻¹, 16.55 m²/g⁻¹, and 12.53 m²/g⁻¹), and structures (FCC) of the synthesized BMNPs were confirmed. The synthesized BMNPs were tested for the catalytic degradation of HIV drugs (STV and ZDV) in the presence of NaBH₄ as a reducing agent in an aqueous medium. For STV and ZDV, the maximum degradation efficiency is approximately 95.76% and 91.45% in 18 min of reaction time by using Chry@Ag-Au BMNPs compared to both Ag-Cu and Au-Cu BMNPs. It is noteworthy that the catalyst could be used five times without a significant loss in its catalytic activity. These BMNPs (20 µg/mL) were determined to have prominent antimicrobial activity against *Escherichia coli*, *Staphylococcus aureus*, *Pseudomonas aeruginosa*, and *Bacillus subtilis* bacteria, as well as fungi such as *Aspergillus niger* and *Candida albicans* respectively. Among them, it was observed that the synthesized Chry@Ag-Au BMNPs had a lethal effect against *Pseudomonas aeruginosa* (20.11 ± 0.05 mm) bacteria and *Aspergillus niger* (12.98 ± 0.05 mm) fungi among all tested bacterial and fungal strains. These biogenic BMNPs synthesized in this study suggest the design of bio-based bimetallic catalysts with high catalytic performance to prevent environmental pollution as well as act as biological agents.

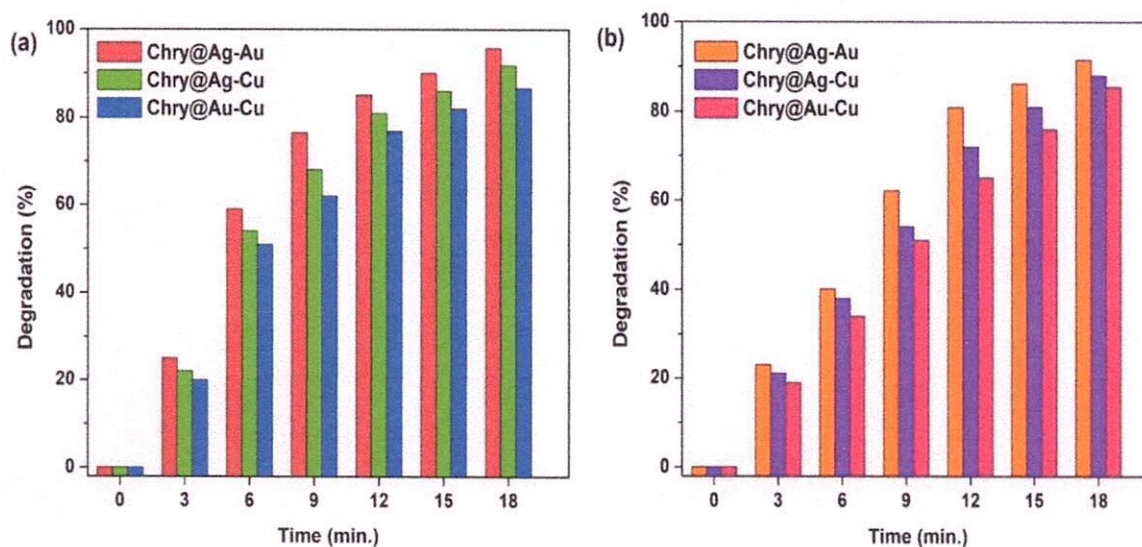


Fig. 9. Catalytic bar degradation images of the HIV drugs such as (a) STV and (b) ZDV by using the synthesized Chry@Ag-Au, Ag-Cu, and Au-Cu BMNPs.



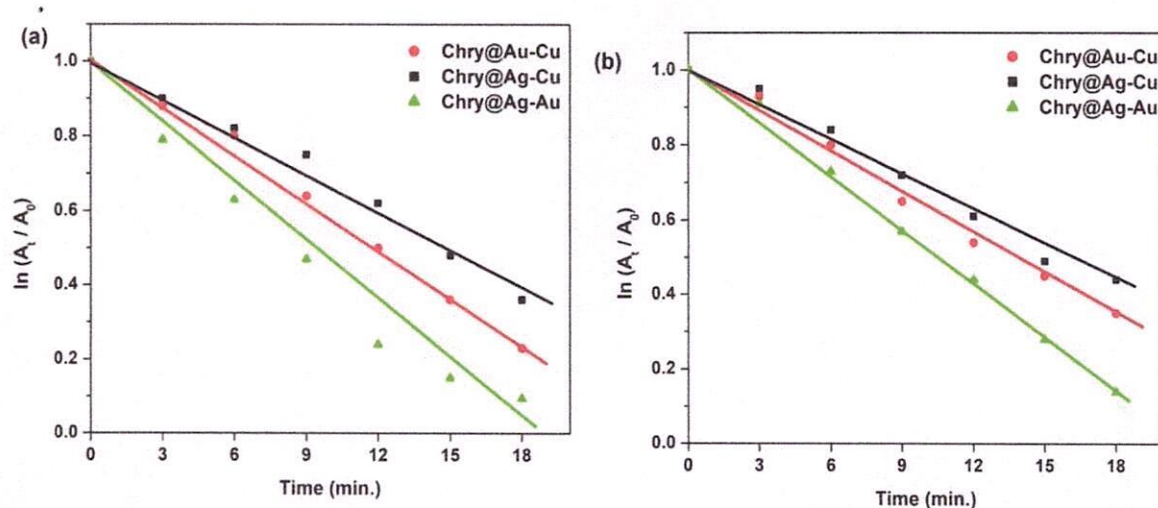


Fig. 10. Catalytic kinetic analysis of the HIV drugs such as (a) STV and (b) ZDV by using the synthesized Chry@Ag-Au, Ag-Cu, and Au-Cu BMNPs.

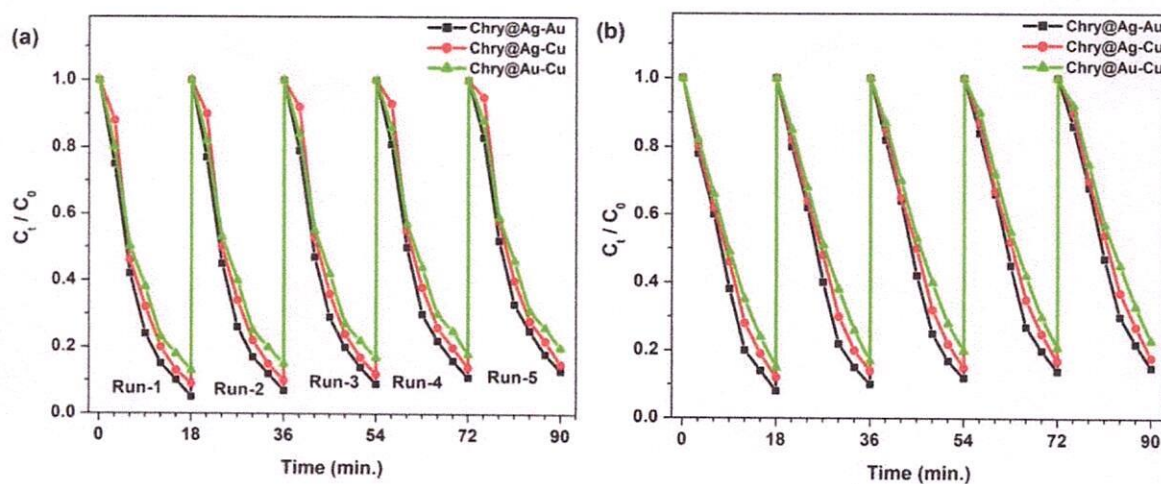


Fig. 11. Reusability study of the synthesized Chry@Ag-Au, Ag-Cu, and Au-Cu BMNPs catalysts in the degradation of (a) STV and (b) ZDV.

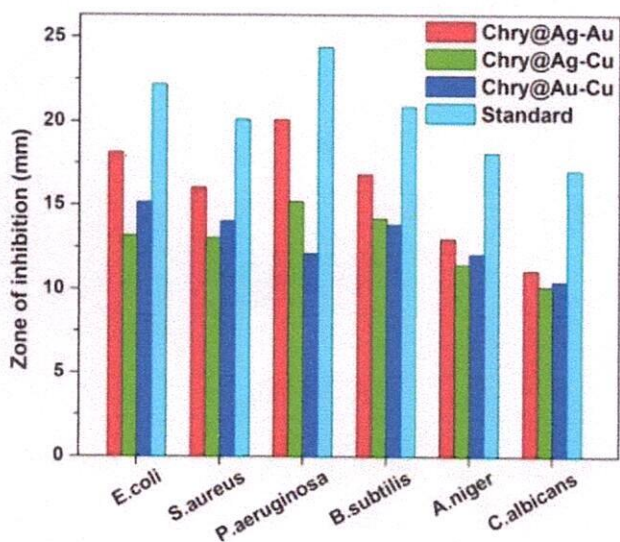


Fig. 12. The measurement of zone of inhibition of several bacteria strains *E. coli*, *S. aureus*, *P. aeruginosa*, and *B. subtilis* as well as fungi strains *A. niger* and *C. albicans* by using the synthesized Chry@Ag-Au, Ag-Cu, and Au-Cu BMNPs.

Declaration of Competing Interest

The authors declare that they have no known competing financial interests or personal relationships that could have appeared to influence the work reported in this paper.

Data availability

No data was used for the research described in the article.

Acknowledgements

The authors are highly grateful to Prof. G. Veerabhadram and Head, Department of Chemistry, Osmania University, Hyderabad, India.

References

- [1] D. Ayodhya, G. Veerabhadram, A review on recent advances in photodegradation of dyes using doped and heterojunction based semiconductor metal sulfide nanostructures for environmental protection, *Mater. Today, Energy* 9 (2018) 83–113.
- [2] K. Bisaria, S. Sinha, R. Singh, H.M. Iqbal, Recent advances in structural modifications of photo-catalysts for organic pollutants degradation—a comprehensive review, *Chemosphere* 284 (2021), 131263.
- [3] W.A. Altowayti, S. Shahir, N. Othman, T.A. Eisa, W.M. Yafooz, A. Al-Dhaqm, C. Y. Soon, I.B. Yahya, N.A. Che Rahim, M. Abaker, A. Ali, The Role of conventional



- methods and artificial intelligence in the wastewater treatment: a comprehensive review, *Processes* 10 (2022) 1832.
- [4] P.S. Kumar, R. Gayathri, B.S. Rathi, A review on adsorptive separation of toxic metals from aquatic system using biochar produced from agro-waste, *Chemosphere* 285 (2021), 131438.
- [5] N. Kapil, S.V. Mayani, K.G. Bhattacharyya, Environmental implications of nanoceramic applications, *Res. Chem.* 5 (2022), 100724.
- [6] M. Behera, J. Nayak, S. Banerjee, S. Chakraborty, S.K. Tripathy, A review on the treatment of textile industry waste effluents towards the development of efficient mitigation strategy: An integrated system design approach, *J. Environ. Chem. Eng.* 9 (2021), 105277.
- [7] D. Ayodhya, G. Veerabhadram, One-pot, aqueous synthesis of multifunctional biogenic Ag NPs for efficient 4-NP reduction, Hg²⁺ detection, bactericidal, and antioxidant activities, *Inorg. Nano Metal Chem.* 51 (2021) 1831–1841.
- [8] H. Sun, S.Y. Lee, S.J. Park, Bimetallic CuPd alloy nanoparticles decorated ZnO nanosheets with enhanced photocatalytic degradation of methyl orange dye, *J. Colloid Interface Sci.* 629 (2023) 87–96.
- [9] J. Wu, H. Yu, W. Liu, C. Dong, M. Wu, C. Zhang, Enhanced degradation of organic pollutant by bimetallic catalysts decorated micromotor in advanced oxidation processes, *J. Environ. Chem. Eng.* 10 (2022), 107034.
- [10] S.M. Padre, S. Kiruthika, S. Mundinamani, Ravikiran, S. Surabhi, J.-R. Jeong, K. M. Eshwarappa, M.S. Murari, V. Shetty, M. Ballal, G. S. c., Mono-and bimetallic nanoparticles for catalytic degradation of hazardous organic dyes and antibacterial applications, *ACS Omega* 7 (39) (2022) 35023–35034.
- [11] D. Ayodhya, A review on recent advances in selective and sensitive detection of heavy toxic metal ions in water using g-C₃N₄-based heterostructured composites, *Mater. Chem. Front.* 6 (18) (2022) 2610–2650.
- [12] D. Ayodhya, A. Ambala, G. Balraj, M.P. Kumar, P. Shyam, Green synthesis of CeO₂ NPs using Manilkara zapota fruit peel extract for photocatalytic treatment of pollutants, antimicrobial, and antidiabetic activities, *Res. Chem.* 4 (2022), 100441.
- [13] D. Ayodhya, G. Veerabhadram, BSA mediated Ag@Bi₂S₃ composites: synthesis, characterization, photodegradation of mixed dyes via metal-semiconductor interface, antimicrobial and antioxidant activities, *Mater. Today Chem.* 17 (2020), 100320.
- [14] S.S. Salem, A. Fouda, Green synthesis of metallic nanoparticles and their prospective biotechnological applications: an overview, *Biological Trace Element Res.* 199 (1) (2021) 344–370.
- [15] S. Raj, S. Sasidharan, T. Tripathi, P. Saudagar, Biofunctionalized Chrysin-conjugated gold nanoparticles neutralize Leishmania parasites with high efficacy, *Inter. J. Bio. Macromol.* 205 (2022) 211–219.
- [16] Y.e. Zhou, M. Zhang, Z. Guo, L. Miao, S.-T. Han, Z. Wang, X. Zhang, H. Zhang, Z. Peng, Recent advances in black phosphorus-based photonics, electronics, sensors and energy devices, *Mater. Horizons* 4 (6) (2017) 997–1019.
- [17] G. Li, W. Zhang, N. Luo, Z. Xue, Q. Hu, W. Zeng, J. Xu, Bimetallic nanocrystals: Structure, controllable synthesis and applications in catalysis, energy and sensing, *Nanomaterials* 11 (2021) 1926.
- [18] P. Verma, Y. Kuwahara, K. Mori, H. Yamashita, Pd/Ag and Pd/Au bimetallic nanocatalysts on mesoporous silica for plasmon-mediated enhanced catalytic activity under visible light irradiation, *J. Mater. Chem. A* 4 (26) (2016) 10142–10150.
- [19] R. Wei, N. Tang, L. Jiang, J. Yang, J. Guo, X. Yuan, J. Liang, Y. Zhu, Z. Wu, H. Li, Bimetallic nanoparticles meet polymeric carbon nitride: Fabrications, catalytic applications and perspectives, *Coord. Chem. Rev.* 462 (2022), 214500.
- [20] M.M. Kumari, J. Jacob, D. Philip, Green synthesis and applications of Au–Ag bimetallic nanoparticles, *Spectrochimica Acta Part A: Molecular and Biomolecular Spectroscopy* 137 (2015) 185–192.
- [21] V. Vilas, D. Philip, J. Mathew, Biosynthesis of Au and Au/Ag alloy nanoparticles using *Coleus aromaticus* essential oil and evaluation of their catalytic, antibacterial and antiradical activities, *J. Mol. Liquids* 221 (2016) 179–189.
- [22] D. Ayodhya, G. Veerabhadram, Green synthesis of garlic extract stabilized Ag@CeO₂ composites for photocatalytic and sonocatalytic degradation of mixed dyes and antimicrobial studies, *J. Mol. Struct.* 1205 (2020), 127611.
- [23] D. Ayodhya, Fabrication of SPR triggered Ag-CuO composite from Cu(II)-Schiff base complex for enhanced visible-light-driven degradation of single and binary-dyes and fluorometric detection of nitroaromatic compounds, *Inorg. Chem. Commun.* 148 (2023), 110295.
- [24] G. Balraj, G. Raju, A.A. Kumar, V. Sumalatha, D. Ayodhya, Facile synthesis and characterization of noble metals decorated g-C₃N₄ (g-C₃N₄/Pt and g-C₃N₄/Pd) nanocomposites for efficient photocatalytic production of Schiff bases, *Res. Chem.* 4 (2022), 100597.
- [25] A. Bansal, J.S. Sekhon, S.S. Verma, Scattering efficiency and LSPR tunability of bimetallic Ag, Au, and Cu nanoparticles, *Plasmonics* 9 (1) (2014) 143–150.
- [26] H. Zhang, C. Wang, H. Li, L. Jiang, D. Men, J. Wang, J. Xiang, Physical process-aided fabrication of periodic Au–M (M= Ag, Cu, Ag–Cu) alloyed nanoparticle arrays with tunable localized surface plasmon resonance and diffraction peaks, *RSC Adv.* 8 (17) (2018) 9134–9140.
- [27] S. Gnanasekar, D. Balakrishnan, P. Seetharaman, P. Arivalagan, R. Chandrasekaran, S. Sivaperumal, Chrysin-anchored silver and gold nanoparticle-reduced graphene oxide composites for breast cancer therapy, *ACS Appl. Nano Mater.* 3 (5) (2020) 4574–4585.
- [28] A. Zielinska-Jurek, E. Kowalska, J.W. Sobczak, W. Lisowski, B. Ohtani, A. Zaleska, Preparation and characterization of monometallic (Au) and bimetallic (Ag/Au) modified-titania photocatalysts activated by visible light, *Appl. Catal. B: Environ.* 101 (2011) 504–514.
- [29] R. Gopalakrishnan, B. Loganathan, K. Raghu, Green synthesis of Au–Ag bimetallic nanocomposites using *Silybum marianum* seed extract and their application as a catalyst, *RSC Adv.* 5 (40) (2015) 31691–31699.
- [30] D. Ayodhya, Ag-SPR and semiconductor interface effect on a ternary CuO@ Ag@ Bi₂S₃ Z-scheme catalyst for enhanced removal of HIV drugs and (photo) catalytic activity, *New J. Chem.* 46 (33) (2022) 15838–15850.
- [31] Y. Mizukoshi, T. Fujimoto, Y. Nagata, R. Oshima, Y. Maeda, Characterization and catalytic activity of core-shell structured gold/palladium bimetallic nanoparticles synthesized by the sonochemical method, *J. Phys. Chem. B.* 104 (25) (2000) 6028–6032.
- [32] H. Zhang, N. Toshima, Synthesis of Au/Pt bimetallic nanoparticles with a Pt-rich shell and their high catalytic activities for aerobic glucose oxidation, *J. Colloid Interface Sci.* 394 (2013) 166–176.
- [33] A. Al-Asfar, Z. Zaheer, E.S. Aazam, Eco-friendly green synthesis of Ag@Fe bimetallic nanoparticles: Antioxidant, antimicrobial and photocatalytic degradation of bromothymol blue, *J. Photochem. Photobiol. B: Biology* 185 (2018) 143–152.
- [34] B.S. Sivamaruthi, V.S. Ramkumar, G. Archunan, C. Chaiyasut, N. Suganthy, Biogenic synthesis of silver palladium bimetallic nanoparticles from fruit extract of *Terminalia chebula*-In vitro evaluation of anticancer and antimicrobial activity, *J. Drug Del. Sci. Technol.* 51 (2019) 139–151.

Principal
 JMJ COLLEGE FOR WOMEN (Autonomous)
 TENALI



Back Propagation Neural Network PO-based Grid Connected Dual PV Management and Reliability Improvement

Vijendra Pratap Singh^{1*}, G.S.S Rao², Sushma Jaiswal³

¹Department of Computer Science & Applications, Mahatma Gandhi Kashi Vidyapith, Varanasi, Uttar Pradesh, India.

²Department of AIML, Nawab Shah Alam Khan College of Engineering and Technology, Malakpeta, Hyderabad, Telangana, India.

³Department of Computer Science and Information Technology, Guru Ghasidas Vishwavidyalaya (A Central University), Bilaspur (C.G.), Chhattisgarh, India.

Received: 05.05.2023

Accepted: 18.05.2023

Published Online: 31.05.2023

Abstract: A single-phase Photovoltaic (PV) system that is based on an Maximum Power Point Tracking (MPPT) and use the perturb and observe algorithm to track the extreme power point. As a consequence of interactions between a variety of semiconductors and changing loads, the input source suffers from power quality concerns such as harmonic distortion, voltage sags, and voltage spikes. These issues are caused by fluctuating loads. As a method for enhancing the excellence of the electricity, the Grid-connected PV and Neural Network System was suggested as a solution. The Perturb and observe algorithm (P&O)-based MPPT technology offers a solution to the issue of partial shadowing, in addition to other unbalanced components that are problematic for PV arrays. Due to the fact that each PV cell in the system's two panels is identical, it

*Correspondence: Assistant Professor, Department of Computer Science & Applications, Mahatma Gandhi Kashi Vidyapith, Varanasi, Uttar Pradesh, India. Email: vijendra@mgkvp.ac.in
<https://doi.org/10.58599/IJSMIEN.2023.1502>
Volume-1, Issue-5, PP:10-23 (2023)



is possible to connect the panels in series in order to generate more power. The output of this PV array can be estimated by taking into account how it reacts to various kinds of irradiation. Back Propagation Neural Network-P&O technology, which also enhances convergence and accuracy, can be rummage-sale to lower the total Harmonic Distortion of photovoltaic array systems.

Key words: Back Propagation Neural Network, Photovoltaic, Perturb and observe algorithm, Maximum Power Point Tracking, Grid.

1. INTRODUCTION

The goal of grid-connected solar power generation systems is to extract as much useful electricity as possible from the sun's energy. Particle swarm optimization using back propagation neural networks and the perturb are two examples. You can choose between these two options. In a variety of setups, the algorithms supply the DC link controller with the reference voltage. This method automatically identifies the extreme power point of the dual PV array by using a BPNN-P&O-based algorithm and a predetermined number of power assessments of the PV system. For short, we'll just call this approach "this method." Data can be automatically retrieved as characteristics using this method. Some examples of this include the I-V curve, radiation, and temperature. The most common approach to capturing this solar energy involves making use of PV cells and modifying their output such that it satisfies our requirements. Solar modules have become significantly more valuable in the field of renewable energy as a result of recent developments in power management made possible by Maximum Power Point Tracking (MPPT) algorithms. Figure 1 depicts the rapid growth of photovoltaic systems into a dependable and flexible source of electricity. The fact that the conversion efficiency for the creation of electric power is quite low (9–17%) is one of the most significant drawbacks of PV generation systems.

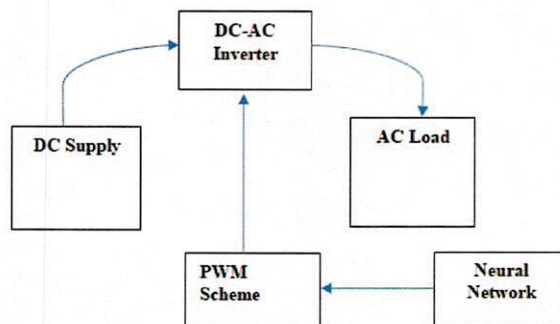


Figure 1. Schematic Representation of a DC-Powered Neural Network

The Biological Problem-Solving Network Model (BPNN) is a mathematical model that is used to represent biological brain networks and the function that these networks play in the process of problem solving. The conclusion is a forecast of the outcome that is calculated using the inputs as well



as the objectives of the training process. There are many different kinds of neural networks, the most common of which being neural networks and layer 1 multilayer perception (MLP) networks. Within the multilayer perceptual network, the processing terminals are linked to one another through weighted connections, and each layer of the network possesses a straightforward sigmoid transfer function with two states. The input, output, and hidden layers of a conventional feed-forward multilayer sensory neural network each serve as the network's three most essential nodes. These levels are also known as "hidden" layers.

When the voltage needs to be increased in a typical step-up scenario, regular DC-DC converters, such as boost converters and fly-back converters, might be utilised to accomplish this task. On the other hand, they are not as helpful when it is necessary to make a major change. Because of the negative impact that using a high turn ratio and duty cycle might have on copper loss, leakage inductance, and conduction loss. If the proper power electronic controllers are utilised, the distributed generation system along with the battery storage can be connected to the primary grid.

2. PREVIOUS RESEARCH WORK

The Prediction Error-Based Power Forecasting (PEBF) method is used to a photovoltaic (PV) system, and it makes use of the grey box neural network that is part of the Photovoltaics for Utility Scale Applications (PVUSA) model [1]. The differential equation-based PVUSA model is first represented in the form of a neural network, which is then constructed. If there is a sufficiently big disparity between the predicted and real powers, the neural network can be configured to train using the PEBF approach, however this will depend on the current state of the system as well as the needs. Uncertainty has been introduced into the operations of distribution networks as a result of the greater integration of photovoltaic (PV) grids. Analytical derivations modelled as line impedance are used for the purpose of studying the effect that a PV site has on the power losses and voltage fluctuations that occur throughout a distribution network that is equipped with PV [2]. Humans have been assigned with the responsibility of studying various placement choices in order to reduce power losses and voltage fluctuations in the network. Particle Swarm Optimization, or P&O, is a method that is used to calculate PV. This method generates a compromise solution that is optimal in the best-case situation. PSCAD/EMTDC, a platform for time-domain simulation, is used in order to incorporate a single PV into a distribution network that operates at 10 kV [3]. When there is a sudden shift in irradiance, which distorts the operating characteristics of the PV system, the P&O algorithm that is employed by the controller has some trouble, but only for a short period of time, in reaching the MPP [4]. However, this issue is only temporary. Nevertheless, by delaying the beginning of MPP tracking once again, the controller is able to improve the accuracy of the algorithm. In addition to this, the oscillation of the terminal voltage caused by the MPP leads to a loss of power. The scientists employ the smallest disruption phase size possible in order to reduce the severity of these tremors. Once more, the minor phase slows down the rate at which the algorithms' first transient occurs and modifies the extent to



which the system is affected by external factors. By combining an INC Algorithm with a Proportional Integral (PI) controller, it is possible to get both reduced rip oscillation throughout the MPP and a good match for transient irradiance fluctuations. These results can be attained by using the algorithm [5].

A Petri Recurrent Wavelet Fuzzy Neural Network (PETRIRWFNN) controller and an easy pre-synchronization estimator are described here as means of achieving the objectives of smooth switching and grid reconnection in a micro grid system. The photovoltaic system, the loads, and the storage system are the components that make up the micro grid [6]. Thanks to the master-slave control architecture, the micro grid can be utilised either in grid-connected mode or in islanded mode. Due to the fact that the master Distributed Generator (DG) uses a different control algorithm based on the mode of operation, the voltage and active power output of the micro grid system experience a momentary drop whenever the modes are switched. The intelligent solar photovoltaic (PV) cell manufacturing process already incorporates standard practises for the automatic detection of issues through the use of smart cameras and sensors that are connected to the IIoT [7]. Extensive research has been done on data-driven detection strategies for the failure of photovoltaic (PV) cells. The subjectivity and fuzziness of human annotation makes robotic fault discovery a difficult task because the data is packed with noise and unexpected ambiguity as a result of human annotation. There are numerous maxima on the power-voltage curve for partially shaded photovoltaic (PV) arrays; the Global Maximum Power Point is one of these maxima. Finding and monitoring the GMPP in each and every conceivable scenario presents a significant obstacle for PV systems that have the efficiency improvement as one of their primary goals [8]. With the goals of improving both speed and accuracy, a novel two-stage global Maximum Power Point Tracking approach has been developed. This method combines the time-tested Hill Climbing algorithm with Artificial Neural Networks. In addition, sensors that measure the temperature or the intensity of the light are unnecessary. In the first step, an analysis of the array IV curve is performed in order to decide where to collect the current-voltage (I-V) curve. This allows for the collection of a smaller number of samples than would be required by a standard feedforward ANN in order to account for variations in temperature and irradiance [9]. Nonlinear power versus voltage characteristics are produced when the triple diode type circuit model solar strings are integrated with the PV array [10]. Therefore, locating the MPP is a difficult and time-consuming task. According to research that was done in the past, there are a broad selection of MPPT procedures that are available for purchase. The MPPT approaches that have received the most research include the classical, meta-heuristic, artificial intelligence, and soft computing efficiency tactics.

3. MATERIALS AND METHOD

The current practise makes use of a modulated Z-source converter, which is paired with single-phase symmetry. Furthermore, direct coupling between solar panels and transformer-less topologies via



impedance source networks is not possible due to the high level of complexity involved. There is a problem with common-mode voltage variance in this technology, but it can be fixed by modifying the modulation techniques or switching patterns. Using a single-phase symmetric Z-source, this method can be implemented in a transformer-less converter with negligible leakage currents. To keep the common-mode voltage stable and the leakage currents to a minimum, photovoltaic applications are using the Highly Efficient and Reliable Concept in tandem with an impedance source network (also called a Z-source network). Due to the switches working at the same frequency as the line, losses are reduced to a minimum even if there are two more active switches than necessary. Particularly impressive is the improvement in harmonic performance and the decrease in leakage currents. The schematic representing the proposed method is shown in Figure 2.

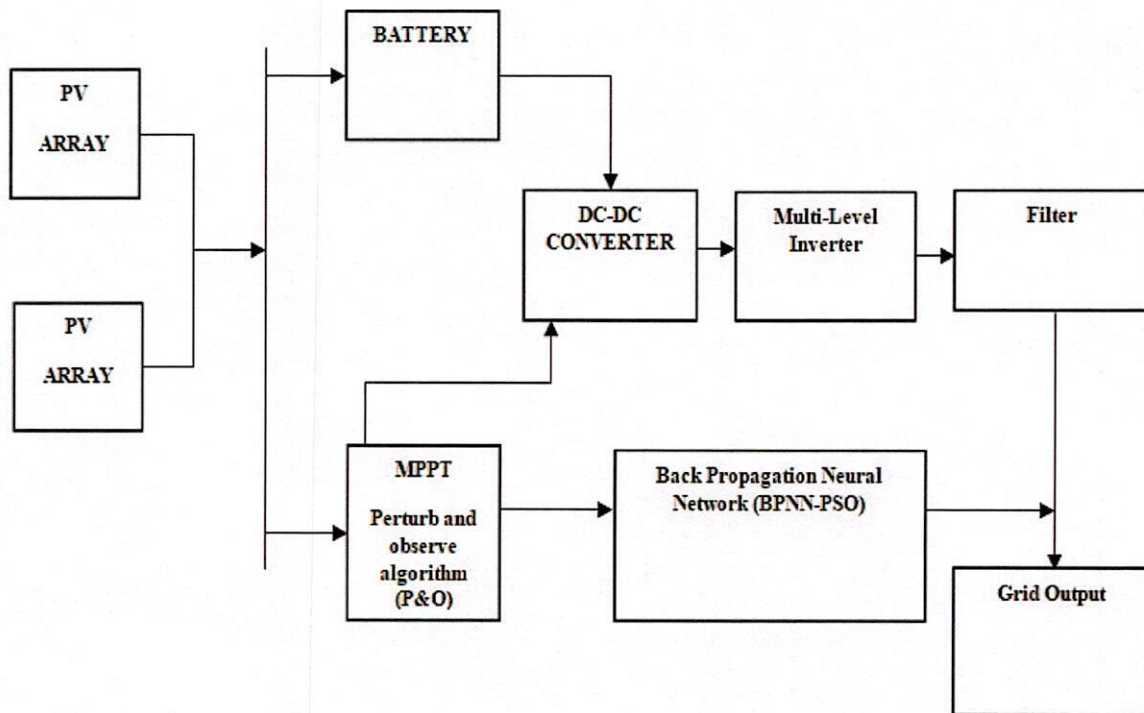


Figure 2. Schematic Representing the proposed method

The proposed method employs Maximum Power Point Tracking (or MPPT for short) to identify flaws and dysfunctions. Each of the three PV (photovoltaic) technologies being used here has its voltage and current closely monitored to prevent it from falling below zero at any time during the input source collection procedure. The condition analysis's P.V. status has deteriorated due to



limitations including limited power and insufficient backup storage. When using a centralised MPPT control system, flaws in solar panels are easy to spot. The DC capacitor supplies a stable voltage to the voltage source converter, and the Multi-level converter changes the DC input voltage into the AC output voltage. A transformer links the VSC's output to the electrical grid. Figure 2 depicts the basic building blocks of a Neural Network that uses Back Propagation. Although there are many layers and nodes in this kind of neural network, just three sorts of layers are distinguished from one another: input, hidden, and output.

3.1. PV Array

Electromagnetic radiation from the sun is a tremendously potent energy source. The wavelength of these rays determines whether they are considered light, radio waves, or something else entirely. Only a tiny fraction of the solar output is transformed into visible light and reaches Earth's surface. Electrons are created when sunlight hits solar cells. Many different kinds of solar cells can absorb and use light of different wavelengths. A solar array is often connected in series with the utility grid to supply electricity. This integrated photovoltaic system includes a solar panel, an inverter, and the necessary gear to connect to the grid for power. Connected systems can be used in a variety of contexts, including the home. Off-grid solar power systems differ from commercial and large-scale solar power plants that are wired into the national electricity grid. Connected devices seamlessly switch over to the associated utility grid as shown in Figure 3. This takes place whenever the energy produced exceeds the energy consumption. A standard rooftop solar system in the United States generates kilowatts of electricity. The average home doesn't need anywhere like this much energy. The output of the reactive power generator must closely match the reactive power voltage level. The system voltage increases when the power factor is positive due to loads with a high capacitance, and decreases when the power factor is negative due to loads with a high inductance. Over or undersupply of reactive power can cause the network voltage to spike or drop, respectively, to unsafe levels, forcing generators to shut down. This leads to a decline in generation and subsequently increases difficulties.

3.2. MPPT Perturb and observe algorithm

The output voltage and current from the PVA are fed into the MPPT system, and the algorithm's job is to determine the reference voltage. You now know what goes into and comes out of the MPPT system. There are two common topologies for control loops in maximum power point tracking systems. The MPPT algorithm block and the comparator that produces the switching pulses are located in the inner loop. The switching pulse generator includes both of these parts. One part of the external control loop, the PI controller, controls the input voltage to the converter. Adjustments to the DC-DC converter's duty cycle are made by the PI controller in an effort to bring the output voltage closer to the dV/dp generated by the MPPT block. In contrast to the MPP block, the MPPT block typically produces a non-zero error signal during operation. While easier to build, this approach fails to keep



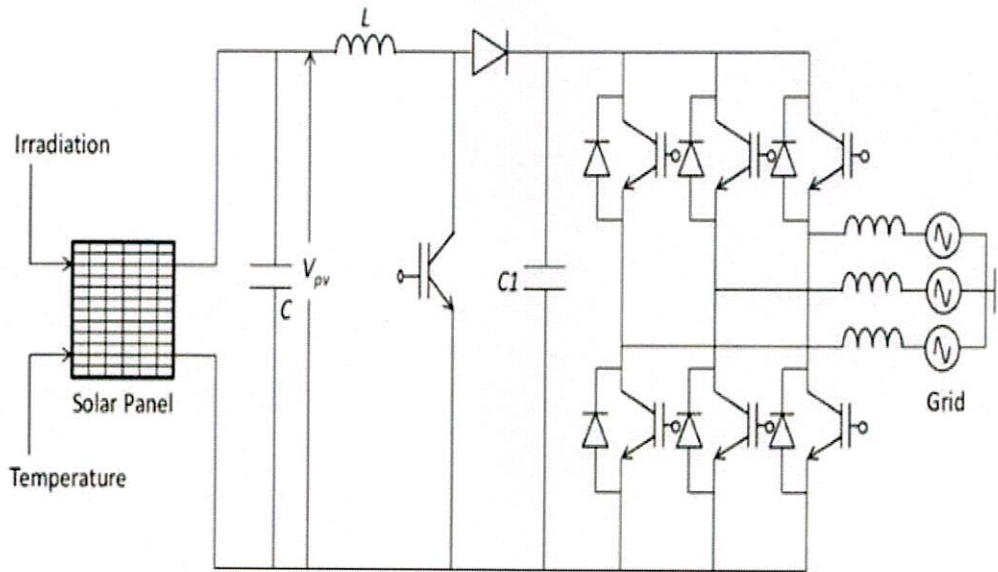


Figure 3. PV Grid-Connected System Circuit Diagram

track of the MPP when there is a sudden change in the radiance. The Observation Graph Generated by the "Perturb and Observe" Algorithm is shown in Figure 4. In photovoltaic (PV) systems, procedures known as Maximum Power Point Tracking (MPPT) are utilised, as depicted in Figure 4, in order to continuously locate the Maximum Power Point (MPP), which is determined by the circumstances of the panel in terms of temperature and irradiance. Because of its ease of use, the Perturb and Observe (P&O) Maximum Power Point Tracking Method is now the most widely used approach to solving the MPPT problem. This is because low-cost implementations typically utilise this approach. P&O's operating point is continuously shifting its location in relation to the MPP, which consumes a portion of the power that is available. It is also common knowledge that when the weather conditions are rapidly changing, the P&O algorithm might become jumbled.

3.3. Back Propagation Neural Network-P&O (BPNN-P&O)

Photovoltaic (PV) systems have a "Maximum Power Point" (MPP) where they generate the most usable electricity within a particular range of irradiance and temperature. Integration of a DC/DC converter with a computational system means the duty cycle can be adjusted in line with the search technique and, implicitly, the converter's input impedance, until the system meets the MPP. The detrimental consequences of the integration on output power will thus be mitigated. This experiment is conducted to identify the functional node using Maximum PowerPoint Tracking. The representation



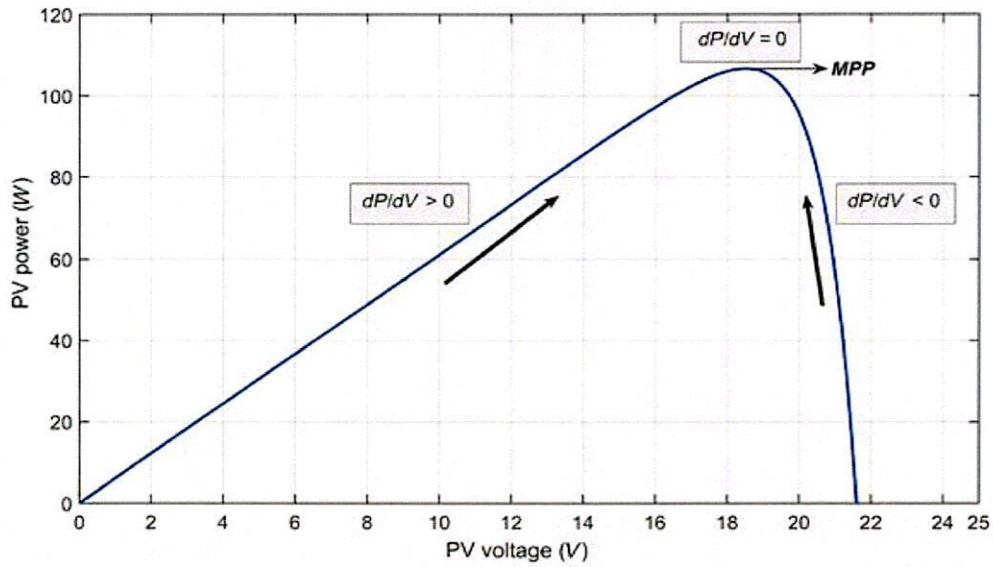


Figure 4. Observation Graph Generated by the "Perturb and Observe" Algorithm

of the fundamental concept of BPNN is shown in Figure 5.

Figure 5 is a representation of the fundamental concept that underpins a back-propagating neural

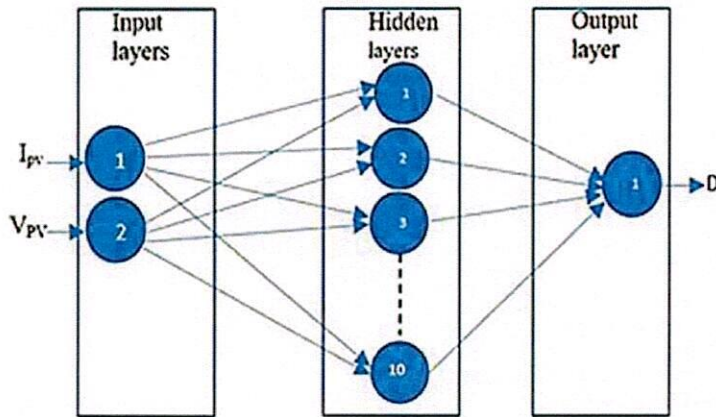


Figure 5. Representation of the fundamental concept of BPNN

network. In a photovoltaic (PV) system, the voltage dV and current dp are as follows: The information collected by the PV systems at a range of temperatures and irradiance levels is sent to the initial layer of the network. The hidden layer, which is the second layer, consists of 10 input levels. These input



layers allow the hidden layer to digest data coming from the input layer and send it on to the output layer. The output layer, which is the third and final layer, is made up of a single linearly triggered action potential duty cycle (D). The sigmoid functions are considered to be its activation functions. Figure 5 depicts the BPNN-P&O approach, which combines the local search power of the BP neural network and the global search capabilities of the P&O. This method aims to find the optimal solution to a problem by looking in many locations simultaneously. This hybrid approach is capable of predicting problems with PV arrays in a more timely and accurate manner. The P&O and the concept of embedding it within deep learning together produce a significant increase in the accuracy of fault-type prediction. During the training phase of an ANN, the duty cycle D is used as the output, while the voltage d and P current d V of the PV array serve as the input variables. These variables correlate to particular solar radiation and environmental temperature conditions. A Mat-lab/Simulink simulation of a PV array that followed the P&O methodology was used to collect the information for this dataset. The Neural Network Toolbox in Mat-lab allows for the construction, training, verification, and testing of neural networks. The training phase will utilise seventy percent of the dataset, while the validation phase will use fifteen percent, and the testing phase will use fifteen percent.

4. RESULTS AND DISCUSSION

Simulation is made using MATLAB/SIMULINK is shown in Figure 6, Circuit diagram is made using blank model of MATLAB and using power-GUI, simulation is executed. By switching properly using a pulse generator, output voltage levels can be generated. An input voltage of 20 Volt is given as voltage at the input side. The pulse generator is set with a switching frequency of 50Hz and the corresponding switching is given Output voltage waveform and gate pulses are observed. As seen in Figure 7, photovoltaic modules or panels, both of which are modelled from a large number of individual fundamental cells. From this point on, any photovoltaic device that is composed of numerous basic cells will be referred to as an array. Because the power supplied by a single module is insufficient for almost all commercial applications, modules are often coupled together to create arrays in order to provide the load. The connections that exist between cells in a module and those that exist between modules in an array are identical. It is also possible to connect modules in parallel or series in order to increase current or voltage respectively. The outcomes of a simulation run in MATLAB/SIMULINK are presented in Figure 6. The schematic for the circuit was produced using a blank model in MATLAB, and the graphical user interface (GUI) of the programme was utilised in order to carry out the simulation. By switching in the appropriate manner using a pulse generator, it is possible to produce the desired voltage levels at the output. A voltage of 20 V is given for the input side of the circuit. The pulse generator receives a switching frequency of 50 Hz as an input, and it produces switching that is matching that frequency. It is possible to observe both the waveform of the output voltage and the gate pulses simultaneously.

The construction of photovoltaic modules or panels, such the ones shown in Figure 7, requires



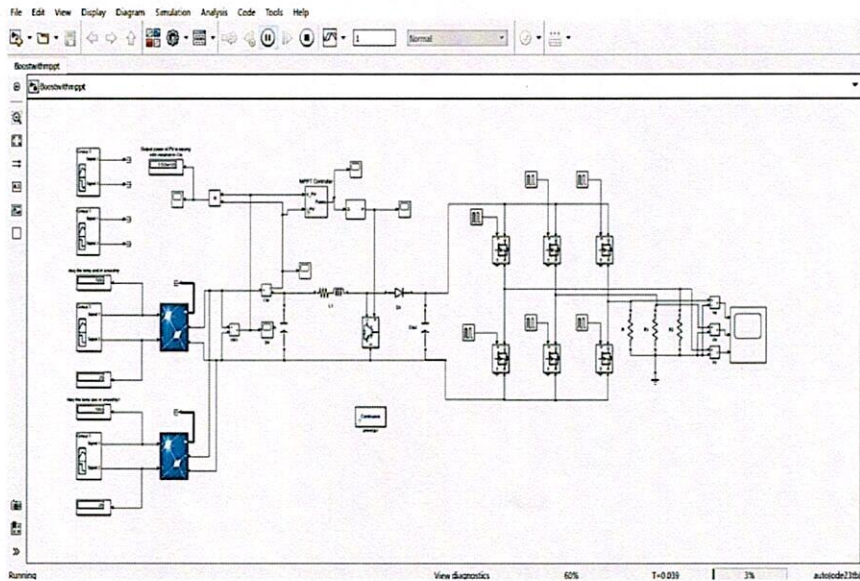


Figure 6. Simulation Implementation of Proposed Method

the modelling of a large number of separate fundamental cells. From this point forward, the term "array" will be used to refer to any solar power system that is made up of a number of separate cells. Because the output of a single module is typically insufficient for use in industrial applications, an array of modules is typically utilised in order to satisfy the demand. Module connections in an array are comparable to cell connections in other structures. Connecting modules in parallel will result in an increase in current, whereas connecting modules in series will result in an increase in voltage.

The Neural Network algorithm preserves all of the data collected from the network during the phase known as the variable screening phase. This phase has the potential to eliminate the influence of any variables that are generating issues for the model. In order to increase the analytical effect of the model and to represent the matrix change of the weight of each variable in the neural network, the practical swarm optimisation approach, also known as P&O, might be used to quantify the significance of the influence of independent variables. This would allow for the expression of the change in the weight of each variable. Therefore, the purpose of this study is to propose a hypertension risk prediction mode that is based on the P&O-BP neural network, and Figure 7 presents the matlab circuit diagram of the Back Propagation Neural Network-P&O. The method is utilised to conduct an analysis of the factors that contribute to the prevalence of hypertension in the region. In high-power, medium-voltage industrial settings, multilevel inverters are utilized as a necessary piece of equipment. Multilevel inverters (MLIs) have a lower level of harmonic distortion compared to ordinary inverters, in addition to having a higher output voltage. The generation of an extensive voltage range using synthesis can make the fabrication of excellent waveforms easier. MLIs can be broken down into three main types on



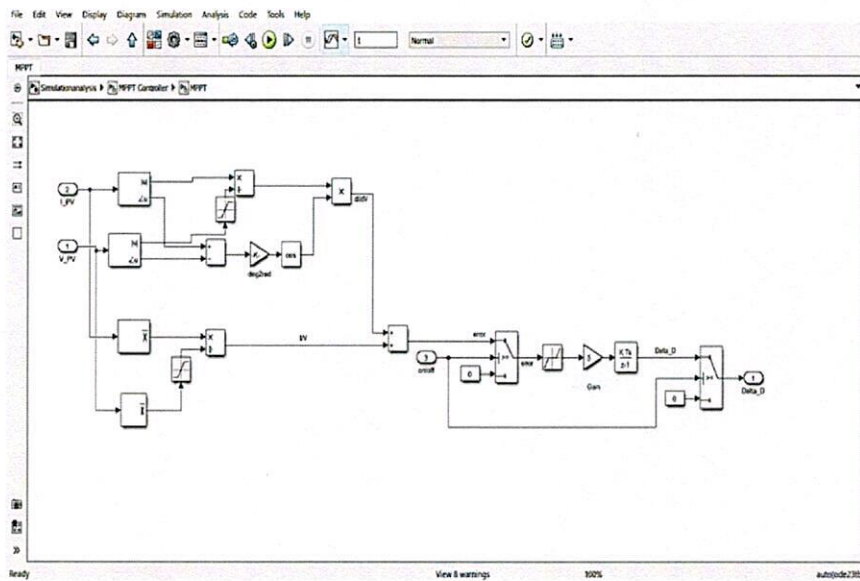


Figure 7. Matlab circuit of Back Propagation Neural Network (BPNN-P&S)

the basis of the components that they make use of. The Multilevel Inverter is the one that needs the least amount of components, such as capacitors and diodes. The system that is depicted in Figure 8 has a variable voltage output that can be set to one of five levels; however, this system is cumbersome and costly because it requires two voltage sources and eight switches. In combination with a multilayer inverter that has been developed to be more efficient and have fewer switches, a renewable source of energy is employed.

In high-power, medium-voltage industrial settings, multilevel inverters are utilized as a necessary piece of equipment. Multilevel inverters (MLIs) have a lower level of harmonic distortion compared to ordinary inverters, in addition to having a higher output voltage. The generation of an extensive voltage range using synthesis can make the fabrication of excellent waveforms easier. MLIs can be broken down into three main types on the basis of the components that they make use of. The Multilevel Inverter is the one that needs the least amount of components, such as capacitors and diodes. The system that is depicted in Figure 9 has a variable voltage output that can be set to one of five levels; however, this system is cumbersome and costly because it requires two voltage sources and eight switches. In combination with a multilayer inverter that has been developed to be more efficient and have fewer switches, a renewable source of energy is employed.

In comparison to the initial value of 4.52%, the total harmonic distortion (THD) that is produced by the proposed technique which can be seen in Figure 10 and is decreased by 1.12%.



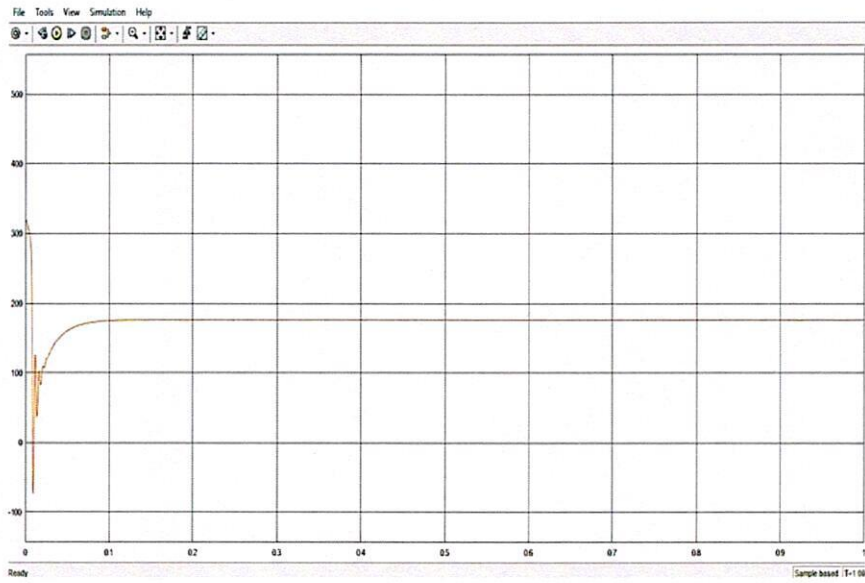


Figure 8. PV output wave from

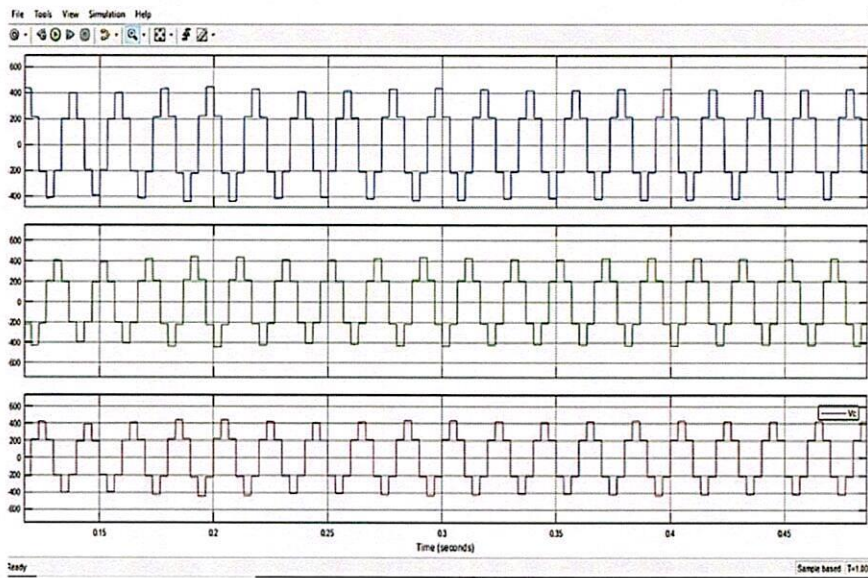


Figure 9. Simulation Output Waveform



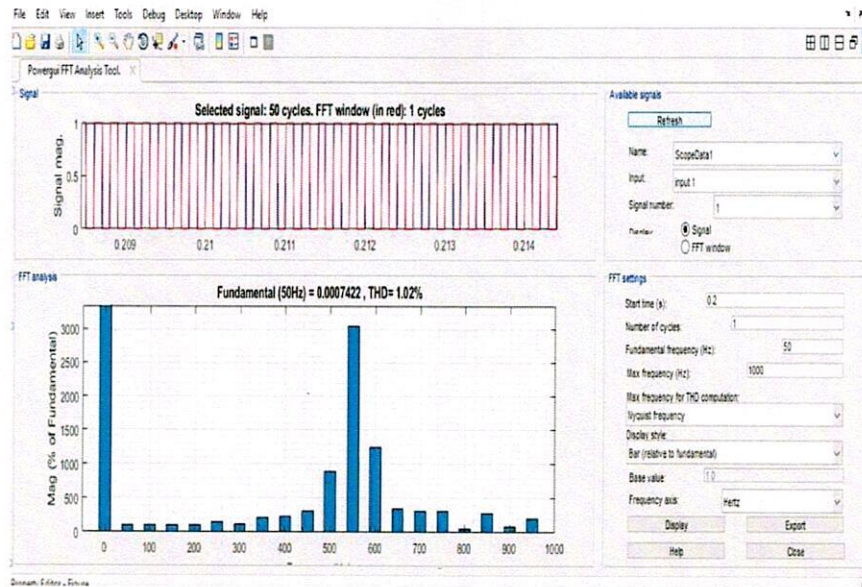


Figure 10. Total Harmonic Distortion

5. CONCLUSION

This study compares and contrasts the P&O approach for the MPPT technology with the Back Propagation Neural Network (BPNN-P&O). These two methods are employed by the Back Propagation Neural Network. Test findings show that the Maximum Power Tracking (MPP) may be achieved by the realistic swarm optimization technique while the PV system is in Peace mode. Since P&O methods are already being implemented, this paves the way for much more power to be extracted. Using the technique supplied by the BP-P&O neural network, it was determined if a particular class of PV system failure had occurred. The input layer is the location of training and the final resting place for the normalized data from the previous layer. The linear function is used in the training layer of the neural network for both learning and data classification. When problems are detected with the PV system, the collected data is sent to the P&O layer, where it is evaluated and classified.

References


- [1] Yuanxiong Guo, Miao Pan, and Yuguang Fang. Optimal power management of residential customers in the smart grid. *IEEE Transactions on Parallel and Distributed Systems*, 23(9):1593–1606, 2012.
- [2] Mostafa F Shaaban, AH Osman, and Mohamed S Hassan. Day-ahead optimal scheduling for demand side management in smart grids. In *2016 European Modelling Symposium (EMS)*, pages 124–129. IEEE, 2016.
- [3] Fathia Chekired, Achour Mahrane, Zoubeyr Samara, Madjid Chikh, Abderrazak Guenounou, and Aissa Meflah. Fuzzy logic energy management for a photovoltaic solar home. *Energy Procedia*, 134:723–730,

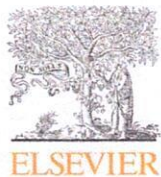


2017.

- [4] Sébastien Bissey, Sébastien Jacques, and Jean-Charles Le Bunetel. The fuzzy logic method to efficiently optimize electricity consumption in individual housing. *Energies*, 10(11):1701, 2017.
- [5] Andoni Saez-de Ibarra, Aitor Milo, Haizea Gaztanaga, Vincent Debusschere, and Seddik Bacha. Co-optimization of storage system sizing and control strategy for intelligent photovoltaic power plants market integration. *IEEE Transactions on Sustainable Energy*, 7(4):1749–1761, 2016.
- [6] I De la Parra, Javier Marcos, Miguel Garcia, and Luis Marroyo. Dynamic ramp-rate control to smooth short-term power fluctuations in large photovoltaic plants using battery storage systems. In *IECON 2016-42nd Annual Conference of the IEEE Industrial Electronics Society*, pages 3052–3057. IEEE, 2016.
- [7] Ridha Benadli, Brahim Khiari, and Anis Sellami. Three-phase grid-connected photovoltaic system with maximum power point tracking technique based on voltage-oriented control and using sliding mode controller. In *IREC2015 The Sixth International Renewable Energy Congress*, pages 1–6. IEEE, 2015.
- [8] Johannes Weniger, Joseph Bergner, and Volker Quaschnig. Integration of pv power and load forecasts into the operation of residential pv battery systems. In *4th Solar integration workshop*, pages 383–390, 2014.
- [9] Bernd Hirschl, Janina Struth, Kai-Philipp Kairies, Matthias Leuthold, Astrid Aretz, Mark Bost, Swantje Gähns, Moritz Cramer, Eva Szczechowicz, Armin Schnettler, et al. Pv-benefit: A critical review of the effect of grid integrated pv-storage-systems. In *Proceedings of the International Renewable Energy Storage Conference (IRES), Berlin, 18.-20. November 2013*. Eurosolar, 2014.
- [10] Fengji Luo, Weicong Kong, Gianluca Ranzi, and Zhao Yang Dong. Optimal home energy management system with demand charge tariff and appliance operational dependencies. *IEEE Transactions on Smart Grid*, 11(1):4–14, 2019.




PRINCIPAL
JMJ COLLEGE FOR WOMEN (Autonomous)
TENALI



Contents lists available at ScienceDirect

Materials Today: Proceedings

journal homepage: www.elsevier.com/locate/matpr

Synthesis of Schiff base stabilized AuNPs for enhanced catalytic degradation of pesticides, Cr(VI) detection, antioxidant, and antimicrobial activities

Sumalatha Vislavath^a, Marri Pradeep Kumar^b, G. Balraj^c, M. Sharath Babu^d, Dasari Ayodhya^{c,*}^aDepartment of Chemistry, J.M.J. College for Women, Tenali 522201, Andhra Pradesh, India^bDepartment of Chemistry, Anurag University, Hyderabad 500088, Telangana, India^cDepartment of Chemistry, University College of Science, Osmania University, Hyderabad 500007, Telangana, India^dDepartment of Chemistry, Sardar Patel College, Secunderabad 500061, Telangana, India

ARTICLE INFO

Article history:

Available online xxx

Keywords:

Schiff base

AuNPs

Pesticides degradation

Cr(VI) sensing

Biological activity

ABSTRACT

In this study, researchers synthesized ultra-small gold nanoparticles (AuNPs) using a Schiff-base and characterized them using several techniques. These Schiff-base stabilized AuNPs were then used for the catalytic reduction of organophosphate pesticides (malathion and parathion) in liquid phase reactions. The researchers achieved a high degradation efficiency of up to 95.06% and 99.1% with the addition of NaBH₄ within a 50-min reaction time for malathion and parathion, respectively. Additionally, the synthesized AuNPs showed selectivity for sensing Cr(VI) metal ions at nanomolar concentrations (10–100 nM) using fluorometric detection.

Copyright © 2023 Elsevier Ltd. All rights reserved.

Selection and peer-review under responsibility of the scientific committee of the 2nd International Conference on Multifunctional Materials.

1. Introduction

Metal nanoparticles (MNPs) containing only a few atoms up to a few hundred are versatile materials with broad applications in area such as optics, electronics, biosensors, biomedicines, and catalysis [1–5]. To produce MNPs, molecular templates and organic ligands have been utilized. When molecular templates other than organic ligands are used, the protected MNPs may lose their catalytic capability due to the almost complete blockage of surface active atoms [3–5]. Therefore, developing an easy, flexible, and effective method to produce ultra-small (<5 nm), highly-dispersed, functionalized, and ultra-stable MNPs is highly desirable.

Schiff bases are versatile organic ligands that form numerous stable complexes when co-ordinated with different transition metal ions, making them important chemical compounds in various fields such as inorganic, analytical, and medicinal chemistry [6,7]. Due to their strong affinity and actual confinement provided by their open, well-isolated, and abundant structure, using MNPs as a platform for the confined growth of MNPs with ultra-small size, high-dispersibility, and high-stability is a promising approach

[8,9]. Thus, encapsulating MNPs within Schiff bases may provide an unusual synergy for developing a new generation of heterogeneous catalysts [9].

Noble-MNPs, such as those made of Au, Ag, and Pt, are considered ingenious forms of nanomaterials due to their unique physicochemical properties [9–12]. Among them, AuNPs are highly-stable nanostructures that possess tunable optical properties and can be prepared in a variety of shapes, making them an attractive subject of scientific and technological research in recent years [4–5,10]. AuNPs have a long history of application in catalytic, sensing, bio-imaging, drug-delivery vehicles, and other fields [13,14]. Additionally, recent studies by Sangappa et al have reported on the catalytic degradation of dyes and other pollutants, as well as the detection of various metal ions using MNPs [15–17]. Based on the previous reports, in this work, we have synthesized and characterized AuNPs using the Schiff base (TMPM4CP) as a reducing and stabilizing agent; and utilized catalytic, sensing, and biological applications.

* Corresponding author.

E-mail address: ayodhyadasari@gmail.com (D. Ayodhya).<https://doi.org/10.1016/j.matpr.2023.05.348>

2214-7853/Copyright © 2023 Elsevier Ltd. All rights reserved.

Selection and peer-review under responsibility of the scientific committee of the 2nd International Conference on Multifunctional Materials.



2. Experimental

2.1. Materials and methods

AR-grade chemicals of $\text{HAuCl}_4 \cdot 3\text{H}_2\text{O}$ (98.5%), 4-(trifluoromethoxy)benzenamine (99%), 5-chloro-2-hydroxybenzaldehyde (98%), NaBH_4 (97.8%), methanol, acetone, and chloroform have been purchased from Merck. Pesticides (MLT and PRT) have been received from Bio-analytical Ltd.

2.2. Synthesis of Schiff base (TMPM4CP; 2-(4-(trifluoromethoxy)phenylimino)methyl)-4-chlorophenol)

The Schiff base (TMPM4CP) was synthesized by mixing the hot methanolic solutions of (25 mL) of 4-(trifluoromethoxy)benzenamine (10 mM) and 5-chloro-2-hydroxybenzaldehyde (10 mM) in 1:1 ratio with stirring and refluxing at 60–70 °C temperature on an oil bath for 2–4 h. The colored precipitates resulted were isolated by filtration and recrystallized from methanol. An outline of synthetic procedure presented in Scheme S1.

2.3. Synthesis of Schiff base capped AuNPs

An equal molar ratio of $\text{HAuCl}_4 \cdot 3\text{H}_2\text{O}$ and NaBH_4 was dissolved in a mixture of ethanol and DDwater in a 100 mL container at pH 7.0. After that, the synthesized TMPM4CP was dissolved in acetone and added to the aqueous solution. The resulting mixture was vigorously stirred for 5 h at 27°C. The completion of the reaction was indicated by a change in the organic layer color from yellow to light-pink indicated the formation of Schiff base stabilized AuNPs.

2.4. Characterizations

UV-vis spectra were recorded using a Shimadzu UV-3600 spectrophotometer (Germany). PL spectra were measured on an RF-5301 PC spectrophotometer. FT-IR spectroscopy was recorded on Bruker, USA. X-ray diffraction (XRD) analysis was carried out using a X'pert Pro diffractometer (Japan). The morphological features were studied using a Tecnaig2 (TEM, Germany).

2.5. Catalytic degradation of pesticides

Here, a mixture of MLT/PRT solution (0.05 mL, 0.5 g/L), freshly prepared NaBH_4 solution (0.05 mL, 0.25 M), and DDwater (2 mL) was prepared in a quartz cell. Next, a solution of catalyst (0.5 mL) was added to the reaction mixture. The maximum absorption of the MLT and PRT solutions was observed at 415 nm and 276 nm, respectively, by UV-vis spectroscopy. The reaction progress was monitored at regular intervals using a UV-vis spectrometer.

2.6. Fluorescence sensing activity

The potential use of the synthesized AuNPs was assessed for the specific detection of Cr(VI) in comparison to other metal ions as per a published protocol [18]. Initially, the samples were spiked with the respective metal-ion solutions (0.001–0.1 mM). The samples (500 mL) were then mixed with a combination of AuNPs (500 mL) and water (500 mL). The resultant solutions were allowed to stabilize at 27°C for 15 min followed by recording of PL spectra. To establish the sensitivity of AuNPs based Cr⁶⁺ sensing, different Cr⁶⁺ concentrations (10–100 nM) were titrated against AuNPs.

2.7. Antimicrobial activities

To evaluate the antimicrobial activity of the Schiff base (TMPM4CP) and AuNPs, and compared with standard compounds by Agal-well diffusion method [19]. Several bacterial strains, including *Staphylococcus aureus*, *Pseudomonas aeruginosa*, *Bacillus subtilis*, and *Escherichia coli*, as well as fungal strains such as *Aspergillus niger* and *Candida albicans*, were employed in this study. The suspended culture was evenly spread on nutrient agar plates, and the solid medium was gently perforated with a corkborer to create-wells. Each well was filled with 100 μL of synthesized AuNPs, and the plates were incubated for 24 h at 37 °C. The antimicrobial activity was measured by determining the diameter of the inhibition zone around the well.

2.8. DPPH antioxidant activity

In DPPH assay, the AuNPs and DPPH were mixed and left to incubate in the dark at 27°C for 30 min, and the optical density was measured at 517 nm. To the mixture, 1.5 mL of 0.1 mM DPPH was added and water was used to adjust the final test tube volume to 2 mL. The linear regression value was calculated using ascorbic acid as the standard. The concentration of Schiff base stabilized AuNPs required to reduce the initial concentration of DPPH by 50% (IC_{50}) under the specified experimental conditions was determined.

3. Results and discussion

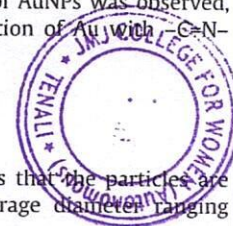
3.1. Optical and structural analysis

UV-vis spectra of the TMPM4CP and AuNPs were displayed in Fig. 1(a) and Fig. S1. The AuNPs were showed the maximum absorption at the range of 510–540 nm due to SPR [19,20]. In addition, TMPM4CP was exhibited the maximum absorbance at the λ of 258 nm and 338 nm, which are assigned to π - π^* and n - π^* transitions of phenyl-ring and chromophore ($-\text{HC}=\text{N}$) group, respectively [21]. Fig. 1(b) shows the PL spectra of TMPM4CP stabilized AuNPs. As shown in Fig. 1(b), TMPM4CP stabilized AuNPs has exhibited a strong emission peak at 594 nm, which is slightly shifted to lower λ , when compared to the Schiff base emission peak. It is the suggesting to the formation of AuNPs.

Fig. 1(c) shows the XRD pattern of the AuNPs, it shows dominant peaks at 38.10, 55.26, 64.12, and 81.54 in the 2θ range which originated for (111), (200), (220), and (311) crystal planes with FCC lattice structure and agree with the previous report [22]. FT-IR analysis was performed on TMPM4CP and AuNPs and displayed in Fig. 1(d) and Fig. S2. The FT-IR spectra of the Schiff base showed various characteristic IR absorption peaks, at 3350 cm^{-1} , 1632 cm^{-1} , 1258 cm^{-1} , 1164 cm^{-1} , and 820 cm^{-1} , which are assigned to $-\text{OH}$, $-\text{C}=\text{N}$, aromatic $\text{C}-\text{H}$, $-\text{C}=\text{O}$, and $\text{C}-\text{O}$ stretching vibrations [23]. The FT-IR spectra of the AuNPs shows that the positions of the bands attributed to azo-methine ($-\text{HC}=\text{N}-$) at 1631 cm^{-1} , $\nu_{\text{C}-\text{O}}$ of carbonyl at 1172 cm^{-1} , $\nu_{\text{C}=\text{O}}$ overlapped amide and ester at 1660 cm^{-1} , $\nu_{\text{asym}}(\text{COO}^-)$ and $\nu_{\text{sym}}(\text{COO}^-)$ at 1430–1520 cm^{-1} respectively. The strong N-H absorption bands were slightly shifted in the FTIR spectra of AuNPs was observed, which may be assigned to the co-ordination of Au with C-N-group [23].

3.2. Morphological analysis

HR-TEM images of AuNPs were reveals that the particles are predominantly spherical shape with average diameter ranging



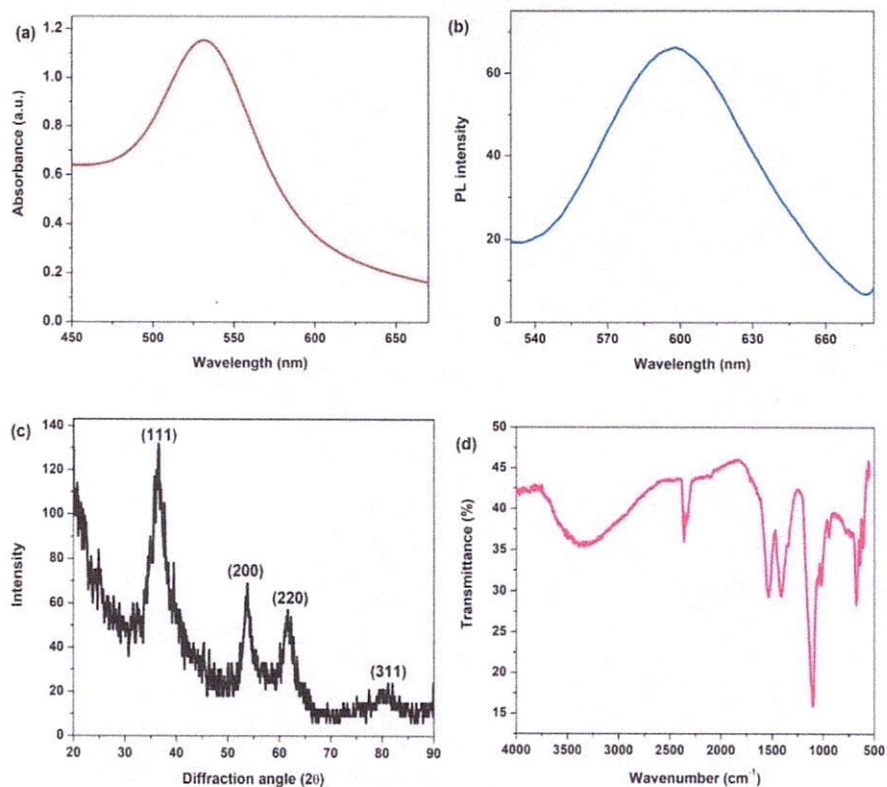


Fig. 1. (a) UV-Vis absorption, (b) PL, (c) XRD, and (d) FTIR spectra of AuNPs.

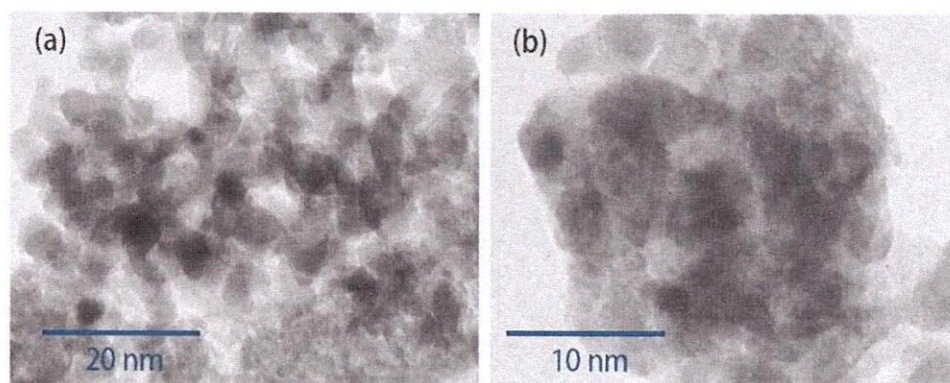


Fig. 2. (a-b) TEM images of AuNPs.

from 4 to 12 nm and highly mono-dispersed in nature without agglomeration (Fig. 2(a-b)).

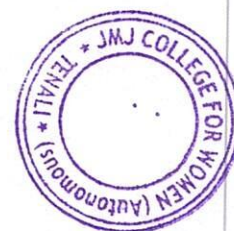
3.3. ^1H NMR, ^{13}C NMR, and ESI-MS

The other characterization techniques including ^1H NMR, ^{13}C NMR, and ESI-MS were analyzed for the confirmation of TMPM4CP formation and it was displayed in Figs. S3–S5.

3.4. Catalytic degradation activity

As depicted in Fig. 3(a), the degradation of MLT and PRT using AuNPs in the presence of NaBH_4 was examined. The results showed that AuNPs were efficient catalysts for the reduction of MLT and PRT in the presence of an excess of NaBH_4 . Typically, MLT and

PRT have unique absorption peaks located at 415 nm and 276 nm, respectively. However, when a miniature amount of AuNPs was added, the absorption peaks of MLT and PRT gradually decreased and vanished after 50 min, indicating as complete degradation. The progress of the reduction reaction was monitored by UV-vis spectrophotometer, which showed a rapid decrease in the intensity of the absorption peaks. The degradation of MLT and PRT increased drastically, reaching about 95.26% and 99.01%, respectively, within 50 min of reaction time (Fig. 3(a)), due to the ultra-small size of the AuNPs [24]. The corresponding value of k calculated from the slope is $1.2812 \times 10^{-3} \text{ min}^{-1}$ and $1.4125 \times 10^{-3} \text{ min}^{-1}$ (Fig. 3(b)).



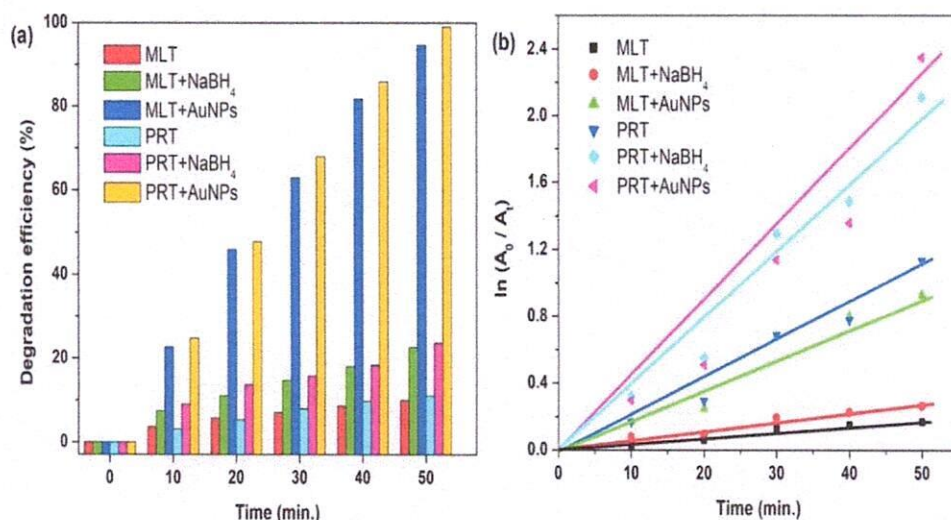


Fig. 3. (a) Catalytic degradation efficiency and (b) kinetic rate constants for the degradation of MLT and PRT using AuNPs.

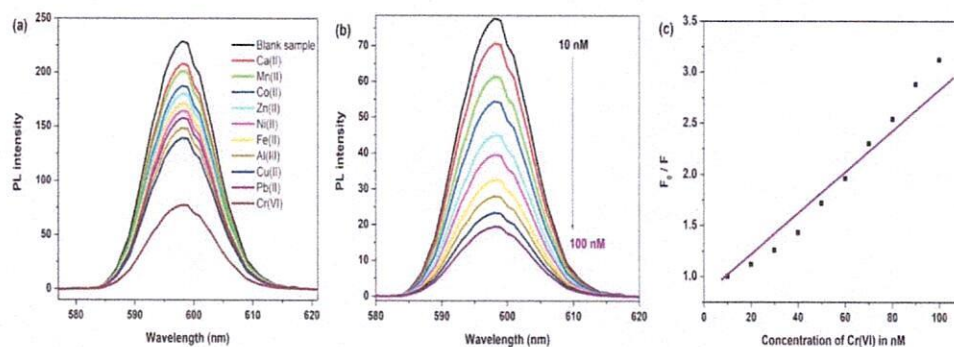


Fig. 4. (a) Fluorescence selective sensing of Cr⁶⁺, (b) sensitive sensing of Cr⁶⁺ in the concentration range of 10–100 nM, and (c) its Stern-Volmer plot using AuNPs.

3.5. Fluorescence sensing activity

In the PL spectra of the detection of Cr⁶⁺ ions, the addition of 10 μ L of an aqueous solution of Zn²⁺, Co²⁺, Ni²⁺, Al³⁺, Mn²⁺, Pb²⁺, Ca²⁺, Cu²⁺, and Fe²⁺ ions to the AuNPs, did not produce any significant fluorescence intensity changes (Fig. 4(a)). However, upon addition of Cr⁶⁺ ions to the solution containing AuNPs and other metal ions, an immediate decrease in PL emission was observed in Fig. 4(b). The results demonstrated that the absorbance of SPR band follows a superior exponential response to Cr⁶⁺ concentrations (10–100 nM) with a regression constant (R^2) of 0.98 as shown in Fig. 4(c).

3.6. Antimicrobial activities

The synthesized AuNPs have superior antimicrobial activities against *Pseudomonas aeruginosa* and *Aspergillus niger* when used in volumes of 10 μ L than TMPM4CP under matching experimental conditions (Fig. 5). On other hand, in the equivalent volumes, the TMPM4CP do not exhibit significant antimicrobial activities against all bacteria and fungi strains. The higher antimicrobial activity of the AuNPs compared to Schiff base may be due to the change in structure or co-ordination and chelating tends to make AuNPs act more powerful and potent bacteriostatic agents, thus inhibiting the growth of the bacteria as well as fungi [25,26].

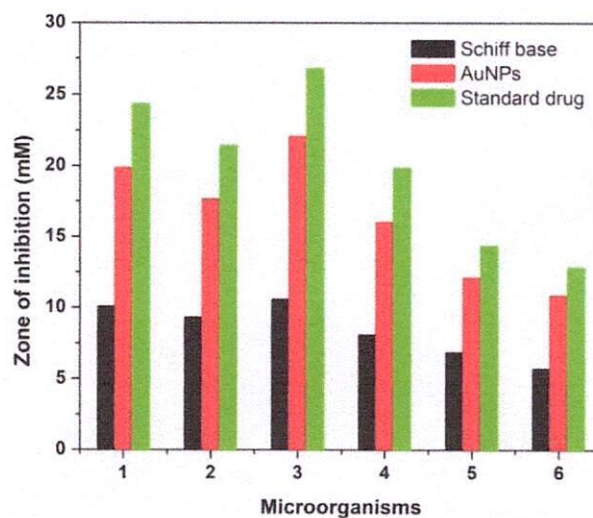


Fig. 5. Antimicrobial activities of the synthesized TMPM4CP and AuNPs: bacteria (1) *Staphylococcus aureus*, (2) *Bacillus subtilis*, (3) *Pseudomonas aeruginosa*, and (4) *Escherichia coli*; and fungi (5) *Aspergillus niger* and (6) *Candida albicans*.

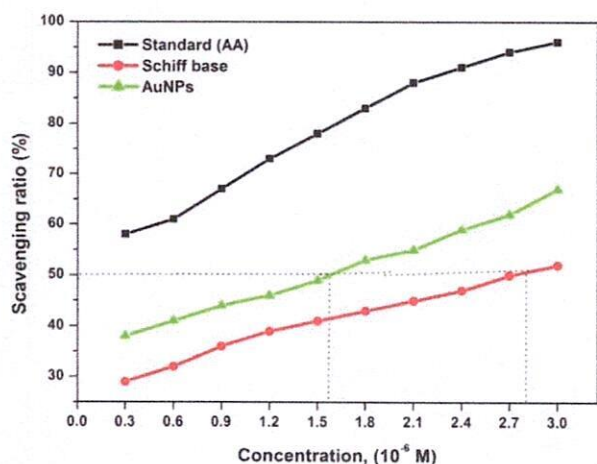


Fig. 6. Antioxidant activity and IC_{50} estimated by DPPH assay using the synthesized TMPM4CP and its stabilized AuNPs.

3.7. Antioxidant activity

In DPPH scavenging activity, the ability of TMPM4CP stabilized AuNPs and TMPM4CP to transport DPPH was analyzed at various concentrations (0.3–3.0 μM). The DPPH free radicals carrying property of the TMPM4CP, the AuNPs, increased significantly with increasing concentrations, as shown in Fig. 6. The AuNPs had a larger surface area and catalytic capabilities, which could have facilitated their antioxidant properties. An IC_{50} value was obtained from the plots of percentage of inhibition with an increase in concentration of the AuNPs ($IC_{50} = 1.58 \mu\text{g}/\text{mL}$) and TMPM4CP ($IC_{50} = 2.81 \mu\text{g}/\text{mL}$), and comparable to standard (ascorbic acid).

4. Conclusions

In summary, we have synthesized and characterized TMPM4CP stabilized AuNPs via the reduction of Au^+ to $\text{Au}(0)$. The AuNPs possess an average diameter of $8 \pm 2 \text{ nm}$ and a fcc structure as determined by XRD and TEM analysis. AuNPs exhibited excellent catalytic properties, with degradation efficiencies of 95.26% and 99.01% observed for MLT and PRT, respectively. Furthermore, we found that our AuNPs were highly selective and sensitive in detecting Cr^{6+} via fluorescence with a concentration range of 10–100 nM. AuNPs also showed superior antimicrobial activity compared to TMPM4CP. Finally, we evaluated the antioxidant potential of AuNPs and found that they exhibited pertinent antioxidant activity.

CRedit authorship contribution statement

Sumalatha Vislavath: Methodology, Investigation, Formal analysis, Conceptualization. **Marri Pradeep Kumar:** . **G. Balraj:** Visualization, Validation. **M. Sharath Babu:** . **Dasari Ayodhya:** Writing – review & editing, Writing – original draft, Visualization, Validation, Supervision, Software, Project administration, Methodology, Investigation, Formal analysis, Data curation, Conceptualization.

Data availability

No data was used for the research described in the article.

Declaration of Competing Interest

The authors declare that they have no known competing financial interests or personal relationships that could have appeared to influence the work reported in this paper.

Acknowledgements

The authors wish to thank the Head, Department of Chemistry, Osmania University, Hyderabad for the excellent support towards research.

Appendix A. Supplementary data

Supplementary data to this article can be found online at <https://doi.org/10.1016/j.matpr.2023.05.348>.

References

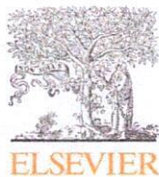
- [1] P.K. Jain, X. Huang, I.H. El-Sayed, M.A. El-Sayed, Noble metals on the nanoscale: optical and photothermal properties and some applications in imaging, sensing, biology, and medicine, *Accou. Chem. Res.* 41 (2008) 1578–1586.
- [2] X. Yang, L. Chen, H. Liu, T. Kurihara, S. Horike, Q. Xu, Encapsulating ultrastable metal nanoparticles within reticular Schiff base nanospaces for enhanced catalytic performance, *Cell Rep. Phys. Sci.* 2 (2021).
- [3] K. Krishna, K.S. Harisha, R. Neelakandan, Y. Sangappa, Fabrication and conductivity study of silver nanoparticles loaded polyvinyl alcohol (PVA-AgNPs) nanofibers, *Mater. Today: Proc.* 42 (2021) 515–520.
- [4] D. Ayodhya, Recent progress on detection of bivalent, trivalent, and hexavalent toxic heavy metal ions in water using metallic nanoparticles: A review, *Res. Chem.* 5 (2023).
- [5] D. Ayodhya, Ag-SPR and semiconductor interface effect on a ternary $\text{CuO@Ag@Bi}_2\text{S}_3$ Z-scheme catalyst for enhanced removal of HIV drugs and (photo) catalytic activity, *New J. Chem.* 46 (2022) 15838–15850.
- [6] A.M. Abu-Dief, I.M. Mohamed, A review on versatile applications of transition metal complexes incorporating Schiff bases, *Beni-suef Univ. J. Basic Appl. Sci.* 4 (2015) 119–133.
- [7] M.S. More, P.G. Joshi, Y.K. Mishra, P.K. Khanna, Metal complexes driven from Schiff bases and semicarbazones for biomedical and allied applications: a review, *Mater. Today Chem.* 14 (2019).
- [8] S. Kannaiyan, K. Kannan, V. Andai, Green synthesis of Phenothiazinium Schiff base and its nano silver complex using egg white as a catalyst under solvent free condition, *Mater. Today: Proc.* 55 (2022) 267–273.
- [9] S. Swami, N. Sharma, A. Agarwala, V. Shrivastava, R. Shrivastava, Schiff base anchored silver nanomaterial: An efficient and selective nano probe for fluoride detection in an aqueous medium, *Mater. Today: Proc.* 43 (2021) 2926–2932.
- [10] F. Amourizi, K. Dashtian, M. Ghaedi, B. Hosseinzadeh, An asymmetric Schiff base-functionalized gold nanoparticle-based colorimetric sensor for Hg^{2+} ion determination: experimental and DFT studies, *Anal. Meth.* 13 (2021) 2603–2611.
- [11] Y. Teng, X. Wang, M. Wang, Q. Liu, Y. Shao, H. Li, C. Liang, X. Chen, H. Wang, A Schiff-base modified Pt nano-catalyst for highly efficient synthesis of aromatic azo compounds, *Catalysts* 9 (2019) 339.
- [12] R. Madhukumar, K.S. Harisha, S. Asha, Y. Wang, Y. Sangappa, Gamma assisted synthesis and characterization of colloidal SF-AgNPs, *InAIP Conf. Proc.* 2100 (2019).
- [13] S.R. Barman, A. Nain, S. Jain, N. Punjabi, S. Mukherji, J. Satija, Dendrimer as a multifunctional capping agent for metal nanoparticles for use in bioimaging, drug delivery and sensor applications, *J. Mater. Chem. B* 6 (2018) 2368–2384.
- [14] K. Nejadi, M. Dadashpour, T. Gharibi, H. Mellatyar, A. Akbarzadeh, Biomedical applications of functionalized gold nanoparticles: a review, *J. Clust. Sci.* 33 (2022) 1–16.
- [15] K.S. Harisha, N. Parushuram, S. Asha, S.B. Suma, B. Narayana, Y. Sangappa, Eco-synthesis of gold nanoparticles by Sericin derived from Bombyx mori silk and catalytic study on degradation of methylene blue, *Part. Sci. Technol.* 39 (2021) 131–140.
- [16] K.S. Harisha, B. Narayana, Y. Sangappa, Highly selective and sensitive colorimetric detection of arsenic (III) in aqueous solution using green synthesized unmodified gold nanoparticles, *J. Dispersion Sci. Technol.* 44 (2023) 132–143.
- [17] H.K. Sanjeevappa, P. Nilgal, R. Rayaraddy, L.J. Martis, S.M. Osman, N. Badiadka, S. Yallappa, Biosynthesized unmodified silver nanoparticles: A colorimetric sensor for detection of Hg^{2+} ions in aqueous solution, *Res. Chem.* 4 (2022) 100507.
- [18] D. Ayodhya, G. Veerabhadram, One-pot, aqueous synthesis of multifunctional biogenic Ag NPs for efficient 4-NP reduction, Hg^{2+} detection, and antioxidant activities, *Inorg. Nano-Metal Chem.* (2023) 1–10.
- [19] D. Ayodhya, G. Veerabhadram, BSA mediated green synthesis, characterization, photodegradation of mixed dyes via metal-semiconductor



- interface, antimicrobial and antioxidant activities, *Mater. Today Chem.* 17 (2020) 100320.
- [20] M.P. Kumar, D. Ayodhya Shivaraj, Novel copper (II) binary complexes with N, O-donor isoxazole Schiff base ligands: Synthesis, characterization, DPPH scavenging, antimicrobial, and DNA binding and cleavage studies, *Res. Chem.* 5 (2023) 100845.
- [21] B. Jarzabek, B. Kaczmarczyk, D. Sek, Characteristic and spectroscopic properties of the Schiff-base model compounds, *Spectrochim Acta Part A: Mol. Biomol. Spectroscopy* 74 (2009) 949–954.
- [22] K.S. Harisha, N. Parushuram, R. Ranjana, L.J. Martis, B. Narayana, Y. Sangappa, Characterization and antibacterial properties of biogenic spherical silver nanoparticles, *Mater. Today: Proc.* 42 (2021) 405–409.
- [23] P. Huang, J. Li, X. Liu, F. Wu, Colorimetric determination of aluminum (III) based on the aggregation of Schiff base-functionalized gold nanoparticles, *Microchim. Acta* 183 (2016) 863–869.
- [24] D. Ayodhya, Fabrication of SPR triggered Ag-CuO composite from Cu(II)-Schiff base complex for enhanced visible-light-driven degradation of single and binary-dyes and fluorometric detection of nitroaromatic compounds, *Inorg. Chem. Commun.* 148 (2023) 110295.
- [25] M. Čonková, V. Montes-García, M. Konopka, A. Ciesielski, P. Samori, A.R. Stefankiewicz, Schiff base capped gold nanoparticles for transition metal cation sensing in organic media, *Chem. Commun.* 58 (2022) 5773–5776.
- [26] K.S. Harisha, M. Shilpa, S. Asha, N. Parushuram, R. Ranjana, B. Narayana, Y. Sangappa, Synthesis of silver nanoparticles using Bombyx mori silk fibroin and antibacterial activity, *InfOP Conf Ser: Mater. Sci. Eng.* 577 (2019) 012008.

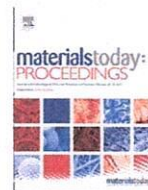
PRINCIPAL
JMJ COLLEGE FOR WOMEN (Autonomous)
TENALI





Contents lists available at ScienceDirect

Materials Today: Proceedings

journal homepage: www.elsevier.com/locate/matpr

Synthesis of Schiff base stabilized AgNPs for enhanced catalytic degradation of antibiotics, Hg(II) detection, antioxidant, and antimicrobial activities

V. Sumalatha^a, Dasari Ayodhya^{b,*}^a Department of Chemistry, J.M.J. College for Women, Tenali-522201, Andhra Pradesh, India^b Department of Chemistry, University College of Science, Osmania University, Hyderabad-500007, Telangana State, India

ARTICLE INFO

Article history:
Available online xxx

Keywords:
AgNPs
Schiff base
SPR
Antibiotic degradation
Hg²⁺ sensing
Biological action

ABSTRACT

The present aim is synthesis of Schiff base (TMPM5MOP), its stabilized silver nanoparticles (AgNPs) with face cubic centered structure and average diameter is approximately 6–14 nm. AgNPs used as catalysts, which is catalytically degrade > 90% of antibiotics such as tetracycline (TC) and ciprofloxacin (Cipro) within the reaction of 0.5 h using sodium borohydride. The selectively and sensitively detected Hg²⁺ ions in an aqueous medium in the presence of AgNPs by fluorometrically. AgNPs are effective against Gram-positive and Gram-negative bacteria. The AgNPs demonstrated a greater aptitude to scavenge DPPH-free-radicals and comparable with standard.

Copyright © 2023 Elsevier Ltd. All rights reserved.

Selection and peer-review under responsibility of the scientific committee of the 2nd International Conference on Multifunctional Materials.

1. Introduction

Nanostructures with reduced dimensions have a greater ratio of surface area to volume compared to their larger counterparts, and possess unique point-to-point connectivity properties that make them particularly sensitive to environmental interactions [1–3]. Compared to other types of low-dimensional nanostructures, metallic nanoparticles (MNPs) are highly adaptable platforms for developing chemical sensors due to their exceptional stability, large surface-to-volume ratio, and unique inter-particle communication capabilities [4–5]. The unique mechanical, chemical, energetic, physical, and analytical properties of MNPs derived from Pt, Ag, and Au have caused difficulties in research due to their distinctive characteristics that distinguish them from other similar materials. Among MNPs, AgNPs with a great attention because its tremendous applications including catalysis, sensing, textiles, cosmetic, biomedical, and food packaging [6–11]. In this context, several researchers were used AgNPs as catalysts, sensors, and biological agents [6–9,12–13]. Additionally, AgNPs due to excessive ROS production and exhibit significant antibacterial and antioxidant activities [14–16]. Herein, we report for the first time,

AgNPs were prepared using TMPM5MOP as Schiff base towards evaluating the catalytic, sensing property, antioxidant, and inhibition of bacterial growth applications.

2. Experimental

2.1. Chemicals

The AR-grade chemicals of AgNO₃ (>98%), NaBH₄ (97.5%), 4-(tri fluoromethoxy)benzenamine, 2-hydroxy-4-methoxy benzaldehyde, methanol (99.85%), acetone (>99%), and chloroform (99.9%) were procured from SDFine Chemicals, India. Antibiotics (TC and Cipro) have been received from Bioanalytical Ltd.

2.2. Synthesis of TMPM5MOP and AgNPs

Schiff base (TMPM5MOP) was fabricated through adding 10 mM, 25 mL of 4-(trifluoromethoxy)benzenamine to 10 mM, 25 mL of 2-hydroxy-4-methoxy benzaldehyde in equal ratio with unremitting stirring and refluxing at 65 °C for 3 h. The obtained precipitate was isolated, filtered, and recrystallised in CH₃OH (Scheme S1). In the fabrication of AgNPs, equal ratio of AgNO₃ and NaBH₄ were added slowly to TMPM5MOP solution and

* Corresponding author.

E-mail address: ayodhyadasari@gmail.com (D. Ayodhya).<https://doi.org/10.1016/j.matpr.2023.05.346>

2214-7853/Copyright © 2023 Elsevier Ltd. All rights reserved.

Selection and peer-review under responsibility of the scientific committee of the 2nd International Conference on Multifunctional Materials.



unremitting stirring for 5 h. The changing in color from light yellow to dark brown is evidence for the formation of AgNPs.

2.3. Characterizations

Morphological features (TEM, TechnaiG2, Germany), crystal structure (XRD, XPertPro, Japan), absorption behavior (UV-3200, Shimadzu, USA), emission properties (RF-5301 PC, UK), and ATR-FTIR (Bruker, KBr pellet, USA) of AgNPs were studied.

2.4. Antibiotics degradation experiment

In a typical procedure, prior to reaction, the suspension (10 mg of catalyst + 10 mg/L of antibiotic solutions (TC; 357 nm and Cipro; 274 and 322 nm) in 100 mL) were mixed under vigorous stirring in absence of light for 0.5 h for homogeneous mixture. Afterthat, the catalytic degradation experiments, the equal aliquots (0.5 mL) of the suspensions were withdrawn at various time intervals and then immediately quenched with methanol. The entire antibiotic degradation reaction pathway was monitored using UV-vis spectrometer.

2.5. Fluorometric detection of Hg(II)

In a detection experiment, Zn^{2+} , Cu^{2+} , Co^{2+} , Cd^{2+} , Ag^+ , Hg^{2+} , Ni^{2+} , Ca^{2+} , Ba^{2+} , and Al^{3+} (100 μ L; 0.1 μ M) were individual mixed to AgNPs (20 μ L; 0.01 M), TMB (20 μ L; 0.01 M), and H_2O_2 (20 μ L; 10 M). The resultant solution was transferred to a quartz cuvette after continuing for 20 min. For the selective detection of Hg^{2+} and other metal ions, 100 mL of various concentrations of Hg^{2+} (ranging from 0.1 to 100 μ M) were added to AgNPs solutions. The mixtures were transferred to a quartz cuvette and recorded PL emission spectra.

2.6. Antimicrobial activity test

100 μ L of microbial cultures were prepared in the nutrient-agar (NA) media for bacteria (*P.aeruginosa*, *E.coli*, *S.aureus*, and *B.subtilis*) and potato-dextrose agar (PDA) for fungi (*A.niger* and *C.albicans*). 8 mm diameter asymmetric Petri plates with 5 wells were formed by punching with stainless steel after solidification of all the plates. 100 μ L of various concentrations of AgNPs (0.2, 0.4, 0.6, and 0.8 μ g/mL) were placed in 4 wells, and one well served as a standard with the same concentration as the negative control. The petrographic plates were incubated for 24 h at 37 °C. The test was conducted in 3 times for each pathogen-containing bacteria and compared to the reference.

2.7. DPPH scavenging test

DPPH was dissolved in 100 mL of methyl alcohol and heated to 20 °C. 2 mL were added from the stock solution to 1 mL of CH_3OH solution containing sample of TMPM5MOP and AgNPs at a nominal concentration of 100 μ g/mL. The DPPH free-radical saving activity was recorded at 517 nm, and the standard benchmark is now set with ascorbic acid.

3. Results and Discussion

3.1. Optical spectra

The absorption bands of TMPM5MOP and AgNPs have a wavelength of 280 and 375 nm; and 431 nm, respectively, while AgNPs have a broad intensity (Fig. 1 and Fig. S1). TMPM5MOP was maximum absorbed at 280 nm was moved towards higher wavelength,

which is confirm that TMPM5MOP is strongly capped with AgNPs. The UV-vis absorption spectra of AgNPs was facade at 431 nm due to the SPR band, which is evidence for the formation of AgNPs. The photoluminescence spectra of TMPM5MOP and AgNPs were measured at $\lambda = 300-600$ nm ($\lambda_{ex} = 380$ nm) and it was displayed in Fig. 1(b). The PL of AgNPs casing the region 520-650 nm (532 nm) is due to the excitation of SPR [17].

3.2. FT-IR spectra

FTIR spectra of TMPM5MOP (Fig. S2) and AgNPs (Fig. 1c) were shown in the strong absorption bands at 1622 cm^{-1} (azo-methine nitrogen) for TMPM5MOP, 1582 cm^{-1} (azo-methine nitrogen interacted with AgNPs) in AgNPs FTIR spectrum [18]. In addition, the absorption bands were appeared at 1319, 1155, and 820 cm^{-1} assigned for -C = O, -C-F, and -C = C bands in the FTIR spectra of TMPM5MOP and AgNPs. In foremost, hydroxyl and imine groups are conspicuous in the IR spectrum act as reducing or capping agents for the fabrication of AgNPs [19].

3.3. XRD study

X-ray diffraction pattern of AgNPs synthesized using TMPM5MOP is shown in Fig. 1(d). The significant peaks in the XRD diffractogram at 2θ values of 38.24° , 44.40° , 64.52° , and 77.51° were discovered to be related to Ag-metal and correspond to (111), (200), (220), and (311) planes of AgNPs (JCPDS card no. 1-1167) [20]. These reflections are in concurrence with Ag-metal, that possesses Fcc cubic structure with high crystallinity.

3.4. TEM

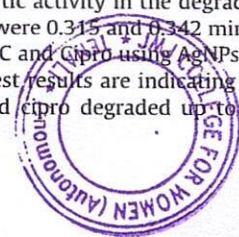
The AgNPs are shown in the TEM images as spherical with irregular shape and size is 5-15 nm (Fig. 2(a-b)). It exhibits the distribution of AgNPs with TMPM5MOP, that might be attributed to complexation between Schiff base and Ag^+ . In addition, the crystalline character of synthesized AgNPs could be observed clearly in TEM image.

3.5. Other spectral analysis

Further characterization techniques including proton NMR, ^{13}C NMR, and mass spectra were analyzed for the confirmation of Schiff base (TMPM5MOP) formation and it was displayed in Fig. S3-S5.

3.6. Catalytic degradation of antibiotics

Fig. 3(a) and Fig. 3(b) shows the degradation of TC and Cipro using AgNPs after 30 min of the reaction in the presence of $NaBH_4$. According to the obtained results, the contribution of Tc and cipro degradation in on the whole degradation using AgNPs was outstanding than without catalyst, hence AgNPs was mostly required to degradation of antibiotics. After 30 min of the reaction, AgNPs adsorbed < 12% of the initial Tc and cipro in presence of AgNPs under identical reaction conditions. Hence, it can be conclude that the AgNPs was responsible for the adsorption of the antibiotic on the surface of catalyst. The degradation efficiency of AgNPs was enormously increased as 88.12% and 90.08% of TC and cipro in 30 min reaction (Fig. 3(c)). The result showed that the prepared AgNPs possessed excellent catalytic activity in the degradation of TC and Cipro. The rate constants were 0.315 and 0.342 min^{-1} were observed for the degradation of TC and Cipro using AgNPs, respectively (Fig. 3(d)). The recycling test results are indicating that the almost similar amount of Tc and cipro degraded up to the 3rd



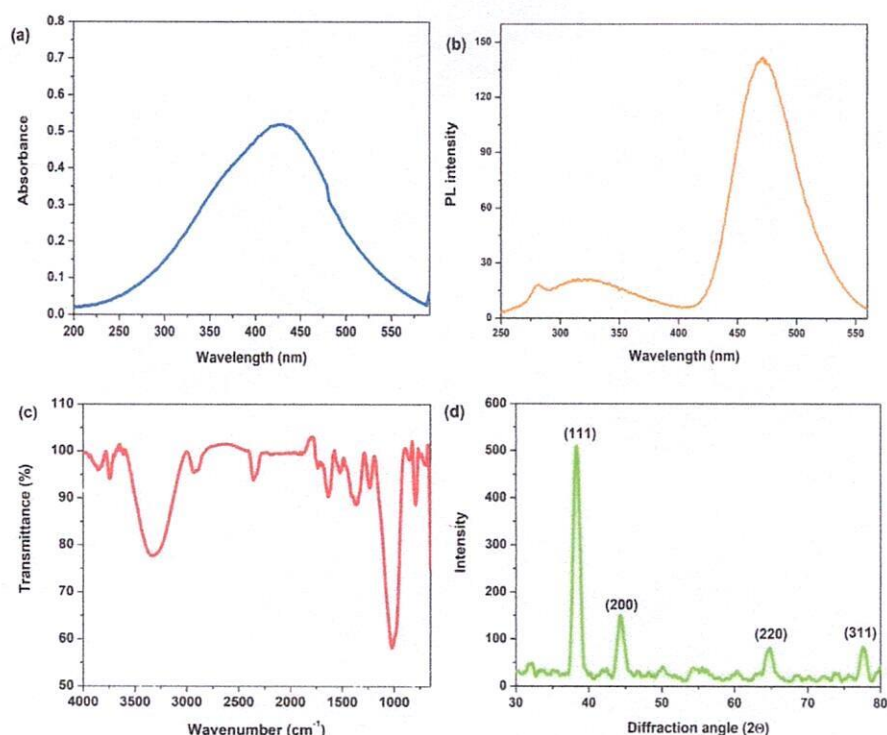


Fig. 1. (a) UV-vis absorption, (b) PL, (c) FTIR, and (d) XRD spectra of AgNPs.

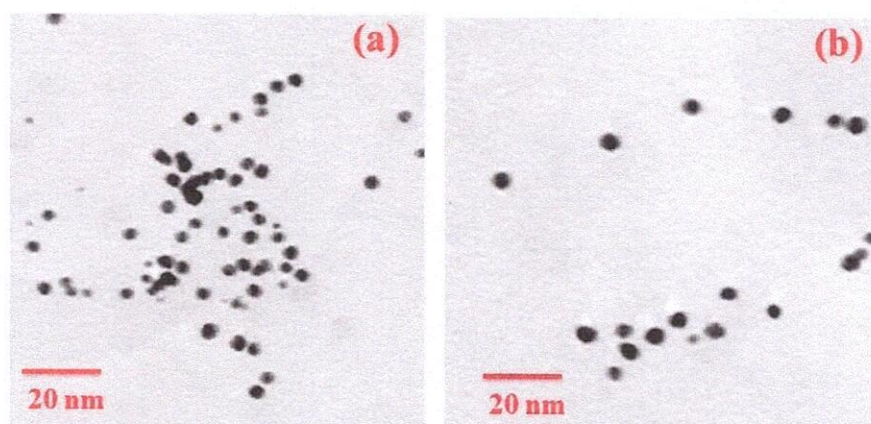


Fig. 2. (a-b) TEM images of AgNPs.

cycle, and only 5% decrement was observed in the 5th cycle as shown in Fig. 3(e).

3.7. Fluorometric detection of Hg^{2+}

In this case, the preset additions (0.5 mL, 10^{-3} mol/L) of individual metal ion solutions were added to 3 mL of AgNPs. Fig. 4(a) depicts the PL emission spectra during detection of Hg^{2+} at 27°C. Then the strength of the SPR-peak changed slightly when the addition of other metal ions (Zn^{2+} , Cu^{2+} , Co^{2+} , Cd^{2+} , Ag^+ , Ni^{2+} , Ca^{2+} , Ba^{2+} , and Al^{3+}) to the AgNPs in aqueous medium. The preserved PL results showed that the addition of a nontrivial addition of the upper metal ions had no effect on the SPR-peak and colour of AgNPs (Fig. 4(b)). In contrast, the SPR characteristic peak vanishes and the colour of the solution changes from yellow to colourless when Hg^{2+} is added to the solution containing AgNPs [21].

3.8. Antimicrobial activity

The antimicrobial results were established as prepared AgNPs shown detached antimicrobial action against pathogenic micro-organisms at 5 $\mu\text{g}/\text{mL}$ concentration and displayed in Fig. 5(a-b). The AgNPs demonstrated notable antibacterial activity in both micro-organisms, however they showed reduced anti-bacterial activity against *E.coli*, *S.aureus*, and *B.subtilis*. Additionally, they showed high activity against *P.aeruginosa*. As well as high antifungal activity was observed against *A. niger* than *c. albicans* under identical experimental conditions. The lipo-solubility property of the at least one molecule contained in AgNPs should be responsible for the degradation of the bacterial cell-membrane and penetrate into the bacterial cell [22–23].



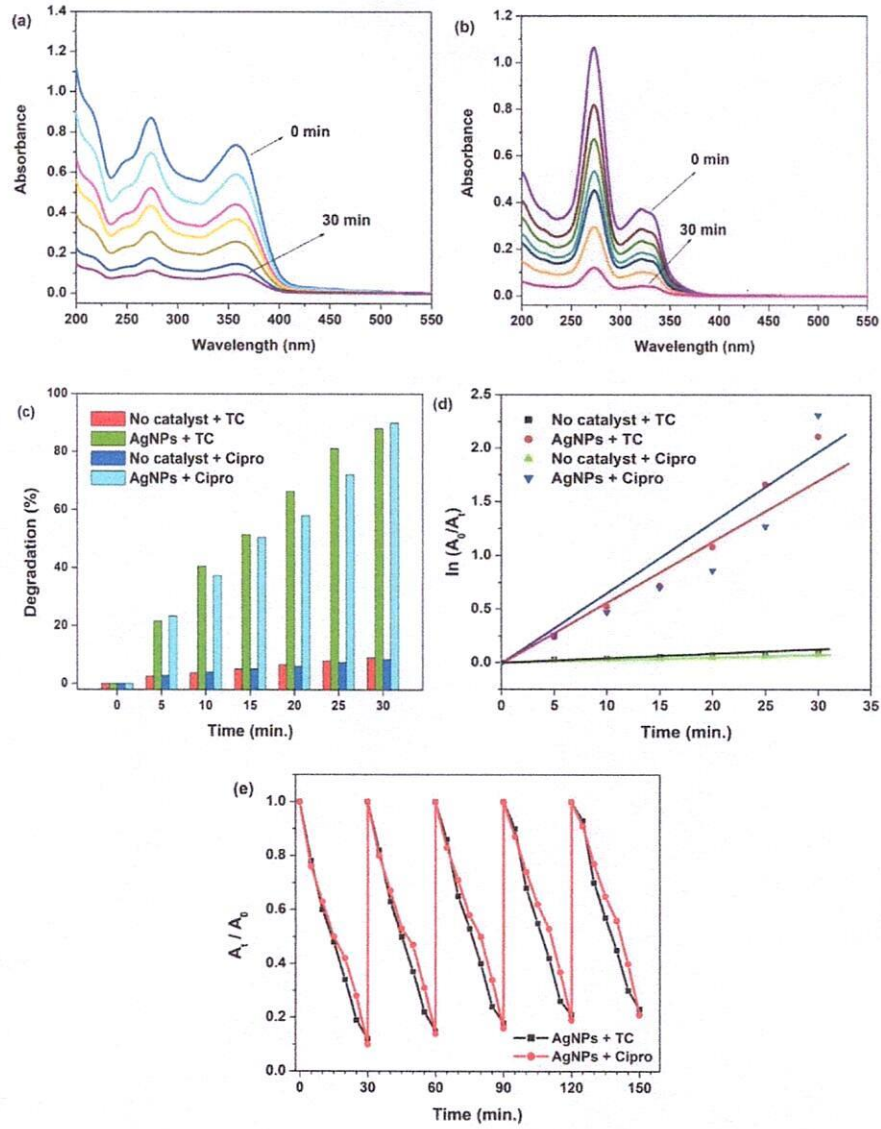


Fig. 3. Catalytic degradation of antibiotics (Tc and cipro) using AgNPs: UV-vis degradation profiles of (a) Tc and (b) cipro; (c) bar diagram; (d) kinetic plot; and (e) recyclability.

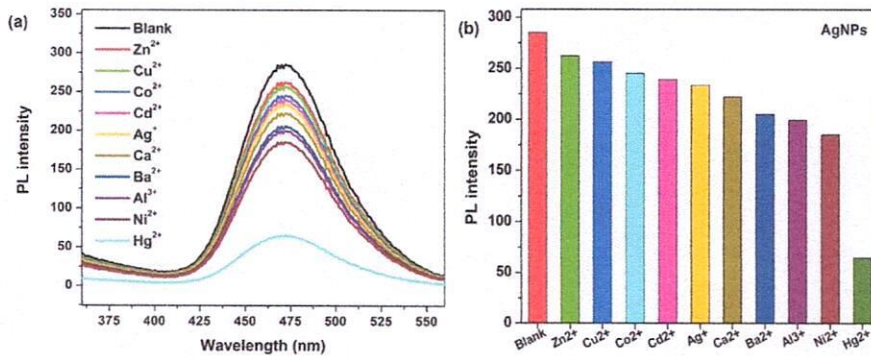


Fig. 4. PL spectra of a) Schiff base capped AgNPs with different metal ions and (b) bar diagram indicating emission intensity at 470 nm.



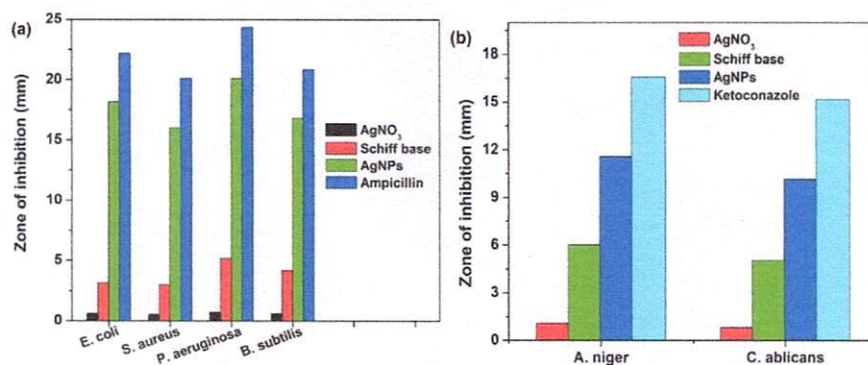


Fig. 5. The bar diagram of the zone of inhibition of bacteria (a) and fungi growth using AgNPs.

3.9. DPPH scavenging activity

DPPH scavenging activity of AgNPs displayed an admirable DPPH scavenging activity with concentrations from 0.5 $\mu\text{g/mL}$ to 3 $\mu\text{g/mL}$ and it was shown in Fig. 6(a). It may be suggested the favor of prominent results due to the functional groups were presented in the Schiff base capped AgNPs and covered by its surface of NPs, high-dispersion, and petite size of the particles based on the previous report [24,25]. The IC_{50} values of TPM5MOP and AgNPs are exhibited at 1.31 and 2.52 $\mu\text{g/mL}$ and displayed in Fig. 6(a). The outcomes are clearly indicated by the fact that AgNPs generated higher DPPH activity (78.18%) than the TPM5MOP (51.20%), in addition to the maximum DPPH activity for standard (Ascorbic acid; 86.11%) as shown in Fig. 6(b). Hence, the scavenging ability of AgNPs for DPPH free radicals showed astonishing activity with the comparison of standard compound.

4. Conclusions

In the conclusions, we have synthesized 2-(4-(trifluoromethoxy)phenylimino)methyl)-5-methoxyphenol and Schiff base capped AgNPs. The synthesized samples were characterized with the confirmation of FCC structure, spherical shape, and size is 10 ± 5 nm. The synthesized AgNPs were tested for the catalytic degradation of TC and Cipro using NaBH_4 as a reducing agent, it shows as almost complete degradation (98%) was observed within 30 min and stable up to 5 cycles. PL spectroscopy was employed to monitor the interaction response between the synthesized AgNPs and an aquatic solution for the determination of Hg^{2+} concentration. Using the disc diffusion method, the synthesized AgNPs demonstrated noteworthy antibacterial and antifungal activity.

The DPPH method indicated that the AgNPs possessed excellent efficacy in scavenging free radicals.

CRediT authorship contribution statement

V. Sumalatha: Methodology, Investigation, Formal analysis, Data curation. **Dasari Ayodhya:** Concept, Methodology, Experiments, Software, Data analysis, Editing, Revision.

Data availability

No data was used for the research described in the article.

Declaration of Competing Interest

The authors declare that they have no known competing financial interests or personal relationships that could have appeared to influence the work reported in this paper.

Acknowledgement

The authors wish to thank the Head, Department of chemistry, Osmania University, Hyderabad for the excellent support toward this research.

Appendix A. Supplementary material

Supplementary data to this article can be found online at <https://doi.org/10.1016/j.matpr.2023.05.346>.

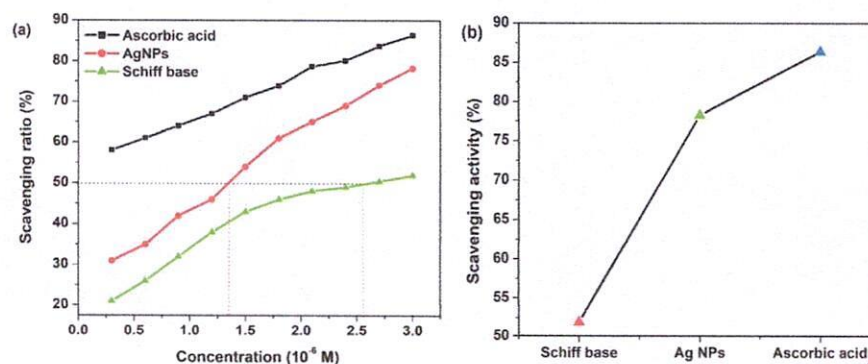


Fig. 6. DPPH radical scavenging activity (%) and (b) IC_{50} values of AgNPs with standard compound.



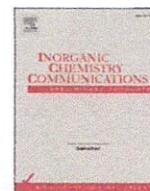
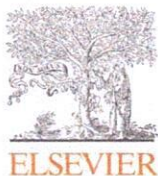
Reference

- [1] J.H. Seo, E. Swinnich, Y.Y. Zhang, M. Kim, Low dimensional freestanding semiconductors for flexible optoelectronics: materials, synthesis, process, and applications, *Mater. Res. Lett.* 8 (2020) 123–144.
- [2] P. Kumari, K.P. Misra, S. Chattopadhyay, S. Samanta, A brief review on transition metal ion doped ZnO nanoparticles and its optoelectronic applications, *Mater. Today Proceed.* 43 (2021) 3297–3302.
- [3] H. Xu, H. Shang, C. Wang, Y. Du, Low-dimensional metallic nanomaterials for advanced electrocatalysis, *Adv. Funct. Mater.* 30 (2020) 2006317.
- [4] C. Burel, O. Ibrahim, E. Marino, H. Bharti, C.B. Murray, B. Donnio, Z. Fakhraai, R. Dreyfus, Tunable plasmonic microcapsules with embedded noble metal nanoparticles for optical microsensing, *ACS Appl. Nano Mater.* 5 (2022) 2828–2838.
- [5] D. Ayodhya, G. Veerabhadram, A review on recent advances in photodegradation of dyes using doped and heterojunction based semiconductor metal sulfide nanostructures for environmental protection, *Mater. Today Energy* 9 (2018) 83–113.
- [6] D. Ayodhya, Ag-SPR and semiconductor interface effect on a ternary $\text{CuO@Ag@Bi}_2\text{S}_3$ Z-scheme catalyst for enhanced removal of HIV drugs and (photo) catalytic activity, *New J. Chem.* 46 (2022) 15838–15850.
- [7] M. Zare-Bidaki, P. Mohammadparast-Tabas, Y. Peyghambari, E. Chamani, M. Siami-Aliabad, S. Mortazavi-Derazkola, Photochemical synthesis of metallic silver nanoparticles using Pistacia khinjuk leaves extract (PKL@ AgNPs) and their applications as an alternative catalytic, antioxidant, antibacterial, and anticancer agents, *Appl. Organomet. Chem.* 36 (2022).
- [8] S. Raj, H. Singh, R. Trivedi, V. Soni, Biogenic synthesis of AgNPs employing Terminalia arjuna leaf extract and its efficacy towards catalytic degradation of organic dyes, *Sci. Rep.* 10 (2020) 9616.
- [9] D. Ayodhya, Fabrication of SPR triggered Ag-cuO composite from Cu(II) -Schiff base complex for enhanced visible-light-driven degradation of single and binary-dyes and fluorometric detection of nitroaromatic compounds, *Inorg. Chem. Commun.* 148 (2023).
- [10] D. Ramachandiran, K. Rajesh, Highly detection of Zn (II) ion sensing and photocatalytic activities of biosynthesized AgNPs using Nilgiranthus ciliatus leaf extract and its properties, *Mater. Res. Bull.* 149 (2022).
- [11] L.H. Silva Martins, M. Rai, j.M. Neto, P.W. Gomes, j.H. Silva, Silver: biomedical applications and adverse effects, In *Biomedical applications of metals* (2018) 113–127. Springer
- [12] S. Kwon, W. Lee, J.W. Choi, N. Bumbudsanpharoke, S. Ko, A facile green fabrication and characterization of cellulose-silver nanoparticle composite sheets for an antimicrobial food packaging, *Front. Nutr.* 8 (2021).
- [13] D. Ayodhya, G. Veerabhadram, One-pot, aqueous synthesis of multifunctional biogenic Ag NPs for efficient 4-NP reduction, Hg^{2+} detection, bactericidal, and antioxidant activities, *Inorg. Nano-Metal Chem.* 51 (2021) 1831–1841.
- [14] S. Chatterjee, X.Y. Lou, F. Liang, Y.W. Yang, Surface-functionalized gold and silver nanoparticles for colorimetric and fluorescent sensing of metal ions and biomolecules, *Coord. Chem. Rev.* 459 (2022).
- [15] E.S. Aazam, W.A. El-Said, Synthesis of copper/nickel nanoparticles using newly synthesized Schiff-base metals complexes and their cytotoxicity/catalytic activities, *Bioorg. Chem.* 57 (2014) 5–12.
- [16] R. Yahya, R.F. Elshaarawy, Recycling Oryza sativa wastes into poly-imidazolium acetic acid-tagged nanocellulose Schiff base supported Pd nanoparticles for applications in cross-coupling reactions, *React. Funct. Polym.* 170 (2022).
- [17] D. Ayodhya, G. Veerabhadram, BSA mediated $\text{Ag@Bi}_2\text{S}_3$ composites: synthesis, characterization, photodegradation of mixed dyes via metal-semiconductor interface, antimicrobial and antioxidant activities, *Mater. Today Chem.* 17 (2020).
- [18] H. Abdolmohammad-Zadeh, Z. Azari, E. Pourbasheer, Fluorescence resonance energy transfer between carbon quantum dots and silver nanoparticles: application to mercuric ion sensing, *Spectrochim. Acta Part A: Mol. Biomol. Spectrosc.* 245 (2021).
- [19] K. Andiappan, A. Sanmugam, E. Deivanayagam, K. Karuppasamy, H.S. Kim, D. Vikraman, In vitro cytotoxicity activity of novel Schiff base ligand-lanthanide complexes, *Sci. Rep.* 8 (2018) 1–12.
- [20] R.A. Abdel-Monem, A.M. Khalil, O.M. Darwesh, A.I. Hashim, S.T. Rabie, Antibacterial properties of carboxymethyl chitosan Schiff-base nanocomposites loaded with silver nanoparticles, *J. Macromol. Sci. Part A 57* (2020) 145–155.
- [21] E.J. Lee, L. Piao, j.K. Kim, Synthesis of silver nanoparticles from the decomposition of silver(I) [bis (alkylthio) methylene] malonate complexes, *Bull. Kor. Chem. Soc.* 33 (2012) 60–64.
- [22] B. Janani, A. Ayed, A.M. Thomas, H.B. Ali, A.M. Elgorban, L.L. Raju, S.S. Khan, UV-vis spectroscopic method for the sensitive and selective detection of mercury by silver nanoparticles in presence of alanine, *Optik* 204 (2020).
- [23] A. Minhaz, N. Khan, N. Jamila, F. Javed, M. Imran, S. Shujah, S.N. Khan, A. Atlas, M.R. Shah, Schiff base stabilized silver nanoparticles as potential sensor for Hg (II) detection, and anticancer and antibacterial agent, *Arabian J. Chem.* 13 (2020) 8898–8908.
- [24] R.A. Abdel-Monem, A.M. Khalil, O.M. Darwesh, A.I. Hashim, S.T. Rabie, Antibacterial properties of carboxymethyl chitosan Schiff-base nanocomposites loaded with silver nanoparticles, *J. Macromol. Sci. Part A 57* (2020) 145–155.
- [25] S. Khorrami, A. Zarepour, A. Zarrabi, Green synthesis of silver nanoparticles at low temperature in a fast pace with unique DPPH radical scavenging and selective cytotoxicity against MCF-7 and BT-20 tumor cell lines, *Biotechnol. Rep.* 24 (2019).




 PRINCIPAL
 JMJ COLLEGE FOR WOMEN (Autonomous)
 TENALI





Short communication

Hydrothermal fabrication of n-CeO₂/p-CuS heterojunction nanocomposite for enhanced photodegradation of pharmaceutical drugs in wastewater under visible-light and fluorometric sensor for detection of uric acid

V. Sumalatha^a, Chilaka Anujya^a, V. Balchander^b, B. Dhanalaxmi^c, Marri Pradeep Kumar^d, Dasari Ayodhya^{e,*}

^a Department of Chemistry, JMJ College for Women, Tenali 522 201, Andhra Pradesh, India

^b Department of Pharmaceutical Engineering, BV Raju Institute of Technology, Narsapur 502 201, Telangana, India

^c University College of Technology, Osmania University, Hyderabad 500 007, Telangana, India

^d Department of Chemistry, Anurag University, Hyderabad 500 088, Telangana, India

^e Department of Chemistry, Osmania University, Hyderabad 500 007, Telangana, India

ARTICLE INFO

Keywords:

n-CeO₂/p-CuS heterojunction
Hydrothermal method
Drugs degradation
Uric acid detection
Wastewater treatment

ABSTRACT

In the present work, n-CeO₂/p-CuS heterostructures have been fabricated by decorating CuS particles on the surface of cerium oxide (CeO₂) nanorods using a hydrothermal method. The optical, structural, and morphological features of CeO₂, copper sulfide (CuS), and n-CeO₂/p-CuS heterostructures were thoroughly characterized using UV–vis, PL, XRD, SEM, and TEM. The UV–vis DRS analysis showed that the n-CeO₂/p-CuS heterojunction exhibited enhanced absorption in the visible region with a band gap of 2.55 eV. XRD and TEM studies revealed that different shaped CuS (12 ± 5 nm) were deposited on the CeO₂ nanorods. The photocatalytic activities of CeO₂, CuS, and n-CeO₂/p-CuS heterostructures were investigated for the degradation of drugs (tetracycline (TC), ciprofloxacin (CF), and capecitabine (CT)) under visible light irradiation. The n-CeO₂/p-CuS heterostructure exhibited the best photocatalytic efficiency for the degradation of these drugs compared to the CeO₂ and CuS NPs, within 25 min of irradiation, due to the interfacial charge transfer effect among the CuS and CeO₂. The better and enhanced photocatalytic efficiency of the n-CeO₂/p-CuS heterostructure was attributed to its high charge separation efficiency, and it remained stable up to 5 cycles without a significant loss of its activity. The empirical data was effectively fitted using the first-order kinetics based on Langmuir–Hinshelwood (L–H) model. Photogenerated e⁻, O₂⁻, and h⁺ were found to be the main active species generated by n-CeO₂/p-CuS to realize simultaneous redox reactions for the effective degradation of drugs. In fluorescence quenching of the uric acid (UA), n-CeO₂/p-CuS showed a concentration range of 10–100 μM and an LOD of 1.214 μM. Additionally, the proposed sensor was successfully used for the detection of UA in human urine samples.

1. Introduction

Antibiotics and uric acid (UA) are biologically active compounds with high hydrophilicity and stability, which allows them to persist in the food chain and water systems, posing severe adverse health consequences for humans [1]. Although antibiotics have undoubtedly helped humans to treat bacterial infections, their large-scale usage has become a serious threat to the ecosystem and human health [1,2]. Second-generation quinolones, such as TC, CF, and CT, are extensively used pharmaceutical drugs due to their good chemical stability and strong inhibition of bacterial growth [3]. However, recent research has

confirmed that drugs are emerging genotoxic contaminants that can harm the ecosystem and human immune system through their acute and chronic toxicities [4]. Therefore, effective removal of these drugs from aqueous environments has become a critical issue [1,5]. Advanced oxidation processes (AOPs), particularly photocatalysis, have been developed as treatment technologies to degrade organic pollutants [6]. Additionally, detecting various analytes with trace amount of concentration in biological fluids is significantly important for early-stage warning of related conditions and for diagnosing patients [7]. Several methods, including high-performance liquid chromatography, mass fragmentography, electrochemical techniques, chemi-luminescence,

* Corresponding author.

E-mail address: ayodhyadasari@gmail.com (D. Ayodhya).

<https://doi.org/10.1016/j.inoche.2023.110962>

Received 31 March 2023; Received in revised form 18 May 2023; Accepted 20 June 2023

Available online 25 June 2023

1387-7003/© 2023 Elsevier B.V. All rights reserved.



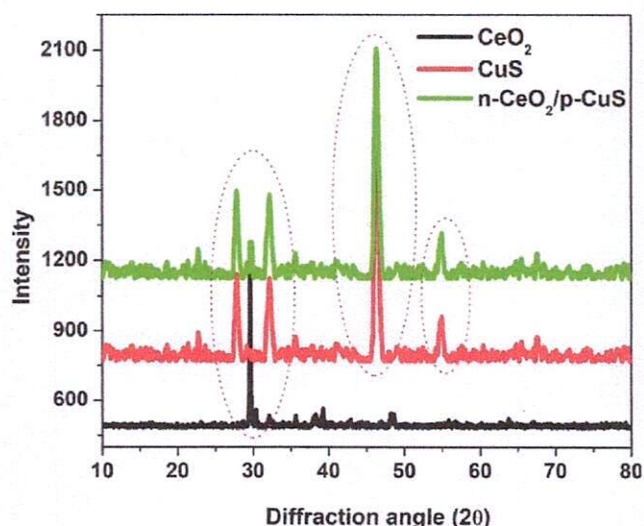


Fig. 1. XRD patterns of the synthesized CeO_2 , CuS , and $n\text{-CeO}_2/p\text{-CuS}$ heterostructures.

and fluorescence methods, have been developed for UA detection [7]. Among these methods, fluorescence sensing is fast, simple, and non-destructive.

The effectiveness of photodegradation of pollutants heavily relies on the quality of the photocatalyst used, making it a critical component in nanotechnology [6]. Therefore, the development of an efficient, stable, and affordable photocatalyst is essential for practical application [8]. Metal oxides or sulfides such as TiO_2 , ZnO , CuO , AgVO_3 , CeO_2 , Ag_3PO_4 , $\text{AgI/Bi}_2\text{O}_3$, Bi_2S_3 , Bi_2MoO_6 , CdS , Cu_2O , and ZnWO_4 are commonly used as photocatalysts [1,2,5–9]. CeO_2 , a rare earth element, has drawn significant attention as a promising n-type photocatalyst due to its unique electronic configuration, catalytic activity, and structural and electronic properties. Its band gap ranges between 2.9 and 3.2 eV, and it exhibits a longer lifetime of photo-generated electron-hole pairs [10]. Moreover, CeO_2 NPs can be easily modified and reconstructed to improve their physicochemical properties, leading to enhanced catalytic activity and stability [10]. The manipulation of CeO_2 NPs surface is a viable strategy to improve their surface characteristics and catalytic performance [10,11].

In recent years, CeO_2 -based materials have emerged as one of the most promising photocatalytic materials due to their narrow band gap (~2.8 eV), excellent reactivity, and stable structure [10–12]. However, the high recombination rate of photogenerated electron-hole pairs has hindered the potential application of CeO_2 in environmental purification [13]. To overcome this limitation, various strategies have been attempted to enhance the visible-light photocatalytic activity of CeO_2 ,

such as combining it with other materials like $\text{SnO}_2/\text{CeO}_2$, $\text{CeO}_2/\text{Cu}_2\text{O}$, CeO_2/CuO , $\text{TiO}_2/\text{CeO}_2$, CeO_2/CdS , $\text{CeO}_2/\text{Bi}_2\text{WO}_6$, $\text{CeO}_2/\text{Y}_2\text{O}_3$, $\text{CeO}_2/\text{BiVO}_4$, $\text{CeO}_2/\text{Fe}_2\text{O}_3$, and BiOBr/CeO_2 , etc [13–18]. Among these strategies, the construction of heterojunctions between CeO_2 and other functional materials has been identified as a promising approach to enhance visible-light photocatalytic activity. CuS , one of the narrow band gap Cu-based semiconductors, has been recently utilized for this purpose due to its non-toxicity, low cost, and easy accessibility [19,20]. It is frequently combined with other photocatalysts to extend the visible-light response capability [19].

While some research has explored the use of CeO_2 combined with metal sulfides for supercapacitor applications, there are currently no articles addressing the photocatalytic degradation of pharmaceutical drugs under visible light irradiation [21,22]. Based on the previous reports, we have fabricated and investigated the photocatalytic activity of CeO_2 , CuS , and $n\text{-CeO}_2/p\text{-CuS}$ heterostructures, which were synthesized through a hydrothermal method. The materials were characterized using various techniques to analyze their optical, structural, and morphological properties. Our findings suggest that the $n\text{-CeO}_2/p\text{-CuS}$ heterostructure demonstrated superior catalytic performance in the degradation of TC, CF, and CT drugs due to its ability to facilitate electron transfer processes. Additionally, the photocatalytic kinetics of the degradation of TC, CF, and CT drugs were analyzed using the Langmuir-Hinshelwood kinetics model. Furthermore, we developed a fluorescence sensor with excellent selectivity, a wide linear detection range, and a low detection limit for UA detection. We successfully applied this sensor to detect UA in human urine samples with satisfactory results.

2. Experimental

2.1. Materials

Copper acetate, cerium nitrate, sodium sulfide, sodium hydroxide and ethanol were purchased from Sigma Aldrich chemicals, India. The pharmaceutical drugs including TC, CF, and CT were purchased from Merck chemicals, India. Phosphate buffered solutions ($\text{NaH}_2\text{PO}_4\text{-Na}_2\text{HPO}_4$), ascorbic acid, uric acid, hippuric acid, picric acid, and salicylic acid were purchased from S D Fine chemicals, India. All the reagents were of analytical grade (99.0%) and used without purification. All aqueous solutions were prepared using double distilled water.

2.2. Synthesis of CeO_2 NPs

CeO_2 NPs were synthesized using cerium nitrate hexahydrate ($\text{Ce}(\text{NO}_3)_3 \cdot 6\text{H}_2\text{O}$) and NaOH in a 1:2 ratio. The procedure involved mixing a 1.0 M solution of $\text{Ce}(\text{NO}_3)_3 \cdot 6\text{H}_2\text{O}$ (4.85 g) with 45 mL of double distilled water while slowly adding a 0.5 M solution of NaOH (1 g) drop wise. The resulting mixture was stirred and agitated while continuously adding a

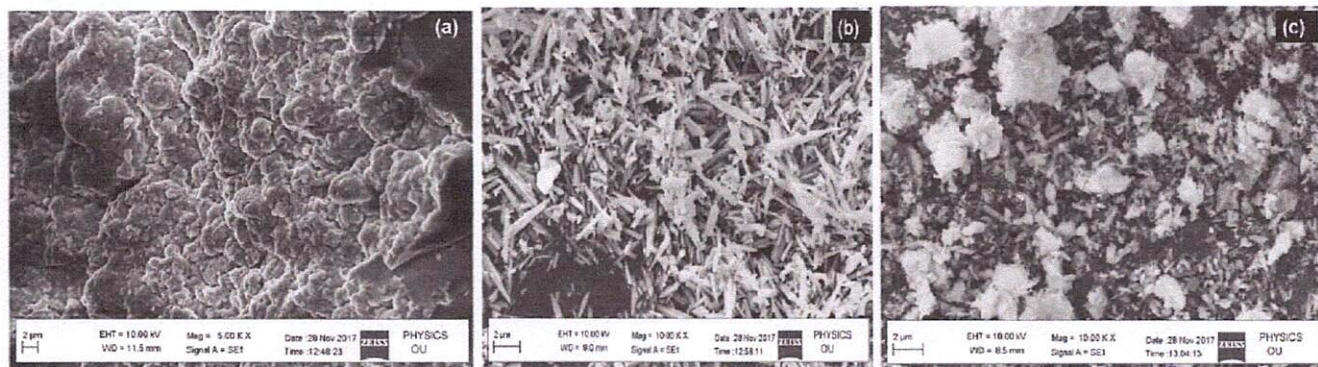


Fig. 2. SEM images of the synthesized (a) CuS , (b) CeO_2 , and (c) $n\text{-CeO}_2/p\text{-CuS}$ heterostructures.



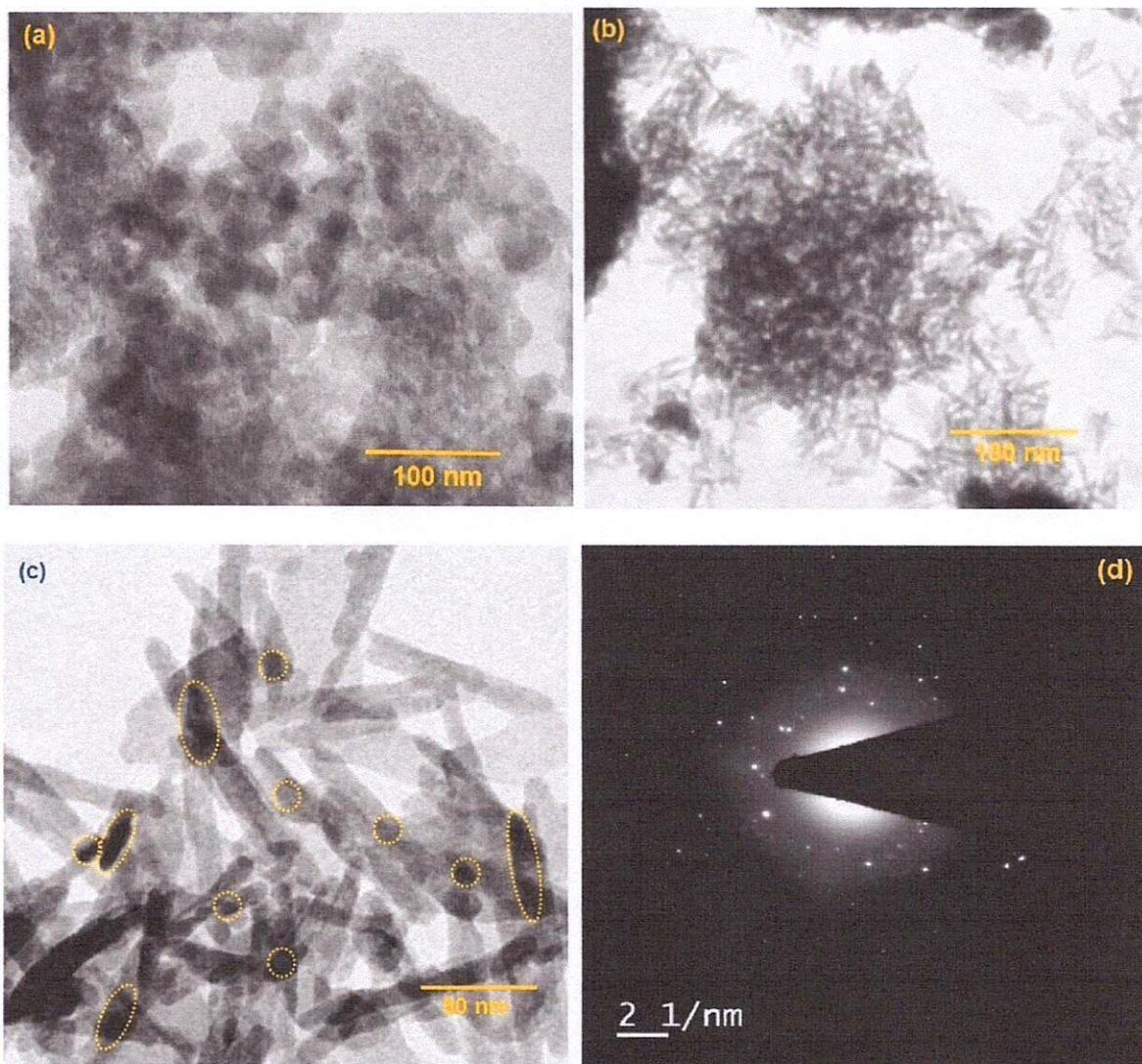


Fig. 3. (a–c) TEM images of the synthesized CeO_2 , CuS , and $\text{n-CeO}_2/\text{p-CuS}$ heterostructures and (d) SAED image of $\text{n-CeO}_2/\text{p-CuS}$ heterostructure.

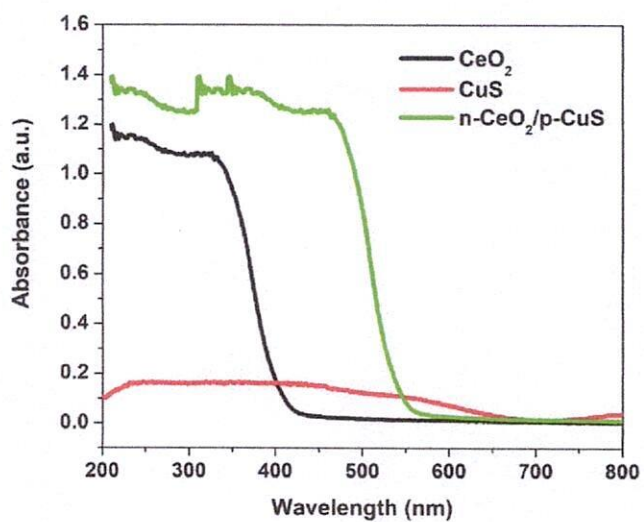


Fig. 4. UV-vis DRS of the synthesized CeO_2 , CuS , and $\text{n-CeO}_2/\text{p-CuS}$ heterostructures.

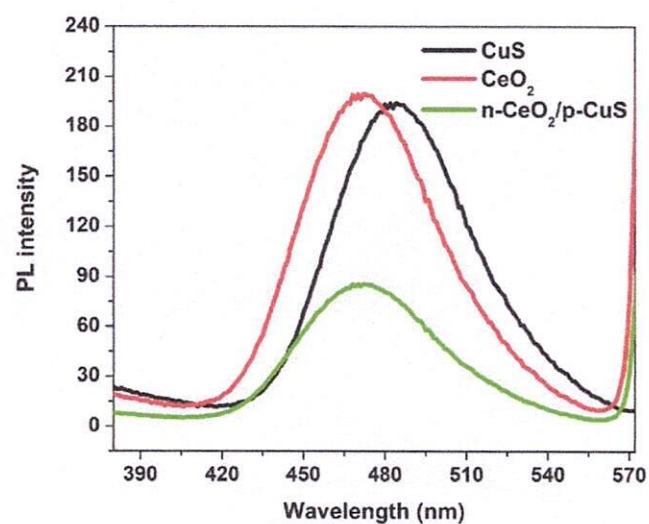
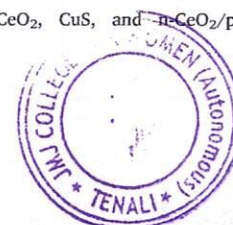


Fig. 5. PL spectra of the synthesized CeO_2 , CuS , and $\text{n-CeO}_2/\text{p-CuS}$ heterostructures.



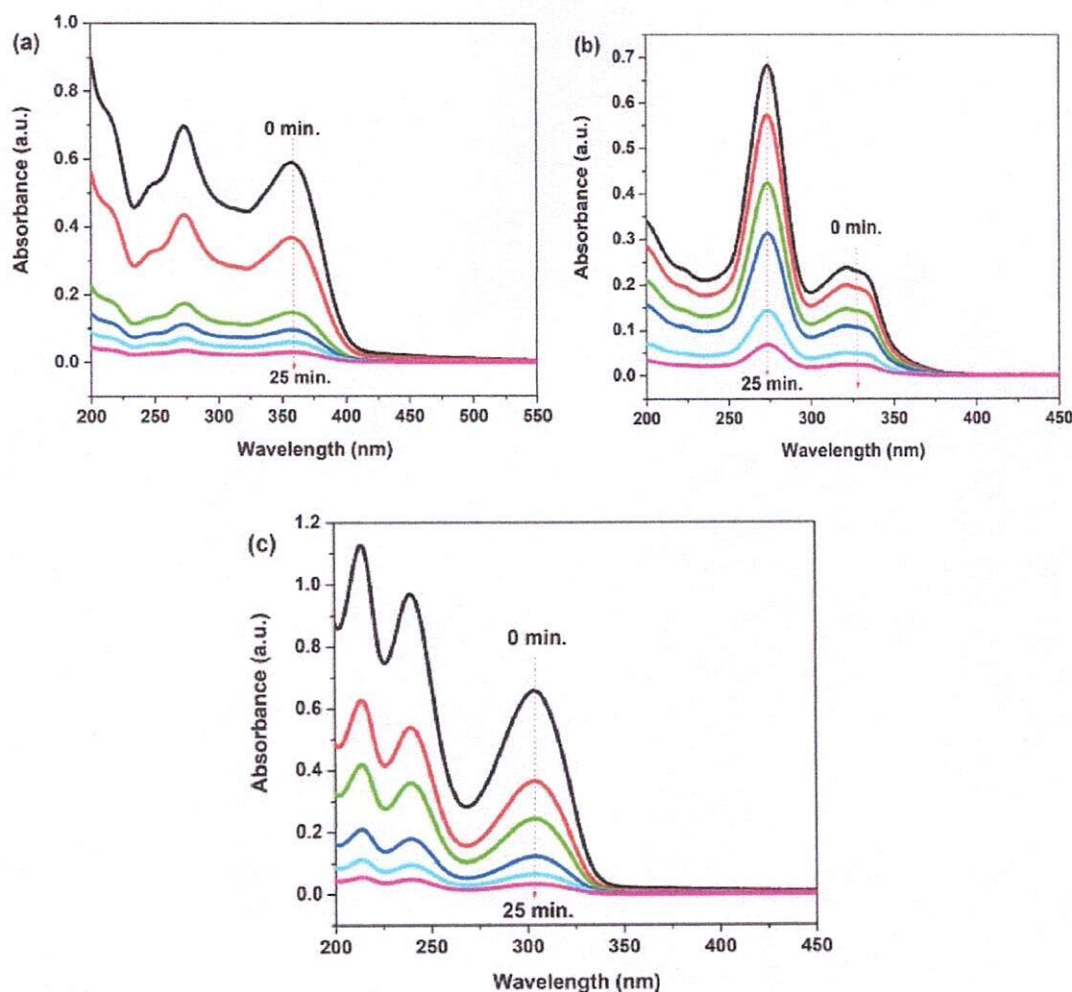


Fig. 6. UV-vis absorption spectra of the photocatalytic degradation of (a) TC, (b) CF, and (c) CT drugs using $n\text{-CeO}_2/p\text{-CuS}$ heterostructures.

0.5 M NaOH (1 g) drop wise. The reaction mixture was then transferred to a Teflon-coated autoclave and heated for 1 h at 120 °C and 15 lbs pressure. The remaining excess NaOH was eliminated by filtering the precipitate using Whatman filter paper and washing it with distilled water and ethanol. The resulting precipitate was dried for 1 h at 100 °C in a hot air oven before being calcined for 2 h at 650 °C to obtain a fine pinkish powder of CeO_2 NPs.

2.3. Synthesis of CuS NPs

According to our previous work [23], CuS NPs were prepared by mixing 25 mL of a 0.1 M aqueous solution of copper acetate dihydrate with 25 mL of a 0.1 M aqueous solution of sodium sulfide. The resulting mixture was placed in a Teflon-coated autoclave and heated for 1 h at 120 °C and 15 lbs pressure. The black solid of CuS products was separated from the solution by repetitive centrifugations, washed with distilled water, dried at 70 °C for 12 h, and finally calcined at 500 °C for 2 h to obtain blackish powder of CuS NPs.

2.4. Synthesis of $n\text{-CeO}_2/p\text{-CuS}$ heterostructures

In the synthesis process of $n\text{-CeO}_2/p\text{-CuS}$ heterostructures through hydrothermal method, 0.068 g of CuS nanoparticles (0.4 mmol) were dispersed in an aqueous solution by sonicating for 10 min after dissolving 0.015 g (0.2 mmol) NaOH and 0.048 g (0.2 mmol) $\text{Ce}(\text{NO}_3)_3 \cdot 6\text{H}_2\text{O}$ in 60 mL of deionized water. The resulting mixture was

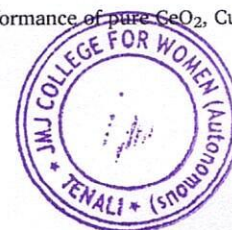
transferred into a Teflon-lined stainless steel autoclave with a capacity of 100 mL, sealed and heated at 150 °C for 12 h in a furnace. The green product was then collected, washed multiple times with deionized water, and finally dried at 70 °C for 4 h in an oven.

2.5. Characterizations

The scanning electron microscopy (SEM, Instrument Zeiss EVO18) was employed to observe the surface morphology of the hetero-junction composite. The crystal nanostructure of $n\text{-CeO}_2/p\text{-CuS}$ heterostructures was analyzed by X-ray diffraction (XRD, X'pert Pro), with $\text{CuK}\alpha$ radiation ($\lambda = 1.540598 \text{ \AA}$) in the 2θ range (10–80°) with a step scan of 0.02°, operating at 45 kV and 40 mA. The UV-3600 PC Shimadzu spectrophotometer was used to investigate the optical properties of the composites. The diffuse reflectance spectra of the samples were measured in the wavelength range of 200–800 nm using a UV-vis spectrophotometer equipped with an integrating sphere accessory, with BaSO_4 as a reference. The fluorescence spectra were recorded on a Shimadzu RF-5301PC spectrofluorometer with an excitation at 325 nm. Transmission electron microscopy (TEM) was carried out using a Tecnai G2 transmission electron microscope operated at an accelerating voltage of 200 kV to further observe the composite's structure.

2.6. Photocatalytic activities

To estimate the photocatalytic performance of pure CeO_2 , CuS, and



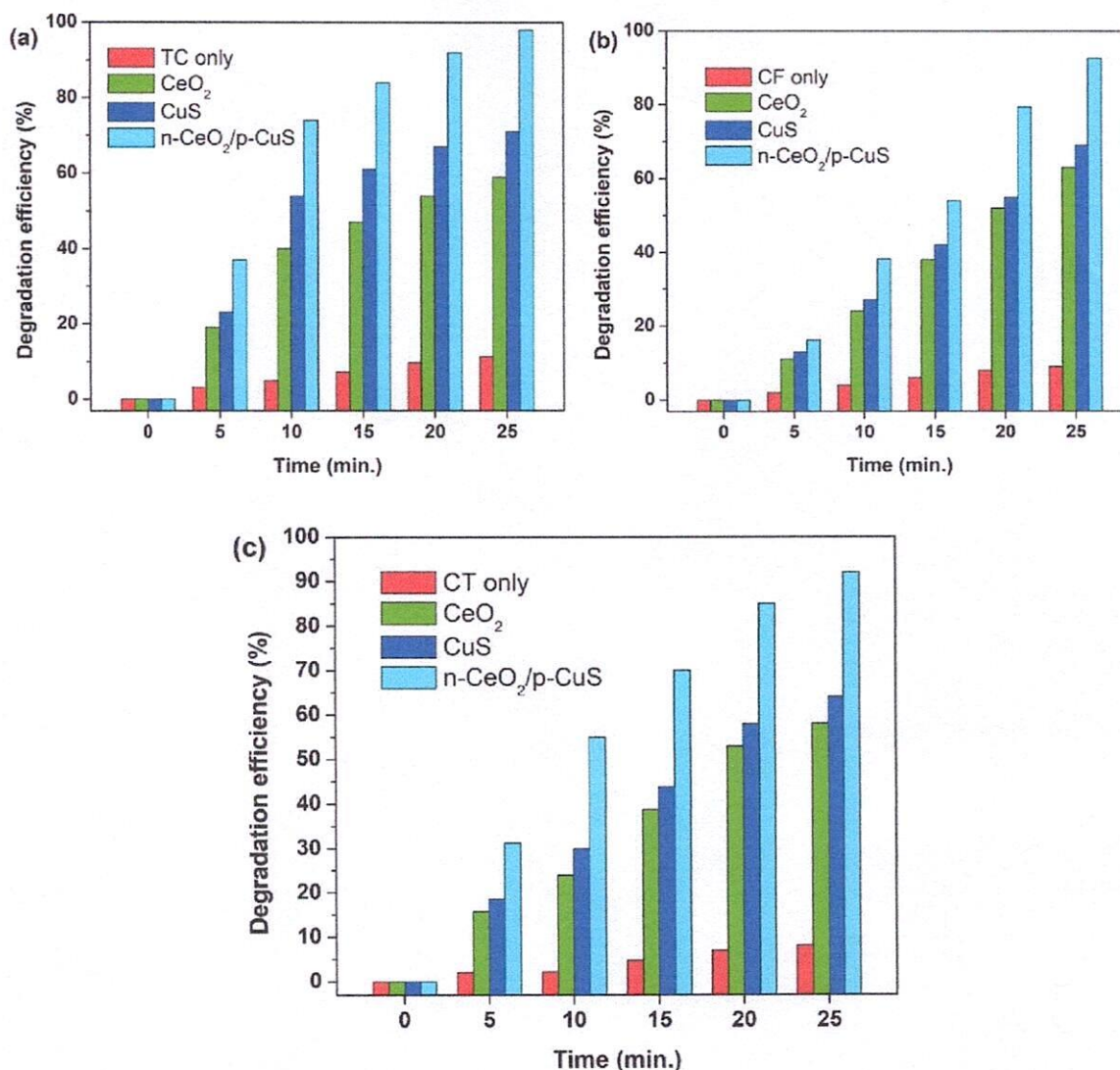


Fig. 7. The bar diagrams of the photocatalytic degradation of (a) TC, (b) CF, and (c) CT drugs using CeO₂, CuS, and n-CeO₂/p-CuS heterostructures.

n-CeO₂/p-CuS heterostructures, the degradation of pharmaceutical pollutants including TC, CF, and CT was carried out. A photocatalytic reactor was utilized to stir 5.8×10^{-5} M of 100 mL drug solution with 0.018 g photocatalyst for 30 min in the dark, followed by irradiation with halogen lamps (Philips, 54 W, $145 \mu\text{W}/\text{cm}^2$). At specific intervals of 5 min, the suspension was withdrawn and centrifuged to separate the solid catalyst. The remaining concentrations of dye solution were measured from the supernatant using a UV-visible spectrometer at the absorption peak of 357 nm and 275 nm for TC, 278 nm for CF, and 305 nm and 241 nm for CT. The degradation efficiency (%) of the drugs at different times was calculated using the following equation [24]:

$$\text{Degradation efficiency (\%)} = \frac{C_0 - C_t}{C_0} \times 100.$$

where C_0 and C_t are initial concentration and remaining concentration of drugs, respectively. The pseudo-first-order kinetics is widely studied and used as a model equation to compare the photocatalytic activity of each photocatalyst, using the following equation [24]:

$$\ln(C_t/C_0) = -kt.$$

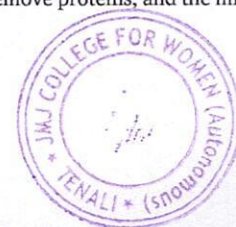
The slope of a linear function gives the value of the apparent rate constant (k , min^{-1}).

2.7. Fluorometric detection of uric acid

In order to assess the selectivity of n-CeO₂/p-CuS heterostructures towards UA over other acids, various acids were utilized, including ascorbic acid (AA), hippuric acid (HA), picric acid (PA), and salicylic acid (SA). The standard solutions of acids were prepared by accurately dissolving specific quantities of the acids in an appropriate volume of 100 mM sodium hydroxide solution, which were then stored in the dark at 4 °C. Additional dilute solutions were prepared each day by accurately diluting just before use. Then, an appropriate volume of the amino acid solution was mixed with n-CeO₂/p-CuS for spectral measurements. Specifically, different concentrations of UA were mixed thoroughly with 100 μL of 10 μM (pH = 7.4) PBS solution and 400 μL n-CeO₂/p-CuS heterostructure (15 nM) at room temperature. The UV-vis spectra of the n-CeO₂/p-CuS heterostructure solution were observed after 5 min. The concentration of UA was quantified via quenching measurement analysis. All experiments were conducted at room temperature.

2.8. Preparation of real samples

A healthy adult male volunteer provided a 1.0 mL urine sample which was subsequently analyzed. The urine sample was mixed with 1.0 mL acetonitrile in a centrifuge tube to remove proteins, and the mixture



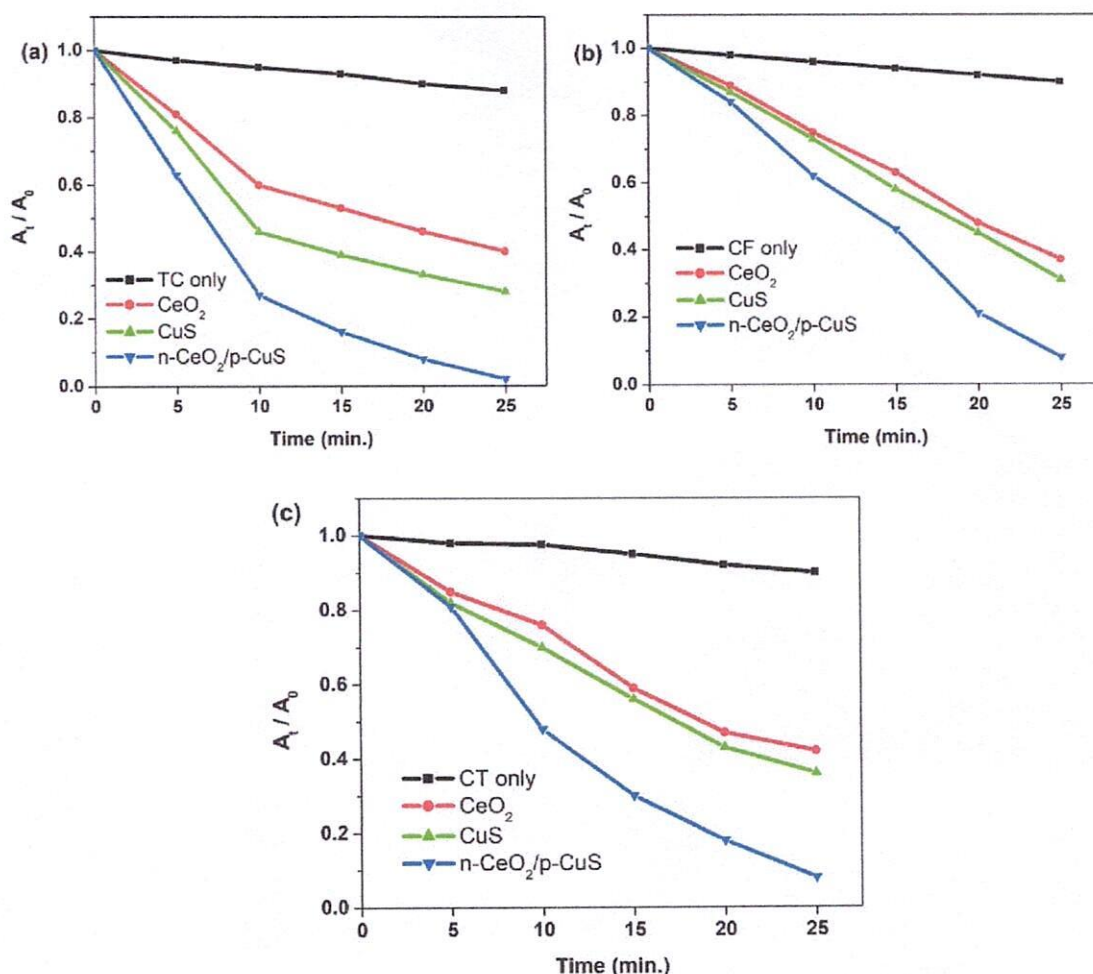


Fig. 8. The plots of A_t/A_0 vs time for the photocatalytic degradation of (a) TC, (b) CF, and (c) CT drugs using CeO_2 , CuS, and n- $CeO_2/p-CuS$ heterostructures.

was then centrifuged at 12,000 rpm for 10 min. The resulting supernatant was filtered through a 0.22 μm filter and dried under vacuum at 50 $^{\circ}C$ for 10 h. Finally, it was diluted to 5 mL with double distilled water before analysis. The diluted human urine sample was then combined with n- $CeO_2/p-CuS$ heterostructure to measure the fluorescence spectrum with an excitation wavelength of 310 nm.

3. Results & discussion

3.1. Structural analysis

The XRD technique was used to analyze the crystalline structures of the prepared materials, including CeO_2 , CuS, and n- $CeO_2/p-CuS$ heterostructures, as depicted in Fig. 1. The diffraction peaks at the 2θ position of 28.45 $^{\circ}$, 33.68 $^{\circ}$, 48.41 $^{\circ}$, 57.85 $^{\circ}$, 59.11 $^{\circ}$, and 69.31 $^{\circ}$ in the XRD pattern of CeO_2 correspond to (111), (200), (220), (311), (222), and (400) crystallographic planes, respectively, and are well matched to JCPDS card no 96-900-9009 [25]. The XRD pattern of CuS NPs shows crystal planes of (100), (102), (103), (006), (110), and (108), indicating the covellite phase with a hexagonal crystal structure. The XRD pattern of n- $CeO_2/p-CuS$ heterostructure demonstrates that it has a cubic phase in good agreement with reference code (JCPDS PDF No 96-900-0524) and is ascribed to the hexagonal phase. The Debye-Scherrer formula was used to estimate the average crystal size of the n- $CeO_2/p-CuS$ heterostructure, which is in the range of 10 ± 3 nm and exhibits a fine crystalline nature.

3.2. Morphological analysis

SEM was used to investigate the morphology and microstructure of the samples, and the resulting images of CeO_2 , CuS, and n- $CeO_2/p-CuS$ heterostructures are displayed in Fig. 2(a-c), respectively. CeO_2 appears as nanorods (Fig. 2b), while CuS particles are spherical in shape (Fig. 2(a)). In the SEM image of the n- $CeO_2/p-CuS$ heterostructure, both spherical particles are observed to be deposited on the surface of the nanorods (Fig. 2(c)), confirming the presence of both CeO_2 and CuS in the n- $CeO_2/p-CuS$ heterostructure material.

To further investigate the morphologies of the synthesized nanomaterials, TEM-SAED analysis was performed. High magnification TEM images of CeO_2 , CuS, and n- $CeO_2/p-CuS$ heterostructure are shown in Fig. 3(a-d). The nanorod-shaped CeO_2 (with a length of approximately 100 nm) and spherical CuS nanoparticles (with a size of about 12 ± 5 nm) are clearly visible in Fig. 3(a-b). The TEM image of the n- $CeO_2/p-CuS$ heterostructure reveals that different shaped CuS particles are uniformly deposited on the surfaces of CeO_2 nanorods, as shown in Fig. 3(c). Fig. 3(d) shows a SAED pattern which indicates that both CuS and CeO_2 particles are polycrystalline, as the reflection spots are on concentric rings. These images clearly exhibit the resolved lattice fringes, which indicate the high crystallinity of the synthesized nanomaterials.

3.3. Optical analysis

The optical properties of the fabricated photocatalysts were



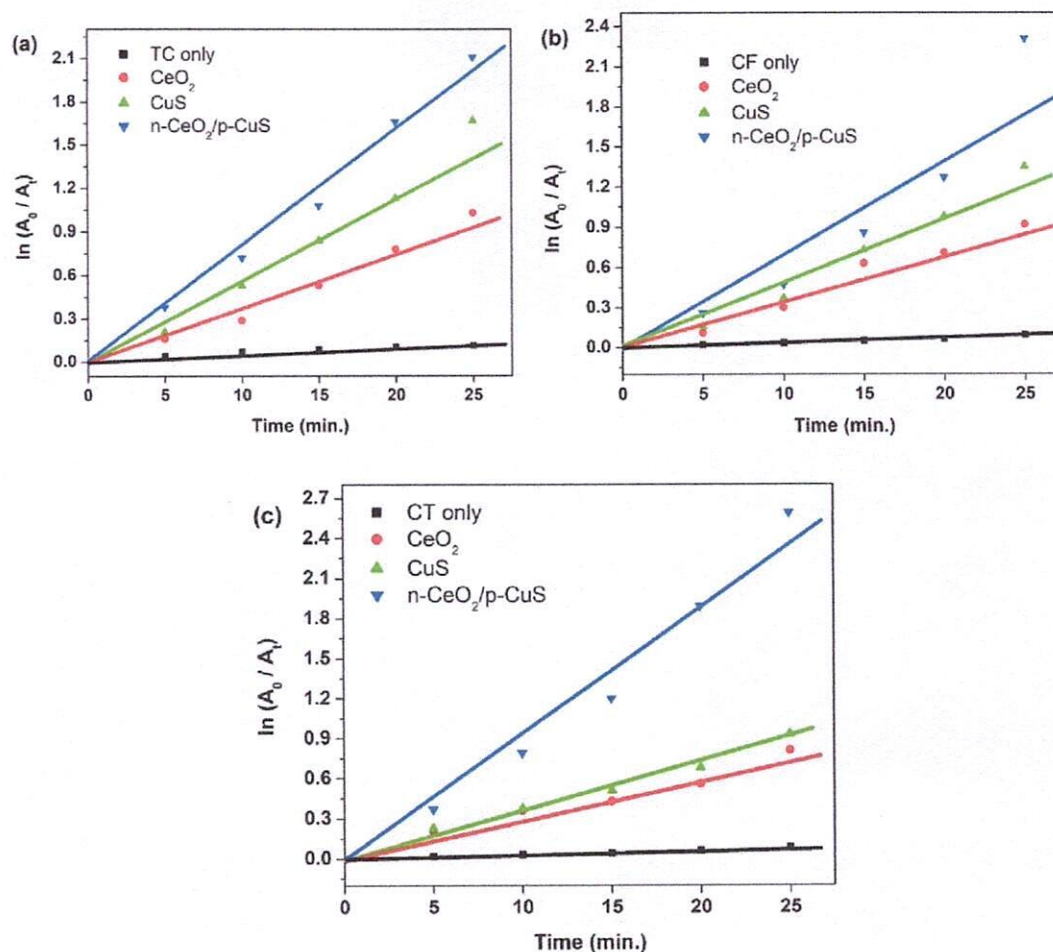


Fig. 9. Kinetic plots for the photocatalytic degradation of (a) TC, (b) CF, and (c) CT drugs using n-CeO₂/p-CuS heterostructures.

Table 1

The photocatalytic degradation parameters of TC, CF, and CT drugs using CeO₂, CuS, and n-CeO₂/p-CuS heterostructures.

S. No.	Catalyst	Dye	Degradation efficiency (%)	Rate constant (min ⁻¹)	Half-life time (min)	R ²
1	No catalyst	TC	11.2	0.0125	55.44	0.99
2	No catalyst	CF	9.1	0.0112	61.87	0.97
3	No catalyst	CT	8.5	0.0105	66.02	0.98
4	CeO ₂	TC	59.1	0.1892	3.66	0.98
5	CuS	TC	71.3	0.3125	2.21	0.99
6	n-CeO ₂ /p-CuS	TC	98.3	0.5214	1.34	0.98
7	CeO ₂	CF	63.6	0.2151	3.22	0.97
8	CuS	CF	69.2	0.3028	2.28	0.99
9	n-CeO ₂ /p-CuS	CF	93.1	0.4925	1.41	0.98
10	CeO ₂	CT	58.2	0.1763	3.93	0.98
11	CuS	CT	74.5	0.3269	2.21	0.97
12	n-CeO ₂ /p-CuS	CT	92.6	0.4893	1.42	0.99

validated using diffuse reflectance spectroscopy analysis. Fig. 4 illustrates the UV-Vis DRS spectra of CeO₂, CuS, and n-CeO₂/p-CuS heterostructures in the range of 250–750 nm. It is evident that unmodified CeO₂ exhibits an absorption edge in the UV region at 415 nm, which is

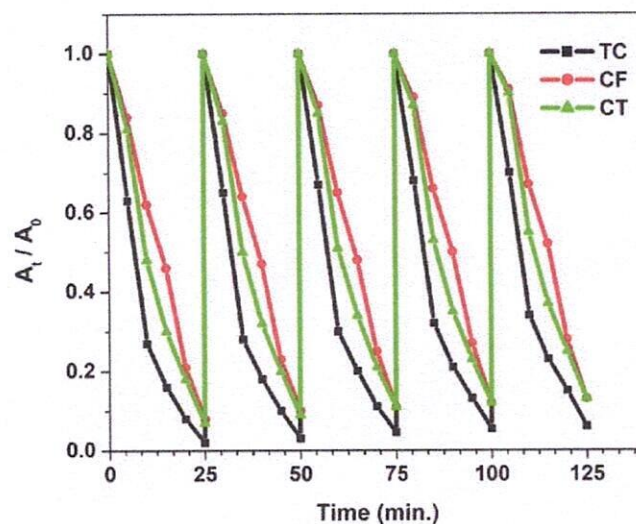


Fig. 10. Stability and recyclability for the photocatalytic degradation of TC, CF, and CT drugs using n-CeO₂/p-CuS heterostructures.

related to electron excitation from the valence band (VB) to the conduction band (CB) across the band gap of 2.98 eV [25]. On the other hand, the absorption spectrum of CuS shows an absorption edge corresponding to a band gap of 1.16–2.24 eV (1.84 eV) [23]. The n-CeO₂/p-

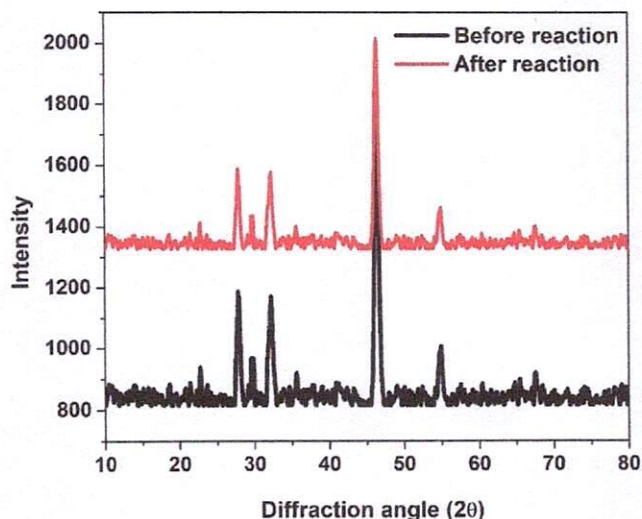


Fig. 11. The powder XRD pattern of the reused n-CeO₂/p-CuS heterostructure as a catalyst (before the reaction and after reaction i.e., 5th cycle).

CuS composite photocatalysts exhibit a shift towards the visible region, and its bandgap is approximately 2.54 eV, which is good agreement with previous report [26]. This indicates that the absorption edge of n-CeO₂/p-CuS composite provides better visible light-harvesting ability than CeO₂, which is expected to enhance the photocatalytic activity under visible light.

Photoluminescence (PL) analysis of CeO₂, CuS, and n-CeO₂/p-CuS heterostructures as presented in Fig. 5. It is crucial in determining the ability of n-CeO₂/p-CuS composites to separate electron/hole pairs and trap charge carriers. PL spectra of CeO₂ exhibit two strong PL bands between 400 and 500 nm, which are attributed to the O2p → Ce4f transition in CeO₂, indicating fast recombination of charge carriers [27]. CuS, on the other hand, shows a moderate signal at 461 nm, indicating low recombination of charge carriers. In the case of n-CeO₂/p-CuS heterostructure, the PL spectrum showed a minimal intense PL signal due to emission quenching [27]. The configuration of CuS on CeO₂ intensively retarded the recombination of charge carriers, which causes higher activity than individual CuS and CeO₂ materials. Therefore, the quenching

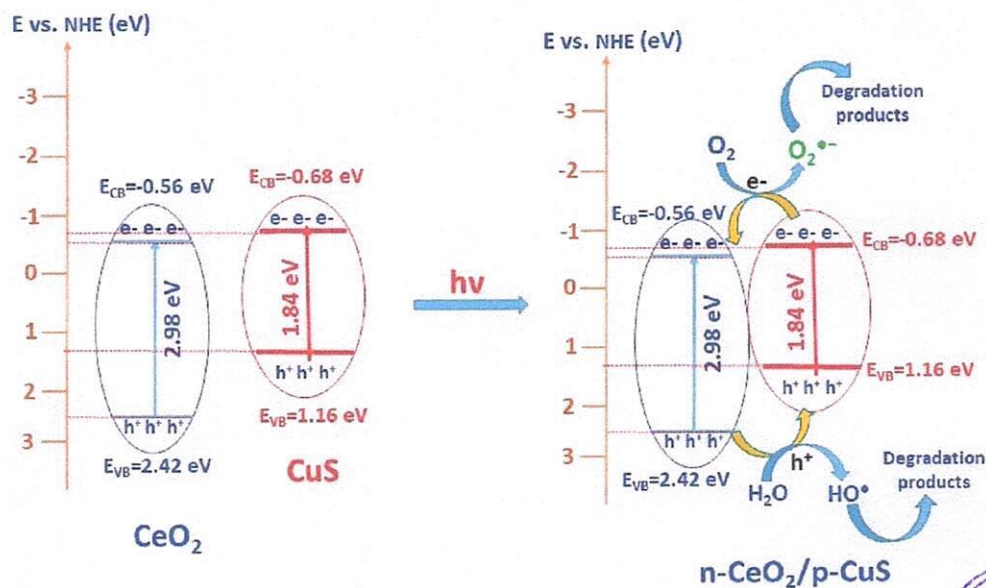
of emission in n-CeO₂/p-CuS heterostructure material confirms the presence of CuS on CeO₂ and its ability to efficiently trap the charge carriers, leading to higher photocatalytic activity than individual CuS and CeO₂ materials.

3.4. Photocatalytic activity

The photocatalytic performance and recycling stability of the synthesized CeO₂, CuS, and n-CeO₂/p-CuS heterostructures were evaluated for the degradation of pharmaceutical drugs (TC, CF, and CT). First, CeO₂ and CuS NPs showed a similar and weak adsorption capacity. Under visible light irradiation, only a small amount (11.2%, 9.1%, and 8.5%) of TC, CF, and CT drugs were degraded in the absence of photocatalyst, respectively. Nevertheless, the n-CeO₂/p-CuS heterostructures could remove efficiently (98.3%, 93.1%, and 92.6%) than the CeO₂ NPs (59.1%, 63.6%, and 58.2%) and CuS NPs (71.3%, 69.2%, and 74.5%) with in 25 min of irradiation, respectively (Fig. 6(a-c)). These results indicated that the n-CeO₂/p-CuS heterostructure have an enormous degrading efficiency under visible light as shown in Fig. 7(a-c) and Fig. 8(a-c). The enhanced photocatalytic activity of the n-CeO₂/p-CuS composite materials observed in this work might be the results from the hindrance of the electron-hole recombination process due to the separation of photogenerated charge carriers between CeO₂ and CuS hetero-junction and the enhancement of light absorption ability of n-CeO₂/p-CuS composite in the visible region.

The degradation efficiency of n-CeO₂/p-CuS heterostructures was studied using the pseudo-first order rate reaction [28]. The degradation rate constant of the n-CeO₂/p-CuS heterostructure was found to be several times higher than that of individual CuS and CeO₂ NPs, reaching maximum under visible light as shown in Fig. 9(a-c) and Table 1. The results suggest that coupling CeO₂ can effectively enhance the photocatalytic activity of CuS under visible light in the n-CeO₂/p-CuS heterostructures. In addition, the formation of n-CeO₂/p-CuS heterostructures allows for efficient transfer of photogenerated e⁻ in the CB from CeO₂ to CuS and parts of h⁺ in the VB in the opposite direction, which is beneficial for separating photogenerated electron holes and enhancing photocatalytic activity.

The recycling ability of n-CeO₂/p-CuS heterostructures was evaluated for the degradation of TC, CF, and CT drugs under visible light irradiation as shown in Fig. 10. The results indicate that the n-CeO₂/p-CuS heterostructures have prominent photocatalytic stability, as the



Scheme 1. Proposed schematic mechanism insight of n-CeO₂/p-CuS heterostructures for the photodegradation of drugs under visible light radiation.

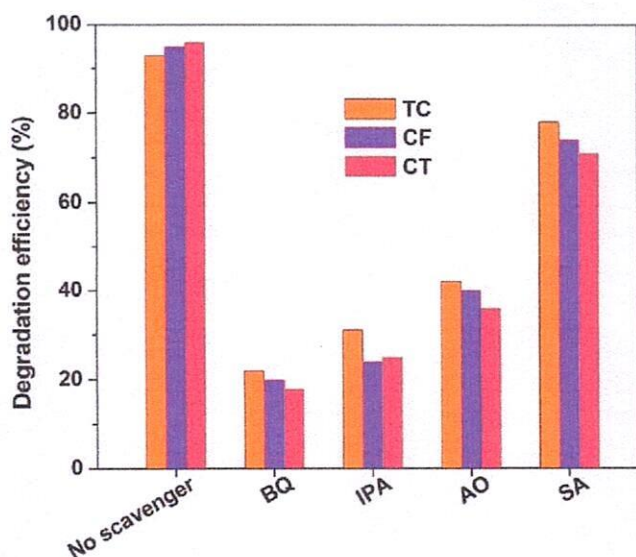


Fig. 12. Effects of different scavengers on the degradation of TC, CF, and CT drugs in the presence of n-CeO₂/p-CuS heterostructure.

complete degradation of all drugs remained unchanged even after 5 cycles. The characterization analysis of n-CeO₂/p-CuS photocatalyst after stability tests were evaluated by carrying out recycling reactions five times for the photodegradation of drugs and results are shown in Fig. 11. No decrease in catalytic activity was observed in the recycling reactions and the XRD patterns of the n-CeO₂/p-CuS composite photocatalyst also showed no change before and after photoreaction. These evidences indicate that the n-CeO₂/p-CuS photocatalysis system has good stability.

3.5. Photocatalytic degradation mechanism

A possible mechanism for the photocatalytic degradation of drugs over the prepared n-CeO₂/p-CuS heterostructures under visible light is shown in Scheme 1. As shown in Scheme 1, the CeO₂ has a lower valence band edge than CuS and as well as it has a higher conduction band edge than CuS. Also, the Fermi level of CeO₂ is located in a much higher position than CuS owing to CeO₂ is an n-type semiconductor, while CuS is a p-type semiconductor. These semiconductors form a p-n heterojunction and the electron transfer occurs from CeO₂ to CuS. By developing internal electric field, the flow of charge carriers generates a depletion layer among CuS (positively charged region) and CeO₂ (negatively charged region) under visible light [26]. The charge separation of the n-CeO₂/p-CuS composite would be increased owing to the internal electric field and band gap alignment. The carriers transfer take place among CeO₂ and CuS owing to their carriers gradient. The electrons are excited from the VB to CB of CuS, leaving behind holes in the VB. The photo-generated electrons in the CB of CuS (-0.68 eV) were rapidly transferred to the CB of CeO₂ (-0.56 eV). The electrons reacted with oxygen (O₂) to produce superoxide radicals ([•]O₂). The electron reduction process of O₂ ($E = (O_2/H_2O_2) = 0.695 \text{ V/NHE}$) lead to form H₂O₂ which could be combined with an electron to form [•]OH [29]. Also, holes in the VB of CeO₂ (+2.42 eV) were rapidly transferred to the VB of CuS (+1.16 eV) and reacted with either water (H₂O) or hydroxyl ions (OH⁻) adsorbed onto the photocatalyst surface to form hydroxyl radicals. All radicals degrade the drug to produce CO₂ and H₂O as harmless substances [30,31].

3.6. Detection of active species in the drugs degradation

It has been recognized that the photogenerated holes and electrons

stemmed from the conduction band and valence band and the subsequently produced radicals are the potential reactive species for the photocatalytic degradation of drugs [32]. In order to reveal the photocatalytic mechanism and investigate the active species involved in the photocatalytic process for n-CeO₂/p-CuS composite, various scavengers are employed to suppress the function of one of the active species generated in the photodegradation process. The [•]OH, [•]O₂, ¹O₂, and h⁺ were examined by adding 1.0 mM benzoquinone (BQ, a quencher of [•]O₂), 1.0 mM isopropanol (IPA, a quencher of [•]OH), 1.0 mM ammonium oxalate (AO, a quencher of h⁺), and 1.0 mM sodium azide (SA, a quencher of ¹O₂), respectively. As illustrated in Fig. 12, the degradation efficiency of BQ quenching declined more than those of IPA and AO, but the photocatalytic degradation of TC, CF, and CT drugs were not influenced by the addition of SA. Thus, the quenching caused by various scavengers revealed that the reactive [•]O₂ was crucial, whereas the [•]OH and h⁺ played minor role in TC, CF, and CT drugs degradation; furthermore, the [•]OH was created through a multistep reduction of [•]O₂.

3.7. Fluorescence detection of uric acid

In the fluorescence detection of acids, along with the sensitivity requirement, high specificity and selectivity is crucial in most scenarios especially in real sample detections. To evaluate the selectivity of the fluorescence sensor of n-CeO₂/p-CuS heterostructure, we measured the fluorescence intensity changes in the presence of the representative acids at different concentrations under the analogous conditions. Among the tested acids, including AA, UA, HA, PA, and SA, only UA significantly affected the fluorescence intensity of the n-CeO₂/p-CuS heterostructure, as shown in Fig. 13(a). These results demonstrate the good selectivity of the n-CeO₂/p-CuS heterostructure-based sensor for UA over other acids.

To assess the sensitivity of the n-CeO₂/p-CuS heterostructure in fluorescence detection of UA, we monitored the fluorescence intensity at 461 nm as a function of UA concentration. As shown in Fig. 13(b-c), the fluorescence emission of the n-CeO₂/p-CuS heterostructure at 461 nm is considerably quenched with increasing UA concentration from 1 to 100 μM, and the limit of detection (LOD) is 1.214 μM. The correlation between fluorescence-quenching efficiency and UA concentration was investigated using the Stern-Volmer formula [33]: $F_0/F = K_{SV} [Q] + 1$, where F₀ and F are the fluorescence intensity of the n-CeO₂/p-CuS heterostructure at 516 nm when immersed in water and UA aqueous solution, respectively; K_{SV} is the quenching constant (M⁻¹); [Q] is the concentration of UA. A good linear relationship was observed between F₀/F and [Q] in the range of 10–100 μM (Fig. 13(d)). The K_{SV} value was calculated to be $7.26 \times 10^3 \text{ M}^{-1}$, indicating that UA has a strong quenching effect on the n-CeO₂/p-CuS heterostructure. Hence, the n-CeO₂/p-CuS heterostructure-based sensor exhibits high sensitivity and selectivity for UA detection.

3.8. Selectivity of proposed fluorescent sensor

Evaluating the selectivity of a fluorescent sensor is crucial for its accurate performance. Therefore, in this study, the effects of various mental ions (K⁺ and Na⁺) and small biological molecules (UA, AA, PA, HA, SA, Glu, Lac, Ala, and Lys) were investigated (Fig. 14) to assess the selectivity of the n-CeO₂/p-CuS heterostructure-based sensor for UA detection. The results revealed that the interfering species mentioned above had a negligible effect on the sensor's performance compared to UA. This high selectivity can be attributed to the strong affinity of uricase for UA. Hence, the proposed fluorescent sensor can detect UA concentration selectively and offer accurate results even when the interfering species are present at high concentrations.

3.9. Real sample analysis

To demonstrate the applicability of the sensor for real-world sample



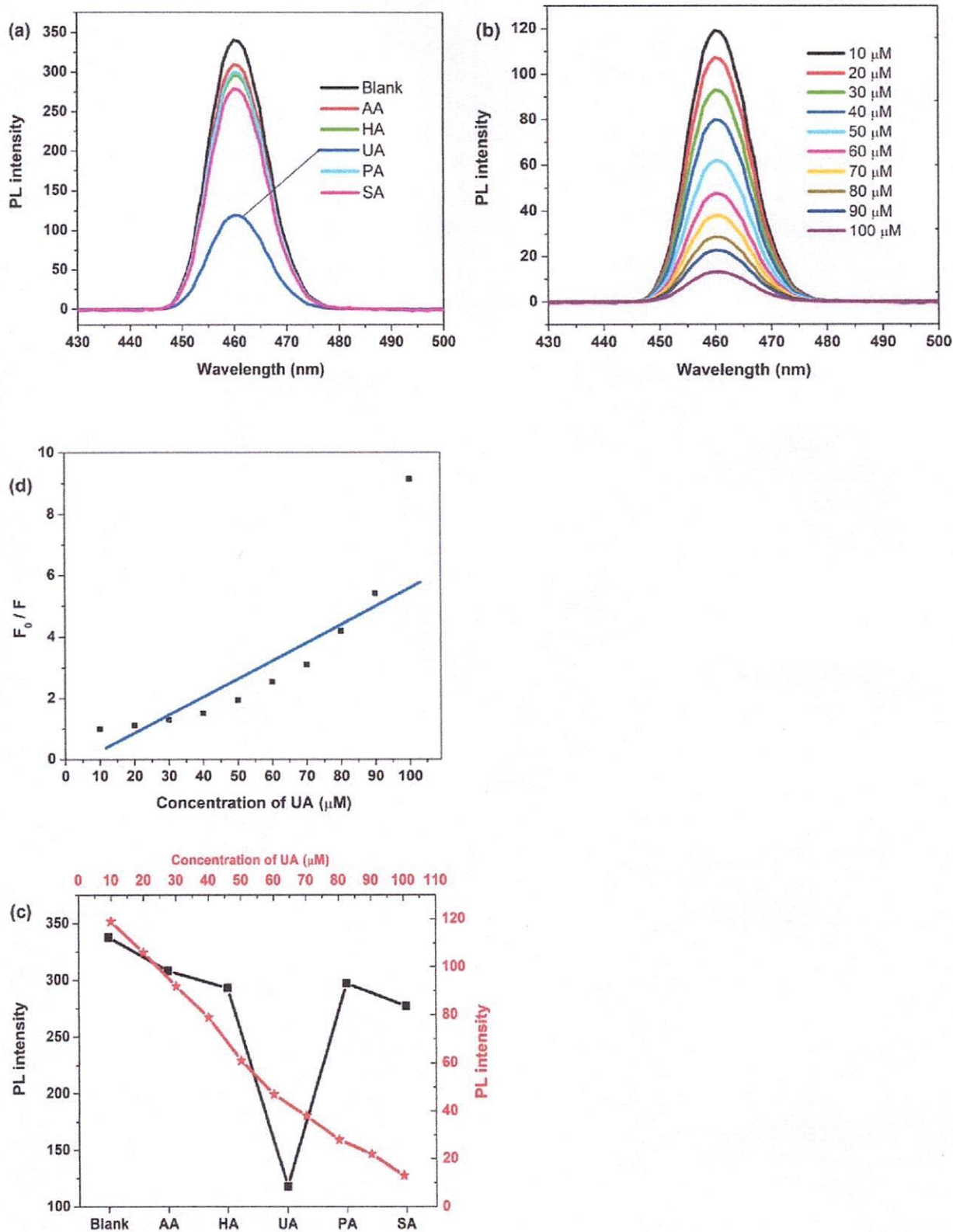


Fig. 13. (a, c) The fluorescence detection of various acids using the synthesized n-CeO₂/p-CuS heterostructure; (b, c) selective sensing of UA from the concentration of 10–100 μM, and (d) Stern-Volmer plot.



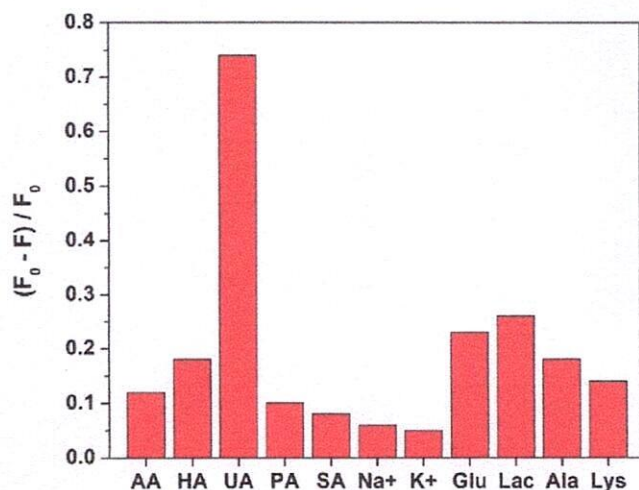


Fig. 14. Selectivity analysis for UA detection by quenched FL intensity of n-CeO₂/p-CuS heterostructure. All the analytes were first incubated with uricase (1.3 U mL⁻¹) in PBS (0.1 M, pH = 7.0) for 45 min at 37 °C bath. The concentration of n-CeO₂/p-CuS heterostructure is 0.02 mg mL⁻¹. The concentration of UA is 10 μM. The concentration of the others is 50 μM.

Table 2
Determination results of UA in human urine samples (n = 3).

UA	Background ± SD (mM)	Added (mM)	Found ± SD (mM)	Recovery (%)
Male urine	1.69 ± 0.04	3.00	5.15 ± 0.06	94.8
Female urine	4.12 ± 0.09	3.00	7.20 ± 0.08	104.3

analysis, human urine samples were collected from healthy adult male volunteers and were tested for the detection of UA. Although a slight detection of UA was observed in the urine samples, the credibility of the method was evaluated using the standard addition method, and the recovery ratios were calculated (Table 2). The results showed satisfactory recoveries with values ranging from 94% to 105% for human urine samples, with relative standard deviations of less than 5% (n = 3). These results demonstrate the potential use of the proposed assay for accurate quantification of UA in aqueous solutions. The high accuracy and precision of this method in practical applications were confirmed by the standard recovery values [34].

4. Conclusions

In this study, CeO₂, CuS, and n-CeO₂/p-CuS heterostructures were successfully synthesized using a hydrothermal method, and their structure, bandgap, morphology, and average diameter were characterized by UV-vis DRS, PL, XRD, SEM, and TEM. The XRD patterns showed that the n-CeO₂/p-CuS heterostructure had a hexagonal phase, while TEM analysis revealed that n-CeO₂/p-CuS heterostructure had CuS deposited on the surface of CeO₂ nanorods with an average diameter of 10 ± 3 nm and a length of ≈100 nm. Visible-light-driven photocatalytic degradation of TC, CF, and CT drugs was studied. As a result, the n-CeO₂/p-CuS heterostructure was an excellent catalyst for visible-light-driven degradation of TC, CF, and CT drugs, with maximum degradation and [•]O₂ being the main active species and [•]OH radical and h⁺ being the minor active species in the degradation process. The n-CeO₂/p-CuS heterostructure also showed excellent selectivity and sensitivity for fluorescence detection of UA, with a LOD of 1.214 μM. The fluorescence emission of the heterostructure at 461 nm was quenched significantly with increasing UA concentration, and a good linear relationship was achieved between I₀/I and [Q]. In addition, interfering

species, such as metal ions (K⁺ and Na⁺) and small biological molecules (AA, PA, HA, and SA, Glu, Lac, Ala, and Lys), were found to be negligible compared with UA, indicating high selectivity. Finally, the n-CeO₂/p-CuS heterostructure was applied to the determination of UA in human urine samples, and standard addition method was used to evaluate the credibility of the method. Satisfying recoveries were obtained, with recoveries ranging from 94 to 105% for human urine samples and relative standard deviations of less than 5% (n = 3). These results demonstrate the potential use of the proposed method for UA quantification in aqueous solutions with excellent accuracy and precision.

Declaration of Competing Interest

The authors declare that they have no known competing financial interests or personal relationships that could have appeared to influence the work reported in this paper.

Data availability

No data was used for the research described in the article.

Acknowledgments

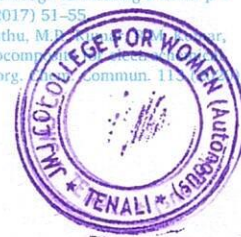
The authors were sincerely thanks to the Head, Department of Chemistry, Osmania University, Hyderabad, India for providing necessary facilities.

Funding

Not applicable.

References

- [1] D. Ayodhya, Ag-SPR and semiconductor interface effect on a ternary CuO@Ag@Bi₂S₃ Z-scheme catalyst for enhanced removal of HIV drugs and (photo) catalytic activity, *New J. Chem.* 46 (2022) 15838–15850.
- [2] X.J. Wen, C.G. Niu, L. Zhang, C. Liang, H. Guo, G.M. Zeng, Photocatalytic degradation of ciprofloxacin by a novel Z-scheme CeO₂-Ag/AgBr photocatalyst: Influencing factors, possible degradation pathways, and mechanism insight, *J. Catal.* 358 (2018) 141–154.
- [3] J. Li, L. Pan, G. Yu, S. Xie, C. Li, D. Lai, Z. Li, F. You, Y. Wang, The synthesis of heterogeneous Fenton-like catalyst using sewage sludge biochar and its application for ciprofloxacin degradation, *Sci. Total Environ.* 654 (2019) 1284–1292.
- [4] J. Li, G. Yu, L. Pan, C. Li, F. You, S. Xie, Y. Wang, J. Ma, X. Shang, Study of ciprofloxacin removal by biochar obtained from used tea leaves, *J. Environ. Sci.* 73 (2018) 20–30.
- [5] A. Kumar, G. Sharma, M. Naushad, T. Ahmad, R.C. Vees, F.J. Stadler, Highly visible active Ag₂CrO₄/Ag/BiFeO₃@RGO nano-junction for photoreduction of CO₂ and photocatalytic removal of ciprofloxacin and bromate ions: The triggering effect of Ag and RGO, *Chem. Eng. J.* 370 (2019) 148–165.
- [6] M. Mousavi-Kamazani, M. Ghodrati, R. Rahmatollahzadeh, Fabrication of Z-scheme flower-like AgI/Bi₂O₃ heterojunctions with enhanced visible light photocatalytic desulfurization under mild conditions, *J. Mater. Sci. Mater. Electron.* 31 (2020) 5622–5634.
- [7] C. Li, Z. Sun, W. Zhang, C. Yu, S. Zheng, Highly efficient g-C₃N₄/TiO₂/kaolinite composite with novel three-dimensional structure and enhanced visible light responding ability towards ciprofloxacin and *S. Aureus*, *Appl. Catal. B* 220 (2018) 272–282.
- [8] M.M. Sabzeheidani, H. Karimi, M. Ghaedi, CeO₂ nanofibers-CdS nanostructures n-n junction with enhanced visible-light photocatalytic activity, *Arab. J. Chem.* 13 (2020) 7583–7597.
- [9] L. Wang, W. Wang, Y. Chen, L. Yao, X. Zhao, H. Shi, M. Cao, Y. Liang, Heterogeneous p-n junction CdS/Cu₂O nanorod arrays: Synthesis and superior visible-light-driven photoelectrochemical performance for hydrogen evolution, *ACS Appl. Mater. Interfaces* 10 (2018) 11652–11662.
- [10] D. Ayodhya, G. Veerabhadram, Green synthesis of garlic extract stabilized Ag@CeO₂ composites for photocatalytic and sonocatalytic degradation of mixed dyes and antimicrobial studies, *J. Mol. Struct.* 1205 (2020), 127611.
- [11] X.J. Wen, C. Zhang, C.G. Niu, L. Zhang, G.M. Zeng, X.G. Zhang, Highly enhanced visible light photocatalytic activity of CeO₂ through fabricating a novel p-n junction BiOBr/CeO₂, *Catal. Commun.* 90 (2017) 51–55.
- [12] G. Manibalan, G. Murugadoss, R. Thangamuthu, M.P. Jayavel, CeO₂-based heterostructure nanocomposites for the determination of L-cysteine biomolecule, *Inorg. Commun.* 11 (2020) 107793.



- [13] M. Mousavi-Kamazani, F. Azizi, Facile sonochemical synthesis of Cu doped CeO₂ nanostructures as a novel dual-functional photocatalytic adsorbent, *Ultrason. Sonochem.* 58 (2019), 104695.
- [14] M. Mousavi-Kamazani, S. Ashrafi, Single-step sonochemical synthesis of Cu₂O-CeO₂ nanocomposites with enhanced photocatalytic oxidative desulfurization, *Ultrason. Sonochem.* 63 (2020), 104948.
- [15] M. Mousavi-Kamazani, R. Reza, F. Beshkar, Facile solvothermal synthesis of CeO₂-CuO nanocomposite photocatalyst using novel precursors with enhanced photocatalytic performance in dye degradation, *J. Inorg. Organomet. Polym. Mater.* 27 (2017) 1342–1350.
- [16] V. Kamari, A. Sharma, N. Kumar, M. Sillanpää, P.R. Makgwane, M. Ahmaruzzaman, A. Hosseini-Bandegharai, M. Rani, P. Chinnumuthu, TiO₂-CeO₂ assisted heterostructures for photocatalytic mitigation of environmental pollutants: A comprehensive study on band gap engineering and mechanistic aspects, *Inorg. Chem. Commun.* 151 (2023), 110564.
- [17] X. Zheng, M. Huang, Y. You, H. Peng, J. Wen, Core-shell structured α -Fe₂O₃@ CeO₂ heterojunction for the enhanced visible-light photocatalytic activity, *Mater. Res. Bull.* 101 (2018) 20–28.
- [18] Q. Mou, Z. Guo, Y. Chai, B. Liu, C. Liu, Visible light assisted production of methanol from CO₂ using CdS@ CeO₂ heterojunction, *J. Photochem. Photobiol. B: Biol.* 219 (2021), 112205.
- [19] D. Ayodhya, G. Veerabhadram, Influence of g-C₃N₄ and g-C₂N₄ nanosheets supported CuS coupled system with effect of pH on the catalytic activity of 4-NP reduction using NaBH₄, *Flat Chem.* 14 (2019), 100088.
- [20] D. Ayodhya, G. Veerabhadram, Preparation, characterization, photocatalytic, sensing and antimicrobial studies of calotropis gigantea leaf extract capped CuS NPs by a green approach, *J. Inorg. Organomet. Polym. Mater.* 27 (2017) 215–230.
- [21] F.Z. Tan, M.T. Ma, W.J. Cai, Y.L. Chen, Y.H. Wang, J.H. Zhou, Synthesis of porous biocarbon supported Ni₃S₄/CeO₂ nanocomposite as high-efficient electrode materials for asymmetric supercapacitors, *J. Saudi Chem. Soc.* 26 (2022), 101530.
- [22] Z. Xue, L. Lv, Y. Tian, S. Tan, Q. Ma, K. Tao, L. Han, Co₃S₄ nanoplate arrays decorated with oxygen-deficient CeO₂ nanoparticles for supercapacitor applications, *ACS Appl. Nano Mater.* 4 (2021) 3033–3043.
- [23] D. Ayodhya, G. Veerabhadram, Facile fabrication, characterization and efficient photocatalytic activity of surfactant free ZnS, CdS and CuS nanoparticles, *J. Sci.: Adv. Mater. Devices* 4 (2019) 381–391.
- [24] D. Ayodhya, Fabrication of SPR triggered Ag-CuO composite from Cu(II)-Schiff base complex for enhanced visible-light-driven degradation of single and binary-dyes and fluorometric detection of nitroaromatic compounds, *Inorg. Chem. Commun.* 148 (2023), 110295.
- [25] D. Ayodhya, A. Ambala, G. Balraj, M.P. Kumar, P. Shyam, Green synthesis of CeO₂ NPs using Manilkara zapota fruit peel extract for photocatalytic treatment of pollutants, antimicrobial, and antidiabetic activities, *Res. Chem.* 4 (2022), 100441.
- [26] M.M. Sabzehmeidani, H. Karimi, M. Ghaedi, Visible light-induced photo-degradation of methylene blue by n-p heterojunction CeO₂/CuS composite based on ribbon-like CeO₂ nanofibers via electrospinning, *Polyhedron* 170 (2019) 160–171.
- [27] W. Li, S. Xie, M. Li, X. Ouyang, G. Cui, X. Lu, Y. Tong, CdS/CeO_x heterostructured nanowires for photocatalytic hydrogen production, *J. Mater. Chem. A* 1 (2013) 4190–4193.
- [28] D. Ayodhya, G. Veerabhadram, A review on recent advances in photodegradation of dyes using doped and heterojunction based semiconductor metal sulfide nanostructures for environmental protection, *Mater. Today Energy* 9 (2018) 83–113.
- [29] D. Ayodhya, V. Sumalatha, R. Gurrapu, M.S. Babu, Catalytic degradation of HIV drugs in water and antimicrobial activity of Chrysin-conjugated Ag-Au, Ag-Cu, and Au-Cu bimetallic nanoparticles, *Res. Chem.* 5 (2023), 100792.
- [30] E.S. Elmolla, M. Chaudhuri, Degradation of amoxicillin, ampicillin and cloxacillin antibiotics in aqueous solution by the UV/ZnO photocatalytic process, *J. Hazard. Mater.* 173 (2010) 445–449.
- [31] J. Luan, Z. Hu, Synthesis, property characterization, and photocatalytic activity of novel visible light-responsive photocatalyst Fe₂BiSbO₇, *Int. J. Photoenergy* 2012 (1–11) (2012), 301954.
- [32] S. Paul, J. Sultana, A. Bhattacharyya, A. Karmakar, S. Chattopadhyay, Investigation of the comparative photovoltaic performance of n-ZnO nanowire/p-Si and n-ZnO nanowire/p-CuO heterojunctions grown by chemical bath deposition method, *Optik* 164 (2018) 745–752.
- [33] V. Sumalatha, D. Ayodhya, Fabrication and characterization of CuO nano-needles from thermal decomposition of Cu(II) metal complex: Fluorometric detection of antibiotics, antioxidant, and antimicrobial activities, *Res. Chem.* 5 (2023), 100821.
- [34] Q. Zheng, L. Xiong, L. Yu, D. Wu, C. Yang, Y. Xiao, An enzyme-free fluorescent sensing platform for the detection of uric acid in human urine, *J. Luminesc.* 236 (2021).

PRINCIPAL
JMJ COLLEGE FOR WOMEN (Autonomous)
TENALI



Combining Lightweight Encryption Methods to Secure IoT Networks

G.S.S Rao^{1*}, K.G.S.Venkatesan², Allanki Sanyasi Rao³

¹Department of AIML, Nawab Shah Alam Khan College of Engineering and Technology, Hyderabad, Telangana, India.

²Department of Computer Science & Engineering, Megha Institute of Engineering and Technology for Women, Hyderabad, Telangana, India.

³Department of Electronics & Communication Engineering, Christu Jyothi Institute of Technology & Science, Jangaon, Telangana, India.

Received: 12.07.2023

Accepted: 20.07.2023

Published Online: 31.07.2023

Abstract: The rapid development of the underlying infrastructure of the internet has permitted the widespread acceptance of a number of emerging technologies that have far-reaching ramifications for current society. As a result of the expansion of the Internet of Things, several new networking protocols and upgrades have been created and implemented. On top of that, there is a significant shortage of financing for the development of information technology applications, as well as critical security problems that jeopardise private data. As if that weren't enough, there are also substantial weaknesses in the data's privacy protection. In spite of the enormous research that has been done, there has not been a single security solution for the IoT network that has been proved to be entirely effective. This is due to the fact that the network of things connected to the Internet of Things has a unique mix of low energy usage, rare materials, sufficient computational power, and considerable operational expenses. As a consequence of this, we consider the modification of the protocol to be a viable and comprehensive strategy for defending Internet of Things devices from cyberattacks. The inclusion of IoT layer-specific security solutions into enhanced code is one of the many ways in which algorithmic enhancements contribute to the accomplishment of this objective. In this study, we propose improving and integrating the DTLS Procedure with the earwiggling mechanism, also then testing the protocol on representative models of

*Correspondence: Professor & HOD, Department of AIML, Nawab Shah Alam Khan College of Engineering and Technology, Hyderabad, Telangana, India. Email: profgssrao@gmail.com
<https://doi.org/10.58599/IJSMEM.2023.1704>
Volume-1, Issue-7, PP:35-45 (2023)



IoT networks to confirm its effectiveness, practicability, economy, and appropriateness. This would be done after the protocol had been tested. These findings will be presented in the form of a paper that will be written up.

Key words: Security networks, Cyber networks security, Wireless sensor networks, Internet of Things.

1. INTRODUCTION

The proliferation of devices that are enabled by the Internet of Things has resulted in a slew of brand-new advancements in networking, as well as in the protocols that govern it. In addition, there is a shortage of resources for the development of applications using information technology, and there are security flaws that pose a significant threat to the information's ability to remain private. In spite of the significant amount of research that has been done, there is not a single security solution that has been shown to be completely successful for the IoT network. This is because the IoT network has a unique combination of characteristics, including great energy efficiency, limited resources, high processing capability, and high operational expenses. Because of this, we feel that an upgrade to the protocol ought to be deemed a feasible and all-encompassing solution for the purpose of safeguarding devices connected to the Internet of Things from cyber assaults. One of the ways in which algorithmic innovations help to the achievement of this goal is via the incorporation of code improvements and security solutions that are particular to certain IoT layers. In this piece, we make the suggestion that the DTLS protocol may be improved by including an overhearing method into it. This would make it possible to have communications that are more secure. After that, we put many different models of Internet of Things networks through a battery of tests to establish whether or not the system is functional, viable, cost-efficient, and acceptable in its current state.

2. IMPROVED DTLS AND OVERHEARING FOR COMPREHENSIVE SECURITY

This is done so that it may take use of both the high level of security offered by asymmetric encryption and the speed offered by symmetric encryption. DTLS is different from TLS since it was designed to work with WSN. To begin, DTLS strengthens the integrity of the encryption by establishing timers on both the server and the client to reattempt transmission of any missed packets. The encryption keys that are used in DTLS are shorter than those that are used in TLS, which makes it simpler to put WSN approaches into practise. Even though it is still in the process of being developed, the Data Transport Layer Security (DTLS) protocol is being tested to secure WSN data from being spoofed and eavesdropped on. Overhearing conversations may be able to assist in the detection and mitigation of DoS attacks, which are known to decrease the availability of the Internet of Things . In particular, distributed denial of service attacks (DDoS) obstruct the delivery of services to legitimate users of the internet of things. This puts a halt to all service operations and results in financial and reputational damages for consumers as well as service providers [1]. Architecture and attack method are the two categories that are most often used for classifying denial of service attacks [2]. The theoretical foundation of an IoT DoS Attack is referred to as architecture, while the operational technique is



referred to as mechanism. UDP flood denial of service attacks that are coordinated by a botnet are presently the norm. Overhearing makes it possible for nodes to eavesdrop on one another and find Bots by identifying the hub of Internet of Things (IoT) communication. Robots will be quarantined as soon as they are detected, and only then will they be employed in an attack Integrity, availability, and secrecy are the three pillars that make up the CIA security triangle [3, 4], which sets these principles as the foundation of information safety and security. Figure 1 also includes the CIA's enhanced Security 6-pointed star, which will (in the near future) have an additional three qualities added [5, 6]. Each ever more advanced characteristic is the consequence of the superposition of the two basic features that are immediately next to it. See Figure 1 for a visual representation of this concept. Three white peaks are marked with uppercase letters to signify the most basic aspects, while three black peaks are labelled with lowercase characters to represent the most comprehensive features.

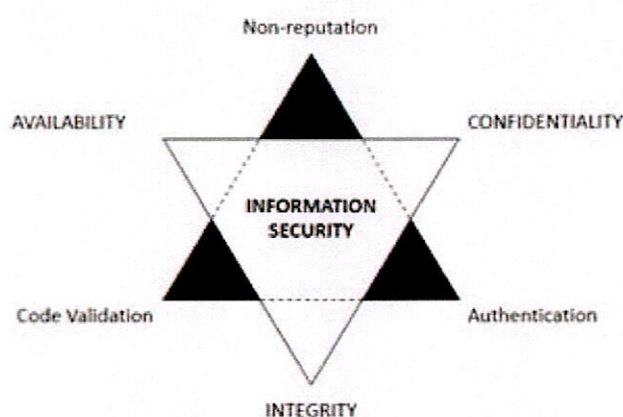


Figure 1. An Early Warning Sign of Safety I.C.I.A. 6-pointed star

If the IoT system's security solution safeguards all three apexes of the security CIA triangle, then the system may rest easy knowing that its most basic qualities, as well as the three that expand from them, are secure. Therefore, the full and entire safety of all critical qualities will be supplied by the DTLS protocol's protection of confidentiality and integrity, in combination with the protection of availability offered by the overhearing mechanism. Because of their susceptibility to denial-of-service attacks, Internet of Things (IoT) systems would benefit greatly from the implementation of both methods. Implementing both the DTLS procedure also the overhearing mechanism will protect IoT systems from virtually every threat currently present, as both have been shown to be effective at preventing data sniffing and spoofing attacks, as well as denial of service attacks via botnet and UDP flood. The all-encompassing security architecture that Yashaswini used consisted of four levels: the application layer, the support layer, the sensor layer, also the transmission layer [7, 8]. A technique for overhearing is implemented in the sensor layer, together with the implementation of the DTLS pro-



ocol in the transmission layer. The spread of these two different solutions over the whole of the IoT infrastructure is shown in Figure 2.

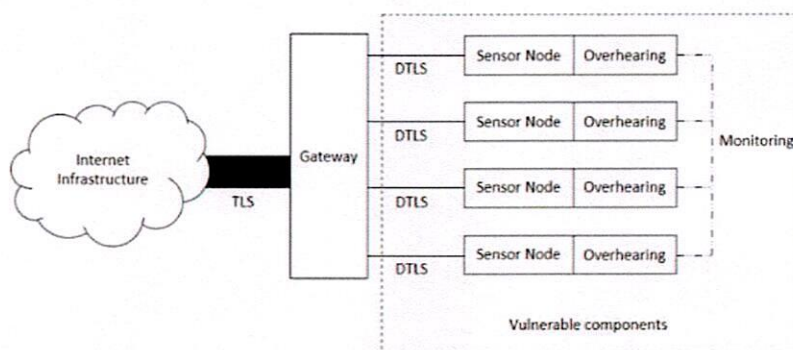


Figure 2. IoT system's DTLS and overhearing hotspots

As can be observed in Figure 2, DTLS and overhearing capabilities are present in the gateway, the sensor node, and the sensor environment. Because of the complex nature of IoT networks, they are more vulnerable to DDoS assaults than traditional networks. Second, there are not yet sufficient security solutions for components that utilise IoT protocols like 6LoWPAN and Zigbee [9], even if the internet is secured by robust security methods like TLS. Despite the robust safeguards in place, this is still the case. Therefore, it is crucial to implement the all-encompassing security solution for these IoT parts.

3. EXTENSIVE SECURITY SOLUTION MODELLING

There are several advantages to using the Contiki Operating System [10], some of which include the fact that it is open-source, the accuracy with which simulations may be visualised, and the friendliness of its interface. Since the overhearing approach has been implemented and tested in the contiki operating system, the paper's simulation may be trusted and relied upon for accuracy and safety. On the other hand, the "tiny-dtls" version of DTLS is already being used in the contiki environment [11, 12]. Cooja is a simulation application for Java code that is used for all aspects of design and deployment in files [13]. In order to install them, we made use of the contiki operating system, and we simulated a denial-of-service attack inside a square-grid wireless sensor network by using UDP Flood and botnet. The findings of the simulation indicate that overhearing is successful when a network is able to maintain regular operation while experiencing a brief decrease in performance [14]. The file framer-802154.c,



Table 1. Overhearing mechanism and the DTLS Protocol

	DTLS	OVERHEARING
Characteristic	Integrity: Stop Attacks From Being Spoof Cryptography, Symmetric and Asymmetric The data-hashing technique ECC's Data Backup System	Each node keeps an eye on the ones around it. Once a "Singularity point from median Algorithm" identifies a bot, the bot is removed from the network.
Target of protection	Confidentiality: halt Attacks Caused by Sniffing	Availability: stop Denial-of-Service Attacks
Zone of safety	The "app" folder is referred to throughout the simulation.	The IEEE 802.15.4-standard nodes are used in the simulation.
Location in "contiki-master"	Folder "tiny-dtls" on folder "apps"	For example, see "core/net/mac"/framer-802154.c.
Location in IoT	Transmission Layer (related to Protocol)	Sensor Layer (related to WSN)

which can be found in the "core/net/mac" portion of the source code that controls network nodes, is where the Overhearing feature of the Contiki OS is really implemented. As a direct consequence of this, the overhearing mechanism safeguards any node that complies with any of the two network standards. The "tiny-dtls" application is the DTLS protocol simulator for the contiki operating system. In spite of this, not all contiki operation simulations are included inside the "tiny-dtls" safety net. Using DTLS to encrypt data on a typical IoT network is not a good idea for a number of reasons, including its high resource needs and the complexity of the encryption algorithms it employs [15]. This is true even in the case when there is no overhearing going on. Memory and computing power of Internet of Things devices might be fairly constrained at times. As a result, a number of DTLS improvements are in the works, all of which are intended to cut down on resource consumption while maintaining the robust security and consistency of the system inside the IoT [16, 17]. The following is an exhaustive summary of all of the newly added features and alterations:

The Internet of Things network nodes are placed at 30-meter intervals on a square grid. The distance between any two nodes on a diagonal is 42 metres, as shown by the Pythagorean Theorem for right triangles. Therefore, the length of the diagonal is around 42 metres between any two nodes. This simulation has a total of 25 nodes, with five endpoints on each of the square's four sides. A more diverse



set of pathways is possible in a network with a grid topology since each node has more neighbours. Each node in this topology may send information directly to its neighbours along any of the three axes of the simulation space (horizontal, vertical, and diagonal). With this configuration, information may be sent from a node at a square topology's corner to three other nodes, from a node on a side to five other nodes, and from a node in the centre to eight other nodes. It is important to note that this simulated experiment did not contain multi-hop capabilities, which enable a node to send to more than one destination. Because of this, it was impossible for a node to send a message to more than one receiver at a time. This topology is shown in Figure 3 for your viewing pleasure.

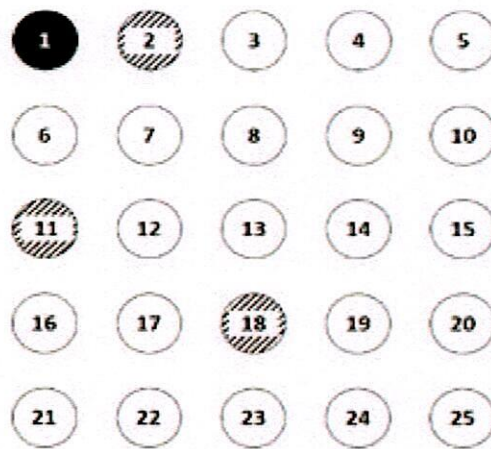


Figure 3. IoT network topology for use in simulated experiments

Figure 3 show client nodes with white backgrounds and black text, whereas the Server nodes have black backgrounds and white text. Figure 3 shows three Bot nodes with a background pattern consisting of a black upward-diagonal line working together to execute a Denial of Service attack against the target server by sending a large number of UDP packets to it. DoS attacks are more successful against an IoT network when the Bots are spread out in a way that takes advantage of their varied positions in the DAG tree and their varying distances from the server node. In other words, when the Bots are distributed in this manner, the DoS attack is more likely to succeed.



4. RESULTS AND DISCUSSION

Wireshark was chosen to do the analysis and assessment of our proposal because it is considered to be one of the most effective applications for researching network protocols via the examination of data obtained from decapsulated packets. Test case TC3, which simulates a network that has DTLS installed, and Test case TC2, which simulates a network that does not have DTLS installed, are both executed in Wireshark. Because MDNS packets were discovered on a network where DTLS had just recently been implemented (depicted with a dark brown marking), it was determined that the DTLS Protocol had been successfully deployed.

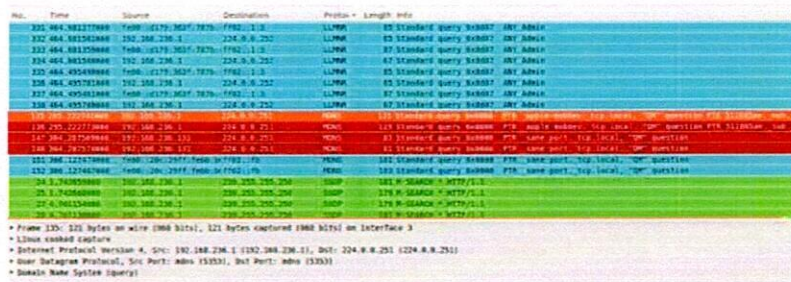


Figure 4. (a) Network installing DTLS

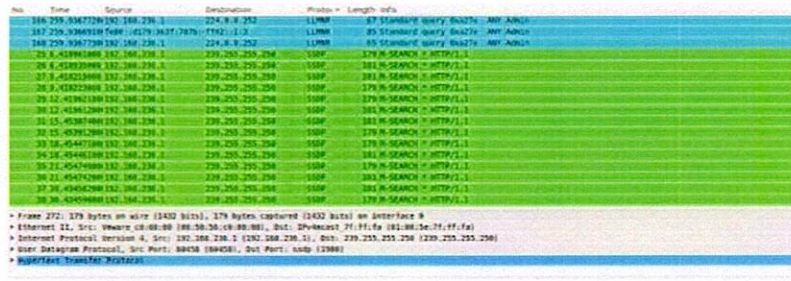


Figure 5. (b) Network without installing DTLS

CPU stands for the amount of power used by the central processing unit throughout the simulation (the value of CPU varies depending on the kind of node), and LPM is the fraction of simulation time that a node spends doing basic operations. We will evaluate the whole WSN based



on three parameters and then calculate an average for each node. The CPU is the amount of power consumed by the CPU during the simulation (the number of CPUs used varies depending on the type of node), and the LPM is the fraction of total simulation time that a node spends performing its core operations. The total value of the WSN will be calculated as the mean of three different metrics collected from throughout the network. Some Sky nodes are used for the simulation, and they only need 1.05 mW for a 5-minute runtime or less than 12.6 mW per hour. Accordingly, for the WSN to function dependably, its energy consumption should be no more than 315 mJ. The results of the research conducted in Time Courses 1 through 6 are summarised in Table 2. Remember that the total of all these results is equivalent to the average value of IoT for that criteria.

WSN. Some Sky nodes, employed in the simulation, need less than 12.6 mW of power over the course of an hour and 1.05 mW over the course of 5 minutes. This means the WSN's energy ingesting necessity be less than 315 mJ if it is towards maintain a constant state of operation. Table 2 displays the experiment's outcomes for all time points from TC1 to TC6. It's important to note that the value shown here is the mean worth of IoT for each standard.

Table 2. WSN Test Case Efficiency

	Mechanics and their current state	PDR (%)	Energy (mJ)	Latency (ms)
TC1	Normal, Overhearing	99.52	177.7	642.44
TC2	Normal, DTLS	99.55	152.18	627.25
TC3	Overload, DTLS	17.58	981.74	51922.21
TC4	Normal, DTLS, Overhearing	96.29	211.57	655.34
TC5	Overload, DTLS, Overhearing	96.04	312.8	783.74
TC6	Overload, Overhearing	97.9	185.14	724.37

Table 2 has several analytical assertions that may be found there. The adoption of a complete safety solution that integrated DTLS also overhearing had a detrimental influence on the typical transmission performance of WSN. In particular, the amount of energy that was used increased noticeably and rapidly within a short period of time. This drop may be attributed, in part, to the use of DTLS and overhearing in combination with several other WSN procedures. Features like as DTLS encryption and overhearing monitoring contributed to an increase in the WSN's power usage. Even though both the PDR and the Latency increased, they were still over the threshold for reliable transmission; as a result, the delay in the WSN's ability to operate was kept to a minimum. The



increase in energy demand did not result in the WSN being overwhelmed .

Because to overhearing, the transmission overload that was brought on by a simulated denial of service attack was reduced. Despite the fact that they were improved, all of the WSN criteria, including the DTLS, continued to have high energy needs. As a component of a comprehensive security solution the DTLS protocol and the overhearing approach will soon be deployed in a genuine Internet of Things system that makes use of Arduino devices.

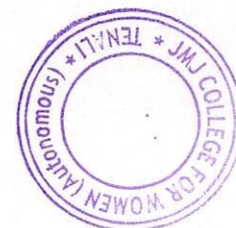
5. CONCLUSION

In this research, we identified three information security aspects that, together referred to as the "CIA security triangle," are required to be guarded against any possible threats that may be posed by an IoT system. These properties include privacy (to stop people from listening in), integrity (to stop people from spoofing), and availability (to stop people from blocking services). Our team created the DTLS Protocol, which protects against attacks such as sniffing and spoofing. Additionally, our team developed the overhearing mechanism, which protects against attacks such as denial of service. The purpose of this research is to spread the word about the all-encompassing security solution that was developed by our group. This solution uses a strengthened version of DTLS at both the transport and the sensing levels. Our response includes location diagram, enhancements to DTLS' resource efficiency to allow for its use on low-power networks. After the theoretical framework has been built, our group will get started with the simulations of the contiki OS experiment. These experiments are being conducted with the intention of finding the sweet spot between DTLS and overhearing, with the end goal of attaining complete security. In addition to that, they will simulate a denial of service attack by using a botnet and a UDP flood. During the packet capture that our team ran, we made use of Wireshark, and the results revealed that simulated WSN conversations were protected with DTLS encryption. The results of WSN performance metrics such as PDR and Latency proved the steady functioning of WSN after the implementation of this complete security solution and passing through a simulated denial of service assault. Even though there are many more obstacles to overcome when establishing a real Internet of Things system as opposed to a simulated one operating on the contiki operating system, the experimental dependability in a real system is far greater.



References

- [1] Bin Yuan, Chen Lin, Huan Zhao, Deqing Zou, Laurence Tianruo Yang, Hai Jin, and Chunming Rong. Secure data transportation with software-defined networking and kn secret sharing for high-confidence iot services. *IEEE Internet of Things Journal*, 7(9):7967–7981, 2020.
- [2] KN Ambili and Jimmy Jose. A secure software defined networking based framework for iot networks. *Cryptology ePrint Archive*, 2020.
- [3] Omar Cheikhrouhou. Secure group communication in wireless sensor networks: a survey. *Journal of Network and Computer Applications*, 61:115–132, 2016.
- [4] Sanjeev Kulkarni, Sachidanand S Joshi, AM Sankpal, and RR Mudholkar. Link stability based multipath video transmission over manet. *International Journal of Distributed and Parallel Systems*, 3(2):133, 2012.
- [5] Sanjeev Kulkarni, Satish H Patil, and RA Patil. Strengths and weakness of present social networks. In *Networking: Proceedings of the International Conference on Computer Applications: 24-27 December 2010, Pondicherry, India*. Research Publishing Services, 2010.
- [6] Haojie Shen, Li Zhuo, and Yingdi Zhao. An efficient motion reference structure based selective encryption algorithm for h. 264 videos. *IET Information Security*, 8(3):199–206, 2014.
- [7] Laurent Eschenauer and Virgil D Gligor. A key-management scheme for distributed sensor networks. In *Proceedings of the 9th ACM Conference on Computer and Communications Security*, pages 41–47, 2002.
- [8] K Sowmya Fathima, S Barker, and S Kulkarni. Analysis of crop yield prediction using data mining technique. *International Research Journal of Engineering and Technology (IRJET)*, 7(05), 2020.
- [9] Ayoub Massoudi, Frédéric Lefebvre, Christophe De Vleeschouwer, Benoit Macq, and J-J Quisquater. Overview on selective encryption of image and video: challenges and perspectives. *Eurasip Journal on information security*, 2008(1):179290, 2008.
- [10] Yijia Cao, Qiang Li, Yi Tan, Yong Li, Yuanyang Chen, Xia Shao, and Yao Zou. A comprehensive review of energy internet: basic concept, operation and planning methods, and research prospects. *Journal of Modern Power Systems and Clean Energy*, 6(3):399–411, 2018.
- [11] Gerard Deepak, M Madiajagan, Sanjeev Kulkarni, Ahmed Najat Ahmed, Anandbabu Gopatoti, and Veeraswamy Ammisetty. Msc-net: Covid-19 detection using deep-q-neural network classification with rfnn-based hybrid whale optimization. *Journal of X-Ray Science and Technology*, (Preprint):1–27, 2023.



- [12] Lein Harn and Ching-Fang Hsu. Predistribution scheme for establishing group keys in wireless sensor networks. *IEEE Sensors Journal*, 15(9):5103–5108, 2015.
- [13] Eraj Khan, Ernst Gabidulin, Bahram Honary, and Hassan Ahmed. Matrix-based memory efficient symmetric key generation and pre-distribution scheme for wireless sensor networks. *IET wireless sensor systems*, 2(2):108–114, 2012.
- [14] Ashwag Albakri, Lein Harn, and Sejun Song. Hierarchical key management scheme with probabilistic security in a wireless sensor network (wsn). *Security and communication networks*, 2019, 2019.
- [15] Chongqing Kang and Liangzhong Yao. Key scientific issues and theoretical research framework for power systems with high proportion of renewable energy. *Automation of electric power systems*, 41(9):2–11, 2017.
- [16] Sanjeev Kulkarnil, Ashok M Sankpal, Ravindra R Mudholkar, et al. Recommendation engine: Matching individual/group profiles for better shopping experience. In *2013 15th International Conference on Advanced Computing Technologies (ICACT)*, pages 1–6. IEEE, 2013.
- [17] Chengshan Wang, Peng Li, Hao Yu, et al. Development and characteristic analysis of flexibility in smart distribution network. *Automation of Electric Power Systems*, 42(10):13–21, 2018.




PRINCIPAL
JMJ COLLEGE FOR WOMEN (Autonomous)
TENALI

Available online at www.sciencedirect.com

Chemical Engineering Research and Design

IChemE

journal homepage: www.elsevier.com/locate/cherd

Fabrication of dual-functional heterostructured p-CuO/n-ZnS nanocomposite for enhanced visible-light active photocatalytic response and fluorometric sensor for selective sensing of thiol-containing amino acids



Marri Pradeep Kumar^a, Aveli Rambabu^b, V. Sumalatha^c, G. Balraj^d,
Dasari Ayodhya^{d,e,*}

^a Department of Chemistry, Anurag University, Hyderabad 500088, Telangana, India

^b Department of Science and Humanities, St Martin's Engineering College, Hyderabad 500100, Telangana, India

^c Department of Chemistry, JMJ College for Women, Tenali 522201, Andhra Pradesh, India

^d Department of Chemistry, Osmania University, Hyderabad 500007, Telangana, India

^e Chemical Group, Intellectual Property India, Patent Office, GST Road, Guindy, Chennai 600032, Tamil Nadu, India

ARTICLE INFO

Article history:

Received 1 June 2023

Received in revised form 19 August 2023

Accepted 21 August 2023

Available online 24 August 2023

Keywords:

P-CuO/n-ZnS heterojunction

Co-precipitation method

Dyes degradation

Amino acids sensing

Detection limit

ABSTRACT

In this study, CuO, ZnS, and p-CuO/n-ZnS heterojunction composites were synthesized using a simple co-precipitation method for investigating their photocatalytic properties for dye degradation and fluorescence sensing of thiol-containing amino acids at room temperature. The synthesized CuO, ZnS, and p-CuO/n-ZnS heterostructures were analyzed using UV-vis, PL, XRD, and TEM. The results showed that the heterostructure exhibited enhanced absorption in the visible light range, and synthesized materials have spherical shape with an average particle size is 12 ± 5 nm. The photocatalytic activities of CuO, ZnS, and p-CuO/n-ZnS heterostructures were evaluated by the degradation of various dyes such as MB, MO, and MR under visible light irradiation. The p-CuO/n-ZnS heterostructure showed the best photocatalytic efficiency, with degradation rates of 98.3%, 94.2%, and 92.8% for MB, MO, and MR dyes, respectively, compared to CuO NPs (72.5%, 75.8%, and 73.5%) and ZnS NPs (76.2%, 79.1%, and 78.3%) within a 35 min of reaction. The enhanced photocatalytic efficiency of the p-CuO/n-ZnS heterostructure was attributed to its high charge separation efficiency, which remained stable for up to five cycles without any significant loss of activity. Furthermore, the p-CuO/n-ZnS heterostructure was used as a fluorescent sensor for detecting thiol-containing amino acids such as cysteine (Cys) and methionine (Met). The results showed that the heterostructure had good sensing performance for Cys and Met within the range of 1–100 μ M, with a detection limit of 2.52 μ M (Cys) and 5.14 μ M (Met) based on the linear calibration range. Moreover, p-CuO/n-ZnS composite was used to detect Met in human serum and urine samples.

© 2023 Institution of Chemical Engineers. Published by Elsevier Ltd. All rights reserved.

* Corresponding author at: Department of Chemistry, Osmania University, Hyderabad 500007, Telangana, India.

E-mail address: ayodhyadasari@gmail.com (D. Ayodhya).

<https://doi.org/10.1016/j.cherd.2023.08.034>

0263-8762/© 2023 Institution of Chemical Engineers. Published by Elsevier Ltd. All rights reserved.



1. Introduction

Designing an efficient hybrid structure photocatalyst for photocatalytic decomposition has been considered a great choice to develop renewable technologies for clean energy production and environmental remediation (Ayodhya, 2023; Chen et al., 2023a; Zhang et al., 2022). For this, the heterogeneous and heterojunction-based photocatalysts can greatly inhibit the recombination of electron-hole pairs, and enhance light utilization rate via broadening the spectral response (Zhang et al., 2017). A typical photocatalytic system requires materials that have an ideal bandgap to effectively harvest a large portion of the solar spectrum, and they must have suitable conduction and valence band edges for targeted reactions (Hu et al., 2020). At the same time, these materials should be abundant, easily accessible and stable in the long term. Semiconductor materials, especially metal oxides and metal sulfides, meet these requirements well. On the other hand, the photocatalytic activities and gas sensitivities are enhanced by using materials with high specific surface area, which provides abundant reactive sites for increasing the adsorption of target species. Some general strategies, such as decreasing particle sizes to nanoscale or designing corresponding two-dimensional nanosheet forms, are employed to increase the surface area (Trang et al., 2020). Among the numerous semiconductors, CuO and ZnS have been widely used as hybrid photocatalysts due to their remarkable photocatalytic activity, appropriate band gap, and stability against photocorrosion (Ayodhya, 2023). Among these hybrid composites, p-n type heterostructure ones present excellent photocatalytic activity (Xiong et al., 2022). The p-n heterostructure possesses a built-in electrical potential in the space charge region from the n-type side to the p-type side, which can direct the carriers to quickly migrate in the opposite direction, leading to effective separation and longer lifetime of charge carriers (Zhu et al., 2022; Xiong et al., 2023).

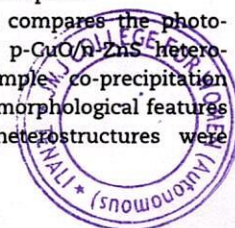
Fluorescent and colorimetric methods have recently gained attention for selective discrimination of amino acids in sensing applications. The various techniques such as indicator-displacement assays, metal complex coordination, specific reactions between probes and amino acids have been widely used for this purpose (Chen et al., 2010). Thiol-containing amino acids serve as important marker molecules in biological systems, with high levels of disulfide cysteine in urine indicating kidney dysfunction, while plasma cysteine levels are linked to Alzheimer's and Parkinson's diseases (Yeom et al., 2022). Accurate determination of thiol levels provides critical insight into physiological functions and disease diagnosis. Several techniques have been described in literature for determination of thiols, including colorimetry, chromatography, spectrophotometry, fluorescent spectrometry, electrochemical methods, and flow injection spectrophotometry (Reliene et al., 2004; Huang et al., 2018; Chen et al., 2023b; Ayodhya and Veerabhadram, 2018; Arshad et al., 2023; de Toledo Fornazari et al., 2005). Among these techniques, fluorescent methods have gained significant attention due to their high sensitivity, low cost, simplicity, and rapid response (Chen et al., 2023b; Ayodhya and Veerabhadram, 2016a; Chen et al., 2021). Based on these reports, we have developed and analyzed a fluorescent sensing method for the detection of amino acids.

In recent years, p-n heterojunctions based semiconductors made of transition metal oxides and metal

sulfides have garnered significant interest in various fields, including optics, optoelectronics, photovoltaics, electrochemistry, and photocatalysis, among others. ZnS is a wide band gap material that exhibits excellent properties, such as n-type conductivity, a direct band gap of approximately 3.37 eV at room temperature, and a high exciton binding energy of 55 meV, which makes excitons thermally stable even at room temperature (Ayodhya and Veerabhadram, 2016b; Pawar et al., 2017). Due to its exceptional fundamental properties, ZnS is used in numerous applications, including sensors, bio-devices, light-emitting diodes, lasers, infrared windows, and flat panel displays (Ayodhya and Veerabhadram, 2016b). In other hand, metal oxides are also promising materials for gas-sensing applications due to their low cost, high stability, and compatibility with microelectronic processing. They are extensively studied for detecting harmful gases such as CO, NH₃, NO₂, ethanol, and acetone (Ayodhya and Veerabhadram, 2020). CuO is a p-type semiconductor that has a narrow band gap of 1.2 eV, excellent stability, and good electrical properties (Ayodhya, 2023; Hajji et al., 2023). It is a compelling option for selective solar absorption as it has high solar absorbency and low thermal emittance (Sumalatha et al., 2023). These two semiconductors are attractive for various applications due to their affordability, abundance, and non-toxicity.

In particular, ZnS can be applied to the fabrication of UV light sensors and gas sensors. Over the past decade, several ZnS nanostructure based gas sensors have been reported including for H₂ sensing (Wan and Wang, 2005; Kim et al., 2012), O₂ sensing (Kolmakov et al., 2005), acetone and ethanol sensing (Park et al., 2013), and glutathione sensing (Wang et al., 2023), etc. On the other hand, ZnS nanostructures-based gas sensors have attracted less attention than metal oxide semiconductor nanostructures-based gas sensors (Wan and Wang, 2005; Kim et al., 2012; Kolmakov et al., 2005; Park et al., 2013; Wang et al., 2023). Further, the various CuO nanostructures including nanoparticles, nanorods/wires, nanoribbons, micro-dandelions, nanoflowers, hollow spheres, nanoplates, spindle, nanofilms, and hierarchical nanostructures have been successfully prepared and some of them were investigated for sensing applications (Yang et al., 2011; Sankaran a and Kumaraguru, 2020; Krishnan et al., 2014). For example, D. Kim et al. reported the detection of hydrogen gas by porous CuO nanowires prepared with carbon nanotube template (Hoa et al., 2010). Leaflet-like CuO nanosheets were found to have highly sensitive sensing to H₂S (Zhang et al., 2010). Very recently, I. Singh et al. prepared CuO nanocrystals with a sol-gel method and investigated their NH₃ sensing performances (Bedi and Singh, 2010). Even though, p-n heterojunction constitutes the vital part of vast majority of electronic devices, the p-CuO/n-ZnS heterojunction composites have not been studied enough. Previous works (Chabane et al., 2015; Park et al., 2016), were mainly focused on the application of p-CuO/n-ZnS hetero-contact for CO, H₂, gas sensors or humidity sensing. However, the efficiency of the hetero-junctions and current transport mechanism are limited by the inevitable presence of defects at the interface and in volume. The level of understanding hetero-junction behavior is far from complete.

The present work examines and compares the photocatalytic and sensing properties of p-CuO/n-ZnS heterojunctions prepared through a simple co-precipitation method. The optical, structural, and morphological features of CuO, ZnS, and p-CuO/n-ZnS heterostructures were



analyzed using various techniques. The p-CuO/n-ZnS heterostructure was found to be an excellent catalyst for the photocatalytic degradation of MB, MO, and MR dyes, owing to the efficient transfer of electrons and the physical detachment of charge carriers upon generation. Additionally, the fluorescent sensing properties of p-CuO/n-ZnS heterojunctions were evaluated for the detection of Cys and Met at nM concentrations.

2. Experimental

2.1. Materials

Zinc acetate ($\text{Zn}(\text{CH}_3\text{COO})_2 \cdot 2 \text{H}_2\text{O}$), copper acetate ($\text{Cu}(\text{CH}_3\text{COO})_2 \cdot 3 \text{H}_2\text{O}$), sodium sulfide (Na_2S), sodium hydroxide (NaOH), methylene blue, methyl orange, methyl red, and ethanol were purchased from Sigma Aldrich chemicals, India. The amino acids including arginine (Arg), asparagine (Asn), aspartic acid (Asp), cysteine (Cys), glutamic acid (Glu), glutamine (Gln), glycine (Gly), histidine (His), isoleucine (Ile), leucine (Leu), lysine (Lys), methionine (Met), phenylalanine (Phe), proline (Pro), serine (Ser), threonine (Thr), tyrosine (Tyr), and tryptophan (Trp) were purchased from Merck chemicals, India. Phosphate buffered solutions (NaH_2PO_4 - Na_2HPO_4) were purchased from S D Fine chemicals, India. All the reagents were of analytical grade (99.0%) and used without purification. All aqueous solutions were prepared using double distilled water.

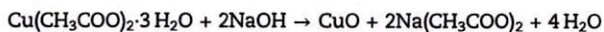
2.2. Synthesis of samples

2.2.1. Synthesis of ZnS NPs

The procedure for the synthesis of ZnS NPs was based on a previous study (Ayodhya and Veerabhadram, 2019), a solution of 0.1 M zinc acetate dihydrate (25 mL) was mixed with 0.1 M sodium sulfide (25 mL) to obtain ZnS NPs. The resulting white solid product was obtained by centrifugation, washed with distilled water, dried at 70 °C for 24 h, and then calcined at 550 °C for 2 h.

2.2.2. Synthesis of CuO NPs

For the synthesis of CuO NPs, a co-precipitation method was employed, according to a previous literature (El-Trass et al., 2012). Copper acetate (25 mM) and sodium hydroxide (100 mM) in ethanol were reacted at 70 °C for 24 h, and then calcined at 550 °C for 2 h resulting in the formation of CuO NPs.



The prepared particles were washed and centrifuged with distilled water, absolute ethanol, and acetone in sequence to remove the by-products and dried in air at room temperature.

2.2.3. Synthesis of p-CuO/n-ZnS heterostructure

To synthesize the p-CuO/n-ZnS heterostructure, 1 g of previously calcined ZnS NPs (at 400 °C for 5 h) was mixed in an aqueous solution of copper acetate (0.2454 g, 8 mol%). The mixture was stirred for 48 h to allow the penetration of copper ions on the ZnS crystal matrix. The supernatant water was evaporated by heating the mixture at 70 °C over a time of 24 h. The resulting product was calcined at 550 °C for 2 h.

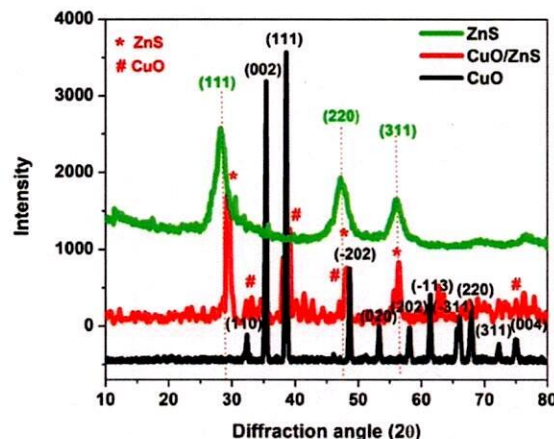


Fig. 1 – XRD patterns of the synthesized CuO, ZnS, and p-CuO/n-ZnS heterostructures.

2.3. Characterizations

The surface morphology of the p-CuO/n-ZnS heterojunction composite was examined using a Tecnai G2 transmission electron microscope operating at an accelerating voltage of 200 kV for Transmission Electron Microscopy (TEM) analysis. The crystal nanostructure of the heterojunction was determined using X-ray diffraction (XRD, X'pert Pro) with $\text{CuK}\alpha$ radiation ($\lambda = 1.540598 \text{ \AA}$) operating at 45 kV and 40 mA in the 2θ range (10–80°) with a step scan of 0.02°. The optical properties of the composites were investigated using a UV-3600 PC Shimadzu spectrophotometer. The diffuse reflectance spectra of the samples were recorded in the wavelength range 200–800 nm using a UV-vis spectrophotometer equipped with an integrating sphere accessory, and BaSO_4 was used as a reference. Fluorescence spectra were recorded on a Shimadzu RF-5301PC spectrofluorometer with an excitation wavelength of 310 nm.

2.4. Photocatalytic activities

The photocatalytic activity of CuO, ZnS, and p-CuO/n-ZnS heterostructures was evaluated by measuring their ability to degrade MB, MO, and MR dyes under visible light irradiation. In this study, 0.02 g of photocatalyst was added to $5.2 \times 10^{-5} \text{ M}$ of 100 mL dye solution, which was stirred in the dark for 30 min in a photocatalytic reactor, and then exposed to halogen lamps (Philips, 54 W, $145 \mu\text{W}/\text{cm}^2$). At specific time intervals (every 5 min), the suspension was withdrawn and centrifuged to separate the solid catalyst. The concentration of the remaining dye solution was measured by a UV-visible spectrometer at the absorption peak of 664 nm (MB), 461 nm (MO), and 492 nm (MR). The degradation efficiency (%) of the dyes at different times was calculated using the following equation:

$$\text{Degradation efficiency (\%)} = \frac{C_0 - C_t}{C_0} \times 100$$

where C_0 and C_t are initial concentration and remaining concentration of dyes, respectively. The pseudo-first-order kinetics is widely studied to compare the photocatalytic activity of each photocatalyst, using the following equation: $\ln(C_t/C_0) = -k t$, wherein, the slope of a linear function gives the value of the apparent rate constant (k , min^{-1}).

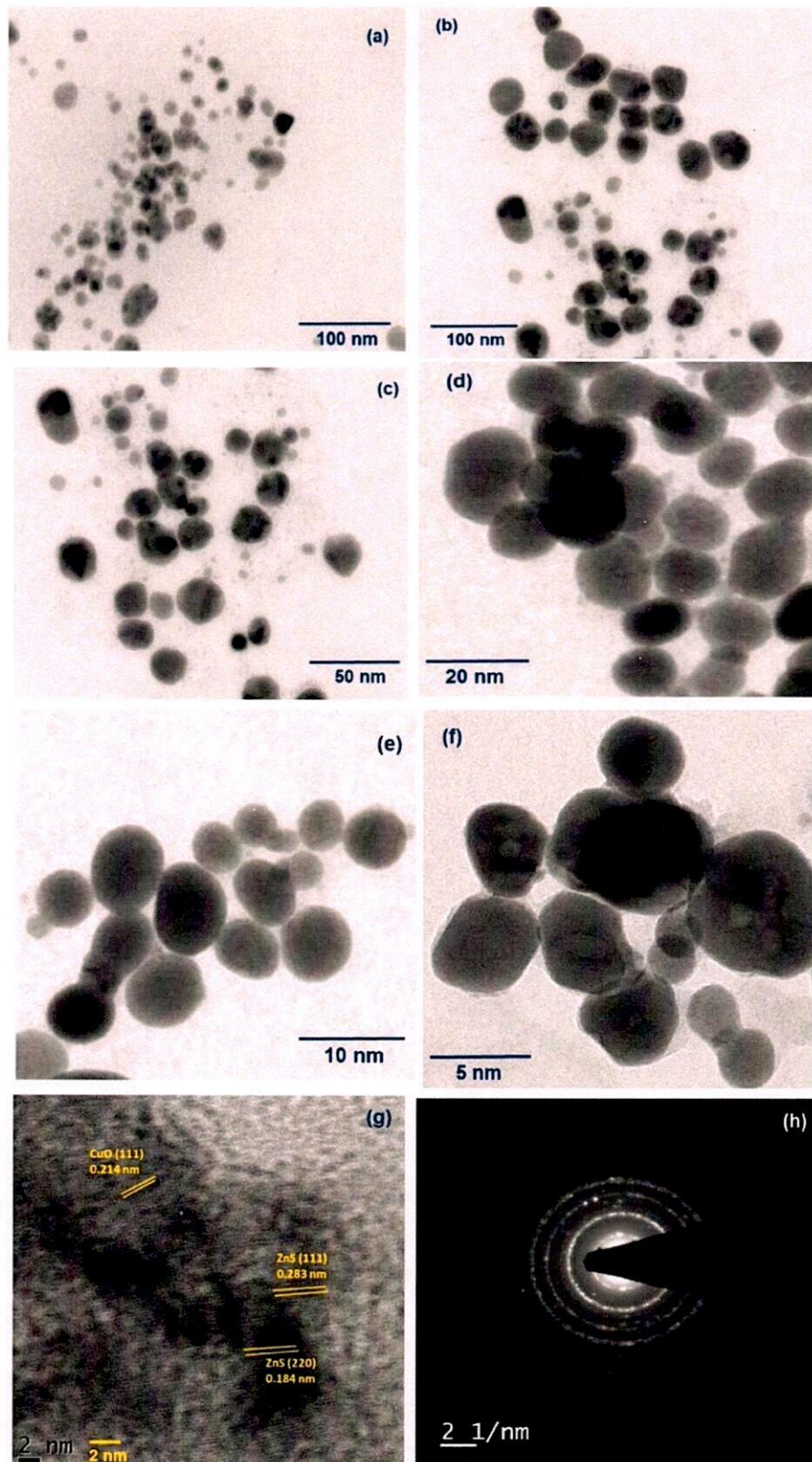
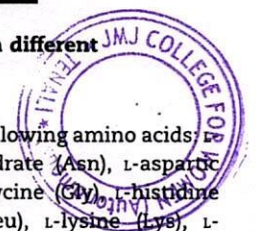


Fig. 2 - (a-g) TEM and HRTEM images of the synthesized CuO, ZnS, and p-CuO/n-ZnS composite with different magnifications, and (h) SAED pattern of p-CuO/n-ZnS heterostructure.

2.5. Fluorometric detection of Cys and Met

In order to study the selective sensing of p-CuO/n-ZnS heterostructure to Cys and Met compared to other α -amino

acids, the experiment employed the following amino acids: arginine (Arg), L-asparagine monohydrate (Asn), L-aspartic acid (Asp), L-glutamic acid (Glu), L-glycine (Gly), L-histidine (His), L-isoleucine (Ile), L-leucine (Leu), L-lysine (Lys), L-



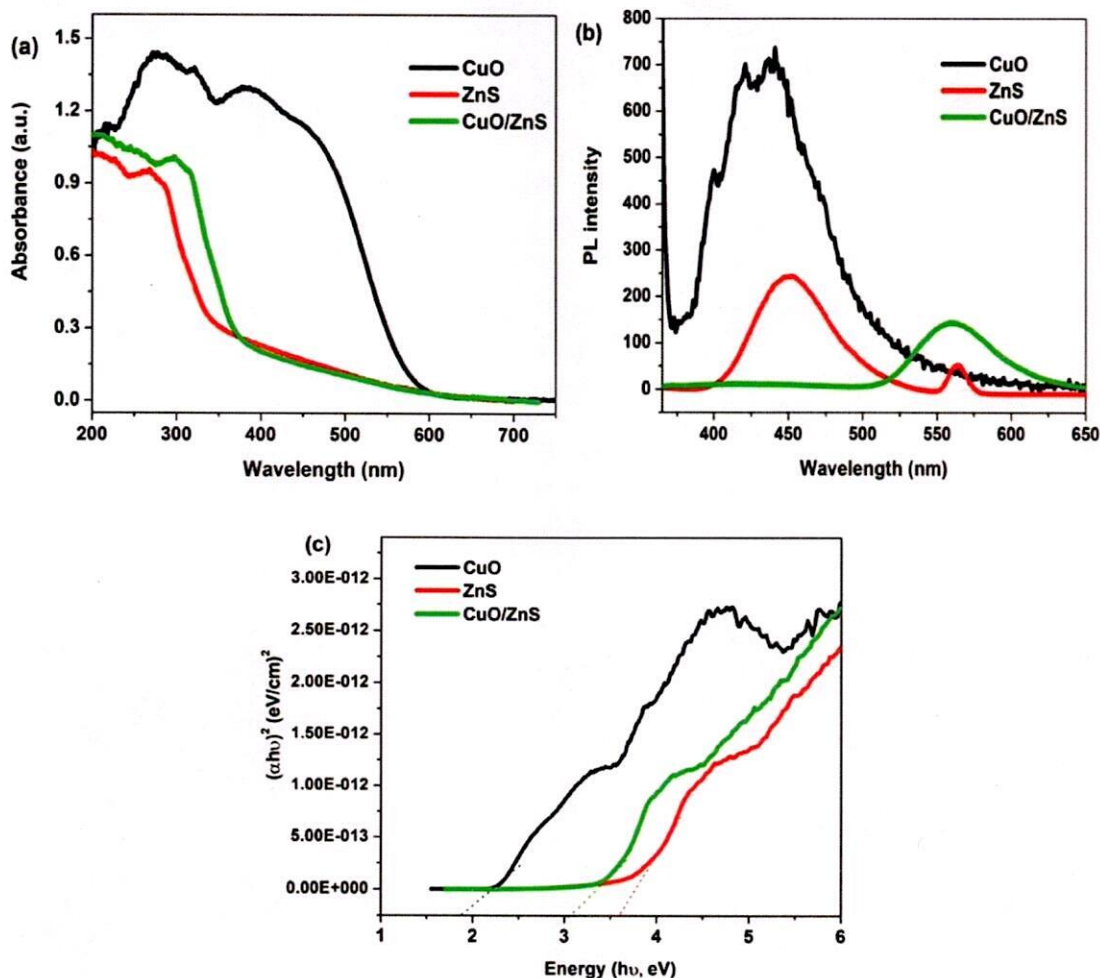


Fig. 3 – (a) UV-vis DRS, (b) PL spectra, and (c) Tauc plot of the synthesized CuO, ZnS, and p-CuO/n-ZnS heterostructures.

phenylalanine (Phe), L-proline (Pro), L-serine (Ser), L-threonine (Thr), L-tryptophan (Trp), and L-tyrosine (Tyr). The amino acids were dissolved in 100 mM sodium hydroxide solution to prepare standard solutions, which were stored at 4 °C in the dark. Dilute solutions were prepared daily before use. Next, the appropriate volume of amino acid solution was mixed with p-CuO/n-ZnS heterostructure for spectral measurements. To quantify the concentration of Cys and Met, different concentrations of these amino acids were mixed with 100 μ L of 10 μ M (pH = 7.4) PBS solution and 400 μ L p-CuO/n-ZnS (15 nM) at room temperature. The PL spectra of the p-CuO/n-ZnS solution were observed after 5 min, and the concentration of Cys and Met was measured using a quenching measurement analysis. All experiments were conducted at room temperature.

2.6. Preparation of real samples

A 1.0 mL human urine sample was obtained from healthy adult male volunteers and processed for analysis. To remove proteins, 1.0 mL of acetonitrile was added to the urine sample in a centrifuge tube, followed by centrifugation at 12,000 rpm for 10 min. The resulting supernatant was filtered through a 0.22 μ m filter and dried under vacuum at 50 °C for 10 h. The dried sample was diluted to 5 mL with double distilled water before analysis.

Human serum was collected from healthy donors of Osmania University dispensary. A 0.5 mL sample of human serum was placed in a centrifuge tube, and 2.0 mL of acetonitrile was added to precipitate proteins. The mixture was vortex-mixed and centrifuged at 12,000 rpm for 15 min. The resulting supernatant was transferred into a 25.0 mL volumetric flask and diluted to the mark with double distilled water. For fluorometric detection, 1.3 μ M Met at different concentrations was mixed with 10 μ L of either the human urine sample or human serum sample. The resulting mixture was added to the p-CuO/n-ZnS solution to obtain a final detective volume of 2 mL.

3. Results & discussion

3.1. Structural analysis

X-ray diffraction (XRD) analysis was employed to assess the phase, composition, and purity of the synthesized CuO, ZnS, and p-CuO/n-ZnS heterostructures. The peaks observed at $2\theta = 32.4^\circ$ (1 1 0), 35.6° (0 0 2), 38.8° (1 1 1), 48.9° (2 0 2), 53.2° (0 2 0), 58.3° (2 0 2), 61.6° (-1 1 3), 66.4° (-3 1 1), 67.9° (2 2 0), 73.8° (3 1 1), and 76.5° (0 0 4) and crystal planes corresponded to the characteristic diffraction peaks of CuO with monoclinic phase (JCPDS No. 45-0937) and their intensities and positions were in agreement with previously reported values (Ayodhya, 2023). The diffraction peaks observed at 28.6° (1 1 0), 35.6° (0 0 2), 38.8° (1 1 1), 48.9° (2 0 2), 53.2° (0 2 0), 58.3° (2 0 2), 61.6° (-1 1 3), 66.4° (-3 1 1), 67.9° (2 2 0), 73.8° (3 1 1), and 76.5° (0 0 4) and crystal planes corresponded to the characteristic diffraction peaks of CuO with monoclinic phase (JCPDS No. 45-0937) and their intensities and positions were in agreement with previously reported values (Ayodhya, 2023). The diffraction peaks observed at 28.6° (1 1 0), 35.6° (0 0 2), 38.8° (1 1 1), 48.9° (2 0 2), 53.2° (0 2 0), 58.3° (2 0 2), 61.6° (-1 1 3), 66.4° (-3 1 1), 67.9° (2 2 0), 73.8° (3 1 1), and 76.5° (0 0 4) and crystal planes corresponded to the characteristic diffraction peaks of CuO with monoclinic phase (JCPDS No. 45-0937) and their intensities and positions were in agreement with previously reported values (Ayodhya, 2023).

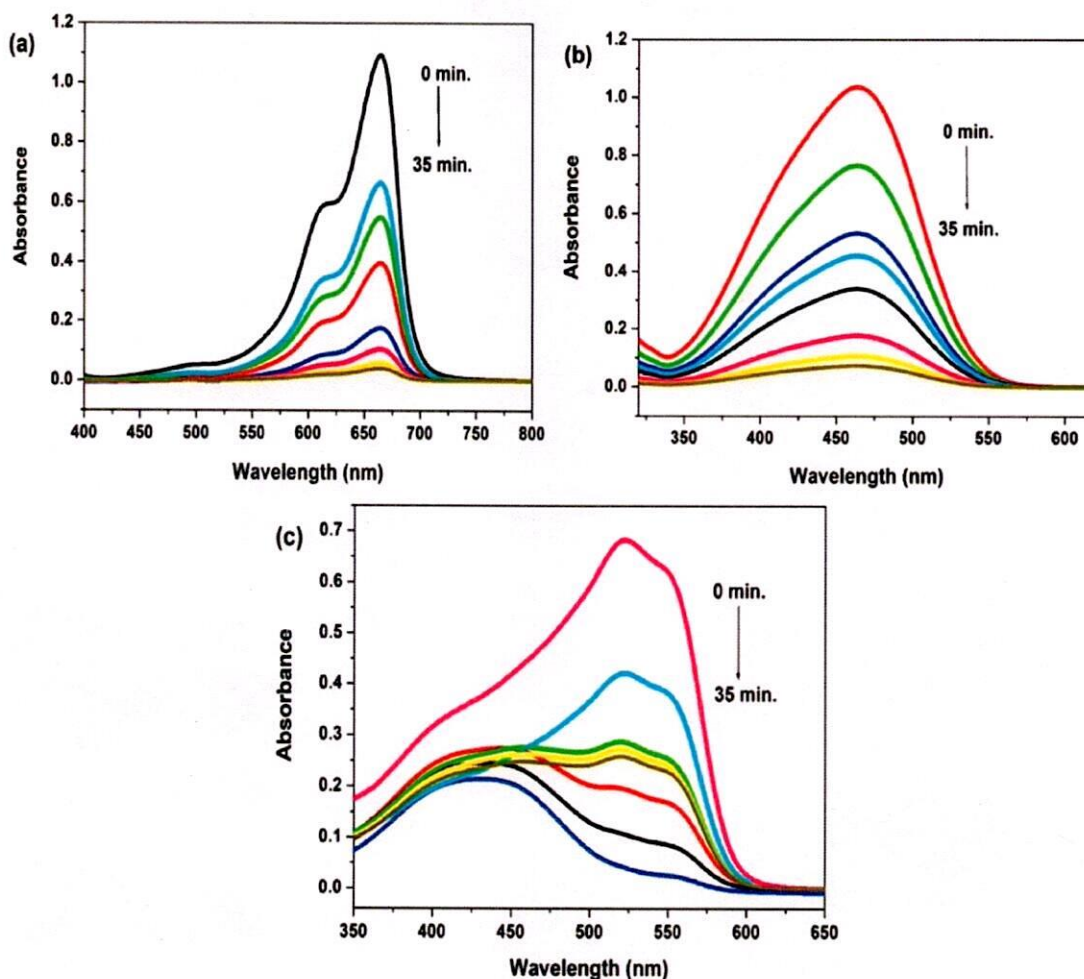


Fig. 4 – UV-vis absorption spectra of the photocatalytic degradation of (a) MB, (b) MO, and (c) MR dyes using p-CuO/n-ZnS heterostructures.

1), 47.6° (2 2 0), and 56.4° (3 1 1) were indexed to ZnS with cubic zinc blend structure (JCPDS No. 05-0566) (Chen et al., 2023a; Goudarzi et al., 2009). From Fig. 1, the XRD pattern of p-CuO/n-ZnS composite, it is noteworthy that the characteristic peak of ZnS in p-CuO/n-ZnS is sharp and perfectly maintains the crystalline phase structure of ZnS, while the characteristic diffraction peak belonging to CuO also appears. Due to the low intensity of the characteristic diffraction peaks of CuO and the high particle dispersion and small particle size in the complex and defects in the lattice structure; which is in agreement with a previous report (Sharma et al., 2017). The average grain size of the p-CuO/n-ZnS heterostructure was estimated at approximately 18 ± 2 nm using the Debye-Scherrer equation.

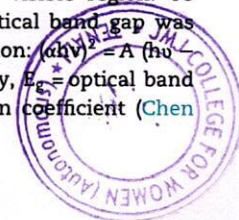
3.2. Morphological analysis

To determine the contact state of CuO with ZnS, the high-resolution morphology image of the p-CuO/n-ZnS sample was examined using TEM. The morphological and structural features of CuO, ZnS, and p-CuO/n-ZnS were observed using TEM images, as shown in Fig. 2(a-g). The TEM images revealed that the ZnS and CuO grains were closely connected, with clear ZnS and CuO lattice fringes indicating the formation of the p-CuO/n-ZnS heterojunction. Fig. 2(g) gives the HRTEM image of p-CuO/n-ZnS heterojunction, which clearly

shows an interface between the ZnS and CuO. The intimate contact between the two sections is conducive to charge transport and separation. The slightly larger *d*-spacing value for the (1 1 1) plane in the ZnS than that in the CuO section is in agreement with the composition contrast between the CuO and ZnS. The p-CuO/n-ZnS heterostructure sample was observed to be a spherical shape and particle size is ≈ 15 nm. Additionally, Fig. 2(h) showed a SAED pattern, which indicated that both ZnS and CuO nanoparticles were polycrystalline as the reflection spots were on concentric rings.

3.3. Optical analysis

To evaluate the optical properties of the photocatalyst, diffuse reflectance spectroscopy analysis was conducted. The UV-vis DRS spectra of CuO, ZnS, and p-CuO/n-ZnS composite from 250 to 750 nm are presented in Fig. 3(a). All samples show an absorption edge at around 300–400 nm, but the p-CuO/n-ZnS heterostructure exhibits stronger absorption under visible light, indicating high utilization efficiency for visible light. While ZnS only absorbs in the UV region and CuO shows absorption throughout the visible region. To calculate valence band position, the optical band gap was determined by the following Tauc equation: $(\alpha h\nu)^2 = A(h\nu - E_g)$, where A = constant, $h\nu$ = light energy, E_g = optical band gap energy, and α = measured absorption coefficient (Chen



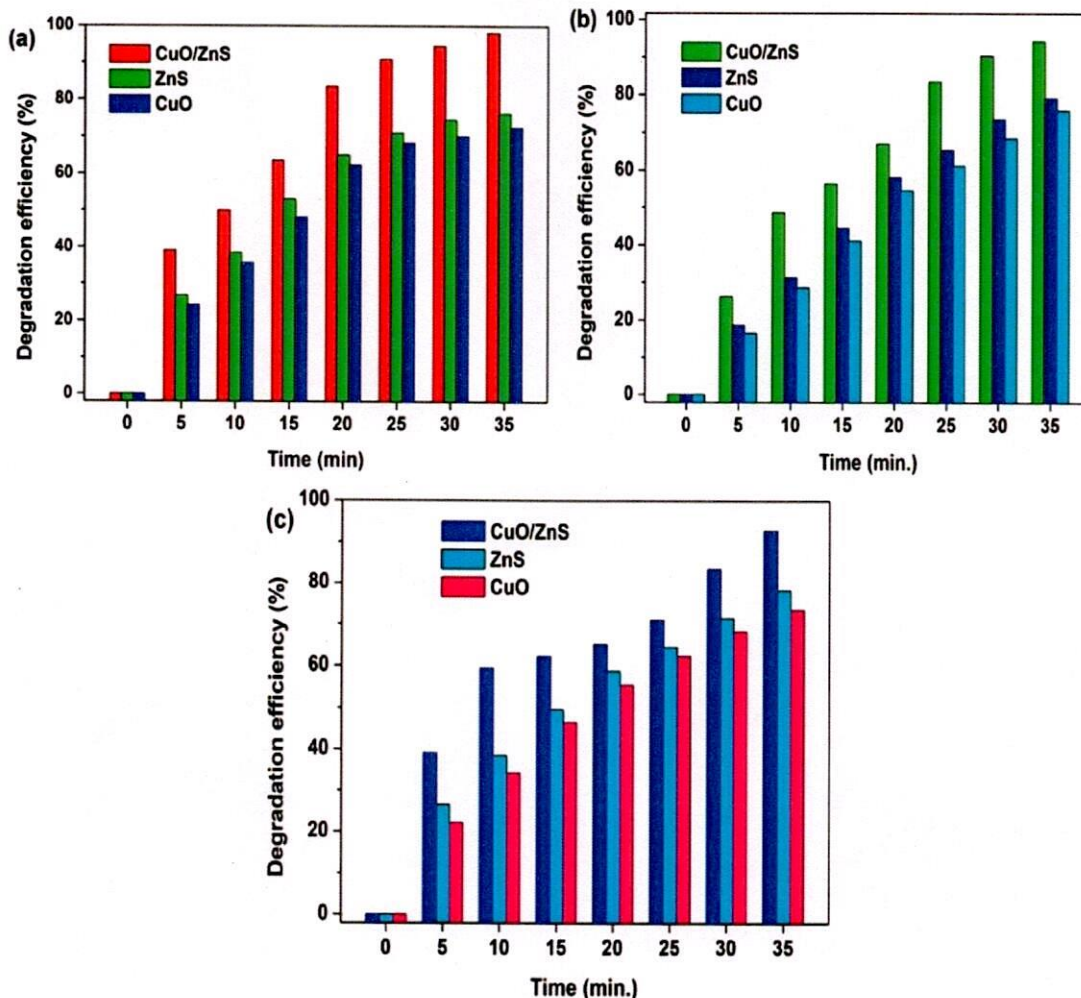


Fig. 5 – The bar diagrams for the comparison of photocatalytic activity of CuO, ZnS, and p-CuO/n-ZnS heterostructures for the degradation of (a) MB, (b) MO, and (c) MR dyes.

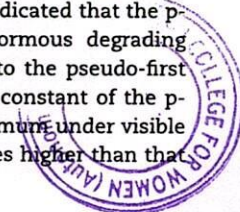
et al., 2011). In the Fig. 3(c), the extrapolation of the Tauc plot on x-intercepts gives the optical band gaps of 1.81 eV, 3.04 eV, and 3.57 eV for CuO, p-CuO/n-ZnS, and ZnS, respectively. The increased utilization efficiency of visible light is an important factor in improving the photocatalytic performance of CuO-based materials (Yang et al., 2015), and it has been shown that this is one of the factors that have improved the photocatalytic performance of p-CuO/n-ZnS composites.

Photoluminescence (PL) analysis is an important method for determining the separation of electron/hole pairs and the ability to trap charge carriers in p-CuO/n-ZnS composites (Fig. 3(b)). The PL spectra show that the PL emission is dependent on the excitation light wavelength in the range of 400–600 nm. Only one strong luminescence peak at about 450 nm and a shoulder peak at about 465 nm were observed from for the CuO NPs excited by 370 nm wavelength, which is good agreement with previous report (Zhao et al., 2015). Yang et al (Yang et al., 2001). has also reported that pure ZnS NPs show the only luminescent peak at 450 nm. It was therefore reasonable to believe that the blue light emission from the ZnS NPs in our work could be attributed to the surface states. However, another broad and weak luminescent peak (about 565 nm) of ZnS NPs has also been observed in our work. In addition, the remarkably quenched PL intensity of the p-CuO/n-ZnS composite indicates a low recombination

efficiency of photogenerated electrons with holes and more effective carrier migration and separation between ZnS and CuO. Therefore, the p-CuO/n-ZnS composite has an excellent photocatalytic behavior is frequently accompanied by higher charge separation efficiency.

3.4. Photocatalytic activity

The photocatalytic performance and recycling stability of the synthesized CuO, ZnS, and p-CuO/n-ZnS heterostructure were evaluated for the degradation of dyes. First, CuO and ZnS NPs showed a similar and weak adsorption capacity. Under visible light irradiation, only a small amount (12.2%, 10.8%, and 8.4%) of MB, MO, and MR dyes were degraded in the absence of photocatalyst, respectively. Nevertheless, the p-CuO/n-ZnS heterostructure could remove efficiently (98.3%, 94.2%, and 92.8%) than the CuO NPs (72.5%, 75.8%, and 73.5%) and ZnS NPs (76.2%, 79.1%, and 78.3%) with in 35 min of irradiation, respectively as shown in Fig. 4(a-c), Fig. 5(a-c), and Fig. 6(a-c). These results indicated that the p-CuO/n-ZnS heterostructure have an enormous degrading efficiency under visible light. According to the pseudo-first order rate reaction, the degradation rate constant of the p-CuO/n-ZnS heterostructure reached maximum under visible light, which is approximately several times higher than that



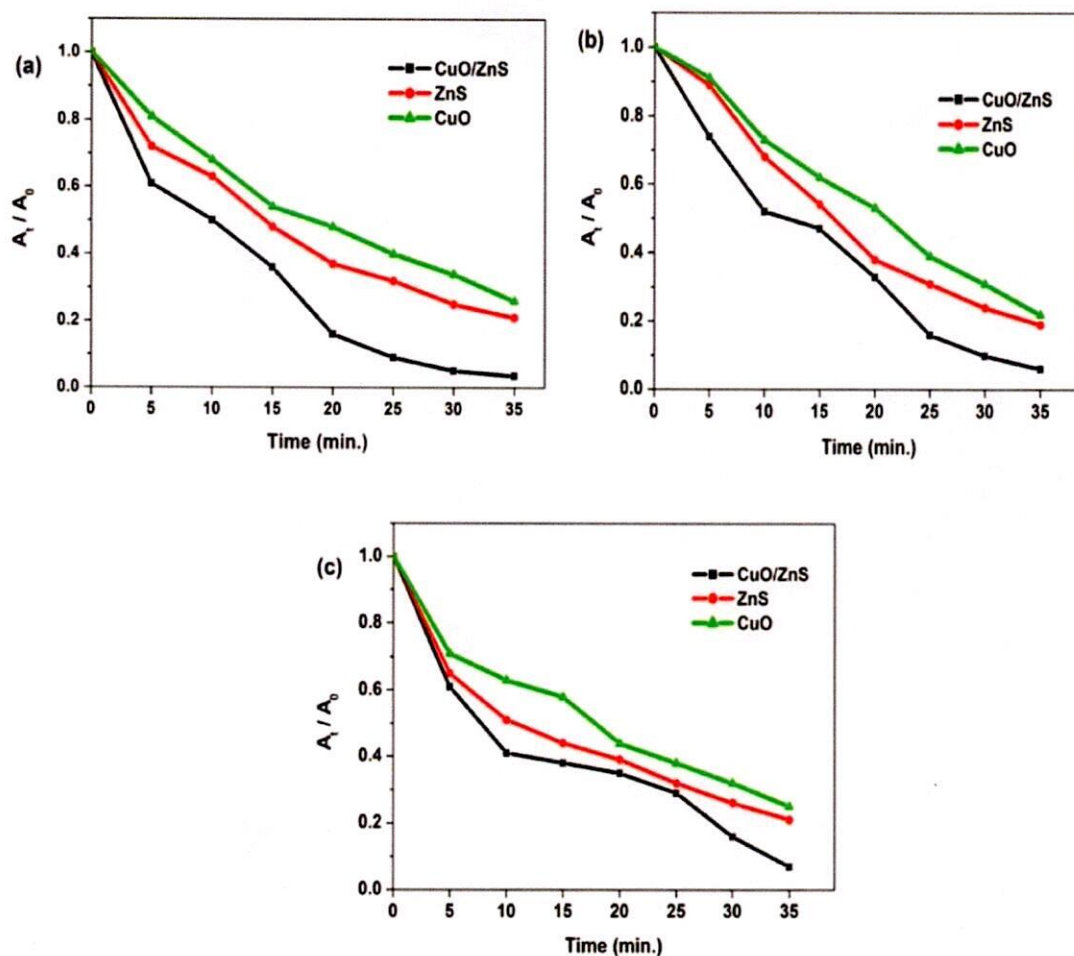


Fig. 6 – The plots of A_t/A_0 vs time for the photocatalytic degradation of (a) MB, (b) MO, and (c) MR dyes using CuO, ZnS, and p-CuO/n-ZnS heterostructures.

of ZnS and CuO NPs (Fig. 7(a-c)). The detailed degradation efficiencies and rate constants for the degradation of dyes were summarized in Table 1. These results indicated that CuO coupling can effectively enhance the photocatalytic activity of ZnS under visible light. In addition, when the p-CuO/n-ZnS heterostructures are formed, photogenerated e^- in the conduction band are easily transferred from CuO to ZnS and parts of h^+ in the valence band are transferred in an opposite direction, which is beneficial for separating photogenerated electron holes to enhance the photocatalytic activity. Fig. 8 shows the recycling ability of p-CuO/n-ZnS heterostructure under visible light for the degradation of MB, MO, and MR dyes. As the number of cycles increases, the time complete degradation is unchanged, which reveals that the p-CuO/n-ZnS heterostructure have prominent photocatalytic stability.

3.5. Detection of active species in the degradation of dyes

To investigate the effect of different active species in the photocatalytic reaction, a series of quenchers were used to scavenge the relevant active species in a manner that mimics the photocatalytic activity test (Yendrapati Taraka et al., 2019). The impact of the $\cdot OH$ radical, $\cdot O_2^-$, 1O_2 , and h^+ were examined by adding 1.0 mM of benzoquinone (BQ), which is a quencher of $\cdot O_2^-$, 1.0 mM of isopropanol (IPA), which is a quencher of $\cdot OH$, 1.0 mM of ammonium oxalate (AO), which

is a quencher of h^+ , and 1.0 mM of sodium azide (SA), which is a quencher of 1O_2 . As shown in Fig. 9, the degradation efficiency of BQ quenching decreased more than that of IPA and AO, but the addition of SA did not affect the photocatalytic degradation of MB, MO, and MR dyes. Therefore, the quenching effect caused by various scavengers indicated that the reactive $\cdot O_2^-$ played a crucial role, whereas the $\cdot OH$ and h^+ played minor roles in the degradation of MB, MO, and MR dyes.

3.6. Photocatalytic degradation mechanism

Despite the experimental efforts to investigate the electronic structure of p-CuO/n-ZnS heterostructure, we were focused on the description of the electronic aspects associated with the electronic excitation which generates the electron-hole pair responsible for the photocatalytic properties. The proposed degradation mechanism for the degradation of dyes using p-CuO/n-ZnS heterostructure was accurately shown in Fig. 10. From Fig. 10, the energy required for excitation of the electron from valence to conduction band is much lower for CuO. One of the main factors which determines the photocatalytic efficiency of semiconductor materials is preventing the recombination of photogenerated pairs (e^-/h^+) during the process, so that they act to produce species with high oxidative capacity of organic molecules. The lower E_g for CuO

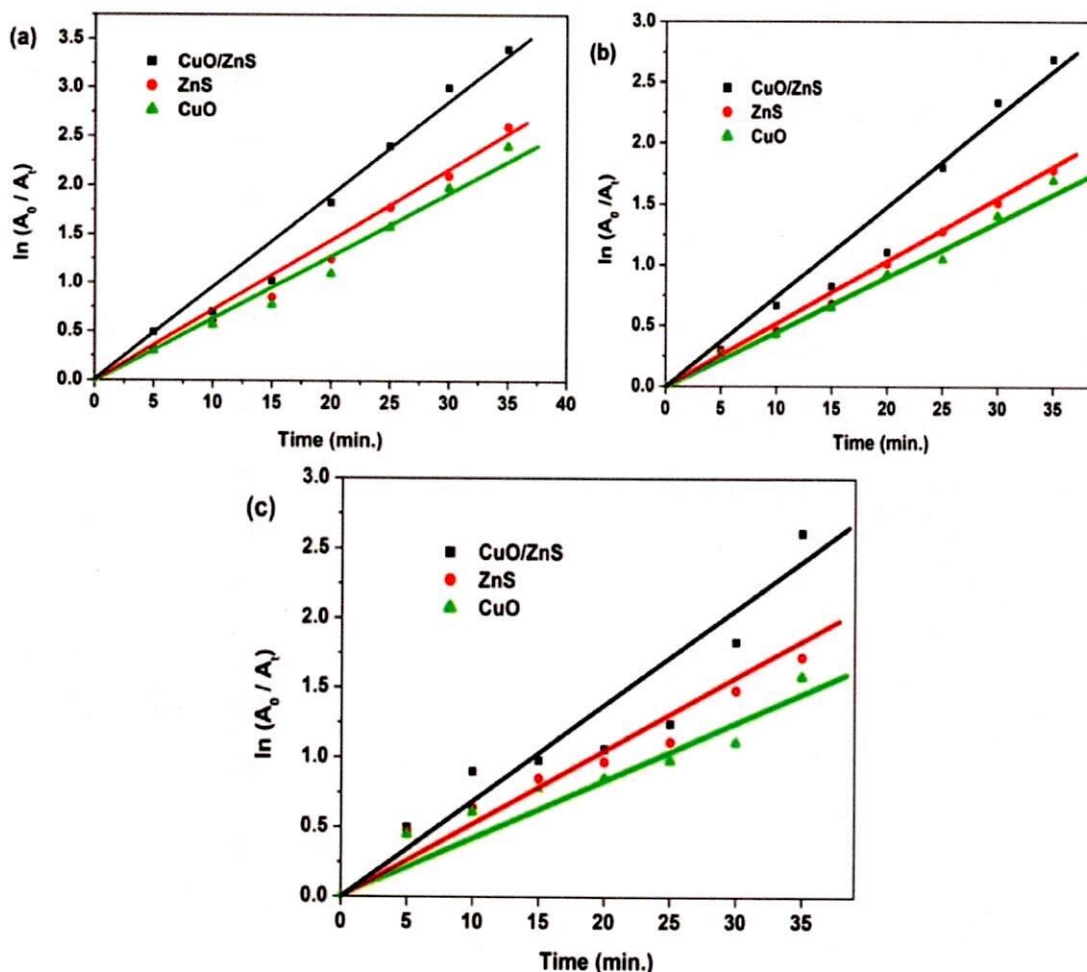


Fig. 7 – The kinetic plots for the photocatalytic degradation of (a) MB, (b) MO, and (c) MR dyes using CuO, ZnS, and p-CuO/n-ZnS heterostructures.

enables a favored recombination for the photogenerated e^-/h^+ pairs during the catalytic process, while ZnS has a higher energy barrier. On the other hand, the formation of the CuO/ZnS heterostructure acts with CuO (p-type) capturing the solar radiation and its excited electrons migrate to the ZnS (n-type) conduction band, performing reduction reactions and generating superoxide species (Paul et al., 2018). Moreover, the electron transfer from CuO conduction band to the ZnS valence band is difficult, allowing the holes present in it to act in generating oxidation reactions, which in turn promote the formation of $\cdot\text{OH}$ and H_2O_2 species with high degradation capacity of pollutants (Yendrapati Taraka et al., 2019; Paul et al., 2018; Ayodhya, 2022).

3.7. Detection of thiol-containing amino acids

In the fluorescence detection of amino acids, along with the sensitivity requirement, high specificity and selectivity is crucial in most scenarios especially in real sample detections. To evaluate the selectivity of the fluorescence sensor of p-CuO/n-ZnS heterostructure, we measured the fluorescence intensity changes in the presence of the representative amino acids at different concentrations under the analogous conditions. Remarkably, among these tested amino acids (Arg, Asn, Asp, Cys, Glu, Gln, Gly, His, Ile, Leu, Lys, Met, Phe, Pro, Ser, Thr, Tyr, and Trp), only Cys and Met have a

significant effect on the fluorescence intensity of the p-CuO/n-ZnS (Fig. 11(a and d)). Thus, the p-CuO/n-ZnS heterostructure-based sensor shows good selectivity for Cys and Met over other amino acids.

To assess the sensitivity of the p-CuO/n-ZnS heterostructure for detecting Cys and Met using fluorescence, we monitored the changes in fluorescence intensity at 560 nm as a function of the concentrations of Cys and Met, as shown in Fig. 11(b-c and e), respectively. The fluorescence emission of the p-CuO/n-ZnS heterostructure at 560 nm exhibited varying responses at different concentration ranges of Cys and Met. As depicted in Fig. 11(b-c), the fluorescence emission of the p-CuO/n-ZnS heterostructure at 560 nm was significantly quenched at Cys and Met concentrations ranging from 1 to 100 μM .

3.8. Possible mechanism for the fluorescence detection of Cys and Met

The fluorescence quenching is usually divided into static quenching and dynamic quenching. The dynamic quenching can be described by Stern–Volmer's equation (Ayodhya, 2023):

$$F_0/F = 1 + K_{sv}[Q],$$

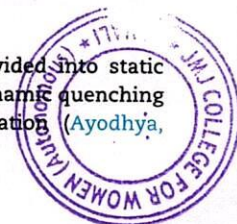


Table 1 – The photocatalytic parameters such as degradation efficiency and rate constants with correlation factor for the photocatalytic degradation of MB, MO, and MR dyes using CuO, ZnS, and p-CuO/n-ZnS heterostructures.

Dye	Catalysts	Degradation efficiency (%)	Rate constant (min ⁻¹)	Half-life time (min)	R ²
MB	No catalyst	12.2	0.0132	52.5	0.98
	CuO	72.5	0.1478	4.68	0.98
	ZnS	76.2	0.1586	4.37	0.99
	P-CuO/n-ZnS	98.3	0.3685	1.88	0.98
MO	No catalyst	10.8	0.0128	54.1	0.97
	CuO	75.8	0.1452	4.77	0.97
	ZnS	79.1	0.1763	3.93	0.99
	P-CuO/n-ZnS	94.2	0.3125	2.22	0.98
MR	No catalyst	8.4	0.0101	68.6	0.98
	CuO	73.5	0.1511	4.58	0.98
	ZnS	78.3	0.1620	4.27	0.97
	P-CuO/n-ZnS	92.8	0.3012	2.30	0.99

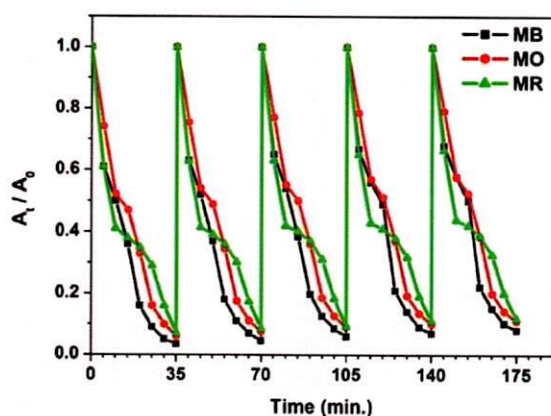


Fig. 8 – Stability and recyclability of p-CuO/n-ZnS heterostructure catalyst for the photocatalytic degradation of MB, MO, and MR dyes.

where F_0 and F are the fluorescence intensities of the p-CuO/n-ZnS heterostructure in the absence and in the presence of a quencher, respectively, $[Q]$ is the concentration of the quencher (Cys and Met), and K_{sv} is the dynamic quenching constant. These results may imply the formation of a non-fluorescence ground state complex between the surface of p-CuO/n-ZnS heterostructure and Cys as well as Met. However, we investigate the emission spectra of p-CuO/n-ZnS heterostructure in the presence of varying Cys and Met concentrations to probe the fluorescence quenching mechanism of Cys and Met (Fig. 11(f)). As shown in Fig. 11(f), the absorption band of p-CuO/n-ZnS heterostructure is changed greatly in the presence of Cys and Met. With increasing the concentration of Cys and Met, the fluorescence emission at 560 nm is decreased gradually, accompanied with an obvious red shift of the absorption peak. Considering the existence of thiol group in Cys and Met; and the observed changes in both absorption and emission spectra of p-CuO/n-ZnS heterostructure. Therefore, we propose that the added Cys and Met interacted directly with p-CuO/n-ZnS heterostructure through the strong thiol-heterostructure interaction.

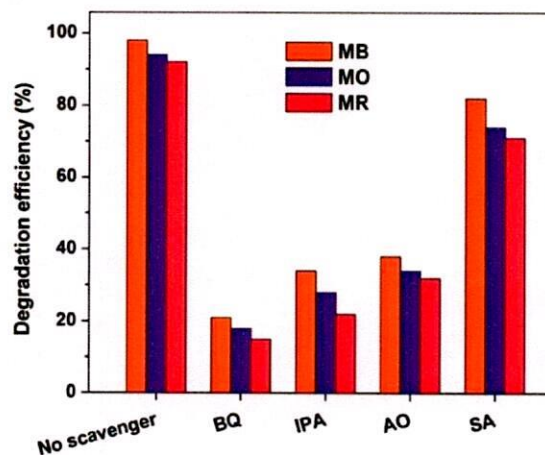


Fig. 9 – Effects of different scavengers on the degradation of MB, MO, and MR dyes in presence of p-CuO/n-ZnS composite.

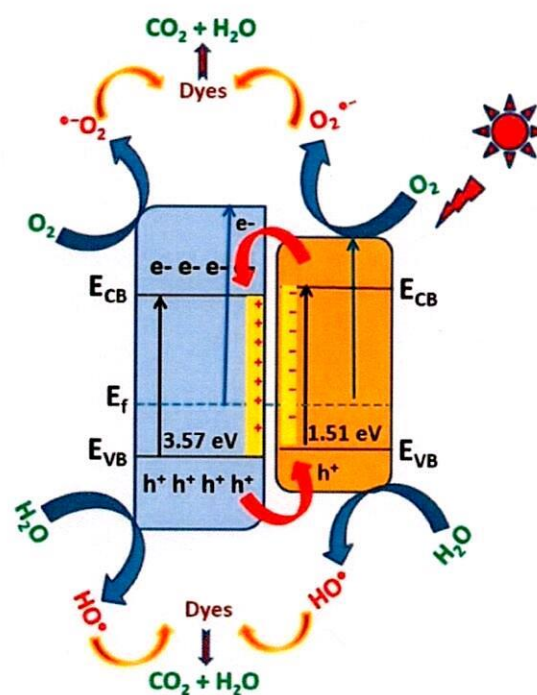


Fig. 10 – Proposed schematic band edge alignment of the p-CuO/n-ZnS heterostructure for the photodegradation of dyes under visible light radiation.

3.9. Real sample analysis

To demonstrate the practicality of the sensor for real sample analysis, it was tested for the determination of Met in human serum and urine samples. Healthy donor human serum was obtained from Osmania University dispensary, while human urine samples were collected from healthy adult male volunteers. The experimental results confirmed the detection of Met in both samples. The reliability of the method was evaluated by applying the standard addition method and calculating the recovery ratios, as presented in Tables 2 and 3. Satisfactory recoveries were achieved in both real samples with the recoveries ranging from 90% to 101% and the relative standard deviations below 5% ($n=3$). These results

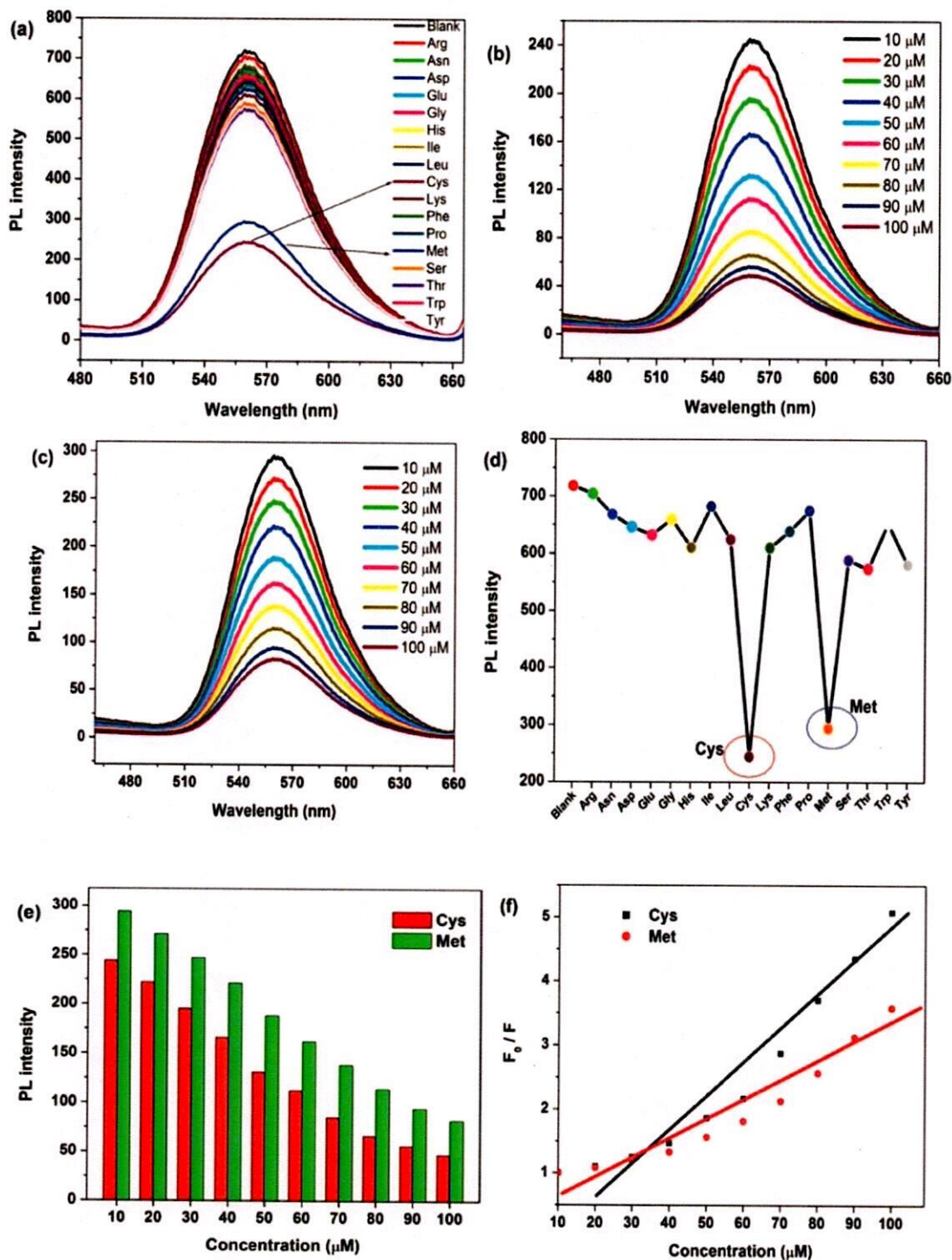


Fig. 11 – (a, d) The fluorescence detection of various thiol-containing amino acids using the synthesized p-CuO/n-ZnS heterostructure and selective sensing of (b, e) Cys and (c, e) Met from the concentration of 10–100 μM , and (f) Stern-Volmer plot.



Table 2 – Determination of Cys in human serum and urine.

S.No	Sample	Concentration of Cys (μM)			
		Spiked	Found	Recovery (%)	RSD (%) (n=3)
1	Serum	1.00	0.98	92.6	0.82
2		2.00	1.53	90.2	0.76
3	Urine	5.00	4.26	101.1	0.41
4		10.00	7.69	97.3	1.01

Table 3 – Determination of Met in human serum and urine.

S.No	Sample	Concentration of Met (μM)			
		Spiked	Found	Recovery (%)	RSD (%) (n=3)
1	Serum	1.00	0.95	90.5	0.72
2		2.00	1.38	91.6	0.63
3	Urine	5.00	4.11	100.3	0.38
4		10.00	7.28	98.5	0.94

demonstrate the dependability of the assay and its potential application for quantifying Met in aqueous solutions.

4. Conclusions

In this study, CuO, ZnS, and p-CuO/n-ZnS heterostructures were synthesized using a simple co-precipitation method, and their structure, electronic, morphological, photocatalytic, and sensing properties were characterized using various experimental and theoretical methods. XRD analysis was revealed the formation of a mixed crystalline phase of CuO and ZnS phases in the p-CuO/n-ZnS heterostructure. From the TEM analysis, the synthesized composites have spherical morphology for CuO, ZnS, and p-CuO/n-ZnS heterostructures with an average particle size is 12 ± 3 nm with a clear formation of heterojunction between CuO and ZnS. The visible-light-driven photocatalytic measurements were studied for the degradation of dyes (MB, MO, and MR), which is indicate that CuO, as a p-type and narrow band-gap sensitizer, can make the n-type ZnS respond to visible light and promote the separation of photogenerated charge carriers by building a p-CuO/n-ZnS heterostructure. The p-CuO/n-ZnS heterostructure exhibited excellent visible-light-driven photocatalytic activity for the degradation of dyes (MB, MO, and MR), with maximum degradation observed and $\cdot\text{O}_2$ identified as the main active species in the degradation process. The fluorescence sensing activity of the p-CuO/n-ZnS heterostructure was selectively quenched in the presence of Cys and Met with a detection limit of $2.52 \mu\text{M}$ (Cys) and $5.14 \mu\text{M}$ (Met), respectively. The p-CuO/n-ZnS heterostructure also demonstrated good selectivity for Cys and Met over other amino acids under identical reaction conditions. Moreover, the long-wavelength emission of the p-CuO/n-ZnS heterostructure made it suitable for monitoring Met in human serum and urine samples.

Funding

Not applicable.

Data Availability

Data will be made available on request.

Declaration of Competing Interest

The authors declare that they have no known competing financial interests or personal relationships that could have appeared to influence the work reported in this paper.

Acknowledgments

The authors were sincerely thanks to the Head, Department of Chemistry, Osmania University, Hyderabad, India for providing necessary facilities.

References

- Arshad, A., Bukhari, M.U., Maqbool, K.Q., Khan, A., Riaz, K., Bermak, A., 2023. Painting sustainable wearables: facile and economical all-recycled dual temperature-motion wearable sensor for monitoring of human temperature and joint movements. *Mater. Today Sustain.* 22, 100395.
- Ayodhya, D., 2022. Ag-SPR and semiconductor interface effect on a ternary CuO@Ag@Bi₂S₃ Z-scheme catalyst for enhanced removal of HIV drugs and (photo) catalytic activity. *N. J. Chem.* 46, 15838–15850.
- Ayodhya, D., 2023. Fabrication of SPR triggered Ag-CuO composite from Cu(II)-Schiff base complex for enhanced visible-light-driven degradation of single and binary-dyes and fluorometric detection of nitroaromatic compounds. *Inorg. Chem. Commun.* 148, 110295.
- Ayodhya, D., Veerabhadram, G., 2016a. Green synthesis, characterization, photocatalytic, fluorescence and antimicrobial activities of Cochlospermum gossypium capped Ag₂S nanoparticles. *J. Photochem. Photobiol. B* 157, 57–69.
- Ayodhya, D., Veerabhadram, G., 2016b. Green synthesis, optical, structural, photocatalytic, fluorescence quenching and degradation studies of ZnS nanoparticles. *J. Fluoresc.* 26, 2165–2175.
- Ayodhya, D., Veerabhadram, G., 2018. Highly efficient sunlight-driven photocatalytic degradation of organic pollutants and fluorescence detection of Hg²⁺ using multifunctional GO-Bi₂S₃ nanostructures. *J. Photochem. Photobiol. A Chem.* 356, 545–555.
- Ayodhya, D., Veerabhadram, G., 2019. Stable and efficient graphitic carbon nitride nanosheet-supported ZnS composite catalysts toward competent catalytic performance for the reduction of 4-nitrophenol using NaBH₄. *Mater. Today Sust.* 5, 100015.
- Ayodhya, D., Veerabhadram, G., 2020. Green synthesis of garlic extract stabilized Ag@CeO₂ composites for photocatalytic and sonocatalytic degradation of mixed dyes and antimicrobial studies. *J. Mol. Struct.* 1205, 127611.
- Bedi, R.K., Singh, I., 2010. Room-temperature ammonia sensor based on cationic surfactant-assisted nanocrystalline CuO. *ACS Appl. Mater. Interfaces* 2, 1361–1368.
- Chabane, L., Zebbar, N., Zeggar, M.L., Aida, M.S., Kechouane, M., Trari, M., 2015. Effects of CuO film thickness on electrical properties of CuO/ZnO and CuO/ZnS hetero-junctions. *Mater. Sci. Semicond. Process.* 40, 840–847.
- Chen, K.K., Chang, Z.H., Chen, Y.Z., Lu, J.J., Liang, J.J., Wang, X.L., 2023b. Transition metal-decorated molybdotellurate-based architectures constructed from flexible pyrazine-pyridine ligand with tuneable electrochemical sensing performance. *Inorg. Chim. Acta* 545, 121250.
- Chen, L., Zheng, L., Wang, F., Yi, S., Liu, D., Huang, X., Chen, R., He, H., 2021. A ratiometric fluorescence sensor based on metal-organic frameworks and quantum dots for detection of ascorbic acid. *Opt. Mater.* 121, 111622.



- Chen, P., Zhang, P., Cui, Y., Fu, X., Wang, Y., 2023a. Recent progress in copper-based inorganic nanostructure photocatalysts: properties, synthesis and photocatalysis applications. *Mater. Today Sustain.* 21, 100276.
- Chen, X., Zhou, Y., Peng, X., Yoon, J., 2010. Fluorescent and colorimetric probes for detection of thiols. *Chem. Soc. Rev.* 39, 2120–2135.
- Chen, X., Liu, L., Yu, P.Y., Mao, S.S., 2011. Increasing solar absorption for photocatalysis with black hydrogenated titanium dioxide nanocrystals. *Science* 331, 746–750.
- El-Trass, A., ElShamy, H., El-Mehasseb, I., El-Kemary, M., 2012. CuO nanoparticles: synthesis, characterization, optical properties and interaction with amino acids. *Appl. Surf. Sci.* 258, 2997–3001.
- Goudarzi, A., Aval, G.M., Park, S.S., Choi, M.C., Sahraei, R., Ullah, M.H., Avane, A., Ha, C.S., 2009. Low-temperature growth of nanocrystalline Mn-doped ZnS thin films prepared by chemical bath deposition and optical properties. *Chem. Mater.* 21, 2375–2385.
- Hajji, M., Ajili, M., Jebbari, N., Loreiro, A.G., Kamoun, N.T., 2023. Photocatalytic performance and solar cell applications of coupled semiconductor CuO–ZnO sprayed thin films: coupling effect between oxides. *Opt. Mater.* 140, 113798.
- Ho, N.D., Van Quy, N., Jung, H., Kim, D., Kim, H., Hong, S.K., 2010. Synthesis of porous CuO nanowires and its application to hydrogen detection. *Sens. Actuators B: Chem.* 146, 266–272.
- Hu, W., Zhang, Q., Luo, K., Yuan, H., Li, J., Xu, M., Xu, S., 2020. Enhanced photocatalytic properties of CuO–ZnO nanocomposites by decoration with Ag nanoparticles. *Ceram. Int.* 46, 24753–24757.
- Huang, P.C., Gao, N., Li, J.F., Wu, F.Y., 2018. Colorimetric detection of methionine based on anti-aggregation of gold nanoparticles in the presence of melamine. *Sens. Actuators B: Chem.* 255, 2779–2784.
- Kim, H., Jin, C., Park, S., Kim, S., Lee, C., 2012. H₂S gas sensing properties of bare and Pd-functionalized CuO nanorods. *Sens. Actuators B: Chem.* 161, 594–599.
- Kolmakov, A., Klenov, D., Lilach, Y., Stemmer, S., Moskovits, M., 2005. Enhanced gas sensing by individual SnO₂ nanowires and nanobelts functionalized with Pd catalyst particles. *Nano Lett.* 5, 667–673.
- Krishnan, S., Haseeb, A.S., Johan, M.R., 2014. Low dimensional CuO nanocomposites synthesis by pulsed wire explosion and their crystal growth mechanism. *Ceram. Int.* 40, 9907–9916.
- Park, S., An, S., Mun, Y., Lee, C., 2013. UV-enhanced NO₂ gas sensing properties of SnO₂-core/ZnO-shell nanowires at room temperature. *ACS Appl. Mater. Interfaces* 5, 4285–4292.
- Park, S., Sun, G.J., Kheel, H., Ko, T., Kim, H.W., Lee, C., 2016. Light-activated NO₂ gas sensing of the networked CuO-decorated ZnS nanowire gas sensor. *Appl. Phys. A* 122, 504.
- Paul, S., Sultana, J., Bhattacharyya, A., Karmakar, A., Chattopadhyay, S., 2018. Investigation of the comparative photovoltaic performance of n-ZnO nanowire/p-Si and n-ZnO nanowire/p-CuO heterojunctions grown by chemical bath deposition method. *Optik* 164, 745–752.
- Pawar, A.S., Mlowe, S., Garje, S.S., Akerman, M.P., Revaprasada, N., 2017. Zinc thiosemicarbazone complexes: single source precursors for alkylamine capped ZnS nanoparticles. *Inorg. Chim. Acta* 463, 7–13.
- Reliene, R., Fischer, E., Schiestl, R.H., 2004. Effect of N-acetyl cysteine on oxidative DNA damage and the frequency of DNA deletions in atm-deficient mice. *Cancer Res* 64, 5148–5153.
- Sankaran, A., Kumaraguru, K., 2020. The novel two step synthesis of CuO/ZnO and CuO/CdO nanocatalysts for enhancement of catalytic activity. *J. Mol. Struct.* 1221, 128772.
- Sharma, A., Dutta, R.K., Roychowdhury, A., Das, D., Goyal, A., Kapoor, A., 2017. Cobalt doped CuO nanoparticles as a highly efficient heterogeneous catalyst for reduction of 4-nitrophenol to 4-aminophenol. *Appl. Catal. A: Gen.* 543, 257–265.
- Sumalatha, V., Ayodhya, D., Balchander, V., 2023. Facile synthesis of hexagonal-shaped CuO NPs from Cu(II)-Schiff base complex for enhanced visible-light-driven degradation of dyes and antimicrobial studies. *Inorg. Chim. Acta* 548, 121358.
- de Toledo Fornazari, A.L., Suarez, W.T., Vieira, H.J., Fatibello-Filho, O., 2005. Flow injection spectrophotometric system for N-acetyl-L-cysteine determination in pharmaceuticals. *Acta Chim. Slov.* 52, 164–167.
- Trang, T.N., Phan, T.B., Nam, N.D., Thu, V.T., 2020. In situ charge transfer at the Ag@ZnO photoelectrochemical interface toward the high photocatalytic performance of H₂ evolution and RhB degradation. *ACS Appl. Mater. Interfaces* 12, 12195–12206.
- Wan, Q., Wang, T.H., 2005. Single-crystalline Sb-doped SnO₂ nanowires: synthesis and gas sensor application. *Chem. Commun.* 30, 3841–3843.
- Wang, X., Zhang, Y., Jin, Y., Wang, S., Zhang, Z., Zhou, T., Zhang, G., Wang, F., 2023. An Off-Off fluorescence sensor based on ZnS quantum dots for detection of glutathione. *J. Photochem. Photobiol. A: Chem.* 435, 114264.
- Xiong, J., Zeng, H.Y., Peng, J.F., Xu, S., Peng, D.Y., Yang, Z.L., 2022. Construction of ultrafine Ag₂S NPs anchored onto 3d network rodlike Bi₂SiO₅ and insight into the photocatalytic mechanism. *Inorg. Chem.* 61, 11387–11398.
- Xiong, J., Zeng, H.Y., Peng, J.F., Wang, L.H., Peng, D.Y., Liu, F.Y., Xu, S., Yang, Z.L., 2023. Fabrication of Cu₂O/ZnTi-LDH pn heterostructure by grafting Cu₂O NPs onto the LDH host layers from Cu-doped ZnTi-LDH and insight into the photocatalytic mechanism. *Compos. Part B: Eng.* 250, 110447.
- Yang, C., Su, X., Xiao, F., Jian, J., Wang, J., 2011. Gas sensing properties of CuO nanorods synthesized by a microwave-assisted hydrothermal method. *Sens. Actuators B: Chem.* 158, 299–303.
- Yang, C., Cao, X., Wang, S., Zhang, L., Xiao, F., Sun, X., Wang, J., 2015. Complex-directed hybridization of CuO/ZnO nanostructures and their gas sensing and photocatalytic properties. *Ceram. Int.* 41, 1749–1756.
- Yang, P., Lü, M., Xü, D., Yuan, D., Zhou, G., 2001. Photoluminescence properties of ZnS nanoparticles co-doped with Pb²⁺ and Cu²⁺. *Chem. Phys. Lett.* 336, 76–80.
- Yendrapati Taraka, T.P., Gautam, A., Jain, S.L., Bojja, S., Pal, U., 2019. Controlled addition of Cu/Zn in hierarchical CuO/ZnO pn heterojunction photocatalyst for high photoreduction of CO₂ to MeOH. *J. CO₂ Util.* 31, 207–214.
- Yeom, G.S., Song, I.H., Park, S.J., Kuwar, A., Nimse, S.B., 2022. Development and application of a fluorescence turn-on probe for the nanomolar cysteine detection in serum and milk samples. *J. Photochem. Photobiol. A: Chem.* 431, 114074.
- Zhang, F., Zhu, A., Luo, Y., Tian, Y., Yang, J., Qin, Y., 2010. CuO nanosheets for sensitive and selective determination of H₂S with high recovery ability. *J. Phys. Chem. C* 114, 19214–19219.
- Zhang, Q.P., Xu, X.N., Liu, Y.T., Xu, M., Deng, S.H., Chen, Y., 2017. A feasible strategy to balance the crystallinity and specific surface area of metal oxide nanocrystals. *Sci. Rep.* 7, 46424.
- Zhang, Q.P., Li, J., Xu, M., 2022. Ag decorated ZnO based nanocomposites for visible light-driven photocatalytic degradation: basic understanding and outlook. *J. Phys. D: Appl. Phys.* 55, 483001.
- Zhao, X., Wang, P., Yan, Z., Ren, N., 2015. Room temperature photoluminescence properties of CuO nanowire arrays. *Opt. Mater.* 42, 544–547.
- Zhu, X., Yan, Y., Wang, Y., Long, T., Wan, J., Sun, C., Guo, Y., 2022. A facile synthesis of Ag₃PO₄/BiPO₄ pn heterostructured composite as a highly efficient photocatalyst for fluoroquinolones degradation. *Environ. Res.* 203, 111843.

Financial Distress Analysis Using The Altman Z Score Model, The Springate Model, And The Grainger Model In The Indian Cement Industry

Dr. Nagella Venkata Ramana¹, Mr. K. Subba Reddy², Dr. M. Sambasivudu³

¹Associate Professor, Department of Management Studies,
Madanapalle Institute of Technology & Science
(Autonomous),

Madanapalle, Annamayya District, Andhra Pradesh, India.

²Assistant Professor, Department of Business Administration,
Annamacharya Institute of Technology and Science,
Rajampet, Annamayya District, Andhra Pradesh, India.

³Head of the Department of Commerce, JMJ College for
Women (Autonomous),
Tenali, Guntur District, Andhra Pradesh, India.

Abstract:

The paper's main objective is financial distress analysis in the cement industry in India, to fulfill the objective of this paper to collect the data from 2019 to 2023 and select 14 cement companies that were listed in NSE. Selected Springate Model, Z Score Model, and Grover Model to achieve the objective of this paper. The result states that Shree Cement Company, ACC, and Star Cement Company have Grey Zone and the remaining selected cement companies are bankrupt as per Altman Z Score, according to Grover score all selected cement companies have not bankrupt and the Spring Model implies Dalmia Cement Company have non-bankrupt and rest of the cement companies have bankrupt. The percentage of accuracy of the Z score is (21.43), the Grover score is (100) and the Spring score is (7.14) and the error percentage of the Z score is 78.57, the Grover score is 0.00 and the Spring score is 92.86.

Key Words: Altman Z Score, Grover Score, Spring Score, and Normality Test.

Introduction



Cement is the most important raw material in the field of construction, it plays an important role in the improvement of the country's infrastructure. China produces the most percentage of cement in the world, it occupies the first position in the world. India was the world's second-largest producer of cement. In February 2023 it increased cement production by 7.3% compared to February 2022.

Any business's main motive is to get maximum profit with minimum cost, the organization must have secure financial stability and utilize all financial, physical, and human resources properly. With the help of financial statements, the company's financial strength condition, and performance. The depth of financial study may provide insight into the company's prospects for success or failure. The different parts of financial statement evaluation mainly serve to enable the accomplishment of the company's goals.

There are many techniques to assess an organization's financial strength, such as the Altman Z Score, Grover Score, and Spring. These models aim to predict the probability that manufacturing companies might file for bankruptcy.

Literature Review

(Mustofa & Fahad Noor, 2020) This focused on solvency and financial distress prediction of Non – Banking Financial Institutions (NBFIs), by using the Fulmer H Score and Springate Z score model. The sample size is 20 Non-Banking Financial Institutions from the Dhaka Stock Exchange. According to the Springate Model, all samples of NBFIs were in financial distress, and as per the Fulmer H Score Model, a few sample NBFIs were in risky zones. It suggested that the Fulmer H Score model is more appropriate than the Springate Z Score model for predicting solvency. The limitation of the study was information not available for all listed NBFIs at the Dhaka Stock Exchange.

(Nurasik et al., 2023) The topic is "Financial Distress Prediction Models: Altman Z-Score Approach". In this topic they concentrated on the prediction of financial distress by applying the Altman Z Score model in Plastic and Packaging Companies. They selected nine manufacturing companies from the listed Indonesia Stock Exchange in packaging and plastic. Based on the result of this study, demonstrated that while some of the selected companies had consistently



endured the financial crisis in the plastics industry, not all of them were in good health.

(Dwi Wahyuni, 2021) In this study, return on assets showed a positive and significant effect on financial distress, the other variables like institutional ownership variables, independent commissioners, board of directors, and leverage had an influence but not significantly on financial distress. Selected a sample of real estate and property sector companies in 2018-19. The researcher selected independent variables (institutional ownership, independent commissioners, number of board of directors) and the dependent variable financial distress for testing the hypothesis in this research.

(Arora & Jiyani, 2022) their study selected Grover's model and Springate's model to guess financial distress and compare between two models which are accurate. All selected sample NBFCs were financially distressed based on the result of the Springate model and inconsistent results given by Grover's model. In between the two models Springate model is more efficient for forecasting financial health.

(Dalvadi & Pandit, 2018) They selected eight public sector enterprises to analyze the financial distress with the help of the Springate model. Four selected public sector companies were in financially worst condition and the rest of the public sector companies were financially healthy.

(Seto, 2022) in his study researcher selected prediction models namely Altman, Springate, Grover, Ohlson, and Zmijewski to study PT. Garuda Indonesia's financial difficulties. The study showed PT. Garuda Indonesia Tbk is in a condition of financial distress or declares bankruptcy between 2018 and 2021.

(Fedorova et al., 2016) in their study they suggested based on the study selected Altman, Fulmer, Springate, Taffler Zmijewski, Saifullin, ISEA, and Zaitseva models for current financial analysis, forecasting financial distress and adoption of efficiency management decisions.

(Dwiningsih et al., 2023) in their study applied the Altman, Springate, and Zmijewski model to predict the financial distress of Bhutan Telecom Limited. The study confirms that Bhutan Telecom Limited was financially healthy during the study period.



(Muzanni & Yuliana, 2021)in this study, researchers selected Descriptive Statistical Analysis, Paired Sample T-Test, Normality Test, Accuracy Test of methods, and Springate and Altman Models to predict the financial distress of PT Eagle MahkotaTbk. In their investigation, the researchers discovered that the Altman model has an error type of 0% and an accuracy rate of 100%, whereas the Springate model has a type error of 33% and an accuracy rate of 67%.

(Sudjiman & Sudjiman, 2019)This study's primary goal is to determine the bankruptcy status of cement businesses listed in Bangladesh. The bankruptcy position was analyzed using the Altman Z score methodology. Out of the selected 8 cement companies, 2 companies were secure regions, 3 companies were grey regions and 3 companies were bankruptcy regions, and positive correlation between 5 independent variables and the dependent variable.

(Yendrawati & Adiwafi, 2020)in their study, the main aim is the accuracy level of financial distress in Altman, Sprinagte, and Zmijewski in the property, building construction, and real estate sectors. The highest accuracy is Altman followed by Zmijewski and Springate models in predicting financial distress of building construction, property, and real estate sectors.

(Ispanggara, 2020)in this study, 152 debtors were analyzed in the category of small and medium enterprises to determine business trends from before the COVID-19 pandemic and during the COVID-19 pandemic by using Altman, Sprigate, Zmijewski, and Grover models. The result indicates down downward trend in business conditions during the COVID-19 pandemic and indicates financial distress condition.

Research Gap

Once critically analyzed the above review of literature, it is said that not much study has been done to predict financial trouble for cement companies in India using the Altman, Springate, Zmijewski, and Grover model. Hence, the researcher attempts to analyze the financial distress by using Grover, Altman, Zmijewski, and Springate model for registered cement companies in India during the period of 2016-17 to 2021-22.



Objective of the study

The primary goal of the research is to use prediction models to analyze the financial difficulties of a subset of Indian cement companies.

Hypothesis

H01: There is no significant difference between sample data of Z Score and normally distributed data

H02: There is no significant difference between the sample data of Grover Score and normal distribution data.

H03:

There is no significant difference between the sample data of Spring Score and normal distribution data.

Research Methodology

The secondary data used in this research study was collected from the annual reports of the selected cement businesses. The researcher has selected fourteen listed top cement companies out of 37 listed cement companies from the National Stock Exchange (NSE). Out of these selected top listed cement companies from NSE.

1. Ultra Tech Cement
2. Ambuja Cements
3. Shree cements
4. Dalmia Cement
5. ACC
6. J. K. Cement
7. Ramco Cement
8. JK Lakshmi Cem
9. India Cement
10. Star Cement
11. Heidelberg Cem
12. Orient Cement
13. Sagar Cement
14. Sanghi Cement

Altman Z-Score Model:

In 1968, Altman became the first researcher to apply the Multiple Discriminant Analysis method. Altman provides the resultant technique well-known as the Altman Z-Score. This method classified the possibility of distress, grey areas, and health for the company.

The Z score formula is as follows:

$$Z = 1.2A + 1.4B + 3.3C + 0.6D + 0.99E$$



Where:

A = Working Capital / Total Assets

B = Retained Earnings / Total Assets

C = EBIT / Total Assets

D = Market Value of Equity / Total Liabilities

E = Sales / Total Assets

Altman Z Score below 1.81 specifies a distress zone – a high likelihood of bankruptcy, between 1.81 and 2.99 signals a grey zone-moderate risk of bankruptcy and more than 2.99 implies a safe zone-low likelihood of bankruptcy.

Grover Score Model:

It is a model formed by redesigning the model of the Altman Z Score. It took A and C of the Altman model and added Profitability Ratio which is ROA.

$$G = 1.650A + 3.404B - 0.016C + 0.057$$

Where:

A = Working Capital / Total Assets

B = EBIT / Total Assets

C = Net Income / Total Assets (ROA)

G Score is less than or equal to -0.02 indicates bankrupt and greater than 0.01 signs not bankrupt.

Springate Model:

It is a type of multiple discriminant analysis that was created in 1978 at Simon Fraser University by Gordon L V. Springate. It uses 19 financial ratios to predict the soundness of a corporation with an accuracy rate of 92.5 percent.

$$S = 1.03A + 3.07B + 0.66C + 0.4D$$

Where:

A = Working Capital / Total Assets

B = Net Profit before Interest and Taxes / Total Assets

C = Net Profit before Taxes / Current Liabilities

D = Sales / Total Assets

A Springate Score is less than 0.862 indicates bankrupt and more than 0.862 signs not bankrupt.

Table No 1 Model of Altman Z Score

Co Name	2019	2020	2021	2022	2023	Average	Result
Ultra	0.9970	1.2256	1.3166	1.4360	1.4128	1.2776	Bankrupt
Ambuja	1.3342	1.3180	1.4472	1.4576	1.5619	1.4238	Bankrupt



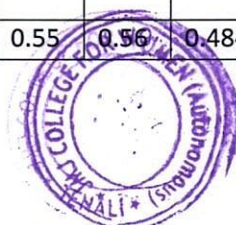
Shree	1.60 58	2.65 47	1.85 21	2.13 46	2.04 56	2.058 6	Grey Zone
Dalmi a	1.24 81	0.81 85	0.67 55	0.73 74	1.51 47	0.998 8	Bankr upt
ACC	1.59 11	1.98 99	1.80 43	1.91 03	1.89 25	1.837 6	Grey Zone
JK	1.32 01	1.34 01	1.52 91	1.45 93	1.45 15	1.420 0	Bankr upt
Ramc o	1.23 43	1.06 73	1.07 62	0.95 11	0.87 57	1.040 9	Bankr upt
JKL	1.06 87	1.37 00	1.65 94	1.93 45	1.98 32	1.603 2	Bankr upt
India	0.77 41	0.61 49	0.73 69	0.66 67	- 0.39 97	0.478 5	Bankr upt
Star	2.73 23	2.50 41	1.98 60	2.18 48	2.24 68	2.330 8	Grey Zone
Heild el	1.55 65	1.69 26	1.68 45	1.78 27	1.49 89	1.643 0	Bankr upt
Orien t	1.15 28	1.25 58	2.55 34	1.89 50	1.56 79	1.685 0	Bankr upt
Sagar	1.01 83	0.92 59	1.57 11	0.77 53	1.22 11	1.102 3	Bankr upt
Sang hi	0.82 95	0.60 55	0.69 55	0.57 25	0.03 66	0.548 0	Bankr upt

Compiled from Annual Reports of Selected Cement Companies in India

Table No. 1 implies the Altman Z Score model of elected cement companies in India during the study period from 2019 to 2023. Shree Cement Company (2.0586), ACC (1.8376), and Star Cement Company (2.3308) have more than 1.81 and less than 2.99 so, these companies have grey zone area and the remaining selected cement companies' average Z Score is less than 1.81 Hence, they have bankrupt during the study period.

Table No 2 Grover Score Model

Co Nam e	2019	2020	2021	2022	2023	Avera ge	Result s
Ultra	0.18 37	0.31 39	0.46 00	0.40 18	0.33 24	0.338 4	Non Bankr upt
Amb	0.44	0.37	0.47	0.55	0.56	0.484	Non



uja	85	09	49	95	67	1	Bankrupt
Shree	0.50 86	0.64 65	0.80 21	0.70 23	0.35 23	0.602 4	Non Bankrupt
Dalmia	0.25 42	0.27 78	0.15 23	0.16 47	0.17 23	0.204 3	Non Bankrupt
ACC	0.28 05	0.72 49	0.69 32	0.79 15	0.49 15	0.596 3	Non Bankrupt
JK	0.39 69	0.44 28	0.64 93	0.45 24	0.38 83	0.466 0	Non Bankrupt
Ramco	0.21 94	0.19 28	0.25 72	0.12 93	0.02 93	0.165 6	Non Bankrupt
JKL	- 0.00 12	0.23 60	0.41 93	0.58 00	0.53 91	0.354 6	Non Bankrupt
India	0.04 13	- 0.05 82	0.02 28	0.02 95	- 0.00 44	0.006 2	Non Bankrupt
Star	1.23 56	1.00 52	0.77 29	0.67 22	0.56 39	0.850 0	Non Bankrupt
Heidelberg	0.47 11	0.59 66	0.56 85	0.66 22	0.39 24	0.538 2	Non Bankrupt
Orient	0.11 42	0.21 85	0.46 02	0.42 52	0.20 63	0.284 9	Non Bankrupt
Sagar	0.10 18	0.08 44	0.52 55	0.21 55	0.14 77	0.209 6	Non Bankrupt
Sanghi	0.15 07	0.06 05	0.12 51	0.00 98	0.30 89	0.131 0	Non Bankrupt

Compiled from Annual Reports of Selected Cement Companies in India

Table No 2 implies the Grover Score Model of selected companies of cement during the period of study. All selected



cement companies' average Grover Score is more than 0.01. Therefore, all companies non-bankrupt in the study period.

Table No 3 Spring Score Model

Co Name	2019	2020	2021	2022	2023	Average	Results
Ultra	0.6297	0.5940	0.7134	1.0291	0.6562	0.7245	Bankrupt
Ambuja	0.4380	0.5313	0.5321	0.3773	0.5000	0.4757	Bankrupt
Shree	0.6340	0.5146	0.8607	0.6429	0.2363	0.5777	Bankrupt
Dalmia	1.5063	4.2500	0.1405	7.7586	6.6129	4.0537	Non Bankrupt
ACC	0.3182	0.4336	0.3890	0.4261	0.2387	0.3612	Bankrupt
JK	0.3296	0.5125	0.6719	0.4697	0.3538	0.4675	Bankrupt
Ramco	0.3444	0.3331	0.4714	0.2883	0.1536	0.3182	Bankrupt
JKL	0.1429	0.3309	0.4194	0.4675	0.3631	0.3448	Bankrupt
India	0.0385	0.0111	0.1272	0.0201	0.2116	0.0817	Bankrupt
Star	1.1483	1.0217	0.5483	0.4506	0.5455	0.7429	Bankrupt
Heidelberg	0.3740	0.4284	0.4261	0.4005	0.1597	0.3577	Bankrupt
Orient	0.1473	0.2845	0.6892	0.6005	0.2388	0.3409	Bankrupt
Sagar	0.1005	0.1196	0.5632	0.2571	0.1112	0.2303	Bankrupt
Sanghi	0.0958	0.0914	0.1767	0.0719	0.4956	0.1863	Bankrupt

Compiled from Annual Reports of Selected Cement Companies in India

Table No. 3 depicts the spring model of selected Indian cement companies during the study period. Dalmia Cement Company's average Spring Score is more than 0.862. So, the company was not bankrupt in the period of study. The rest of



the selected cement companies are bankrupt because the average Spring Score is less than 0.862.

Table No 4 Descriptive Statistics

Values	Models		
	Z-Score	Grover-Score	Springate-Score
Mean	1.3892	0.3737	0.6617
Median	1.4219	0.3465	0.3595
Variance	0.280	0.052	0.988
Std. Deviation	0.52923	0.22852	0.99414
Minimum	0.48	0.01	0.08
Maximum	2.33	0.85	4.05
Range	1.85	0.84	3.97
Std. Error	0.14144	0.06107	0.26570

Source: Computed Value

Table No 4 depicts descriptive statistics of prediction financial distress models viz., Z-Score, Grover-Score, and Springate-Score Models. Z Score of mean and median is more than the mean and median of Grover and Springate. The variance and standard deviation of Springate are more than that of the Z Score and Grover Score. The minimum Z Score is the highest value compared to Grover and Springate, and the maximum value of Springate is the highest compared to other models. The range and Standard Error value of Springate are more than the Z Score and Grover Score values.

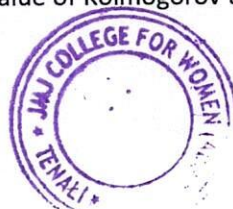
Table No 5 Normality Test

Model	Kolmogorov-Smirnov ^a			Shapiro - Wilk		
	Statistic	df	Sig.	Statistic	df	Sig
Z Score	0.095	14	0.200*	0.978	14	0.962
Grove Score	0.121	14	0.200*	0.974	14	0.925
SpringateScore	0.396	14	0.000	0.473	14	0.000

• This is a lower bound of the true significance.

a. Lilliefors Significant Correction

Table No 5 implies the normality test of Z score, Grover score, and Spring score significant value of Kolmogorov and Shapiro.



The null hypotheses H01 and H02 were accepted due to the significant value of the Grover score and Z score being more than 0.05%. The null hypothesis H03 is rejected as the Spring score significant value is less than 0.05%.

Table No 6 Results of Potential Bankruptcy of Fear Level Prediction

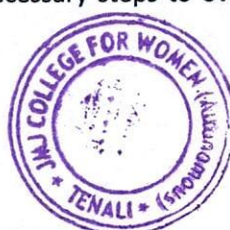
Prediction	Methods		
	Z - Score	Grover - Score	Springate - Score
Bankrupt	11	0	13
Grey	3	0	0
Non Bankrupt	0	14	1
Total Samples	14	14	14
% Accuracy	21.43	100	7.14
% Error Type	78.57	0	92.86

Source: Processing of Data Outcome

The Altman Z-Score model implies that 11 businesses have the potential to file for bankruptcy, 3 have a gray area, and no business has ever filed for bankruptcy. The model of Altman Z-Score has an accuracy rate of 21.43% with an error type of 78.57%. Grover Score forecasts 14 firms that have no bankruptcy, with an accuracy rate of 100%. As per Springate Score, 13 companies were bankrupt and one company was nonbankrupt. The accuracy rate of 7.14% and the error type of 92.86%.

Conclusion

Based on the study of financial distress analysis by using a model of Altman Z score, Grover score, and Spring score model from 2019 to 2023. Z Score model predicts 3 companies as grey zone and 11 companies as bankrupt companies, with an accuracy rate of 21.43% with a 78.57% error type, as per the Grover score model 14 companies are nonbankrupt, rate of accuracy of 100% with an error type of 0% and Spring score model states one company nonbankrupt and 13 companies were bankrupt precision rate of 7.14% and type of error 92.86%. Based on the conclusion this study can imply that investors are owners of the capital can know the signals of company failure or not, creditors are lenders of the company can know the health condition of the company and management can take necessary steps to overcome the risk of bankruptcy.

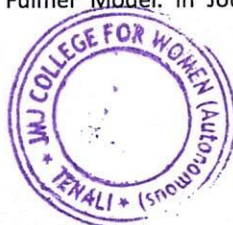


References

1. Alareeni, B. A., & Branson, J. (2012). Predicting Listed Companies' Failure in Jordan Using Altman Models: A Case Study. In *International Journal of Business and Management* (Vol. 8, Issue 1, pp. 113–126).
<https://doi.org/10.5539/ijbm.v8n1p113>
2. Altman, E. I., Haldeman, R. G., & Narayanan, P. (1977). ZETATM analysis A new model to identify bankruptcy risk of corporations. In *Journal of Banking and Finance* (Vol. 1, Issue 1, pp. 29–54). [https://doi.org/10.1016/0378-4266\(77\)90017-6](https://doi.org/10.1016/0378-4266(77)90017-6)
3. Aminian, A., Mousazade, H., & Khoshkho, O. I. (2016). Investigate the Ability of the Bankruptcy Prediction Models of Altman and Springate and Zmijewski and Grover in the Tehran Stock Exchange. In *Mediterranean Journal of Social Sciences* (Vol. 7, Issue 4, pp. 208–214).
<https://doi.org/10.5901/mjss.2016.v7n4s1p208>
4. Arora, M. N., & Jiyani, C. (2022). An Analysis of Efficacy of Financial Distress Prediction Springate and Grover Model. In *GAP iNTERDISCIPLINARITIES: Vol. V* (Issue IV, pp. 74–77).
5. Author, C., Harry Prasetyo, D., Fatma, A., & Author, C. (2019). Prediction Analysis of Financial Distress Potential By Comparing Altman, Springate, And Zmijewski Models In Indonesia Eximbank. In *American International Journal of Business Management (AIJBM) ISSN* (Vol. 2, Issue 5, pp. 10–18). www.aijbm.com
6. Dalvadi, Y. M., & Pandit, J. B. (2018). An Analysis of Financial Distress of Selected Public Sector Enterprises of India using Springate Score Model. In *Journal of Commerce & Trade* (Vol. 13, Issue 1, p. 105). <https://doi.org/10.26703/jct.v13i1-15>
7. Dwi Wahyuni, P. (2021). Determinants of Financial Distress Prediction Using Springate Model: Based on Gcg and Financial Indicators. In *South East Asia Journal of Contemporary Business, Economics and Law* (Vol. 24, Issue 2, pp. 120–129).
8. Dwiningsih, S., Yahya, M. Z., & Info, A. (2023). Analysis of Springate Method and the Altman Z-Score Method for Predicting the Financial Distress (Vol. 1, Issue 1, pp. 59–68).
9. Fedorova, E. A., Dovzhenko, S. E., & Fedorov, F. Y. (2016). Bankruptcy-prediction models for Russian enterprises: Specific sector-related characteristics. In *Studies on Russian Economic Development* (Vol. 27, Issue 3, pp. 254–261).
<https://doi.org/10.1134/S1075700716030060>
10. Hantono, H. (2019). Predicting Financial Distress Using Altman Score, Grover Score, Springate Score, and Zmijewski Score (Case Study on Consumer Goods Company). In *Accountability* (Vol. 8, Issue 1, p. 1).
<https://doi.org/10.32400/ja.23354.8.1.2019.1-16>
11. Hertina, D., Kusmayadi, D., & Yulaeha. (2020). Comparative Analysis of the Altman, Springate, and Zmijewski Models as Predicting Financial Distress. In *Journal of Archaeology Of*



- Egypt/Egyptology (Vol. 17, Issue 5, pp. 552–561).
www.economy.okezone.com
12. Hoque, E., Hossain, T., & Saha, T. (2022). Predicting the Bankruptcy of Cement Companies in Bangladesh: A Study on Dhaka Stock Exchange. In *International Journal of Business, Economics and Management* (Vol. 9, Issue 5, pp. 162–174).
<https://doi.org/10.18488/62.v9i5.3207>
 13. Imanzadeh, P., Maran-Jouri, M., & Sepehri, P. (2011). A study of the application of Springate and Zmijewski bankruptcy prediction models in firms accepted in the tehran stock exchange. In *Australian Journal of Basic and Applied Sciences* (Vol. 5, Issue 11, pp. 1546–1550).
 14. Ispanggara, R. (2020). Financial Distress Analysis using Altman, Springate, Zmijewski , and Grover Models for Small and Medium Enterprises Debtor During the Covid-19.
 15. Lestari, R. M. E., Situmorang, M., Pratama, M. I. P., & Bon, A. T. (2021). Financial distress analysis using altman (Z-score), springate (S-Score), zmijewski (X-Score), and Grover (G-Score) models in the tourism, hospitality, and restaurant subsectors listed on the Indonesia stock exchange period 2015-2019. In *Proceedings of the International Conference on Industrial Engineering and Operations Management* (pp. 4249–4259).
 16. Mustofa, S., & Fahad Noor, M. (2020). Predicting Solvency of Non-Banking Financial Institutions in Bangladesh by Using Springate Fulmer Model. In *Turk Turizm Arastirmalari Dergisi* (Vol. 2, Issue 1, pp. 51–69).
<https://doi.org/10.26677/tr1010.2020.427>
 17. Muzanni, M., & Yuliana, I. (2021). Comparative Analysis of Altman, Springate, and Zmijewski Models in Predicting the Bankruptcy of Retail Companies in Indonesia and Singapore. In *TIJAB (The International Journal of Applied Business)* (Vol. 5, Issue 1, p. 81). <https://doi.org/10.20473/tijab.v5.i1.2021.81-93>
 18. Nurasik, Abidin, F. I. N., Hasanah, E., & Rizal, A. (2023). Financial Distress Prediction Models: Altman Z-Score Approach (Vol. 1, pp. 398–408). Atlantis Press SARL.
https://doi.org/10.2991/978-2-38476-052-7_44
 19. Setiawan, C., & Rafiani, T. T. (2021). Financial Distress Prediction Models: Case Study of Textile Industry in Indonesia. In *International Journal of Entrepreneurship* (Vol. 25, Issue 4, p. 9264).
 20. Seto, A. A. (2022). Altman Z-Score Model, Springate, Grover, Ohlson, and Zmijweski to Assess the Financial Distress Potential of PT. Garuda Indonesia Tbk During and After the Covid-19 Pandemic. In *Enrichment: Journal of Management* (Vol. 12, Issue 5, pp. 3819–3826).
www.enrichment.iocspublisher.org
 21. Shalih, R. A., & Kusumawati, F. (2019). Prediction of Financial Distress in Manufacturing Company: A Comparative Analysis of Springate Model and Fulmer Model. In *Journal of Auditing,*



- Finance, and Forensic Accounting (Vol. 7, Issue 2, pp. 63–72).
<https://doi.org/10.21107/jaffa.v7i2.6717>
22. Sudjiman, L. S., & Sudjiman, P. E. (2019). The Accuracy of Springate and Zmijewski in Predicting Financial Distress in Cosmetic and Household Subsector Companies. In Abstract Proceedings International Scholars Conference (Vol. 7, Issue 1, pp. 1343–1358). <https://doi.org/10.35974/isc.v7i1.2067>
23. Voda, A. D., Dobrotă, G., Țircă, D. M., Dumitrașcu, D. D., & Dobrotă, D. (2021). Corporate bankruptcy and insolvency prediction model. In Technological and Economic Development of Economy (Vol. 27, Issue 5, pp. 1039–1056). <https://doi.org/10.3846/tede.2021.15106>
24. Wahyudi, H., Prastyowati, A. H., & ... (2021). Altman Z-Score, Springate, and Zmijewski Methods' Analysis for Predicting Financial Distress In Manufacturing Companies Listed On The Indonesia Stock Exchange. In International Conference On Economics And Business (pp. 393–404).
25. Yendrawati, R., & Adiwafi, N. (2020). Comparative analysis of Z-score, Springate, and Zmijewski models in predicting financial distress conditions. In Journal of Contemporary Accounting (Vol. 2, Issue 2, pp. 72–80).
<https://doi.org/10.20885/jca.vol2.iss2.art2>



Principal
J.M.J. COLLEGE FOR WOMEN (Autonomous)
TENALI - 522 202

Class Consciousness in the Novel *The Space Between Us* by Thrity Umrigar

Dr. S. Mary Sophia Rani*¹

Kadapa, India

Abstract-

“Her presence was slight, and went unnoticed. But when illness or indisposition kept her away, she was seen everywhere; in the dirty cups and saucers, upon the dusty furniture, in the sheets of unmade beds.” (Mistry 64)

The above statement tells about the toil of a housemaid in a family. Her sense of sacrifice and suffering for the welfare of the family deserves all appreciation and her role is pivotal. But she remains a victim of age-old subjugation. The writers of the South Asian fiction probe the different aspects of domestic servants. The problems that confront middle class family servants are illiteracy, protectorate, obligation, rapport and aging. Like other Asian writers Thrity Umrigar also touches the issues of domestic servants in her second novel *The Space Between Us* (2006). It is about the relationship between employer and servant. In her debut novel, *Bombay Time* (2001) she focuses on the Parsi Indian middle-class families within an apartment, where all the residents are Parsis and their disparate memories, experiences of disappointments, shattered dreams, betrayals, pangs of separation by death and regret due to wrong decisions. Brad Watson, author of *The Heaven of Mercury*, reviewed and labeled her work as ‘bitter sweet novel’. Whereas in this novel *The Space Between Us*, she shifts her focus on gender, class and how they play a dominant role between the lives of two women.

Index Terms- Class Consciousness, domestic servants, illiteracy, shattered dreams and betrayals.

INTRODUCTION

The novel *The Space Between Us* is about the relationship between two women, in fact it is a relationship between an employer and a maid whose intimacy gradually increased and ran smoothly for some time until these women have recognized their status. The most important factor which portrays a woman’s destiny, her survival and her fate is clearly portrayed by the author. In a conversation with Thrity Umrigar in the Post Script of the novel, she stated that “it is impossible to have two human beings work and live in a contained domestic space all day long and not form some kind of a bond or human connection” (P.S. 7).

The two protagonists of this novel Sera Dubash, a Parsi woman of upper middle class family and Bhima the domestic servant of Dubash family, who has been working for decades. The novel is author’s mouth piece, powerful, creative and evocative. Umrigar portraying the pain, pleasure, suffering, memories of flashback and the bond between these two women. Both belong to different classes. Their class division is dependent upon certain modes of lifestyle, attitude and behaviour. There are different ways of marginalization in which Sera and Bhima are treated in their respective classes. They have few choices in their individual roles and are entrapped in the inescapable cage of the “woman-wife-mother.” In their journey of life, both Sera and Bhima follow the particular class pattern where power and wealth play a significant role and the family honour and welfare are the primary concern. This class division never allows them to cross their boundaries and they remain trapped in the clutches of traditions and manners of their familial position.

These two women, Bhima and Sera experience similar situations in their lives; death, abuse or absence of husband enduring shame and disappointment, their love for their children and hope for their future. The only element that separate them is class. The two women pull on at opposite ends at the socio-economic spectrum of Bombay city.

Sera was brought up in an independent environment of Bombay. Being a single daughter of scientist, she enjoyed an extraordinary position in her paternal home. An educated and self-sustained woman, Sera was treated as an individual and the woman of self-respect. Her liberal upbringing and education provide her the option of selecting her spouse independently. Anjana Sen Gupta in her book *Women on the Move* asserts;

“Her self-choice marriage is expected to provide opportunities for intellectual growth, intimacy in relationship, a sense of companionship and opportunity for self-expressions” (Sengupta 23).

Sera is portrayed as an acquiescent character, who never raised her voice against her husband. A modern and well educated Sera learnt to obey and compromise to all hurdles in her life. Gradually, she understands her place in Feroz’s home as that of an ‘unpaid servant.’ She compromises with and adjusts to her marginalized status in the home. The repeated abuse that Sera has suffered in love makes her so vulnerable that she feels empty as a woman. The emptiness of Sera’s marital relation makes her crave for motherhood. Motherhood offers familial and social compensation to Sera. Dinaz’s birth not only gives her a chance to experience the joy of childbirth and nurture but it also furnishes her with a sense of accomplishment and belonging that is observed by Nancy Friday;

“When one woman gives birth to another, to someone like her, they are linked together for life in a special way”. (Friday 39)

Sera’s misery is distinctly witnessed by Bhima, the maid of Dubash family, who lives in the slum of Mumbai. She uses some natural herbs to heal the stain of Feroz’s violation. “Sera remembers the blow and the balm; the tormentor and the healer: Feroz and Bhima”. The way he acts with his wife depends on his mother. Banu, who is interloper of Sera’s life. Her action is like a spy or an informer. She always has a lidless eye on her daughter-in-law’s every movement in the house and tells Feroz every day when he returns from office. The only bliss Sera has in her life is her daughter Dinaz. She always thinks about her daughter that;

“She is the only bright spot in my life anymore, she thought..... The rest of them- Feroz and his mother- they have ruined her life.” (184)

The only person in Sera’s life, who knew that her husband’s abuses occasionally flew like ‘black vultures’ over the desert of her body is her maid, friend and well-wisher Bhima. She knew more about the strangeness of her marriage than any family member of friends. Though she is illiterate and servant, she advises Sera about Feroz’s cruelty.

Bhima, a sixty-five years old, a slum dweller, who is wrinkled and scooped out, a sign of her abject poverty, who is illiterate and stoic, a sign of the sub-culture of poverty she was born into, and who struggles to live with the company of Maya, her orphaned granddaughter, in a mud-floored squalid slum by working as a housemaid for Sera on a daily routine.

Bhima is an illiterate and stoic became a sign of wretched poverty. There is no scale for Bhima’s pain, there is no hope for Maya’s future, and their lives are deceived, subjugated, exploited, oppressed and blamed. Bhima and Maya live in a mud floored squalid slum, her routine job starts every morning leaving her small shanty in the ghetto to tend Sera Dubash’s home. The novel is set on a passive height. Bhima whose story begins and ends in the novel, is a spokesperson of that wide support system of workers without whom most middle class households of India would collapse; individuals who touched upon the lives of their privileged employers intimately but themselves remain peripheral and insignificant entities in any deeper and meaningful sense in those lives.

Bhima is also proud mother of two children, Amit and Pooja. All is well till her husband is maimed in an industrial accident and the factory administration refuses to own responsibility for the accident and pay compensation. The accountant of the factory visits their home and takes Bhima’s signature on a blank paper, which later used to deny any benefits to Gopal. The official plays tricks with marginalized people, withholding the truth from them and conspiring with the rich to defraud the couple. He takes advantage of their trust and lack of education and negotiates to safeguard the interests of the owners. This incident becomes the main cause of their suffering and Gopal gradually slips into alcoholism. Gopal accused Bhima of accountant treachery:

“Everything else has been taken from me, Bhima- my hands, my employment, my pride. Please don’t take one thing away from me. I’m not like those other drunken fools. I know when to stop”. (234)

One day Gopal absconds with their only son Amit and Bhima to meet the challenges of the world. He had struck her like a viper and moreover he had stolen the brightest and shiniest object in her life (their son Amit). He left Bhima and Pooja as ‘an abandoned pair of shoes.’ (147) She brings up her daughter Pooja and arranges her marriage to Raju. After the wedding Pooja leaves for Delhi with her husband but the mother-daughter relation is sustained beyond the constraints of place. All this while, Bhima says busy with

her daily routine in the Dubash household, then catastrophe strikes when Raju and Pooja are diagnosed with AIDS. Pooja has contracted the dreaded disease from her husband. The knowledge devastates the young couple. As an illiterate Bhima said:

And after this second funeral, after Pooja turns into ashes before my cursed eyes, after I have witnessed the horror of my own child dying before me, I will want to melt like ice, I will want to crumble like sand, I will want to dissolve like sugar in a glass of water. I will want to stop existing. (147)

Bhima is a grandmother and she raises Maya affectionately with the support of Sera who takes the responsibility to provide her a good education. Maya's admission into a school and the prospects of a bright future are like miracles to Bhima. She believes that her degree would get them out of an autocratic Bombay slums, guaranteeing Maya a better life away from servitude. Sera and Bhima's experiences as mothers and grandmother thus, provide them diverse experiences of identity, power, happiness, suffering and pain. The pain in Bhima's words:

Once I had two children, and now I will have none. One dead, the other disappeared, vanished, stolen from me by my cockroach of a husband. And a mother without children is not a mother at all, and if I am not a mother, then I am nothing. Nothing. I am like a sugar dissolved in a glass of water. Or, I am like salt, which disappears when you cook with it. I am salt. Without my children, I cease to exist. (147)

Sera never noticed Bhima appearing old, exhausted and diffident. Not even when Gopal had left and he takes with him the most precious thing (her son Amit) in her life. She had been scared then, no question about that situation, but she knew she was still responsible for Pooja, and that responsibility towards her daughter had strengthened and kept her from falling apart. Sera said; "No, Gopal may have broken Bhima's back, but Maya had broken her spirit (43)".

Maya is the only granddaughter of Bhima, she rescued her from death's door and promised to Pooja to look after Maya. Bhima lost everything in her life. Maya is the only bright spot in her life; who had come to her as an orphan and grown up to be a brilliant and aspiring young girl; she is the only flesh and blood family member she still had near her.

Such a bright and brilliant girl, Maya becoming a mother at seventeen, which ruins her bright future. She refuses when Bhima mentioned about abortion. Maya was the only first person in Bhima's family to attend college. The bright path that raised before Maya. She does not reveal the father of unborn baby who had brought so much worry into their lives. Bhima thinks about her granddaughter that she is just a silly and immature girl, she has no idea how the pit of fate would swallow her up if she went ahead and without a father to support her would spoil her life.

The situation is aggravated when Maya declines unfathomably to reveal the identity of the man. To avoid social disgrace, it seems necessary to Sera and Bhima that Maya should abort. For, it is not possible to take either responsibility. Bhima is completely shattered at this turn of events and now it is Sera who assumes the position of the supporter. Sera and Bhima seek to find the father of the unborn child but they fail. In these circumstances, the intimacy between Sera and Bhima takes the shape of a sisterhood where both the servant negotiates in their equal capacity as women and try to make a protective nest for Maya.

Bhima plays an important role in Dubash family, but what happens in their 'dichotomous and cherished relationship' is that when Bhima is encountered the truth of Maya's pregnancy, Sera is found guilty as her own son-in-law is the cause of Maya's unborn baby. Though Sera knew Bhima is truthful because of their previous acquaintance still Sera could not stand by Bhima's side. Sera opted to save her daughter Dinaz marital life by supporting Viraf. Sera is not willing to put her daughter's life into risk by standing on the side of truth and prioritising the rapport which Sera had built all these years. Through this situation one can come to know that the subject of marriage or marital life of a girl is given a highest place in society and it has a strong impact on woman, where people got tuned that marital life is the only prospect for a woman and if no marriage takes place for a woman she is considered as ill fated, scorned, misunderstood and questioned by society.

Apart from friendship, Thrity Umrigar highlighted the subjugation of poor, the power suppressing the powerless. Because Bhima is poor, she is not able to sue against Viraf nor does she have the strength to go against Sera's family.

When Sera shifts to her new home and Bhima undertakes to work at Sera's new home in addition to working at the Dubash household. Bhima appreciate that Sera and Dinaz treat her as a person, overlooking the fact that she is needed to eat separately and using different crockery from the family. Sera and Bhima conscious of the class difference between them and they accept their different lots in life with the nonchalance founded on the acceptance of tradition. The class-supremacy and its impact on individuals is noticeable and false class consciousness is followed by a full awareness of the true situation and of understanding the nature of their position. Bhima cannot sit on the furniture which she cleans every day and Sera upholds this class disparity as even the thought of Bhima sitting on their furniture repulses Sera. She cannot to see Dinaz embracing Bhima and she has to, "suppress the urge to order her daughter to go and wash her hands (29)". Though Sera calls Bhima, "my Bhima", and talks about her proprietarily (19)". Sera sits on a chair at the table while Bhima squats on her haunches on the floor nearby. On the other hand, she cannot but admire Bhima for her conduct and character and when one of her neighbours states that, "Sera is rewarded in heaven for the way she treats Bhima" she replies wryly, "heaven has nothing to do it, Bhima is a decent person and a good worker." (44) However the conditioning of the rigid social structure keeps them apart in the sphere beyond that of the mistress-servant. She has never visited Bhima's house which is located less than a fifteen minutes walk away. She bridges the gap fleetingly only once on the day when Bhima is unwell. On entering Bhima's home she feels as, "If she had entered another universe." (113) And wants to run away from that place and escape back to her sanity house.

The relationship between these women in many ways highlights the space between them which is concretized by the material difference at their homes-one a rich apartment and the other a small room in a slum. Swapna Krishna in a review of *The Space Between Us* states;

"The reader hopes that Sera will reach out to Bhima and try to connect with her on their common ground because they really could help one another. But unfortunately, that isn't the way that class works". (Krishna)

With the experience of earlier betrayals, Bhima is immediately able to deduce that it is Viraf who is responsible for their misery and pain. She notices that he tries to hide behind his wife and mother-in-law. She recalls how he treated Maya playfully without any class difference and now he is the man who ruptures the lives of her and her granddaughter. He pushed the blame for their indiscretion upon Maya alone. Here again patriarchy plays a vital role as he uses his machismo and cunning to safeguard his position by undermining Maya's;

"listen, Maya, he said softly. I was thinking...thinking about what...just happened, about what you did. Yes, that was a bad thing you did, tempting me like that, taking advantage of me while I was in a weak mood". (279)

Now he clearly uses different tools of negotiation-intrigue and threats, to protect himself and his reputation. He relegates Maya to the position of the temptress and the sub-servient. Taking full advantage of patriarchy, "a system of social structure and practices in which men dominate, oppress and exploit women," he cheats Maya and Bhima and Dinaz and Sera equally. (Walby 142)

Bhima's silence, her surly behaviour towards Viraf and her refusal to speak to him threaten him and provoke a negative response from him because he is aware that Bhima knows the reality and she holds the power to save or ruin his life. In psychological terms human beings feel two types of threats in their life which are elucidated by Paul Gilbert as "external and internal". External threats are threats that are perceived to lie outside of the self. Internal threats relate to the emergence of internal experiences that negatively impact on "self-evaluations, self-identity and self-presentation" (14). He is clearly vulnerable to both threats. To hide his misdeeds and self-protection, he uses negative negotiation and cunningly sets a trap for Bhima. He falsely tells Sera that Bhima has stolen seven hundred rupees from his cupboard. Bhima is completely shocked at his statement and she realizes that he must have planned it for weeks. She retaliates angrily, "I'll tell the story about your evil, how you ruined my family's reputation, how you stained my family's honour. Just open your mouth to the police, and I'll show you what I'm made of, you dirty dog" (301). Sera is shocked and confused at this development of Bhima. She is not able to understand the situation and her inner voice which gives her support and encouragement on many occasions fails to guide her at this critical moment. So she silently she sits on the sofa with a stricken look on her face.

As the situation builds to a crucial breakpoint, under relational obligations Sera is not able to show her resentment directly to Viraf, but it spontaneously appears in relation to Bhima when she calls Viraf a dog. She bursts out authoritatively, like a mistress not a friend, and tells Bhima, “control yourself have gone mad, talking in this low class way? don’t forget who you’re talking to” (301)

It is manifest at this juncture that class-consciousness again seems to play a vital role as Sera fails to negotiate beyond class boundaries and acts solely to protect her family and its honour. On the other hand, her action can also be explicated in line with the psychological effects of her dependency of Viraf and her only daughter Dinaz. This dependence leads to lack of self-esteem, lack of confidence, and the inability to take decisions. Sera turns towards Viraf inquiringly to know the truth from him even as Bhima expects Sera to take her side.

As a matter of fact, Sera clearly realizes that Viraf is lying. She recognizes that lines of hierarchy and kinship are clearly drawn between her and Bhima. They now shape their complex relationship. Sera seems to consciously choose conduct aimed at creating and maintaining family harmony. However, at a deeper level it is a mother’s protective instinct for her daughter that is driving her. Her reference to Dinaz is an oblique way of explaining that her behaviour is goaded by her concern for the wellbeing of her daughter.

Here Sera uses her class power to marginalize Bhima to protect her daughter’s life but in her rage Bhima only perceives it as a dastardly betrayal. To her Sera appears to choose family over friendship and class over sisterhood. Sera has to sacrifice Bhima to protect Dinaz and orders Bhima out from her life and from her home with the cryptic remark “Get out of my sight” (303). At these words of Sera, Bhima hears the resentment in her voice and she aware of the whole situation. But she notices the film of sweat on his face and a look of satisfaction and victory towards her. Sera’s action is painful for both Sera and Bhima and both are victims of Viraf’s villainy. Sera loses a friend and confidante and Bhima is bereft of Sera’s emotional, physical and psychological support. Natasha Mann comments;

For more than twenty years they have lived through each other’s pains and losses, and have been subject to secrets hidden even from their relatives, so that they have become bound by- if not friendship –then kindness, compassion and intimate knowledge. Only when a crisis occurs are they forced to choose their true allegiances (Mann)

Therefore, the long bonding between Sera and Bhima is overcome by Sera’s maternal instinct for Dinaz. In this situation Bhima’s silence about the seduction and abuse of Maya speaks volumes about her attachment to Sera. The difference in the choices they make opens a yawning space between them. Finally, Sera choose to save her daughter’s life and she believe her son-in-law’s “obvious lie” over Bhima’s “obvious truth”. (311) Ligaya Mishan observes in her review:

In the classic upstairs-downstairs story, you always have a sneaking suspicion that downstairs, freed of corsets and etiquette, the servants are having a lot more fun than their prim, monocle masters. But no such palliative exists in the world of Thrity Umrigar’s second novel, which examines the class divide... through the relationship of mistress and her servant. ([http:// www.umrigar.com/space-between.html](http://www.umrigar.com/space-between.html))

Henceforth, Sera and Bhima move in opposite directions; Sera moves inward to her family and home whereas Bhima steps out to an uncertain future. In the process of marginalization between man and woman and between woman and woman, Sera is cast in the image of a woman who is inward and diffident. She is willing to sacrifice her relationship with Bhima for the sake of peace and family relations. Thus, the seeds of marginalization produce the ‘class war’ where both Sera and Bhima are still form an ideal, democratic and liberated model of life where they have their own say in their particular position. Umrigar’s compassionate understanding of realities does not propel her to stretch her imagination towards the scope of proposing any mode of activism within her narratology.

At the end of the novel, it is Bhima who stands apart for her extraordinary strength and human resilience to withstand the terrible odds and pleasures when everything seems to be lost in a world like that of urbanized Mumbai where anonymity seems to be the hallmark of the poor of India. In contemporary India, there are innumerable Bhima who, as domestic servant, continue to scrub and clean the houses of Sera’s but cannot claim equality of fellowship, if not status. This is one of the modern travesties and tragedies of India.

There are many women like Sera, Bhima, Dinaz and Maya. The lives of these four women are ruined because of one man Viraf. In the roles of mothers Sera and Bhima want to save their daughters marital lives. In the course of saving her Dinaz's life sera sacrificing her life time companion Bhima. Feminist critic Uma Chakravathy rightly remarks:

"Class divides women. It extraordinarily succeeds in dividing women, in erasing a possibility of sisterhood. Such sisterhood can emerge only when we eliminate class and caste". (271)

This oppression of woman is not being tried to be understood or is purportedly connived at because women hold social security for their children and themselves before their individuality and try to avoid the social stigma of being marked as an abandoned woman. This weak point has given strength to patriarchal male dominance which is universally present.

To explore this class difference Umrigar briefly skims the concept of the subaltern. Bhima is a member of the subaltern class that labours in order to survive. In the polemics of heterogeneity, Gayatri Spivak includes: "the oppressed subject" and "the people of inferior rank." Notwithstanding the consciousness of class distinction, Sera and Bhima are able to negotiate around it to forge and sustain a strong bonding. In their relationship there is no need even of a verbal exchange and they share an "unspoken language, this intimacy that has developed between them over the years." (17) Sera helps Maya to pursue higher education and she takes the initiative to enroll her in college. Maya is also attached to Sera and several times comes to work for the Dubash family, particularly in the absence of her grandmother. In this all-women world Sera, Dinaz, Bhima, and Maya follow as easy rhythm from which Feroz is excluded. When Bhima's husband Gopal was admitted in the hospital, Sera and Feroz visited and enquired with the hospital staff and which compelled them to administer a new dose of anti-biotic to Gopal which helped him immensely for his speedy recovery. The power of education, wealth, position and of courses his Parsi heritage all are reflected in his high-handed attitude.

"I work for the TATA's, you understand? Do you know what pull we have with the hospital administration? One word from me and you will be out on the streets with you. And what's more I will make bloody sure not one other hospital in Bombay hires you (218)".

Bhima who was a witness to all this first that the air of confidence and power which Feroz Seth possessed, which made even the doctor in rubber slippers bow down in servility, was due to education. But later she realized that it was the easy grace and elegance which most Parsis possessed which prompted others to follow their order like meek lambs. Bhima both perplexed and happy wonders.

Sera understand Bhima's moods and she even appreciates Bhima's silence as there a lot is conveyed through Bhima's quiet gestures. Both share a very good bonding so good that even Sera had given half of her place to Bhima in her heart. Though Sera is well aware of the fact that Bhima maintained a decent sense of hygiene compared to other maids who lived in the near-by slums she is totally repulsed by her daughter's closeness to Bhima. In fact ever since Sera had known Bhima, she was quite aware of the fact that Bhima took a fifteen minute break at 4.00 p.m to tidy herself. "Her daily ministrations compelled Sera, who then became aware of her own-sour-smelling body, to stop whatever she was doing and freshen up". (29)

In fact, Bhima had been Sera's only companion at times when she was shaken up by the physical abuse meted out by her husband Feroz and soul-wrenching humiliation inflicted by Banu, her mother-in-law. Another reason as to why Bhima though a confidant of Sera is kept at a distance was that Sera had rarely come across such close master-servant behavior pattern in her own parental house or society in which she mingled.

The same attitude or behaviour which Sera have towards Bhima can be seen practiced by many upper caste Hindus especially among the Brahmin community. Even though the members might be highly educated and technology savvy many of them still keep servants at a bay and separate utensils are maintained for the use of the servant.

Dinaz presents a total resistance and challenge to the class consciousness by wholeheartedly accepting Bhima as an elderly mother-figure whom she adores. Though both parents are apprehensive about Dinaz's strange fascination to Bhima they keep quiet for the fear that Dinaz will openly blurt out and accuse of practicing caste-prejudice like that the Brahmin community. She always tells to her mother;

"You tell all your friends that Bhima is like a family member, that you couldn't live without her". (27)



And Dinaz accused her parents' discrimination towards Bhima. The women from the lower class are often stereotyped as attempting to hook men using their wily charms. It is because of the interiorisation of this stereotype that Sera in 'The Space between Us' refuses to believe Bhima when the latter blurts out the truth that it was Sera's son-in-law, Viraf who had raped Maya. In spite of several pleas by Bhima that Maya is innocent, Sera throws out Bhima out of her house. In case of any problem in which people from two opposite classes are involved, it is always the people from the lower class who are blamed, deemed guilty and left to suffer the consequences. Sera too blame Maya and redeem her son-in-law from the accusations. She insults Maya;

"What your Maya did is her business... She can be whore with fifty men for all I care. Just don't involve my family in her sickness. I've done all I could for that girl. Now I wash my hands of the whole family... get out of my sight". (303)

Bhima is not scared about losing her employment in Sera's house. Bhima did not gave up she went up to Sera to ask justice for her Maya's innocence. Through Sera and Bhima, one can see that in a tradition bound country like India, marriage, family and a girl's chastity becomes a primary aspect for a woman. Sera was stand on Viraf's side by pushing all the blame on Maya. But, she will never forget the words of Bhima and that words caw in her ears like crows and distress her in the sweaty and sleepless nights. Moreover, she ever be able to look at her only daughter's innocent, laughing face again and not think of Viraf's deceit.

The novel pulls on at opposite ends at the socio-economic spectrum of Mumbai city. The lasting impact the novel upon the reader's psyche is the way this two characters-one a victim of human cruelty, and the other, a victim of poverty and marginalization, survive the onslaught of a male dominated world and the condescendingly gossiping world of men and women with strength and fortitude. The way Umrigar juxtaposes contradictory thoughts, realities, and emotions is scintillating and soul-impacting, ushering in a compunctious catharsis. The title of the novel is so apt that it speaks of the spaces that ensure affinities and spaces that create distances vis-à-vis different relationships among characters in the novel. The soul-mate affinities of the space between Sera and Bhima are limitless but the cultural and class distances of the space between them are governed by Sera's background of birth, wealth, and status. Bhima is more an object of Sera's benediction and benefaction though she, as a subject, gives a valuable emotional support to Sera in the context of the predicament she lives with. Though the kindness Sera extends towards the wellbeing of Bhima and Maya has some therapeutic effect, to treat Bhima as an equal is an unacceptable proposition to Sera because of her 'upper-middle-class skin'. Sera even admires the way Dinaz appreciate Bhima but she has also the temerity to chide and caution her daughter against her rapport with Bhima. Thus, Umrigar imagined India is a reflection of the trajectory of class discrimination between the privileged and powerful and the poor and literature. Told from the point of view of the old woman, the story tellingly portrays the vicious circle in which the poor like Bhima are caught.

What makes Sera be kind to Bhima? Is it the experience of innumerable humiliations she had to undergo under her abusive husband and cruel mother-in-law then, or is it a sign of her moral and spiritual solidarity with the cause of the poor and marginalized? The answer is obviously the first one as the novelist implies. The bond of gender relationship both sera and Bhima maintain have their source of strength in their awareness of the crushing conjugal disappointments both of them have to endure. Sera is not capable of opting for a revolutionary step which would enable her to treat Bhima as an equal. Her bond of womanhood or feminine psyche does not transcend or eliminate the man-made barriers such as engendered poverty and deep-rooted class disparities India is destined to endure despite the progress achieved on several counts. This is why she is a more a type than an individual. Therefore, the poor are bound to be there everywhere and at all times-now and times to come, because of the citizenry in general believe, as Sera does, in certain constricting boundaries that perpetuate class considerations. The lyrical touch with which the novelist handles emotions of the central characters, the tragic beauty connoted by her narrative art, and the feminine psyche of the novelist enlightened by life-experiences in contemporary India contribute to the richness and the variety of new canonical trends set by women writers in India's post-nationalist modern literature.

Umrigar imagined Bhima is both an individual and type, and the real Bhima is known to the novelist by virtue of her childhood and teenage upbringing in Mumbai. In one of her radio conversations, Umrigar speaks of her hopes that one day she would meet her real Bhima, perhaps the one who worked for her house when she was living in India, but who is no more within the vicinity of her family apartment in Mumbai. The novel is aptly dedicated to the real Bhima and the millions like Bhima, critics have noticed similarities

of perception in Alice Walker's *The Color Purple*, Maya Angelou's *I know why the Caged Bird Sings*, Khaled Hosseini's *The Kite Runner*, and Rupa Bajwa's *The Sari Shop* but the blunt realism and compassionate aesthetics with which Umrigar presents the contemporary India through personal stories is uniquely Parsi-Indian. In Umrigar's words about Bhima:

"I loved Bhima, because I had just declared myself a Socialist and Bhima was my own private laboratory, my personal experiment, on whom to try out my newly discovered theories of social justice and the proletariat and the revolution". (P.S Umrigar)

Thus this novel is about women's strength, identity, survival, poverty, education, family and gender role are all explored. "It is dark, but inside Bhima's heart it is Dawn."(312). Thrity Umrigar projected Bhima as a woman of strong character who in spite of poverty and low status did not hesitate to fight for her granddaughter's cause at the cost of losing her livelihood and straining the long standing relationship between her mistress and her. At the end of the novel Bhima stands apart an extraordinary strength and human resilience to withstand the terrible odds and pressures when everything seems to be lost in the world.

Gender and the division of class, it is a theme that has interested me- haunted me, even- for as long as I can remember. One of the reasons I have always loved Bombay is because it is a city riddled with contradictions and paradox. In an apartment in a small corner of the city, I grew up experiencing a microcosm of this larger paradox- this strange tug-of war between intimacy and unfamiliarity; between awareness and blindness. (<http://www.umrigar.com/space-between.html>)

REFERENCES

1. Mistry, Rohinton. *Family Matters*. London: Faber, 2002.
2. Umrigar, Thrity. *The Space Between Us*. New Delhi: Harper Collins, 2005. Print.
3. Sengupta, Anjana. *Women on the Move: Socio-Cultural Dimensions Influencing Status of Rural Women*. Calcutta: Minerva, 2000. Print. Pp. 609
4. Beauvoir, Simon de. *The Second Sex*. Trans H.M. Parshley, London: Four Square Books Limited, 1961. Print. Pp. 609
5. Friday, Nancy. *My Mother/My Self*. New York: Bantam, 1987. Print .Pp. 39
6. Umrigar, Thrity. *Bombay Time*. New York: Picador, 2001.
7. Walby, Sylvia. "Structuring Patriarchal societies." *Sociology: introductory Readings*: Ed. Anthony Giddens and Philip W. Sutton. 3rd ed. Cambridge: Polity.P,2010. 142-148. Print.
8. Mann, Natasha. "Bombay Mix in the Home." Rev. of *The Space Between Us*, by Thrity Umrigar. *The Scotsman* (n.d.): n. pag. Web 5 July 2012
9. [http:// www.umrigar.com/space-between.html](http://www.umrigar.com/space-between.html)

PRINCIPAL
JMJC COLLEGE FOR WOMEN (Autonomous)
TENALI

